

# **HYPOXIA-ACTIVATED SMALL MOLECULE- INDUCED GENE EXPRESSION**



Thesis submitted for the degree of:  
DPHIL IN CHEMICAL BIOLOGY

**SARAH LOUISE COLLINS**

Exeter College, University of Oxford  
Trinity Term 2018

*Under the supervision of:*

Professor Stuart J. Conway (Oxford)

Professor Ester M. Hammond (Oxford)

Dr Laure Bouchez (Novartis)





**SCHOOL OF CHEMISTRY**  
**DECLARATION OF AUTHORSHIP**

**Name:** SARAH LOUISE COLLINS

**Candidate number:** 761382

**College:** EXETER

**Supervisor:** PROFESSOR STUART CONWAY  
PROFESSOR ESTER HAMMOND

**Title of thesis:** HYPOXIA-ACTIVATED SMALL MOLECULE-INDUCED GENE EXPRESSION

*Please tick to confirm the following:*

- |  |                                     |
|--|-------------------------------------|
| I have read and understood the University's disciplinary regulations concerning conduct in examinations and, in particular, the regulations on plagiarism.   | <input checked="" type="checkbox"/> |
| I have read and understood the Education Committee's information and guidance on academic good practice and plagiarism at <a href="https://www.ox.ac.uk/students/academic/guidance/skills?wssl=1">https://www.ox.ac.uk/students/academic/guidance/skills?wssl=1</a> .  | <input checked="" type="checkbox"/> |
| The dissertation I am submitting is entirely my own work except where otherwise indicated.   | <input checked="" type="checkbox"/> |
| It has not been submitted, either partially or in full, either for this Honour School or qualification or for another Honour School or qualification of this University (except where the Special Regulations for the subject permit this), or for a qualification at any other institution.   | <input checked="" type="checkbox"/> |
| I have clearly indicated the presence of all material I have quoted from other sources, including any diagrams, charts, tables, or graphs.   | <input checked="" type="checkbox"/> |
| I have clearly indicated the presence of all paraphrased material with appropriate references.   | <input checked="" type="checkbox"/> |
| I have acknowledged appropriately any assistance I have received in addition to that provided by my supervisor.  | <input checked="" type="checkbox"/> |
| I have not copied from the work of any other candidate.  | <input checked="" type="checkbox"/> |
| I have not used the services of any agency providing specimen, model or ghostwritten work in the preparation of this thesis/dissertation/extended essay/assignment/project/other submitted work. (See also section 2.4 of Statute XI on University Discipline under which members of the University are prohibited from providing material of this nature for candidates in examinations at this University or elsewhere: <a href="http://www.admin.ox.ac.uk/statutes/352-051a.shtml">http://www.admin.ox.ac.uk/statutes/352-051a.shtml</a> ). | <input checked="" type="checkbox"/> |
| I agree to retain an electronic copy of this work until the publication of my final examination result, except where submission in hand-written format is permitted.   | <input checked="" type="checkbox"/> |
| I agree to make any such electronic copy available to the examiners should it be necessary to confirm my word count or to check for plagiarism.  | <input checked="" type="checkbox"/> |

Candidate's signature: ..... Date: .....





# ABSTRACT

Hypoxia, conditions of insufficient oxygen, can occur in a wide variety of biological environments, including solid tumours, bacterial biofilms, and plants. Hypoxic tumours are associated with aggressive tumour phenotypes, increased resistance to radio- and chemotherapy, and poor patient prognosis. In biofilms, low oxygen delivery to cells causes significant reduction in bacterial growth rates, which increases resistance to antibiotics. Plants most commonly become hypoxic through flooding, which negatively impacts crop yields. Consequently, tools to study hypoxia are crucial. Hypoxia-activated prodrugs offer the ability to deliver compounds selectively to regions of hypoxia, through attachment of bioreductive groups, (e.g. 4 nitrobenzyl moiety). Oxygen-dependent nitroreductase enzymes catalyse reduction of the nitro group to form a radical nitro anion, which is re-oxidised back to the nitro group in the presence of oxygen. Under hypoxic conditions, this futile REDOX cycling cannot occur. The nitro anion radical is further reduced to form a hydroxylamine or amine; subsequent fragmentation releases the drug.

This work combines the concept of hypoxia-activated prodrugs with an IPTG-inducible gene expression system in *BL21 (DE3) E. coli* bacteria. We hypothesised that protecting IPTG **76** with a bioreductive group would inhibit IPTG-induced expression. Only under hypoxic conditions will reduction of the bioreductive group, release of IPTG **76** and induction of gene expression occur.

First, a hypoxia-activated resorufin-based fluorophore was employed to determine whether hypoxia-dependent bioreduction of a nitroaryl group would take place in bacteria using the *BL21 (DE3)* strain of *E. coli*. Then a range of derivatives of IPTG, protected with a bioreductive group were synthesised and analysed for their ability to undergo reduction and fragmentation to release IPTG **76**. Using, sfGFP as a reporter gene, these were then tested for their ability to induce hypoxia-dependent gene expression in *BL21 (DE3) E. coli*. Through fluorescence and western blot analysis, compound **94** was shown to induce expression of sfGFP in a hypoxia-dependent manner (Figure 1). This work represents a proof-of-concept system for hypoxia-

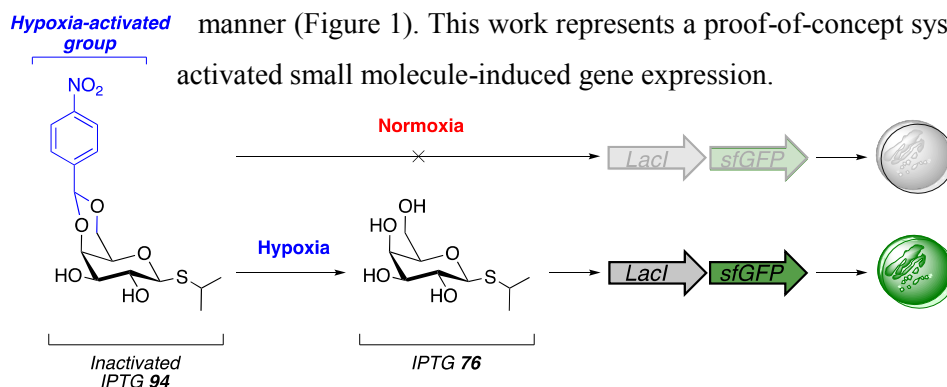


**Figure 1:** Hypoxia-activated small molecule induced gene expression. Compound **94** selectively induces expression of sfGFP in hypoxia.



*To Jesse,  
My thoughts are with you and your family.  
p.s. Sorry I didn't pick a better dye*



---

# TABLE OF CONTENTS

---

<b>ABSTRACT</b>	<b>i</b>
<b>ACKNOWLEDGMENTS</b>	<b>xi</b>
<b>ABBREVIATIONS</b>	<b>xiii</b>
<b>CHAPTER 1: INTRODUCTION</b>	<b>1</b>
<b>1.1. Introduction</b>	<b>1</b>
<b>1.2. Hypoxia and Solid Tumours</b>	<b>2</b>
1.2.1. Cancer	2
1.2.2. Development of Tumour Hypoxia	3
1.2.3. Implications of Tumour Hypoxia	6
1.2.4. Treating Tumour Hypoxia	8
<b>1.3. Hypoxia and Biofilms</b>	<b>10</b>
1.3.1. Biofilms	10
1.3.2. Formation of Biofilms	10
1.3.3. Causes and Implications of Hypoxia in Biofilms	12
<b>1.4. Hypoxia and Plants</b>	<b>14</b>
1.4.1. Causes and Implications of Hypoxia in Plants	16
1.4.2. Biotechnological Approaches to Overcome Plant Hypoxia	17
<b>1.5. Targeting Hypoxia</b>	<b>18</b>
1.5.1. Hypoxia-Activated Prodrugs (HAPs)	18
1.5.2. Mechanism of Activation and Hypoxia-Selectivity of HAPs	19
1.5.3. Classes of HAPs	20
1.5.4. Molecularly Targeted HAPs	30
1.5.5. Imaging Hypoxia with HAPs	33
<b>1.6. Gene Expression Systems</b>	<b>38</b>
1.6.1. Inducible Gene Expression Systems	39
1.6.2. Small Molecule-Induced Gene Expression Systems	40
<b>1.7. Aims</b>	<b>43</b>

<b>CHAPTER 2: A RESORUFIN-BASED HYPOXIA-ACTIVATED FLUORESCENT PROBE</b>	<b>45</b>
<b>2.1. Introduction and Aims</b>	<b>45</b>
<b>2.2. Hypoxia-Activated Fluorescent Probes</b>	<b>46</b>
<b>2.3. Evaluation of <b>63</b> as a Hypoxia-Activated Probe</b>	<b>47</b>
2.3.1. Synthesis of <b>63</b>	47
2.3.2. Zinc/NH <sub>4</sub> Cl Reduction of <b>63</b>	47
2.3.3. Cytochrome P450:NADPH Reductase Treatment of <b>63</b>	49
2.3.4. Cellular Analysis of <b>63</b>	50
<b>2.4. Evaluation of <b>79</b> as an Alternative Hypoxia-Activated Probe</b>	<b>52</b>
2.4.1. Synthesis <b>79</b>	53
2.4.2. Fluorescence Analysis of <b>79</b>	53
2.4.3. Zinc/NH <sub>4</sub> Cl Reduction of <b>79</b>	53
2.4.4. Cytochrome P450:NADPH Reductase Treatment of <b>79</b>	55
2.4.5. Cellular Analysis of <b>79</b>	57
<b>2.5. Conclusion</b>	<b>59</b>
<b>CHAPTER 3: SYNTHESIS OF HYPOXIA-ACTIVATED INDUCERS FOR AN IPTG-INDUCIBLE EXPRESSION SYSTEM</b>	<b>61</b>
<b>3.1. Introduction and Aims</b>	<b>61</b>
3.1.1. Analysis of LacI/IPTG Binding interactions	63
3.1.2. Design of Hypoxia-Activated Inducers	64
<b>3.2. Synthesis of a UV-Active Inducer of the <i>lac</i> Promoter</b>	<b>66</b>
3.2.1. Choice of Inducer	66
3.2.2. Synthesis of <b>103</b> and <b>104</b>	68
3.2.3. Analysis of Gene Expression	70
<b>3.3. Synthetic Strategy</b>	<b>72</b>
<b>3.4. Optimisation of 4-Nitrobenzyl Alkylation</b>	<b>73</b>
<b>3.5. Synthesis of 2-Position Protected Inducers</b>	<b>80</b>
<b>3.6. Synthesis of 3-Position Protected Inducers</b>	<b>82</b>
3.6.1. Routes 1 and 2 <i>via</i> Ester Protecting Groups	82
3.6.2. Route 3 <i>via</i> Selective Fmoc protection of the C3-OH Group	88
3.6.3. Route 4 <i>via</i> Direct Alkylation of Unprotected Galactopyranosides	90
<b>3.7. Synthesis of 4-Position Protected Inducers</b>	<b>93</b>
3.7.1. Route 1 <i>via</i> Regioselective Ring Opening of <b>127</b>	93
3.7.2. Route 2 <i>via</i> Tin-Mediated Regioselective Acylation	95
3.7.3. Route 3 <i>via</i> Ester Protecting Groups	98
3.7.4. Route 4 <i>via</i> Butane-1,2-Diacetal	100

<b>3.8. Synthesis of 6-Position Protected Inducers</b>	<b>104</b>
3.8.1. Route 1 <i>via</i> Deprotection of a 6-Position Silyl Ether	104
3.8.2. Route 2 <i>via</i> Alkylation of <b>129</b>	106
<b>3.9. Synthesis of 4,6-Acetal Protected Inducers</b>	<b>108</b>
3.9.1. Synthesis of 4-Nitrobenzylidene 4,6-Acetal Inducers	110
3.9.2. Synthesis of 2-Nitroimidazole 4,6-Acetal IPTG	112
3.9.3. Synthesis of 5-Nitrothiophene 4,6-Acetal IPTG	113
<b>3.10. Conclusion</b>	<b>114</b>
<b><u>CHAPTER 4: HYPOXIA-ACTIVATED SMALL MOLECULE-INDUCED GENE EXPRESSION</u></b>	<b><u>119</u></b>
<b>4.1. Introduction and Aims</b>	<b>119</b>
<b>4.2. Reduction and Bioreduction Analysis of <b>123</b>–<b>127</b></b>	<b>120</b>
4.2.1. Zinc/NH <sub>4</sub> Cl Reduction of <b>123</b> – <b>127</b>	120
4.2.2. Cytochrome P450:NADPH Reductase Treatment of <b>123</b> – <b>127</b>	122
<b>4.3. Hypoxia-Activated Gene Expression in <i>BL21 (DE3)</i> Bacteria</b>	<b>124</b>
4.3.1. Choice of Reporter System for Gene Expression	124
4.3.2. Flavin-Binding Fluorescent Proteins	126
4.3.3. Expression of pNIC28-iLOV and pNIC28-creiLOV	127
4.3.4. Expression of pT5-iLOV	130
4.3.5. Expression of pNIC28-sfGFP	131
4.3.6. Hypoxia-Dependent Expression of pNIC28-sfGFP	133
<b>4.4. Postulated Mechanism for Hypoxia-Activation of <b>94</b></b>	<b>138</b>
4.4.1. Mechanism 1: Fragmentation <i>via</i> a Hemi-Acetal to Release IPTG	140
4.4.2. Mechanism 2: Hemi-Acetal <b>301</b> Induces Gene Expression	141
<b>4.5. Steps Towards Hypoxia-Dependent Gene Expression in Mammalian Cells</b>	<b>143</b>
4.5.1. IPTG-Inducible Expression of sfGFP in Mammalian Cells	144
4.5.2. Improving Mammalian Cell Permeability	148
4.5.3. Investigation of Hypoxia-Dependent Gene Expression with a 2-Nitroimidazole Bioreductive Inducer	152
<b>4.6. Conclusion</b>	<b>155</b>
<b><u>CHAPTER 5: CONCLUSIONS AND FUTURE WORK</u></b>	<b><u>159</u></b>
<b>5.1. Conclusions</b>	<b>159</b>
<b>5.2. Future Work</b>	<b>161</b>
5.2.1. Modulating the Rate of IPTG Release	161
5.2.2. Translation Into Mammalian Cells	162
5.2.3. Considering Alternative Gene Expression Systems	163
<b>5.3. Concluding Remarks</b>	<b>164</b>

<b>CHAPTER 6: EXPERIMENTAL</b>	<b>165</b>
<b>6.1. General Chemical Methods</b>	<b>165</b>
<b>6.2. Synthetic Methods</b>	<b>170</b>
6.2.1. Synthesis of Resorufin-Based Probes	170
6.2.2. Synthesis of UV-Active Inducers	172
6.2.3. Optimisation of 4-Nitrobenzyl Alkylation Reaction	178
6.2.4. Synthesis of 2-Protected Galactopyranosides	181
6.2.5. Synthesis of 3-Protected Galactopyranosides	191
6.2.6. Synthesis of 4-Protected Galactopyranosides	207
6.2.7. Synthesis of 6-Protected Galactopyranosides	221
6.2.8. Synthesis of 4,6-Acetal Protected Galactopyranosides	233
<b>6.3. General Biological Methods</b>	<b>246</b>
6.3.1. Chemicals and Cell Culture Reagents	246
6.3.2. Bacterial Cell Culture	247
6.3.3. Mammalian Cell Culture	248
6.3.4. Cryopreservation of Cell Lines	248
6.3.5. Hypoxia Treatment	249
6.3.6. Cell lysis and SDS–PAGE Electrophoresis	250
6.3.7. Western blot	250
6.3.8. Fluorometric Analysis	251
6.3.9. HPLC-MS Analysis	252
6.3.10. Fluorescence Microscopy	253
6.3.11. DNA Transfection	254
6.3.12. Statistical Analysis	254
<b>6.4. Molecular Biology</b>	<b>256</b>
6.4.1. Primers	256
6.4.2. Constructs	257
6.4.3. Preparation of Competent <i>E. coli</i>	257
6.4.4. Cloning	258
6.4.5. Agarose Gel Electrophoresis	260
6.4.6. Extraction of DNA from Agarose Gels	261
6.4.7. Transformation of Bacteria	261
6.4.8. Extraction of Plasmid DNA from Bacterial Cells	261
6.4.9. Determination of DNA Concentration	262
6.4.10. DNA Sequencing	262



<b>6.5. Procedures for Biological Evaluation of Compounds</b>	<b>263</b>
6.5.1. Zinc Reduction	263
6.5.2. Enzyme Assays	264
6.5.3. Cellular Analysis of <b>63</b> and <b>79</b>	265
6.5.4. Analysis of Alternative Inducers <b>103</b> and <b>104</b>	266
6.5.5. GFP Fluorescence Recovery	266
6.5.6. Procedure for Bacterial Hypoxia-Induced Gene Expression	267
6.5.7. Disc Assay Analysis of the Oxygen Dependency of <b>94</b>	267
<b>REFERENCES</b>	<b>269</b>
<b>APPENDICES</b>	<b>289</b>
<b>A. DNA Sequences for Fluorescent Proteins</b>	<b>289</b>
<b>B. Plasmid Maps</b>	<b>290</b>
<b>C. Selected NMR Spectra</b>	<b>300</b>
<b>D. Image Permissions</b>	<b>405</b>



---

# ACKNOWLEDGMENTS

---

First, I would like to thank my two supervisors: Stuart and Ester. Stuart – thank you for accepting me into your group and for your support and patience, especially at the start. I have enjoyed our running chats in the lab and science chats on runs! Also, I hear you had a pretty cool idea while at Caltech... Ester – I am incredibly grateful to you for welcoming me into your lab and for letting me bring my “bugs” up the hill (even if I do insist on calling them cells). Thank you for your down-to-earth advice and for teaching me not only to approach problems from a more biological perspective but also to stop overcomplicating things! Thank you to the BBSRC and Novartis for funding and to Laure for giving me the fantastic opportunity to work in her lab at NIBR in Basel.

I would also like to thank Alix, and especially Lisa, for giving up so much of their time over the years to help me with the HPLC in Oncology. Thank you also to all the staff in both the CRL and ORCRB, whose work behind the scenes keep the departments functioning as well as they do.

My experience over the past four years has been shaped by the many people I have worked with across both research groups. Thank you all for the many interesting discussions and fun times both in the lab and out. Thank you also to everyone who read chapters, sometimes at very short notice. Special mention to all the SJC runners who have shared my love of running, joined me on runs, and even maybe made marathon running seem like not such a crazy idea (Amy, Mus, Joe, Coco, Ewen, Alex, Amélie and Stuart). It definitely makes the amount of cake we manage to put away seem more acceptable! Larissa, thank you for brightening up G12, keeping me company during columns, and sharing my organising habits. It also makes me laugh that we enjoy the same puzzles! Catherine, you are one of the most kind-hearted people I know. Never stop smiling...or being our crazy cat lady and Coco, thanks for being a great desk buddy (although I think I’ll be finding stickers on things for a long time to come!) Ewen, thank you not only for your advice about everything chemistry-related but also for your willingness to listen and talk to me about a

## *Acknowledgments*

whole range of non-science-topics. Thank you also to my biology teachers: Anthony, who taught me aseptic techniques, bacterial cell culture and cloning, and Ishna, who taught me mammalian cell culture. In addition, thank you to everyone in Ester's lab who helped with the biology aspects of my project, whether it be through splitting me a flask of cells, taking something into the Bactron or getting in touch with your inner chemist to take a time point. ;) Lingbing, thank you for sharing your extensive sugar-chemistry knowledge with me. From that first question about glycosylations to showing me your latest lab technique, you have taught me so much. Your friendship is very special to me and I am so happy that everything is working out for you in Japan. Amélie, you really helped me to find my feet in Oxford and I couldn't have asked for a better friend to do my PhD alongside. Thank you for all the wonderful times in Oxford, Paris, Basel, and now California. I look forward to wherever our next adventure takes us.

Away from the lab, thank you to my Durham friends for some great trips and weekends away. Although we are now scattered around the world, I'm sure whenever we meet up we will always end up talking, walking, and talking some more!

Martin, when I arrived at that flat on Cowley Road, I wasn't really sure what any of my new housemates would be like. Who'd have thought that, more than three years later, we'd be where we are now? Thank you for your support, always making me laugh, and, of course, the tea and baking. Whatever we do, wherever we go next, I'm glad you are a factor! :P Love you.

Lastly, thank you to my amazing family who have supported and encouraged me every step of the way. Josh, Peter, Zoe (and the newest addition, Rose ☺), thank you for always believing in me, even when you had no idea what I was doing! Peter, thank you also for being our football coach – it was great to spend so much time with you that year. Thanks also to Aurora for being my comfort during thesis writing. Finally, Mum and Dad: this journey started a long time before I even set foot in Oxford. Thank you for your unconditional love and support through school, university and now my PhD. From putting up with my tears to celebrating the happy moments, thank you for always being there.

---

# ABBREVIATIONS

---

<b>× <i>g</i></b>	times gravity
<b>4-TsOH</b>	4-toluenesulfonic acid
<b>Ac</b>	acetyl
<b>aq.</b>	aqueous
<b>ATP</b>	adenosine triphosphate
<b>BDA</b>	butane-1,2-diacetal
<b>Bn</b>	benzyl
<b>Bz</b>	benzoyl
<b>C2-OH</b>	2-position hydroxyl group
<b>C3-OH</b>	3-position hydroxyl group
<b>C4-OH</b>	4-position hydroxyl group
<b>C6-OH</b>	6-position hydroxyl group
<b>CDA</b>	cyclohexane-1,2-diacetal
<b>CF</b>	cystic fibrosis
<b>conc.</b>	concentrated
<b>COSY</b>	homonuclear correlation spectroscopy
<b>CYP</b>	cytochrome P450
<b>DAPI</b>	4',6-diamidino-2-phenylindole dihydrochloride
<b>DBU</b>	1,8-diazabicyclo[5.4.0]undec-7-ene
<b>DMAP</b>	<i>N,N</i> -dimethyl-4-aminopyridine
<b>DMEM</b>	Dulbecco's modified Eagle's medium
<b>DMF</b>	dimethylformamide
<b>DMNB</b>	4,5-dimethoxy-2-nitrobenzyl
<b>DMSO</b>	dimethyl sulfoxide
<b>DNA</b>	deoxyribonucleic acid
<b><i>E. coli</i></b>	<i>Escherichia coli</i>

## Abbreviations

<b>EGFR</b>	epidermal growth factor receptor
<b>EPS</b>	extracellular polymeric substance
<b>eq.</b>	equivalents
<b>ESI</b>	electrospray ionisation
<b>FbFP</b>	flavin-binding fluorescent protein
<b>FBS</b>	foetal bovine serum
<b>Fmoc</b>	fluorenylmethyloxycarbonyl
<b>g</b>	gram(s)
<b>G-DEPT</b>	gene-directed enzyme prodrug therapy
<b>GFP</b>	green fluorescent protein
<b>GLUT</b>	glucose transporter
<b>h</b>	hour(s)
<b>HAP</b>	hypoxia-activated prodrug
<b>HBOT</b>	hyperbaric oxygen therapy
<b>HCR</b>	hypoxic cytotoxicity ratios
<b>HIF-1</b>	hypoxia inducible factor 1
<b>HMBC</b>	heteronuclear multiple-bond correlation
<b>HPLC</b>	high-performance liquid chromatography
<b>HRE</b>	hypoxia response element
<b>HRMS</b>	high resolution mass spectrometry
<b>HSQC</b>	heteronuclear single quantum coherence
<b>Hz</b>	hertz
<b>ICT</b>	intramolecular charge transfer
<b><i>i</i>Pr</b>	<i>iso</i> -propyl
<b>IPTG</b>	isopropyl 1-thio- $\beta$ -D-galactopyranoside
<b>IR</b>	infrared
<b><i>J</i></b>	coupling constant
<b>LacI</b>	<i>lac</i> repressor
<b><i>lacO</i></b>	<i>lac</i> operator
<b>LF2000</b>	lipofectamine 2000
<b>LF3000</b>	lipofectamine 3000
<b>lit.</b>	literature value

<b>LOV</b>	light, oxygen, or voltage
<b>LRMS</b>	low resolution mass spectrometry
<b>M</b>	molar
<b>MCS</b>	multiple cloning site
<b>Me</b>	methyl
<b>MeCN</b>	acetonitrile
<b>MeOH</b>	methanol
<b>mg</b>	milligram(s)
<b>MHz</b>	megahertz
<b>min</b>	minute(s)
<b>mL</b>	millilitre(s)
<b>mp</b>	melting point
<b>MRI</b>	magnetic resonance imaging
<b>MS</b>	mass spectrometry
<b>Ms</b>	methanesulfonyl (or: mesyl)
<b>MS</b>	molecular sieves
<b>NAD(P)H</b>	nicotinamide adenine dinucleotide (phosphate)
<b>NHE</b>	normal hydrogen electrode
<b>NIBR</b>	Novartis Institute for Biomedical Research
<b>NIR</b>	near infrared
<b>NMR</b>	nuclear magnetic resonance
<b>NOESY</b>	nuclear Overhauser effect spectroscopy
<b>NP</b>	normal phase
<b>NQO1</b>	NAD(P):quinone oxidoreductase
<b>NSCLC</b>	non-small cell lung carcinomas
<b>OD</b>	optical density
<b>OER</b>	oxygen enhancement ratio
<b>PAMPA</b>	parallel artificial membrane permeation assay
<b>PARP</b>	poly(ADP-ribose) polymerase
<b>PBS</b>	phosphate-buffered saline
<b>PDB ID</b>	protein data bank identification
<b>PE</b>	petroleum ether

## Abbreviations

<b>PET</b>	positron-emission tomography
<b>PFA</b>	paraformaldehyde
<b>Ph</b>	phenyl
<b>PNB</b>	4-nitrobenzyl
<b>pO<sub>2</sub></b>	partial pressure of oxygen
<b>ppm</b>	parts per million
<b>R<sub>f</sub></b>	retention factor
<b>RNA</b>	ribonucleic acid
<b>RP</b>	reversed phase
<b>RT</b>	room temperature
<b>rtTA</b>	reverse tetracycline-controlled transactivator
<b>sat.</b>	saturated
<b><i>sept</i></b>	septet
<b>sfGFP</b>	superfolder green fluorescent protein
<b>SM</b>	starting material
<b>SNARF</b>	seminaphthorhodafluors
<b>TBAB</b>	tetrabutylammonium bromide
<b>TBAF</b>	tetrabutylammonium fluoride
<b>TBDMS</b>	<i>tert</i> -butyldimethylsilyl
<b>TBDPS</b>	<i>tert</i> -butyldiphenylsilyl
<b>TBS</b>	tris-buffered saline
<b><sup>t</sup>Bu</b>	<i>tert</i> -butyl
<b><i>tetO</i></b>	tetracycline operator
<b>TetR</b>	tetracycline repressor
<b>Tf</b>	trifluoromethanesulfonate (triflate)
<b>TFA</b>	trifluoroacetic acid
<b>THF</b>	tetrahydrofuran
<b>TKI</b>	tyrosine kinase inhibitor
<b>TLC</b>	thin layer chromatography
<b>TMS</b>	tetramethylsilane
<b>TPZ</b>	tirapazamine
<b>Ts</b>	4-toluenesulfonyl (tosyl)



<b>v/v</b>	volume per unit volume (1% = 1 mL/100 mL)
<b>w/v</b>	weight per unit volume (1% = 1 g/100 mL)



---

# CHAPTER 1

## INTRODUCTION

---

### 1.1. Introduction

The ability to produce a sufficient amount of energy to maintain normal cellular function is essential for the survival of all organisms. This energy is usually generated and stored in the form of adenosine triphosphate (ATP), which contains a high-energy phosphate bond that is used to power physicochemical reactions in living cells.<sup>1</sup> Production of ATP in a cell occurs primarily through either oxidative phosphorylation or anaerobic glycolysis, although a third pathway (aerobic glycolysis, also known as the Warburg effect) has also been described in proliferating cancer cells (Figure 1.1).<sup>2,3</sup> Oxygen serves as the final electron acceptor in oxidative phosphorylation, which is more efficient and generates more ATP than glycolysis.<sup>4</sup> Furthermore, an analysis of the metabolic network across more than 70 genomes suggested that molecular oxygen is involved in more than 350 reactions, making it one of the most-utilised compounds in eukaryotic cellular metabolism.<sup>5</sup> It is clear that oxygen is an essential factor for most multicellular life to exist; many multicellular organisms would not be sustained by energy produced from anaerobic glycolysis alone.<sup>1,6</sup>

Hypoxia, conditions of insufficient oxygen, can occur in a number of biological environments including solid tumours,<sup>7</sup> bacterial biofilms,<sup>8</sup> and plants.<sup>9</sup> Hypoxia is primarily caused by an inadequate oxygen supply to support cellular function.<sup>10,11</sup> In this chapter, the causes and consequences of hypoxia in each of these settings will be considered in turn. Next, the use of bioreductive prodrugs to target and image hypoxia will be discussed. Finally, the last section of this chapter will focus on inducible gene expression systems and how the principle of bioreductive

prodrugs could be applied to such systems to control gene expression in a hypoxia-dependent manner.

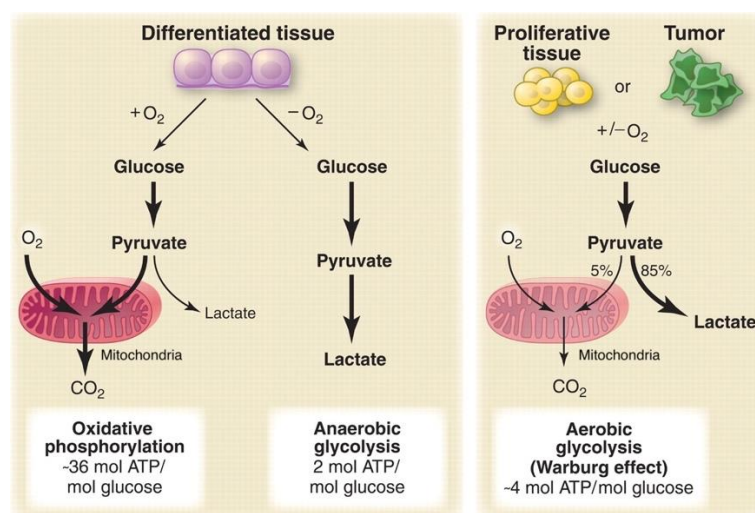


**Figure 1.1:** Schematic representation of the differences between oxidative phosphorylation, anaerobic glycolysis, and aerobic glycolysis (Warburg effect). Figure reprinted from M. G. V. Heiden, L. C. Cantley, C. B. Thompson, *Science* **2009**, 324, 1029–1033 with permission from AAAS.<sup>2</sup>

## 1.2. Hypoxia and Solid Tumours

### 1.2.1. Cancer

Cancer is the term used to describe a collection of related diseases characterised by the growth of abnormal cells, which divide without control (neoplasia) and can invade nearby tissues. It is second only to cardiovascular disease as a cause of death worldwide.<sup>12</sup> In 2012, an estimated 8.2 million people died from cancer with a further 14.1 million new cases diagnosed.<sup>13</sup> Despite significant research efforts into improving the understanding of cancer biology, based on recent trends in major cancers, the number of new diagnoses is expected to increase to 22.2 million each year by 2030.<sup>14</sup>

The complexity and diversity of different cancers makes treatment of cancer patients challenging. Indeed, there are over 100 distinct types of cancer, many of which also have subtypes found within different organs.<sup>15</sup> Although all cancers result from somatic mutations, the causes and exact nature of these mutations varies across the vast range of different cancer types.<sup>16,17</sup> To understand

what causes normal cells to become tumourigenic, in 2000 Hanahan and Weinberg proposed six “hallmarks of cancer”, which describe key alterations in cell physiology that are common to all cancers, and which allow cancer cells to survive, proliferate, and disseminate.<sup>15</sup> This list was subsequently expanded to include two emerging hallmarks (altering cellular metabolism to support neoplastic growth and the ability to avoid immunological destruction) and two enabling characteristics (genomic instability and tumour-induced inflammation). The enabling characteristics facilitate acquisition of the other eight hallmarks by tumour cells (Figure 1.2).<sup>18</sup> Together these concepts have helped to direct many areas of cancer research, providing a solid foundation for improving our understanding of the biology of cancer.

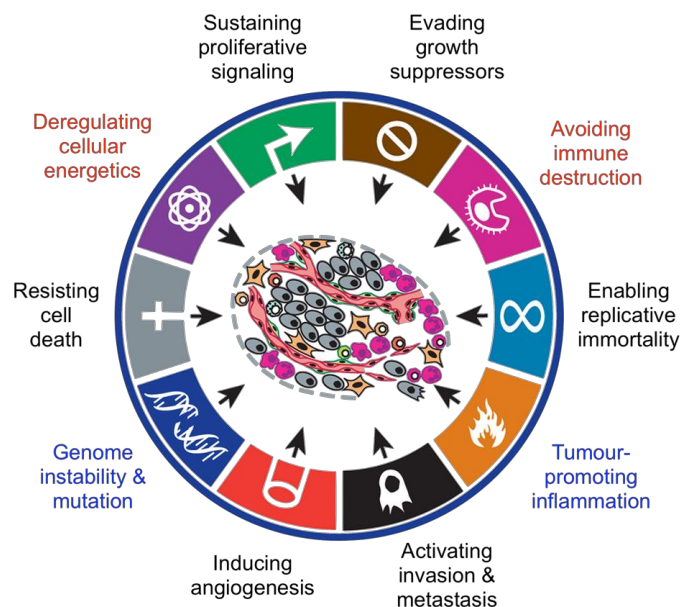


**Figure 1.2:** Illustration showing the original six hallmarks of cancer (black), described by Hanahan and Weinman,<sup>15</sup> the two additional emerging hallmarks (red), and two enabling factors (blue). Figure adapted and reprinted from D. Hanahan, R. A. Weinberg, *Cell* **2011**, *144*, 646–674 with permission from Elsevier, License No. 4423610377962.<sup>18</sup>

### 1.2.2. Development of Tumour Hypoxia

The order and mechanisms by which cancers acquire these hallmarks are strongly influenced by the tumour microenvironment, which consists of normal cells, molecules, and blood vessels that surround and feed a tumour cell. In many solid tumours, it is characterised by regions of hypoxia.<sup>19,20</sup> Hypoxic tumours are associated with aggressive tumour phenotypes, increased

genomic instability and metastases, resistance to radio- and chemotherapy, and, consequently, poor patient prognosis.<sup>21–23</sup>

Tumour hypoxia results from an imbalance between oxygen supply and oxygen consumption.<sup>24</sup> Rapidly proliferating cells have increased energy requirements to fuel their cell growth and division, which results in an increase in their oxygen consumption.<sup>24</sup> To cope with this increased demand for oxygen, the tumour can initiate the formation of new blood vessels in a process known as angiogenesis.<sup>25,26</sup> However, whereas normal, healthy tissues are supplied by blood vessels that are highly organised into definitive venules, arterioles, and capillaries, the newly formed tumour vasculature is abnormal and chaotic. Furthermore, the tumour blood vessels are architecturally different, characterised by irregular shapes, dead-ends, sluggish blood flow, and leakiness.<sup>25,27</sup> Consequently, the supply of oxygen to parts of the tumour becomes limited and regions of hypoxia develop.

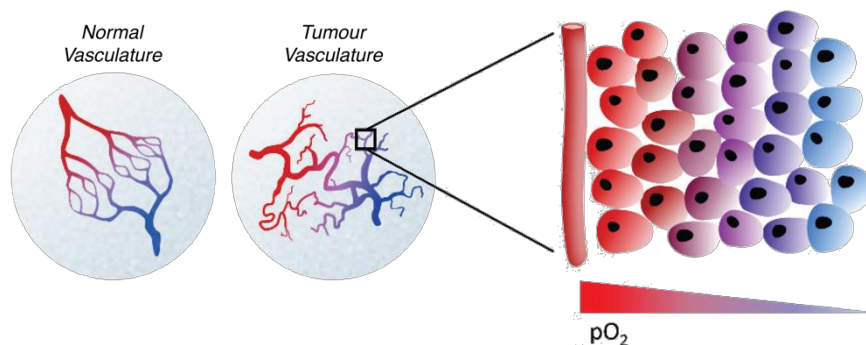


**Figure 1.3:** Diagram showing hypoxia in the tumour microenvironment. Tumour cells are characterised by a disordered vasculature. When the high rate of tumour growth cannot be sustained by tumour angiogenesis, cells distal to the blood vessel have a limited supply of oxygen, resulting in regions of hypoxia. Figure adapted and reprinted from S. Ramachandran, J. Ient, E.-L. Göttgens, A. Krieg, E. Hammond, *Genes* **2015**, 6, 935–956.<sup>28</sup>

Two pathways have been described for the development of hypoxia in solid tumours: diffusion-limited and perfusion-limited. In diffusion-limited hypoxia, oxygen is unable to diffuse through respiring cells farther than  $\sim 150\ \mu\text{m}$  from functional blood vessels, resulting in chronically hypoxic regions.<sup>29</sup> Consequently, the further away from the vasculature the cells in the tumour are, the more hypoxic they become (Figure 1.3).<sup>24,29,30</sup> In perfusion-limited hypoxia, acutely hypoxic regions are caused by transient changes in blood flow;<sup>30,31</sup> the reoxygenation of cells following reperfusion of microvessels is known as cycling hypoxia.<sup>32,33</sup>

Although normoxia is usually taken to be the oxygen partial pressure ( $\text{pO}_2$ ) of air (21%), the normal physiological  $\text{pO}_2$ , known as physioxia, varies between different tissues, according to their metabolic requirements and functional status.<sup>34</sup> This makes it difficult to define an absolute  $\text{pO}_2$  value that can be considered hypoxic, although there appears to be a critical  $\text{pO}_2$  value at 1% oxygen;  $\text{pO}_2$  values below this point are associated with adverse effects caused by reduced oxygen.<sup>7,11,34</sup> Both chronic and cycling hypoxia can occur in solid tumours and, consequently, the oxygen tension in tumours is dynamic and highly heterogeneous, ranging between approximately 8% and 0.02%.<sup>21</sup> All human tumours have been shown to have median oxygen levels lower than their normal tissue of origin, highlighting the presence of hypoxic regions across the diverse range of solid tumours (Table 1.1).<sup>21,35,36</sup>

**Table 1.1:** Median partial pressures of oxygen ( $\text{pO}_2$ ) in various tumour cell types compared with the normal values in their tissue of origin.<sup>36</sup>

Tumour Type	Normal $\text{pO}_2$ (Median % $\text{O}_2$ )	Tumour $\text{pO}_2$ (Median % $\text{O}_2$ )
Brain	4.6	1.7
Breast	8.5	1.5
Cervical	5.5	1.2
Renal (Kidney)	9.5	1.3
Liver	4.0–7.3	0.8
Non-small-cell lung cancer	5.6	2.2
Pancreas	7.5	0.3
Rectal carcinoma	3.9	1.8

### 1.2.3. Implications of Tumour Hypoxia

The clinical implications of tumour hypoxia for the treatment of cancers are well documented and instances of poor patient prognosis have been observed in a number of trials.<sup>22,23,37</sup> For example, in a study on a population of patients with advanced cancer of the uterine cervix, tumour oxygenation status was the strongest independent predictor of overall and disease-free survival. Patients with a median  $pO_2 < 10$  mmHg (1.3%  $O_2$ ) had a survival rate of 40%; this was half the survival rate of patients who had a median  $pO_2 > 10$  mmHg (1.3%  $O_2$ ) (Figure 1.4).<sup>38</sup> A similar effect has also been observed in studies on patients with skin cancer,<sup>39</sup> head and neck cancer,<sup>40,41</sup> and in human soft tissue sarcoma.<sup>42,43</sup>

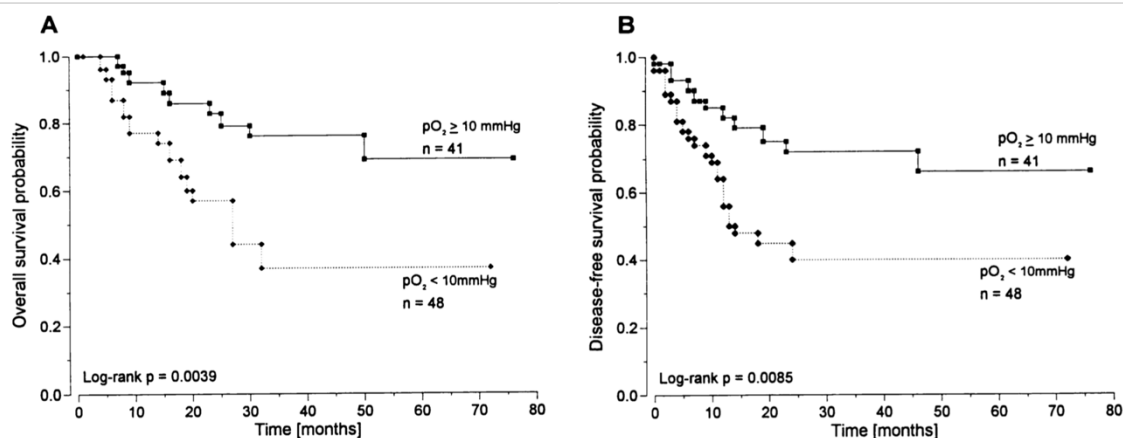


**Figure 1.4:** A) Overall and B) disease-free survival probabilities calculated with the Kaplan-Meier method for 89 patients treated with curative intent stratified for tumour oxygenation from a study on a population of patients with advanced cancer of the uterine cervix. Figure adapted and reprinted from M. Höckel, K. Schlenger, B. Aral, M. Mitze, U. Schaffer, P. Vaupel, *Cancer Res.* **1996**, *56*, 4509–4515 with permission from the AACR, License No. 4425301420715.<sup>38</sup>

There are a number of reasons why hypoxic tumours are difficult to treat using radio- or chemotherapy.<sup>44,45</sup> Radiotherapy relies on molecular oxygen, which is a powerful radiosensitiser, to be effective. Both acute and chronic hypoxia increase resistance to radiotherapy (X- and  $\gamma$ -radiation),<sup>46,47</sup> while severely hypoxic cells ( $< 0.1\%$   $O_2$ ) require a 2.5–3 times higher dose of radiation than cells that were well-oxygenated at the time of treatment (Figure 1.5).<sup>48</sup>



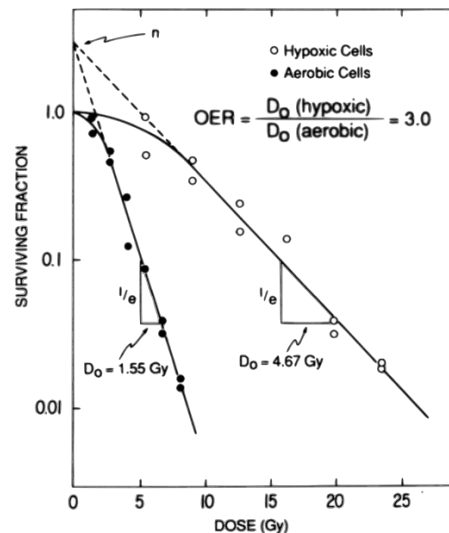


**Figure 1.5:** Survival curves for hypoxic and aerobic cells in cell culture show the oxygen enhancement effect (OER). Exponentially growing EMT6 mouse mammary tumour cells were irradiated under aerobic conditions or were made severely hypoxic just before and during irradiation with 250 kV X-rays. Cell survival was measured immediately after irradiation using a colony formation assay. The hypoxic cells are three times as resistant to irradiation as the aerobic cells. Figure reprinted from S. Rockwell, I. T. Dobrucki, E. Y. Kim, S. T. Marrison, V. T. Vu, *Curr. Mol. Med.* **2009**, 9, 442–458 with permission from Eureka Science, License No. 4427700610567.<sup>44</sup>

The increased radiation dose required to produce an equivalent effect in hypoxic samples compared with well-oxygenated samples is termed the oxygen enhancement effect and has been explained through the oxygen fixation hypothesis.<sup>49–51</sup> For oxygen to act as a radiosensitiser, it must be present during or up to 5 ms after irradiation.<sup>49,52</sup> Radiation interacts either with DNA directly or with intracellular water to form highly-reactive free radicals, which can, in turn, induce DNA damage. These free radicals also react with oxygen, “fixing” the damage through the formation of peroxide radicals, which are much more damaging and difficult for the cell to repair. In the absence of oxygen, these peroxide radicals do not form and the initial DNA damage will be readily repaired by the cell.<sup>49–51</sup>

Chemotherapy is also dependent on a number of factors to be effective. In general, hypoxic cells are resistant to most anticancer drugs.<sup>53</sup> Due to the inefficient vasculature of solid tumours, many areas of the tumour are poorly supplied with blood vessels. Consequently, this same feature that prevents the penetration of oxygen in diffusion-limited hypoxia also affects diffusion of the drug

into the tumour. Chemotherapeutic agents must diffuse relatively long distances through the extravascular compartment to reach their targets; cells further from the blood vessel receive a lower dose of drug and, therefore, survive.<sup>54,55</sup> Furthermore, many anticancer drugs target rapidly dividing cells. However, cell proliferation is inhibited by hypoxia and, consequently, the effectiveness of the drug is reduced.<sup>27,56</sup>

#### 1.2.4. Treating Tumour Hypoxia

Hypoxia is a major clinical challenge in the treatment of patients with solid tumours and a variety of strategies have been investigated to improve treatments. Some approaches, such as the use of hyperbaric oxygen therapy (HBOT) or radiosensitisers, have focused on increasing the effectiveness of radiotherapy.<sup>57</sup> In HBOT, patients breathe air enriched with oxygen prior to radiation. This increases the dissolved oxygen concentration in blood plasma, which in turn increases the local concentration at the tumour.<sup>58</sup> Alternatively, radiosensitisers, which mimic the effect of oxygen in radiotherapy, have been employed. The majority of these radiosensitisers are based on a nitroimidazole scaffold (Figure 1.6). Early work utilised 2-nitroimidazole derivatives, such as misonidazole **1**. However, the toxicity of 2-nitroimidazoles at high concentrations resulted in severe side effects, such as delayed peripheral neuropathy and, at acceptable doses, a maximum oxygen enhancement ratio of only 1.5–2.0 was achieved.<sup>57</sup> Subsequent work has focused on 5-nitroimidazoles, such as nimorazole **2**, which has been shown to significantly improve the effect of radiotherapy in patients with head and neck tumours.<sup>59</sup>

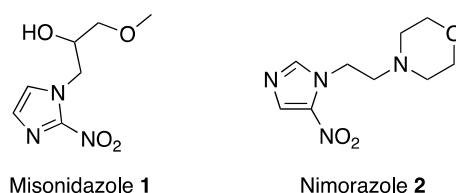


**Figure 1.6:** Structures of the radiosensitisers misonidazole **1** and nimorazole **2**.

A third strategy aims to selectively kill hypoxic cells by specifically targeting the hypoxic fraction of tumour cells. Hypoxic tumours present a unique phenotype and microenvironment that can be exploited in therapeutics to reduce toxicity to normal tissues. For example, following its

stabilisation in hypoxia, the hypoxia-inducible factor 1 (HIF-1) activates transcription of several genes that are involved in many important aspects of cancer biology, including angiogenesis, cell survival, and invasion. This provides an opportunity for molecularly targeted therapeutics: in this case, small molecule inhibitors aimed at exploiting biochemical responses to hypoxia (See Section 1.5.4). In particular, inhibition of HIF-1, or any of its target genes, is an attractive therapeutic strategy that is specific to tumour cells.<sup>53,60,61</sup>

Another approach to specifically target hypoxic tumour cells includes gene-directed enzyme prodrug therapy (G-DEPT). This method uses selective expression of a prodrug-activating enzyme in tumour cells alongside concurrent administration of a non-toxic prodrug; the expressed enzyme converts the prodrug to the active, toxic drug inside the tumour cell (Figure 1.7).<sup>62</sup> Methods for selective delivery of the prodrug-activating enzyme to tumour cells include placing it downstream of the hypoxia response element (HRE), thereby controlling its expression with HIF-1,<sup>63</sup> or the use of recombinant obligate anaerobic bacteria, which have been shown to preferentially accumulate in tumours.<sup>64</sup>

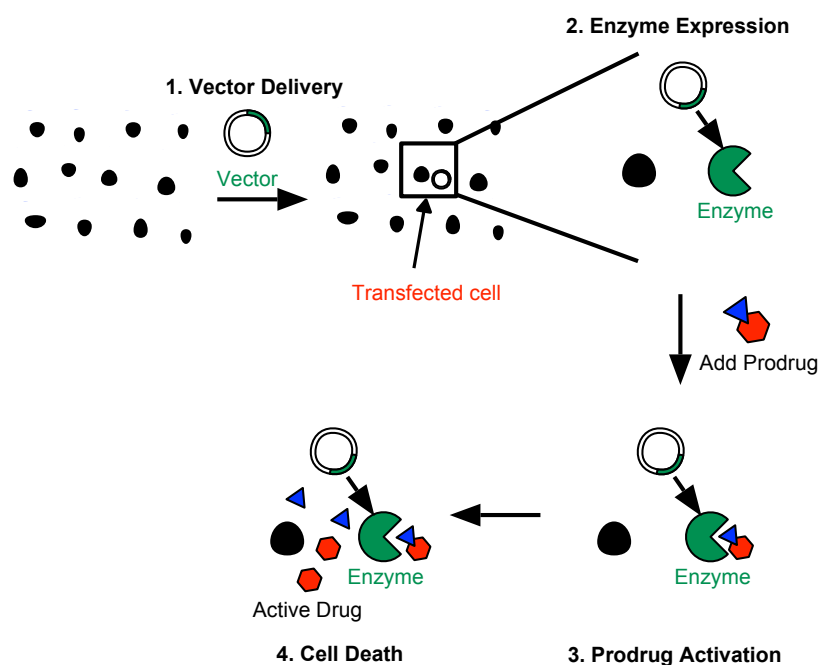


**Figure 1.7:** Schematic representation of the mechanism of action in G-DEPT. A prodrug-activating enzyme is selectively expressed in tumour cells with concurrent administration of a non-toxic prodrug; the enzyme converts the nontoxic prodrug into its cytotoxic form resulting in the death of the transfected cancer cells.

Lastly, alternative prodrugs are being developed that directly exploit the chemically reducing conditions found in hypoxic regions.<sup>65</sup> The use of this bioreductive prodrug strategy to target, image, and treat hypoxia will be discussed in more detail in Section 1.5.1.

### **1.3. Hypoxia and Biofilms**

#### **1.3.1. Biofilms**

A second biological setting where hypoxia is important is in biofilms. A microbial biofilm is a dense, sessile population of microorganisms, irreversibly attached to a surface and embedded in an extracellular polymeric substance (EPS) matrix that is usually secreted by the microorganism itself.<sup>66,67</sup> The microorganisms must also exhibit an altered phenotype, with respect to growth rate and gene transcription, compared with the planktonic form; these changes are referred to as the “biofilm phenotype”.<sup>68</sup> Evidence of biofilm formation from early fossil records suggests that the first prokaryotic biofilms existed more than three billion years ago.<sup>69,70</sup> It is now known that organisms from each of the Archaea, Bacteria, and Fungi kingdoms are all capable of forming biofilms.<sup>66,71</sup> Biofilms can adhere to almost any surface, resulting in serious, harmful effects in a range of natural, medical, and industrial settings.<sup>72</sup> For example, biofilms have been implicated in more than 80% of bacterial infections in humans,<sup>73</sup> including a number of chronic infections such as periodontitis (gum disease),<sup>74</sup> ulcers,<sup>75</sup> and cystic fibrosis (CF).<sup>76–79</sup> They also commonly form on medical devices, such as catheters, artificial joints, and heart valves.<sup>66,67,80–84</sup> In an industrial setting, biofilm formation in water and sewage pipes or on the hull of ships can cause water contamination and erosion.<sup>67,72,85</sup>

#### **1.3.2. Formation of Biofilms**

It has been proposed that not only are nearly all bacteria capable of forming a biofilm, but also that a significant portion of their lifetime is spent within a biofilm community.<sup>86</sup> Studies into the underlying molecular mechanisms that dictate biofilm formation have shown that these pathways can vary between different species or even within strains of the same species.<sup>72</sup> Despite this, there are a number of characteristics, including morphology and macroscopic arrangement, that are shared between all biofilms. Guided by microscopic analysis, these have led to the generalisation

of the process of biofilm formation into five discrete stages, each with its own unique phenotype (Figure 1.8).<sup>86,87</sup> Interestingly, a similar series of stages have also been described in fungi biofilm formation.<sup>88</sup>

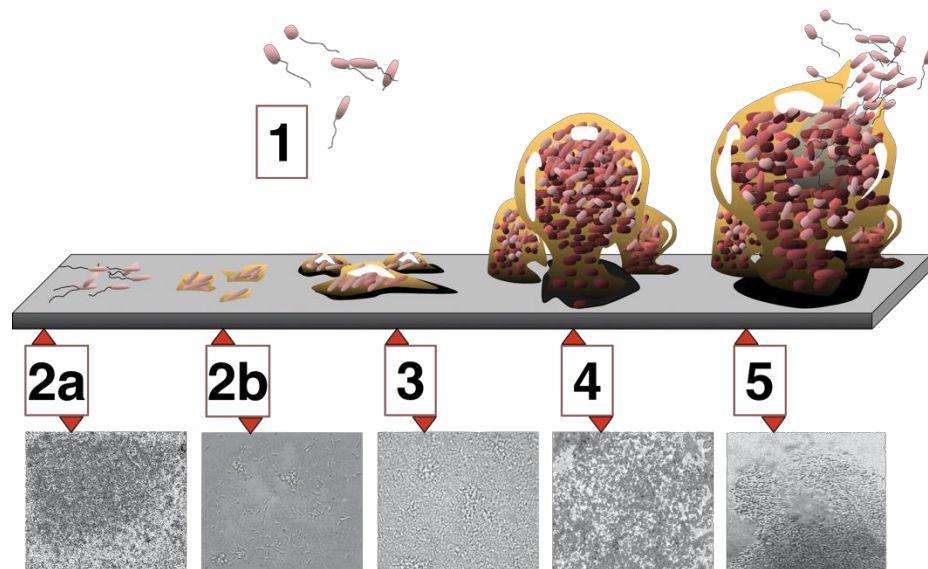


**Figure 1.8:** Schematic representation of the five stages of biofilm development. 1) planktonic; 2) attachment, which is further subdivided into reversible (2a) and irreversible (2b) attachment; 3) microcolony formation; 4) macrocolony formation; 5) dispersion. The photomicrographs show a developing *Pseudomonas aeruginosa* biofilm. All photomicrographs are shown to same scale. Figure adapted and reprinted from D. Monroe, *PLoS Biol.* **2007**, 5, e307.<sup>89</sup>

The five stages of biofilm development are: planktonic; attachment, which is further subdivided into reversible and irreversible attachment; microcolony formation; macrocolony formation; and dispersion. The transition from planktonic (suspension) growth to a sessile, biofilm community is initiated by environmental factors.<sup>90</sup> Although the environmental signals varies among species, one of the key features that promotes adherence of planktonic bacteria to a surface is the presence of high shear forces, which are believed to increase the frequency of bacteria-surface interactions. Biofilms formed at high shear are more resistant to mechanical breakage.<sup>68</sup> The initial, reversible, attachment phase is controlled by a balance of repulsive and attractive forces, such as van der Waals forces and steric or electrostatic interactions.<sup>91</sup> Only those bacteria that can withstand these repulsive forces will become permanently attached. This process is particularly favoured by motile bacteria, which can use their flagella to maintain surface contacts.<sup>91,92</sup>

Following irreversible attachment, the biofilm starts to mature, forming discrete cell-clusters, known as microcolonies.<sup>86</sup> This stage is associated with a number of gene expression changes, including upregulation of factors involved in formation of the EPS matrix, which ultimately will account for approximately 90% of the biofilm mass.<sup>92,93</sup> The microcolonies continue to grow until they become macrocolonies with a characteristic shape.<sup>86</sup> The final stage, dispersion, occurs when bacteria detach from the macrocolony, either through shear forces or in response to environmental changes. These bacteria have re-entered the planktonic growth phase and can disperse and colonise new locations.<sup>94</sup>

### **1.3.3. Causes and Implications of Hypoxia in Biofilms**

Biofilms provide microorganisms with a protected mode of growth compared with the planktonic form. This results in increased resistance to a number of stresses including ultraviolet (UV) damage,<sup>95</sup> desiccation,<sup>96</sup> pH gradients,<sup>97</sup> and, critically, antibiotics.<sup>98–100</sup> Indeed the extreme tolerance of biofilms to antimicrobial agents is considered to be a defining feature of biofilms.<sup>76</sup> This resistance has been attributed to two main mechanisms: poor diffusion of antimicrobial agents through the EPS matrix and the reduction in bacteria growth rate, which is caused by nutrient limitation.<sup>98,101</sup> Since many antimicrobials are dependent on cell division, this slow growth reduces their effectiveness.

The restricted movement of nutrients, signalling compounds, bacterial waste, and metabolic substrates, such as oxygen, through the biofilm results concentration gradients that create microenvironments in the biofilm.<sup>101</sup> In particular, regions of hypoxia occur at the centre of the biofilm due to an imbalance between oxygen consumption by cells in the upper layers and the diffusion rate of oxygen through the EPS matrix. This has been confirmed through the use of oxygen electrodes to measure oxygen concentration profiles in biofilms.<sup>102–104</sup> For example, in a 220 µm biofilm, the concentration of oxygen was found to decrease rapidly with increasing depth with a maximum penetration into the biofilm of approximately 150 µm; beyond this point the oxygen concentration was below 0.1 mg/L.<sup>102</sup>

One of the most important implications of hypoxia in biofilms is that limiting oxygen delivery to cells causes significant reduction in bacterial growth rates, an effect which was hypothesised to contribute to the increased resistance of hypoxic biofilms to antibiotics. To confirm this, Walters *et al.* investigated whether the effectiveness of two antibiotics, ciprofloxacin **3** or tobramycin **4** (Figure 1.9), was more affected by antibiotic distribution through the biofilm or by oxygen concentration. They found that even distribution of the drug throughout the biofilm had no effect on the rate of bacterial death. Conversely, antibiotic activity was detected in the aerobic regions, close to the air interface, but not in the oxygen deficient regions at the core.<sup>103</sup> Similar results were obtained by Borriello *et al.*, who found that oxygen limitation could explain more than 70% of the protection afforded to hypoxic biofilms for a range of different antibiotics.<sup>105</sup>

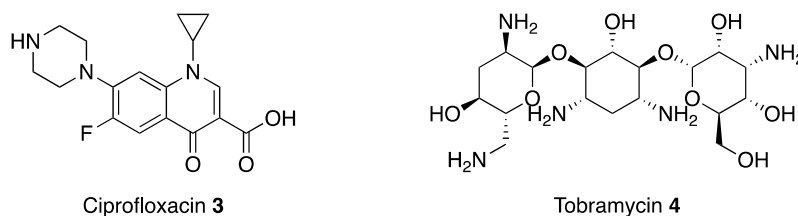


**Figure 1.9:** Structures of the antibiotics ciprofloxacin **3** and tobramycin **4**.

At a clinical level, decreased oxygen concentrations, such as those found in the airway plugs of cystic fibrosis patients, have been shown increase biofilm formation, due to increased polysaccharide expression that promotes surface-adhesion.<sup>106,107</sup> Consequently, it is clear that hypoxia not only impacts biofilm survival under a range of environmental stresses, but can also contribute to its formation in the first place. It is hoped that better understanding the mechanisms behind the role of hypoxia in biofilms will enable the development of new, targeted, and more effective therapeutics.<sup>79</sup>

## **1.4. Hypoxia and Plants**

The last biologically relevant context of hypoxia that will be discussed focuses on plant hypoxia. Like many other organisms, plants are obligate aerobes, dependent on oxygen both for aerobic metabolism and as a substrate in many other metabolic reactions, including fatty acid desaturation and the synthesis of phytohormones (e.g. ethylene, abscisic acid or gibberellins).<sup>108</sup> The primary source of free oxygen on Earth is oxygenic photosynthesis, the process by which green plants, algae, and cyanobacteria split molecules of water into hydrogen and oxygen.<sup>109</sup> Despite their important role in this process, plants have no specialised active-transport mechanism to distribute oxygen to organs, relying on passive processes, such as diffusion and convection.<sup>9,110</sup> Hypoxia arises when diffusion from the environment cannot satisfy the metabolic demand.<sup>9</sup> The concentration of oxygen varies substantially in tissues, forming steep gradients, based on how far the cells are from the oxygen supply and the metabolic demands of the cell. In general, the oxygen concentration is lowest at the points closest to the centre of plant organs. It also varies according to the amount of light (since photosynthesising tissue generates oxygen), type of tissue and extent of growth during development (Figure 1.10).<sup>108,111</sup> Under optimal oxygenation conditions, these gradients are expected and relatively benign. Conversely, when oxygen availability from the environment is reduced, the hypoxic regions become larger and have more severe consequences, which can ultimately lead to cell death.<sup>108</sup>



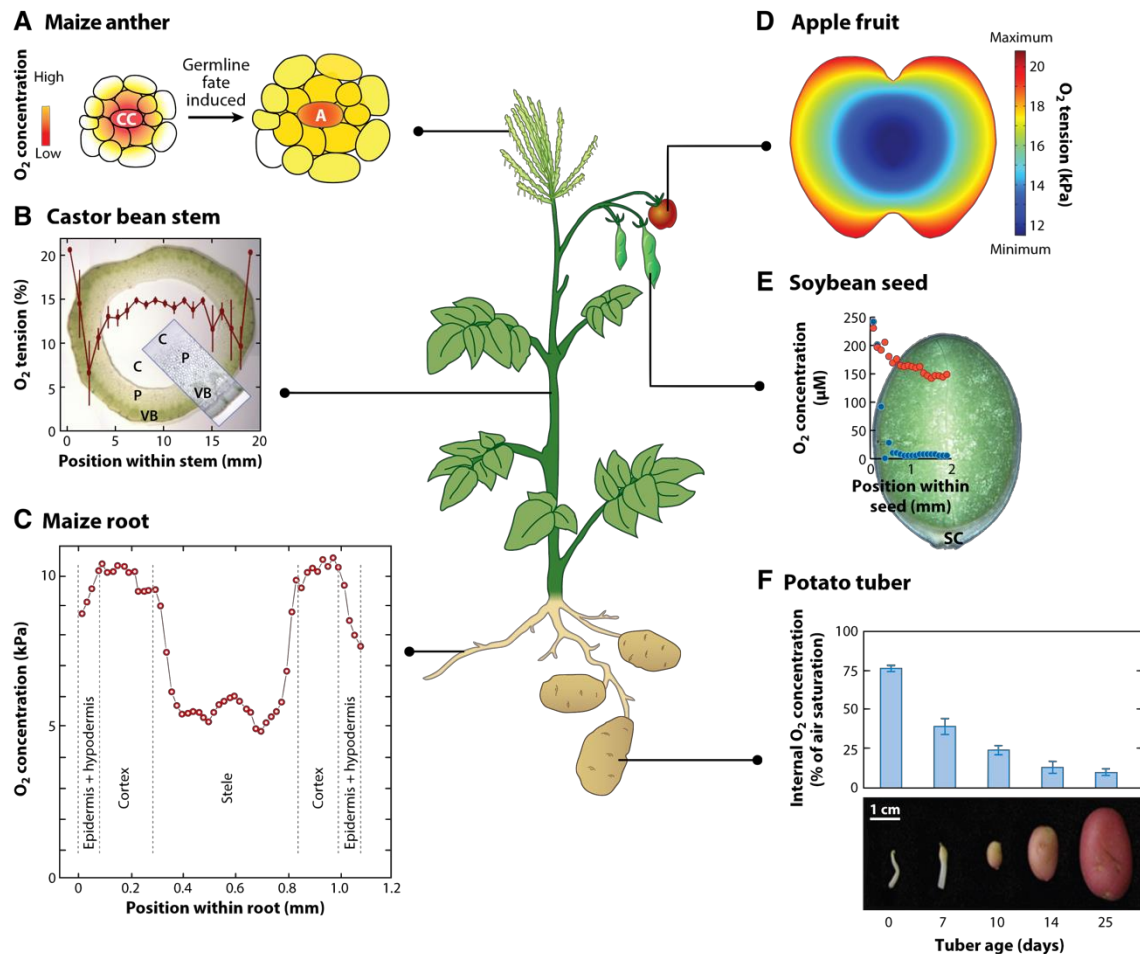


**Figure 1.10:** Oxygen gradients inside plant tissues. A) Oxygen concentration in maize anthers. Hypoxia is thought to be actively induced within the tissue by the activation of alternative respiration pathways that use molecular oxygen to dissipate REDOX energy as heat rather than to convert it into ATP. A = archesporial cells; CC = central cells (CC) into archesporial cells. B) Oxygen profile as measured using a microsensor through a castor bean (*Ricinus communis*) stem. Gas is transported through the hollow centre with the result that the outer parenchymal (P) and vascular bundle (VB) tissues become hypoxic. C) Radial oxygen profile across the primary root of maize. The oxygen concentration is higher in the cortex than in the surrounding tissues of the rhizodermis and the stele. D) Model of the oxygen partial pressure distribution along the vertical axis of an apple fruit. Gas transport through bulky fruit tissue is mediated mainly *via* an extensive network of gas-filled apoplasmic spaces between the cells. E) Oxygen distribution map of soybean seeds measured under light (red circles) or dark (blue circles) conditions. The oxygen concentration is higher in light conditions due to the photosynthetic activity of the cotyledon within the developing green seed. F) Internal oxygen levels in the cores of tubers at different developmental stages. The oxygen concentration decreases as tuber size increases. Figure reprinted from J. T. van Dongen, F. Licausi, *Annu. Rev. Plant Biol.* **2015**, 66, 345–367 with permission from Annual Reviews, License No. 4427700866199.<sup>108</sup>

#### 1.4.1. Causes and Implications of Hypoxia in Plants

Although there are a number of causes of hypoxia in plants, including anatomical structures, which limit the permeability of oxygen,<sup>112</sup> compact soil,<sup>113</sup> ice crusts,<sup>114</sup> and irrigation,<sup>115</sup> the primary cause is flooding.<sup>116</sup> Statistically, floods are the most common (40%) and widespread of all natural disasters.<sup>117</sup> Flooding, and in particular the associated hypoxic stress, has serious implications for crop yields in a wide variety of plants. Worldwide, over 22 million hectares of rice-cultivable area, which account for 18% of the global rice supply, are vulnerable to flooding.<sup>118</sup> A study in South East Asia, where 15% of total maize growing area is affected by floods and water logging, found that grain yields were reduced between 20–50%, depending on the genotype of the maize plant.<sup>119</sup> Similarly, a study in Western Australia on the effects of low, moderate, or severe waterlogging on wheat grain yield in 17 different wheat varieties found that, on average, grain yields were reduced by 10%, 25%, and 65%, respectively.<sup>120</sup> Furthermore, in Australia, the annual losses due to reductions in cereal crop yields has been valued at >11 million Australian dollars.<sup>121</sup>

The precise impact of flooding is highly dependent on both the extent of flooding and the type of plant. In general, there are three degrees of flooding: waterlogging, partial, and complete submergence (Figure 1.11). Waterlogging is defined as a condition of the soil where excess water limits gas diffusion; usually, only the root goes underwater.<sup>122</sup> In partial submergence, the portion of the plant that is underwater extends to include the shoot; in complete submergence, the whole plant is underwater.<sup>118</sup> Plants are diverse in their ability to withstand flooding, ranging from submergence sensitive species, such as *Arabidopsis thaliana*, *Zea mays* (maize), and *Solanum tuberosum* (potato), to submergence tolerant species, such as *Oryza sativa* (rice), and *Rumex palustris* (marsh dock).<sup>123</sup>

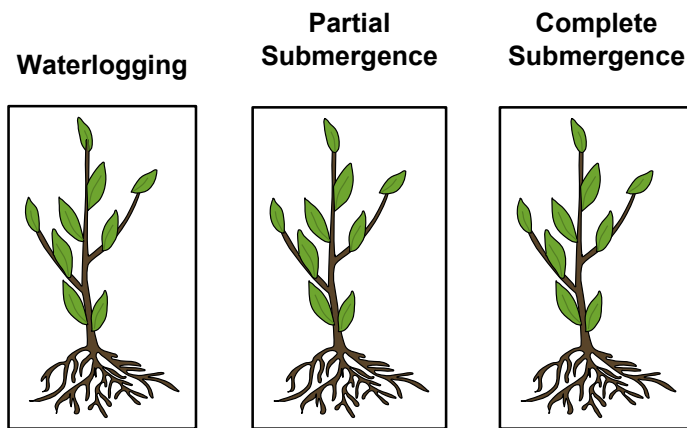


**Figure 1.11:** Representation of the three different degrees of flooding experienced by plants: waterlogging, partial submergence, and complete submergence.

The main reason why flooding is so detrimental to plants is because gases such as oxygen, carbon dioxide and ethylene diffuse very slowly in water. This results in significantly reduced gas exchange between plants and their environment, which in turn causes a decrease in the intracellular oxygen levels.<sup>116</sup> These reduced oxygen levels lead to one of the most severe problems encountered by flooded plants: restricted aerobic respiration, which reduces the rate of energy production by 65–97%.<sup>124,125</sup> In fully submerged plants, water turbidity can also inhibit photosynthesis, which further limits oxygen.<sup>126</sup>

#### 1.4.2. Biotechnological Approaches to Overcome Plant Hypoxia

In both submergence sensitive and submergence tolerant plants, flooding-induced hypoxia results in a myriad of molecular responses, which either rearrange the cellular metabolism to cope with a deficiency in ATP, or provoke structural changes, such as aerenchyma formation or rapid stem elongation.<sup>108,127,128</sup> Aerenchyma are soft tissues that form air spaces, which allow an increase in gas exchange, while stem elongation helps the plant to reach the water surface, thereby increasing access to oxygen. There is a huge genetic diversity in the different species of plants that can tolerate flooding and it is hoped that better understanding of the molecular mechanisms behind these responses will enable development of agricultural tools that can be applied to limit the effects of flooding on crops yields.<sup>116,129</sup>

In the short term, approaches such as improving land drainage or direct treatment of crops, such as the addition of nitrogen fertilisers, have been successful at reducing the impact of flooding. However, the long term aim is to use biotechnological methods to create plants that are inherently tolerant to hypoxia.<sup>129</sup> For example, Vartapetian *et al.* identified that glucose-stimulated glycolysis protected plant cells from hypoxia, even in plants that were not considered to be submergence tolerant.<sup>130</sup> These results demonstrated the importance of anaerobic metabolism to hypoxia tolerance. Subsequently, *in vitro* selection of hypoxia-tolerant wheat cells in the absence of glucose led to development of an entire plant that was resistant to root flooding.<sup>129</sup> It is now feasible that the use of genetic engineering combined with new knowledge about the mechanisms behind plant adaptations to hypoxia will enable development of new hypoxia-tolerant crop species.

## 1.5. Targeting Hypoxia

It is clear that hypoxia has negative implications in a diverse range of biological settings and, in each case, it presents a unique challenge. A similarly diverse range of approaches is required to cope with the specific demands of hypoxia in each of these settings and it is impossible to apply a single technique universally. Many of these methods have been mentioned above in the context in which they were first investigated. However, one approach, namely the use of bioreductive prodrugs is of particular relevance to this project. Bioreductive prodrugs were primarily developed as an alternative therapeutic strategy to target the hypoxic fraction of cancer cells and therefore, it is this application that will be expanded on here.

### 1.5.1. Hypoxia-Activated Prodrugs (HAPs)

Hypoxia-activated prodrugs (HAPs) are non-toxic, biologically inactive molecules that are converted into an active drug by enzymatic reduction in hypoxic tissues.<sup>131</sup> HAPs offer the ability to deliver compounds selectively to regions of hypoxia through attachment of a bioreductive moiety, which masks the active drug.<sup>132</sup> The structure of HAPs has been described using a general modular structure consisting of the effector (active drug or imaging agent), linker, and trigger

(bio-reductive moiety) (Figure 1.12).<sup>133</sup> The increased control over drug delivery also gives HAPs the potential to reduce the toxic side effects associated with many current cancer therapies.

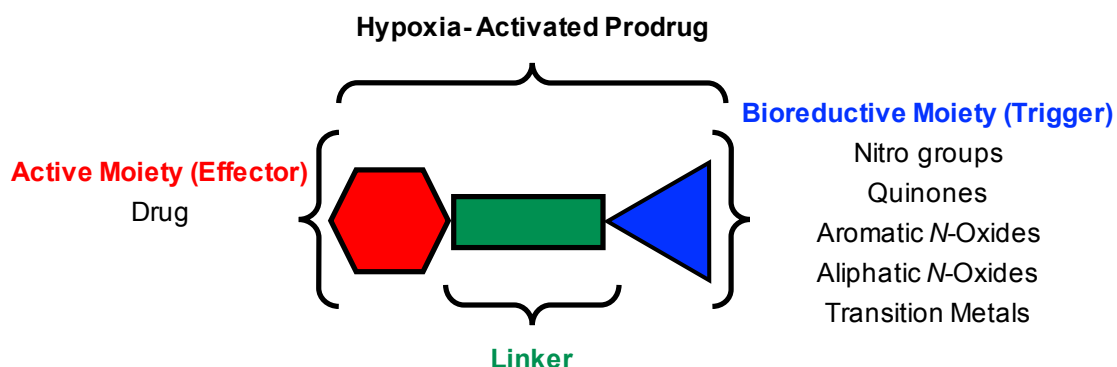


**Figure 1.12:** General structure of a hypoxia-activated prodrug. Attachment of a bio-reductive moiety masks the functionality of the active drug or imaging agent. To date, five different classes of bio-reductive groups have been used to protect a range of drugs or imaging agents.<sup>131</sup>

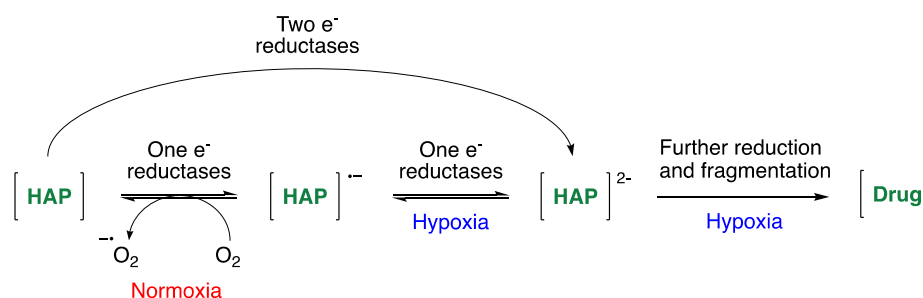
### 1.5.2. Mechanism of Activation and Hypoxia-Selectivity of HAPs

HAPs are activated by enzyme-mediated reductions, catalysed by endogenous human cellular oxidoreductases.<sup>134</sup> To be selective for hypoxic microenvironment, this activation must not happen in well-oxygenated tissues. There are two main mechanisms that confer hypoxia-selectivity on HAPs: inhibition or reversal of the activation process by oxygen and elevated expression of oxidoreductases in hypoxia.<sup>135</sup>

First, many HAPs are activated under conditions of low oxygen *via* the general mechanism, shown in Scheme 1.1. Cellular one-electron reductases catalyse reduction of the HAP to form a radical anion. In the presence of oxygen, the initial radical anion is back-oxidised to reform the parent HAP and superoxide ( $O_2^{\cdot-}$ ). These radical species are readily detoxified by host mechanisms. Under hypoxic conditions, this futile REDOX cycling cannot occur and the radical anion is further reduced; subsequent fragmentation releases the drug (Scheme 1.1). This reversal of the initial reduction step by molecular oxygen restricts prodrug activation in non-hypoxic tissues.<sup>135,136</sup>

Alternatively, some prodrugs, the most notable of which is AQ4N **30** (See Section 1.5.3), are reduced by concerted sequential two-electron reductions.<sup>137</sup> These reduction steps occur in an

oxygen-independent manner, by-passing the oxygen-sensitive prodrug radical. As a result, such drugs have the potential for off-target activation in normal tissues and selectivity is usually dependent on overexpression of the oxidoreductases under hypoxic conditions.<sup>131,135</sup> The mechanism and specific enzyme responsible for activation of HAPs depends on the nature of the HAP itself, including which class of bioreductive moiety was employed.<sup>138</sup>



**Scheme 1.1:** General mechanism for the metabolic activation of bioreductive prodrugs. Cellular one-electron reductases reduce the HAP to form a prodrug radical anion intermediate. In the presence of oxygen, this initial radical anion is quenched. Further reduction, and in some cases fragmentation, under hypoxic conditions results in activation of the HAP. Some prodrugs are also reduced by a concerted two-electron reduction, which by-passes the oxygen-sensitive prodrug radical.<sup>131</sup>

### 1.5.3. Classes of HAPs

To date, five different functional groups have been used as the bioreductive “trigger” moiety of HAPs: nitro(hetero)aromatics, quinones, aromatic *N*-Oxides, aliphatic *N*-Oxides, and transition metal complexes.<sup>131</sup> These have been further grouped into two classes according to how readily they are reduced under hypoxic conditions. Class I HAPs, which include quinones and *N*-oxides, are activated under relatively mild hypoxia, whereas Class II HAPs, which include the nitroaromatics, typically require more severe hypoxia.<sup>139</sup> Some of the oxygen dependencies for different therapies and biological responses to hypoxia are illustrated in Figure 1.13. In theory, knowledge of both the oxygen requirements for different therapies and the degree of hypoxia at the core of the solid tumour could potentially dictate the choice of hypoxia-targeted therapy. However, in practise, methods to non-disruptively and accurately quantify the oxygenation status

of tumour cells do not exist and more research on the efficacy of HAPs would be required to make this a reality.<sup>131</sup>

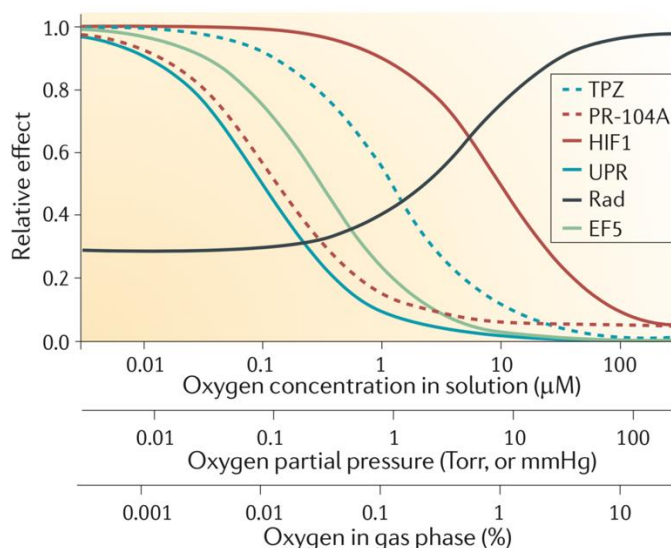


**Figure 1.13:** Schematic representation of quantitative oxygen dependencies for ionising radiation, bioreductive activation of prodrugs and imaging agents, and biological responses to hypoxia. Three commonly used units for oxygen concentration are shown on the x axis, assuming that the culture medium is in equilibrium with humidified gas mixtures at atmospheric pressure. TPZ = tirapazamine; UPR = Unfolded protein response; Rad = ionising radiation; EF5 = etanidazole pentafluoride. Figure adapted and reprinted from W. R. Wilson, M. P. Hay, *Nat. Rev. Cancer* **2011**, *11*, 393–410 with permission from Springer Nature, License No. 4426021475169.<sup>131</sup>

### Nitroaromatics

The discovery that oxygen is able to inhibit enzyme-mediated one-electron reduction of nitroaryl groups represents one of the earliest advances in the development of bioreductive prodrugs.<sup>140</sup> Subsequently, it was shown that the 2-nitroimidazole, misonidazole **1**, which had initially been developed as a radiosensitiser, was also able to effect significant hypoxia-selective cytotoxicity.<sup>141</sup> This led to the development of a range of nitroaromatic groups that are sensitive to bioreduction, including nitrofurans **5**, nitrothiophenes **6**, both 2-nitromidazoles **7** and 5-nitroimidazoles **8**, and nitrobenzyls **9** (Figure 1.14).

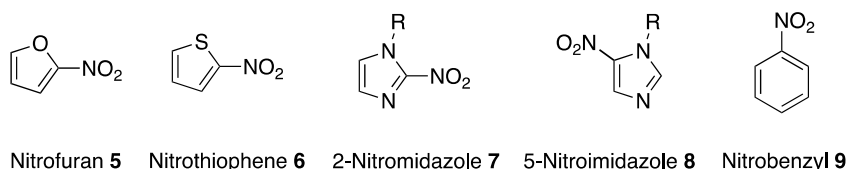
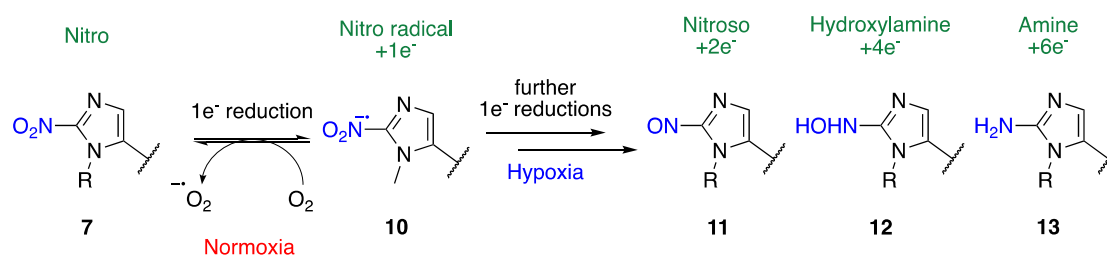


**Figure 1.14:** Structures of some nitroaromatic groups that are sensitive to bioreduction. R = alkyl.<sup>132</sup>

Each of these nitroaryl bioreductive groups is activated by reduction of the nitro group, which is catalysed by one-electron reductases. As in the general mechanism for the activation of HAPs, described above, the initial one-electron reduction generates a radical nitro anion **10**, which in the presence of oxygen is rapidly quenched to reform the nitro group. In hypoxia, further sequential reductions result in formation of the nitroso **11**, hydroxylamine **12** or amine **13** derivatives (Scheme 1.2).<sup>138</sup>



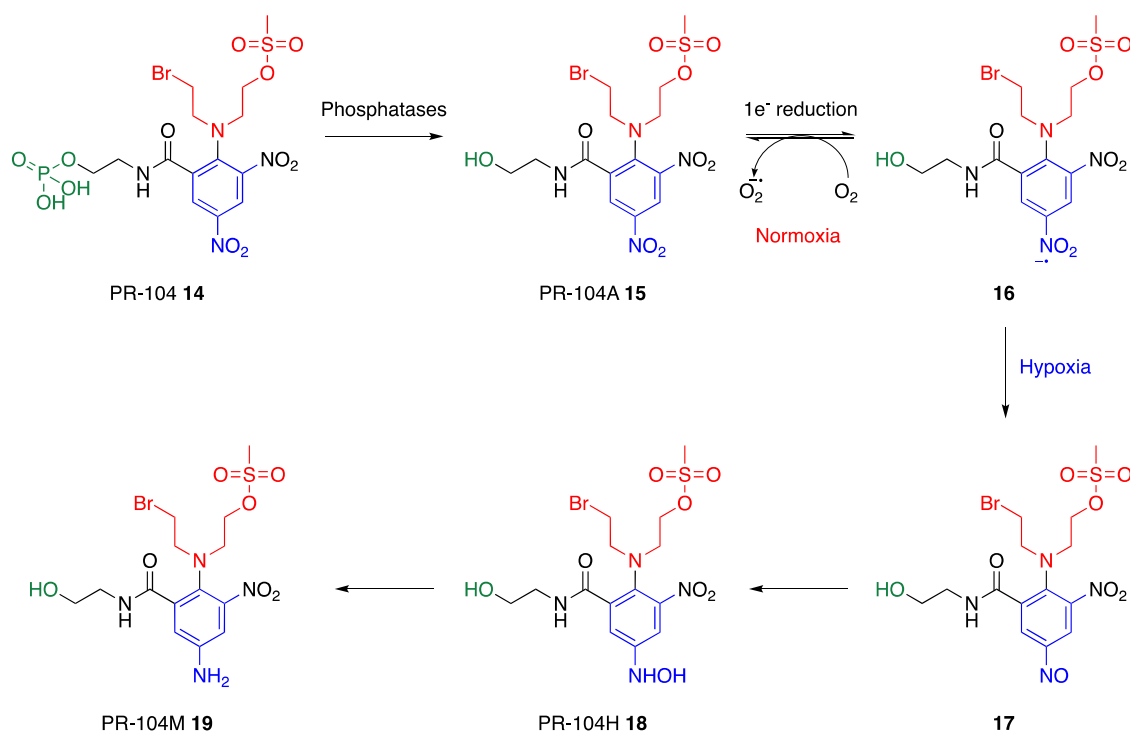
**Scheme 1.2:** General mechanism for the bioreductive activation of nitroaromatics. An initial one-electron reduction generates a nitro radical anion **10**, which is quenched by molecular oxygen under normoxic conditions. Further one-electron reductions afford the nitroso **11**, hydroxylamine **12**, or amine **13** derivatives. The *N*-alkyl-2-nitroimidazole group is used as a representative example. R = alkyl.

The reduction of the nitro group to the hydroxylamine or amine groups results in a change in electron-density, which has been exploited in two main ways: either as bioreductive components embedded in molecules or as groups to trigger fragmentation.<sup>132</sup>

The first method is exemplified by the DNA alkylating agent PR-104 **14**. PR-104 **14** is administered as a phosphate “pre-prodrug”, which is cleaved to the alcohol, PR-104A **15**, by intracellular phosphatases. PR-104A **15** undergoes sequential one-electron reductions, which convert the 4-nitro group to the 4-hydroxylamine, PR-104H **18** and 4-amine, PR-104M **19** via the



4-nitroso intermediate **17** (Scheme 1.3).<sup>135</sup> PR-104H **18** and PR-104M **19** form DNA interstrand cross-links, which kill the tumour cells.<sup>142</sup>

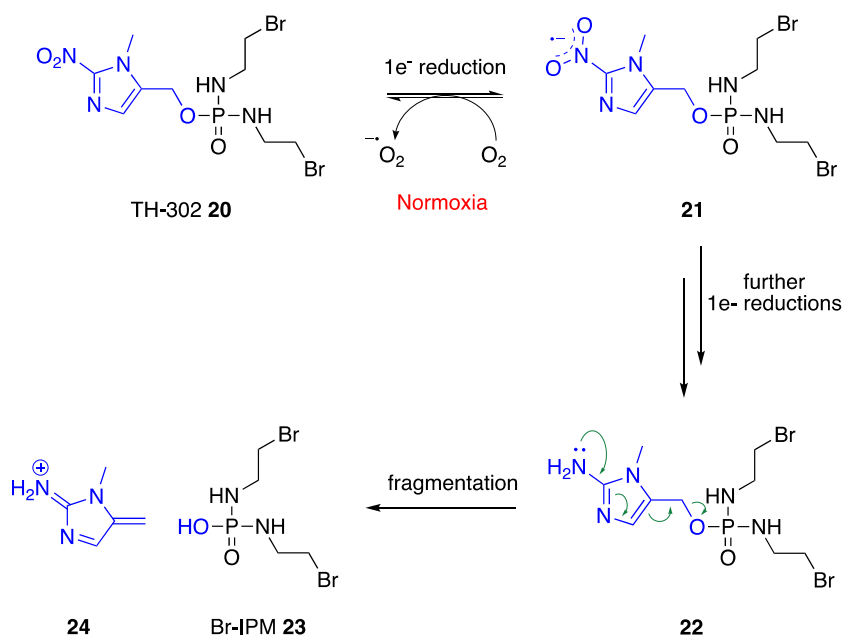


**Scheme 1.3:** Mechanism for reductive activation of PR-104 **14**. The “pre-prodrug” PR-104 **14** is hydrolysed by phosphatases to form the bioreductive prodrug PR-104A **15**. One-electron reduction generates a nitro radical intermediate **16**, which is back-oxidised to the nitro **15** in the presence of oxygen. Further reductions under hypoxia afford the DNA cross-linkers PR-104H **18** and PR-104M **19**. Blue = bioreductive moiety; green = phosphate pre-prodrug moiety; red = DNA damaging nitrogen mustard.<sup>143</sup>

Selectivity for hypoxic cells is primarily conferred through one-electron reductases, CYP:P450 reductase and FOXRED2, which generate the radical anion **16**, which is quenched in the presence of oxygen.<sup>144,145</sup> Some activity under normoxic conditions, attributed to two-electron reduction by an aldo-keto reductase, AKR1C3, has also been observed.<sup>146</sup> Although success in phase I clinical trials was affected by dose-limiting toxicities in a number of cases, PR-104 **14** showed promise for the treatment of acute leukaemias and a phase I/II study of PR104 in both acute myeloid leukaemia and acute lymphoblastic leukaemia is underway.<sup>135,147,148</sup>

In the second group of nitroaromatic-based HAPs, the change in electron density, which occurs following reduction of the nitro group to form the hydroxylamine or amine derivative, promotes fragmentation to release its cargo. This “trigger” functionality has been the focus of a number of HAPs, the most advanced of which is Evofosfamide (TH-302) **20**.

TH-302 **20** was first reported in 2008 and functions through release of a highly toxic DNA crosslinking agent in hypoxia.<sup>149</sup> As with other nitroaromatics, an initial one-electron reduction forms a radical nitro anion **21** that is quenched in the presence of oxygen. Under hypoxic conditions, further reduction reactions form the amine derivative **22**; subsequent fragmentation of amine **22** releases bromo-isophosphoramidate mustard (Br-IPM) **23** (Scheme 1.4). Br-IPM **23** is a potent DNA cross-linking agent that is particularly effective against cell lines that are deficient in homology-dependent DNA repair pathways.<sup>150</sup>



**Scheme 1.4:** Mechanism for reductive activation of TH-302 **20**. One-electron reduction generates a nitro radical intermediate **21**, which is back-oxidised to the nitro group in the presence of oxygen. Further reductions under hypoxia afford the amine **22**, which undergoes fragmentation to release the DNA cross-linker Br-IPM **23**. Blue = bioreductive moiety.<sup>150</sup>

TH-302 **20** exhibits a 550-fold *in vitro* selectivity towards hypoxic over oxygenated cells.<sup>150</sup>

Results from phase I and phase II clinical trials were largely positive; TH-302 **20** was well-tolerated and promising clinical activity was observed for treatments in combination with

chemotherapy.<sup>135,151–153</sup> Unfortunately, initial results from a phase III clinical trial on the use of TH-302 **20** to treat soft tissue sarcoma showed no significant effect of TH-302 **20** combination therapies.<sup>154</sup>

## Quinones

The first bioreductive quinones were discovered through the observation that mitomycin C **25**, a widely-used quinone-based anticancer drug, displayed increased toxicity to hypoxic cells (Figure 1.15). Mitomycin C **25** functions as a DNA cross-linking agent. It is now known that enzymic reduction of mitomycin to the hydroquinone form, facilitates protonation of the aziridine nitrogen, increasing its reactivity and promoting intracellular alkylation.<sup>155–157</sup>

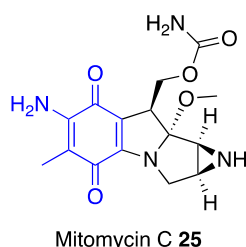
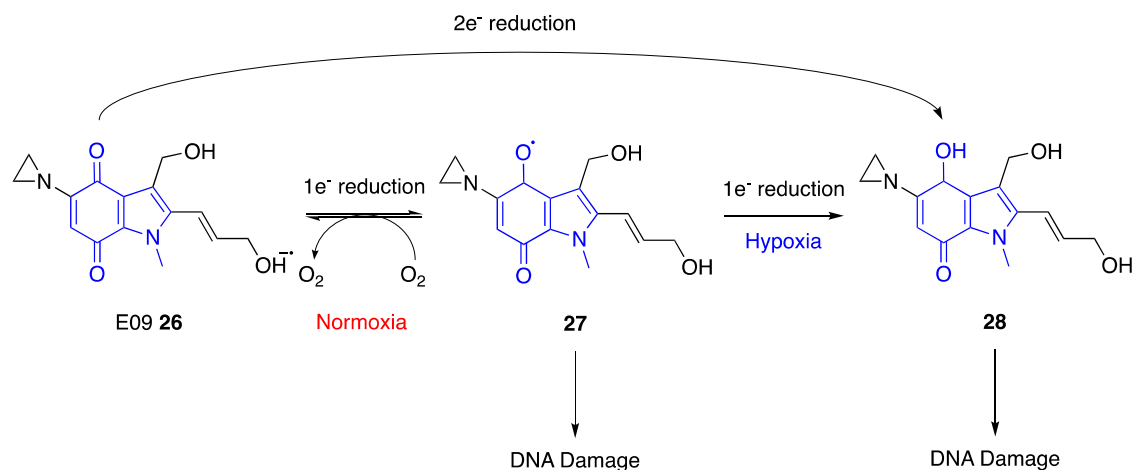


**Figure 1.15:** Structure of mitomycin C **25**.

Unfortunately, the *in vitro* cytotoxicity of mitomycin C in hypoxia was less than five-fold greater than that in normoxic cells.<sup>138</sup> Subsequently, a novel series of quinone-based alkylating agents, derived from mitomycin C **25**, was developed. This resulted in identification of EO9 (Apaziquone) **26**, which exhibited a 30-fold improved cytotoxicity in hypoxic cells compared with normoxic cells.<sup>138,158</sup> As with mitomycin C **25**, activation of EO9 **26** consists of two sequential one-electron reductions: first to the semiquinone **27** and second to the hydroquinone **28** (Scheme 1.5).<sup>131</sup>

EO9 **26** is also a substrate for NAD(P)H:quinone oxidoreductase (NQO1), which catalyses the two-electron reduction of quinones. This means that NQO1 reduction by-passes the oxygen-sensitive semiquinone step, activating EO9 **26** equally in both normoxic and hypoxic cells. Thus, selectivity over normoxic cells is only observed when either the cell line expresses negligible NQO1 or the hypoxic tumour cell overexpresses NQO1.<sup>135,159</sup>



**Scheme 1.5:** Mechanism for reductive activation of the indolequinone bioactive prodrug, EO9 **26**. One-electron reduction generates the semiquinone radical **27**, which in the presence of oxygen back-oxidised to the parent compound. In the absence of oxygen, the free radical is stabilised and undergoes a further one-electron reduction to generate the hydroquinone species **28**, leading to DNA damage. Blue = bioactive moiety.<sup>135</sup>

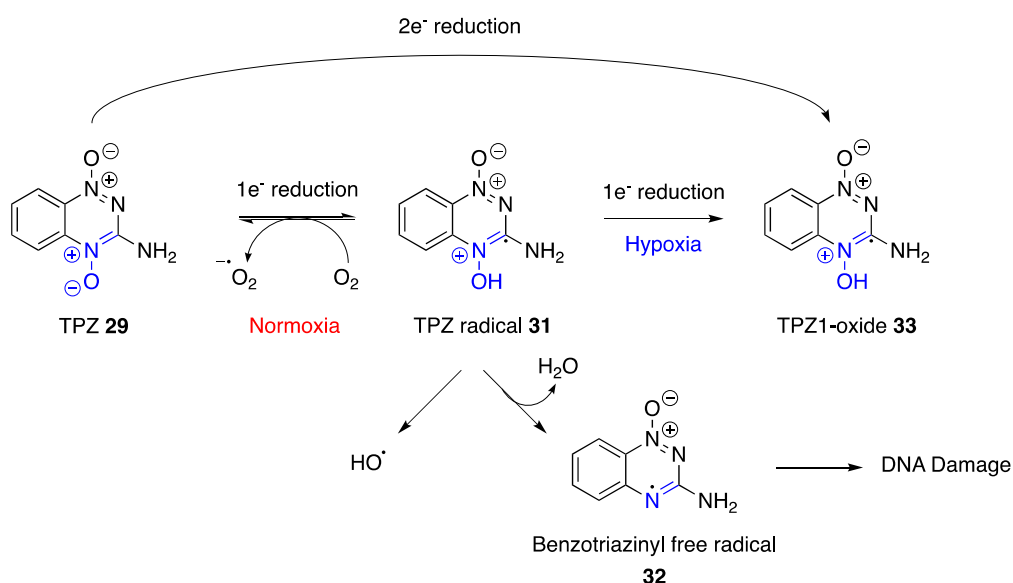
Nevertheless, EO9 **26** was selected for evaluation in a series of phase I clinical trials but, unfortunately, it failed to show any significant clinical activity.<sup>159</sup> This was attributed in part to its poor pharmacokinetic properties. EO9 **26** has rapid clearance and an extremely short half-life of 0.8 to 19 min at the maximum tolerated dose. Consequently, EO9 **26** is now being investigated for use in bladder cancer, where it can be administered locally, thereby circumventing the problem of its poor pharmacokinetics. Recent results from phase III clinical trials suggested that EO9 **26** did not perform statistically better than placebo treatment, although some improvements were observed and a further phase III trial, based on these results, is currently underway.<sup>143</sup>

### ***N*-Oxides**

There are two key *N*-oxide based bioactive prodrugs that have been investigated as potential HAPs: Tirapazamine (TPZ) **29**, an aromatic *N*-oxide, and AQ4N (Banoxantrone) **30**, an aliphatic *N*-oxide.

TPZ was originally developed in 1986 and is now one of the most extensively studied HAPs in the clinic.<sup>134,160</sup> TPZ **29** is primarily reduced by one-electron reductases to form the TPZ radical **31**. As with many HAPs, selectivity arises due to the quenching of this radical by

molecular oxygen. Under hypoxic conditions, the radical undergoes spontaneous conversion to either a hydroxyl or benzotriazinyl free radical **32**;<sup>161</sup> it is these radical species that are responsible for the toxicity of TPZ **29**, inducing DNA damage, such as DNA breaks and complex lesions. Additionally, although the two-electron reductase NQO1 can also reduce TPZ **29**, this reaction by-passes the toxic TPZ radical **31**, forming TPZ1-oxide **33**, which is considered to be relatively non-toxic (Scheme 1.6).<sup>162</sup>



**Scheme 1.6:** Mechanism for reductive activation of the aromatic *N*-oxide TPZ **29**. TPZ **29** is primarily reduced by one-electron reductases to form the TPZ radical **31**, which in the presence of oxygen are back-oxidised to the parent compound. Further reductions in hypoxia generate a DNA-reactive benzotriazinyl free radical **32**. Blue = bioreductive moiety.<sup>135</sup>

As a result, TPZ **29** exhibits excellent selectivity over normoxic cells, with hypoxic cytotoxicity ratios (HCR) of 50–200 observed in cells in culture.<sup>163</sup> However, despite these promising *in vitro* results, TPZ **29** has performed poorly in clinical trials. In three independent trials of non-small cell lung cancer (NSCLC), head and neck cancer, and cervical cancer, no survival advantage was conferred by adding TPZ **29** to chemotherapy or radiotherapy.<sup>164–166</sup> This was hypothesised to be due to the rapid metabolism of TPZ **29** and novel analogues with improved pharmacokinetic properties are being developed.<sup>167</sup> Of these, CEN-209 **34** (formerly SN30000), is the most promising and is likely to enter phase I clinical trials soon (Figure 1.16).<sup>168</sup>

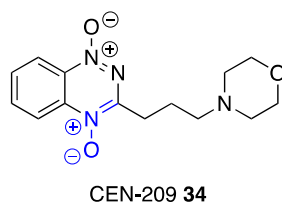
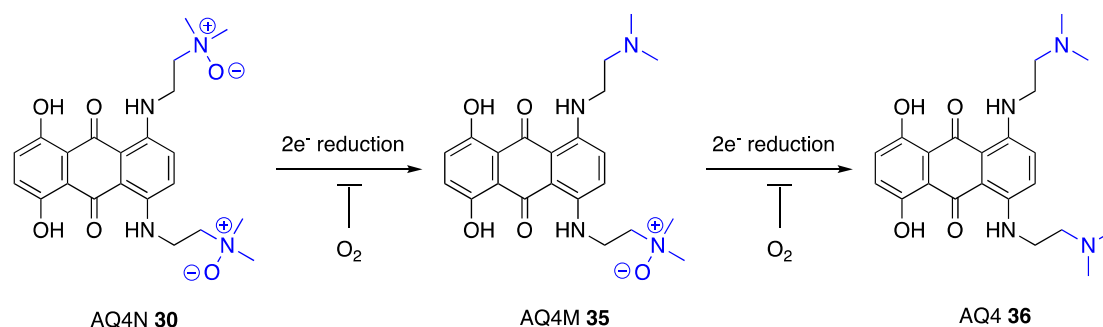


**Figure 1.16:** Structure of CEN-209 **34**, a novel analogue of TPZ **29**, which is predicted to have improved pharmacokinetic properties.<sup>135</sup>

Unlike many HAPs, the aliphatic *N*-oxide AQ4N **30**, is activated by sequential two-electron reduction reactions to form AQ4 **36** via the mono-*N*-oxide intermediate AQ4M **35** (Scheme 1.7). The reduction reactions are catalysed by haem-containing reductases, such as CYP2S1 and CYP2W1 and inducible nitric oxide synthase (iNOS).<sup>169,170</sup> This process is inhibited by oxygen, which outcompetes AQ4N **30** for the haem centre of the reductases, thereby conferring hypoxia-selectivity on the activation of AQ4N **30**.<sup>137</sup>



**Scheme 1.7:** Mechanism for reductive activation of the aliphatic *N*-oxide AQ4N **30**. AQ4N **30** undergoes sequential two-electron reductions to form AQ4M **35** and, subsequently, AQ4 **36**, which is a DNA intercalator. This process is inhibited by oxygen, which outcompetes AQ4N **30** for the haem centre of the reductases. Blue = bio-reductive moiety.<sup>135</sup>

AQ4 **36** is a DNA intercalator with a high DNA binding affinity. It also acts as a topoisomerase II inhibitor, which prevents hypoxic cells from repopulating the tumour during periods of re-oxygenation between treatments. In comparison, the AQ4N **30** prodrug cannot form these strong interactions with the DNA.<sup>135</sup> This is primarily due to the highly repulsive electrostatic interaction between the negative charge in the AQ4N **30** *N*-oxide moiety and the phosphates in the DNA backbone.<sup>137</sup> As a result, AQ4N **30** has negligible cytotoxicity in a wide range of cancer cell

lines.<sup>137</sup> AQ4 **36** is also able to diffuse into neighbouring cells, where it exerts bystander effects, resulting in death of the proximal cells.<sup>171</sup>

AQ4N **30** also has a positive effect when combined with radiation or chemotherapy agents, including cyclophosphamide, cisplatin and thiotepa, *in vivo*.<sup>172,173</sup> For example, addition of AQ4N **30** prior to radiation treatment increased the amount of DNA damage observed after 24 hours than either radiation or AQ4N **30** alone.<sup>174</sup> In the clinic, AQ4N **30** was very well tolerated – no dose-limiting toxic effects were observed – and high intratumoural concentrations of AQ4 **36** were detected.<sup>175,176</sup> OCT1002 **37**, an deuterium-containing analogue of AQ4N **30**, is now being developed by OncoTherics (Figure 1.17).<sup>177</sup>

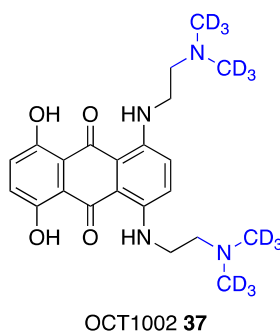


**Figure 1.17:** Structure of OCT1002 **37**, a deuterium-containing analogue of AQ4N **30**.

These studies highlight that, to date, no HAP has been approved for use in humans. Nevertheless, the examples described here suggest a number of ways in which the different classes of bioreductive prodrugs can be exploited to target regions of hypoxia. The work described in this dissertation focuses on the use of nitroaryl HAPs to release target molecules under hypoxic conditions. This approach has also been applied to release both molecularly targeted HAPs and imaging agents.

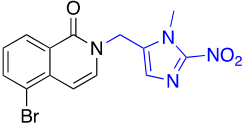
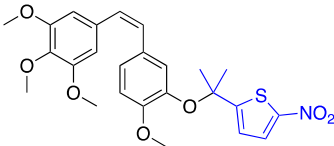
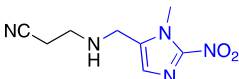
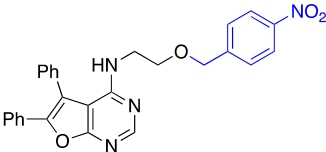
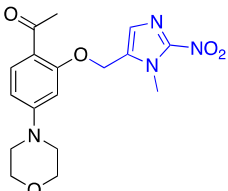
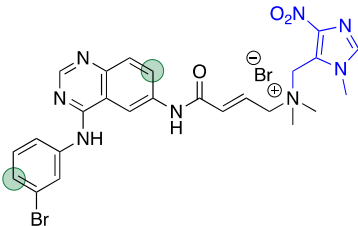
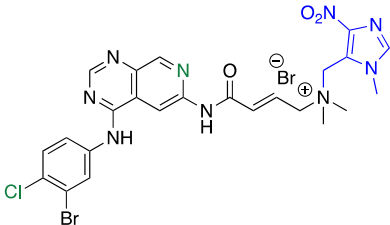
#### 1.5.4. Molecularly Targeted HAPs

Although new targets for anti-cancer drugs are continually being identified, the most successful drugs are still those which target DNA. These drugs can also induce DNA damage in proliferating normal tissues and, therefore, are associated with high levels of toxicity.<sup>131</sup> It was hoped that selectively activating a therapeutic agent directly in hypoxic cells would limit some of these off-target effects. However, many of these drugs can also diffuse into and damage neighbouring cells. This is known as the by-stander effect.<sup>138</sup> Therefore, it is preferable to design HAPs, in which the released drug is more toxic to hypoxic tumour cells than to normal cells. This new class of HAPs, known as molecularly targeted HAPs, is based on the use of small molecule inhibitors that are aimed at exploiting biochemical responses to hypoxia.<sup>178</sup> This approach necessitates identification of both the most useful molecular targets in hypoxic cells and the most appropriate bioreductive group.<sup>131</sup>

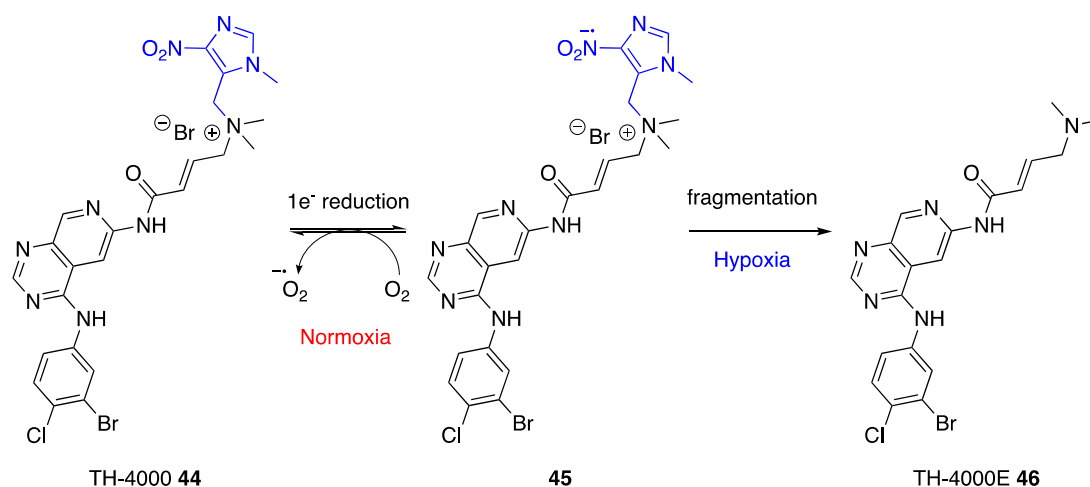
Compound **38**, which targeted poly(ADP-ribose) polymerase (PARP), is one of the earliest examples of a molecularly targeted HAP.<sup>179</sup> PARP1 is involved in the repair of single-stranded DNA breaks and, therefore, inhibiting PARP increases radiosensitivity. A number of molecularly targeted bioreductive prodrugs that target a wide range of cellular pathways have since been developed. The structures of some of these HAPs that employ nitroaromatics as a “trigger” group and their tumour targets are given in Table 1.2.



**Table 1.2:** Structures of some molecularly targeted bioreductive prodrugs that employ nitroaromatics as a “trigger” group and their tumour targets. The bioreductive moiety is shown in blue. SAR studies on SN29966 **43** resulted in development of TH-4000 **44**. The key changes in structure are shown in green

HAP	Structure	Target	Ref
38		PARP1	179
39		Tubulin	180
40		Lysyl oxidase (LOX)	181
CH-01 <b>41</b>		Chk1/Aurora A	182
BCCA621C <b>42</b>		DNA-protein kinase	183
SN29966 <b>43</b>		EGFR	184
TH-4000 <b>44</b>		EGFR	185

Of these, the most clinically advanced molecularly targeted HAP is TH-4000 **44**, which employs a 4-nitroimidazole bio-reductive moiety.<sup>185</sup> TH-4000 **44** was originally developed as a result of structure activity relationship (SAR) studies on SR29966 **43**, a hypoxia-activated irreversible epidermal growth factor receptor (EGFR) tyrosine kinase inhibitor (TKI).<sup>184,186</sup> Under hypoxic conditions, one-electron nitroreductases reduce the nitroimidazole to form the radical nitro anion **45**, which is believed to fragment directly (without further reductions to the hydroxylamine or amine derivatives) to release TH-4000E **46** (Scheme 1.8).



**Scheme 1.8:** Mechanism of reductive activation of TH-4000 **44**. One-electron nitroreductases reduce the 4-nitroimidazole group to form the radical nitro anion **45**, which fragments to release TH-4000E **46**. Blue = bio-reductive moiety.

Existing EGFR TKIs, such as erlotinib **47** and gefitinib **48** (Figure 1.18), which are approved for use in NSCLC, have been shown to be particularly effective against mutant EGFR. Promisingly, phase I trials showed that TH-4000 **44** was more effective than erlotinib against NSCLC xenografts with wild-type and mutant EGFR.<sup>187,188</sup> TH-4000 was advanced into two parallel phase II clinical trials against EGFR-mutant, T790M-negative patients with advanced NSCLC (NCT02454842) and metastatic squamous cell carcinoma of the head and neck or skin (NCT02449681). However, both of these clinical trials have now been terminated due to a lack of efficacy.<sup>189,190</sup>

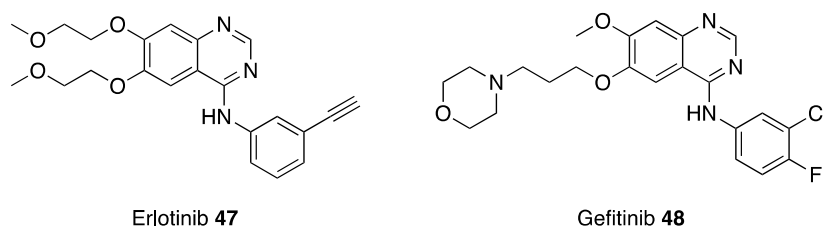
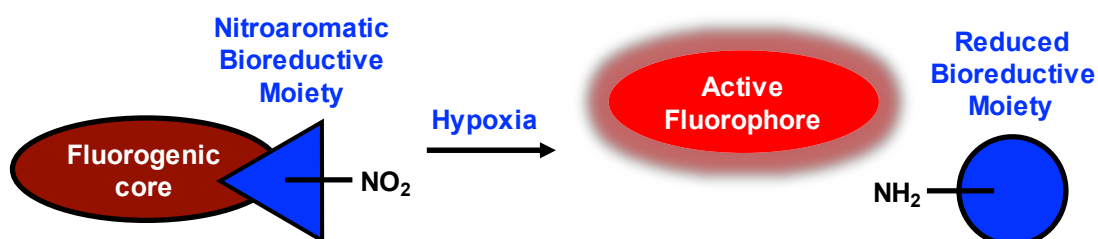


**Figure 1.18:** Structures of erlotinib **47** and gefitinib **48**, EGFR TKIs that are currently approved for the treatment of NSCLC.<sup>191</sup>

Despite the lack of clinical success in the use HAPs to target tumours, the research to date has highlighted and developed a number of important concepts. In particular, the use of bioreductive nitroaryl groups to release compounds selectively in hypoxia has been applied to release alternative biologically active compounds, such as imaging agents.

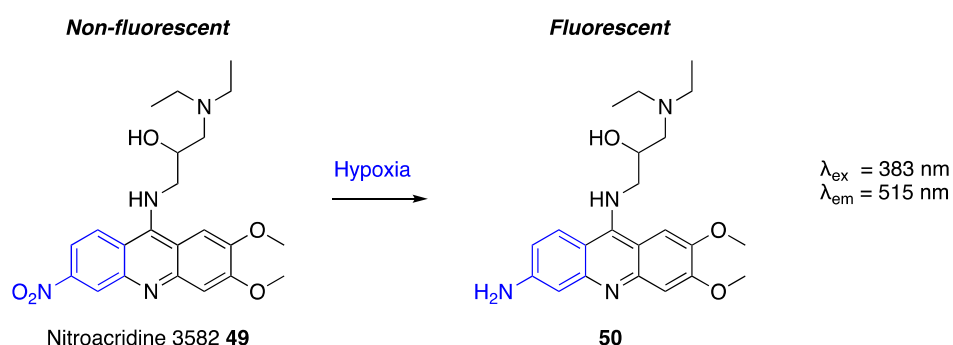
#### 1.5.5. Imaging Hypoxia with HAPs

One key consideration in the application of HAPs is determining when the use of hypoxia-activated prodrugs is appropriate. Consequently, the ability to visualise hypoxia *in situ* is a powerful tool for the evaluation of hypoxia in complex physiological environments. Although historically hypoxia was measured by inserting a fine needle electrode into a readily accessible tumour site, it is preferable to use non-invasive approaches, such as hypoxia-sensitive probes, to illustrate the heterogeneity of hypoxia throughout the tumour.<sup>192</sup> A number of different techniques to visualise hypoxia have been investigated, including those based on optical imaging, positron-emission tomography (PET), magnetic resonance imaging (MRI), and photoacoustic imaging. Only those that employ a nitroaromatic bioreductive group, which fragments under hypoxic conditions to release an active fluorophore, will be considered here (Scheme 1.9).<sup>192</sup>



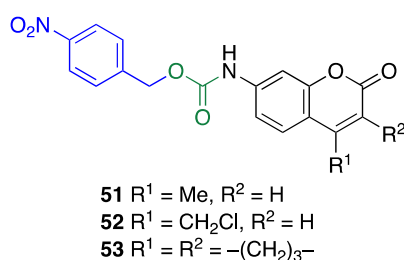
**Scheme 1.9:** Schematic showing the principle of bioreductive activation of imaging agents under hypoxia.

Fluorescence probes are favourable due to their high resolution, high sensitivity and non-invasiveness.<sup>193</sup> Early nitroaromatic-based probes incorporated the nitro group into their core, whereupon reduction to the amine restored fluorescence. This “switch-on” fluorescence is exemplified by nitroacridine-3582 **49**, which was shown to undergo reduction to the amine in hypoxia affording the fluorescent product **50** (Scheme 1.10).<sup>194–196</sup>



**Scheme 1.10:** Reduction of nitroacridine-3582 **49** to **50**, results in a “switch-on” fluorescence.

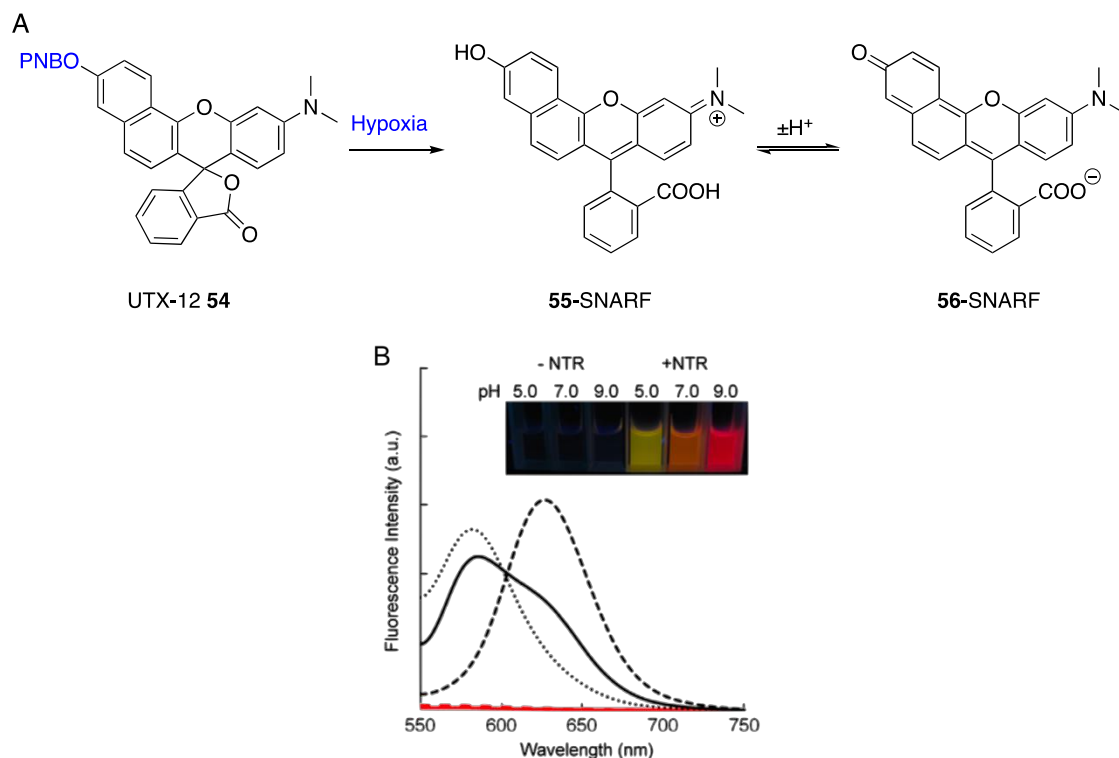
Over the last 20 years an alternative approach, in which reduction of the nitroaromatic induces fragmentation to release a fluorescent molecule, has also gained interest. The first proof-of-concept work focused on 7-hydroxylamine coumarin derivatives **51–53**, protected with a 4-nitrobenzyl bio-reductive group attached *via* a carbamate linker. However, this work was hampered by poor insolubility in aqueous media and short excitation wavelengths (<450 nm), which precluded full analysis of these compounds (Figure 1.19).<sup>197</sup>



**Figure 1.19:** Structures of the bioreductive 7-hydroxylamine coumarin derivatives, proposed by James *et al.* as potential detectors of nitroreductase activity. Blue = bioreductive moiety; green = carbamate linker.<sup>197</sup>

Subsequently, a novel hypoxia-activated probe UTX-12 **54** that released a pH sensor, based on the seminaphthorhodafluors (SNARF) scaffold was developed and used to visualise hypoxia in

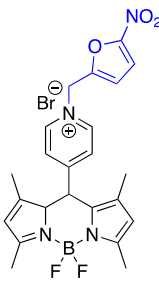
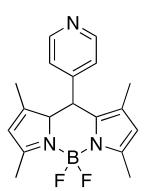
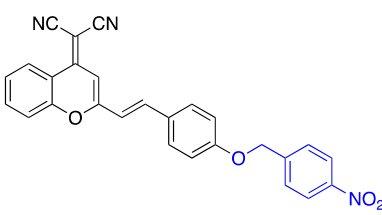
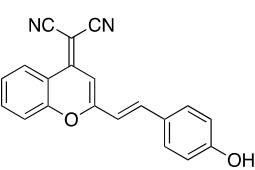
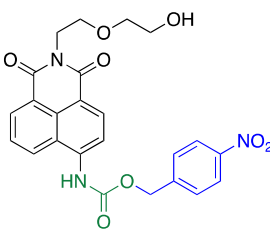
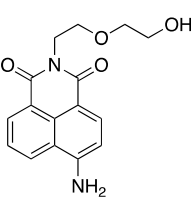
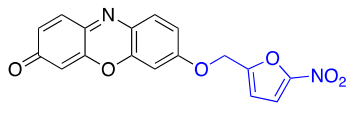
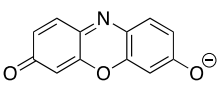
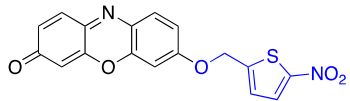
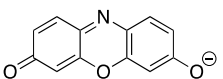
V79 cells. Under hypoxic conditions UTX-12 **54** fragments to release **55**-SNARF or **56**-SNARF, which interconvert under acidic or basic conditions resulting in a pH dependent fluorescence response (Figure 1.20).<sup>193</sup>

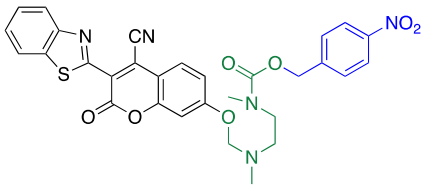
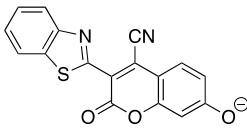
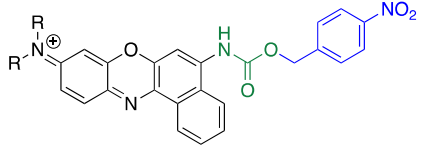
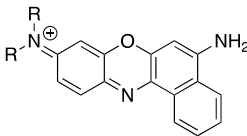
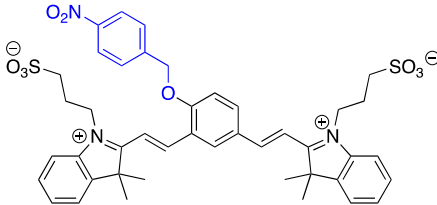
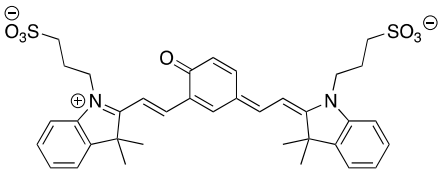
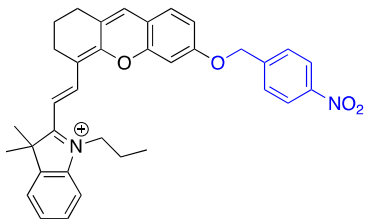
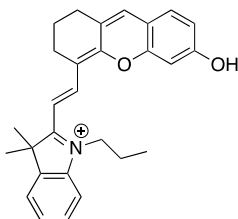
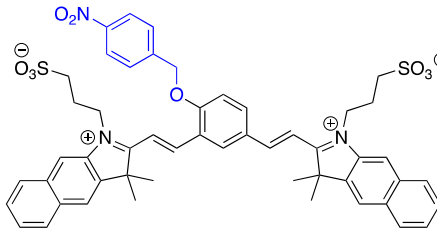
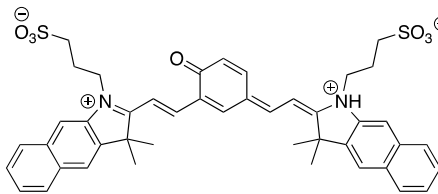


**Figure 1.20:** A) Scheme showing hypoxia-dependent activation of UTX-12 **54**, to release SNARF in the form of **55** or **56**, which exhibit a pH dependent fluorescence response. B) Fluorescence spectra showing pH dependence of UTX-12 in the presence (black) or absence (red) of NTR.  $\lambda_{\text{ex}} = 534 \text{ nm}$ ; pH 5.0 = dot line, pH 7.0 solid line, and pH 9.0 = dashed line. Inset: Photograph of the ratiometric fluorescent response in different pH conditions with or without NTR. Figure adapted and reprinted from E. Nakata, Y. Yukimachi, H. Kariyazono, S. Im, C. Abe, Y. Uto, H. Maezawa, T. Hashimoto, Y. Okamoto, H. Hori, *Bioorg. Med. Chem.* **2009**, *17*, 6952–6958 with permission from Elsevier, License No. 4427170951206.<sup>193</sup>

Similarly, a number of other probes that release a range of fluorescent molecules have been developed (Table 1.3). It is interesting to note that, compared with molecularly targeted HAPs, where the nitroimidazole bioreductive moiety predominates, the majority of these imaging agents employ the 4-nitrobenzyl group either directly or *via* a linker.

**Table 1.3:** Structures of probes for imaging of hypoxia, which use a nitroaromatic bioreductive group that fragments under hypoxic conditions to release an active fluorophore. The excitation and emission wavelengths reported in the original publication are indicated. Blue = bioreductive moiety; green = linkers.

Compound	Fluorophore	$\lambda_{\text{ex}}$ nm	$\lambda_{\text{em}}$ nm	Ref.
 <p><b>57</b></p>	 <p><b>58</b></p>	470	520	198
 <p><b>59</b></p>	 <p><b>60</b></p>	480	534	199
 <p><b>RHP 61</b></p>	 <p><b>RHF 62</b></p>	410	550	200
 <p><b>63</b></p>	 <p><b>Resorufin 64</b></p>	550	585	201
 <p><b>65</b></p>	 <p><b>Resorufin 64</b></p>	550	585	202

Compound	Fluorophore	$\lambda_{\text{ex}}$ nm	$\lambda_{\text{em}}$ nm	Ref.
 <b>66</b>	 <b>67</b>	500	595	203
 <b>NBP 68</b>	 <b>NBF 69</b>	580	658	204
 <b>70</b>	 <b>71</b>	590	708	205
 <b>72</b>	 <b>HPXI 73</b>	670	705	206
 <b>74</b>	 <b>75</b>	605	720	207

One drawback to many of these fluorescent probes is that they have maximum absorption/fluorescence peaks in the UV or visible region of spectrum. These short, high energy wavelengths are unfavourable due to tissue damage, poor penetration and autofluorescence. Therefore, it is preferable to use near infrared (NIR, 650–900 nm) light, which causes minimal

biological damage, can travel up to centimetres through tissues, and exhibits almost no autofluorescence, maximising the signal-to-background ratio.<sup>208</sup>

In 2013, compound **70**, the first sensor with fluorescence emission more than 700 nm, was reported.<sup>205</sup> This molecule contains a cyanine core, which upon deprotection of the 4-nitrobenzyl group, affords a phenolate, whose negative charge can be delocalised to nitrogen atoms forming a conjugated  $\pi$ -electron system.<sup>205</sup> A similar hemi-cyanine probe **72** was also found to exhibit favourable NIR fluorescence.<sup>206</sup> Finally, further development of **70** to **74** extended both the excitation and emission wavelengths further into the NIR region (Table 1.3).<sup>207</sup>

These examples highlight the wide range of substrates that can be protected with a bioreductive group, suggesting that the approach is highly applicable in a number of different biological settings. In this work, the concept was extended to inducible expression systems, which will be introduced next.

## 1.6. Gene Expression Systems

In 1977, pioneering work by Itakura *et al.* demonstrated recombinant expression of human somatostatin, a growth hormone inhibiting hormone, in *Escherichia coli* (*E. coli*).<sup>209</sup> Since then, the ability to overexpress a desired gene of choice, under conditions predetermined by the user, has become an important tool in biological and medicinal chemistry.<sup>210</sup> For example, insulin, used to treat diabetes, was the first commercial healthcare product to be produced by recombinant DNA technology.<sup>211</sup> Recombinant protein expression using a wide selection of organisms, including bacteria, yeast, and animal cells, has enabled the purification and characterisation of an enormous range of functional proteins from across the whole spectrum of living organisms.<sup>210,212</sup> However, although this technology has greatly facilitated the biochemical characterisation of purified proteins, there is still a significant benefit to being able to study the biological role of proteins in a cellular setting. This can be accomplished through the use of inducible gene expression systems.



### 1.6.1. Inducible Gene Expression Systems

Inducible gene expression is defined as the ability to control gene expression through a cell's response to an environmental stimulus, such as the addition of a chemical, temperature shifts, manipulation of pH, osmolarity, or depletion of certain nutrients.<sup>213</sup> The main advantage of inducible gene expression systems is that they avoid the increased metabolic burden associated with constitutive gene expression, allowing spatial and/or temporal control of gene expression.<sup>212</sup> In recombinant protein production, this allows production of the target protein to be delayed until a desired cell density has been obtained, resulting in increased protein yields.<sup>212</sup> Alternatively, inducible control of gene expression can facilitate the analysis of genes, which are toxic when expressed constitutively or at specific stages of development.<sup>214</sup>

Current techniques for inducible control of gene expression *in vitro* include cloning of the gene of interest downstream of environmentally-induced promoters (e.g. genes inserted downstream of the HRE will be up-regulated in response to hypoxia), or utilisation of small molecule-induction systems (e.g. isopropyl 1-thio- $\beta$ -D-galactopyranoside (IPTG) **76** or tetracycline **77** induction; Figure 1.21). The promoter can be an endogenous promoter, present in the host cell, where it is likely to also control expression of a number of other genes, or it can originate from an alternative species and be adapted to be functional in a different organism. Taking the regulatory elements from a different organism is advantageous because it minimises the basal expression level in the uninduced state, allowing more refined control of gene expression.<sup>214,215</sup> The use of small molecule-induction systems to control gene expression will be the focus for the rest of the chapter.

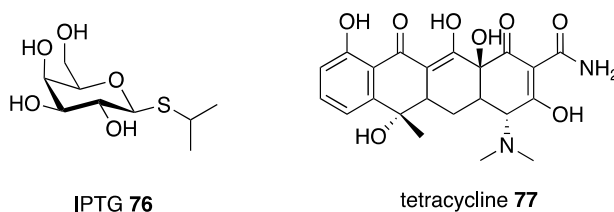


**Figure 1.21:** Structures of small molecule-inducers IPTG **76** and tetracycline **77**.

### 1.6.2. Small Molecule-Induced Gene Expression Systems

Small molecule-induction systems rely on the addition of a exogenous small molecule (the inducer), which interacts with regulatory elements inside the cell to switch gene expression on (or off).<sup>214</sup> There are several key criteria, which must be satisfied for an inducible system to be useful.<sup>214,216</sup> First, it must be specific, only responding to the desired exogenous small molecule and not endogenous factors present in the cell. Second, it should also exhibit low basal expression in the uninduced state but rapid expression of high levels upon addition of the inducer. The difference between the basal activity in the absence of inducer and the maximally induced state is known as the dynamic range of the induction.<sup>216</sup> It is also beneficial for there to be a dose-dependent response, which allows for more precise control of expression levels. Finally, the small molecule must be membrane permeable, able to enter the cell and interact with the regulatory protein.<sup>214,216</sup> Analysis of induction levels is complicated by the stochastic nature of expression in a single cell. Often significant heterogeneity is observed within a population of cells, with each cell having different expression levels according the specific intracellular inducer concentration that it experiences.<sup>217</sup>

**Table 1.4:** Examples of small molecule-inducible gene expression systems.

	Regulatory Element	Inducer	Origin	Ref.
AlcR	Transcriptional activator	Acetaldehyde	<i>A. nidulans</i>	218
ArgR	Transcriptional repressor	L-Arginine	<i>C. pneumoniae</i>	219
BirA	Biotin ligase	Biotin	<i>E. coli</i>	220
CymR	Transcriptional repressor	Cumate	<i>P. putida</i>	221
MphR	Transcriptional repressor	Erythromycin	<i>E. coli</i>	222
LacI	Repressor protein	IPTG	<i>E. coli</i>	223
HdnoR	Transcriptional repressor	6-Hydroxynicotine	<i>A. nicotinovorans</i>	224
PPAR $\gamma$	Transcription factor	Rosiglitazone	<i>H. sapiens</i>	225
TetR	Transcriptional repressor	Tetracycline	<i>E. coli</i>	226
HucR	Transcriptional repressor	Uric acid	<i>D. radiodurans</i>	227
AraC	Transcriptional activator	Arabinose	<i>E. coli</i>	228

A number of small molecule regulatory systems have been developed for inducible gene expression, some of which are shown in Table 1.4. Many of these regulate gene expression through the interaction of the inducer with an intracellular regulatory protein. These interactions either turn on an activator or turn off a repressor (Figure 1.22).<sup>216</sup>

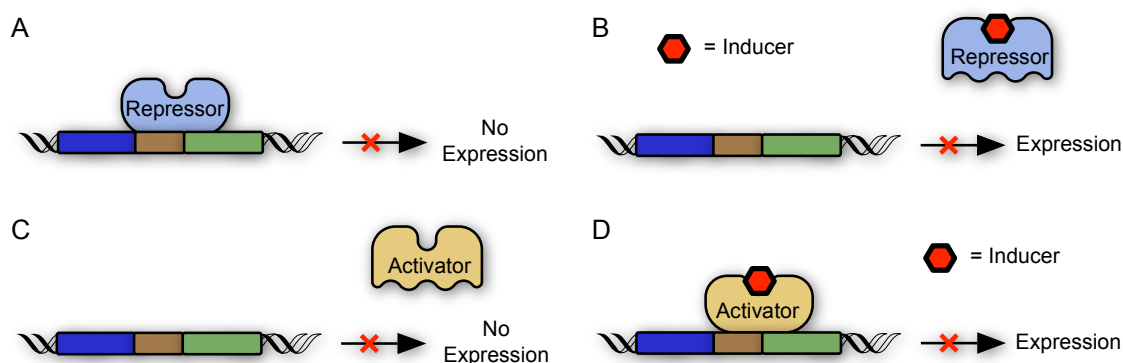


**Figure 1.22:** Schematic showing induction of repressor- (A/B) and activator- (C/D) controlled gene expression. A) In the absence of an inducer, a repressor protein binds to the DNA, inhibiting gene expression. B) Addition of an inducer causes dissociation of the repressor from the DNA; gene expression is de-repressed. C) In the absence of an inducer, the presence of an activator protein is insufficient to enable gene expression. D) Addition of an inducer enables binding of the activator to the DNA; gene expression is activated.

Of these, IPTG-inducible expression of a *LacI/lacO*-controlled promoter and tetracycline-induced expression of a TetR-controlled promoter are two important inducible gene expression systems that have found widespread use in the control of gene expression in bacteria or mammalian cells, respectively.<sup>214,229</sup>

## LacI

One of the most commonly used systems to control gene expression in bacteria is based on the *lac* promoter. In the absence of an inducer, the *lac* repressor (LacI), which is constitutively expressed, binds to a sequence of DNA adjacent to the promoter, known as the *lac* operator (*lacO*). This interaction prevents RNA polymerase from binding to *lacO* and initiating transcription. Following addition of an inducer, usually IPTG **76**, it binds to LacI and induces a conformation change, which causes LacI to dissociate from the DNA. RNA polymerase is then

able to bind to the promoter and initiate transcription, resulting in translation of the downstream gene (Figure 1.23).<sup>230</sup>

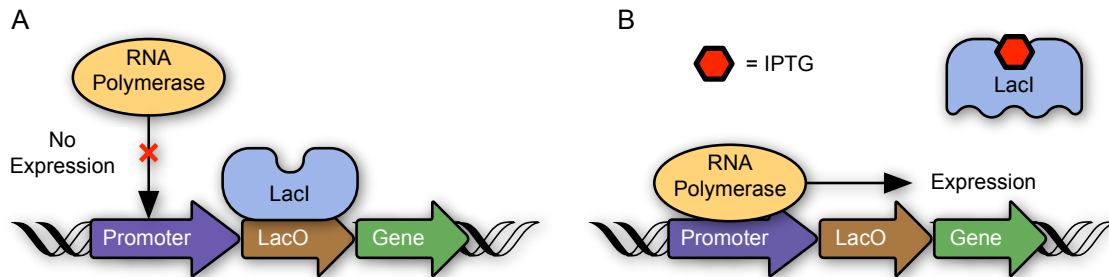


**Figure 1.23:** Schematic showing IPTG-inducible expression. A) In the absence of IPTG **76**, the *lac* repressor (LacI), which is constitutively expressed, binds to the operator sequence (*lacO*). This interaction prevents RNA polymerase from binding, inhibiting transcription. B) Following addition of an inducer, IPTG **76**, it binds to LacI and induces a conformational change, which causes LacI to dissociate from the DNA. This allows RNA polymerase to bind and transcribe the downstream gene.

## TetR

Tetracycline-inducible expression utilises three components: a tetracycline operator sequence (*tetO*), the tetracycline repressor (TetR) and tetracycline. In its native form, tetracycline exerts negative control of gene expression: binding of TetR to *tetO* requires the binding of tetracycline to TetR.<sup>231</sup> Consequently, expression is constitutively active until addition of tetracycline turns it off. This is known as the “tetracycline off” system.<sup>232</sup> However, this system was subsequently engineered to invert the phenotype, such that addition of tetracycline results in expression, not repression, of the gene of interest. This is known as the “tetracycline on” system and is controlled by a reverse tetracycline-controlled transactivator (rtTA) (Figure 1.24).<sup>226</sup>

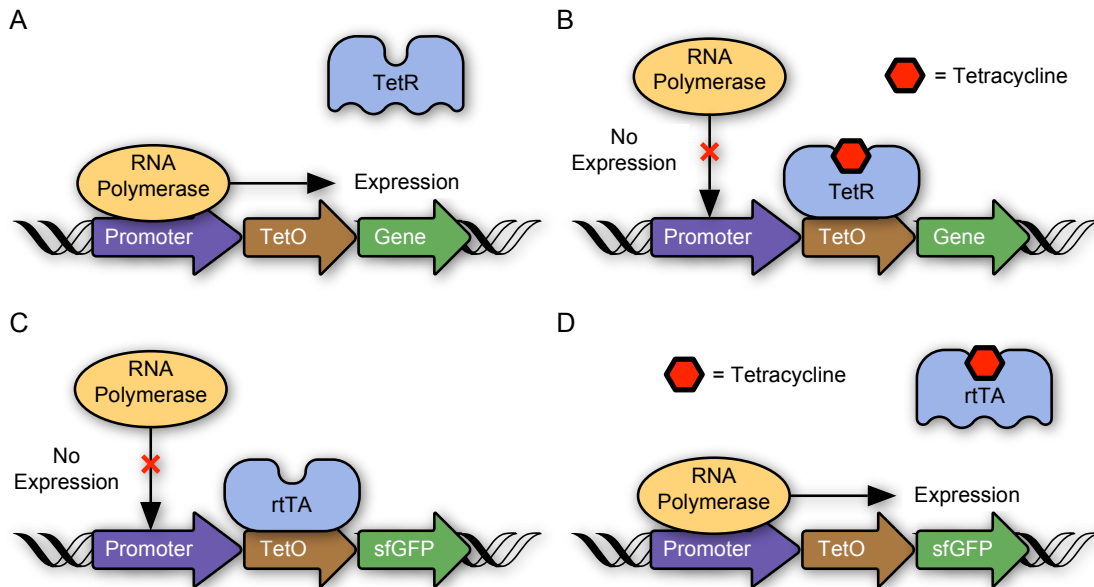


**Figure 1.24:** Schematic showing “tetracycline on” (A/B) and “tetracycline off” (C/D) regulation of gene expression. Tetracycline on: A) In the absence of tetracycline, TetR cannot bind to *tetO*, resulting in constitutive gene expression. B) Addition of tetracycline, which binds to TetR, allows TetR to bind to *tetO*, repressing gene expression. Tetracycline off: C) In the absence of tetracycline, rtTA binds to *tetO*, inhibiting gene expression. D) Addition of tetracycline causes TetR to dissociate from *tetO*, resulting in an increase in gene expression.

### 1.7. Aims

Given the numerous negative implications of hypoxia in a number of areas that are of fundamental importance for human health, including cancer therapies and biofilm antibiotic resistance, it is clear that chemical tools to study hypoxia are vital. We have previously developed tools to target<sup>182,233</sup> and image<sup>234</sup> hypoxia, which function by exploiting the reducing chemical environment that is characteristic of hypoxia. It is becoming increasingly preferable to exert additional levels of control over small molecule-induced expression systems. This has led to the development of more complex induction systems where the small molecule itself must be activated before expression, such as light-activated release of IPTG **76**,<sup>235,236</sup> which will be discussed further in Section 3.1.2. The primary aim of this project was to demonstrate hypoxic control over small molecule-induced gene expression. Accordingly, this work combines the concept of hypoxia-activated prodrugs with an IPTG-inducible gene expression system to achieve hypoxia-activated small molecule-induced gene expression in *BL21 (DE3)* bacteria (Figure 1.25).

To accomplish this, the project was broken down into three key stages. First, *BL21 (DE3)* bacteria were chosen as a model system. Therefore, it was necessary to determine whether bacteria are able to reduce nitroaryl groups in a hypoxia-dependent manner, similar to that observed in mammalian cells (Chapter 2). Next, a range of hypoxia-activated derivatives of IPTG were identified and targeted for synthesis (Chapter 3). Finally, each compound was tested for its ability to induce hypoxia-dependent gene expression in *E. coli* (Chapter 4).

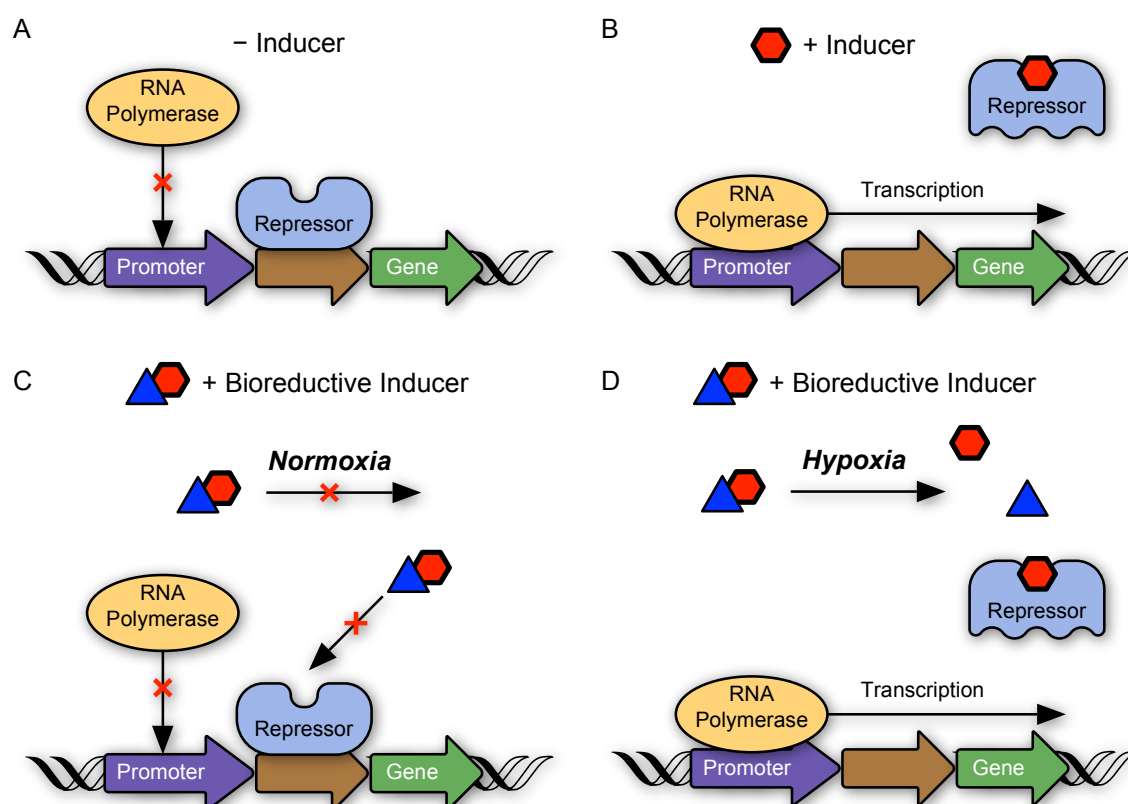


**Figure 1.25:** Schematic representation showing the concept of hypoxia-activated gene expression. A) Under uninduced conditions, a constitutively expressed repressor protein prevents binding of RNA polymerase and the downstream gene of interest is not expressed. B) Addition of an inducer (red hexagon), which binds to the repressor protein, results in dissociation of the repressor protein from the DNA. Subsequently, RNA polymerase binds and the downstream gene of interest is expressed. C) Addition of an inducer (red hexagon), protected with a bio-reductive group (blue triangle) is unable to bind to the repressor. In normoxia, the bio-reductive inducer is stable and there is no expression of the downstream gene of interest. D) In hypoxia, reduction of the bio-reductive group and fragmentation to release the inducer results in hypoxia-dependent induction of gene expression.

---

# CHAPTER 2

## A RESORUFIN-BASED HYPOXIA-ACTIVATED FLUORESCENT PROBE

---

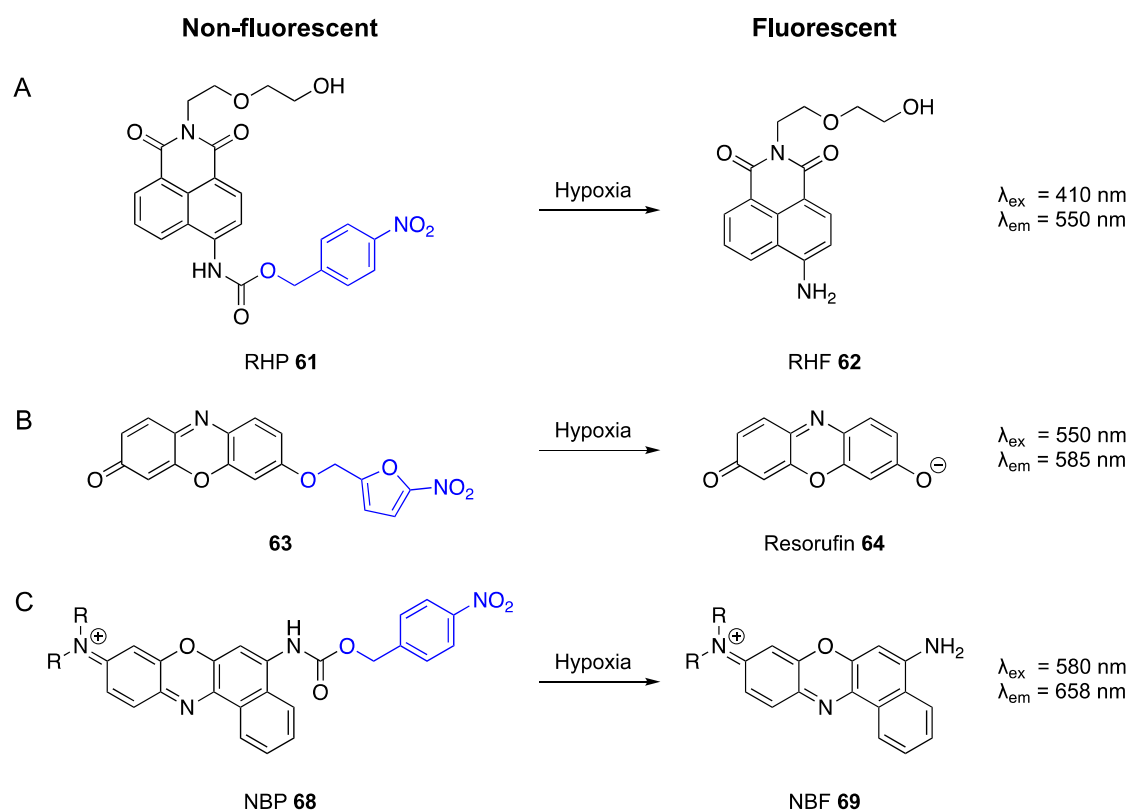
### 2.1. Introduction and Aims

To demonstrate the principle of molecular-controlled hypoxia-activated gene expression it was first necessary to choose a system, in which a plasmid encoding a protein of our choice could be readily incorporated. Due to the ease and speed with which bacteria can be manipulated, we chose to employ bacteria as a model organism.<sup>210</sup> However, hypoxia-activated prodrugs and imaging agents have primarily been studied in the context of mammalian cells and, in particular, hypoxic tumour cells.<sup>192</sup> In mammalian cells, oxygen-sensitive, one-electron nitroreductases have been implicated in bioactivation of nitroaryl HAPs<sup>131,237,238</sup> but the response of bacteria to hypoxia is largely unstudied with most research focusing on how *E. coli* sense oxygen and the associated metabolic shift between aerobic and anaerobic growth.<sup>239–241</sup> Due to their use in gene-directed enzyme prodrug therapy (G-DEPT, See Section 1.2.4),<sup>62,242</sup> the most well studied nitroreductases in bacteria are the *E. coli* oxygen-insensitive nitroreductases, NfsA and NfsB. These enzymes reduce a range of polynitroaromatic compounds in an oxygen-independent manner.<sup>243</sup> This observation suggests that there may be an innate ability for *E. coli*, which express these enzymes, to reduce nitroaryl compounds even in the presence of oxygen. Therefore, to be able to use bacteria as a model organism, it was first important to determine whether bacteria are able to reduce nitroaryl groups in a hypoxia-dependent manner, similar to that observed in mammalian cells.<sup>244</sup>

The aim of the work in this chapter was to develop a fluorescent probe that would enable the investigation of bacterial hypoxia-dependent bioreduction of nitroaromatic-based HAPs. As such, this work lays the foundation for the remainder of this dissertation, which focuses on the use of *E. coli* to develop small molecule-induced hypoxia-activated gene expression.

## 2.2. Hypoxia-Activated Fluorescent Probes

There are a variety of nitro-containing protected fluorophores that have been published as detectors of either nitroreductase activity or hypoxia, or both (See Section 1.5.5). Some examples, each containing a nitroaromatic that, upon reduction, fragments to release the corresponding fluorophore, are shown in Scheme 2.1.



**Scheme 2.1:** Literature examples of nitro-aromatic probes for detection of nitroreductase activity and hypoxia. The excitation and emission wavelengths reported in the original publication are indicated. A) **61**, a probe based on an intramolecular charge transfer (ICT) mechanism;<sup>200</sup> B) **63**, a resorufin-based probe;<sup>201</sup> C) **68**, a Nile Blue-based probe.<sup>204</sup> Blue = bioreductive moiety.

Compound **63** consists of a resorufin core **64** directly attached to a 5-nitrofuran moiety, while both **61** and **68** contain a 4-nitrobenzyl moiety attached *via* a carbamate linker to the amine of

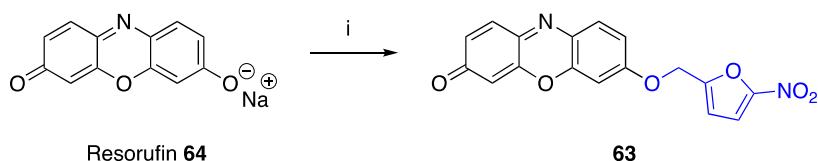


either a 4-amino-1,8-naphthalimide-based (RHF **62**) or Nile Blue-based (NBF **69**) chromophore, respectively.<sup>200,201,204</sup> Of these, **63** was chosen for our purposes due to the ready-availability of starting materials and an apparently straightforward one-step synthesis required to attach the hypoxia-activated group *via* an ether bond at the 7-hydroxyl group. Alkylation at the 7-hydroxyl group quenches the fluorescence ( $\lambda_{550/585}$  nm) of resorufin **64**; fluorescence is restored upon reduction and subsequent fragmentation of the probe, providing a sensitive technique for the detection of resorufin **64** release.

## 2.3. Evaluation of **63** as a Hypoxia-Activated Probe

### 2.3.1. Synthesis of **63**

Compound **63** was synthesised according to the literature procedure<sup>201</sup> from commercially available resorufin **64** and 2-bromomethyl-4-nitrofuran **78** in DMF (Scheme 2.2).



**Scheme 2.2:** Synthesis of **63**. *Reagents and conditions:* i) 2-bromomethyl-5-nitrofuran **78**,  $K_2CO_3$ , DMF, 40 °C, 2 h, 51%. Blue = bioreductive moiety.

### 2.3.2. Zinc/ $NH_4Cl$ Reduction of **63**

Following synthesis of **63**, it was next necessary to confirm that **63** fragments upon reduction of the nitro group to release resorufin **64**. Therefore, **63** was subjected to our previously developed sequence of chemical and biochemical reduction assays.<sup>132</sup> First, **63** was treated with zinc and ammonium chloride in DMF, as summarised in Table 2.1. Compound **63** forms an orange solution in DMF, whereas resorufin **64** is pink. Consequently, the reduction and fragmentation can be qualitatively followed by observing a colour change from orange to pink.

**Table 2.1:** Summary of reaction conditions for chemical reduction of **63**.

Entry	Equivalents Zn	Equivalents NH <sub>4</sub> Cl	Conditions	Reduction Rate / min
1	36	1.2	Aqueous	-
2	36	12	Aqueous	<5
3	10	10	Aqueous	15
4	5	10	Anhydrous	30

No reaction was observed with 1.2 equivalents of aqueous ammonium chloride (Table 2.1, Entry 1); however, increasing the number of equivalents of aqueous ammonium chloride 10-fold, resulted in an almost instantaneous colour change from orange to pink, presumed to be due to rapid release of resorufin **64**. This was confirmed by HPLC-MS analysis of an aliquot taken after 5 minutes, which showed that only resorufin **64** was present in the reaction mixture (Figure 2.1).

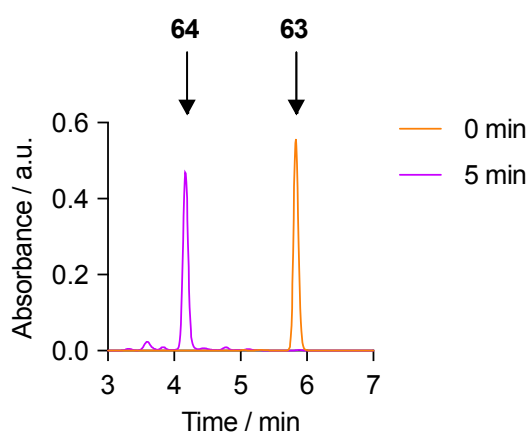


**Figure 2.1:** HPLC-MS traces showing analysis of aliquots of **63** following reduction with Zn/NH<sub>4</sub>Cl in DMF according to Table 2.1, Entry 2. Rapid release of resorufin **64** is observed after 5 min reduction.

Reducing the number of equivalents of zinc from 36 to 10 (Table 2.1, Entry 3) slowed this colour change, suggesting that the reduction and fragmentation was occurring over a longer time period of 15 minutes (Figure 2.2). However, there was still evidence of fragmentation in the reduction reaction solution, whereas previous reactions in the group had only detected fragmentation after a sample of the reduction reaction mixture was added to phosphate buffer.<sup>244</sup>

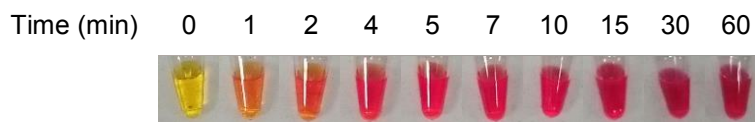


**Figure 2.2:** A photograph showing aliquots of **63** following treatment with Zn/NH<sub>4</sub>Cl in DMF for 1 h according to Table 2.1, Entry 3. The pink colour indicates increasing amounts of fragmentation product **64**.

It was hypothesised that the high water solubility of resorufin **64** would favour fragmentation in non-anhydrous conditions. Accordingly, when the reduction was repeated with solid ammonium chloride and anhydrous DMF (Table 2.1, Entry 4), the colour change to pink was only observed after 5  $\mu$ L of the aliquot taken after 60 minutes was added to 95  $\mu$ L phosphate buffer (Figure 2.3). These data suggest that when **63** is reduced, it fragments under aqueous conditions to release resorufin **64**.



**Figure 2.3:** A photograph showing aliquots of **63** following treatment under anhydrous conditions with Zn/NH<sub>4</sub>Cl in DMF for 1 h according to Table 2.1, Entry 4. The pink colour, indicating the presence of fragmentation product **64**, is only present after a sample of the aliquot taken after 60 min was added to phosphate buffer.

### 2.3.3. Cytochrome P450:NADPH Reductase Treatment of **63**

The next step was to determine whether **63** is enzymatically reduced under hypoxic conditions in a cell-free environment. For this we used an enzymatic assay, which employs human cytochrome P450 (CYP450):NADPH reductase enzymes with an NADPH regeneration system.<sup>132</sup> CYP450:NADPH reductase enzymes catalyse the single-electron reduction of nitro compounds and have previously been shown to be involved in bioreduction of nitroaromatic compounds under hypoxic conditions.<sup>237,238</sup>

Compound **63** was treated with CYP450:NADPH reductase enzymes under normoxic (21% O<sub>2</sub>; Figure 2.4A) and hypoxic (<0.1% O<sub>2</sub>; Figure 2.4B) conditions for 6 hours. Samples taken at

various time points were analysed by HPLC-MS to determine the concentrations of **63** and released resorufin **64**.

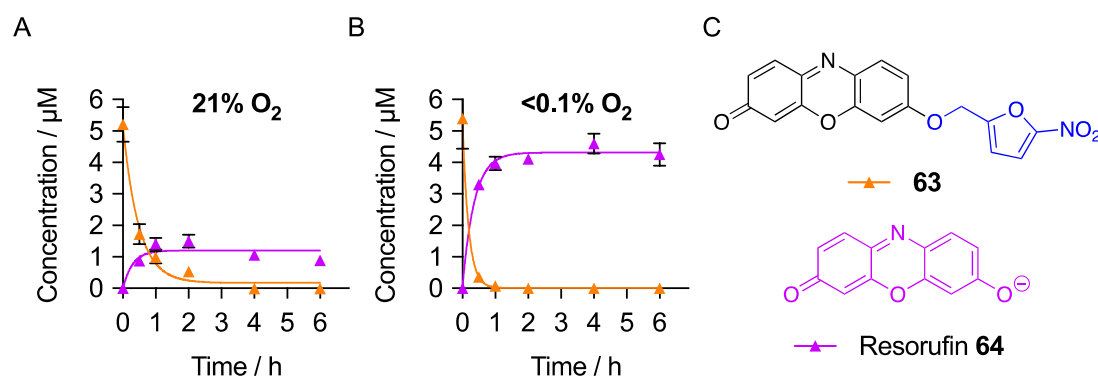


**Figure 2.4:** Compound **63** (5 μM) was treated with CYP450:NADPH reductase enzymes under A) normoxic (21% O<sub>2</sub>) and B) hypoxic (<0.1% O<sub>2</sub>) conditions over 6 h. Aliquots were taken at the time indicated and analysed by HPLC. C) Structures of probe **63** and resorufin **64**. Blue = bio-reductive moiety.

Under hypoxic conditions, **63** was rapidly reduced with a concomitant increase in resorufin **64**. However, a reduction in **63** and an increase in resorufin **64** was also observed in the normoxic samples. Although the fragmentation in normoxia occurred at a slower rate than in hypoxia, these data suggested that in the presence of CYP450:NADPH reductase enzymes, **63** is unstable in normoxic conditions.

### 2.3.4. Cellular Analysis of **63**

For the probe to be used as a reliable fluorescent tool to ascertain whether bacteria can reduce nitroaromatics in a hypoxia-dependent manner, it is essential that it is stable under normoxic conditions. Compound **63** has previously been reported as a probe for selective imaging of the hypoxic status of tumour cells.<sup>201</sup> Therefore, despite the instability observed in our enzyme assay, it was decided to further investigate the bacterial stability of **63** in our hands.

The *BL21 (DE3)* strain of *E. coli*<sup>245</sup> is a popular strain for recombinant expression of proteins in bacteria<sup>210</sup> and was chosen for these studies. For comparison with a mammalian cell line, the human liver cancer cell line, HepG2, which has been used for hypoxic imaging previously in the group, was chosen.<sup>234</sup>

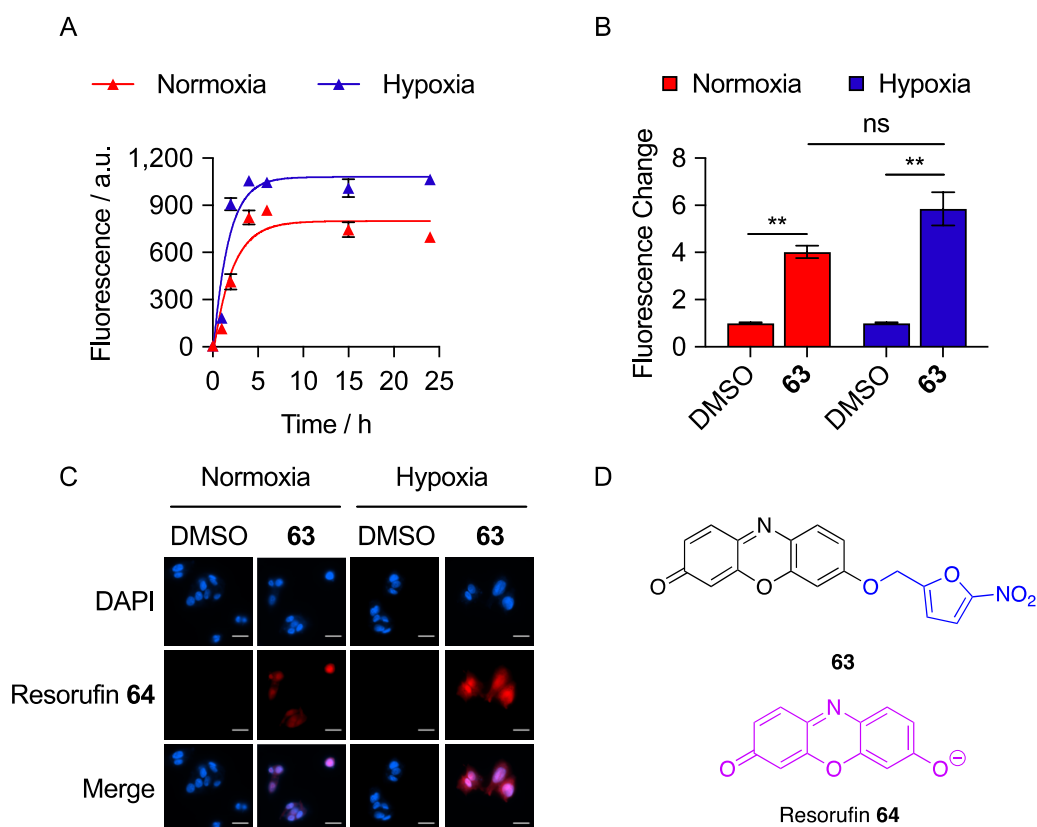


**Figure 2.5:** Compound **63** is unstable and susceptible to bioreduction under both normoxic and hypoxic conditions. A) *BL21 (DE3)* bacteria were treated with **63** (5  $\mu$ M) under normoxic (21%  $O_2$ ) and hypoxic (<0.1%  $O_2$ ) conditions over 24 h. Samples were analysed by fluorescence ( $\lambda_{ex}$  = 550 nm;  $\lambda_{em}$  = 585 nm). B–C) Quantification of pixel intensity (B) and representative images (C) of HepG2 cells ( $3 \times 10^5$ ) treated with **63** (5  $\mu$ M) under normoxic (21%  $O_2$ ) and hypoxic (<0.1%  $O_2$ ) conditions for 6 h. Cells were fixed and observed by fluorescence microscopy. DAPI (blue) was used as a nuclear stain. Scale bars represent 25  $\mu$ M. In both bacteria and HepG2 cells, an increase in fluorescence was observed in both normoxic and hypoxic conditions D) Structures of probe **63** and resorufin **64**. Blue = bioreductive moiety.

*BL21 (DE3)* bacteria were incubated with **63** under either normoxic (21%  $O_2$ ) or hypoxic (<0.1%  $O_2$ ) conditions for 0–24 hours and analysed for an increase in fluorescence due to release of resorufin **64**. Bacteria in both normoxia and hypoxia showed a rapid increase in fluorescence until saturation was reached after 5 hours (Figure 2.5A). Similarly, HepG2 cells were treated with **63** under either normoxic or hypoxic conditions for 6 hours and analysed using fluorescence microscopy. After this time a significant increase in fluorescence was observed in both the normoxia- and the hypoxia-treated samples (Figure 2.5B/C). Taken together with the CYP450:NADPH reductase assay, these data suggest that **63** undergoes bioreduction in both

normoxia and hypoxia. Consequently, it was decided that **63** was too unstable, and therefore inappropriate, to be used as a probe to analyse hypoxia-specific bio-reduction of nitroaromatics in *E. coli*.

## 2.4. Evaluation of **79** as an Alternative Hypoxia-Activated Probe

Having observed that **63** underwent bio-reduction both in normoxia and hypoxia, an alternative nitroaromatic containing probe that would be more stable in normoxic conditions, but still be susceptible to reduction and fragmentation under hypoxic conditions, was sought. There are a variety of nitroaryl groups that have been investigated in the context of hypoxia-activated prodrugs.<sup>132,179,246</sup> The chemical reduction potentials  $E(\text{ArNO}_2/\text{ArNO}_2^-)$  vs the normal hydrogen electrode (NHE) under physiological conditions of some of these have been estimated (Figure 1.14) and these values are hypothesised to be indicative for how readily a group is reduced under hypoxic conditions in a biological setting.<sup>132,247</sup>

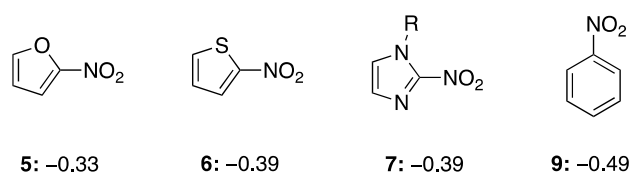


**Figure 2.6:** Estimated values of reduction potentials  $E(\text{ArNO}_2/\text{ArNO}_2^-)$  vs NHE in water at pH 7 of some commonly used nitroaryl systems; R = alkyl or hydroxyalkyl.<sup>247</sup>

As can be seen from these values, the 4-nitrobenzyl group **9** has a lower reduction potential ( $-0.49 \text{ V}$  vs  $-0.33 \text{ V}$ ) than the 5-nitrofuran group **5** and is, therefore, expected to require lower oxygen concentrations to be bio-reduced.<sup>132</sup> It was hypothesised that an analogous compound, **79**, comprising the 4-nitrobenzyl group attached to resorufin **64**, would be a more suitable probe (Figure 2.7).

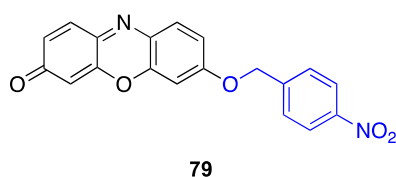
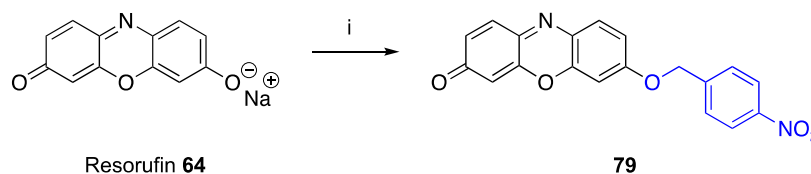


**Figure 2.7:** Structure of the proposed alternative hypoxia-activated fluorescent probe, **79**. Blue = bio-reductive moiety.

### 2.4.1. Synthesis 79

Compound **79** was synthesised in a similar manner to **63**, using 4-nitrobenzyl bromide **80** instead of 2-bromomethyl-4-nitrofur **78**. Additionally, in this case **79** was isolated in high purity by crystallisation from dichloromethane.



**Scheme 2.3:** Synthesis of **79**. *Reagents and conditions:* i) 4-NO<sub>2</sub>BnBr **80**, K<sub>2</sub>CO<sub>3</sub>, DMF, 100 °C, 17 h, 34%. Blue = bioreductive moiety.

### 2.4.2. Fluorescence Analysis of 79

In order for **79** to be a useful probe, it must be non-fluorescent until reduction and fragmentation releases **64**. Fluorescence analysis confirmed that **79** exhibits negligible fluorescence compared to free resorufin **64** (Figure 2.8). Therefore, **79** was next analysed in a manner similar to that used for **63** by applying our previously developed sequence of chemical and biochemical reduction assays.<sup>132</sup>

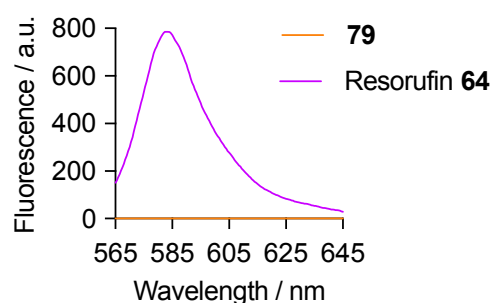


**Figure 2.8:** Fluorescence spectra for **64** (0.5 μM in PBS) and **79** (1 μM in PBS); λ<sub>ex</sub> = 550 nm.

### 2.4.3. Zinc/NH<sub>4</sub>Cl Reduction of 79

First, **79** was treated with zinc and ammonium chloride in DMF (Table 2.2) and evaluated both visually using the change in reaction colour from orange to pink and by HPLC-MS.

**Table 2.2:** Summary of reaction conditions for chemical reduction of **79**.

Entry	Equivalents Zn	Equivalents NH <sub>4</sub> Cl	Conditions	Reduction Rate (min)
1	36	1.2	Aqueous	-
2	36	13	Aqueous	<5
3	5	10	Anhydrous	60

As before, no change was observed with 1.2 equivalents of ammonium chloride (Table 2.2, Entry 1), while increasing the number of equivalents of ammonium chloride 10-fold (Table 2.2, Entry 2) resulted in an almost instantaneous colour change from orange to pink, suggesting rapid reduction and release of resorufin **64**. Performing the reaction under anhydrous conditions (Table 2.2, Entry 3) again delayed release of resorufin **64** until a sample of the reduction reaction mixture was added to phosphate buffer (Figure 2.9A). HPLC-MS analysis of the reduction reaction showed a decrease in **79** over time with only partial release of resorufin **64** (Figure 2.9B). This small increase in resorufin **64** could be due to fragmentation on the column, which uses aqueous formic acid as the polar eluent. When a sample of the aliquot taken after 60 minutes reduction was added to phosphate buffer, complete conversion to resorufin **64** was observed (Figure 2.9C/D). Together, these data show that when **79** is reduced, it fragments under aqueous conditions to release resorufin **64**.



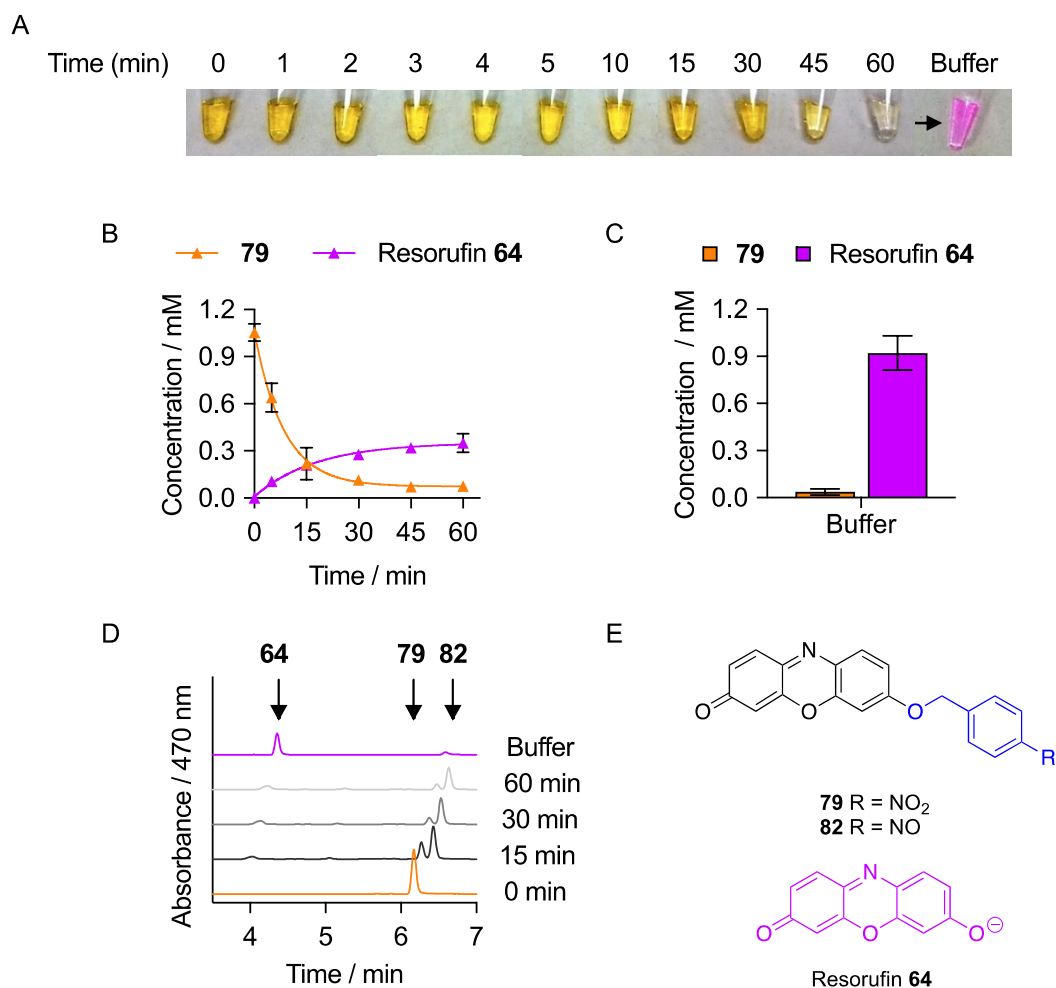


**Figure 2.9:** Zn/NH<sub>4</sub>Cl reduction of **79**. A) Compound **79** was treated with Zn/NH<sub>4</sub>Cl over 60 min according to Table 2.2, Entry 3. Addition of an aliquot taken after 60 min to phosphate buffer results in a formation of a pink solution, suggesting release of resorufin **64**. B–C) Conditions as in (A). HPLC-MS analysis of chemical reduction (B) and fragmentation (C) of **79**. The concentration of **79** decreases over time with only partial release of resorufin **64**. When a sample of the aliquot taken after 60 min reduction was added to phosphate buffer, complete conversion to resorufin **64** is observed. D) Conditions as in (A). Representative HPLC traces showing reduction of **79** via nitroso intermediate **82** and fragmentation to release resorufin **64**. E) Structures of the nitro probe **79**, nitroso intermediate **82**, and resorufin **64**. Blue = bioreductive moiety.

#### 2.4.4. Cytochrome P450:NADPH Reductase Treatment of **79**

Compound **79** was next treated with CYP450:NADPH reductase enzymes over 48 hours under normoxic (21% O<sub>2</sub>; Figure 2.10A) and hypoxic (<0.1% O<sub>2</sub>; Figure 2.10B) conditions to determine its stability to enzyme-mediated reduction under normoxic conditions and whether it

would fragment to release resorufin **64** under hypoxic conditions. Samples taken at the time points shown were analysed by HPLC-MS to determine the concentrations of **79** and released resorufin **64**.

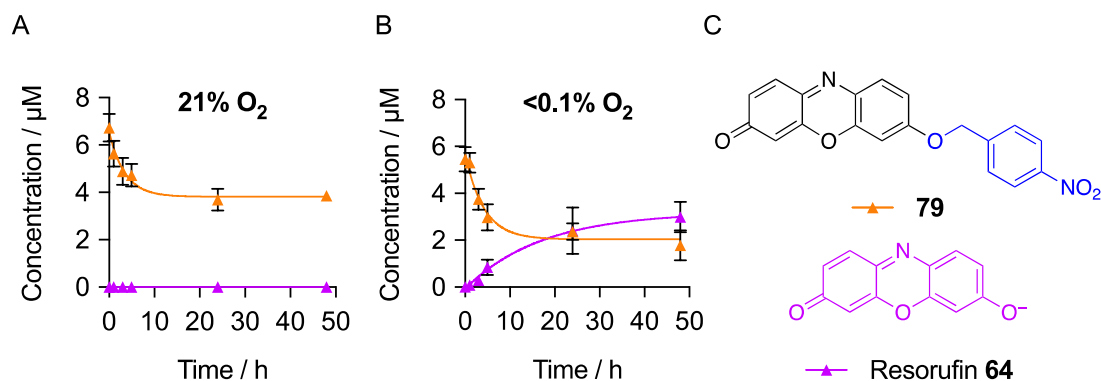
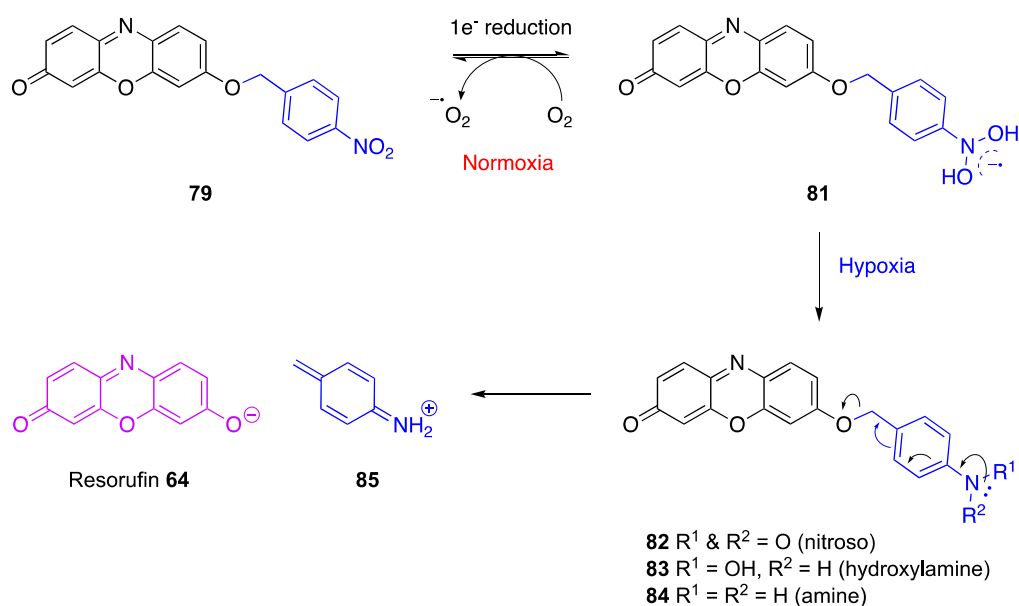


**Figure 2.10:** Compound **79** (5  $\mu\text{M}$ ) was treated with CYP450:NADPH reductase enzymes under A) normoxic (21% O<sub>2</sub>) and B) hypoxic (<0.1% O<sub>2</sub>) conditions over 48 h. Aliquots were taken at the time indicated and analysed by HPLC. C) Structures of probe **79** and resorufin **64**. Blue = bioreductive moiety.

Under normoxic conditions, no formation of resorufin **64** was detected by HPLC-MS even after 48 hours. Conversely, under hypoxic conditions, the concentration of **79** was reduced over time with a corresponding increase in released resorufin **64**. This result suggests that, when treated with CYP450:NADPH reductase enzymes, **79** can undergo hypoxia-dependent reduction resulting in fragmentation to release resorufin **64** (Scheme 2.4). It is also worth noting that in both the chemical and enzymatic reduction assays, reduction and fragmentation of **79** occurred more slowly than reduction and fragmentation of **63**. This observation suggests that, as expected, the nitrobenzyl derivative of resorufin **64** is more stable than the nitrofuranyl derivative.



**Scheme 2.4:** Mechanism of hypoxia-dependent activation of **79**.<sup>132</sup> Under hypoxic conditions, the nitro group is reduced to form an electron-donating substituent, which induces fragmentation and releases resorufin **64**. Blue = bioreductive moiety.

#### 2.4.5. Cellular Analysis of **79**

Having shown that **79** undergoes hypoxia-dependent reduction and fragmentation when treated with CYP450:NADPH reductase enzymes, it could then be used in a cellular setting to determine whether hypoxia-dependent bioreduction of a nitroaryl group takes place in *BL21 (DE3)* bacteria.

First, to confirm that **79** is stable under normoxic conditions and bioreduced under hypoxic conditions to release resorufin **64** as expected in a mammalian cell line, HepG2 cells were again used for comparison. The human colorectal carcinoma cell line, HCT116, which have also previously been used in the group for hypoxic imaging,<sup>234</sup> were also employed. HepG2 and HCT116 were treated with **79** under either normoxic (21% O<sub>2</sub>) or hypoxic (<0.1% O<sub>2</sub>) conditions for 24 hours and analysed by fluorescence microscopy (Figure 2.11). Promisingly after this time, no fluorescence was observed in the normoxia samples. Conversely a 1.8-fold increase (HepG2) and a 3.8-fold increase (HCT116), relative to the respective DMSO controls, were observed in the hypoxic samples. This result suggested that **79** is stable under normoxic conditions and fragments under hypoxic conditions to release resorufin **64** and, therefore, would be appropriate to assess bioreduction of nitroaromatics in *BL21 (DE3)*.

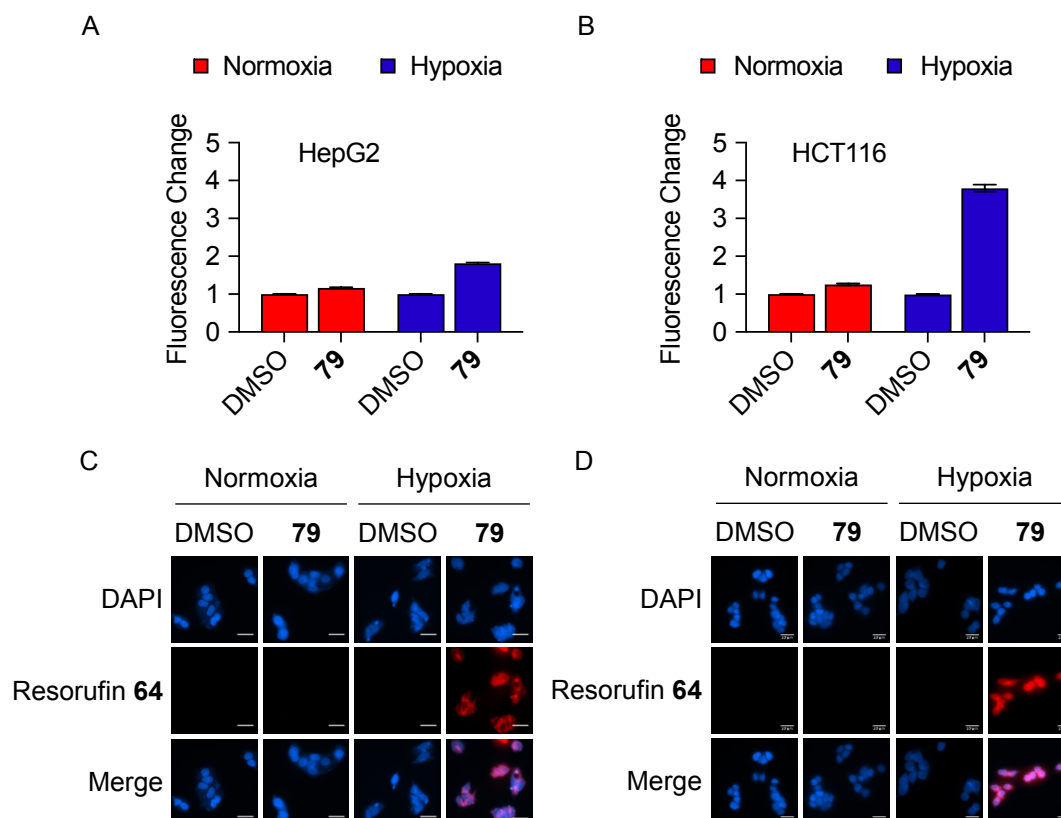


**Figure 2.11:** Quantification (A/B) and representative images (C/D) of HepG2 cells (A/C) and HCT116 cells (B/D) treated with **79** (5  $\mu$ M) under normoxic (21% O<sub>2</sub>) and hypoxic (<0.1% O<sub>2</sub>) conditions for 24 h. Cells were fixed and observed by fluorescence microscopy. DAPI (blue) was used as a nuclear stain. Scale bars represent 25  $\mu$ M. In both cell lines, an increase in fluorescence is only observed in hypoxic conditions.

*BL21 (DE3)* bacteria were next treated with **79** under normoxic (21%) and hypoxic (<0.1%) conditions and analysed at the time points indicated over 24 hours (Figure 2.12). After 24 hours, a 7-fold increase in fluorescence compared to that in normoxic conditions was observed (Figure 2.12).

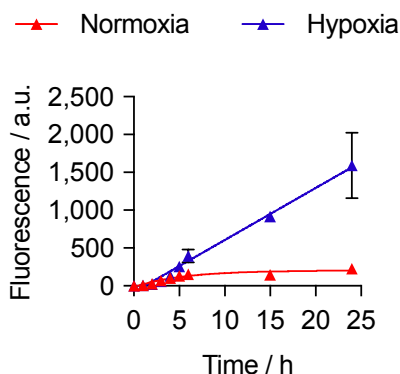


**Figure 2.12:** *BL21 (DE3)* bacteria were treated with **79** (5  $\mu$ M) under normoxic (21% O<sub>2</sub>) and hypoxic (<0.1% O<sub>2</sub>) conditions over 24 h. Samples were analysed by fluorescence ( $\lambda_{\text{ex}}$ : 550 nm;  $\lambda_{\text{em}}$ : 585 nm).

Taken together, these data indicate that bioreduction of **79** and subsequent fragmentation to release resorufin **64** occurs selectively in hypoxia in bacterial cells, in a manner that is similar to that observed in human cells. Consequently, it was concluded that other nitroaryl HAPs would function in a similar manner and, therefore, that *BL21 (DE3)* would be a suitable model organism for development of small molecule-induced hypoxia-activated gene expression.

## 2.5. Conclusion

In conclusion, a fluorescent probe that would determine whether or not bacteria cells can effect hypoxia-specific reduction of nitroaryl HAPs was sought. Initially, compound **63**, a previously reported detector of nitroreductase activity was assessed; however, in our hands **63** was found to be unstable under normoxic conditions and, therefore, unsuitable for our purposes. Consequently compound **79**, a nitrobenzyl based analogue of **63** was synthesised and shown to be a novel hypoxia-activated fluorescent probe. Compound **79** was used to show that in *BL21 (DE3)* bacteria, there is a hypoxia-dependent reduction and release of resorufin **64**. This suggested that *BL21 (DE3)* bacteria would be a suitable model organism for development of our technology for small molecule-induced hypoxia-activated gene expression. This is the first example of hypoxia-dependent bioreduction of nitroaryl groups in *E. coli*. Future chapters will build on this work, discussing the synthesis (Chapter 3) and analysis (Chapter 4) of a range of potential hypoxia-activated inducers of gene expression.



---

# CHAPTER 3

## SYNTHESIS OF HYPOXIA-ACTIVATED INDUCERS FOR AN IPTG-INDUCIBLE EXPRESSION SYSTEM

---

### 3.1. Introduction and Aims

A number of small molecule regulatory systems have been developed for inducible gene expression (See Section 1.6.2). This project focused on IPTG-inducible gene expression, which is based on the *lac* promoter. In the absence of an inducer, the *lac* repressor (LacI), which is constitutively expressed, binds to a specific sequence of DNA adjacent to the promoter, known as the *lac* operator (*lacO*). This interaction prevents RNA polymerase from binding to *lacO* and initiating transcription. Following addition of an inducer, usually IPTG **76**, it binds to LacI and induces a conformation change, which causes LacI to dissociate from the DNA. RNA polymerase is then able to bind to the promoter and initiate transcription, resulting in translation of the downstream gene (Figure 1.23).<sup>230</sup>

It was hypothesised that protecting IPTG **76** with a bioreductive group would prevent binding of IPTG **76** to LacI, inhibiting its biological activity. Bioreduction and fragmentation will release IPTG **76**, resulting in transcription and subsequent translation of the downstream gene or genes, thereby placing them under the control of hypoxia (Figure 3.2).

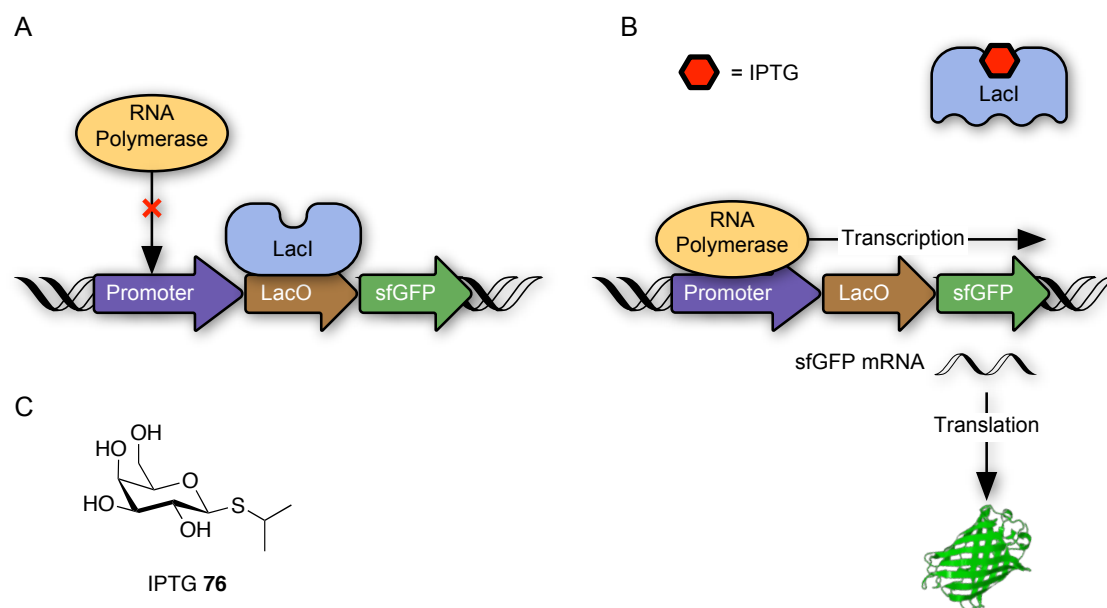


**Figure 3.1:** Schematic showing IPTG-inducible expression of sfGFP. A) In the absence of IPTG 76, the *lac* repressor (LacI), which is constitutively expressed, binds to the operator sequence (*lacO*). This interaction prevents RNA polymerase from binding, inhibiting transcription. B) Following addition of an inducer, IPTG 76, it binds to LacI and induces a conformational change, which causes LacI to dissociate from the DNA. This allows RNA polymerase to bind and transcribe the downstream gene. C) Chemical structure of IPTG 76.

The aim of the work described in this chapter was to design and synthesise potential inducers of gene expression that are specific for hypoxic conditions. Accordingly, the synthesis of a range of derivatives of IPTG that are protected with a bioreductive moiety will be discussed.

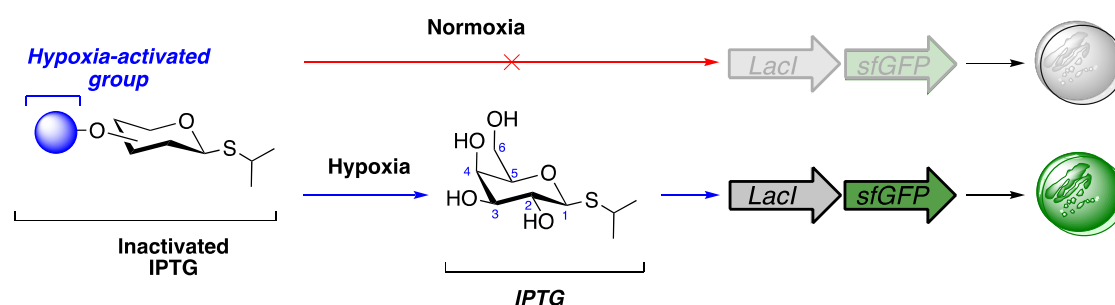


**Figure 3.2:** The concept of using hypoxia-activated IPTG to place the *lac* repressor, and hence gene expression, under the control of hypoxia. Blue = bioreductive moiety; sfGFP is shown as a representative gene.



### 3.1.1. Analysis of LacI/IPTG Binding interactions

A key consideration in the design of hypoxia-activated inducers for IPTG-inducible expression is that attachment of a bioreductive moiety to IPTG **76** must prevent IPTG **76** from binding to LacI. Analysis of a 2.0 Å resolution X-ray crystal structure of a dimeric LacI with IPTG **76** bound has identified a number of key binding interactions between IPTG **76** and LacI (PDB ID: 2P9H)<sup>248</sup> (Figure 3.3). These interactions predominantly comprise an extensive hydrogen-bonding network between the hydroxyl groups on the sugar and the amino acid side chains of the repressor.<sup>248</sup>

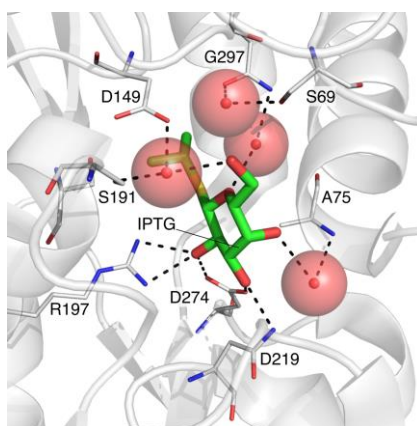


**Figure 3.3:** X-ray crystal structure of IPTG **76** (carbon = green) bound to the *E. coli lac* repressor (LacI), showing important hydrogen bonding interactions (black dashed lines) (PDB ID: 2P9H).<sup>248</sup> Figure generated using PyMOL.

The 2-position (C2-OH) and 3-position (C3-OH) hydroxyl groups form direct hydrogen bonds with the side chains of Arg-197, Asn-246 and Asp-274, which are located in the C-terminal subdomain. The 4-position (C4-OH) hydroxyl group forms a water-mediated hydrogen bond to both the backbone nitrogen of Ala-75 and the side chain of Asn-246. Water-mediated interactions between the 6-position (C6-OH) hydroxyl group and the side chains of Ser-69, Asp-149 and Asn-125, which are located on the N-terminal domain, and Ser-191 and Ser-193 in the C-terminal domain, are also crucial for inducer activity.<sup>248</sup> For example, whilst 2-nitrophenyl 1-thio-β-D-galactopyranoside **107** increases gene expression levels, 2-nitrophenyl 1-thio-β-D-fucoside **115**, which does not contain the C6-OH group, reduces gene expression levels (Figure 3.4).<sup>249</sup> Furthermore, removing or epimerising either the C2-OH or C3-OH groups prevents binding of IPTG **76** to LacI.<sup>249,250</sup>

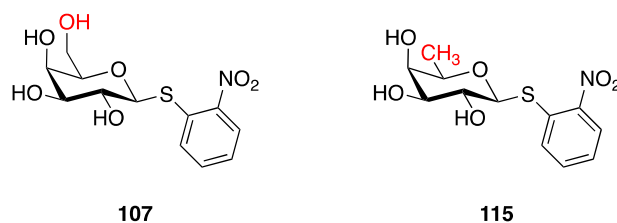


**Figure 3.4:** Structures of **107**, which increases, and **115**, which decreases gene expression levels. Compounds **107** and **115** differ only in the presence or absence of a C6-OH group. The inability of **115** to induce gene expression, suggests that the C6-OH group is essential for inducer activity.

### 3.1.2. Design of Hypoxia-Activated Inducers

Given that all of the hydroxyl groups of IPTG **76** form hydrogen bonding interactions with the protein, either directly or through water molecules, it was unclear which was the optimal position for inclusion of the bioreductive group. It was hypothesised that protection of any of the free hydroxyl groups with a hypoxia-activated group could inhibit formation of the LacI/IPTG complex. Although a variety of nitroaryl hypoxia-activated groups can be used,<sup>132,179,246</sup> this project focused on the use of the 4-nitrobenzyl group that had been employed in the initial resorufin studies (Chapter 2). Consequently, analogues of IPTG, protected with a 4-nitrobenzyl group at the 2- (**86**), 3- (**87**), 4- (**88**), and 6- (**89**) positions, were identified as potential hypoxia-activated inducers of gene expression and targeted for synthesis (Figure 3.5).

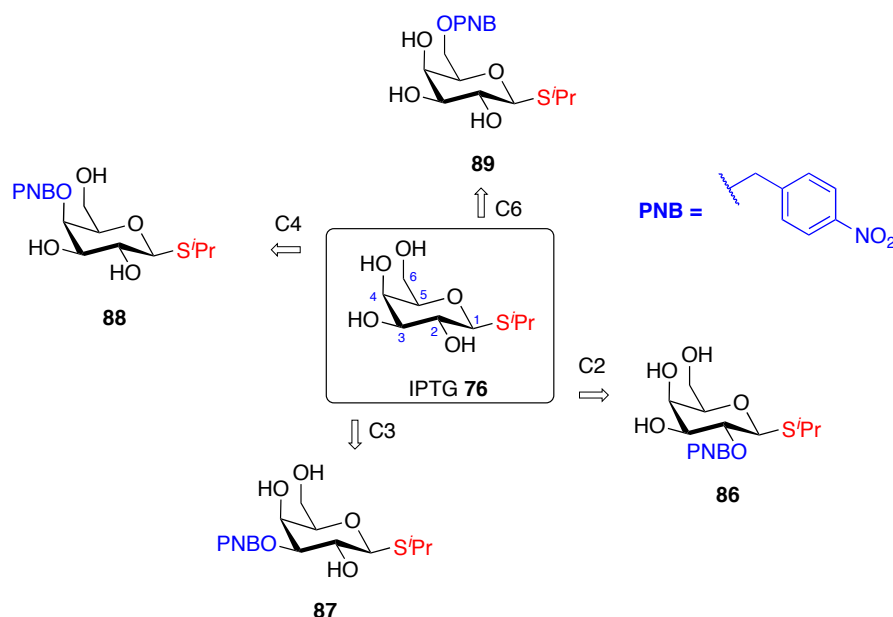
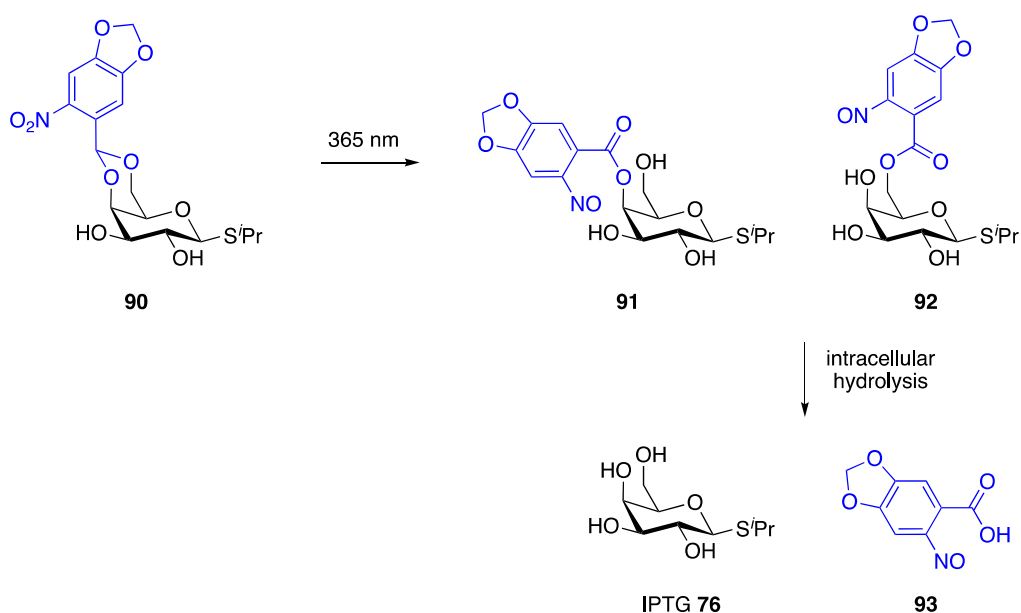


**Figure 3.5:** Structures of analogues of IPTG **86–89** that were identified as potential hypoxia-activated inducers of gene expression. Blue = bioreductive group.

One further compound was also of interest following the work of Young and Deiters into light-activation of gene expression.<sup>235,236</sup> In their work, formation of a 1,3-dioxolan between the C4-OH and the C6-OH groups with a photolysable 6-nitropiperonal afforded **90**, which is unable to form the LacI/IPTG complex. Irradiation at 365 nm converts **90** to esters **91** and **92** which are hydrolysed by intracellular esterases to release IPTG **76** (Scheme 3.1).



**Scheme 3.1:** Structure and schematic of activation of a light-activated caged IPTG **90**. Irradiation of **90**, followed by intracellular hydrolysis of the esters **91** and **92** yields IPTG **76**.<sup>236</sup>

It was hypothesised that an analogous derivative of IPTG (**94**, Figure 3.6), containing a bio-reductive group formed *via* an acetal linkage between the C4-OH and the C6-OH groups, would also be unable to bind to LacI. This compound is not expected to induce gene expression until exposure to hypoxic conditions results in reduction and fragmentation to release IPTG **76**.

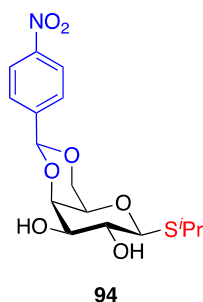


**Figure 3.6:** Structure of an alternative hypoxia-activated inducer of gene expression **94** based on the light-activated compound **90**.<sup>236</sup>

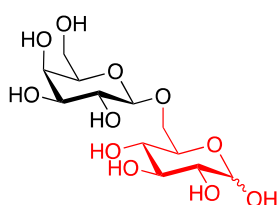
### 3.2. Synthesis of a UV-Active Inducer of the *lac* Promoter

As the most commonly used synthetic inducer of the *lac* promoter, it was preferable to design hypoxia-activated inducers based on IPTG **76**. Downstream analysis (Chapter 4) of these compounds will follow our previously developed sequence of chemical and biochemical reduction assays.<sup>132</sup> However, IPTG **76** cannot be easily visualised by UV absorption. Therefore, in order to facilitate HPLC detection of released compounds in the chemical and enzymatic reduction assays, it was decided to synthesise analogues of IPTG containing a UV-active moiety.

Although, in principle, any group that would confer UV absorption activity could be used, it was preferable to use one in which the free compound was still an inducer of the *lac* promoter as this would enable its use in both the enzymatic assays and bacterial induction experiments. Therefore, the first aim was to synthesise an alternative inducer of the *lac* promoter that contains a UV active chromophore.

#### 3.2.1. Choice of Inducer

The natural inducer of the *lac* promoter is allolactose **95**, which consists of D-galactose and D-glucose linked through a  $\beta$ -1,6 glycosidic bond (Figure 3.7).<sup>251</sup>

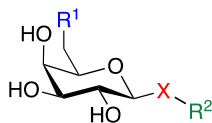


Allolactose **95**

**Figure 3.7:** Structure of allolactose **95**, the natural inducer of the *lac* operon. The anomeric glucose moiety is shown in red.

Early studies, which investigated effecting ligands of LacI, identified a number of alternative  $\beta$ -D-galactoside based compounds, which either increased or decreased levels of gene expression.<sup>252</sup> This showed that a number of different functional groups can be tolerated at the anomeric position. Some examples of these compounds are shown in Table 3.1.

**Table 3.1:** Structures of some galactose-based compounds, shown to be inducers, anti-inducers or neutral ligands of the *lac* repressor.<sup>249</sup>



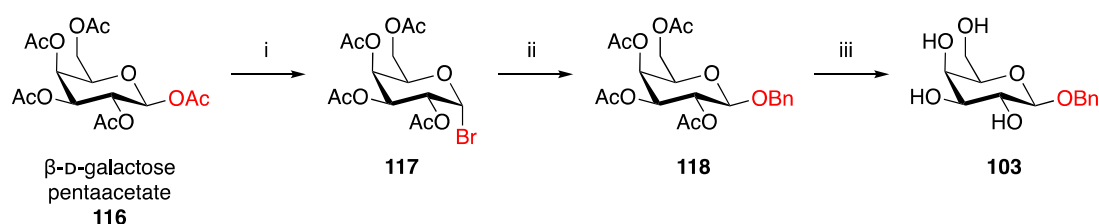
Compound	R <sup>1</sup>	X	R <sup>2</sup>
Inducers			
<b>96</b>	OH	O	Me
<b>97</b>	OH	S	Me
<b>98</b>	OH	S	<sup>n</sup> Pr
<b>99</b>	OH	O	<sup>i</sup> Pr
<b>100</b>	OH	S	<sup>i</sup> Pr
<b>101</b>	OH	O	<sup>n</sup> Bu
<b>102</b>	OH	S	<sup>n</sup> Bu
<b>103</b>	OH	O	Bn
<b>104</b>	OH	S	Bn
<b>105</b>	OH	O	4-NH <sub>2</sub> Ph
<b>106</b>	OH	S	4-NH <sub>2</sub> Ph
<b>107</b>	OH	S	2-NO <sub>2</sub> Ph
<b>108</b>	OH	O	4-NO <sub>2</sub> Ph
<b>109</b>	OH	S	4-NO <sub>2</sub> Ph
<b>110</b>	H	O	H
Neutral			
<b>111</b>	OH	O	2-NO <sub>2</sub> Ph
Anti-Inducers			
<b>112</b>	OH	O	Ph
<b>113</b>	OH	S	Ph
<b>114</b>	H	O	2-NO <sub>2</sub> Ph
<b>115</b>	H	S	2-NO <sub>2</sub> Ph

These ligands have been classified as either inducers or anti-inducers, according to whether they destabilise or stabilise or the repressor-operator (LacI-*lacO*) complex, respectively. One neutral ligand, which binds to the repressor without affecting the stability of the LacI-*lacO* complex was also identified.<sup>249,252–254</sup>

Of the ligands classified as inducers, those that do not contain an aromatic moiety (**96–102** and **110**) were not appropriate for our purposes and could be immediately disregarded. It was also decided that ligands containing either an amino-aromatic (**105**, **106**) or a nitro-aromatic (**107–109**) anomeric group would be avoided due to their similarity to the nitrobenzyl hypoxia-activated protecting group. Therefore, compounds **103** and **104**, which each contain an anomeric benzyl group were identified as potential inducers and targeted for synthesis and analysis of their ability to induce expression of GFP at a range of concentrations in comparison to IPTG **76**.

### 3.2.2. Synthesis of **103** and **104**

Compound **103** was synthesised in three steps from  $\beta$ -D-galactose pentaacetate **116**, according to Scheme 3.2.



**Scheme 3.2:** Synthesis of **103**. *Reagents and conditions:* i) HBr (33 wt.% in AcOH), 0 °C–RT, 2.5–16 h, 55–96%; ii) BnOH, Ag<sub>2</sub>CO<sub>3</sub>, 4 Å MS, dark, CH<sub>2</sub>Cl<sub>2</sub>, RT, 24 h; iii) NaOMe, MeOH, RT, 1–24 h, 64–84% (2 steps).

Bromination at the anomeric position with HBr afforded **117** as the  $\alpha$ -anomer, as determined from the coupling constants of the 1-position proton. Initially, the reaction was carried out overnight and a 55% yield was obtained due to formation of the dibrominated by-product **119** (Figure 3.8). Reducing the reaction time to 2.5 hours avoided formation of this unwanted by-product and increased the yield to 96%.

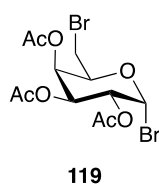
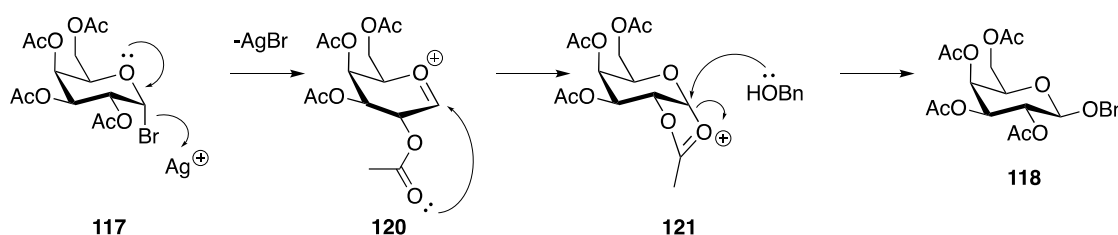


**Figure 3.8:** Structure of the dibrominated by-product that formed when **116** was reacted with HBr in AcOH overnight.

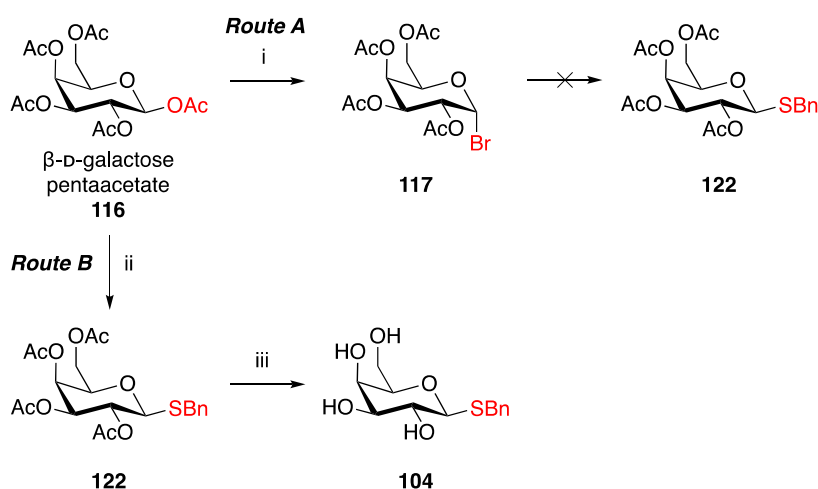
Subsequent Koenigs-Knorr glycosylation<sup>255</sup> with silver carbonate and benzyl alcohol in dichloromethane yielded the  $\beta$ -anomer **118** preferentially, due to neighbouring group participation of the 2-*O*-acetyl protecting group. Following elimination of silver bromide, the cyclic oxonium ion **121** forms, shielding the  $\alpha$ -face of the molecule. Benzyl alcohol then reacts from the *trans*-face, in this case resulting in selective formation of the  $\beta$ -anomer **118** (Scheme 3.3).<sup>256–258</sup>

No further purification beyond filtration of the reaction mixture through Celite® to remove molecular sieves and precipitated silver bromide was required. The crude product was deprotected using standard Zemplén deacetylation conditions, of sodium methoxide in methanol, to afford **103**.<sup>259</sup> With four equivalents of benzyl alcohol, consistent yields of 64–74% were obtained over the two steps on scales ranging from 1–4 g. Increasing the number of equivalents of benzyl alcohol to eight in the glycosylation step improved the overall yield of **103** to 84%.



**Scheme 3.3:** Mechanism of the Koenigs-Knorr glycosylation reaction, showing neighbouring group participation of the 2-*O*-acetyl protecting group to afford only the  $\beta$ -anomer **118**.

For the synthesis of **104**, initially a similar route to that employed for the synthesis of **103** was attempted (Scheme 3.4, Route A). However, during glycosylation of **117** with benzyl mercaptan, addition of the thiol to silver carbonate resulted in formation of an unreactive black precipitate. Thioglycosides are commonly prepared directly from per-*O*-acetylated sugars through Lewis acid-promoted glycosylation with the appropriate thiol.<sup>260</sup> Applying these conditions, using  $\text{BF}_3 \cdot \text{Et}_2\text{O}$  as the Lewis acid, afforded **122** as the  $\beta$ -anomer, as determined from the coupling constants of the 1-position proton, directly from  $\beta$ -D-galactose pentaacetate **116**. Finally, deprotection of the acetyl groups *via* Zemplén deacetylation<sup>259</sup> yielded **104** (Scheme 3.4, Route B).



**Scheme 3.4:** Synthesis of **104**. *Reagents and conditions:* i) HBr (33 wt.% in AcOH), 0 °C–RT, 2.5–16 h, 55–96%; ii) BnSH, BF<sub>3</sub>·Et<sub>2</sub>O, 4 Å MS, CH<sub>2</sub>Cl<sub>2</sub>, –78 °C–RT, 6 h, 62% iii) NaOMe, MeOH, RT, 18 h, 93%.

### 3.2.3. Analysis of Gene Expression

Following synthesis of **103** and **104**, the next step was to compare the ability of each compound to induce gene expression with that of IPTG **76**. For consistency, the same reporter gene was chosen for this experiment as was used for subsequent gene expression experiments under hypoxic conditions (See Chapter 4). Therefore, the superfolder green fluorescent protein (sfGFP), which is a fast-folding version of GFP,<sup>261</sup> was inserted downstream of an IPTG-inducible promoter in the pNIC28-Bsa4 expression vector<sup>262</sup> and the resulting plasmid was transformed into *BL21 (DE3) E. coli*. Transformed bacteria were incubated with **103** or **104** at concentrations ranging from 1 mM to 15 mM for 24 hours. DMSO and IPTG **76** (1 mM) were included as controls (Figure 3.9).

A gradual increase in fluorescence was observed with increasing concentrations of **104** (Figure 3.9A/B). However, even at 15 mM **104**, the amount of fluorescence detected was very low, indicating only low levels of sfGFP expression (Figure 3.9A/B). On the other hand, visible fluorescence was observed at all concentrations of **103** tested (Figure 3.9A), although there was no significant change as the concentration of **103** was increased (Figure 3.9B). These data suggest that the maximum level of gene expression induced with **103** is one third of the amount that is induced with 1 mM IPTG **76** (Figure 3.9B).



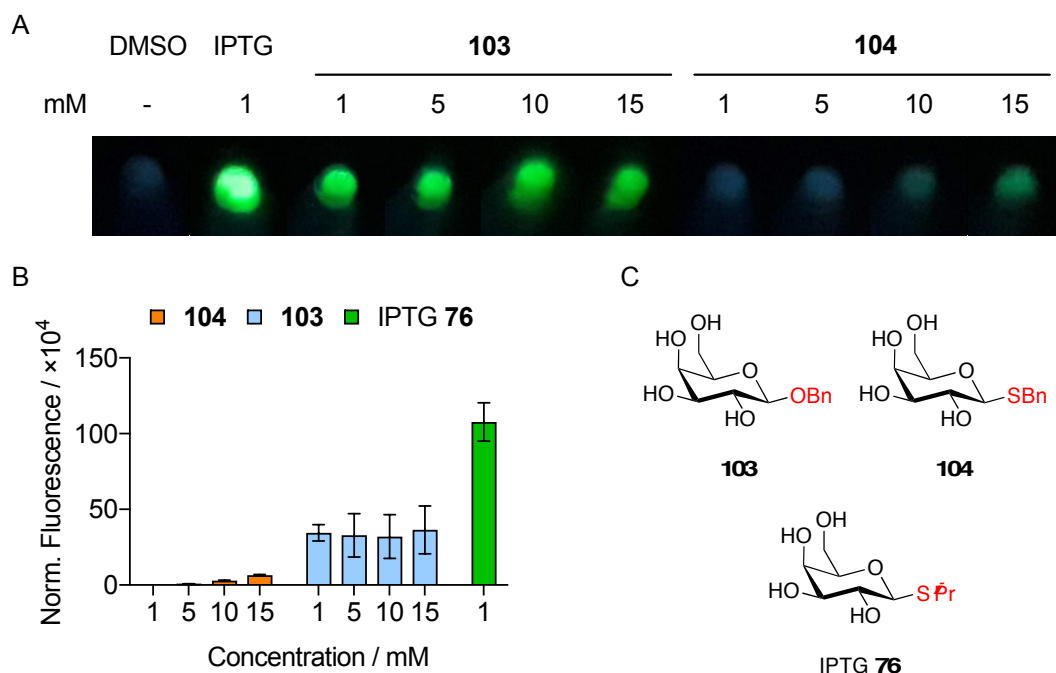


**Figure 3.9:** Analysis of the induction ability of **103** and **104** at concentrations ranging from 1–15 mM in comparison with **76**. A) *BL21 (DE3) pNIC28-sfGFP* were treated with DMSO, IPTG **76** (1 mM), **103** (1, 5, 10, 15 mM), and **104** (1, 5, 10, 15 mM) for 24 h. Bacterial samples were pelleted and imaged under a UV lamp ( $\lambda_{\text{ex}} = 365$  nm). Visible fluorescence was observed for all concentrations of **76** and **103**, but only for the highest concentrations of **104**. B) Conditions as in (A). Samples were analysed by fluorescence ( $\lambda_{\text{ex}} = 485$  nm,  $\lambda_{\text{em}} = 520$  nm, PBS). Fluorescence was divided by the optical density at 600 nm. C) Structures of **103** and **104** and IPTG **76**.

Therefore, compound **103** was selected as a suitable alternative core to IPTG **76** for HPLC analysis of the products from the chemical and biochemical reduction assays; for cellular experiments, it was decided to continue to use the more potent and metabolically stable inducer, IPTG **76**. Accordingly, the corresponding benzyl analogues, protected with a 4-nitrobenzyl group at the 2- (**123**), 3- (**124**), 4- (**125**), and 6- (**126**) positions, and the 4,6-acetal compound **127**, were also targeted for synthesis (Figure 3.10).

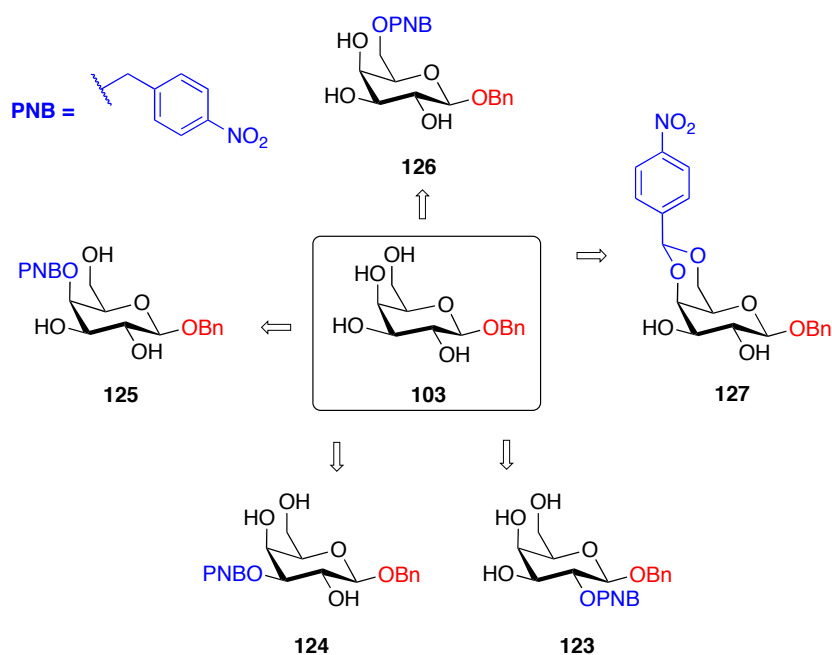


**Figure 3.10:** Structures of hypoxia-activated derivatives **123–127** for HPLC analysis of chemical and biochemical reduction assays. Each compound contains a UV-active benzyl moiety at the anomeric position to facilitate HPLC detection of released compounds. Blue = bioreductive moiety.

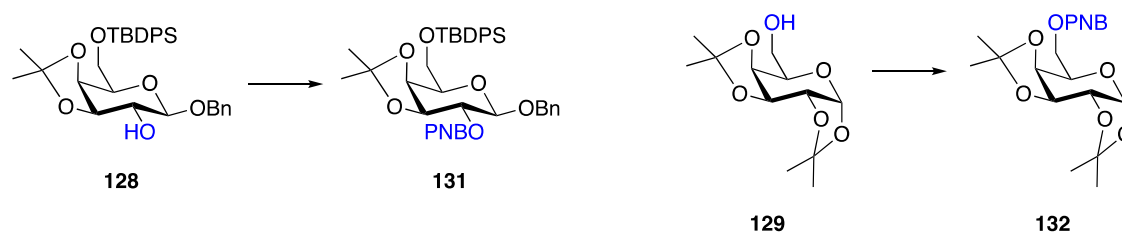
### 3.3. Synthetic Strategy

The synthesis of the potential hypoxia-activated inducers of gene expression identified in Section 3.1.2 can be broken down into three discrete stages: protection of the free sugar to afford key intermediates featuring one free hydroxyl group; coupling of this hydroxyl to a 4-nitrobenzyl hypoxia-activated group; and deprotection to yield the hypoxia-activated protected inducer. The alkylation reaction to attach a 4-nitrobenzyl group was found to be particularly problematic and will be discussed first. The remaining two stages for protection and deprotection of each galactoside will then be discussed in the context of which position was alkylated with the 4-nitrobenzyl bioreductive group. During optimisation of the protecting group strategies for synthesis of hypoxia-activated inducers of gene expression, compounds with either an anomeric benzyl (analogues of **103**) or thioisopropyl group (analogues of IPTG **76**) were used.

### 3.4. Optimisation of 4-Nitrobenzyl Alkylation

The first problem to be addressed was the alkylation of a sugar hydroxyl with a hypoxia-activated 4-nitrobenzyl group, which is critical to the whole project. Alkylation reactions were performed on intermediate **128**, the synthesis of which is described in detail in Section 3.5, or on commercially available 1,2:3,4-di-*O*-isopropylidene- $\alpha$ -D-galactopyranoside **129**. Both of these model compounds contain acetonide protecting groups, although **129** has an unprotected primary hydroxyl compared to the free secondary hydroxyl found in **128**.

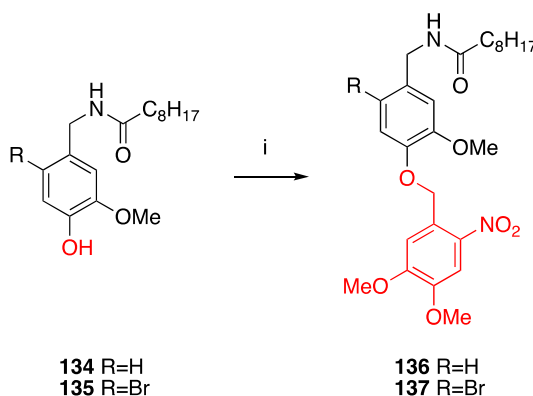
Typically, benzyl ethers can be readily formed *via* the Williamson ether synthesis, using a strong base in polar, aprotic solvents.<sup>263–265</sup> Initial deprotonation of the alcohol affords the alkoxide, which reacts with benzyl bromide **130** to yield the corresponding benzyl ether. When alkylation of both **128** and **129** was attempted using sodium hydride as the base, DMF as the solvent and replacing benzyl bromide **130** with either 4-nitrobenzyl bromide **80** or 4-nitrobenzyl iodide **133**, no reaction was observed (Table 3.2, Entries 1–4). In each case, the reaction was characterised by a plethora of by-products, as observed by TLC and these were also present when 4-nitrobenzyl bromide **80** was added to a solution of sodium hydride in DMF in the absence of substrate. This observation suggests that inherent instability of the reagent under the reaction conditions was the primary cause for the lack of reactivity.<sup>266</sup>

**Table 3.2:** Summary of conditions that were investigated during optimisation of the 4-nitrobenzyl alkylation reaction.

Entry	Substrate	Reagent	Eq.	Solvent	Temp. °C	Yield %
1	<b>128</b>	4-NO <sub>2</sub> BnBr <b>80</b> NaH	1.5 1.5	DMF	0–40	0
2	<b>128</b>	4-NO <sub>2</sub> BnI <b>133</b> NaH	2.0 1.8	DMF	0–RT	0
3	<b>129</b>	4-NO <sub>2</sub> BnBr <b>80</b> NaH	1.3 1.3	DMF	0–RT	0
4	<b>129</b>	4-NO <sub>2</sub> BnI <b>133</b> NaH	1.8 1.5	DMF	0–RT	0
5	<b>129</b>	4-NO <sub>2</sub> BnBr <b>80</b> <sup>t</sup> BuOK	1.1 1.1	THF	RT	0 <sup>b</sup>
6 <sup>d,e</sup>	<b>129</b>	4-NO <sub>2</sub> BnBr <b>80</b> Ag <sub>2</sub> O	1.1 1.1	CH <sub>2</sub> Cl <sub>2</sub>	RT	0
7 <sup>d,e</sup>	<b>129</b>	4-NO <sub>2</sub> BnBr <b>80</b> Ag <sub>2</sub> O	2.0 2.0	DMF	60	0
8 <sup>d,e</sup>	<b>129</b>	4-NO <sub>2</sub> BnBr <b>80</b> Ag <sub>2</sub> O	1.1 1.1	Cyclohexane	RT–40– 60	55 <sup>a</sup>
9 <sup>d,e</sup>	<b>129</b>	4-NO <sub>2</sub> BnBr <b>80</b> Ag <sub>2</sub> O	2.0 2.0	Cyclohexane	Reflux	0
10 <sup>d,e</sup>	<b>129</b>	4-NO <sub>2</sub> BnBr <b>80</b> Et <sub>3</sub> N Ag <sub>2</sub> O	1.1 1.1 1.1	CHCl <sub>3</sub>	Reflux	0
11 <sup>d,f</sup>	<b>129</b>	1) AgOTf 4-NO <sub>2</sub> BnBr <b>80</b> 2) 2,4,6-collidine	1.1 1.1 1.3	CH <sub>2</sub> Cl <sub>2</sub>	1) –78 2) RT	0
12	<b>128</b>	4-NO <sub>2</sub> BnBr <b>80</b> 1 M NaOH (aq.) <sup>n</sup> Bu <sub>4</sub> NHSO <sub>4</sub>	1.5 1.5 1.5	CH <sub>2</sub> Cl <sub>2</sub>	Reflux	72 <sup>a</sup>

Entry	Substrate	Reagent	Eq.	Solvent	Temp. °C	Yield %
13	<b>129</b>	4-NO <sub>2</sub> BnBr <b>80</b> 1 M NaOH (aq.) <sup>t</sup> Bu <sub>4</sub> NHSO <sub>4</sub>	1.2 2.0 1.2	CH <sub>2</sub> Cl <sub>2</sub>	Reflux	0 <sup>c</sup>
14	<b>129</b>	<b>151</b> TfOH	2 0.3	CH <sub>2</sub> Cl <sub>2</sub> :Cyclohexane (1:2)	RT	0 <sup>g</sup>
15 <sup>d,e</sup>	<b>129</b>	4-NO <sub>2</sub> BnBr <b>80</b> Freshly prepared Ag <sub>2</sub> O	1.5 1.5	Cyclohexane	Reflux	99 <sup>h</sup>
16 <sup>d,e</sup>	<b>128</b>	4-NO <sub>2</sub> BnBr <b>80</b> Freshly prepared Ag <sub>2</sub> O	1.5 1.5	Cyclohexane	Reflux	91 <sup>i</sup>

<sup>a</sup>Incomplete conversion, multiple impurities unable to be removed from product; <sup>b</sup>product underwent rapid breakdown under the reaction conditions; <sup>c</sup>negligible mass recovery; <sup>d</sup>reactions performed in the dark; <sup>e</sup>added 4 Å molecular sieves (powder); <sup>f</sup>*in situ* generation of 4-NO<sub>2</sub>BnOTf, followed by addition of **129** and 2,4,6-collidine; <sup>g</sup>product was identified as **152**; <sup>h</sup>NMR conversion; <sup>i</sup>isolated yield. PNB = 4-nitrobenzyl.

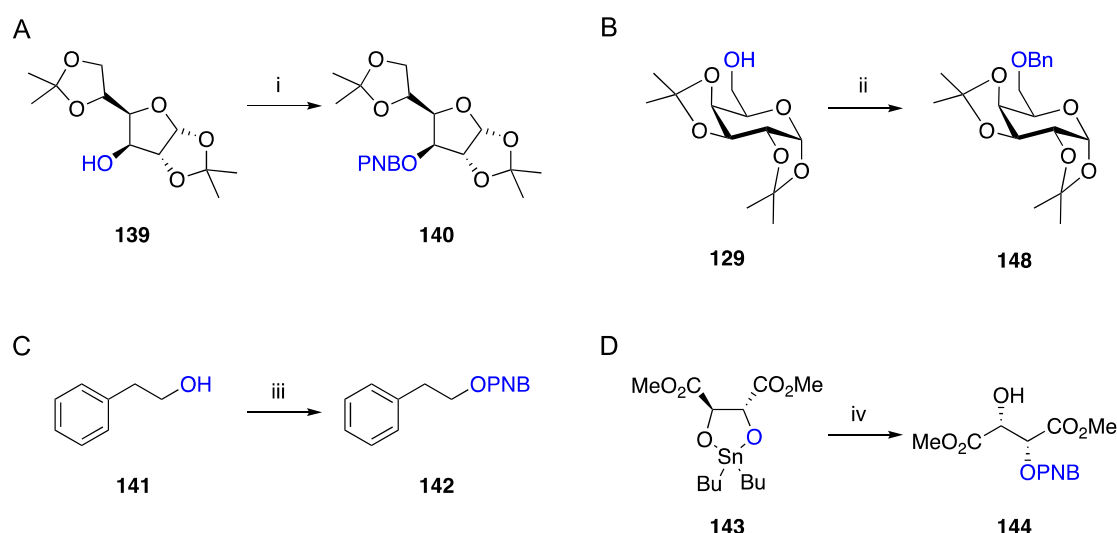


**Scheme 3.5:** Reaction scheme showing previous work in the group to attach the DMNB caging group.<sup>267</sup> *Reagents and conditions:* i) <sup>t</sup>BuOK, 4,5-dimethoxy-2-nitrobenzyl bromide, THF, RT, **136**: 57%; **137**: 55%.<sup>267</sup>

Previous work in the group has used potassium *tert*-butoxide as the base in THF to attach a similar nitro-containing moiety, 4,5-dimethoxy-2-nitrobenzyl (DMNB), to substituted phenols **134** and **135**, yielding **136** and **137** (Scheme 3.5).<sup>267</sup> However, applying these conditions to 4-nitrobenzyl alkylation resulted in initial formation of the desired ether product, followed by its rapid degradation under the reaction conditions (Table 3.2, Entry 5). When both 4-nitrobenzyl bromide

**80** and 4,5-dimethoxy-2-nitrobenzyl bromide were treated with potassium tert-butoxide in THF, 4,5-dimethoxy-2-nitrobenzyl bromide was found to be stable to the reaction conditions, whereas 4-nitrobenzyl bromide **80** broke down rapidly, as determined by TLC. This difference in stability likely accounts in part for the difference in success between these two reactions.

It has been reported that traditional Williamson ether synthesis conditions, such as those trialled here, are unsuitable for introduction of 4-nitrobenzyl groups; both 4-nitrobenzyl bromide **80** and the resulting ethers have been shown to undergo rapid decomposition in the presence of strong bases in polar solvents.<sup>268</sup> However, a variety of other methods have been used for the synthesis of 4-nitrobenzyl ethers in moderate to excellent yields. These include reaction of alcohols with 4-nitrobenzyl bromide **80** and silver oxide in non-polar solvents (Scheme 3.6A),<sup>269</sup> the use of silver triflate to generate 4-nitrobenzyl triflate **138** *in situ* (Scheme 3.6B, Scheme 3.6C),<sup>269,270</sup> and monoalkylation of diols *via* stannylene acetal formation in the presence of caesium fluoride (Scheme 3.6D).<sup>271</sup>

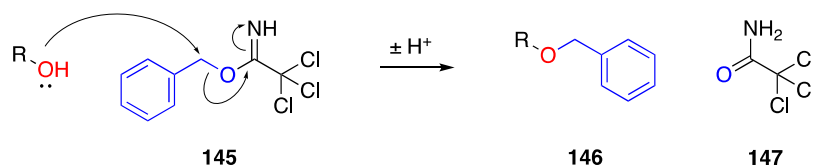


**Scheme 3.6:** Summary of reaction conditions from the literature that have been shown to be successful for formation of 4-nitrobenzyl ethers. Conditions described in (B) for alkylation with benzyl bromide **130** were adapted in (C) for alkylation with 4-nitrobenzyl bromide **80**. *Reagents and conditions:* i) 4-NO<sub>2</sub>BnBr **80**, Ag<sub>2</sub>O, 3 Å MS, benzene, RT, 48 h, 91%;<sup>272</sup> ii) BnOH, AgOTf, 2,6-di-*tert*-butylpyridine, CH<sub>2</sub>Cl<sub>2</sub>, -70 °C, 30 min, 93%;<sup>270</sup> iii) 4-NO<sub>2</sub>BnBr **80**, AgOTf, -70 °C, then **141**, 2,4,6-collidine, CH<sub>2</sub>Cl<sub>2</sub>, 91%;<sup>269</sup> iv) 4-NO<sub>2</sub>BnBr **80**, CsF, 93%.<sup>271</sup> PNB = 4-nitrobenzyl.

It was presumed that the absence of a neighbouring free hydroxyl group in either **128** or **129** would preclude formation of the stannylene acetal;<sup>271</sup> therefore, the silver conditions were investigated first. Based on the original literature,<sup>269,272</sup> initial reactions were performed at room temperature in dichloromethane but there was little evidence of any reaction occurring (Table 3.2, Entry 6). Promisingly, under these conditions, there was no indication of decomposition of 4-nitrobenzyl bromide **80**. On the other hand,<sup>268</sup> when the reaction was attempted in DMF under these mild silver oxide conditions, rapid degradation of 4-nitrobenzyl bromide **80** was observed by TLC. Changing the solvent to cyclohexane resulted in slow formation of a new product, as observed by TLC, although the reaction mixture still predominantly consisted of starting material **129**. In an attempt to drive the reaction further towards completion, the temperature was gradually increased first to 40 °C and then to 60 °C. Although compound **132** was identified as the main product, it could only be isolated along with an unknown impurity (Table 3.2, Entry 8). Encouraged by these results, the reaction was repeated in cyclohexane with heating under reflux from the start but in this instance, no reaction was observed at all (Table 3.2, Entry 9). An alternative reaction with 4-nitrobenzyl iodide **133**, silver oxide and triethylamine in chloroform (Table 3.2, Entry 10) was also attempted. Unfortunately, despite apparent formation of silver iodide, which precipitated from the reaction mixture, product **132** was not formed. Application of the method developed by Berry and Hall<sup>270</sup> and adapted by Fukase et al.,<sup>269</sup> which involves *in situ* generation of 4-nitrobenzyl triflate **138**, was also unsuccessful (Table 3.2, Entry 11).

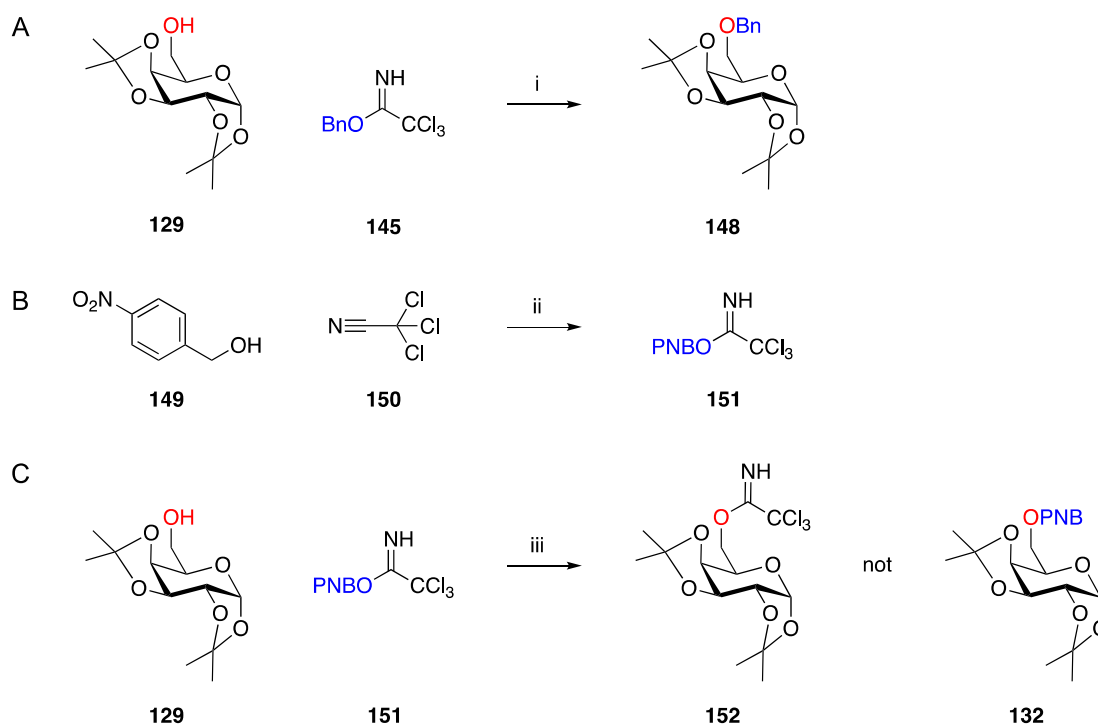
Some success was had with aqueous 1 M NaOH in dichloromethane for the alkylation of **128** (Table 3.2, Entry 12). This method was based on phase transfer catalysis, which was originally employed in the monobenylation of diols.<sup>273</sup> However, the reaction did not go to completion and coelution of impurities during purification meant that this approach was not pursued further. Additionally, when this reaction was repeated with **129** as the substrate, no reaction was observed (Table 3.2, Entry 13).

At this point, due to the low success and poor reproducibility of conditions trialled thus far, alternative methods were investigated. Benzyl-2,2,2-trichloroacetimidate **145** has previously been used for the formation of benzyl ethers **146** under acidic conditions (Scheme 3.7).<sup>274,275</sup>



**Scheme 3.7:** Mechanism for the formation of benzyl ethers **146** using benzyl-2,2,2-trichloroacetimidate **145** under acidic conditions.

Given the high sensitivity of 4-nitrobenzyl ethers to base, these acidic conditions were a promising approach. A test reaction of **129** with **145** afforded **148** in 51% yield and confirmed the stability of the isopropylidene groups under these reaction conditions (Scheme 3.8A).

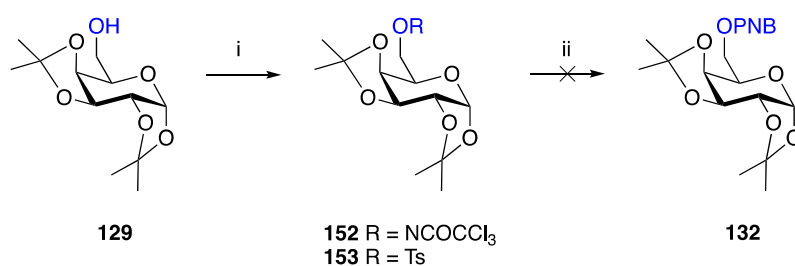


**Scheme 3.8:** A) Benzylation of **129** with benzyl-2,2,2-trichloroacetimidate **145**. B) Synthesis of **151**. C) Reaction of **129** with 4-nitrobenzyl-2,2,2-trichloroacetimidate **151** afforded **152** and not the expected product **132**. *Reagents and conditions:* i) **145**, TfOH, CH<sub>2</sub>Cl<sub>2</sub>:cyclohexane (1:2), RT, 1 h, 51%; ii) 4-NO<sub>2</sub>BnOH, CCl<sub>3</sub>CN, DBU, CH<sub>2</sub>Cl<sub>2</sub>, RT, 15 min, 95%; iii) **151**, TfOH, CH<sub>2</sub>Cl<sub>2</sub>:cyclohexane (1:2), RT, 48 h. PNB = 4-nitrobenzyl.



Encouraged by this result, 4-nitrobenzyl-2,2,2-trichloroacetimidate **151** was synthesised from 4-nitrobenzyl alcohol **149** and trichloroacetonitrile **150** (Scheme 3.8B). However, reaction of **129** with **151** under the same acidic conditions afforded **152** as the major product and not the desired 4-nitrobenzyl ether **132** (Scheme 3.8C), indicating that the use of **151** is unsuitable for the formation of 4-nitrobenzyl ethers.

Following the lack of success in alkylating the sugar hydroxyl group directly, it was hypothesised that converting the hydroxyl group into a good leaving group followed by displacement with 4-nitrobenzyl alcohol would afford the 4-nitrobenzyl ether (Scheme 3.9). Although **129** could be readily converted into both the trichloroacetimidate **152** and tosylate **153**, the subsequent displacement reactions were unsuccessful (Table 3.3).



**Scheme 3.9:** Proposed alternative route towards PNB-protected glycosides. The primary C6-OH group was converted into a good leaving group; however, displacement with 4-nitrobenzyl alcohol **149** to afford the 4-nitrobenzyl ether **132** was unsuccessful. *Reagents and conditions:* i) **152**: NCCCl<sub>3</sub> **150**, DBU, CH<sub>2</sub>Cl<sub>2</sub>, RT, 30 min, 89%; **153**: 4-TsCl, pyridine, 0 °C–RT, 21 h, 99%; ii) See Table 3.3.

**Table 3.3:** Summary of reaction conditions that were tested for the displacement of a good leaving group with 4-nitrobenzyl alcohol **149**.

Entry	Substrate	Reagent	Eq.	Solvent	Temp. °C	Yield %
1	<b>153</b>	4-NO <sub>2</sub> BnOH <b>149</b> Et <sub>3</sub> N	2.0 2.0	CH <sub>2</sub> Cl <sub>2</sub>	40	0 <sup>a</sup>
2	<b>153</b>	4-NO <sub>2</sub> BnOH <b>149</b> Et <sub>3</sub> N	2.0 2.0	DMF	60	0 <sup>a</sup>
3	<b>152</b>	4-NO <sub>2</sub> BnOH <b>149</b> TfOH	2.0 0.3	CH <sub>2</sub> Cl <sub>2</sub> :cyclohexane (1:2)	Reflux	0 <sup>b</sup>

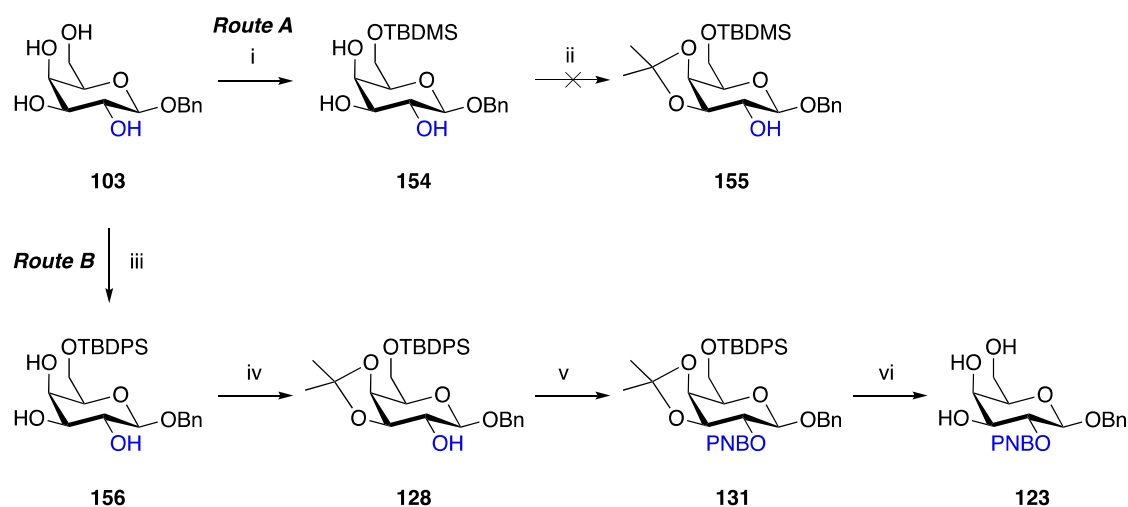
<sup>a</sup>no reaction; <sup>b</sup>product isolated in a 1:0.8 ratio with an unknown impurity, as determined by <sup>1</sup>H NMR.

Further investigation into the silver oxide-mediated reaction conditions discussed above suggested that it may be necessary to prepare silver oxide fresh prior to use.<sup>276</sup> This was accomplished by dropwise addition of excess aqueous 1 M NaOH to an aqueous solution of silver nitrate and filtration of the resulting brown precipitate. Remarkably when freshly prepared silver oxide was used, complete conversion of **129** to **132** was observed for the first time (Table 3.2, Entry 15). Furthermore, this reaction was also highly effective for the conversion of **128** to **131** (Table 3.2, Entry 16). Consequently, these optimised silver oxide conditions were selected as the most appropriate for alkylation of free sugar hydroxyl and applied to the synthesis of each hypoxia-activated protected-inducer.

### 3.5. Synthesis of 2-Position Protected Inducers

The synthesis of 2-position protected inducers was based on a previously reported synthesis for the selective protection of galactose derivatives (Scheme 3.10, Route A).<sup>277</sup> Initial protection of the primary hydroxyl group of **103** with TBDMSCl afforded **154**. During formation of an isopropylidene group between the *cis* C3-OH and C4-OH groups to form **155**, the acidic conditions employed resulted in concomitant deprotection of the TBDMS group. Therefore, the primary hydroxyl was instead protected with the more stable TBDPS group,<sup>278,279</sup> forming **156**.

Subsequent isopropylidene formation yielded **128** in 99% yield. Applying the silver oxide conditions described above for 4-nitrobenzyl alkylation at the free 2-position afforded **131**.



**Scheme 3.10:** Synthesis of **123**. *Reagents and conditions:* i) TBDMSCl, pyridine, RT, 3 h, 36%; ii)  $C(CH_3)_2(OCH_3)_2$ , 4-TsOH·H<sub>2</sub>O, acetone, 40 °C; iii) TBDPSCl, imidazole, DMF, RT, 4–5 h, 53–81%; iv)  $C(CH_3)_2(OCH_3)_2$ , 4-TsOH·H<sub>2</sub>O, acetone, 40 °C, 2 h, 93–99%; v) 4-NO<sub>2</sub>BnBr **80**, Ag<sub>2</sub>O, 4 Å MS, dark, cyclohexane, reflux, 16 h, 91%; vi) AcCl, MeOH, RT, 33 h, 59%. PNB = 4-nitrobenzyl.

A small scale test reaction, in which **131** was treated with 1 M tetrabutylammonium fluoride (TBAF) in THF afforded only **157**, resulting from loss of both the silyl and 4-nitrobenzyl groups (Figure 3.11). Although TBAF in THF is commonly used to deprotect silyl groups,<sup>264,280,281</sup> it is likely that the basicity of the fluoride ion, especially under anhydrous conditions, resulted in deprotection of the base-sensitive 4-nitrobenzyl ether in **131**.<sup>282</sup>

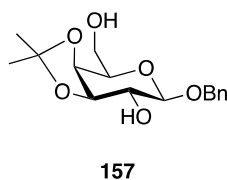
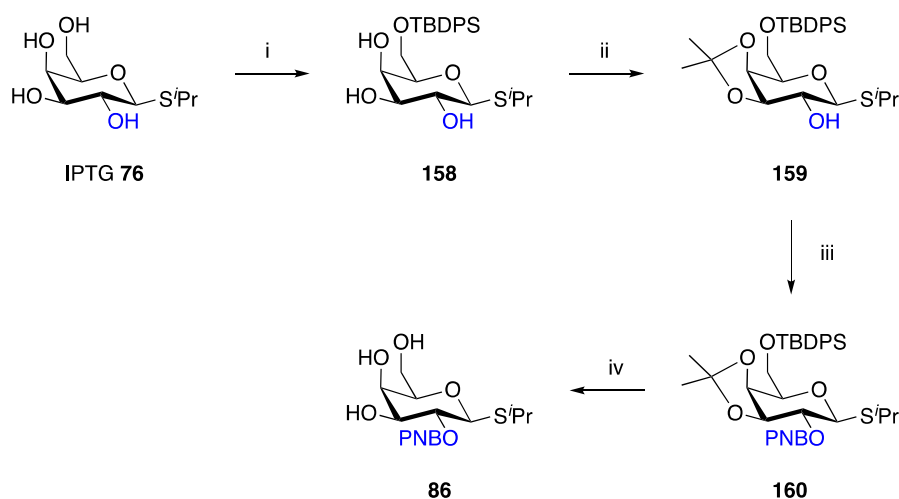


**Figure 3.11:** Structure of the compound formed when **131** was treated with TBAF in THF, resulting from deprotection of the silyl and 4-nitrobenzyl groups.

Consequently, an alternative deprotection method that uses a substoichiometric amount of acetyl chloride in anhydrous methanol, generating HCl *in situ*, was employed.<sup>283</sup> Compound **131** was treated with 0.15 equivalents of acetyl chloride in methanol, resulting in slow formation of fully

deprotected **123**. Increasing the number of equivalents of acetyl chloride to 0.6 equivalents accelerated the reaction, affording **123** in 59% yield.

Having developed a synthetic route to 2-position protected inducers, this strategy was next applied to the synthesis of **86** from IPTG **76**. TBDPS protection of the primary C6-OH group (**158**) and subsequent acetonide formation afforded **159**, which was alkylated with the optimised silver oxide conditions to yield **160**. The acetyl chloride/methanol deprotection conditions have been reported to be compatible with an anomeric thiol group and could therefore be applied to this synthesis.<sup>283</sup> Accordingly, the final deprotection step with acetyl chloride in methanol, with the addition of dichloromethane as a co-solvent to improve the solubility of the starting material, afforded **86** in 85% yield (Scheme 3.11).



**Scheme 3.11:** Synthesis of **86**. *Reagents and conditions:* i) TBDPSCl, imidazole, DMF, RT, 7 h, 59%; ii)  $C(CH_3)_2(OCH_3)_2$ , 4-TsOH·H<sub>2</sub>O, acetone, RT, 1–2 h, 93–99%; iii) 4-NO<sub>2</sub>BnBr **80**, Ag<sub>2</sub>O, 4 Å MS, dark, cyclohexane, reflux, 17.5 h, 87%; iv) AcCl, CH<sub>2</sub>Cl<sub>2</sub>:MeOH (2:1), RT, 15 h, 85%. PNB = 4-nitrobenzyl.

### 3.6. Synthesis of 3-Position Protected Inducers

#### 3.6.1. Routes 1 and 2 via Ester Protecting Groups

The first route for the synthesis of 3-position protected inducers was based on previous work in which 2-methylphenylthioglycosides were used as glycosyl building blocks and a range of glycosyl acceptors were synthesised.<sup>284</sup> These acceptors included **161**, which consists of a benzoyl protected galactopyranoside with a free hydroxyl group at the 3-position. It was hypothesised that

the analogous compounds **162** and **163**, with an anomeric benzyl or thioisopropyl group, respectively, would be appropriate intermediates for alkylation at the 3-position with the 4-nitrobenzyl bioreductive group (Figure 3.12).

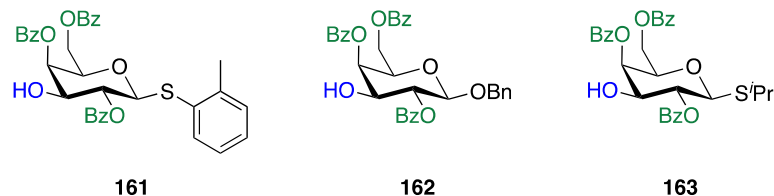
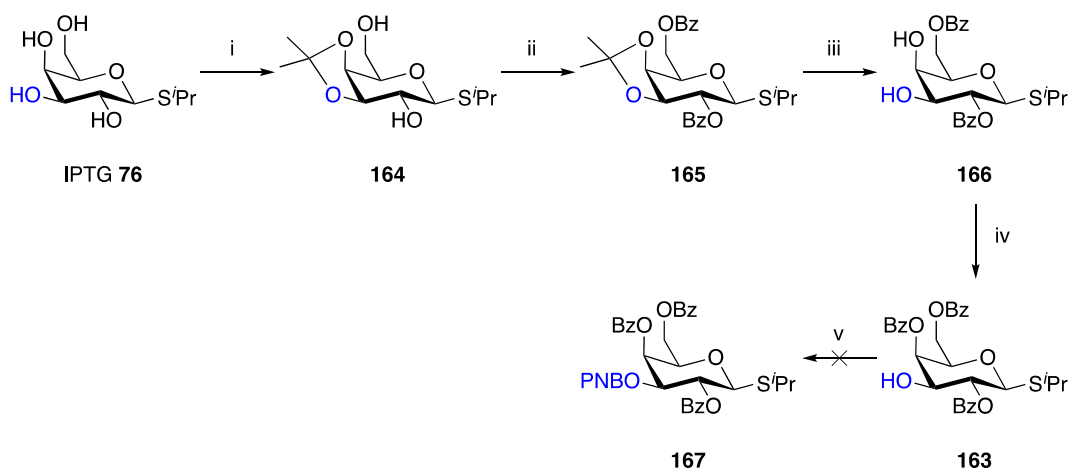


**Figure 3.12:** Structures of the previously reported 2-methylphenyl 1-thio-β-D-galactopyranoside **161**<sup>284</sup> with a free C3-OH group and the analogous precursors containing an anomeric benzyl **162** or thioisopropyl **163** group.

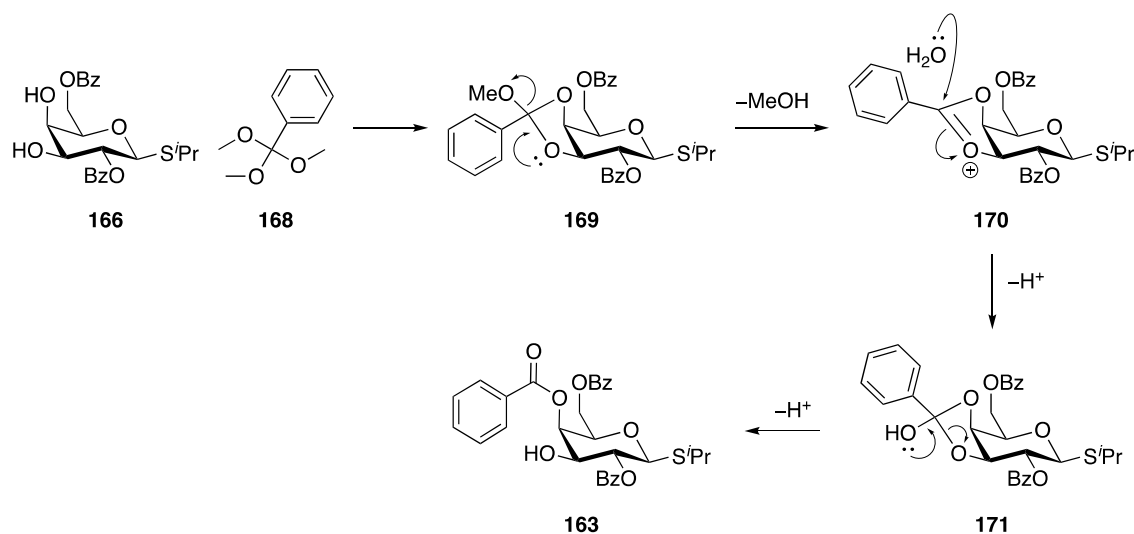
Compound **163** was synthesised in four steps from IPTG **76** (Scheme 3.12). Selective acetonide formation at the *cis* C3-OH and C4-OH groups of the free sugar afforded **164**. Benzoylation of the C2-OH and C6-OH groups to obtain **165** and subsequent deprotection of the isopropylidene protecting group yielded **166**.



**Scheme 3.12:** Route 1 towards the synthesis of 3-position protected inducers. *Reagents and conditions:* i) 2,2-Dimethoxypropane, 4-TsOH·H<sub>2</sub>O, acetone, RT, 2.5 days; then MeOH: H<sub>2</sub>O (10:1), reflux, 24 h, 49%; ii) Benzoyl chloride, 4-DMAP, pyridine, 0 °C, 0.5–1 h then RT, 2–4 h, 84–98%; iii) Dowex<sup>®</sup> 50WX8, MeOH, RT, 27 h, then 1 M HCl (aq.), RT, 15 h, 88%; iv) PhC(OMe)<sub>3</sub>, (±)-CSA, CH<sub>2</sub>Cl<sub>2</sub>, RT, 30 min; then AcOH (90% aq.), RT, 2 h, 79%; v) 4-NO<sub>2</sub>BnBr **80**, Ag<sub>2</sub>O, 4 Å MS, dark, cyclohexane, reflux. PNB = 4-nitrobenzyl.

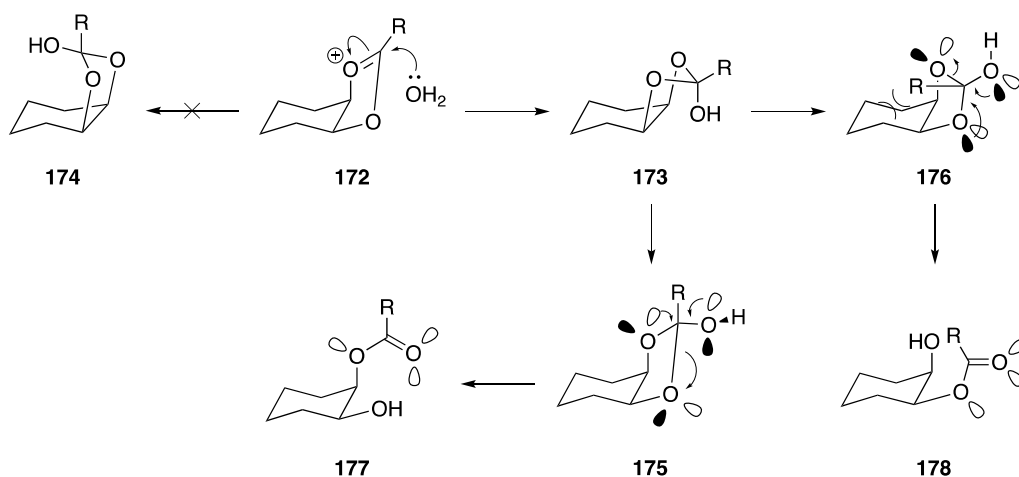
To selectively protect the axial C4-OH group with a benzoyl moiety, **166** was treated with trimethyl orthobenzoate **168** to form the 3,4-(methylorthobenzyloxy) intermediate **169** *in situ*.

Subsequent acid-catalysed hydrolysis of this intermediate *via* the dioxolenium cation **170** and tetrahedral intermediate **171** afforded **163** (Scheme 3.13).



**Scheme 3.13:** Reaction mechanism for formation of the axial 4-*O*-benzoyl ester, following hydrolysis of the orthoester **169**.<sup>285–288</sup>

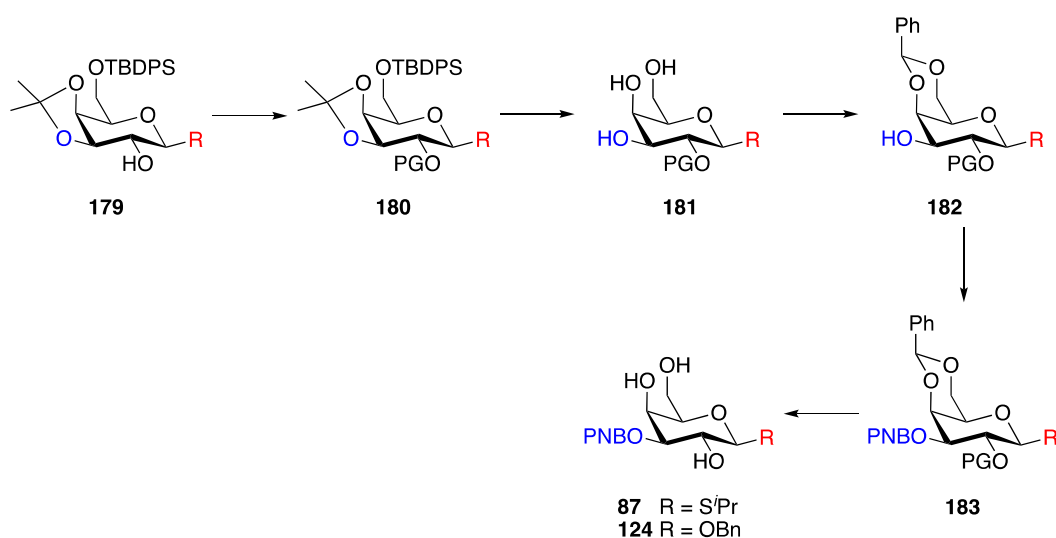
The hydrolysis of dioxolenium ions fused to 6-membered rings with one oxygen axial and the other oxygen equatorial is known to form the “axial ester-equatorial alcohol” preferentially.<sup>285–288</sup> From the dioxolenium ion **172**, nucleophilic attack of the water molecule can occur on either face. However, due to steric hindrance from the ring, formation of hemi-orthoester **173** is favoured over **174**. Hemi-orthoester **173** can take the conformation of either **175** or **176**, which break down to form either the axial (**177**) or equatorial (**178**) esters, respectively. Due to steric clashes, the formation of **176** is disfavoured when R is not a proton, and the axial ester **177** is formed preferentially (Scheme 3.14).<sup>287</sup>



**Scheme 3.14:** Mechanistic explanation for the preferential formation of the axial ester from a dioxolenium ion. Scheme adapted from *Stereoelectronic Effects in Organic Chemistry*.<sup>287</sup>

Although there are a number of examples of silver oxide-catalysed alkylation reactions in the presence of ester functional groups,<sup>289–291</sup> applying the optimised silver oxide conditions described above to the alkylation of **163** to form **167** was unsuccessful due to deprotection of the benzoyl groups under the reaction conditions.

In parallel, an alternative synthetic strategy was investigated, using **179**, which had been synthesised as an intermediate in the synthesis of 2-position protected inducers. It was hypothesised that protection of the C2-OH group, deprotection of the 6-position TBDPS and the 3,4-acetonide protecting groups, and reprotection of the C4-OH and C6-OH groups would afford an appropriate intermediate that could be alkylated and deprotected to afford **87** and **124** (Scheme 3.15).

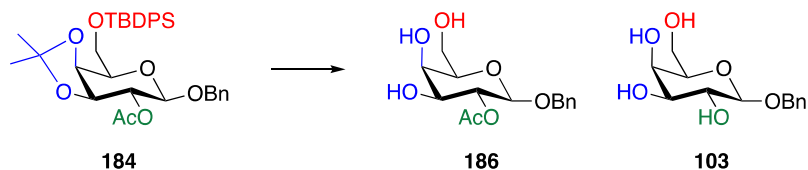


**Scheme 3.15:** Proposed route 2 towards the synthesis of 3-position protected inducers **87** and **124** from **179**, which was synthesised as an intermediate in the synthesis of 2-position protected inducers. PG = protecting group; PNB = 4-nitrobenzyl.

Acetyl protection of the C2-OH group of **128** afforded **184** in 99% yield. Initially, formation of **186** by simultaneous deprotection of the silyl and acetonide protecting groups was attempted using acetyl chloride in methanol which was successful for the deprotection of **131** and **160**. However, under these conditions deprotection of the acetyl group was also observed, resulting in isolation of both **186** and **103** in a molar ratio of 1:0.7 (**186:103**) (Table 3.4, Entry 1). Repeating the reaction under more stringently anhydrous conditions did not solve this problem. Furthermore, it was observed that formation of **103** began to occur before all the starting material **184** had been consumed and a longer reaction time resulted in an increase in the ratio of **186:103** to 1:2.5 (Table 3.4, Entry 2). Deprotection of acetyl groups under these mild acidic conditions has previously been reported.<sup>292</sup>



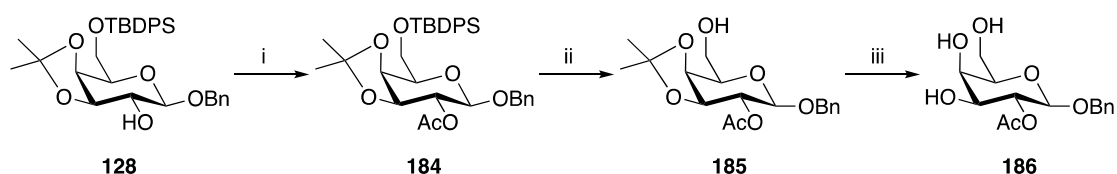
**Table 3.4:** Summary of reaction conditions and molar ratios observed for the deprotection of **184** to **186** with formation of **103** as a by-product.



Entry	AcCl eq.	Solvent	Time h	Ratio 186:103
1	0.6	MeOH	15.5	1.0:0.7 <sup>a</sup>
2	0.6	MeOH:CH <sub>2</sub> Cl <sub>2</sub> (2:1)	72	1.0:2.5 <sup>b</sup>

<sup>a</sup>based on isolated yields; <sup>b</sup>based on NMR ratio.

Alternatively, stepwise deprotection, first with TBAF in THF to remove the TBDPS (**185**) then Dowex<sup>®</sup> 50WX8 (H<sup>+</sup>) in methanol to remove the acetone afforded 15 mg of **186** in a 55% yield over two steps (Scheme 3.16). Additionally, it was thought that **185** formed during this stepwise deprotection would have been a useful intermediate towards the synthesis of 6-position protected inducers. Unfortunately, at this stage, ester deprotection during the 4-nitrobenzyl alkylation reaction with silver oxide on alternative substrates **163** (Section 3.6.1) and **226** (Section 3.7.3) had been observed. As it was likely that this would also occur during alkylation of both **185** and **186**, instead of scaling up this route, alternative strategies were investigated.

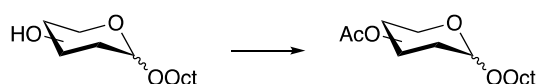


**Scheme 3.16:** Route 2 towards the synthesis of a 3-position protected inducer from **128**. *Reagents and conditions:* i) Ac<sub>2</sub>O, pyridine, RT, 15 h, 99%; ii) TBAF, THF, RT, 1 h, 70%; iii) Dowex<sup>®</sup> 50WX8 (H<sup>+</sup>), MeOH, RT, 17.5 h, 79%.

### 3.6.2. Route 3 *via* Selective Fmoc protection of the C3-OH Group

The third strategy for the synthesis of 3-position protected inducers sought to avoid base-labile protecting groups. This strategy was based on a number of studies that have investigated the relative intrinsic reactivities of secondary hydroxyl groups in different sugars, and which have been recently reviewed.<sup>293</sup> Of particular interest was the observation that 4-DMAP-catalysed acylation of unprotected octyl D-glucopyranoside with a limiting amount of acylating agent afforded predominantly either the 3-OAc or 4-OAc product. Despite the C6-OH group being the most sterically unhindered, the 6-OAc product was formed only in small quantities (Table 3.5, Entries 1 and 2). Different ratios of acetylation between the hydroxyl groups were observed when either octyl D-mannopyranoside (Table 3.5, Entries 3 and 4) or octyl D-galactopyranoside (Table 3.5, Entries 5 and 6) were treated with acetic anhydride under the same conditions. Interestingly, in all cases, negligible amounts of 2-OAc product was formed.<sup>294</sup> These data suggest that 4-DMAP-catalysed acylation can be used to protect hydroxyl groups other than the C2-OH group. This observation has been exploited in the regioselective acylation of C3-OH groups in a number of examples.<sup>295–298</sup>

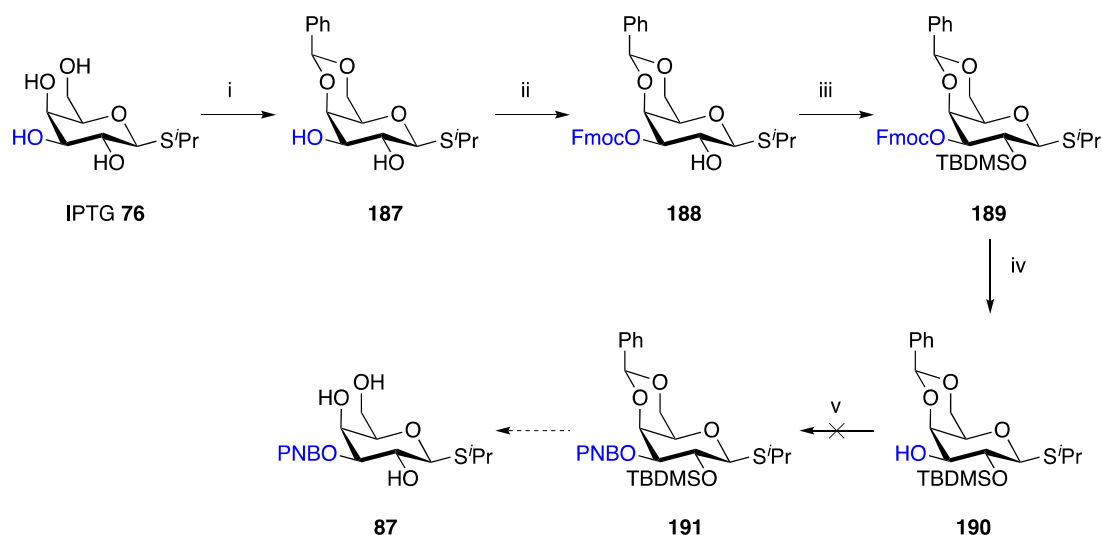
**Table 3.5:** Summary of 4-DMAP-catalysed acetylation of monosaccharides investigated by Kurahashi *et al.*, showing the relative reactivities of each hydroxyl when a limiting amount of acylating agent was used.<sup>294</sup>



Entry	Substrate	2-OAc	3-OAc	4-OAc	6-OAc	Total Yield (%) <sup>a</sup>
1	Octyl $\alpha$ -Glc	-	25	61	14	98
2	Octyl $\beta$ -Glc	2	42	37	19	100
3	Octyl $\alpha$ -Man	7	16	40	37	75
4	Octyl $\beta$ -Man	-	22	46	32	72
5	Octyl $\alpha$ -Gal	-	14 <sup>b</sup>	28 <sup>b</sup>	58	73
6	Octyl $\beta$ -Gal	-	16 <sup>b</sup>	14 <sup>b</sup>	70	81

<sup>a</sup>NMR conversion relative to the initial amount of Ac<sub>2</sub>O; <sup>b</sup>Product ratio could not be determined accurately due to poor separation of signals. *Reagents and conditions:* Ac<sub>2</sub>O (0.7 eq.), 4-DMAP (0.05 eq.) K<sub>2</sub>CO<sub>3</sub>, CHCl<sub>3</sub>, RT, 1 h.

As can be seen from Table 3.5, the reactivity of the hydroxyl groups for galactose is  $C6-OH > C4-OH \approx C3-OH > C2-OH$ . Therefore, in order to avoid unwanted acylation at the C4-OH or C6-OH groups, these positions of IPTG **76** were first protected with a benzylidene protecting group, yielding **187** (Scheme 3.17).



**Scheme 3.17:** Route 3 towards synthesis of 3-position protected inducer **87**. *Reagents and conditions:* i)  $\text{PhCH}(\text{OMe})_2$ , 4-TsOH·H<sub>2</sub>O, CH<sub>2</sub>Cl<sub>2</sub>, RT, 1 h, 95%; ii) FmocCl, DMAP, pyridine, 0 °C, 2 h then RT, 14–20.5 h, 55–62%; iii) TBDMSOTf, 2,6-lutidine, CH<sub>2</sub>Cl<sub>2</sub>, RT, 19.5 h, 86–99%; iv) Et<sub>3</sub>N, CH<sub>2</sub>Cl<sub>2</sub>, RT, 11–22 h, 79–84%; v) 4-NO<sub>2</sub>BnBr **80**, Ag<sub>2</sub>O, 4 Å MS, dark, cyclohexane, reflux. PNB = 4-nitrobenzyl.

9-Fluorenylmethyloxycarbonyl chloride (FmocCl) has previously been used to selectively protect the C3-OH group of benzylidene protected galactopyranosides.<sup>295,296,298</sup> Furthermore, it has been noted that increasing the steric bulky of the acylating agent, increases the selectivity of the reaction.<sup>299</sup> Accordingly, treatment of **187** with FmocCl and 4-DMAP in pyridine afforded **188** in 62% yield. When the reaction was repeated on a larger scale, the yield of **188** decreased to 55% due to formation of a by-product identified as **192** in 31% yield, resulting from addition of Fmoc to both free hydroxyl groups (Figure 3.13).

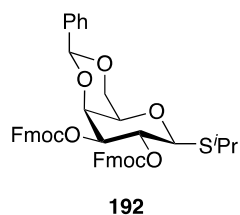


**Figure 3.13:** Structure of the by-product formed when the synthesis of **188** was scaled up to 2 g.

Installation of a TBDMS group on the free C2-OH group, using conditions previously developed within the group,<sup>300</sup> afforded **189** in 86–99% yield. Subsequent deprotection of the 3-OFmoc group with triethylamine in dichloromethane yielded **190** (Scheme 3.17). However, again, applying the silver oxide conditions to the alkylation of **190** failed to yield any of the desired alkylation product, **191**. Surprisingly the major product isolated was identified through <sup>1</sup>H NMR and mass spectrometry to be **193** (Figure 3.14). It is possible that the C3-OH group was too sterically hindered to react efficiently under these conditions and, therefore, a fourth route was investigated.

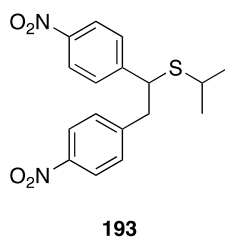
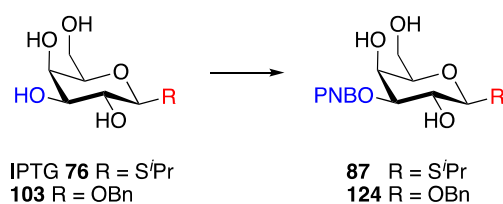


**Figure 3.14:** Structure of the major product formed from the attempted alkylation of **190** with 4-nitrobenzyl bromide **80** and silver oxide in cyclohexane.

### 3.6.3. Route 4 *via* Direct Alkylation of Unprotected Galactopyranosides

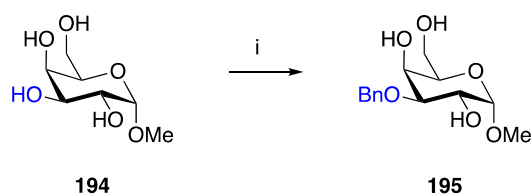
There are a number of methods for regioselective alkylation of unprotected monosaccharides.<sup>264,293,301</sup> Many of these involve pre-activation of the sugar and a range of reagents, which promote regioselectivity, have been developed for this purpose.<sup>301–305</sup> One of the most widely applied methods uses stannylene acetals, which are traditionally pre-formed using stoichiometric quantities of tin prior to addition of the alkylating agent.<sup>286,293,306</sup> These regioselective benzylation reactions are typically performed using a two-step, one-pot strategy in which initial formation of the dibutylstannylene acetal *in situ* is followed by addition of the benzyl bromide **130** alkylation agent. Formation of the dibutylstannylene acetal generates water as a

by-product, which must be removed to drive the reaction forwards. This method is disadvantageous due to the high toxicity of organotin compounds and the potential difficulty in removing residual tin even after purification.<sup>307</sup> To reduce the toxicity of these reactions, catalytic conditions which use substoichiometric amounts of organotin reagent have been developed.<sup>308,309</sup> In the case of galactose, benzylation occurs on the C3-OH group and it was hypothesised that similar conditions could be used to directly alkylate IPTG **76** and **103** to afford **87** and **124**, respectively (Scheme 3.18).



**Scheme 3.18:** Proposed route for direct alkylation of IPTG **76** and **103** to afford **87** and **124**, respectively, using catalytic amounts of dibutyl tin oxide.<sup>308</sup>  $R = \text{S}'\text{Pr}$  or  $\text{OBn}$ ; PNB = 4-nitrobenzyl.

To confirm the selectivity of the reaction, conditions developed by Xu *et al.* were applied to the regioselective benzylation of **194** as a test substrate.<sup>308</sup> Promisingly, alkylation of **194** with dibutyl tin oxide, potassium carbonate, tetrabutylammonium bromide and benzyl bromide **130** afforded **195** in 40% yield (Scheme 3.19).<sup>308</sup> It was next investigated whether these conditions would be applicable to direct alkylation of the C3-OH group with 4-nitrobenzyl bromide **80**. When the reaction was repeated, substituting benzyl bromide **130** with 4-nitrobenzyl bromide **80**, only starting material was recovered.



**Scheme 3.19:** Selective benzylation of a test substrate **194** to afford **195** according to the reaction conditions described by Xu *et al.*<sup>308</sup> *Reagents and conditions:* i)  $\text{Bu}_2\text{SnO}$ , toluene, 100 °C, 1 h; then  $\text{K}_2\text{CO}_3$ , TBAB,  $\text{BnBr}$  **130**,  $\text{MeCN}:\text{DMF}$  (10:1), 80 °C, 2.5 h, 40%.

A recent publication demonstrated the use of an iron catalyst,  $[\text{Fe}(\text{dibm})_3]$  **196**, that can effect the same selectivity as dibutyl tin oxide but without the associated toxicity (Figure 3.15).<sup>310,311</sup> It was hypothesised that this catalyst could be applied to the synthesis of 3-position protected inducers **87** and **124**.

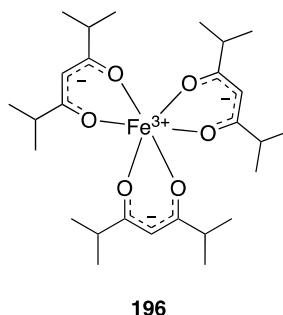
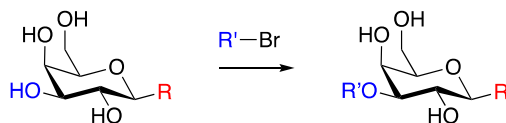


**Figure 3.15:** Structure of an iron catalyst,  $[\text{Fe}(\text{dibm})_3]$  **196**,<sup>311</sup> reported to effect regioselective alkylation of diols and polyols.<sup>310</sup>

The reported alkylation conditions were first applied to benzylation at the 3-position of **103** to confirm that the reported selectivity was observed (Table 3.6, Entry 1) and, subsequently, to **76** to ensure that the reaction was amenable to thioglycosides (Table 3.6, Entry 2). In both cases, the corresponding 3-*O*-benzylated product was obtained. Furthermore, unlike with the tin chemistry, substituting benzyl bromide **130** with 4-nitrobenzyl bromide **80** led to formation of **87** and **124** directly from **76** and **103**, respectively (Table 3.6, Entries 3 and 4), albeit in lower yields.

**Table 3.6:** Synthesis of 3-*O*-alkylated galactopyranosides, using the iron-catalyst [Fe(dibm)<sub>3</sub>] **196** to direct the regioselectivity of the alkylation reaction.



Entry	Scale mg SM	R	R'	Time h	Product	Yield %
1	50	OBn	Bn	15	<b>197</b>	45
2	50	S <sup>i</sup> Pr	Bn	22	<b>198</b>	43
3	50	OBn	4-NO <sub>2</sub> Bn	22	<b>124</b>	37
4	50	S <sup>i</sup> Pr	4-NO <sub>2</sub> Bn	22	<b>87</b>	35
5	300	OBn	4-NO <sub>2</sub> Bn	17.5	<b>124</b>	28
6	300	S <sup>i</sup> Pr	4-NO <sub>2</sub> Bn	24	<b>87</b>	38

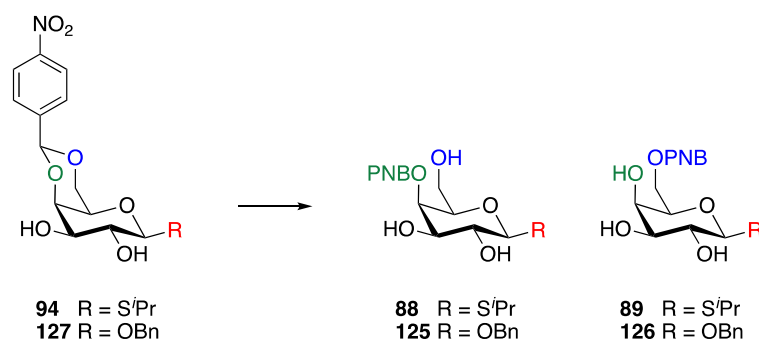
Reagents and conditions: [Fe(dibm)<sub>3</sub>] **196**, K<sub>2</sub>CO<sub>3</sub>, MeCN:DMF (9:1), 80 °C.

Although the yields are not as high as those reported in the original paper, the one step, direct alkylation reaction was preferable to a multi-step protection and deprotection reaction sequence. The loss of yield can be attributed to the fact that in each case, the reaction did not go to completion, even after increasing both the reaction time and the catalyst load. Finally, the reactions to yield **87** and **124** were repeated on a larger scale to obtain enough compound for future biological studies (Table 3.6, Entries 5 and 6).

### 3.7. Synthesis of 4-Position Protected Inducers

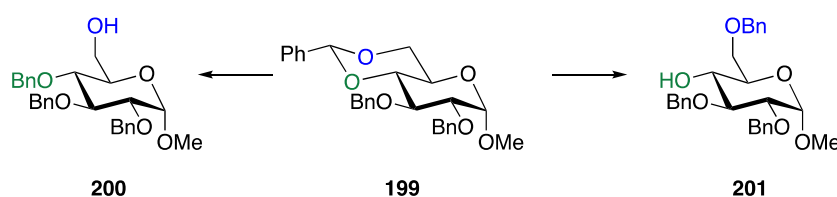
#### 3.7.1. Route 1 *via* Regioselective Ring Opening of **127**

For the synthesis of 4-position protected inducers **88** and **125**, it was initially hypothesised that regioselective ring opening of the 4-nitrobenzylidene acetals **94** and **127**, which had previously been synthesised as potential hypoxia-activated inducers (Section 3.9.1), would be the most direct route (Scheme 3.20).



**Scheme 3.20:** Proposed route 1 for regioselective ring opening of **94** and **127** to afford **88** or **89** and **125** or **126**, respectively. R = S<sup>i</sup>Pr or OBn; PNB = 4-nitrobenzyl.

There is a wealth of literature around the regioselectivity of reductive 4,6-*O*-benzylidene acetal ring-opening reactions, and the synthetic and mechanistic aspects of these were reviewed in 2011.<sup>312</sup> Many of the reported conditions have been optimised for ring opening of methyl 2,3-di-*O*-benzyl-4,6-*O*-benzylidene- $\alpha$ -D-glucopyranoside **199** to afford either the 4-*O*-benzyl ether **200** or the 6-*O*-benzyl ether **201** (Scheme 3.21). When applied to the ring opening of galactose-based 4,6-acetals, under many of these conditions, regioisomeric mixtures were obtained.<sup>312</sup> Nevertheless, there are some conditions, predominantly based on the use of borane-THF, which have been shown to be selective for formation of the 4-*O*-benzyl ether from 4,6-*O*-benzylidene galactopyranosides.<sup>313–316</sup>

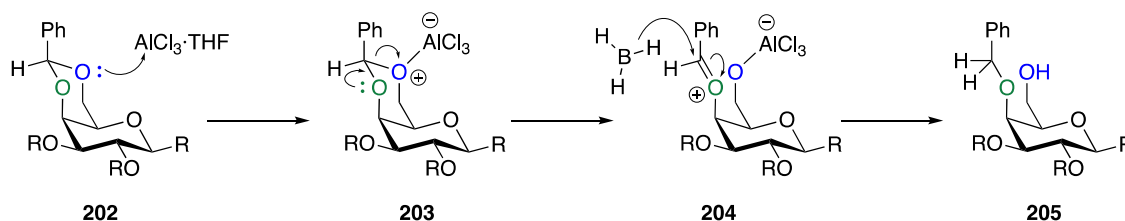


**Scheme 3.21:** The regioselective ring opening of benzylidene acetal **199** to afford either the 4- (**200**) or 6- (**201**) position benzyl ether is frequently used as a standard substrate for comparison between different methods.<sup>312</sup>

The regioselectivity of reductive openings of benzylidene acetals is directed by both the reducing agent and the solvent.<sup>312,317</sup> In non-polar solvents, such as toluene, the Lewis acid (e.g. AlCl<sub>3</sub>) is not solvated and rapidly coordinates to the more nucleophilic primary C6-OH group; borane reacts at the C4-OH group to afford the 4-*O*-benzyl product. In polar solvents, such as THF, the solvent fully solvates the Lewis acid, reducing its activity and slowing the reaction rate. With



non-activated reducing agents, such as borane-THF, the Lewis acid preferentially coordinates to the primary hydroxyl affording the same selectivity as in non-polar solvents (Scheme 3.22). When the borane reducing agent is activated, for example as the borane·dimethylamine complex, it can coordinate to the primary C6-OH group preferentially ahead of the Lewis acid, resulting in the inverse selectivity.<sup>312,317</sup>



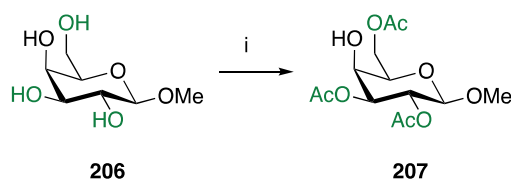
**Scheme 3.22:** Mechanistic explanation for formation of 4-*O*-benzyl ethers from 4,6-*O*-benzylidene acetals with borane and a Lewis acid catalyst in THF.<sup>312,317</sup>

Conditions employing borane-tetrahydrofuran complex and cobalt(II) chloride have previously been used in the group for regioselective reductive ring-opening reactions to yield the 4-*O*-benzyl ether.<sup>316,318</sup> When these conditions were applied for regioselective ring-opening of **127**, the reaction failed to proceed and resulted in recovery of starting material. Similarly low reactivities when attempting to reductively open 4-nitrobenzylidene acetals have also been reported.<sup>319</sup> This effect is mostly likely due to the increased electron deficiency of the 4-nitrobenzylidene system in comparison with either the benzylidene or 4-methoxybenzylidene systems. There are no reported examples in the literature of such a reaction and this strategy was not pursued further.

### 3.7.2. Route 2 via Tin-Mediated Regioselective Acylation

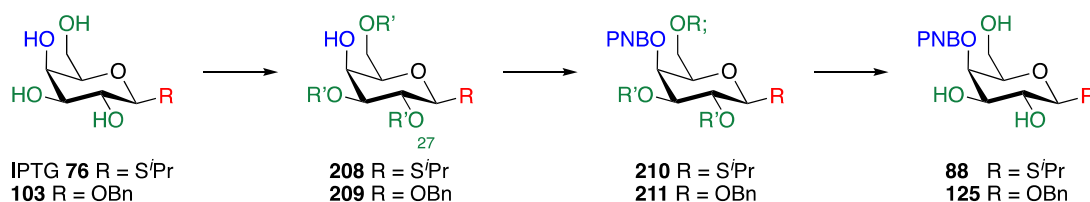
The next strategy investigated the use of organotin reagents, including tributyl tin oxide and dibutyl tin oxide, which have frequently been used to obtain monosubstituted compounds directly from unprotected or partially protected carbohydrates.<sup>320–322</sup> It has been reported that using an excess of organotin reagent can promote multiple substitution of sugars with a substitution pattern that is controlled by the specific reaction conditions, such as choice of reagent and temperature.<sup>323,324</sup> For example, following formation of a stannylene acetal from an unprotected galactopyranoside **206** with 3.3 equivalents of dibutyltin oxide, addition of 3.3 equivalents of

acetic anhydride in toluene yielded the corresponding 2,3,6-*O*-acetylated product **207** (Scheme 3.23).<sup>324</sup>



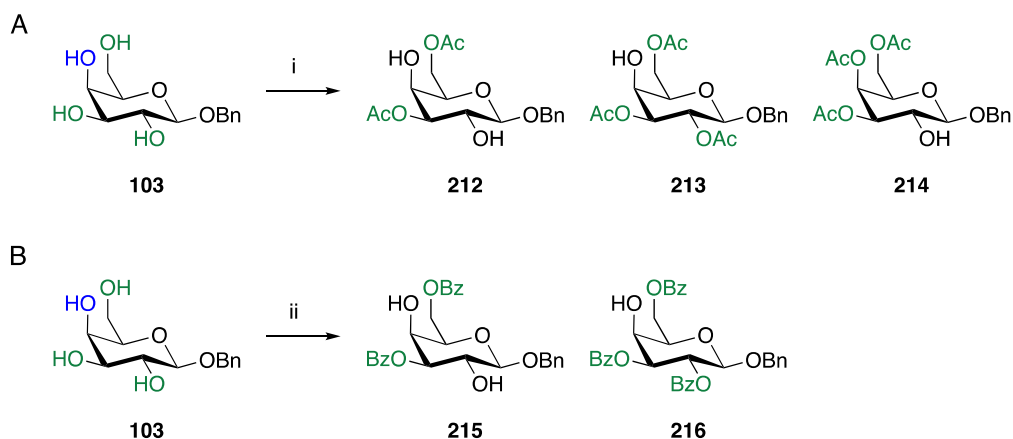
**Scheme 3.23:** Direct formation of a 2,3,6-tri-*O*-acetylated galactopyranoside from the unprotected precursor using excess of dibutyltin oxide and acetic anhydride. *Reagents and conditions:* i) Bu<sub>2</sub>SnO (3.3 eq.), MeOH, 70 °C, 2 h, then Ac<sub>2</sub>O (3.3. eq.), toluene, 0 °C–RT, 6 h, 70%.<sup>324</sup>

Similarly, it was expected that 3,6-*O*-benzoylated galactopyranosides could be synthesised through an analogous reaction with benzoyl chloride.<sup>323</sup> Consequently, the next route that was investigated sought to use these regioselective acylation reactions to afford intermediates **208** and **209** from IPTG **76** and **103**. The intermediates would then be alkylated with 4-nitrobenzyl bromide **80** to yield **210** and **211**, and, finally, deacylated to yield 4-position protected inducers **88** and **125** (Scheme 3.24).



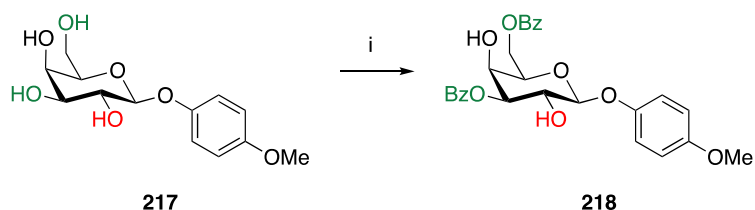
**Scheme 3.24:** Proposed route 2 for synthesis of 4-position protected inducers **88** and **125** from **76** and **103**, via stannylene acetal mediated formation of 2,3,6-tri-*O*-acetyl intermediates **208** and **209**, respectively. R = S'Pr or OBn; R' = acyl group; PNB = 4-nitrobenzyl.

Initial efforts to acetylate **103** under these conditions were unsuccessful and resulted in formation of 3,6-di-*O*-acetylated compound **212** as the major product (44% yield) with tri-*O*-acetylated compounds **213** and **214** formed in 17% and 3% yield, respectively (Scheme 3.25A). Similarly, despite a three-fold excess of benzoyl chloride, benzoylation reactions with **103** afforded 3,6-di-*O*-benzoylated product **215** as the major product (82%) with tri-*O*-benzoylated compound **216** formed in only 12% yield. (Scheme 3.25B).



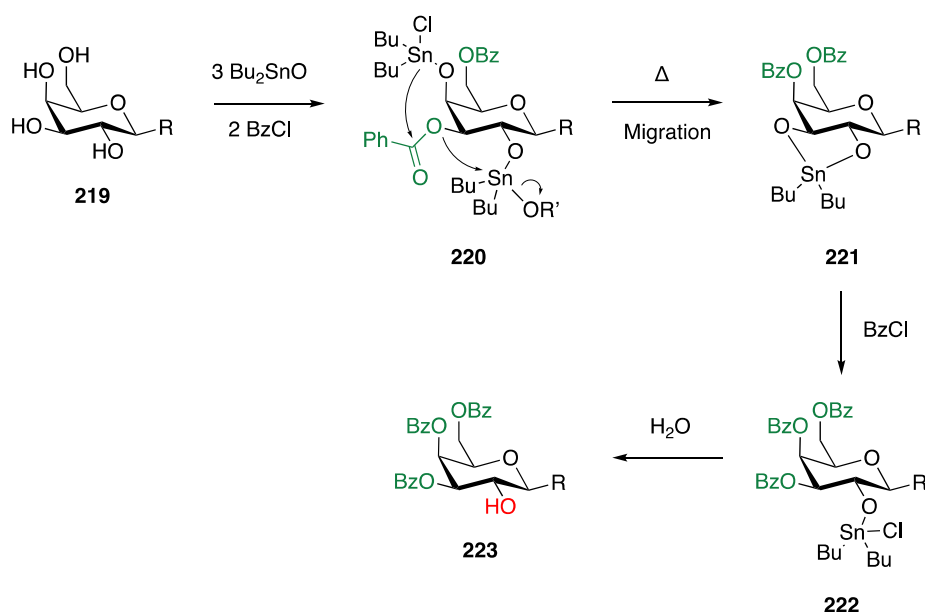
**Scheme 3.25:** Reaction of **103** with excess of dibutyltin oxide and A) acetic anhydride and B) benzoyl chloride. *Reagents and conditions:* i)  $\text{Bu}_2\text{SnO}$ , MeOH, reflux, 2 h, then  $\text{Ac}_2\text{O}$ , toluene,  $0\text{ }^\circ\text{C}$ –RT, 1 h, **212**: 44%, **213**: 17%, **214**: 3%; ii)  $\text{Bu}_2\text{SnO}$ , MeOH, reflux, 2 h, then  $\text{BzCl}$ , toluene,  $0\text{ }^\circ\text{C}$ , 2 h, **215**: 82%, **216**: 12%.

This benzoylation pattern has been previously observed by Zhang and Wohl, who treated galactopyranoside **217** with benzoyl chloride, obtaining **218** in 93% yield (Scheme 3.26).<sup>323</sup>



**Scheme 3.26:** Literature example of formation of the di-benzoylated product **218**, when **217** was treated with an excess of benzoyl chloride, following formation of a dibutyl stannylene acetal. *Reagents and conditions:* i)  $\text{Bu}_2\text{SnO}$  (3.0 eq.), toluene:benzene (1:1) reflux, then  $\text{BzCl}$  (3.3 eq.), RT, 5 h, 93%.<sup>323</sup>

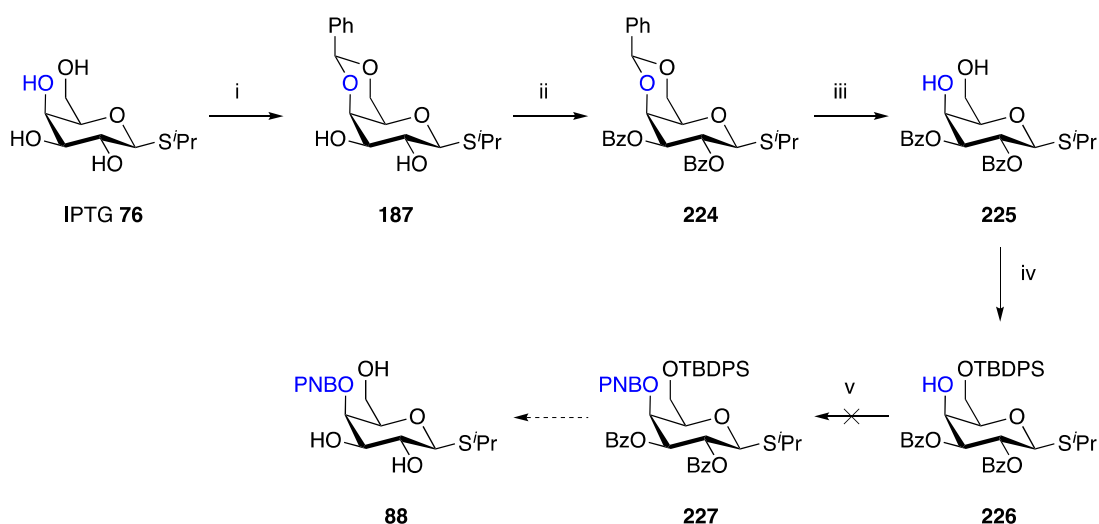
Unfortunately, it has also been shown that increasing the temperature of these reactions in an attempt to drive the formation of the 2,3,6-tri-*O*-benzoylated compound favours formation of the 3,4,6-tri-*O*-acylated product due to benzoyl migration from the 3-position to the 4-position and re-benzoylation of the C3-OH group (Scheme 3.27).<sup>323</sup> Therefore, due to these difficulties in formation of the desired 2,3,6-tri-*O*-acylated compounds an alternative route was investigated.



**Scheme 3.27:** Mechanistic explanation for the formation of 3,4,6-tri-*O*-benzoylated galactopyranosides when free galactopyranosides are heated with an excess of benzoyl chloride, following formation of a dibutyl stannylene acetal. Benzoylation at the 3- and 6-positions is rapid. Heat promotes migration of the 3-*O*-benzoyl to the C4-OH group. The resulting stannylene acetal reacts to reform the 3-*O*-benzoyl ester, which is hydrolysed to afford 3,4,6-tri-*O*-benzoylated galactopyranosides.<sup>323</sup>

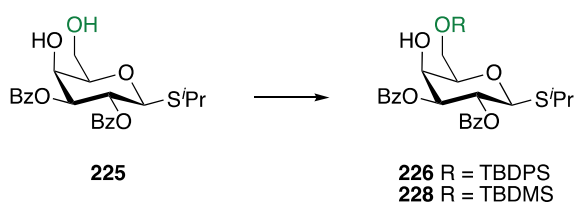
### 3.7.3. Route 3 via Ester Protecting Groups

The third route that was investigated towards synthesis of a 4-position protected inducer is outlined in Scheme 3.28. In a similar manner to the first route attempted towards the synthesis of 3-position protected inducers (see Section 3.6.1), benzylidene protection of the C4-OH and C6-OH groups afforded **187**, which was subsequently benzoylated at the remaining free C2-OH and C3-OH groups to form **224**. Deprotection of the benzylidene acetal was initially attempted with trifluoroacetic acid (90% in water) and, although it appeared that there had been full consumption of **224** by TLC analysis, **225** was only isolated in a 48% yield, along with recovery of 35% of starting material **224**. Changing the deprotection conditions from TFA to acetic acid (80% in water) afforded **225** in an 87% yield.



**Scheme 3.28:** Proposed route 3 towards synthesis of a 4-position protected inducer. *Reagents and conditions:* i)  $\text{PhCH(OMe)}_2$ , 4-TsOH,  $\text{CH}_2\text{Cl}_2$ , RT, 1 h, 95%; ii)  $\text{BzCl}$ , 4-DMAP, pyridine,  $0\text{ }^\circ\text{C}$ –RT, 2 h, 85%; iii) AcOH (80% in water),  $60\text{ }^\circ\text{C}$ , 48 h, 87%; iv)  $\text{TBDPSCl}$ , 4-DMAP, pyridine,  $50\text{ }^\circ\text{C}$ , 30 min, 79%; v) 4- $\text{NO}_2\text{BnBr}$  **80**,  $\text{Ag}_2\text{O}$ , 4 Å MS, dark, cyclohexane, reflux. PNB = 4-nitrobenzyl.

Silyl protection of the primary hydroxyl was attempted using conditions that had previously been employed for TBDPS (Table 3.7, Entry 1) or TBDMS (Table 3.7, Entry 2) protection of the C6-OH group. In both cases, these were unsuccessful and only starting material **225** was recovered. Increasing the temperature to  $50\text{ }^\circ\text{C}$  and adding 4-DMAP as a catalyst (Table 3.7, Entry 3) afforded **226** in 79% yield.

**Table 3.7:** Summary of conditions tested for silyl protection of the primary hydroxyl of **225**.

Entry	Reagent	Eq.	Solvent	Temp. °C	Yield %
1	TBDPSCI	1.2	DMF	RT	0
	Imidazole	2.5			
2	TBDMSCI	1.1	Pyridine	0–RT	0
	Imidazole	1.5			
3	TBDPSCI	2.3	Pyridine	50	79
	4-DMAP	0.4			

Subsequent attempts to alkylate the C4-OH group with silver oxide and 4-nitrobenzyl bromide **80** in cyclohexane resulted in deprotection of the benzoyl protecting groups. This result is consistent with the loss of benzoyl protecting groups observed during the analogous reaction for alkylation of **163** (Section 3.6.1) and confirms the lability of acyl groups under these silver oxide conditions.

#### 3.7.4. Route 4 *via* Butane-1,2-Diacetal

Consequently, it was necessary to find an alternative protecting group strategy that did not involve any base-labile protecting groups. 1,2-Diacetals have become important protecting groups for 1,2-*trans*-diequatorial diols in cyclic systems.<sup>325</sup> The selectivity of these diacetals is based on the stabilising anomeric effect that results from having the two methoxy groups axial, while sterically demanding groups are placed in the more favourable equatorial positions. Initially, cyclohexane-1,2-diacetals (CDA) were used as protecting groups in carbohydrate syntheses (Figure 3.16A).<sup>326</sup> More recently, other 1,2-diacetals, including butane-1,2-diacetal (BDA) (Figure 3.16B), have increased in popularity. A variety of these 1,2-diacetals have been used to effect selective protection of hydroxyl functionality in both carbohydrate synthesis and in the syntheses of complex natural products.<sup>325–328</sup>

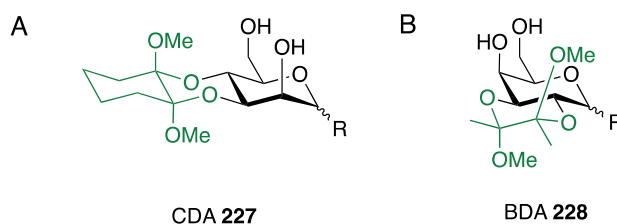
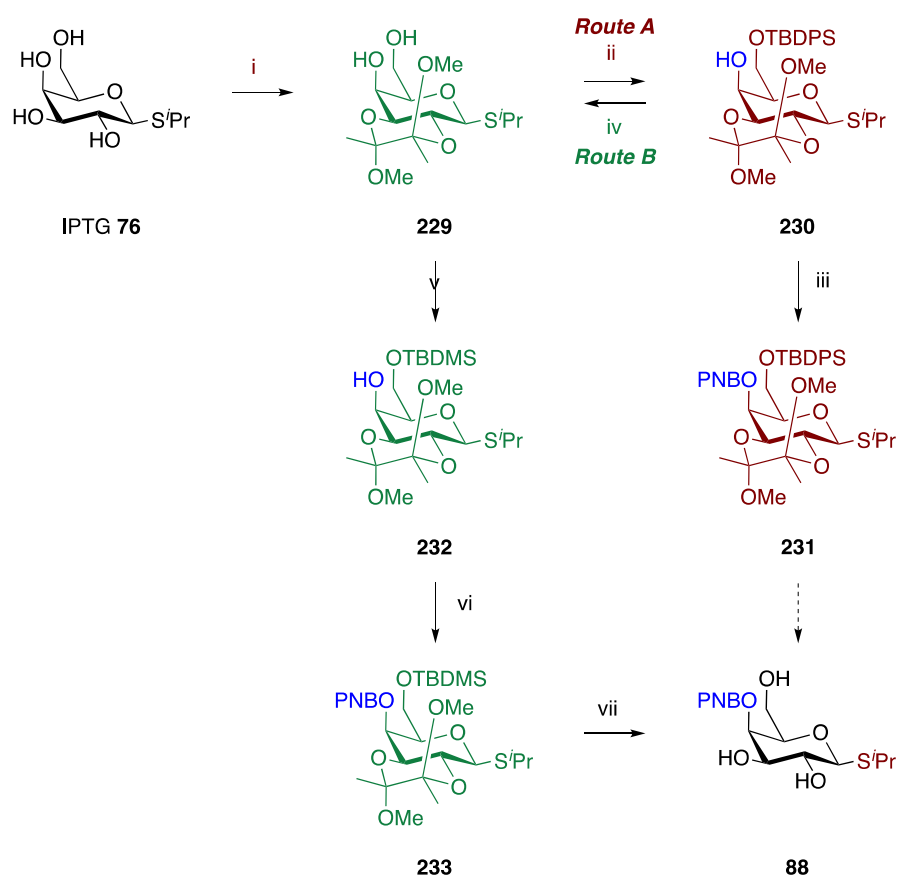


**Figure 3.16:** Examples of 1,2-diacetal protecting groups. A) a cyclohexane-1,2-diacetal (CDA) protected mannopyranoside **227**; B) a butane-1,2-diacetal (BDA) galactopyranoside **228**.

It was hypothesised that the BDA protecting group would protect the *trans* C2-OH and C3-OH groups in a manner analogous to isopropylidene protection of the *cis* C3-OH and C4-OH groups. Silyl protection of the primary C6-OH group would afford an intermediate with a free C4-OH group that could be alkylated to form the 4-nitrobenzyl ether.

Typically, 1,2-diacetals are formed by heating a diol or polyol under reflux with an excess of the appropriate dione, trimethylorthoformate, and ( $\pm$ )-CSA in methanol. Accordingly, IPTG **76** was treated under these conditions with butane-2,3-dione, forming the 2,3-BDA protected intermediate **229**. Purification of **229** was challenging due to formation of an unidentified by-product that co-eluted with the desired product during column chromatography. It was found that this impurity could be removed in the next step; TBDPS protection of the primary C6-OH group afforded **230** as a colourless solid. Applying the previously developed silver oxide conditions to alkylate **230** with 4-nitrobenzyl bromide **80** did not give full conversion to **231**. Efforts to drive the reaction to completion by increasing the reaction time and the number of equivalents of both silver oxide and 4-nitrobenzyl bromide **80** had no effect. Furthermore, purification of **231** by column chromatography was frequently only partially successful, due to coelution of an unidentified by-product. Pure **231** was only obtained on one occasion, albeit in a very low 8% yield, with concomitant recovery of 58% of starting material **230**.

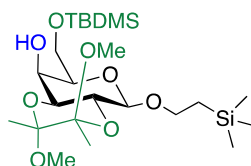


**Scheme 3.29:** Route 4 towards the synthesis of 4-position protected inducer **88**. *Reagents and conditions:* i) 2,3-Butanedione, ( $\pm$ )-CSA,  $\text{CH}(\text{OMe})_3$ , MeOH, reflux, 17.5 h; ii) TBDPSCl, 4-DMAP, pyridine, 50 °C, 7 h, 45% (2 steps); iii) 4- $\text{NO}_2\text{BnBr}$  **80**,  $\text{Ag}_2\text{O}$ , 4 Å MS, dark, cyclohexane, reflux, 19 h, 8%; iv) TBAF, THF, RT, 2 h, 84%; v) TBDMSCl, 4-DMAP, pyridine, 0 °C–RT, 43.5 h, 99%; vi) 4- $\text{NO}_2\text{BnBr}$  **80**,  $\text{Ag}_2\text{O}$ , 4 Å MS, dark, cyclohexane, reflux, 39 h; vii) AcOH (80% in water), reflux, 2.5 h, 19% (2 steps). PNB = 4-nitrobenzyl.

It was hoped that deprotection of **231** to afford **88** would facilitate purification. Previously acetyl chloride in methanol:dichloromethane (1:2), which generates HCl *in situ*, had been used to deprotect **131** and **160**, which contain the acid labile acetonide and TBDPS moieties. However, the increased stability of the BDA-protecting group compared with an acetonide meant that under these conditions, only TBDPS was deprotected; the BDA group was unaffected. In general, BDA protecting groups are removed with aqueous trifluoroacetic acid.<sup>329–332</sup> Unfortunately, deprotection of **231** with TFA:H<sub>2</sub>O (9:1) in dichloromethane resulted in negligible overall yields (Scheme 3.29, Route A).



It was hypothesised that the primary problem with 4-nitrobenzyl alkylation was a combination of the lower reactivity of the axial C4-OH group, in comparison with the C2-OH, C3-OH, and C6-OH groups and the presence of two bulky protecting groups. Recently, Liu *et al.* synthesised a galactopyranoside **234**, protected at the 2- and 3-positions with BDA and at the 6-position with a TBDMS group (Figure 3.17).

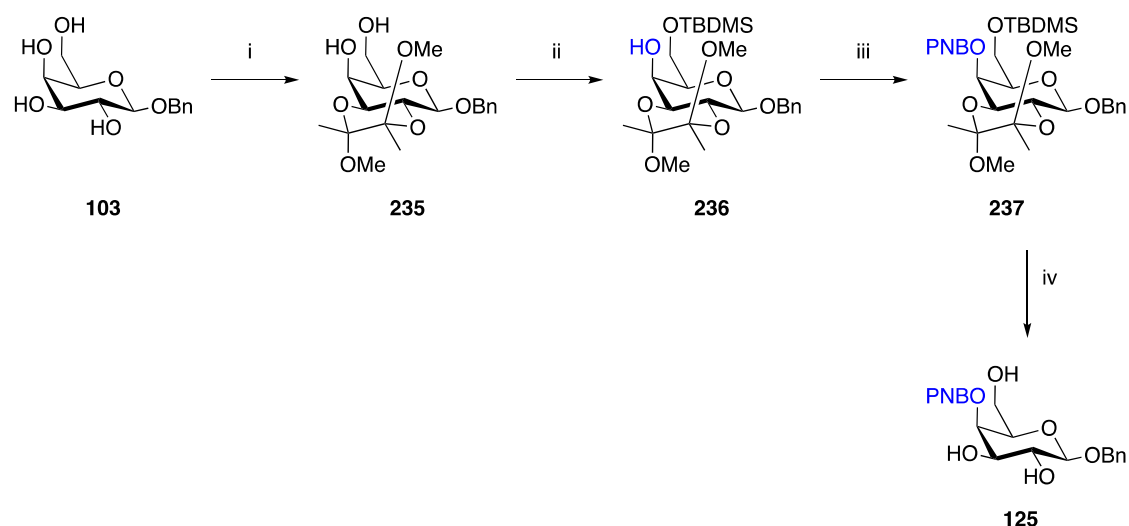


**234**

**Figure 3.17:** Structure of the precursor **234** synthesised by Liu *et al.*<sup>333</sup>

This intermediate was subjected to a variety of alkylation reactions, including alkylation with 4-nitrobenzyl, at the C4-OH group.<sup>333</sup> This compound differs from IPTG **76** only in the group at the anomeric position, suggesting that replacing the 6-position TBDPS protecting group with TBDMS might facilitate the 4-nitrobenzyl alkylation reaction by relieving some of the steric bulk around the reaction centre. Deprotection of TBDPS with TBAF in THF to yield **229** followed by reprotection with TBDMSCl in pyridine afforded **232**. Unfortunately, again, the alkylation reaction with 4-nitrobenzyl bromide **80** under the silver oxide conditions did not reach completion. Formation of **233** and subsequent deprotection with acetic acid (80% in water)<sup>334</sup> as a milder acid than TFA afforded **88** in 19% yield over two steps (Scheme 3.29, Route B).

Having synthesised **88**, these conditions were next applied to the synthesis of 4-position protected benzyl galactose **125**. Protection of the C2-OH and C3-OH groups with 2,3-butanedione yielded **235**; subsequent protection of the C6-OH group with TBDMS afforded **236**. Again, the alkylation reaction to form the 4-nitrobenzyl ether **237** was problematic and did not reach completion. Nevertheless, a sufficient quantity of **237** was isolated and deprotected with acetic acid (80% in water) without further purification to afford **125** in 28% yield over two steps (Scheme 3.30).

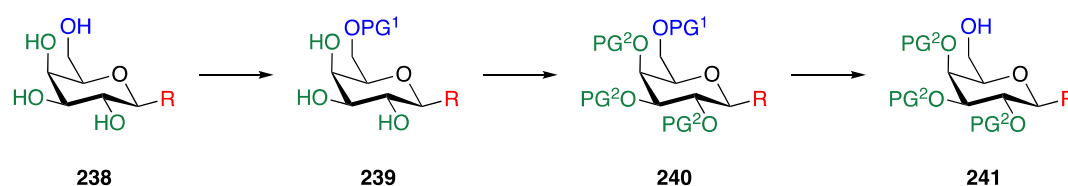


**Scheme 3.30:** Synthesis of 4-PNB protected benzyl galactopyranoside **125**. *Reagents and conditions:* i) 2,3-Butanedione, ( $\pm$ )-CSA, CH(OMe)<sub>3</sub>, MeOH, reflux, 15.5 h, 62%; ii) TBDMSCl, 4-DMAP, pyridine, 0 °C–RT, 3.5 h, 81%; iii) 4-NO<sub>2</sub>BnBr **80**, Ag<sub>2</sub>O, 3 Å MS, dark, cyclohexane, reflux, 68 h; iv) AcOH (80% in water), 80 °C to 100 °C, 1 h, 28% (2 steps). PNB = 4-nitrobenzyl.

### 3.8. Synthesis of 6-Position Protected Inducers

#### 3.8.1. Route 1 *via* Deprotection of a 6-Position Silyl Ether

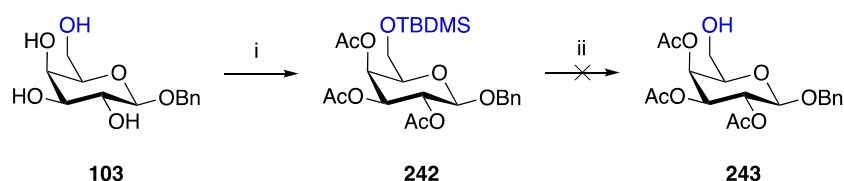
The first route that was investigated for the syntheses of 6-position protected inducers **89** and **126** focused on selective protection of the primary hydroxyl (**239**), orthogonal protection of the remaining free secondary hydroxyls (**240**), and finally deprotection of the primary hydroxyl to afford an intermediate with the C6-OH group free (**241**) (Scheme 3.31).



**Scheme 3.31:** Proposed strategy for the synthesis of 6-position protected inducers. R = S<sup>i</sup>Pr or OBn; PG<sup>1</sup> and PG<sup>2</sup> are orthogonal protecting groups.

There are a number of similar protecting group manipulations described in the literature. These predominantly consist of silyl or trityl protection of the C6-OH group and benzyl ether or ester protection of the C2-OH, C3-OH and C4-OH groups.<sup>335–342</sup> Compounds that contained a benzyl protecting group were unsuitable, since deprotection of the benzyl ether would also be expected

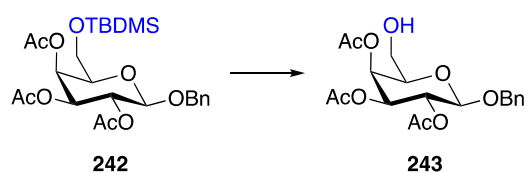
to remove the 4-nitrobenzyl group. For the compounds containing secondary ester protecting groups, a one pot procedure for direct silyl ether formation and acetylation has been reported.<sup>343</sup> Therefore it was decided to synthesise **242** and to deprotect the TBDMS protecting group. Compound **242** was readily synthesised *via* initial formation of the primary TBDMS ether, followed by acetyl protection of the remaining free three hydroxyl groups (Scheme 3.32).



**Scheme 3.32:** Attempted synthesis of **243**, *via* deprotection of the TBDMS group on the primary C6-OH group. *Reagents and conditions:* i) TBDMSCl, pyridine, RT, 3.5 h, then Ac<sub>2</sub>O, pyridine, RT, 2 h, 80%; ii) See Table 3.8).

Deprotection of the TBMDS group to form **243** was attempted using a variety of conditions including, basic conditions buffered with acetic acid (Table 3.8, Entry 1),<sup>343</sup> acidic conditions (Table 3.8, Entry 2)<sup>344</sup> and enzyme-mediated deacetylation (Table 3.8, Entry 3).<sup>345,346</sup> In each case, these were unsuccessful due to migration of the acetyl groups. The migration of acetyl groups is a known problem in carbohydrate chemistry.<sup>347–350</sup> It was concluded that **242** was inherently unstable and therefore unsuitable as an intermediate for the synthesis of **126**.

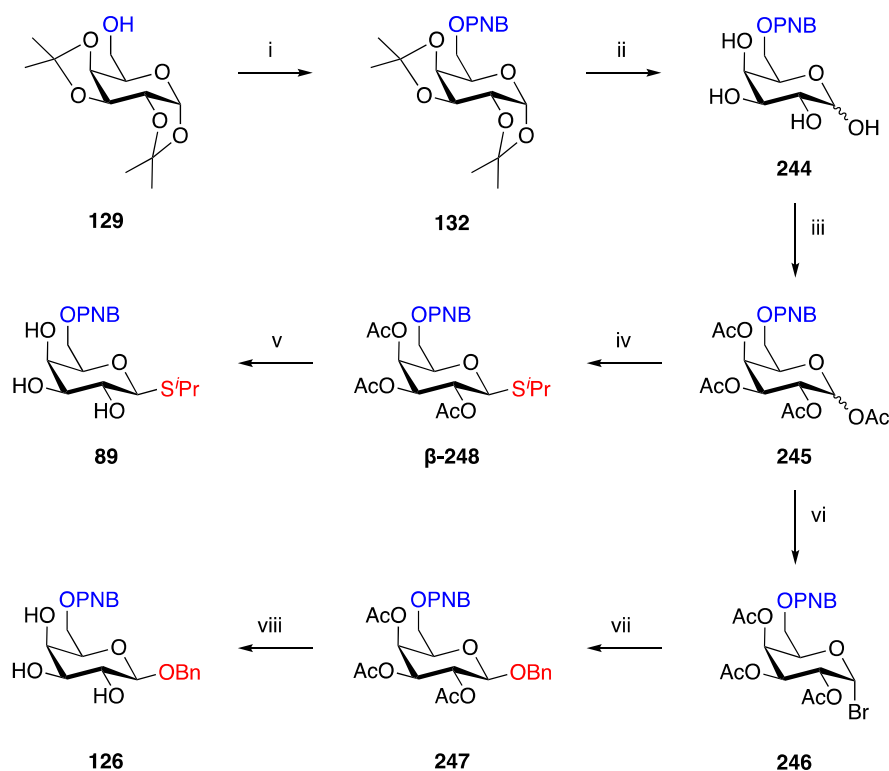
**Table 3.8:** Summary of reaction conditions for the deprotection of the primary 6-position TBDMS group to yield **243**.



Entry	Reagent	Eq.	Solvent	Temp. °C	Yield %
1	TBAF	5.0	THF	RT	0
2	TFA (80% aq.)	10.0	-	RT	0
3	Lipozyme TL IM "butanol	166 mg/(mmol <b>242</b> ) 1.2	Toluene	42	0

3.8.2. Route 2 *via* Alkylation of **129**

During earlier investigations into the alkylation reaction with 4-nitrobenzyl bromide **80**, commercially available **129** was used as a test substrate. Compound **129** contains a single, free C6-OH group and it was hypothesised that following alkylation to form **132**, this compound could be readily transformed into both **89** and **126** (Scheme 3.33).



**Scheme 3.33:** Synthesis of **89** and **126**. *Reagents and conditions:* i) 4-NO<sub>2</sub>BnBr **80**, Ag<sub>2</sub>O, 4 Å MS, cyclohexane, dark, reflux, 15 h; ii) TFA (80% aq.), RT, 30 min; iii) Ac<sub>2</sub>O, pyridine, RT, 21–72 h, 52–68% (3 steps); iv) <sup>i</sup>PrSH, BF<sub>3</sub>·Et<sub>2</sub>O, 4 Å MS, CH<sub>2</sub>Cl<sub>2</sub>, RT, 24–48 h, 25–44%; v) NaOMe, MeOH, RT, 16 h, 79%; vi) HBr (33 wt.% in AcOH), RT, 0.5–2 h, 78–88%; vii) BnOH, AgCO<sub>3</sub>, 4 Å MS, dark, CH<sub>2</sub>Cl<sub>2</sub>, RT, 9 h; viii) NaOMe, MeOH, 19.5 h, 76% (2 steps). PNB = 4-nitrobenzyl.

To facilitate purification after alkylation, **132** was directly deprotected with TFA (80% in water) to form **244**. The exposed hydroxyl groups were then immediately reprotected with acetyl groups, yielding a mixture of  $\alpha/\beta$ -**245** in a yield that ranged from 43–68% over three steps ( $n = 3$ ). Interestingly, the first time the reaction sequence was performed, **245** was isolated with an anomeric ratio of 2:1 ( $\alpha:\beta$ ), as determined by <sup>1</sup>H NMR. This ratio was expected to be due to the

anomeric effect, which stabilises the axial conformation.<sup>351</sup> However, each time the reaction was repeated an anomeric ratio of 1:1.5 ( $\alpha$ : $\beta$ ) was formed (Figure 3.18). This different ratio was unlikely to affect downstream glycosylation reactions, since, as before (see Section 3.2.2) the acetyl protecting groups, positioned on the C2-OH group adjacent to the anomeric position, had been selected to enhance selectivity for the  $\beta$ -anomer during glycosylation.

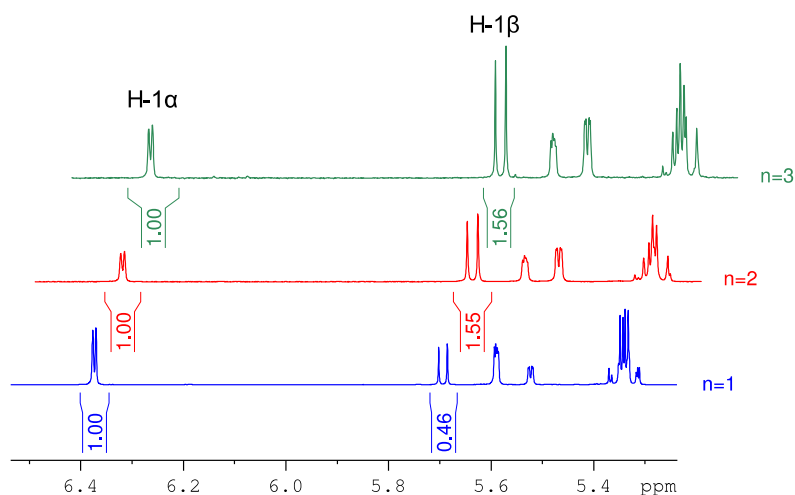


**Figure 3.18:**  $^1\text{H}$  NMR spectra ( $\text{CDCl}_3$ , 400 MHz) of **245**, taken from three different reactions, showing the different ratios of  $\alpha$ : $\beta$ -anomers, using integration from the 1-position proton for each anomer.

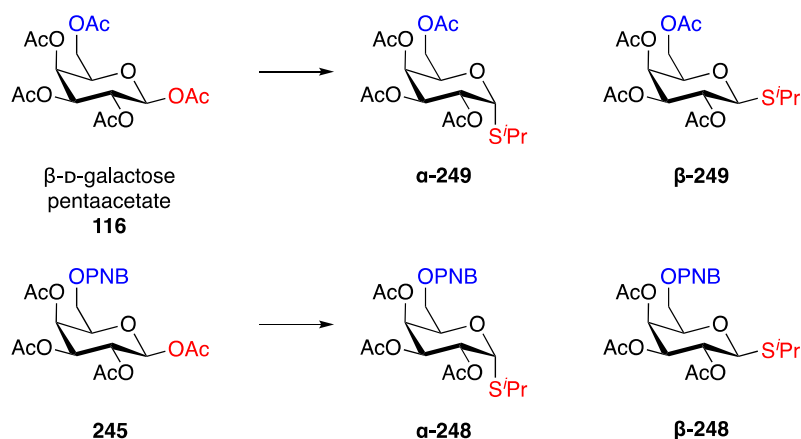
Compound **126** was synthesised following an identical procedure to that employed for the synthesis of **103** from **116**. Bromination at the anomeric position afforded the galactopyranosyl bromide **246**, which was glycosylated with benzyl alcohol to form **247** as the  $\beta$ -anomer. Direct deprotection of the acetyl groups under standard Zemplén deacetylation conditions<sup>259</sup> yielded **126**.

Similarly, the synthesis of **89** was attempted using conditions that had been successful during the synthesis of **76**. Previously, glycosylation of **116** with 2-propanethiol and  $\text{BF}_3 \cdot \text{Et}_2\text{O}$  afforded **249** exclusively as the  $\beta$ -anomer (Table 3.9, Entry 1). However, when these conditions were applied to the synthesis of  $\beta$ -**248**, the reaction was found to proceed significantly more slowly with formation of the  $\alpha$ -anomer ( $\alpha$ -**248**) as a by-product (Table 3.9, Entry 2). Although increasing both the reaction time and the number of equivalents of thiol and  $\text{BF}_3 \cdot \text{Et}_2\text{O}$  reduced the amount of

**$\alpha$ -248** isolated, a large quantity of starting material was still recovered (Table 3.9, Entry 3).

Deprotection of  **$\beta$ -248** proceeded as expected to yield **89** in 79% yield.

**Table 3.9:** Summary of anomeric ratios and recovered starting material (SM) obtained during glycosylation reactions of the appropriate glycosyl donor to form **248** and **249**.



Entry	Substrate	<sup>i</sup> PrSH eq.	BF <sub>3</sub> ·Et <sub>2</sub> O eq.	Time h	$\alpha^b$ %	$\beta^b$ %	SM <sup>b</sup> %
1	<b>116</b>	1.5	2	5	0	71 <sup>a</sup>	0
2	<b>245</b>	3	3	24	19	25	31
3	<b>245</b>	4	4	48	6	44	38

*Reagents and conditions:* <sup>i</sup>PrSH, BF<sub>3</sub>·Et<sub>2</sub>O, 4 Å MS, CH<sub>2</sub>Cl<sub>2</sub>, -78 °C–RT. <sup>a</sup>yield after deprotection to **76** (two steps); <sup>b</sup>isolated yields. PNB = 4-nitrobenzyl.

### 3.9. Synthesis of 4,6-Acetal Protected Inducers

To synthesise the 4,6-acetal protected inducers, it was hypothesised that analogous chemistry to that used for the synthesis of 4,6-benzylidene acetals could be used. The introduction of the benzylidene functional group in carbohydrate chemistry is well established.<sup>264</sup> In the case of polyols, protection of 1,3-diols to form the corresponding benzylidene acetal is thermodynamically favoured over that of 1,2-diols, due to reduced steric clashes between the exposed protons and to the fact that the benzyl group can be positioned equatorially (Figure 3.19).<sup>264</sup>

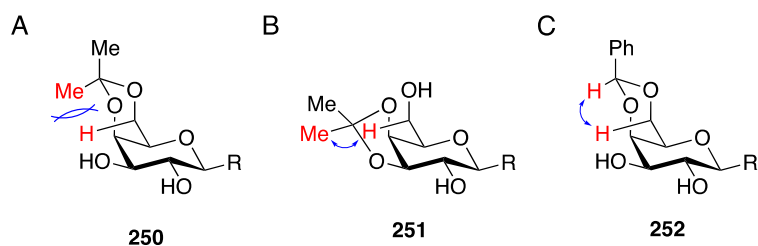


**Figure 3.19:** The formation of 1,3-diols is preferred over 1,2-diols when using benzylidene protecting group compared with the isopropylidene protecting group. A) When  $\text{Me}_2\text{CO}$  is reacted to form the 1,3-acetal **250**, one of the methyl groups must be axial. This cyclic acetal is destabilised by butane-gauche interactions. B) When  $\text{Me}_2\text{CO}$  is reacted to form the 1,2-acetal **251**, the shape of the 5-membered ring acetal is such that the distance between the Me group and proton is larger and the corresponding butane-gauche interactions are smaller. C) When  $\text{PhHCO}$  is reacted to form the 1,3-acetal **252**, the phenyl group can be positioned equatorially, with the proton positioned axially; this reduces steric interactions, and **252** forms preferentially.

There are three methods most frequently employed for the synthesis of benzylidene acetals from unprotected sugars: the use of zinc chloride and benzaldehyde,<sup>352</sup> acid-catalysed transacetalisation using benzaldehyde dimethyl acetal,<sup>353,354</sup> and base-catalysed reaction with  $\alpha,\alpha$ -dibromotoluene.<sup>312</sup> These acetals can usually be readily synthesised in one step from unprotected sugars; therefore, it was decided to also synthesise IPTG derivatives **253** and **254** containing the alternative bioreductive groups 2-nitroimidazole and 5-nitrothiophene, respectively, to allow for direct comparison with the 4-nitrobenzyl compound **94** (Figure 3.20).

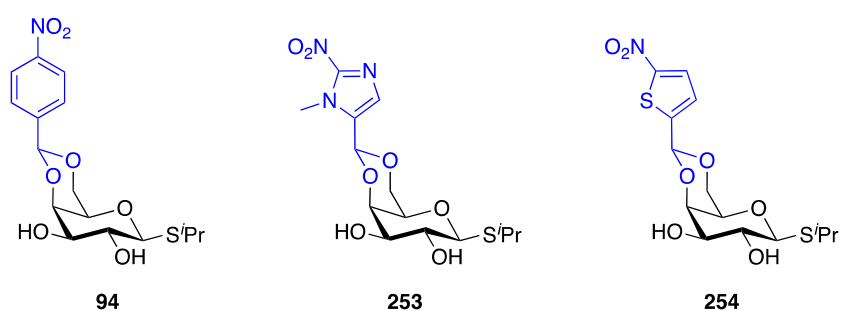
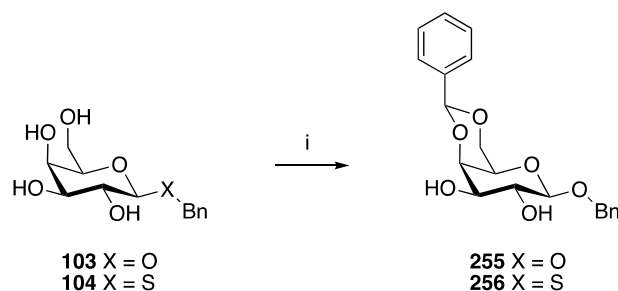


**Figure 3.20:** Structures of IPTG derivatives, containing different bioreductive groups: **94**: 4-nitrobenzyl; **253**: 2-nitroimidazole; **254**: 5-nitrothiophene.

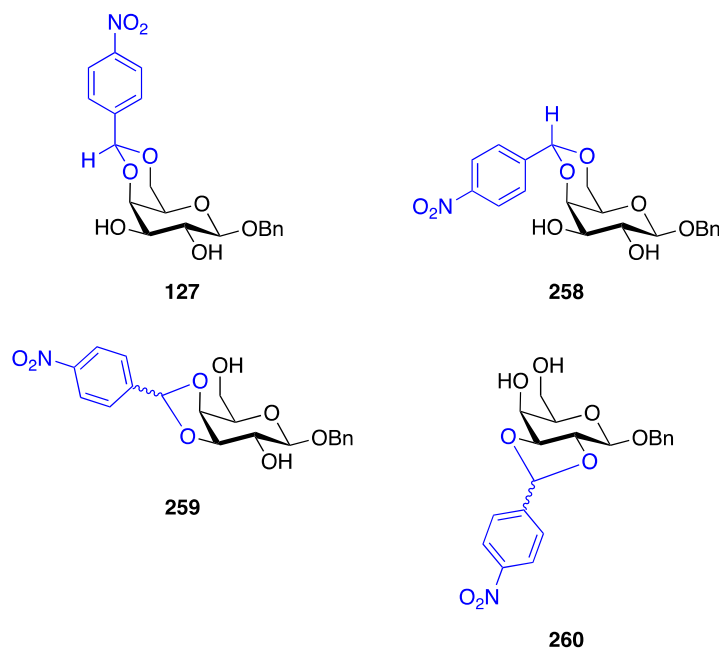
### 3.9.1. Synthesis of 4-Nitrobenzylidene 4,6-Acetal Inducers

The synthesis of **127** was initially based on a previously published procedure for the synthesis of galactose 4,6-*O*-benzylidene derivatives<sup>355,356</sup> that had been employed successfully in the synthesis of **255** and **256** (Scheme 3.34).



**Scheme 3.34:** Synthesis of **255** and **256**. *Reagents and conditions:* i)  $\text{PhCH(OMe)}_2$ , 4-TsOH·H<sub>2</sub>O, MeCN, RT, 1 h, **256**: 81%, **255**: 59%.

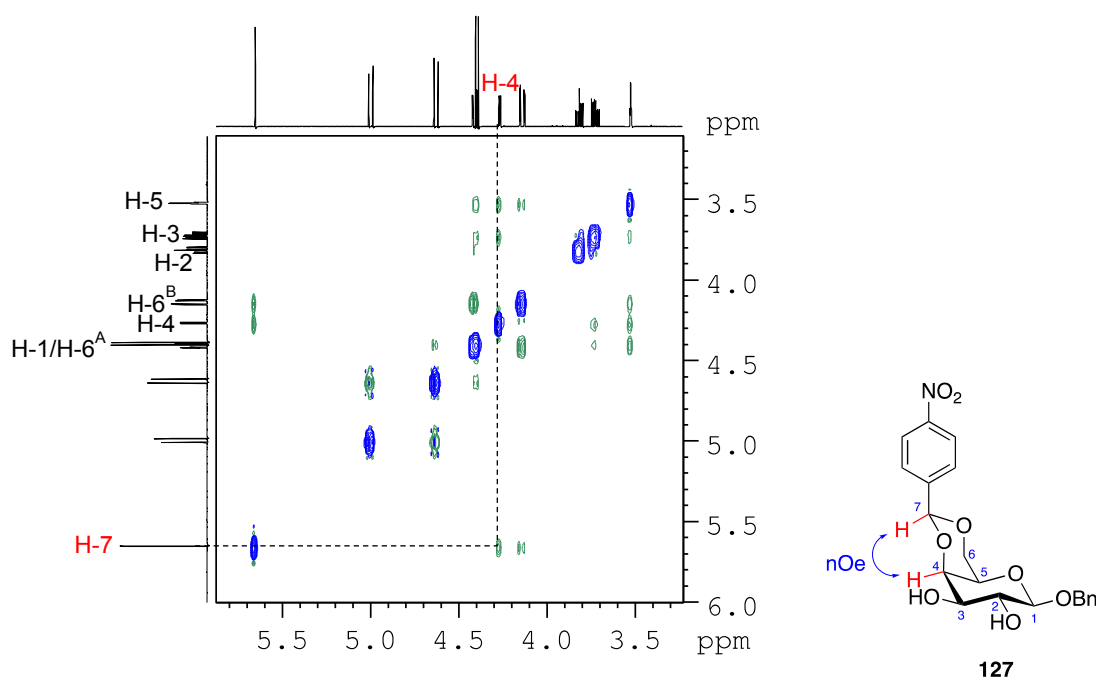
Applying these conditions to the synthesis of **127** (Table 3.10, Entry 1), substituting benzaldehyde dimethyl acetal with 4-nitrobenzaldehyde dimethyl acetal **257**, resulted in formation of a variety of regio- and stereoisomers, due to acetal formation at different positions around the ring, as confirmed by <sup>1</sup>H-<sup>13</sup>C HMBC (Figure 3.21).



**Figure 3.21:** Structures of the regio- and stereoisomers isolated from reaction of **103** with 4-nitrobenzaldehyde dimethyl acetal, according to Table 3.10, Entry 1.

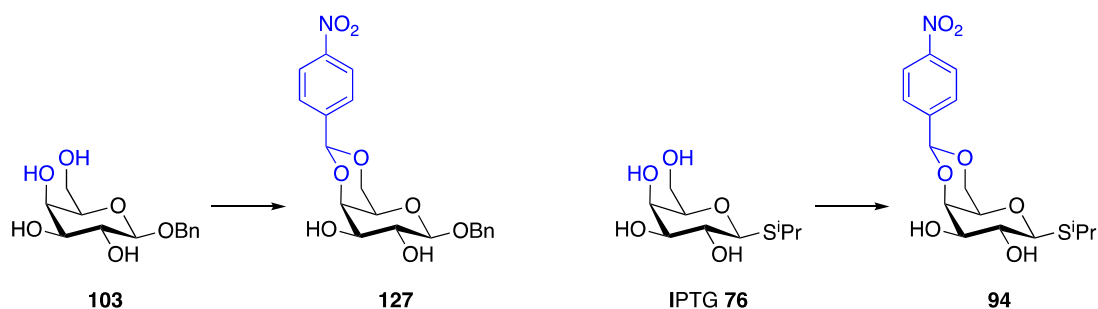


To distinguish between the stereoisomers **127** and **258**, Nuclear Overhauser Effect Spectroscopy (NOESY) was employed. This experiment identified a through space correlation between the equatorial 4-position proton and the 7-position proton of the 4-nitrobenzylidene group in **127** (Figure 3.22).



**Figure 3.22:** The 2D Nuclear Overhauser Spectroscopy (NOESY) spectrum ( $\text{CDCl}_3$ , 500 MHz) for **127**, showing the through space correlation between the equatorial 4-position proton and the 7-position proton of the 4-nitrobenzylidene group.

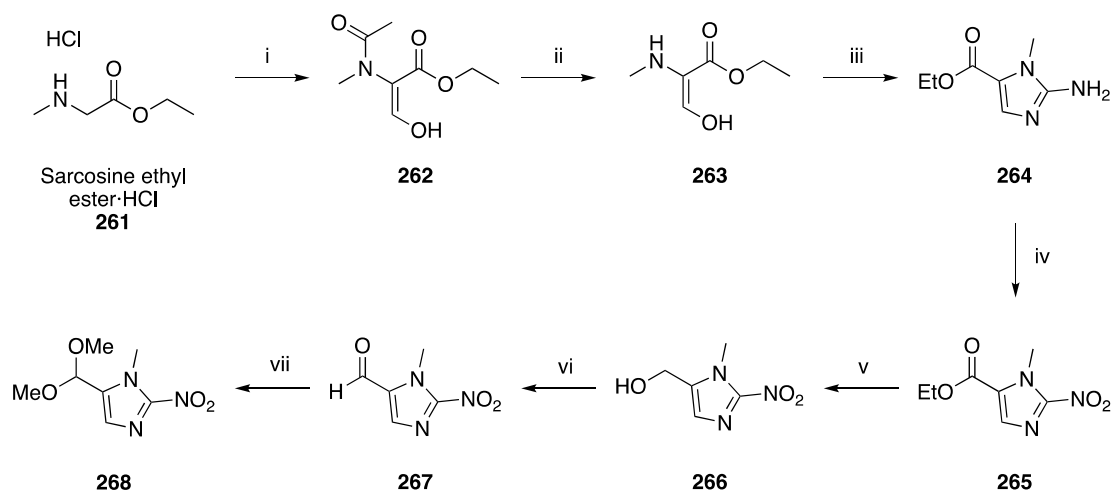
Smith *et al.* have reported the use of indium triflate to mediate formation of cyclic acetals in high yields, under solvent free conditions, and have shown its applicability for a range of substituted acetals, including **257**.<sup>357</sup> Therefore, these conditions were trialled for the synthesis of **127** (Table 3.10, Entry 2). Although the yield increased to 38%, as before, a range of regioisomers were isolated as side products. It was therefore decided, that whilst a sufficient quantity of **127** had been purified for our purposes, alternative conditions would be preferable for the synthesis of **94**. Acid-catalysed acetal formation with either ( $\pm$ )-CSA in  $\text{DMF}$ <sup>358</sup> (Table 3.10, Entry 3) or 4-TsOH  $\cdot$   $\text{H}_2\text{O}$  in dichloromethane<sup>359</sup> (Table 3.10, Entry 4) afforded improved yields of **94**.

**Table 3.10:** Summary of reaction conditions for the synthesis of the 4,6-acetal 4-nitrobenzylidene compounds **94** and **127**.

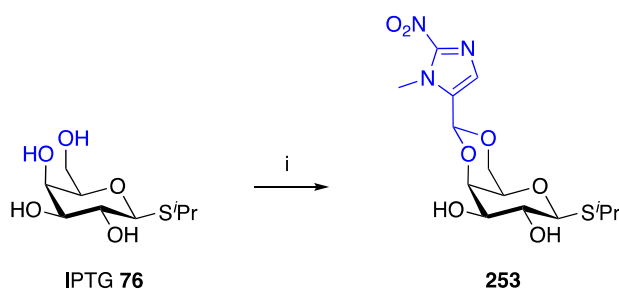
Entry	Substrate	Reagent	Eq.	Solvent	Temp. °C	Yield %
1	<b>103</b>	4-NO <sub>2</sub> Ph(OMe) <sub>2</sub> 4-TsOH·H <sub>2</sub> O	1.1 0.1	MeCN	RT	28
2	<b>103</b>	4-NO <sub>2</sub> Ph(OMe) <sub>3</sub> In(OTf) <sub>3</sub>	15 0.25	-	RT	38
3	<b>76</b>	4-NO <sub>2</sub> Ph(OMe) <sub>3</sub> (±)-CSA	2.0 0.04	DMF	60	58
4	<b>76</b>	4-NO <sub>2</sub> Ph(OMe) <sub>3</sub> 4-TsOH·H <sub>2</sub> O	1.7 0.04	CH <sub>2</sub> Cl <sub>2</sub>	RT	59

### 3.9.2. Synthesis of 2-Nitroimidazole 4,6-Acetal IPTG

For the synthesis of **253**, it was first necessary to synthesise the 2-nitroimidazole transacetalisation reagent **268** (Scheme 3.35). The 2-nitroimidazole aldehyde **267** was synthesised in four steps from sarcosine ethyl ester hydrochloride **261**, according to conditions previously developed in our lab.<sup>233</sup> Briefly, in a one pot reaction **261** was formylated at both the  $\alpha$ -carbon and secondary amine to afford intermediate **262**, the amine formyl group was removed with aqueous HCl to form **263**, and cyclisation upon treatment with cyanamide under reflux yielded **264**. Diazotisation with a saturated aqueous solution of sodium nitrite afforded **265**, which was reduced to the alcohol **266** with sodium borohydride in THF. Re-oxidation to the aldehyde with manganese dioxide afforded **267**, which was converted to the dimethyl acetal **268** with trimethyl orthoformate in methanol. Subsequently, reaction of **268** with IPTG **76**, employing the conditions that had previously been used for the synthesis of **94**, yielded **253** in 73% yield (Scheme 3.36).



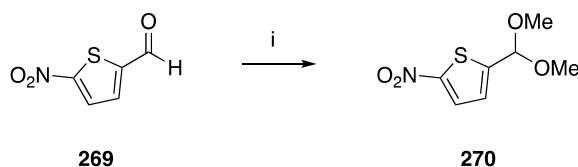
**Scheme 3.35:** Synthesis of **268**.<sup>233</sup> *Reagents and conditions:* i) EtOCHO, NaH, THF, 45 min–4.5 h; ii) conc. aq. HCl, EtOH, reflux, 2 h; iii) NH<sub>2</sub>CN, EtOH, H<sub>2</sub>O, pH 3, reflux, 1.5 h; 23–50% (three steps); iv) NaNO<sub>2</sub>, AcOH, 0 °C–RT, 2–16 h, 50–59%; v) NaBH<sub>4</sub>, MeOH, THF, 0 °C, 45 min then RT, 2–5 h, 60–92%; vi) MnO<sub>2</sub>, CHCl<sub>3</sub>, reflux, 16 h, 79%; vii) CH(OMe)<sub>3</sub>, 4-TsOH·H<sub>2</sub>O, MeOH, reflux, 14 h, 85%.



**Scheme 3.36:** Synthesis of **253**. *Reagents and conditions:* i) **268**, 4-TsOH·H<sub>2</sub>O, CH<sub>2</sub>Cl<sub>2</sub>, reflux, 7.5 h, 73%.

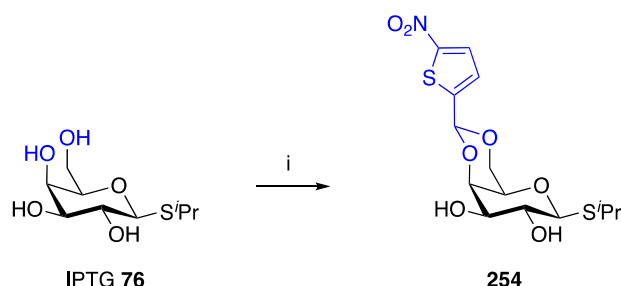
### 3.9.3. Synthesis of 5-Nitrothiophene 4,6-Acetal IPTG

For the synthesis of **254** the 5-nitrothiophene transacetalisation reagent **270** was synthesised in one step from 5-nitro-2-thiophenecarboxaldehyde **269** (Scheme 3.37).



**Scheme 3.37:** Synthesis of **270**. *Reagents and conditions:* i) CH(OMe)<sub>3</sub>, 4-TsOH·H<sub>2</sub>O, MeOH, reflux, 16 h, 96%.

Compound **270** was then reacted with **76**, using the same conditions as described above, affording **254** in 62% yield (Scheme 3.38).



**Scheme 3.38:** Synthesis of **254**. *Reagents and conditions:* i) **270**, 4-TsOH·H<sub>2</sub>O, CH<sub>2</sub>Cl<sub>2</sub>, reflux, 22 h, 62%.

### 3.10. Conclusion

In conclusion, the aim of the work described in this chapter was to synthesise derivatives of IPTG that could function as hypoxia-activated inducers of gene expression. Additionally, in order to facilitate downstream biological analysis of these compounds, an alternative group of analogues, each containing an anomeric UV-active moiety, was sought.

First, in order to identify an alternative inducer to IPTG **76** that contained an anomeric UV-active group, **103** and **104** were synthesised. These compounds were analysed for their ability to induce expression of sfGFP under normoxic conditions. It was found that **103** was a more potent inducer than **104**; therefore, derivatives containing an anomeric benzyl group were targeted for synthesis.

Analysis of a 2 Å crystal structure of IPTG **76** bound to the *lac* repressor suggested that all of the hydroxyl groups of IPTG **76** formed important interactions with the protein either directly or through water-mediated hydrogen bonds. As such, it was unclear where the optimal position for inclusion of a bioreductive protecting group would be and it was decided to synthesis derivatives of IPTG, protected at each of the free hydroxyl groups (2-, 3-, 4-, 6- position). Additionally, based on previous work on light-activated derivatives of IPTG by Young and Deiter,<sup>236</sup> compounds **94**, **127**, **253** and **254**, each containing a bioreductive moiety attached *via* an acetal linkage, were designed as alternative hypoxia-activated inducers of gene expression (Figure 3.23).

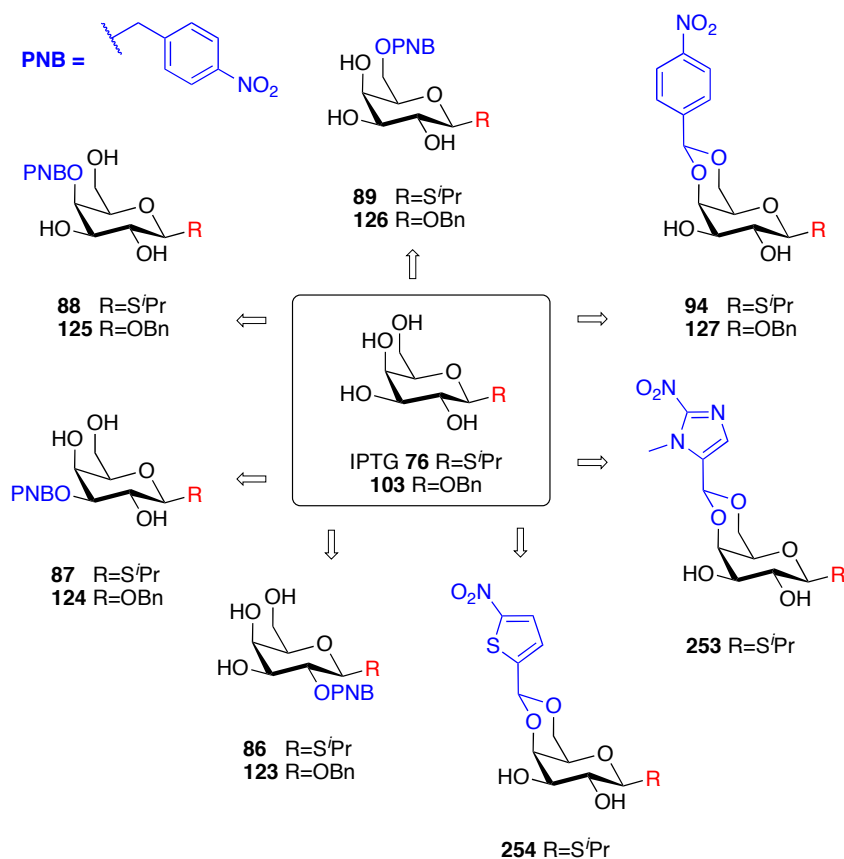
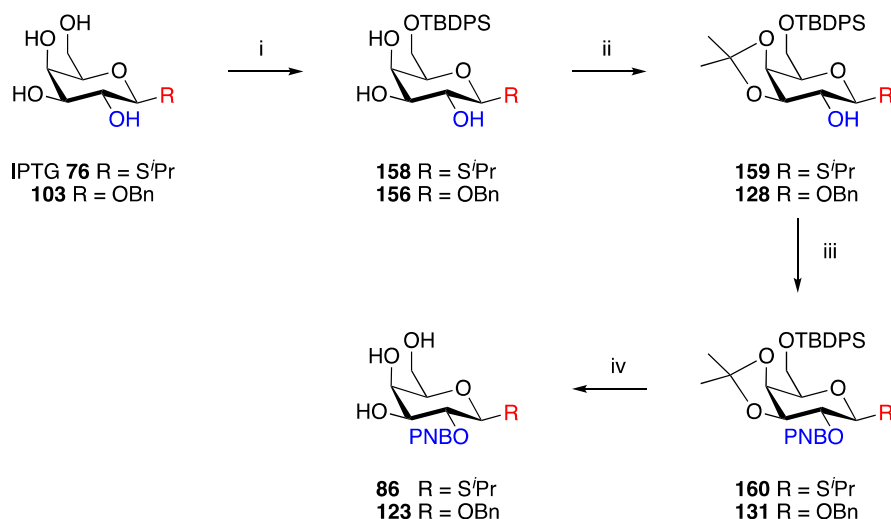


**Figure 3.23:** Overview of potential hypoxia-activated inducers of gene expression, containing either an anomeric benzyl or anomeric thioisopropyl group, the syntheses of which were described in this chapter. R = S<sup>i</sup>Pr or OBn.

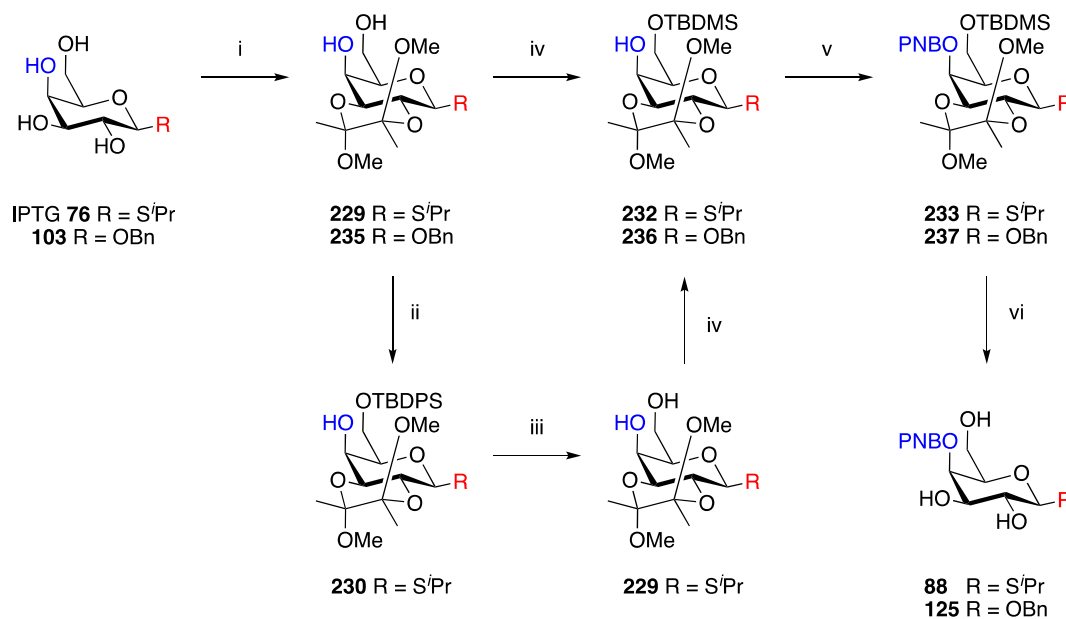
A number of methods were investigated for attachment of a bioreductive 4-nitrobenzyl group and the use of freshly prepared silver oxide in cyclohexane was identified as the most appropriate for our purposes.

A range of protecting group strategies were then explored for the synthesis of each compound and it was found that the silver oxide alkylation conditions precluded the use of base labile protecting groups, such as acetyl or benzoyl groups.

Accordingly, 2- (**86** and **123**) and 4-position (**88** and **125**) protected inducers were synthesised by silyl protection of the primary C6-OH group and acetal protection of either the *cis* C3-OH and C4-OH groups (2-position inducers. Scheme 3.39) or the *trans* C2-OH and C3-OH groups (4-position inducers, Scheme 3.40).

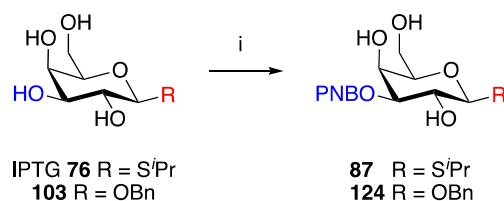


**Scheme 3.39:** Synthesis of 2-position protected inducers **86** and **123**. *Reagents and conditions:* i) TBDPSCl, imidazole, DMF, RT, **158**: 7 h, 59%, **156**: 4–5 h, 53–81%; ii) C(CH<sub>3</sub>)<sub>2</sub>(OCH<sub>3</sub>)<sub>2</sub>, 4-TsOH·H<sub>2</sub>O, acetone, RT, **159**: 1–2 h, 93–99%, **128**: 2 h, 93–99%; iii) 4-NO<sub>2</sub>BnBr **80**, Ag<sub>2</sub>O, 4 Å MS, dark, cyclohexane, reflux, **160**: 17.5 h, 87%, **131**: 16 h, 91%; iv) AcCl, RT, **86**: CH<sub>2</sub>Cl<sub>2</sub>:MeOH (2:1), 15 h, 85%, **123**: MeOH, 33 h, 59%. R = S'Pr or OBn; PNB = 4-nitrobenzyl.

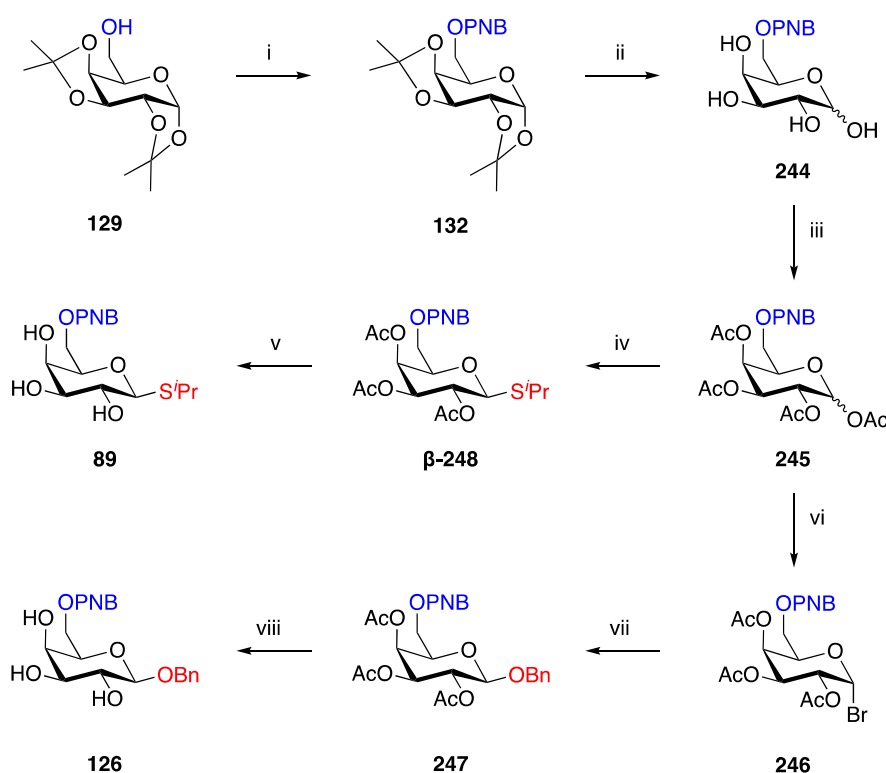


**Scheme 3.40:** Synthesis of 4-position protected inducers **88** and **125**. *Reagents and conditions:* i) 2,3-Butanedione, (±)-CSA, CH(OMe)<sub>3</sub>, MeOH, reflux, **235**: 15.5 h, 62%, **229**: 17.5 h then ii) TBDPSCl, 4-DMAP, pyridine, 50 °C, 7 h, **230**: 45% (2 steps); iii) TBAF, THF, RT, 2 h, 84%; iv) TBDMSCl, 4-DMAP, pyridine, 0 °C–RT, **232**: 43.5 h, 99%, **236**: 3.5 h, 81%; v) 4-NO<sub>2</sub>BnBr **80**, Ag<sub>2</sub>O, cyclohexane, dark, reflux, **233**: 4 Å MS, 39 h, **237**: 3 Å MS, 68 h; vi) AcOH (80% in water), **88**: reflux, 2.5 h, 19% (2 steps), **125**: 80–100 °C, 1 h, 28% (2 steps). R = S'Pr or OBn; PNB = 4-nitrobenzyl.

Inducers **87** and **124**, protected at the 3-position, were synthesised directly from unprotected galactopyranosides **76** and **103**, though the use of an iron catalyst [Fe(dibm)<sub>3</sub>] (Scheme 3.41).



**Scheme 3.41:** Synthesis of 3-position protected inducers **87** and **124**. *Reagents and conditions:* [Fe(dibm)<sub>3</sub>] **196**, K<sub>2</sub>CO<sub>3</sub>, MeCN:DMF (9:1), 80 °C, **87**: 22–24 h, 35–38%, **124**: 17.5–22 h, 28–37%. R = S<sup>i</sup>Pr or OBn; PNB = 4-nitrobenzyl.

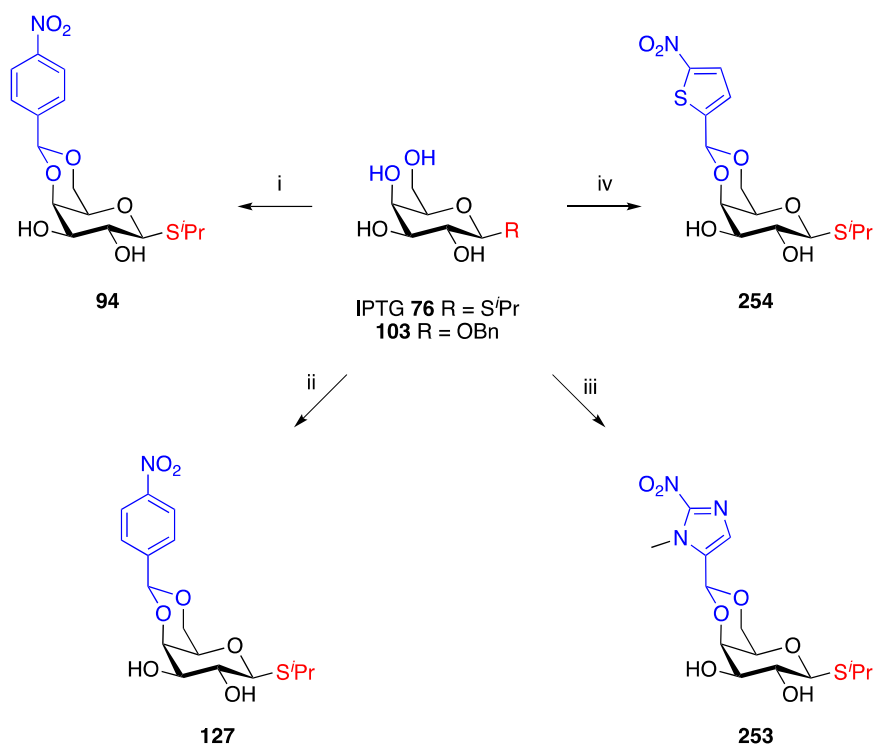


**Scheme 3.42:** Synthesis of 6-position protected inducers **89** and **126**. *Reagents and conditions:* i) 4-NO<sub>2</sub>BnBr **80**, Ag<sub>2</sub>O, 4 Å MS, cyclohexane, dark, reflux, 15 h; ii) TFA (80% aq.), RT, 30 min; iii) Ac<sub>2</sub>O, pyridine, RT, 21–72 h, 52–68% (3 steps); iv) <sup>t</sup>PrSH, BF<sub>3</sub>·Et<sub>2</sub>O, 4 Å MS, CH<sub>2</sub>Cl<sub>2</sub>, RT, 24–48 h, 25–44%; v) NaOMe, MeOH, RT, 16 h, 79%; vi) HBr (33 wt.% in AcOH), RT, 0.5–2 h, 78–88%; vii) BnOH, AgCO<sub>3</sub>, 4 Å MS, dark, CH<sub>2</sub>Cl<sub>2</sub>, RT, 9 h; viii) NaOMe, MeOH, 19.5 h, 76% (2 steps). PNB = 4-nitrobenzyl.

For the synthesis of 6-position protected inducers **89** and **126**, a commercially available 1,2:3,4-di-*O*-isopropylidene galactopyranoside **129** was first alkylated with a 4-nitrobenzyl

group. Then, following standard protecting group manipulations, glycosylation at the anomeric position and deprotection of the acetyl protecting groups afforded **89** and **126** (Scheme 3.42).

Finally, the 4,6-acetal bioreductively-protected inducers **94**, **127**, **253** and **254** were synthesised *via* direct acetal formation from unprotected galactopyranosides **76** and **103** with the appropriate dimethoxy transacetalisation reagent (Scheme 3.43).



**Scheme 3.43:** Synthesis of 4,6-acetal protected inducers **94**, **127**, **253**, and **254**. *Reagents and conditions:* i) 4-NO<sub>2</sub>Ph(OMe)<sub>3</sub>, In(OTf)<sub>3</sub>, RT, 17.5 h, 38%; ii) 4-NO<sub>2</sub>Ph(OMe)<sub>3</sub>, (±)-CSA, RT, CH<sub>2</sub>Cl<sub>2</sub>, 23 h, 59%; iii) **268**, 4-TsOH·H<sub>2</sub>O, CH<sub>2</sub>Cl<sub>2</sub>, reflux, 7.5 h, 73%; iv) **270**, 4-TsOH·H<sub>2</sub>O, CH<sub>2</sub>Cl<sub>2</sub>, reflux, 22 h, 62%. R = S<sup>i</sup>Pr or OBn.

Having developed synthetic routes towards all of the targeted potential hypoxia-activated inducers of gene expression, the next step was to analyse them for their ability to undergo bioreduction and to induce gene expression in a cellular setting, specifically under hypoxic conditions. These experiments will be discussed in Chapter 4.



---

# CHAPTER 4

## HYPOXIA-ACTIVATED SMALL MOLECULE-INDUCED GENE EXPRESSION

---

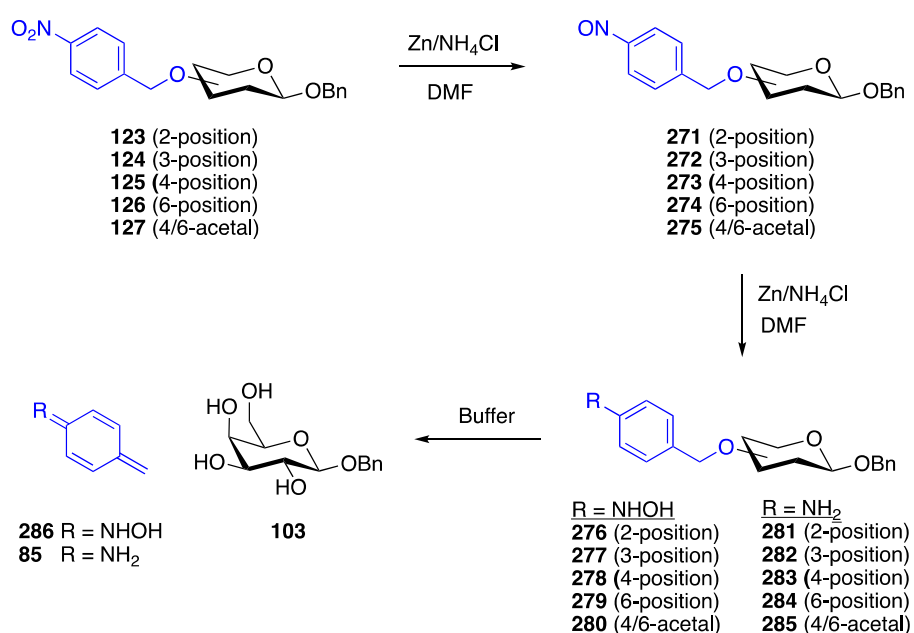
### 4.1. Introduction and Aims

Following the synthesis of potential hypoxia-activated inducers of gene expression **86–89** and **94** and their benzyl analogues **123–127** (Chapter 3, Figure 3.23), the next step was to evaluate these compounds for their ability to induce gene expression in a hypoxia-dependent manner. This chapter will focus on the biological evaluation of each compounds. To determine whether the compounds fragment as expected, our standard series of reduction and bio-reduction assays for analysis of HAPs was followed.<sup>132</sup> The compounds were then analysed in a bacterial setting for hypoxia-dependent gene expression. The last section will discuss steps taken towards transferring the technology into mammalian cancer cell lines.

## 4.2. Reduction and Bioreduction Analysis of 123–127

### 4.2.1. Zinc/ $\text{NH}_4\text{Cl}$ Reduction of 123–127

The first step in the analysis of bioreductive compounds employs reduction with zinc and ammonium chloride in DMF (Scheme 4.1). Compounds **123–127** were treated with zinc and ammonium chloride in DMF over 60 minutes. In each case, a mixture of nitroso **271–275** and hydroxylamine **276–280** intermediates was formed. When an aliquot, taken after 60 minutes of reduction, was added to phosphate buffer, complete loss of the hydroxylamine derivatives **276–280** with a corresponding increase in **103** was observed (Figure 4.1). This demonstrates that, following reduction of the nitro group, fragmentation to release **103** occurs under aqueous conditions.



**Scheme 4.1:** Zinc reduction of 4-nitrobenzyl protected compounds. Reduction proceeds *via* the nitroso (**271–275**) intermediate to form either the hydroxylamine (**276–280**) or amine (**281–285**) derivatives, which are expected to fragment in phosphate buffer to release **103**.

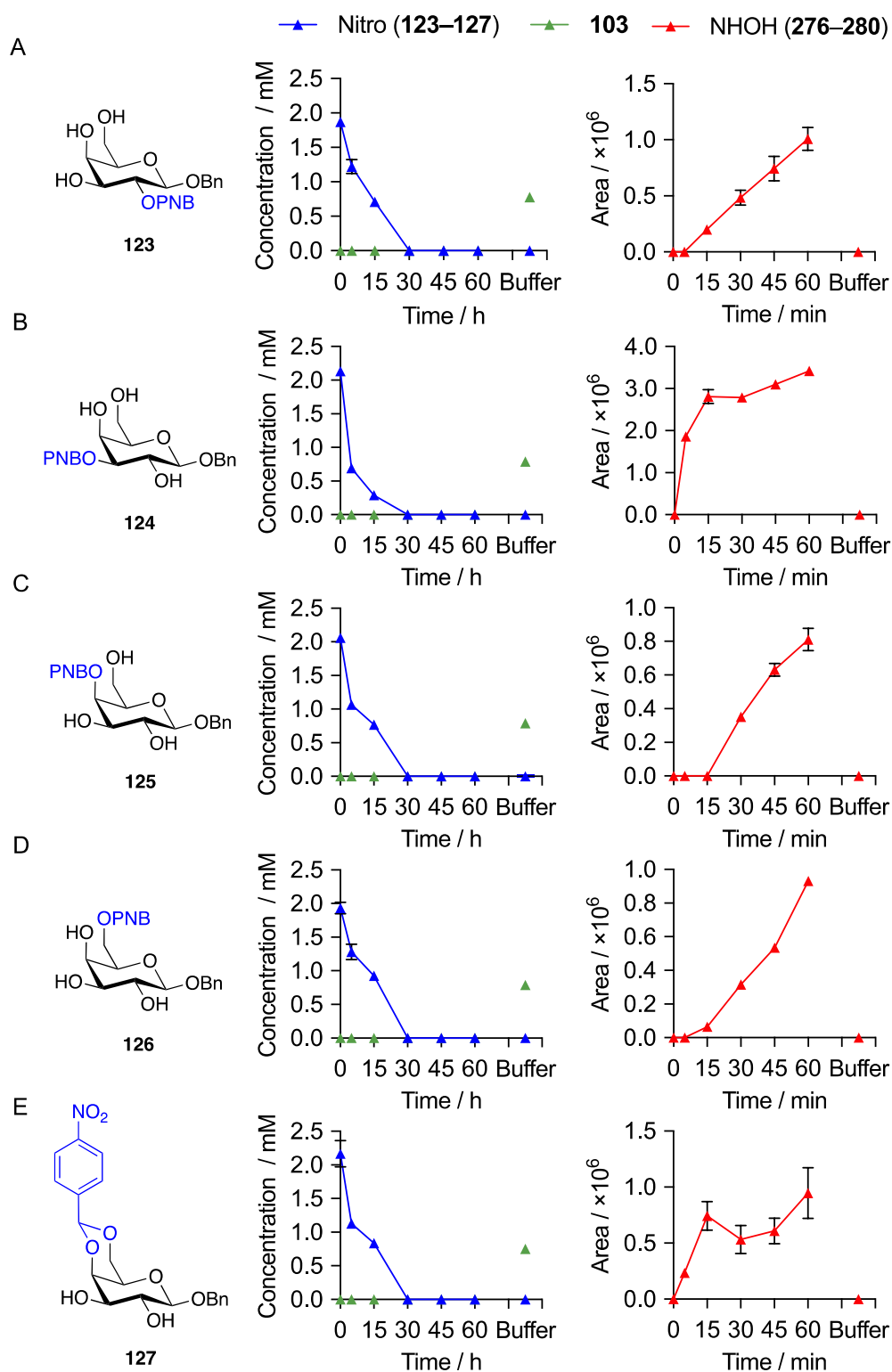


**Figure 4.1:** A–E) Compounds **123–127** (2 mM) were treated with Zn/NH<sub>4</sub>Cl in DMF over 60 min. Aliquots taken at the time indicated were analysed by HPLC-MS. In each case, reduction of the nitro compounds **123–127** and formation of the corresponding hydroxylamine derivatives **276–280** was observed. Addition of a sample of the reduction reaction mixture, taken after 60 min, to buffer resulted in fragmentation of the hydroxylamine derivatives to release **103**. PNB = 4-nitrobenzyl.

#### 4.2.2. Cytochrome P450:NADPH Reductase Treatment of 123–127

Compounds **123–127** were next treated with CYP450:NADPH reductase enzymes in phosphate buffer under normoxic (21% O<sub>2</sub>) and hypoxic (<0.1% O<sub>2</sub>) conditions.<sup>132</sup> Samples taken at the time points indicated were analysed by HPLC-MS.

For all compounds (**123–127**) no changes were detected after 48 hours in the normoxia samples, suggesting that all of the compounds are stable to normoxic conditions. On the other hand, under hypoxic conditions, reduction to the hydroxylamine **276–280** and amine **281–285** derivatives, followed by fragmentation to release 10–20% **103** was observed (Figure 4.3). It should be noted that when **127** was tested at a concentration of 10  $\mu$ M, negligible release of **103** was detected (Figure 4.2). This suggests that, in this enzyme assay, the acetal is a less effective substrate for the enzyme and that the compound fragments more slowly than compounds **123–126**. To overcome this detection problem, and to determine whether any fragmentation was occurring, compound **127** was assessed at a concentration of 20  $\mu$ M (Figure 4.3E). For the ether compounds **123–126**, the differing amounts of each compound released can be attributed to the difference in enzyme activity on these substrates, as the leaving group ability of each of the hydroxyl groups, and hence propensity of the compound to fragment, is expected to be very similar.

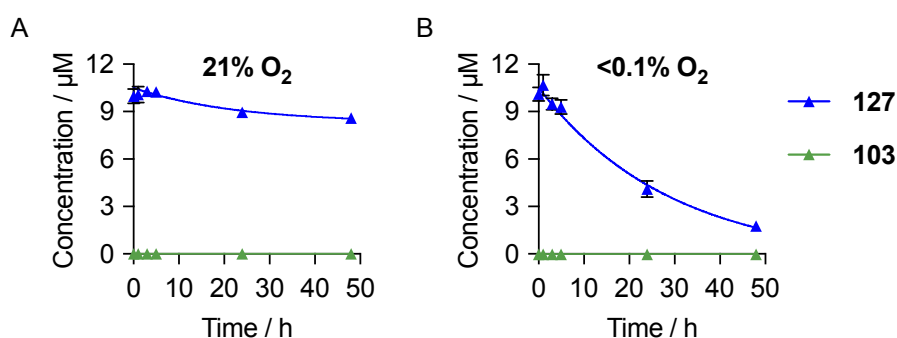


**Figure 4.2:** Compound **127** (10  $\mu$ M) was treated with CYP450:NADPH reductase enzymes under A) normoxic (21% O<sub>2</sub>) and B) hypoxic (<0.1% O<sub>2</sub>) conditions over 48 h. Aliquots taken at the time indicated were analysed by HPLC-MS. Although **127** was stable in normoxia (21% O<sub>2</sub>) and selectively reduced in hypoxia (<0.1% O<sub>2</sub>), release of **103** was not detected.

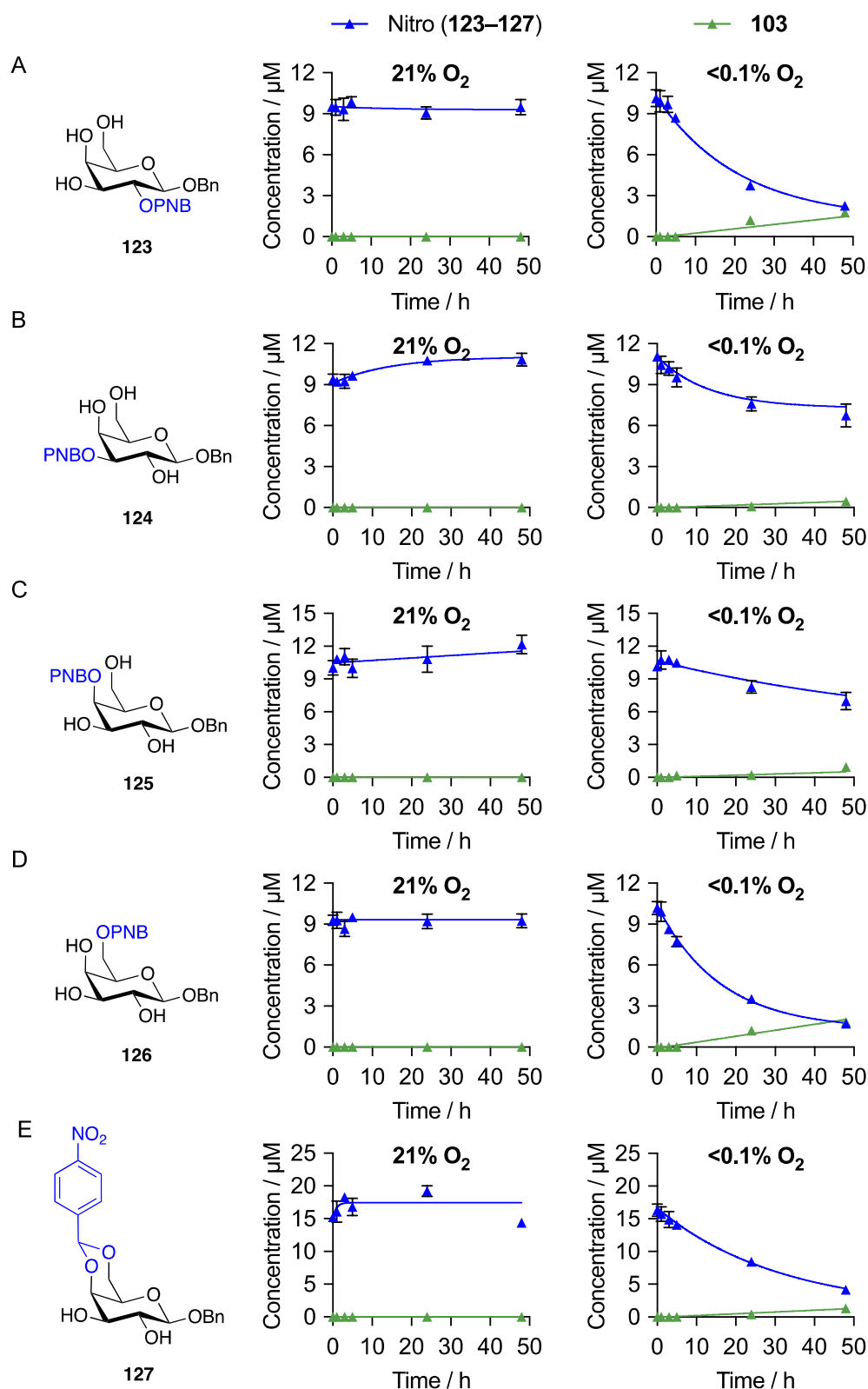


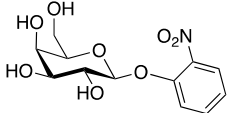
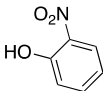
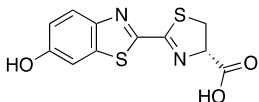
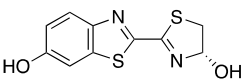
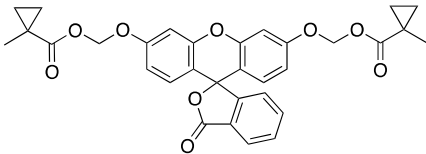
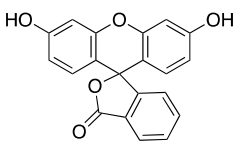
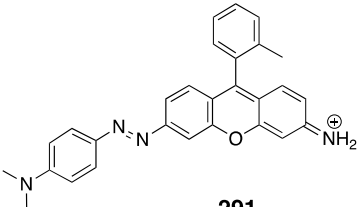
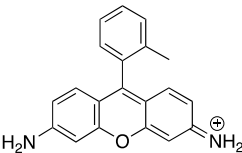
**Figure 4.3:** Compounds **123–127** are reduced selectively in hypoxia. A–E) Compounds **123–126** (10 μM) and **127** (20 μM) were treated with CYP450:NADPH reductase enzymes under normoxic (21% O<sub>2</sub>) and hypoxic (<0.1% O<sub>2</sub>) conditions over 48 h. Aliquots taken at the time indicated were analysed by HPLC-MS. All compounds were stable in normoxia (21% O<sub>2</sub>) but were selectively reduced in hypoxia (<0.1% O<sub>2</sub>), releasing 10–20% **103**.

### 4.3. Hypoxia-Activated Gene Expression in *BL21 (DE3)* Bacteria

#### 4.3.1. Choice of Reporter System for Gene Expression

Given that all compounds underwent hypoxia-dependent reduction and fragmentation, the next step was to evaluate their ability to selectively induce gene expression under hypoxic conditions. The first consideration for these experiments was the choice of reporter gene, which would determine the readout for successful gene expression. There are a number of reporter systems that are used to detect gene expression. These typically rely on either expression of an enzyme, which reacts with an exogenous substrate to form a product that is readily detected, or direct expression of a fluorescent protein.<sup>360</sup> Some examples of these enzyme substrate pairs are shown in Table 4.1.

**Table 4.1:** Literature examples of enzyme-substrate pairs that are used in reporter systems for gene expression.

Enzyme	Substrate	Product	Detection Method
$\beta$ -Galactosidase <sup>361</sup>	 <b>111</b>	 <b>286</b>	Absorbance $\lambda_{\text{max}} = 420 \text{ nm}$
Luciferase <sup>362</sup>	 <b>D-Luciferin 287</b>	 <b>Oxyluciferin 288</b>	Luminescence $\lambda_{\text{max}} = 560 \text{ nm}$
Porcine Liver Esterase <sup>363</sup>	 <b>289</b>	 <b>290</b>	Fluorescence $\lambda_{\text{ex}} = 490 \text{ nm}$ $\lambda_{\text{em}} = 525 \text{ nm}$
Azoreductase <sup>364</sup>	 <b>291</b>	 <b>292</b>	Fluorescence $\lambda_{\text{ex}} = 498 \text{ nm}$ $\lambda_{\text{em}} = 515 - 600 \text{ nm}$

Enzyme substrate pairs only provide an indirect readout of gene expression due to their requirement for secondary activation of an exogenous substrate that must be added to the

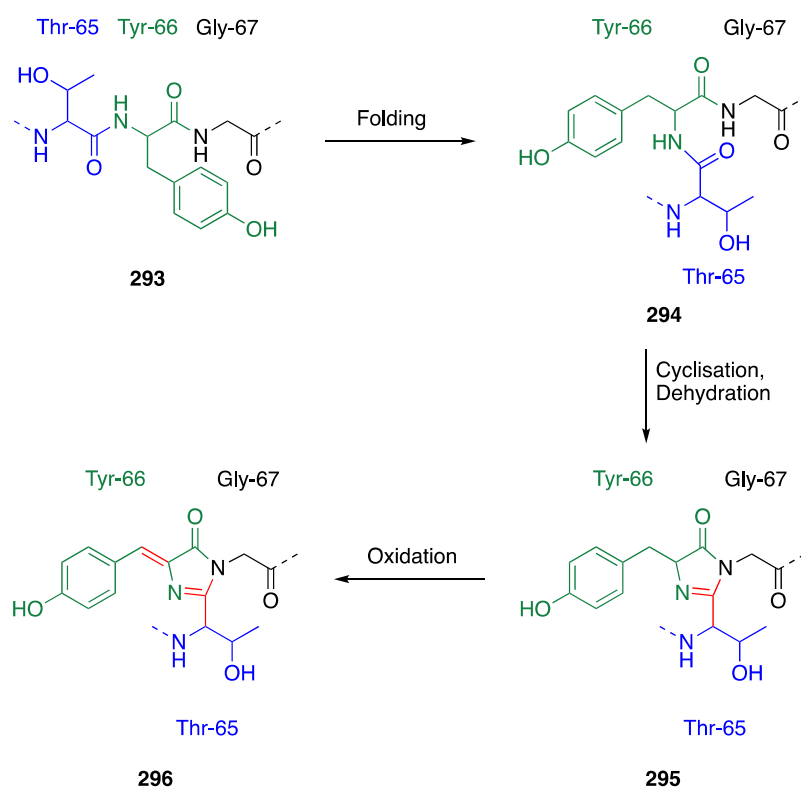
experiment. Therefore, it was decided that, for our purposes, it would be preferable to directly express a fluorescent protein and use fluorescence measurements as the primary indicator of gene expression.

A green fluorescent protein (GFP) was first isolated from *Aequorea victoria* in 1962<sup>365</sup> and, along with other fluorescent proteins derived from GFP, is now one of the mostly widely employed fluorescent proteins in biology (Table 4.2).<sup>366,367</sup>

**Table 4.2:** Summary of the most commonly employed GFP-based fluorescent proteins.<sup>367</sup>

Name	$\lambda_{\text{ex}}$ max nm	$\lambda_{\text{em}}$ max nm	Quantum Yield	Relative Brightness % of EGFP
mTagBFP	399	456	0.63	98
mTurquoise	434	474	0.84	75
mEGFP	488	507	0.60	100
mVenus	515	528	0.57	156
mCherry	587	610	0.22	47
mKate2	588	633	0.40	74

However, the use of GFP and its derivatives in hypoxia is complicated by their intrinsic dependence on molecular oxygen.<sup>368,369</sup> The chromophore of GFP is formed from three residues: Ser-65, Tyr-66, and Gly-67 **293**. Chromophore formation occurs in a three-step intramolecular reaction: protein folding **294**, cyclisation of the tripeptide through nucleophilic attack of Gly-67 amide on the Ser-65 carbonyl to form the imidazolinone **295**, and finally dehydrogenation of the  $\alpha,\beta$  bond of Tyr-66 by molecular oxygen, to form a conjugated system between the aromatic group and imidazolinone (**296**) (Scheme 4.2).<sup>366,369,370</sup> Furthermore, this oxygen-mediated dehydrogenation step is the slowest step of chromophore formation, meaning that, typically, a substantial reoxygenation period is required.<sup>370</sup> Therefore, initially fluorescent proteins without this dependence on molecular oxygen were investigated.



**Scheme 4.2:** Mechanism for GFP chromophore formation. Folding of the protein positions the Gly-67 amide for nucleophilic attack on the Ser-65 carbonyl to form the imidazolinone **295**. Dehydrogenation of the  $\alpha,\beta$  bond of Tyr-66 by molecular oxygen forms a conjugated system between the aromatic group and imidazolinone.<sup>369,370</sup>

#### 4.3.2. Flavin-Binding Fluorescent Proteins

The most promising class of alternative fluorescent proteins are those based on the flavin-binding light, oxygen, or voltage (LOV) sensing domain (FbFPs).<sup>371</sup> Developments in this class of fluorescent proteins, and their advantages and disadvantages have been reviewed recently.<sup>372,373</sup> FbFPs are smaller than GFP (typically between 12 and 16 kDa for FbFPs compared with 27 kDa for GFP),<sup>372</sup> exhibit fast maturation of fluorescence,<sup>374</sup> and, crucially, fluoresce in an oxygen-independent manner.<sup>375</sup>

Initially, two FbFPs, iLOV<sup>376</sup> and creiLOV,<sup>377</sup> were chosen as potential reporters for gene expression. iLOV is a monomeric protein (12.1 kDa) that was first derived from the LOV domain of phototropin (a blue light receptor) in *Arabidopsis thaliana*. It is reported to have greater brightness and enhanced tolerance to variations in temperature and pH compared with other reported FbFPs, such as EcFbFP and PpFbFP.<sup>374,375</sup> Recently, creiLOV, a novel FbFP, engineered



from *Chlamydomonas reinhardtii*, was identified. Like iLOV, it is monomeric (13.0 kDa) and exhibits high levels of thermal stability. It is also brighter, has a higher quantum yield and improved pH tolerance compared with iLOV. However, overexpression of medium to high levels of creiLOV was shown to impose a greater metabolic burden on cells, which resulted in drastically reduced growth rate.<sup>377</sup> Coding sequences corresponding to iLOV and creiLOV were purchased from ThermoFisher Scientific (GeneArt Strings) and inserted downstream of an IPTG-inducible promoter in the pNIC28-Bsa4 expression vector (Section 6.4).<sup>262</sup> The resulting plasmids were transformed into *BL21 (DE3) E. coli*.

#### **4.3.3. Expression of pNIC28-iLOV and pNIC28-creiLOV**

First, expression of iLOV and creiLOV with IPTG **76** under both normoxic (21%) and hypoxic (<0.1%) conditions was investigated. Promisingly, when *BL21 (DE3)* pNIC28-iLOV bacteria and *BL21 (DE3)* pNIC28-creiLOV bacteria were incubated with 1 mM IPTG **76** for 5 hours, there was comparable fluorescence between the normoxic and hypoxic treated cells. (Figure 4.4A, Figure 4.4C). Western blot analysis indicated that there were similar levels of iLOV expression between the normoxic and hypoxic induced samples, suggesting that fluorescence could be used as a reliable measure for iLOV expression (Figure 4.4B, Figure 4.4D).

## iLOV

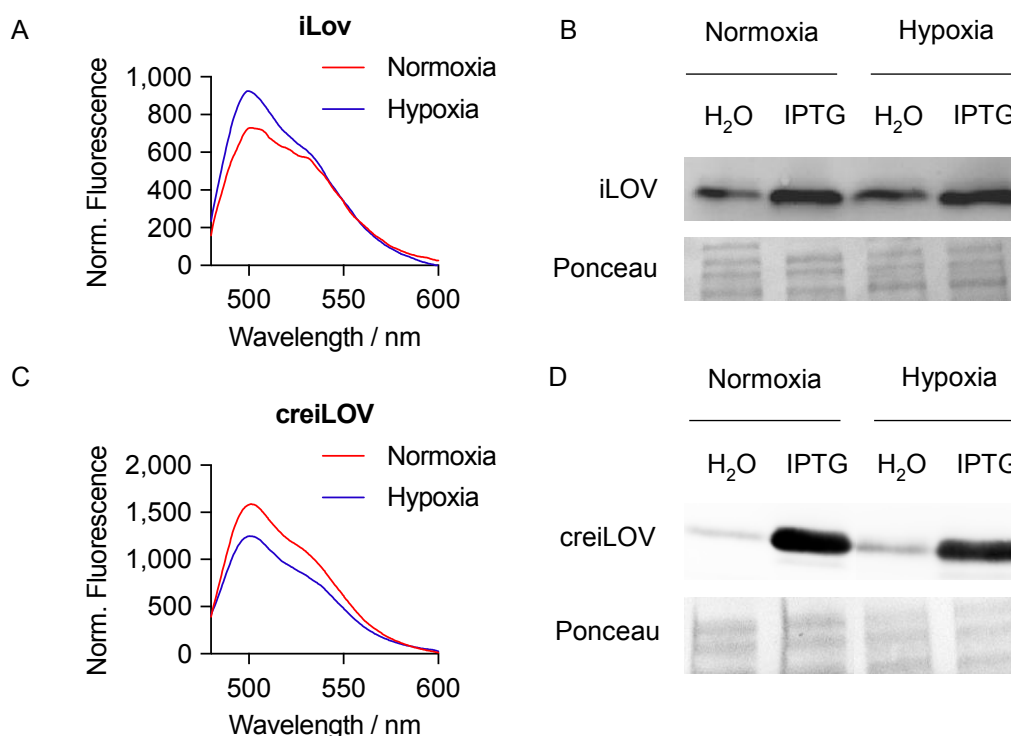


**Figure 4.4:** Overexpression of iLOV (A/B) and creiLOV (C/D) shows comparable fluorescence under normoxic and hypoxic conditions after 5 h induction. A/C) Fluorescence spectra of induced cells. *BL21 (DE3)* pNIC28-iLOV bacteria (A) or *BL21 (DE3)* pNIC28-creiLOV bacteria (C) were treated with water or IPTG **76** (1 mM) for 5 h under normoxic (21% O<sub>2</sub>) or hypoxic (<0.1% O<sub>2</sub>) conditions. Samples were analysed by fluorescence ( $\lambda_{\text{ex}} = 450 \text{ nm}$ , PBS). Fluorescence was divided by the optical density at 600 nm and adjusted for background fluorescence by subtracting the fluorescence of uninduced cells from that of induced cells. Normoxic and hypoxic samples show similar levels of fluorescence. B/D) Conditions as in (A/C). Western blot analysis of induced and uninduced bacteria. Ponceau staining is shown as a loading control. Both uninduced and induced cells show expression of iLOV, although a greater amount of iLOV is detected for induced cells.

Higher levels of fluorescence were observed in the creiLOV samples than in the iLOV samples, suggesting that, as reported, creiLOV is brighter than iLOV. Unfortunately, in both cases there was a high level of background expression in uninduced cells (Figure 4.5), which also grew noticeably more slowly than non-transformed bacteria. Furthermore, when *BL21 (DE3)* pNIC28-creiLOV bacteria were treated with DMSO or IPTG **76** for 24 hours, which was hypothesised to be a more appropriate time frame than 5 hours for hypoxia-activated gene

expression, only small differences in fluorescence between the uninduced and induced samples were observed (Figure 4.6). Potential hypoxia-activated inducers **86–89** and **94** are unlikely to induce levels of gene expression higher than that observed with free IPTG **76**. The absence of large increases in fluorescence upon induction with IPTG **76** was expected to make it more difficult to detect any fluorescence changes during analysis of **86–89** and **94**. Consequently, it was concluded that the pNIC28-iLOV and pNIC28-creiLOV expression vectors were unsuitable for our purposes.

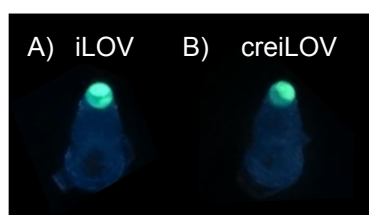


**Figure 4.5:** Background expression of A) iLOV (left) and B) creiLOV (right). 1 mL of an overnight culture of *BL21 (DE3)* pNIC28-iLOV or *BL21 (DE3)* pNIC28-creiLOV was pelleted and visualised under UV light ( $\lambda_{\text{ex}} = 365 \text{ nm}$ ). In both cases, fluorescence was observed despite the absence of IPTG **76**.

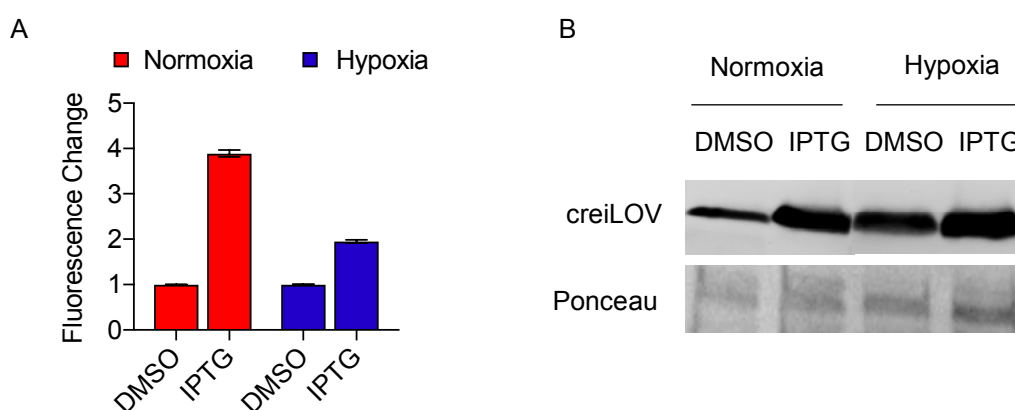


**Figure 4.6:** Small increases in creiLOV expression are observed between induced and uninduced samples after 24 h induction. A) *BL21 (DE3)* pNIC28-creiLOV bacteria were treated with DMSO or IPTG **76** (1 mM) for 24 h under normoxic (21% O<sub>2</sub>) or hypoxic (<0.1% O<sub>2</sub>) conditions. Samples were analysed by fluorescence ( $\lambda_{\text{ex}} = 485 \text{ nm}$ ;  $\lambda_{\text{em}} = 520 \text{ nm}$ , PBS). Fluorescence was divided by the optical density at 600 nm and normalised to the relevant DMSO control. B) Conditions as in (A). Western blot analysis of induced and uninduced bacteria. Ponceau staining is shown as a loading control.

#### 4.3.4. Expression of pT5-iLOV

There are a number of changes that can be made to the expression vector in order to reduce background expression, including changing the promoter of the gene of interest,<sup>378–380</sup> changing the sequence of *lacO*,<sup>381,382</sup> or increasing the strength of the promoter of the LacI gene.<sup>210,383</sup> These changes either affect the strength of LacI binding to *lacO* or change the total number of LacI molecules present in the cell, resulting in tighter repression in the uninduced state. An alternative promoter, based on a T5 promoter that has been employed in studies of FbFPs under hypoxic conditions, was designed and cloned into the pNIC28-vector in place of the previous T7 promoter (Section 6.4).<sup>374,377</sup> This promoter incorporated one *lacO* sequence within the promoter and a second, symmetrical *lacOP* sequence directly downstream of the promoter.<sup>210</sup> The symmetrical *lacOP* sequence has been shown to stabilise the binding of LacI to *lacO*, thereby decreasing background expression (Figure 4.7).<sup>382</sup> The resulting plasmid, designated pT5-iLOV, was transformed into both *BL21 (DE3)* bacteria.

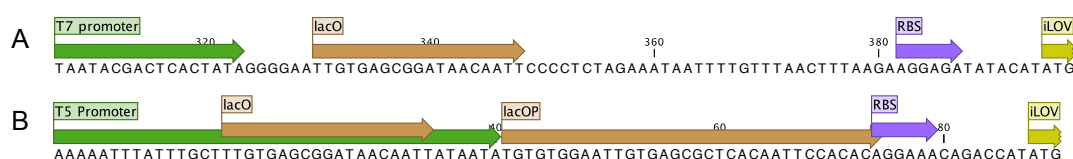


**Figure 4.7:** Design of the T5 promoter. A) T7 promoter present on the pNIC28-vector. B) T5 promoter, containing an additional *lacOP* sequence downstream of the promoter sequence.

Although these changes successfully reduced background expression, the increased affinity of LacI for *lacO* meant that derepression upon addition of IPTG **76** was less efficient. In particular, in hypoxia, only low levels of iLOV induction were observed (Figure 4.8). Therefore, it was concluded that this vector was unsuitable for our purposes.

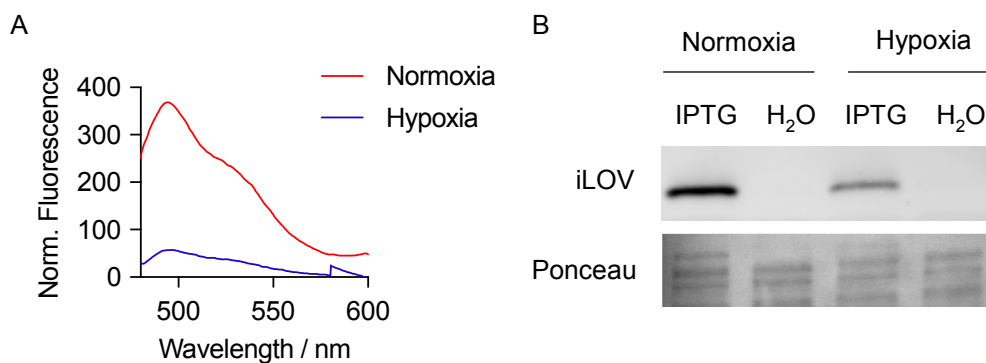


**Figure 4.8:** Overexpression of iLOV under normoxic (21% O<sub>2</sub>) and hypoxic (<0.1% O<sub>2</sub>) conditions after 24 h induction. A) *BL21 (DE3)* pT5-iLOV bacteria were treated with water or IPTG **76** (1 mM) for 24 h under normoxic or hypoxic conditions. Samples were analysed by fluorescence ( $\lambda_{\text{ex}} = 450$  nm, PBS). Fluorescence was divided by the optical density at 600 nm and adjusted for background fluorescence by subtracting the fluorescence of uninduced cells from that of induced cells. B) Conditions as in (A). Western blot analysis of uninduced and induced bacteria. Ponceau staining is shown as a loading control. No background expression is observed, however, the IPTG-treated hypoxic samples show reduced expression levels compared with the IPTG-treated normoxic samples.

#### 4.3.5. Expression of pNIC28-sfGFP

Due to the low fluorescence of the FbFP proteins observed in induced bacteria compared with uninduced bacteria, an alternative reporter protein was investigated. Despite the associated problems with GFP in hypoxia (see Section 4.3.1), there are a variety of mutations that have been made to the GFP sequence that enhance maturation rates upon reoxygenation.<sup>261</sup> In particular, a superfolder GFP (sfGFP) has been reported to recover >95% of its initial fluorescence within four minutes, when allowed to refold following denaturation with urea. The initial rate of fluorescence recovery for sfGFP was also approximately 3.5-fold faster than an unmutated reporter GFP.<sup>261</sup> Therefore, sfGFP was chosen as the reporter of gene expression and inserted downstream of an IPTG-inducible promoter in the pNIC28-Bsa4 expression vector (Section 6.4).<sup>262</sup> The resulting plasmid was transformed into *BL21 (DE3)*.

The first step was to confirm that sfGFP could be induced with IPTG **76** under both normoxic (21%) and hypoxic (<0.1%) conditions, that there was minimal background expression, and that there was sufficient fluorescence recovery in the hypoxic samples to use fluorescence as a

measure for sfGFP expression. Promisingly, when *BL21 (DE3)* pNIC28-sfGFP bacteria were incubated with IPTG **76** or DMSO for 24 hours under both normoxic and hypoxic conditions, high levels of sfGFP induction were observed in the IPTG-treated samples, with low levels of background expression in the uninduced DMSO control samples (Figure 4.9). However, despite similar levels of sfGFP expression, as determined by western blot analysis (Figure 4.9B), significantly lower fluorescence was observed for the hypoxic samples than for the normoxic samples (Figure 4.9A). This is likely due to insufficient time for sfGFP chromophore formation between the end of the experiment, when the hypoxic samples are first exposed to oxygen, and measurement of the fluorescence.

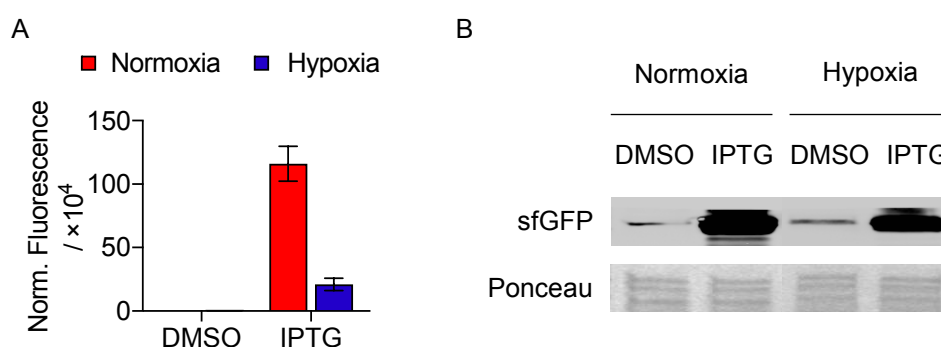


**Figure 4.9:** Overexpression of sfGFP in normoxia (21% O<sub>2</sub>) and hypoxia (<0.1% O<sub>2</sub>). A) *BL21 (DE3)* pNIC28-sfGFP bacteria were treated with DMSO or IPTG **76** (1 mM) for 24 h in normoxia or hypoxia. Samples were analysed using fluorescence ( $\lambda_{\text{ex}} = 485$  nm;  $\lambda_{\text{em}} = 520$  nm, PBS). Fluorescence was divided by the optical density at 600 nm. The IPTG-treated hypoxic samples show reduced fluorescence levels compared with the IPTG-treated normoxic samples. B) Conditions as in (A). Western blot analysis of uninduced and induced bacteria. Ponceau staining is shown as a loading control. High levels of sfGFP induction were observed in the IPTG **76** samples with low levels of background expression in the uninduced DMSO control samples.

To allow for sufficient time for fluorescence recovery in the hypoxic samples, an additional incubation step in normoxia was included. To determine the optimal time for this incubation, after *BL21 (DE3)* pNIC28-sfGFP had been treated with DMSO or IPTG **76** for 24 hours, all samples were transferred to normoxia and incubated at 37 °C for 0–150 minutes (Figure 4.10). No change in fluorescence was observed for the normoxia samples, suggesting that the additional incubation time does not affect expression levels or fluorescence of sfGFP. In comparison, a rapid increase

in fluorescence was observed for the hypoxic samples. After 30 minutes at 21% O<sub>2</sub>, the fluorescence of the hypoxia samples was equivalent to approximately 50% of that of the normoxia samples and after 60 minutes there was no significant difference between them (Figure 4.10A). However, after 30 minutes, the total amount of sfGFP in the hypoxia samples also started to increase, as determined by western blot analysis (Figure 4.10B). Therefore, a 30-minute reoxygenation period, which would allow enough time for fluorescence recovery in the hypoxia samples, without affecting overall expression levels, was chosen and included at the end of each experiment.

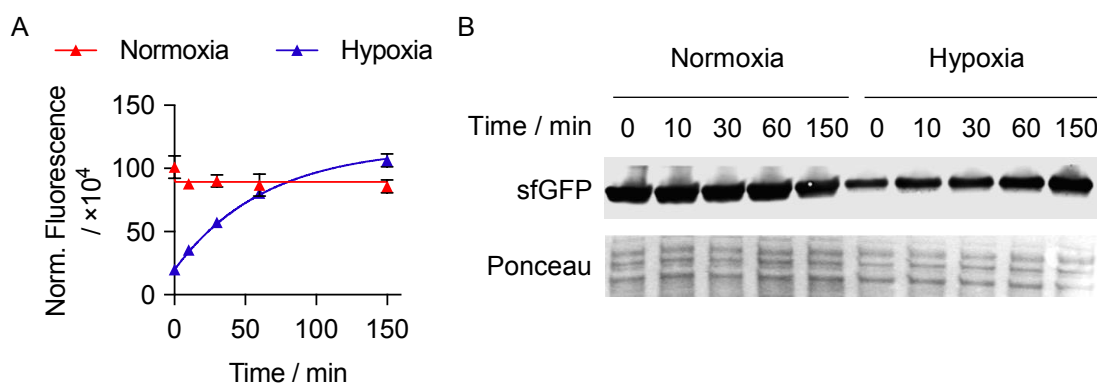


**Figure 4.10:** Fluorescence recovery of sfGFP upon reoxygenation of hypoxia-treated bacteria. A) *BL21 (DE3)* pNIC28-sfGFP bacteria were treated with IPTG **76** (1 mM) for 24 h under normoxic or hypoxic conditions. After this time, all samples were transferred to normoxic conditions and incubated for the time period indicated. Samples were analysed by fluorescence ( $\lambda_{\text{ex}} = 485 \text{ nm}$ ;  $\lambda_{\text{em}} = 520 \text{ nm}$ , PBS). Fluorescence was divided by the optical density at 600 nm. Rapid fluorescence recovery was observed for the hypoxia samples. B) Conditions as in (A). Western blot analysis of sfGFP expression in reoxygenated bacteria. Ponceau staining is shown as a loading control. After 30 min, the total amount of sfGFP in the hypoxia samples started to increase.

#### 4.3.6. Hypoxia-Dependent Expression of pNIC28-sfGFP

Having identified a reporter gene that could be used to reliably detect gene expression under our conditions, compounds **86–89** and **94** (Figure 4.11) were next tested for their ability to induce gene expression of sfGFP in a hypoxia-dependent manner. It was expected that, if the 4-nitrobenzyl group inhibits binding to LacI, no sfGFP expression would be observed in normoxia (21% O<sub>2</sub>), while in hypoxia (<0.1% O<sub>2</sub>), fragmentation to release IPTG **76** would induce sfGFP

expression and consequently an increase in fluorescence would be observed. The 2-nitroimidazole **253** and 5-nitrothiophene **254** analogues of **94** were also included for analysis.

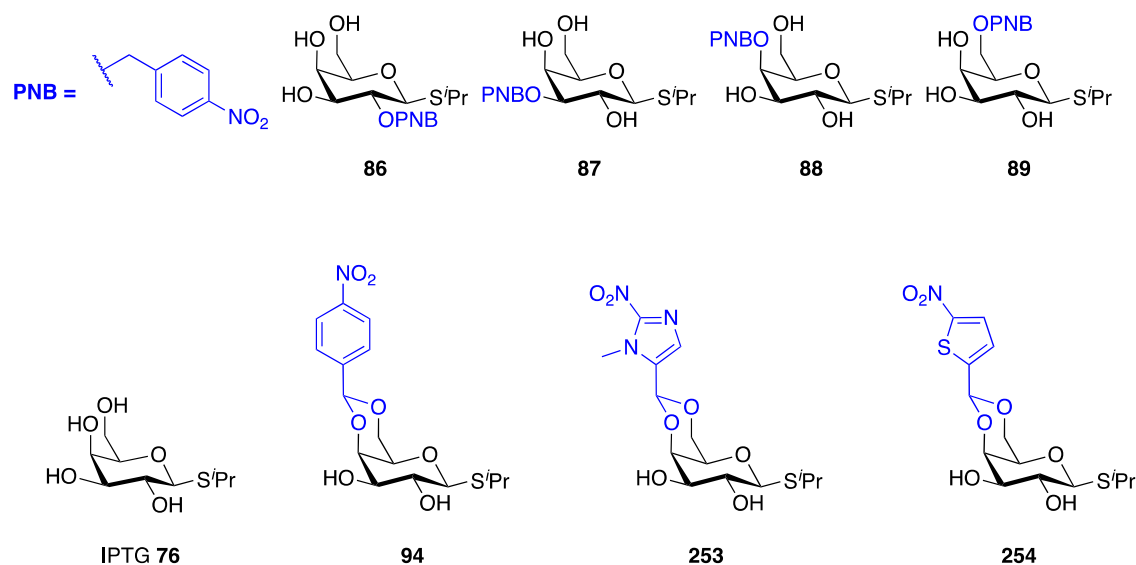


**Figure 4.11:** Structures of IPTG **76** and potential hypoxia-activated inducers of gene expression **86–89**, **94**, **253** and **254**.

*BL21 (DE3)* pNIC28-sfGFP were incubated with each compound under normoxic or hypoxic conditions for 24 hours. Western blot analysis and fluorescence studies (Figure 4.12A–D) showed that both **89** and **254** induced sfGFP expression under normoxic conditions. In the case of **89**, this result indicates that the 4-nitrobenzyl group can be accommodated by LacI at the 6-position and does not inhibit binding of IPTG **76** to the promoter. Inspection of the X-ray crystal structure shows that the 6-position of IPTG **76** is oriented towards a pocket that is likely to be occupied by the glucose moiety of allolactose, the endogenous ligand for LacI. Compound **254** contains a 5-nitrothiophene bio-reductive group, which is predicted to undergo more rapid bio-reduction and fragmentation than either the 4-nitrobenzyl or the 2-nitroimidazole groups.<sup>180,247</sup> Therefore, it is likely that bio-reduction and fragmentation of **254** occurs in normoxia, resulting in the expression of sfGFP observed.



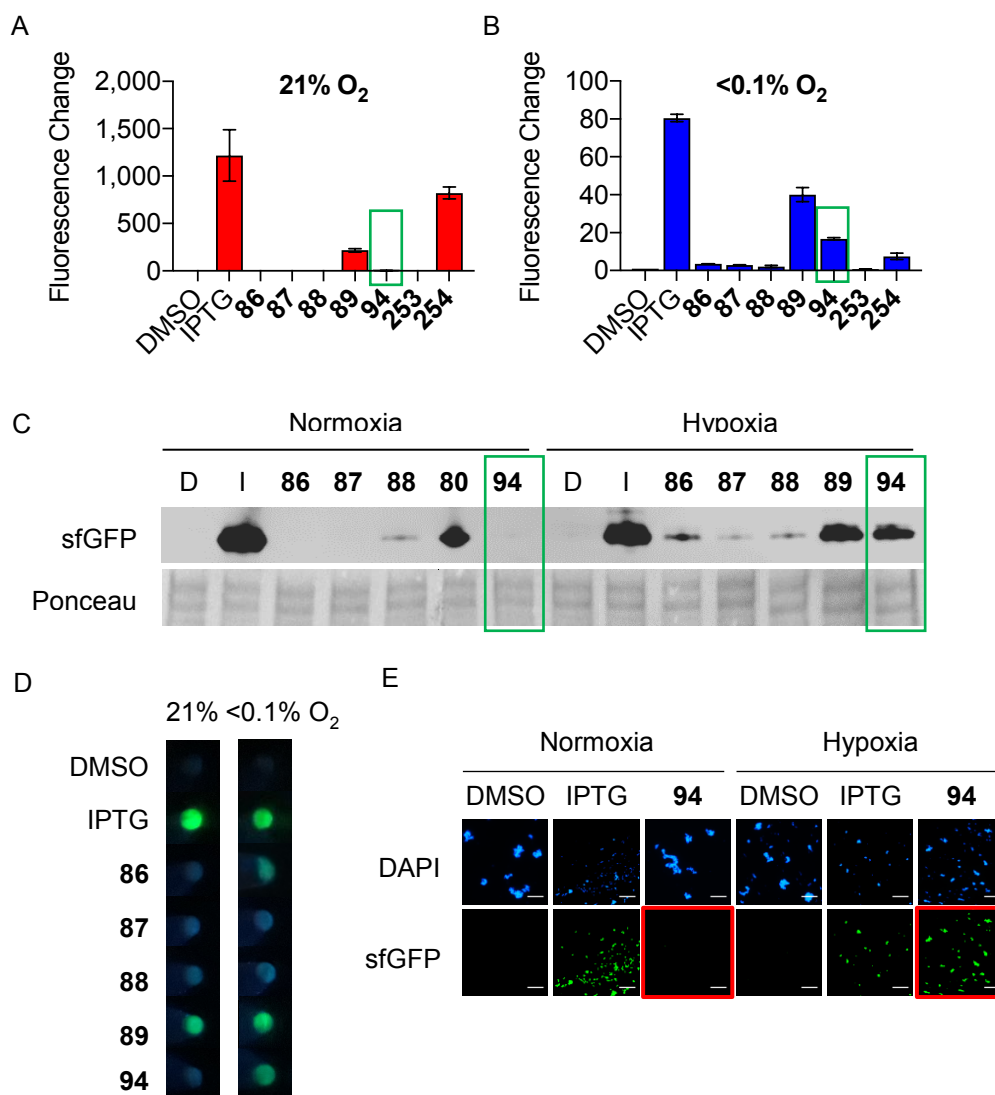


**Figure 4.12:** Compound **94** induces gene expression selectively in hypoxia in *BL21 (DE3)* bacteria. A) *BL21 (DE3)* pNIC28-sfGFP were treated with DMSO (D), IPTG **76** (I) or hypoxia-activated IPTG derivatives **86–89**, **94**, **253**, and **254** (1 mM) for 24 h under normoxic (21% O<sub>2</sub>) conditions. Samples were analysed by fluorescence ( $\lambda_{\text{ex}} = 485 \text{ nm}$ ,  $\lambda_{\text{em}} = 520 \text{ nm}$ , PBS). Fluorescence was divided by the optical density at 600 nm and normalised to the relevant DMSO control. IPTG **76**, **89** and **254** showed an increase in fluorescence under these conditions. B) Conditions as in (A), except treatment under hypoxic (<0.1% O<sub>2</sub>) conditions. IPTG **76**, **89**, **94** and **254** show an increase in fluorescence, indicating that compound **94** is able to induce sfGFP production selectively in hypoxia. C) Conditions as in (A/B). Samples were analysed by western blot. Ponceau staining is shown as a loading control. The results mirror those observed by fluorescence. D) Conditions as in (A/B). Bacterial samples were pelleted and imaged under a UV lamp ( $\lambda_{\text{ex}} = 365 \text{ nm}$ ), showing the hypoxia-dependent production of sfGFP promoted by **94**. E) Conditions as in (A/B). Samples were suspended in PBS and visualised by fluorescence microscopy. DAPI (blue) was used as a nucleic acid stain. Scale bars represent 25  $\mu\text{M}$ .

Although the 2-nitroimidazole acetal compound **253** did not induce sfGFP expression in normoxia, treatment with **253** under hypoxic conditions, resulted in substantial bacterial death. The 2-nitroimidazole group has known antibiotic activity.<sup>384</sup> As such, it is possible that under hypoxic conditions, a 2-nitromidazole derivative with similar antimicrobial activity is being released and causing the observed bacterial death.

Promisingly, the 4-nitrobenzyl ether derivatives **86**, **87** and **88** showed no induction of sfGFP expression in normoxia. This result is consistent with the X-ray crystal structure, which indicated that substitutions at these positions would not be tolerated. However, none of these compounds caused significant increase in sfGFP expression in hypoxia, indicating that significant quantities of IPTG **76** are not being released (Figure 4.12A–D). This is consistent with the data obtained in the enzyme assay, which also showed that low levels of the parent compound were released.

The 4-nitrobenzyl acetal **94** showed no sfGFP expression in normoxia, but displayed a substantial increase in fluorescence in hypoxia, with a corresponding increase in the amount of sfGFP detected by western blot (Figure 4.12A–D). Cellular imaging experiments also confirmed that **94** does not induce sfGFP expression in *BL21 (DE3)* pNIC28-sfGFP in normoxia but leads to significant expression of sfGFP in hypoxia (Figure 4.12E).

To determine the rate of activation of gene expression with **94** under hypoxic conditions, a time course experiment was carried out. *BL21 (DE3)* pNIC28-sfGFP were incubated with **94** for 0–24 hours under normoxic and hypoxic conditions. Fluorescence analysis showed that after an initial lag, hypothesised to be caused by the activation step required to release IPTG **76**, sfGFP expression rapidly increased with time until saturation was reached after 24 hours (Figure 4.13A). Consistent with this hypothesis, this lag was not observed when free IPTG **76** was added (Figure 4.13B).

The oxygen dependency of the hypoxia-activated gene expression with **94** was investigated. While negligible sfGFP expression was observed at 1% O<sub>2</sub>, there was partial induction at

0.5% O<sub>2</sub>, and high levels of expression at 0.1% O<sub>2</sub>, demonstrating the oxygen dependency of the response (Figure 4.14).

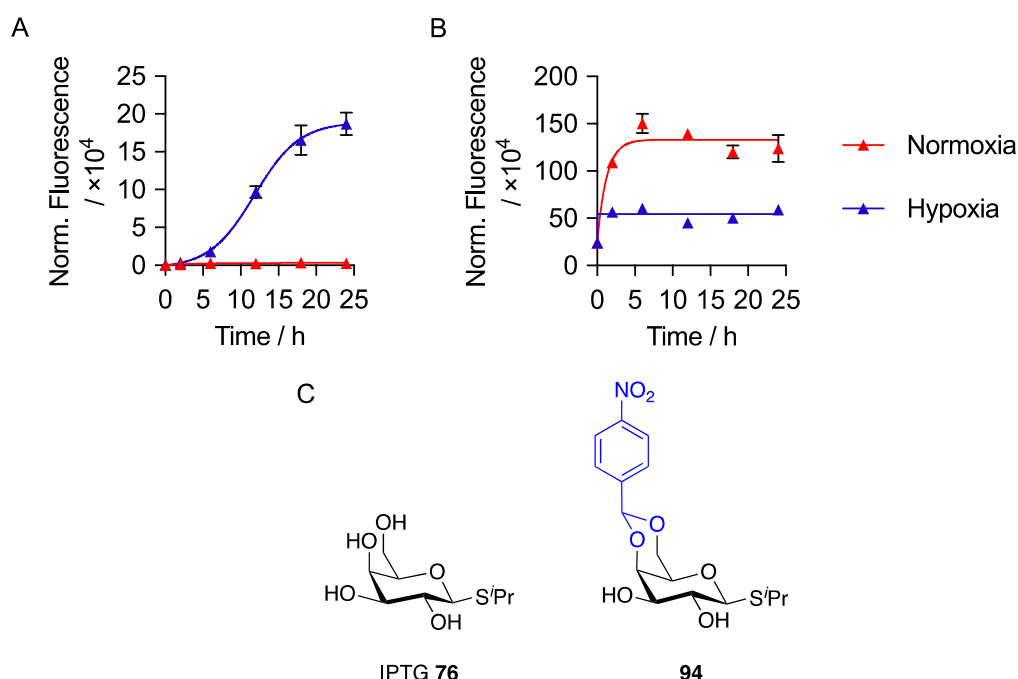


**Figure 4.13:** Time course analysis of sfGFP induction with IPTG **76** and **94**. A) *BL21 (DE3)* pNIC28-sfGFP bacteria were treated with **94** (1 mM) under normoxic (21% O<sub>2</sub>) and hypoxic (<0.1% O<sub>2</sub>) conditions over 24 h. Samples, taken at the time points indicated, were analysed by fluorescence ( $\lambda_{\text{ex}} = 485 \text{ nm}$ ,  $\lambda_{\text{em}} = 520 \text{ nm}$ , PBS). After an initial lag period, rapid induction of sfGFP expression was observed until saturation was reached after 24 h. Fluorescence was divided by the optical density at 600 nm. B) Conditions as in (A), except treatment with IPTG **76** (1 mM). C) Structures of IPTG **76** and **94**.

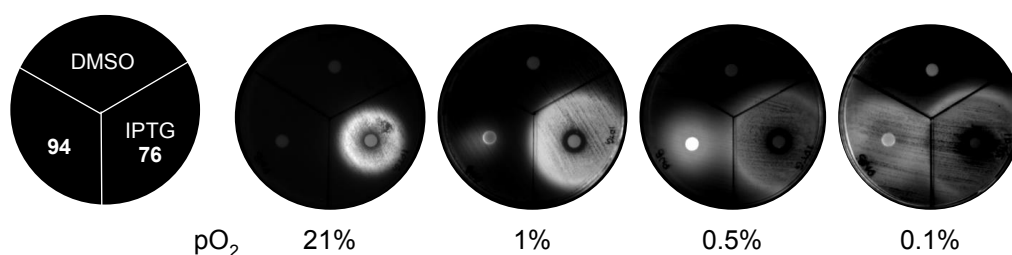
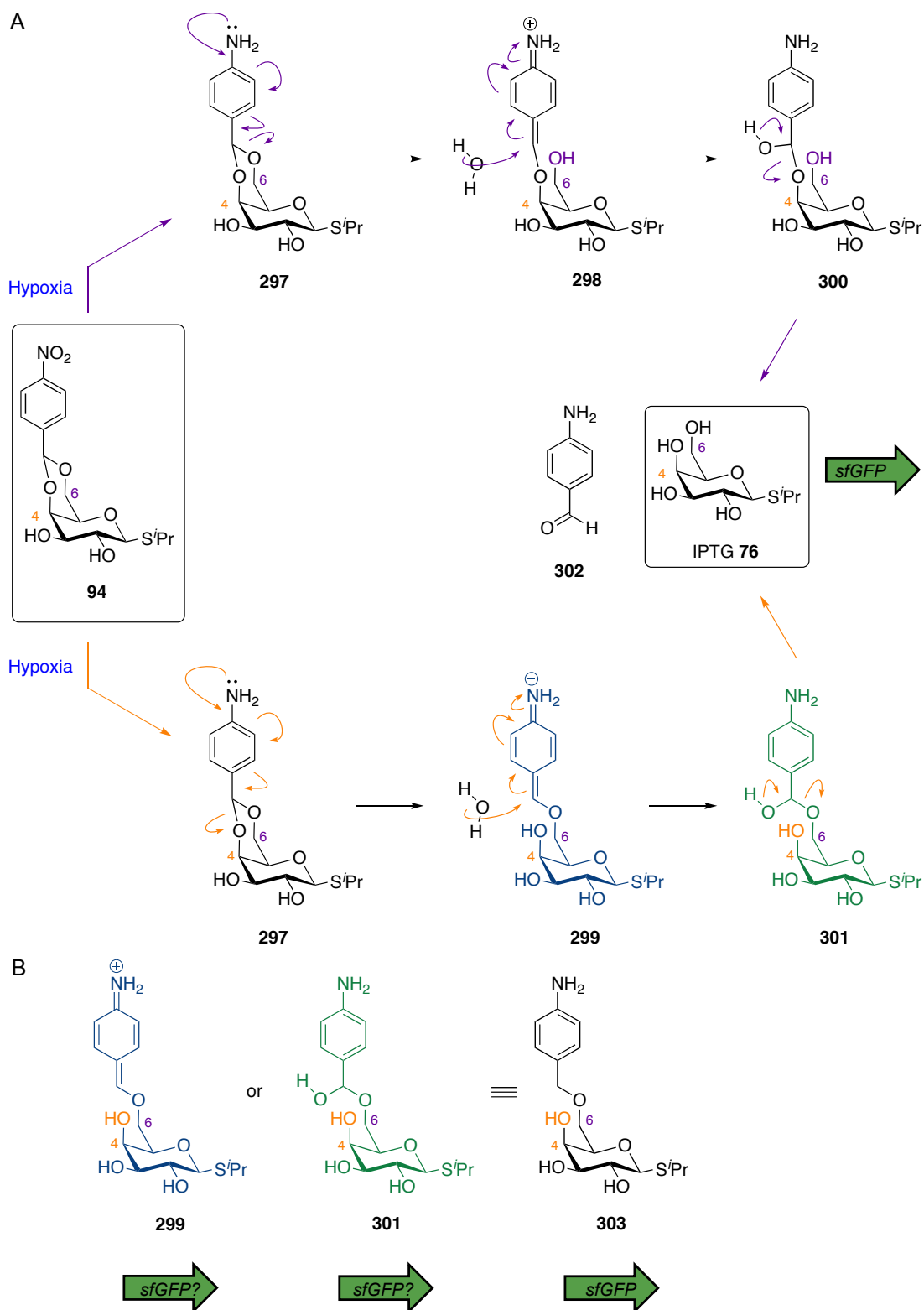


**Figure 4.14:** Oxygen dependency of hypoxia-activated gene expression with **94**. *BL21 (DE3)* pNIC28-sfGFP bacteria were spread on 2× YT agar plates. A disc coated with DMSO, IPTG **76**, or **94** (10 mM) was placed in each third. The plates were incubated at the required oxygen tension for 24 h and then imaged by fluorescence. No sfGFP expression was observed at 1% O<sub>2</sub>, there was partial induction at 0.5% O<sub>2</sub>, and high levels of expression at 0.1% O<sub>2</sub>.

#### 4.4. Postulated Mechanism for Hypoxia-Activation of **94**

While the enzyme-based assays showed similar release of **103** from both the nitrobenzyl ethers **123–125** and acetal-based compound **127**, in a cellular setting, the acetal-based compound **94** showed significantly more induction of sfGFP expression than the corresponding ether compounds **86–88**. To date, examples of hypoxia-activated prodrugs have been reported that consist of an active drug attached to a bioreductive group either directly or *via* a linker moiety.<sup>192,385,386</sup> To our knowledge, there are no previous examples of acetal-based bioreductive groups and we propose that this structural difference accounts for the higher activation observed in bacteria. To explain this difference in cellular activity, two possible mechanisms for bioreductive activation of **94** were investigated (Scheme 4.3).



**Scheme 4.3:** Proposed mechanisms for hypoxia-dependent bioreductive activation of **94**. A) Fragmentation of **94**, affords hemi-acetals **300** and **301**, which collapse to release IPTG **76** and 4-aminobenzaldehyde **302**. B) Compounds **299** or **301** may also induce gene expression, as an analogue **303** was shown to induce production of sfGFP in *BL21 (DE3)* pNIC28-sfGFP bacteria.

#### 4.4.1. Mechanism 1: Fragmentation *via* a Hemi-Acetal to Release IPTG

In the first mechanism (Scheme 4.3A), it is proposed that reduction in hypoxia to form to the corresponding amine **297** is followed by one or both of two possible fragmentation pathways. These result in extended enol-ether-like systems attached to either the 4- (**298**) or the 6- (**299**) position. It is possible that these systems are intercepted by water or other endogenous nucleophiles (e.g. glutathione) to give the hemi-acetals **300** and **301** (or equivalent), which collapse to release IPTG **76** and 4-aminobenzaldehyde **302**.

To test this theory, the HPLC traces for **127** (the benzyl analogue of **94**) treated with CYP450:NADPH reductase enzymes under 21% O<sub>2</sub> and <0.1% O<sub>2</sub> were analysed for the presence of **302**. 4-Aminobenzaldehyde **302** was only observed in the hypoxic samples (Figure 4.15), supporting the mechanism proposed in Scheme 4.8A.

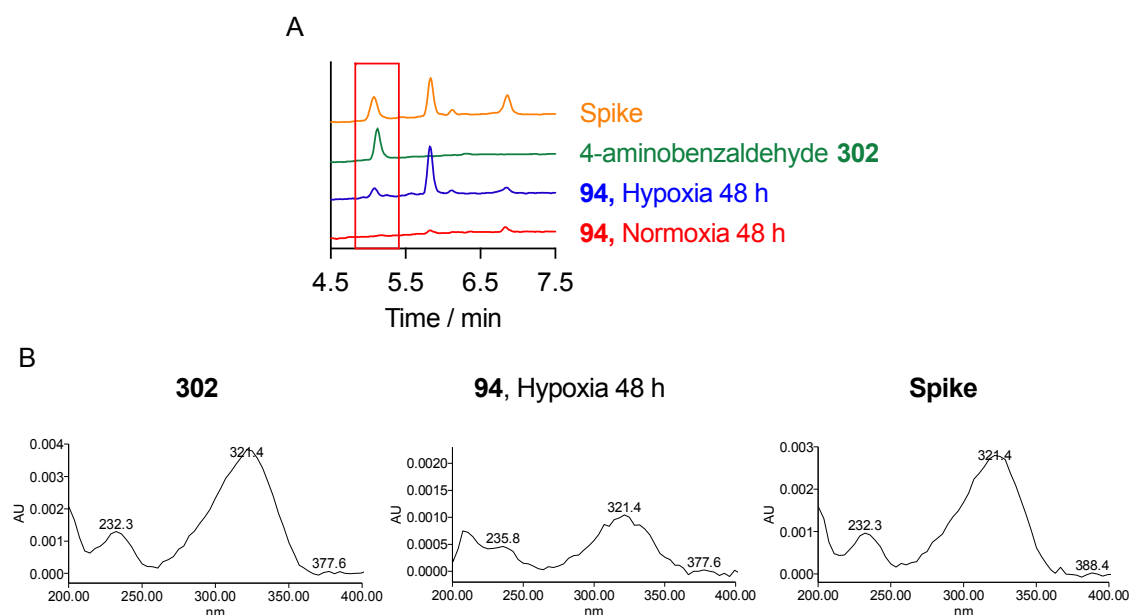
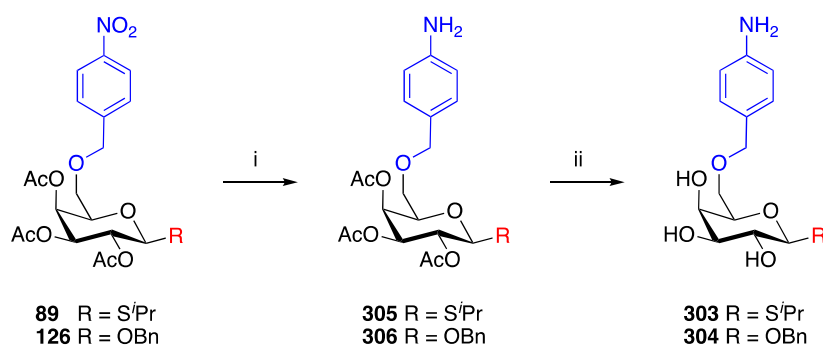


**Figure 4.15:** Compound **127** fragments under hypoxic conditions to release 4-aminobenzaldehyde **302**. A) Compound **127** (20 μM) was treated with CYP450:NADPH reductase enzymes under normoxic (21% O<sub>2</sub>) and hypoxic (<0.1% O<sub>2</sub>) conditions. Aliquots taken after 48 h were analysed by HPLC-MS ( $\lambda_{320}$ ). The hypoxic samples were spiked with 4-aminobenzaldehyde **302** to confirm the presence of **302** in the hypoxic samples. B) Conditions as in (A). UV spectra for the peak at 5.1 min (red box).

#### 4.4.2. Mechanism 2: Hemi-Acetal **301** Induces Gene Expression

The second proposed mechanism is based on the observation that **89**, in which the 4-nitrobenzyl group is attached to the 6-position of IPTG **76**, induced gene expression in 21% O<sub>2</sub>. Therefore, it is feasible that compounds **299** or **301**, which result from reduction and initial fragmentation of **94** are also able to induce gene expression (Scheme 4.3B). This hypothesis is difficult to test directly, due to the predicted instability of **299** and **301**. Compound **303**, the 6-*O*-(4-aminobenzyl) derivative of IPTG, was identified as an analogue of **299** and **301** and targeted for synthesis. To facilitate analysis of the stability of the 4-aminobenzyl ether under aqueous conditions by HPLC, **304**, the 6-*O*-(4-aminobenzyl) derivative of **103**, containing an anomeric benzyl moiety, was also synthesised.

Compounds **303** and **304** were synthesised *via* an identical synthetic route. Reduction of the nitro group of the acetylated 6-*O*-(4-nitrobenzyl) derivatives **248** and **247** to form the amines **305** and **306** was accomplished with palladium-catalysed hydrogenation. Final deprotection under standard Zemplén deacetylation conditions afforded **303** and **304** (Scheme 4.4).



**Scheme 4.4:** Synthesis of **303** and **304**. *Reagents and conditions:* i) Pd/C, H<sub>2</sub>, EtOAc, RT, **305**: 1.5 h, 93%; **306**: 2.5 h, 99%; ii) NaOMe, MeOH, RT, **303**: 1 h, 82%; **304**: 3 h, 29%.

Compound **304** was stirred in phosphate buffer for 24 hours and samples taken at the time points indicated were analysed using HPLC-MS. The concentration of **304** did not significantly change over the course of the experiment, although 5 μM **103** was detected after 24 hours (Figure 4.16). This suggests that **304** is stable under aqueous conditions with negligible fragmentation to release **103** and, consequently, that **303** will also be stable for the duration of the induction experiment.

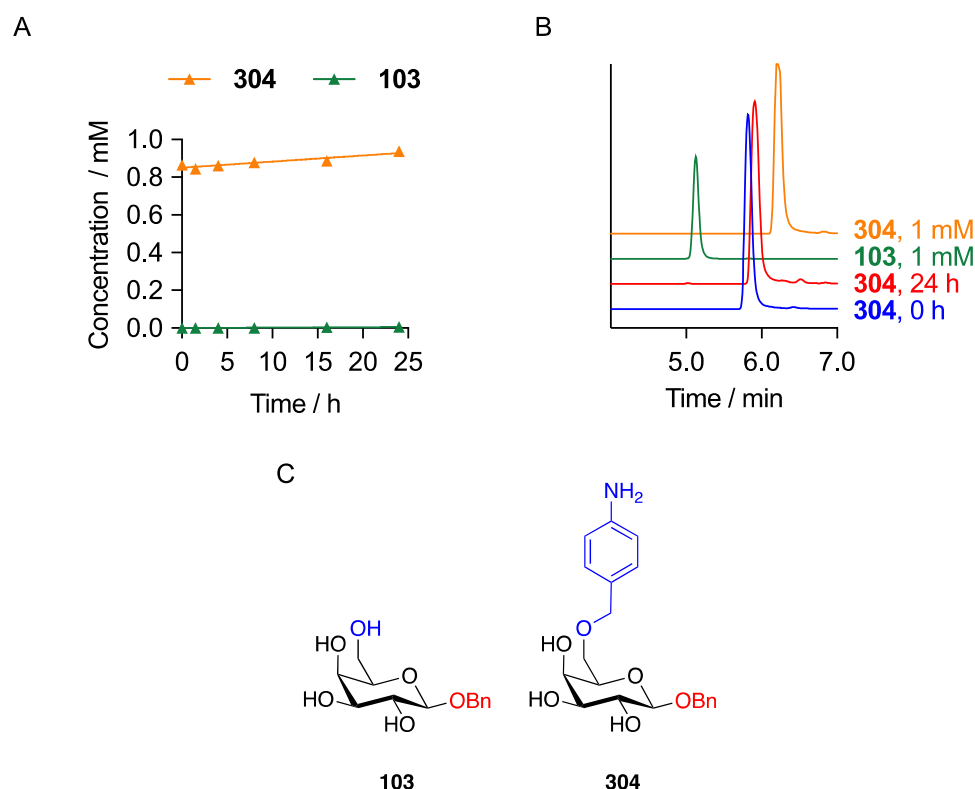


**Figure 4.16:** Compound **304** is stable under aqueous conditions. A) Compound **304** (1 mM) was stirred in phosphate buffer at 37 °C for 24 h. Time points taken at the indicated times were analysed by HPLC-MS ( $\lambda = 205$  nm). The concentration of **304** did not significantly change during this time period, although 5  $\mu$ M **103** was detected after 24 h. This suggests that **304** is stable under aqueous conditions with negligible fragmentation to release **103**. B) Conditions as in (A). Representative HPLC traces of samples taken after 0 h and 24 h, as well as standards for **103** and **304** (1 mM,  $\lambda = 205$  nm). C) Structures of **103** and **304**.

Having shown the stability of the 6-aminobenzyl group under aqueous conditions, **303** was next incubated with *BL21 (DE3)* pNIC28-sfGFP bacteria under either normoxic (21% O<sub>2</sub>) or hypoxic (<0.1% O<sub>2</sub>) conditions for 24 hours. Induction of sfGFP expression was observed in both conditions (Figure 4.17A/B). Additionally, to confirm that expected release of 5  $\mu$ M IPTG **76** is insufficient to induce gene expression, a calibration curve for IPTG induction was performed. Expression of sfGFP rapidly increased with increasing concentrations of IPTG **76** until saturation was reached at 50  $\mu$ M (Figure 4.17C). From these data, it is clear that the amount of sfGFP observed following induction with **303** is greater than can be accounted for by release of 5  $\mu$ M IPTG **76** under these conditions. This suggests that **303** is able to bind LacI and induce gene expression.



Taken together, these studies into the mechanism of activation of **94** suggest that there are two possible mechanisms by which bioreduction of **94** can induce gene expression, accounting for its greater activity in bacteria than the ether compounds **86–89**.

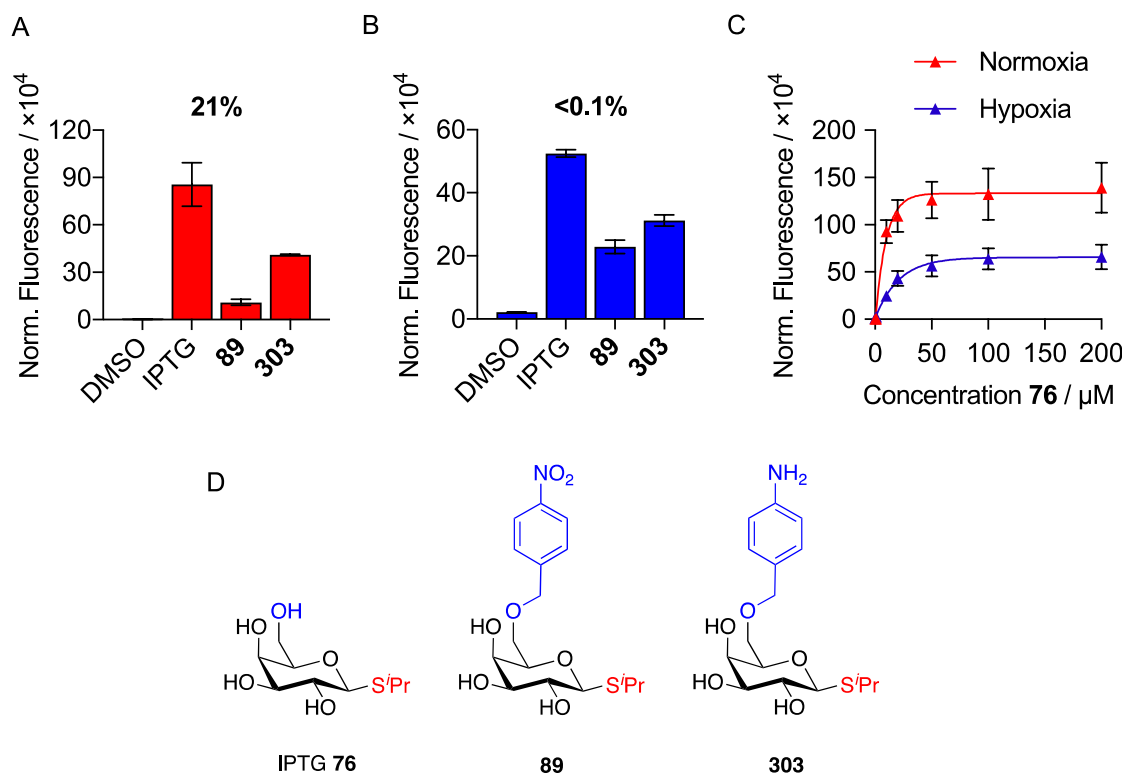


**Figure 4.17:** Compound **303** induces sfGFP expression in both normoxic and hypoxic conditions. A) *BL21 (DE3)* pNIC28-sfGFP were treated with DMSO, IPTG **76**, **89** or **303** (1 mM) for 24 h under normoxic (21% O<sub>2</sub>) conditions. Samples were analysed by fluorescence ( $\lambda_{\text{ex}} = 485$  nm,  $\lambda_{\text{em}} = 520$  nm, PBS). Fluorescence was divided by the optical density at 600 nm. B) Conditions as in (A), except treatment under hypoxic (<0.1% O<sub>2</sub>) conditions. C) IPTG calibration curve for induction of sfGFP expression. *BL21 (DE3)* pNIC28-sfGFP bacteria were treated with IPTG **76** at the indicated concentrations for 24 h under normoxic or hypoxic conditions. Samples were analysed by fluorescence ( $\lambda_{\text{ex}} = 485$  nm;  $\lambda_{\text{em}} = 520$  nm, PBS). Fluorescence was divided by the optical density at 600 nm. D) Structures of IPTG **76**, **89** and **303**.

#### 4.5. Steps Towards Hypoxia-Dependent Gene Expression in Mammalian Cells

The work so far has demonstrated a proof-of-concept system, which places genes under the control of a hypoxia-activated inducer in bacteria cells. While this is especially relevant for the study of biofilms, hypoxia is found in many biological contexts, including hypoxic tumours and

plants (See Chapter 1). Focus was next placed on transferring the system to human cancer cell lines. During this process, two key challenges were encountered. First, IPTG-inducible expression is dependent on the presence of both LacI (which, in eukaryotic cells, must also translocate to the nucleus) and promoters that are controlled by a *lacO* sequence. Neither of these components are endogenously present in mammalian cells and must be introduced before IPTG-inducible expression is possible. Second, the synthesised hypoxia-activated inducers were found to exhibit very low membrane permeability. The remainder of this chapter will discuss the steps taken towards overcoming these challenges.

#### 4.5.1. IPTG-Inducible Expression of sfGFP in Mammalian Cells

It has been shown that the *lac* operon is functional in mammalian cells<sup>387</sup> and this has enabled the use of IPTG-inducible expression in a variety of contexts, both *in vitro*<sup>388–390</sup> and *in vivo*.<sup>391,392</sup> Plasmids have been developed that contain the required components optimised for IPTG-inducible expression in mammalian cells.<sup>223</sup> The LacSwitchII inducible mammalian expression system (Agilent) comprises three plasmids: pCMV-LacI, pOPRSVI/MCS, and pOPI3CAT. pCMV-LacI allows for constitutive expression of LacI, which is targeted to the nucleus by a SV40 nuclear localisation sequence. The gene of interest can be cloned into either of the expression plasmids, pOPRSVI/MCS or pOPI3CAT, which contain *lacO* sequences, inserted at various positions. The primary difference between pOPRSVI/MCS and pOPI3CAT is in the number and position of the *lacO* sequences (Appendix B). sfGFP was inserted into both pOPRSVI/MCS or pOPI3CAT to form the expression plasmids, pOPRSVI-sfGFP and pOPI3-sfGFP, respectively (Section 6.4).

Since IPTG-inducible expression is only possible when both LacI and the expression plasmid are present, transfection with only the expression plasmid should result in constitutive expression of sfGFP, regardless of the experimental conditions. On the other hand, co-transfection with both pCMV-LacI and one of the expression plasmids should result in sfGFP expression only when the cells are treated with IPTG **76**. Accordingly, HepG2 cells were transiently transfected with different combinations of plasmids and treated with either DMSO or IPTG **76**. Green

fluorescence, indicating expression of sfGFP, was observed in the cells transfected with only pOPRSVI-sfGFP or pOPI3-sfGFP. Furthermore, cells co-transfected with pCMV-LacI and either pOPRSVI-sfGFP or pOPI3-sfGFP showed fluorescence only in the IPTG-treated samples (Figure 4.18). This suggests that expression of LacI is successfully repressing gene expression until induction with IPTG **76**. In general, pOPI3-sfGFP transfected more efficiently than pOPRSVI-sfGFP and was chosen for subsequent experiments.

Although, IPTG-inducible expression of sfGFP was achieved in HepG2 cells, the transfection efficiency was very low (<10%). In transient transfections, the optimal time for expression of transgenes varies according to many factors including the cell line, genes to be expressed, and the method of transfection.<sup>393</sup> To determine the optimal experimental conditions for our purposes, different transfection times and transfection reagents were investigated (Figure 4.19).

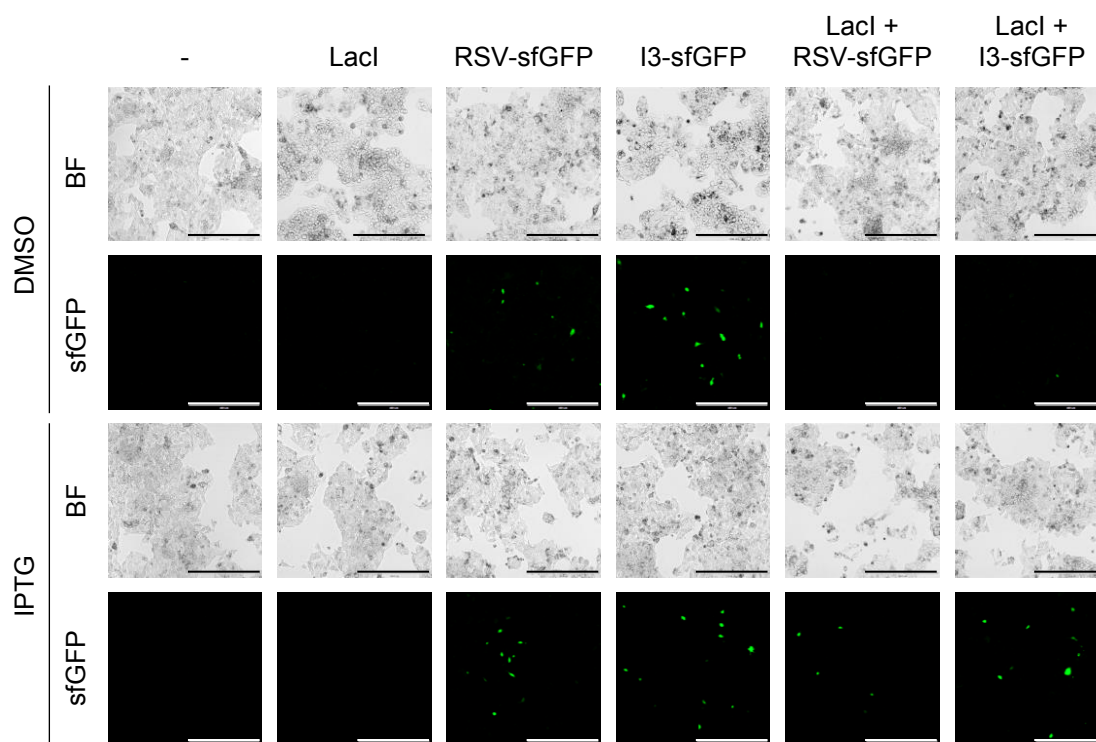


**Figure 4.18:** Transient transfection of HepG2 with pCMV-LacI and either pOPRSVI-sfGFP or pOPI3-sfGFP results in IPTG-inducible gene expression. HepG2 cells ( $0.3 \times 10^6$ ) were transiently transfected with pCMV-LacI, pOPRSVI-sfGFP, pOPI3-sfGFP, or a combination of pCMV-LacI and either pOPRSVI-sfGFP or pOPI3-sfGFP (plasmid ratio 1:1). After 48 h, the media was replaced with fresh media containing either DMSO or IPTG **76** (1 mM) and the cells were incubated for a further 24 h. Samples were analysed by fluorescence microscopy ( $\lambda_{\text{ex}} = 480 \text{ nm}$ ,  $\lambda_{\text{em}} = 517 \text{ nm}$ ). The brightfield (BF) images are shown above the corresponding samples. Scale bars represent 400  $\mu\text{M}$ . sfGFP expression is observed in the samples transfected with only pOPRSVI-sfGFP or pOPI3-sfGFP and in the presence of IPTG **76** in the samples cotransfected with pCMV-LacI and pOPRSVI-sfGFP or pOPI3-sfGFP.

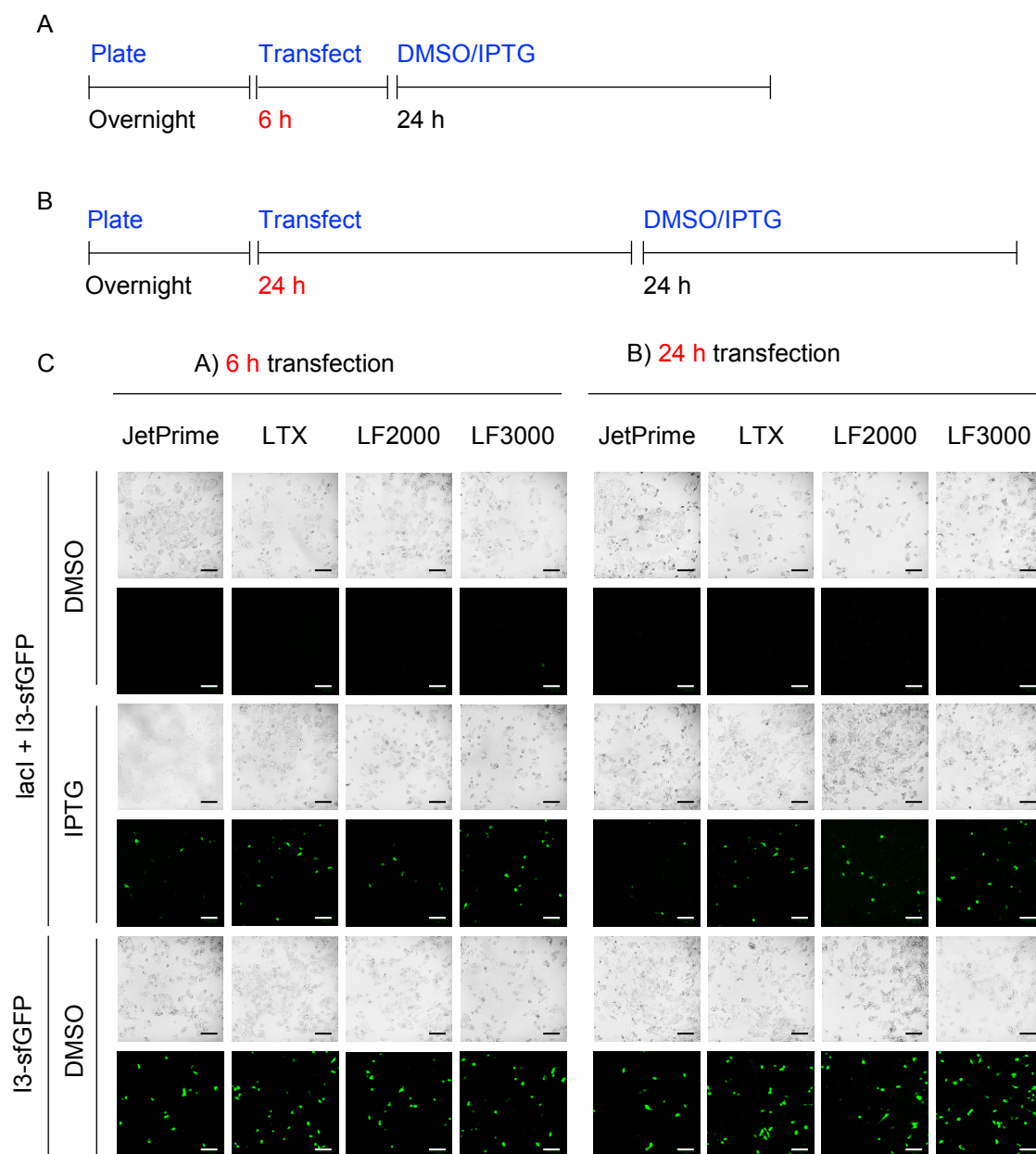


**Figure 4.19:** Investigation of different transfection time frames and transfection reagents for transient IPTG-inducible expression in HepG2. A/B) Schematics showing the timings for each step in the expression protocol. C) HepG2 cells ( $8 \times 10^4$ ) were transiently transfected with pOPI3-sfGFP or cotransfected with pCMV-LacI:pOPI3-sfGFP (1:1), using the transfection reagents indicated. After 6 h or 24 h, the media was replaced with fresh media containing either DMSO or IPTG **76** (1 mM) and the cells were incubated for a further 24 h. Samples were analysed by fluorescence microscopy ( $\lambda_{\text{ex}} = 480 \text{ nm}$ ,  $\lambda_{\text{em}} = 517 \text{ nm}$ ). The brightfield (BF) images are shown above the corresponding samples. Scale bars represent 100  $\mu\text{M}$ . Qualitatively, HepG2 cells transfected with LF3000 for 24 h showed the highest transfection efficiency.

HepG2 cells were transfected with either JetPrime, Lipofectamine LTX, Lipofectamine 2000 (LF2000) or Lipofectamine 3000 (LF3000) and the complexes were removed after either 6 hours

or 24 hours (Figure 4.19). After this time, cells were treated with either DMSO or IPTG **76** for 24 hours and analysed for fluorescence. In each case, similar transfection efficiencies were observed although, qualitatively, HepG2 cells transfected with LF3000 for 24 hours showed the highest transfection efficiency (Figure 4.19C).

While adequate transfection levels were obtained for cells transfected with only pOPI3-sfGFP (i.e. constitutive expression of sfGFP), consistently low levels of sfGFP expression were observed for co-transfected cells (i.e. IPTG-inducible expression of sfGFP). The pOPI3-sfGFP expression vector contains three *lacO* sequences. For expression of sfGFP, none of these *lacO* sequences can be bound to LacI; therefore, there must be a sufficient amount of IPTG **76** present in the nucleus to minimise the number of molecules of LacI that are available for binding to the *lacO* sequence. Consequently, it is possible that, rather than poor transfection efficiency, expression of LacI is too high to allow complete derepression with the amount of IPTG **76** added, resulting in low sfGFP expression levels. Although either increasing the concentration of IPTG **76** or decreasing the expression levels of LacI could be considered, the concentration of IPTG **76** was already high (1 mM) and reducing the ratio of pCMV-LacI:pOPI3-sfGFP increases the chance that some transfected cells will take up pOPI3-sfGFP without pCMV-LacI. This would result in false positive cells due to constitutive expression of sfGFP. Therefore, neither of these solutions were appropriate for our purposes. Future work will focus on generating a stable cell line that expresses both pCMV-LacI and pOPI3-sfGFP. This will reduce the number of variables involved in the experiment by eliminating the transient transfection step.

#### 4.5.2. Improving Mammalian Cell Permeability

The other challenge was the membrane permeability of the synthesised hypoxia-activated inducers. In general large, uncharged polar molecules exhibit poor membrane permeability.<sup>394</sup> Sugars, such as glucose and galactose, are typically transported into cells by the glucose transporter (GLUT) family of transporters.<sup>395</sup> However, protection of IPTG **76** with a bioreductive moiety may prevent recognition by these transporters, making diffusion through the membrane the primary means of transport into the cell.

First, the membrane permeabilities of **86**, **94**, **253** and **254** were analysed in the parallel artificial membrane permeation assay (PAMPA) at Novartis Institute for Biomedical Research (NIBR).<sup>396–399</sup> This assay uses an *in vitro* model for passive diffusion to measure permeability of a compound across an artificial membrane and classifies a compound as either low permeability ( $\log P_{\text{app}} < -5.00$  cm/s) or high permeability ( $\log P_{\text{app}} > -5.00$  cm/s). For each compound  $\log P_{\text{app}}$  values of less than  $-5.3$  cm/s (the detection limit in this assay) were obtained, suggesting that, at least *via* passive diffusion mechanisms, uptake of **86**, **94**, **253** and **254** across cell membranes was likely to be very poor. Since **94** induced the highest levels of hypoxia-dependent gene expression in *E. coli* bacteria (Section 4.3.6), **94** was chosen for analysis in a cellular setting. The human cancer cell lines HCT116 and HepG2, which had previously been used during bioreductive analysis of resorufin-based probes **63** and **79** (Chapter 2), were treated with **94** for 6 hours. After this time, samples taken from either the media or cell lysate were analysed by HPLC-MS. Negligible compound was extracted from the cells, while concentrations that were not significantly different to the starting concentrations were observed in the media sample. This suggests that only a small amount, if any, of **94** is being taken up into the cell (Figure 4.20).

There are a number of methods that are employed to improve the membrane permeability of bioactive compounds, including enhancing small molecule lipophilicity, by masking polar regions of the compound,<sup>400,401</sup> and conversion to prodrugs, which are designed to target specific membrane carrier proteins.<sup>394,402</sup> Previously, the use of acetyl groups to mask the hydroxyls of trehalose, a disaccharide, resulted in accumulation of acetylated trehalose into cells, where it was hydrolysed to release trehalose.<sup>403</sup> It was hypothesised that similar acetyl protection of the hydroxyl groups of **94** would reduce their hydrophilicity and improve uptake *via* passive diffusion mechanisms.

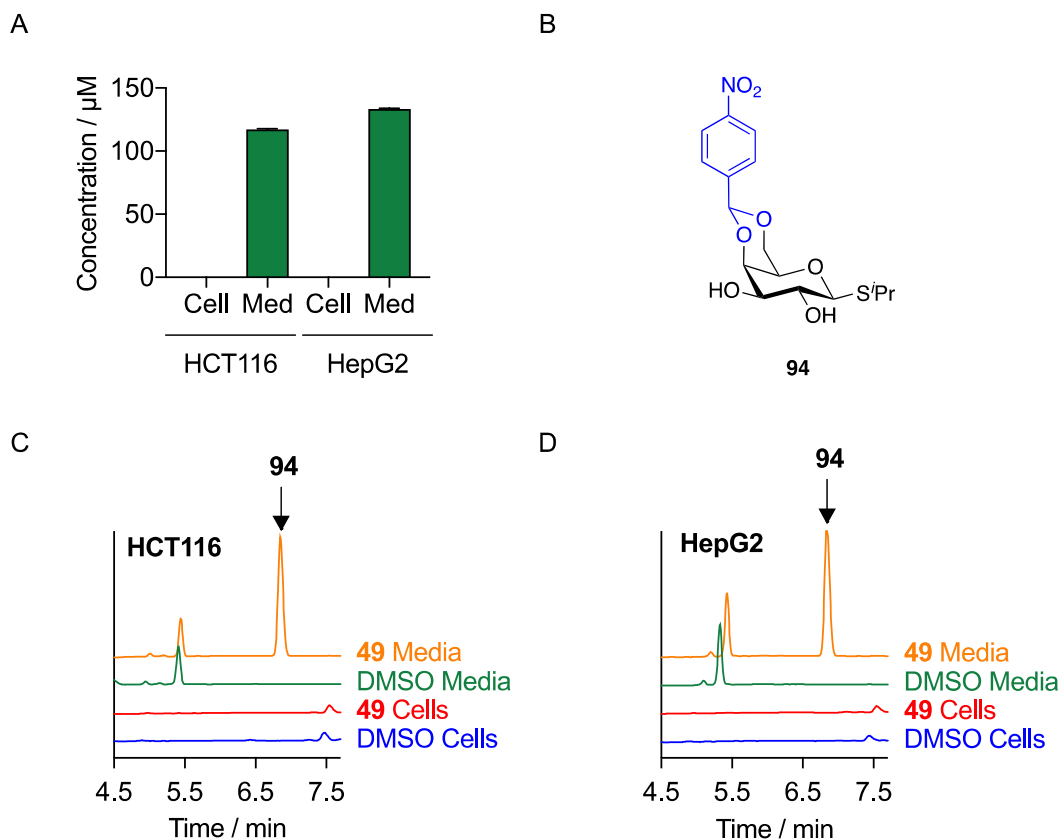
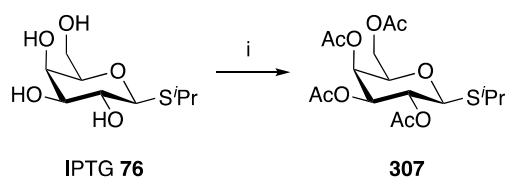


**Figure 4.20:** Compound **94** has low membrane permeability in HCT116 and HepG2 cancer cell lines. A) Concentrations of **94** in HCT116 and HepG2 cell lysates ( $0.3 \times 10^6$  cells) and the corresponding media samples. Cells were treated with **94** ( $100 \mu\text{M}$ ) for 6 h and lysed with MeCN:MeOH (1:1). Samples were analysed by HPLC-MS. B) Structure of **94**. C) Conditions as in (A). Representative HPLC traces of media and cell lysates for HCT116 ( $\lambda = 270 \text{ nm}$ ). D) Conditions as in (A). Representative HPLC traces of media and cell lysates for HepG2 ( $\lambda = 270 \text{ nm}$ ). Negligible **94** is observed in the cell lysate samples.

One drawback to this ester prodrug strategy is the introduction of an additional activation step (hydrolysis of the acetyl groups) required before IPTG **76** is released and gene expression induced. Therefore, IPTG **76** was first acetylated to form **307** and investigated for its ability to induce gene expression. Compound **307** was readily synthesised in one step from IPTG **76** with acetic anhydride in pyridine (Scheme 4.5). HepG2 cells, transfected with pCMV-LacI and pOPI3-sfGFP (Section 4.5.1), were treated with IPTG **76** or acetylated IPTG **307** and analysed for production of sfGFP by fluorescence. In both cases, there was an increase in the number of fluorescent cells compared with the DMSO-treated control cells, indicating that both IPTG **76** and acetylated IPTG **307** can induce gene expression in HepG2 (Figure 4.21).





**Scheme 4.5:** Synthesis of tetra-*O*-acetyl IPTG **307**. *Reagents and conditions:* Ac<sub>2</sub>O, pyridine, RT, 3 h, 90%.

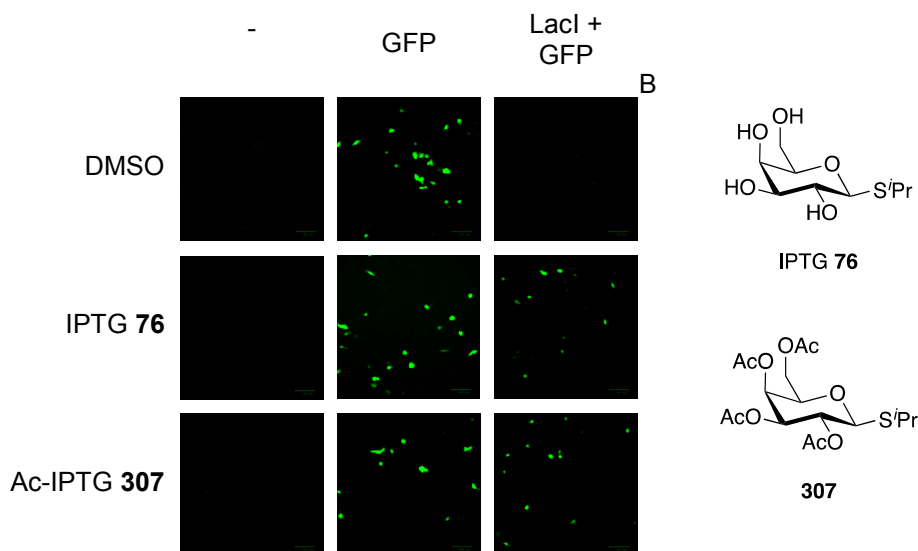
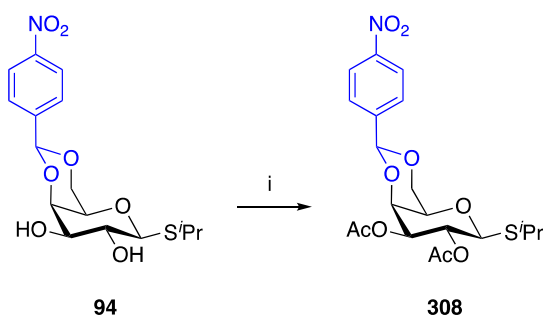


**Figure 4.21:** Acetylated IPTG **307** is able to induce gene expression in IPTG-inducible HepG2 cells. A) HepG2 cells ( $0.1 \times 10^6$ ) were transiently transfected with pOPI3-sfGFP or pCMV-LacI:pOPI3-sfGFP (1:1). After 24 h, the media was replaced with fresh media containing either DMSO, **76** or **307** (500  $\mu$ M) and the cells were incubated for a further 24 h. Samples were analysed by fluorescence microscopy ( $\lambda_{\text{ex}} = 480$  nm,  $\lambda_{\text{em}} = 517$  nm). Scale bars represent 100  $\mu$ M. Expression of sfGFP is induced in the cells treated with **76** and **307**. B) Structures of IPTG **76** and acetylated-IPTG **307**.



**Scheme 4.6:** Synthesis of acetyl protected inducer **308**. *Reagents and conditions:* Ac<sub>2</sub>O, pyridine, RT, 3 h, 99%.

Encouraged by these results, compound **94** was acetylated with acetic anhydride in pyridine to afford **308**, (Scheme 4.6). Cell lysates of HepG2 cells, treated with **308** for 24 hours under normoxic or hypoxic conditions, were analysed by HPLC-MS. Although an increase in the intracellular concentration of **308** was observed (Figure 4.22A), under these conditions, **94** was not detected, suggesting that the acetyl groups were not being hydrolysed. Furthermore, there was no difference between the normoxic and hypoxic samples suggesting that hypoxia-dependent bioreduction of the 4-nitrobenzylidene group was not occurring. Compound **94** was therefore deemed to be unsuitable for further analysis of hypoxia-activated gene expression in mammalian cells.

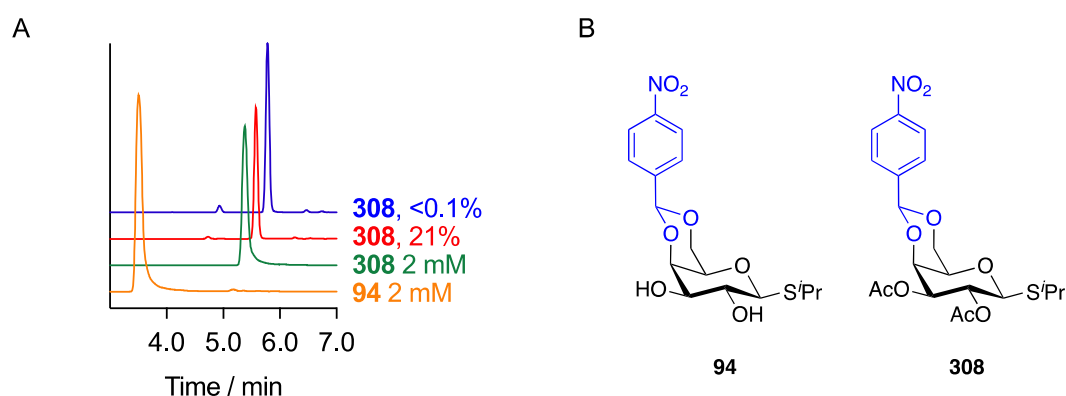
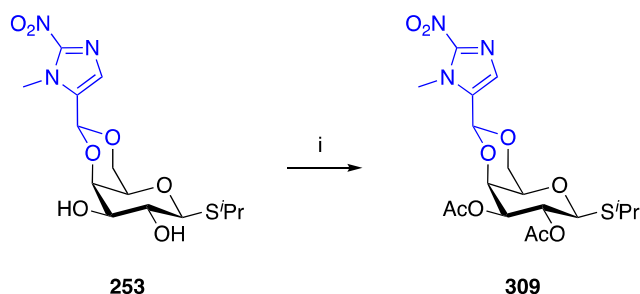


**Figure 4.22:** Compound **308** exhibits improved membrane permeability in HepG2 cells. A) Representative HPLC trace of HepG2 cell lysates ( $0.8 \times 10^6$  cells), following treatment with **308** (1 mM) for 24 h ( $\lambda = 270$  nm). Cells were lysed with MeCN:H<sub>2</sub>O (1:1). An increase in the intracellular concentration of **308** was observed, although release of **94** was not detected. B) Structures of **94** and **308**.

#### 4.5.3. Investigation of Hypoxia-Dependent Gene Expression with a 2-Nitroimidazole Bioreductive Inducer

Previous work in the group has shown that, of the bioreductive groups investigated in mammalian cancer cell lines, the 2-nitroimidazole bioreductive group provides an optimum balance between bioreduction in hypoxia and stability in normoxia; the 4-nitrobenzyl was found to be too stable in hypoxia, while the 5-nitrothiophene was too labile in normoxia. Having observed that **308**, which contains a 4-nitrobenzylidene group, was stable over 24 hours in hypoxic conditions in HepG2

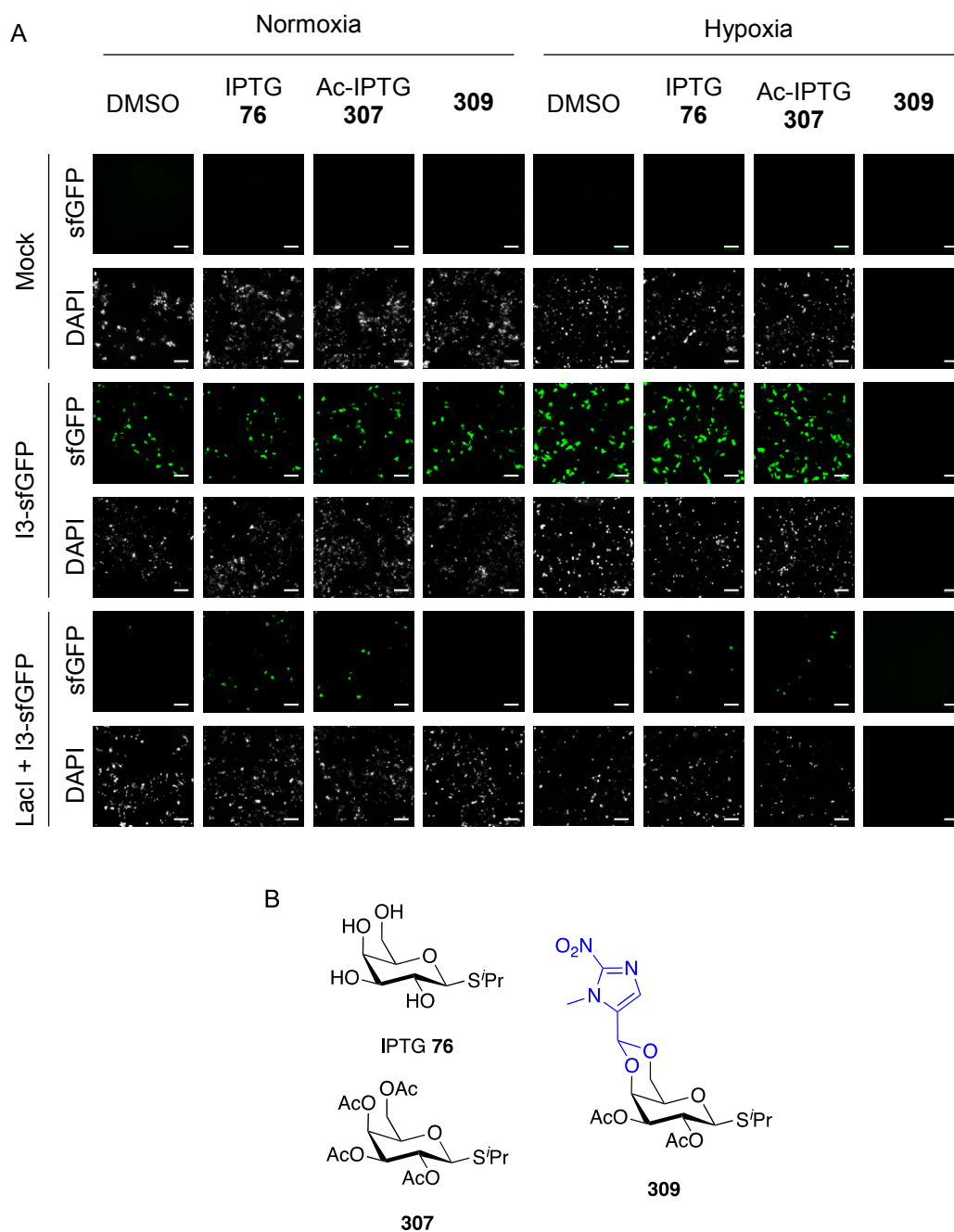
cells, it was hypothesised that the 2-nitroimidazole analogue **253** would be more appropriate for hypoxia-dependent gene expression in mammalian cells. Compound **253** had previously been tested in *BL21 (DE3)* pNIC28-sfGFP bacteria but was found to be toxic under hypoxic conditions. As before, to improve the membrane permeability of **253**, the 2- and 3- hydroxyl groups were protected with acetyl groups, yielding **309** (Scheme 4.7).



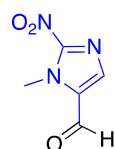
**Scheme 4.7:** Synthesis of acetyl protected inducer **309**. *Reagents and conditions:* Ac<sub>2</sub>O, pyridine, RT, 15 h, 94%.

HepG2 cells, transfected with pCMV-LacI and pOPI3-sfGFP (Section 4.5.1), were treated with IPTG **76**, acetylated IPTG **307**, and **309** under normoxic and hypoxic conditions. Samples were analysed for production of sfGFP by fluorescence. Although **309** did not induce sfGFP expression in normoxia, treatment with **309** under hypoxic conditions, resulted in death of all cells (Figure 4.23). This is similar to the toxicity observed when *BL21 (DE3)* pNIC28-sfGFP were treated with **253** under hypoxic conditions (Section 4.3.6). Adams *et al.* investigated the toxicity of a range of nitroaryl compounds, including the 2-nitroimidazole aldehyde **267** (Figure 4.24), towards hypoxic mammalian cells and found that the one-electron reduction potential was a key determinant of hypoxic-cell toxicity.<sup>404</sup> Compounds with a similar electron reduction potential but that did not contain a nitro group did not display the same toxicity to hypoxic cells. They proposed that a nitro group in a structure of high electron affinity is responsible for the observed toxicity towards hypoxic cells and that any of the sequence of reduction products may be responsible for the cytotoxicity. Based on the mechanism proposed for the fragmentation of **94** (Section 4.4.1), it is possible that reduction and fragmentation under hypoxic conditions releases the 2-nitroimidazole aldehyde **314** and that this product contributes to the toxicity observed in hypoxia (Scheme 4.8). Due to its high toxicity towards hypoxic cells, compound **309** was

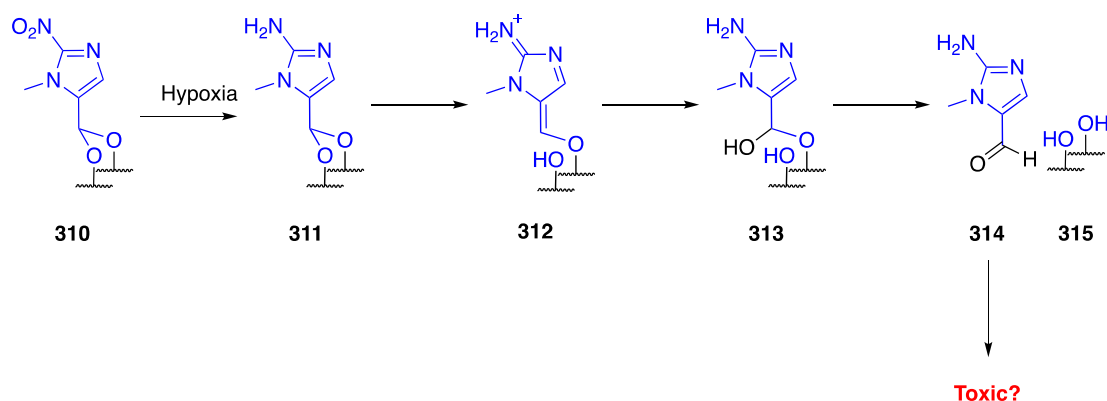
unsuitable for our studies into hypoxic-dependent gene expression in mammalian cells and was not pursued further.



**Figure 4.23:** Compound **309** is toxic to HepG2 cells under hypoxic conditions. A) HepG2 cells ( $8 \times 10^4$ – $15 \times 10^4$  cells) were transfected with pOPI3-sfGFP or pCMV-LacI:pOPI3-sfGFP (1:1). After 24 h, the media was replaced with fresh media containing DMSO, **76**, **307** or **309** (1 mM) and the cells were incubated for a further 24 h under either normoxic (21% O<sub>2</sub>) or hypoxic (<0.1% O<sub>2</sub>) conditions. Samples were analysed by fluorescence ( $\lambda_{\text{ex}} = 480$  nm,  $\lambda_{\text{em}} = 517$  nm). DAPI (blue) was used as a nuclear stain. Scale bars represent 100  $\mu$ M. B) Structures of IPTG **76**, acetylated-IPTG **307** and **309**.

**267**

**Figure 4.24:** Structure of the 2-nitroimidazole aldehyde **267** investigated by Adams *et al.*, during their studies into the toxicity of nitroaryl compounds towards hypoxic mammalian cells.<sup>404</sup>



**Scheme 4.8:** Potential mechanism for fragmentation of 2-nitroimidazole acetals following bioreduction under hypoxic conditions.

#### 4.6. Conclusion

The aim of this chapter was to determine whether the potential hypoxia-activated inducers, synthesised in Chapter 3 (Figure 4.25), are able to induce gene expression in a hypoxia-dependent manner. Compounds **123–127** were analysed in our standard series of reduction and bioreduction assays for analysis of HAPs.<sup>132</sup> In all cases, reduction with zinc and ammonium chloride in DMF resulted in formation of the hydroxylamine intermediate. Upon addition of a sample taken after 60 minutes of reduction to buffer, the hydroxylamine intermediate fragmented to release **103**. Furthermore, when **123–127** were treated with CYP450:NADPH reductase enzymes under both normoxic and hypoxic conditions, reduction and fragmentation to release **103** was only observed in the hypoxia-treated samples.

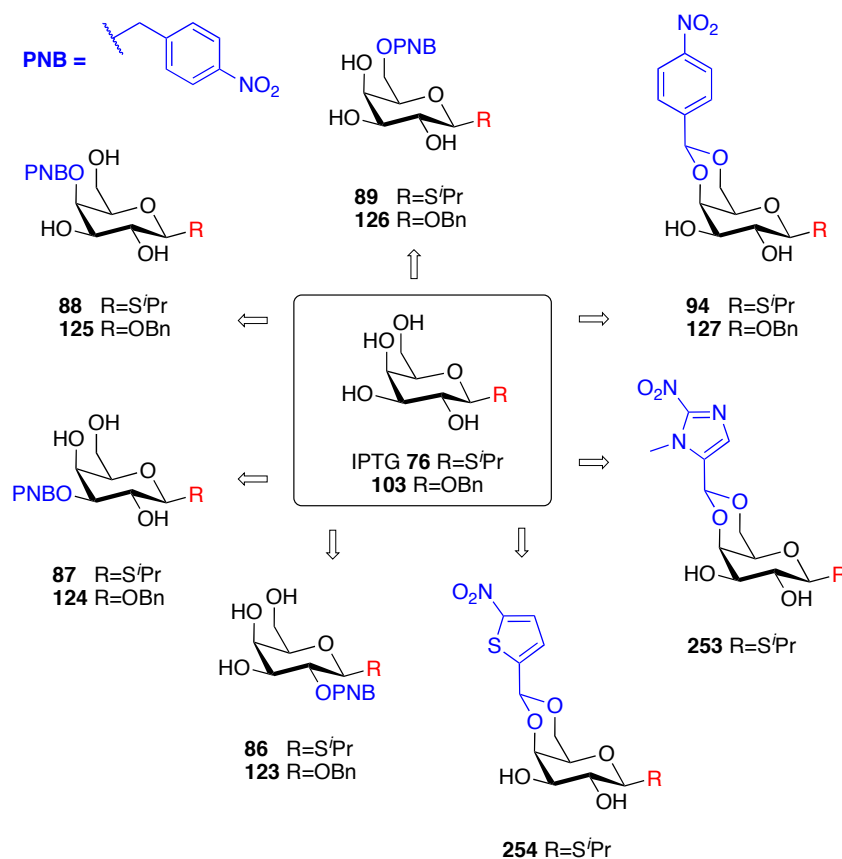


**Figure 4.25:** Structures of the potential hypoxia-activated inducers of gene expression, containing either an anomeric benzyl or thioisopropyl group, synthesised in Chapter 3.

Initially, the FMN-based fluorescent proteins (FbFPs), iLOV and creiLOV, were investigated as potential reporters for gene expression due to their ability to fluoresce in an oxygen independent manner. However, expression of these proteins in *E. coli* treated with IPTG **76** was not bright enough to be easily detected over the background signal from uninduced *E. coli*. As a result, sfGFP, a superfolder GFP, which can rapidly recover fluorescence upon reoxygenation, was chosen as the reporter gene. Compounds **86–89**, **94**, **253**, and **254** were next incubated with *BL21 (DE3)* pNIC38-sfGFP. It was found that **89** and **254** induced sfGFP expression in normoxic conditions, while **253** was toxic to bacterial cells under hypoxic conditions. Although compounds **86–88** and **94** did not induce gene expression in normoxic conditions, significant expression of sfGFP in hypoxia was only observed for the acetal compound **94**. A time course study showed that, after an initial lag period, expression of sfGFP increased rapidly until saturation was reached after 24 hours. Lastly, analysis of the oxygen-dependency of the response suggested that while

no sfGFP expression was observed at 1% O<sub>2</sub>, there was partial induction at 0.5% O<sub>2</sub>, and high levels of expression at 0.1% O<sub>2</sub>.

Investigations into the mechanism of activation suggested that there are two possible pathways. In the first, initial reduction and fragmentation forms a hemi-acetal intermediate **301**, which collapses to release 4-aminobenzaldehyde **302** and IPTG **76**. The second proposed pathway is based on the fact that **89** induced gene expression in normoxia. Initial reduction and fragmentation forms **299** or **301**, which may also be able to bind to LacI and induce gene expression. Taken together, these data have demonstrated the first example of hypoxia-dependent small molecule-induced gene expression in *BL21 (DE3) E. coli*.

Following the success of hypoxia-dependent expression in *E. coli* bacteria, focus was next placed on transferring the technology into mammalian cancer cells. Through the use of plasmids that contain the required components optimised for IPTG-inducible expression in mammalian cells,<sup>223</sup> IPTG-inducible expression was achieved in HepG2 cells, although the levels of sfGFP expression were consistently low in IPTG-induced samples. Furthermore, the hypoxia-activated inducers were found to have very low membrane permeability. To increase the membrane permeability of these compounds, the free hydroxyl groups were protected with acetyl protecting groups. Although this did successfully increase the membrane permeabilities, intracellular hydrolysis of the acetyl groups was slow. Additionally, the 4-nitrobenzyl acetal compound **308** was not significantly reduced in hypoxic conditions, suggesting the 4-nitrobenzyl group would be unsuitable for use in mammalian cells. Unfortunately, the more labile 2-nitroimidazole compound **309** was toxic to hypoxic cells and was, therefore, also unsuitable for our studies into hypoxic-dependent gene expression in mammalian cells. Thus far, steps towards transferring the technology into mammalian cells have encountered a number of challenges. Overcoming these challenges will be the primary focus of future work.





---

# CHAPTER 5

## CONCLUSIONS AND FUTURE WORK

---

### 5.1. Conclusions

The primary aim of the work described in this dissertation was to develop a technology for hypoxia-activated small molecule-induced gene expression. Building on previous work in the group, in which tools have been developed to target<sup>182,233</sup> and image<sup>234</sup> hypoxia, this work combined the concept of hypoxia-activated prodrugs with an IPTG-inducible gene expression system to achieve hypoxia-dependent gene expression in *BL21 (DE3)* bacteria.

*BL21 (DE3)* bacteria were chosen as a model system due to the ease and speed with which bacteria can be manipulated. Therefore, to determine whether *BL21 (DE3)* bacteria are able to reduce nitroaryl groups in a hypoxia-dependent manner, similar to that observed in mammalian cells, a fluorescent probe **79** (Figure 2.7, p52), comprising a 4-nitrobenzyl group attached to resorufin **64** dye was employed (Chapter 2). The ability of compound **79** to function as a hypoxia-dependent probe was first assessed through a series of chemical and enzymatic assays and found to be suitable for use in a cellular setting. Subsequently, compound **79** was incubated with either mammalian cancer cell lines (HepG2 and HCT116) and *BL21 (DE3)* bacteria. In both cases, a hypoxia dependent reduction and release of resorufin **64** was observed (Figure 2.11, p58; Figure 2.12, p59). This represents the first example of hypoxia-dependent bioreduction of nitroaryl groups in *E. coli* and suggested that *E. coli* would be a suitable model system, in which to develop hypoxia-activated small molecule-induced gene expression. Therefore, this work laid the foundation for the remainder of this dissertation.

The next step was to identify and to synthesise potential hypoxia-activated inducers of gene expression (Chapter 3). A key consideration in the design of these hypoxia-activated inducers for IPTG-inducible expression was that attachment of a bioreductive moiety to IPTG **76** must prevent IPTG **76** from binding to LacI. However, it was unclear from the crystal structure of IPTG **76** bound to LacI, where the optimal position for inclusion of a bioreductive protecting group would be and it was decided to synthesis derivatives of IPTG, protected at each of the free hydroxyl groups (2-, 3-, 4-, 6- position). In addition to these ether derivatives, an additional class of HAPs (**94**, **253** and **254**), containing a bioreductive group formed via an acetal linkage between the 4- and 6-position hydroxyl groups, was also synthesised. Finally, in order to facilitate downstream biological analysis of these compounds, analogues containing an anomeric UV-active moiety, were also synthesised (Figure 3.23, p115).

Following the synthesis of these potential hypoxia-activated inducers of gene expression **86–89** and **94** and their benzyl analogues **123–127**, the compounds were next evaluated for their ability to induce gene expression in a hypoxia-dependent manner (Chapter 4). All compounds were shown to be stable to CYP450:NADPH reductase enzymes in normoxia, while in hypoxia reduction to the hydroxylamine and amine derivatives, followed by fragmentation to release 10–20% **103** was observed. Although the enzyme-based assays showed similar release of IPTG **76** from both the 4-nitrobenzyl ether compounds and acetal compound, in a cellular setting, only compound **94** was found to successfully induce significant levels of sfGFP expression selectively in hypoxia (Figure 4.12, p135). To account for this difference in activity, we proposed two putative mechanisms by which bioreduction of **94** can induce expression. This work demonstrated the first example of hypoxia-dependent small molecule-induced gene expression in *BL21 (DE3) E. coli*. As it stands, this work will allow the investigation of hypoxia- activated gene expression in bacteria, which has especially significant implications in the study of biofilms. Additionally, to our knowledge, there are no previous examples of an acetal-based bioreductive compound, which opens the possibility to the development of a new class of hypoxia-activated prodrugs and imaging agents.

## 5.2. Future Work

The work described here represents a proof-of concept system for hypoxia-activated small molecule-induced gene expression. Thus far, it has only been shown to work in bacteria, but hypoxia is found in many biological contexts, including hypoxic tumours and plants. The approach presented here also activates gene expression relatively slowly (on the order of hours). Consequently, there are two important directions, which are of immediate interest for future investigations: modification of the bioreduction potential to modulate the rate of IPTG **76** release and further work on transferring the technology into alternative systems including human and/or plant cells. A third approach, in which the hypoxia-activated prodrug strategy could be applied to an alternative small molecule-controlled gene expression will also be discussed.

### 5.2.1. Modulating the Rate of IPTG Release

In the context of this work, increasing the rate of IPTG **76** release is expected to increase the speed with which gene expression is activated. It is generally accepted that there are two factors, which control fragmentation of HAPs to release a cargo molecule: variation in the choice of bioreductive group and decreasing the pKa of the leaving group.<sup>132</sup>

In the first approach, alteration of the bioreductive group (i.e. by replacing a nitrobenzyl with a nitroimidazole or nitrothiophenes moiety) is expected to increase the rate of reduction in hypoxia. However, this introduces the additional possibility that reduction of the nitroaryl group will occur under normoxic conditions, as was observed for the nitrothiophene acetal **254** (Section 4.3.6). Furthermore, in the context of this work, the nitroimidazole acetal **253** was found to be highly toxic to both bacteria and mammalian cells under hypoxic conditions (Sections 4.3.6 & 4.5.3). It is possible that these drawbacks are unique to the acetal-based bioreductive prodrug system employed. Therefore, alternative ether-based inducers, as the 2-nitroimidazole- (**316**) or 5-nitrothiophene- (**317**) based derivatives, may be more suitable for inducing rapid gene expression under hypoxic conditions (Figure 5.1).

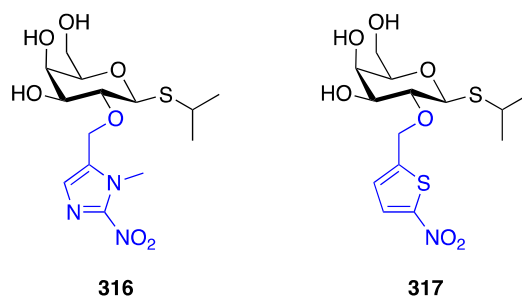


**Figure 5.1:** Structures of potential alternative ether-based inducers, containing either a 2-nitroimidazole **316** or 5-nitrothiophene **317** bioreductive group.

Alternatively, it has been shown that introducing electron-donating substituents, such as a *mono*-methyl or *gem*-dimethyl, at the benzylic position of the bioreductive moiety, increases the rate of fragmentation.<sup>405</sup> This approach is advantageous, because it is not expected to affect the reduction potential of the bioreductive group, which should help to reduce undesired reduction under normoxic conditions. Consequently, a third alternative inducer, such as **318**, which includes a *gem*-dimethyl-4-nitrobenzyl group also has the potential to increase the rate of activation of gene expression (Figure 5.2).

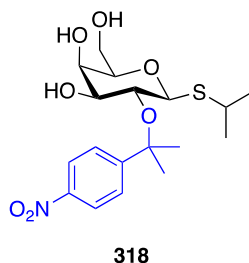


**Figure 5.2:** Structure of a potential alternative inducer **318**, containing a *gem*-dimethyl-4-nitrobenzyl bioreductive group.

### 5.2.2. Translation Into Mammalian Cells

Initial steps taken towards translating the system to mammalian cell lines encountered a number of challenges including the requirement for the presence of both LacI and promoters that are controlled by a *lacO* sequence, neither of which are endogenously present in mammalian cells, and the poor membrane permeability of the hypoxia-activated compounds (Section 4.5). The use of acetyl protecting groups was shown to improve the membrane permeability of **94** and **253**. However, to overcome the challenge of introducing two endogenous components, future work

should focus on generating a stable cell line that both expresses LacI and contains *lacO*-controlled genes. This will reduce the number of variables involved in the experiment by eliminating the transient transfection step. A FACS-based approach, using the LacSwitchII system, has been shown to be an efficient technique for the generation of inducible cell lines and would be highly applicable here.<sup>406</sup>

### 5.2.3. Considering Alternative Gene Expression Systems

Finally, the work described in this dissertation has focused on the IPTG-inducible system for gene expression and, although this has been shown to work in bacteria, there are a number of alternative small molecule-controlled gene induction systems, which could have been chosen (Section 1.6.2). For example, one such system uses a repressor (CymR) that was taken from the *p-cym* and *p-cmt* operons found in *Pseudomonas putida* and can be induced with 4-isopropylbenzoic acid **319** (cumic acid) (Figure 5.3A).<sup>407</sup> Similarly to IPTG/*lacO* controlled gene expression, CymR binds to an operator sequence (*CuO*); upon induction, cumic acid **319** binds the repressor, which then dissociates from the DNA, allowing transcription of the downstream gene. The main advantage of the cumate system over IPTG-inducible expression is that lower levels of inducer can be used (50  $\mu$ M cumic acid **319** compared with 1 mM IPTG **76**). Additionally, it is likely that a bioreductively protected cumic acid **319** will be more membrane-permeable than the galactose-based inducers. However, there is no known crystal structure of cumic acid **319** bound to CymR, which complicates prediction of where is the optimal position to functionalise with a bioreductive moiety. Extensive SAR studies around the ability of analogues of cumic acid **319** to induce gene expression have suggested that the carboxylic acid moiety is essential for binding to the repressor. Consequently, attaching a bioreductive moiety *via* an ester-functionality (**320**) could inhibit binding to the repressor. Additionally, inclusion of a *mono*-methyl (**321**) or *gem*-dimethyl (**322**) group at the benzylic position may help to prevent ester hydrolysis by intracellular esterases, reducing the likelihood of hypoxia-independent activation (Figure 5.3B). It should be noted that, like IPTG-inducible expression, this approach also requires incorporation of two exogenous components (CymR and *CuO*) into the system of interest. Commercially available systems, which

deliver CymR and a *CuO*-controlled gene-of-interest in one lentivector, are available (System Bioscience) and this approach may help to overcome the challenges encountered regarding efficient co-transfection of both components.

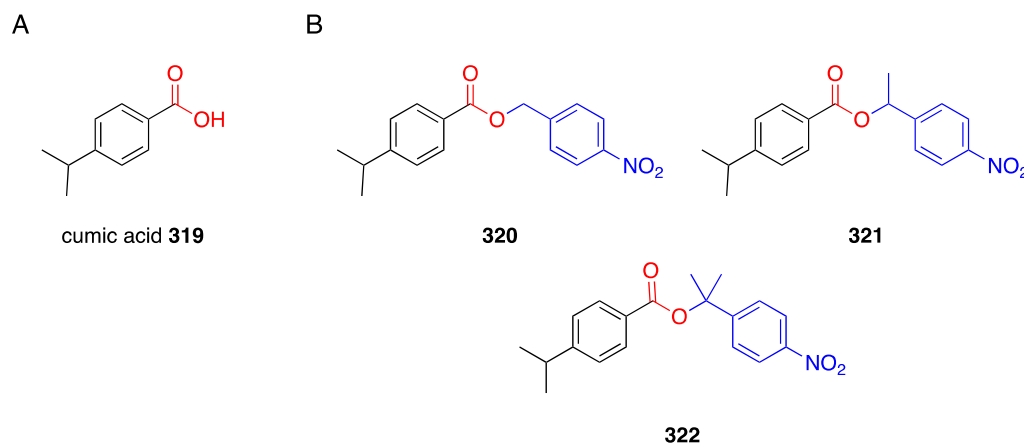


**Figure 5.3:** A) Structure of cumic acid **319**, which can be used to induce CymR/*CuO*-controlled gene expression. The carboxylic acid moiety, which is essential for induction is shown in red. B) Structures of the proposed bioreductive inducers of the CymR/*CuO* expression system. Blue = bioreductive group.

### 5.3. Concluding Remarks

It is clear that hypoxia has numerous negative implications in a number of areas that are of fundamental importance, including cancer therapies, biofilm antibiotic resistance, and agriculture, and that chemical tools to study hypoxia are vital. Whilst hypoxia-induced gene expression has previously been achieved using environmental-driven promoters (such as HRE in mammalian cells), the hypoxia-activated small molecule-induced gene expression system developed here has the potential to be a widely applicable tool in number of biologically important contexts. Altering the hypoxia-sensing group would also offer the ability to control the degree of hypoxia required for, and the kinetics of, gene induction. It could also conceivably be extended to regulate the production of any given protein of choice, without the requirement to re-develop the prodrug strategy. Further development of tools such as these will enable greater understanding of the role of individual proteins in the hypoxia-driven complexities that underlie a wide variety of systems. This knowledge will provide an important contribution towards development of novel strategies, which aim to minimise the impact of hypoxia in these biologically-important settings.

---

# CHAPTER 6

## EXPERIMENTAL

---

### 6.1. General Chemical Methods

#### Chemicals

Chemicals were purchased from Acros Organics, Alfa Aesar, Apollo Scientific, Fisher Scientific, Fluka, Fluorochem, Merck or Sigma Aldrich and were used without further purification. Silver oxide was freshly prepared prior to use by dropwise addition of excess aqueous 1 M NaOH to an aqueous solution of silver nitrate. The resulting solid brown precipitate was filtered, washed with water then acetone and dried *in vacuo*.

**Brine** refers to a saturated, aqueous solution of sodium chloride. **Hexane** refers to a mixture of hexane isomers. **Petroleum ether** refers to the fraction boiling between 40–60 °C. Molecular sieves were activated in an oven at 400 °C. Unless otherwise stated, **phosphate buffer** refers to an aqueous solution of 50 mM NaH<sub>2</sub>PO<sub>4</sub>/Na<sub>2</sub>HPO<sub>4</sub> and 150 mM NaCl at pH 7.4. Celite® refers to Celite®545 filter aid, treated with sodium carbonate, flux-calcined, which was purchased from Sigma Aldrich. **Concentrated aqueous HCl** refers to a 37% (w/w) solution of hydrochloric acid in water.

#### Solvent Purification

Where appropriate and if not otherwise stated, all non-aqueous reactions were carried out under an inert atmosphere of argon, using flame-dried glassware. **Anhydrous solvents** were obtained under the following conditions: acetonitrile, dichloromethane, diethyl ether and DMF were dried by passing them through a column of active basic alumina according to Grubbs' procedure<sup>408</sup> and stored over activated 3 Å molecular sieves under argon. Pyridine was stirred over potassium

hydroxide, distilled from calcium hydride and stored over activated 3 Å molecular sieves under argon. Anhydrous THF was either distilled from sodium metal, using benzophenone as an indicator or dried by passing through a column of active basic alumina according to Grubbs' procedure<sup>408</sup> and stored over activated 3 Å molecular sieves under argon. Anhydrous methanol was purchased from Sigma Aldrich UK in SureSeal™ bottles and used without further purification.

### Analytical Thin Layer Chromatography

Thin layer chromatography (TLC) was performed on normal phase Merck silica gel 60 F254 aluminium-supported thin layer chromatography sheets. Spots were visualised by either absorption under UV light (254 nm), exposure to iodine vapour or thermal development after dipping into either a solution of ammonium molybdate in sulfuric acid or an aqueous solution of potassium permanganate.

### Reaction Monitoring

Reaction progress was monitored at appropriate times by TLC analysis.

### Silica Gel Flash Column Chromatography

Normal phase silica gel flash column chromatography was performed manually using Geduran Silicagel 60 (40–63 µm) under a positive pressure of compressed nitrogen.

### Concentration *in vacuo*

*In vacuo* refers to the removal of solvents under reduced pressure using a Büchi™ rotary evaporator in a water bath at 40 °C, unless otherwise specified. Vacuum transfer refers to the removal of solvents on a manifold linked to a high vacuum pump at room temperature.

### NMR

<sup>1</sup>H NMR spectra were recorded on a Bruker AVIIIHD 400 (400 MHz), a Bruker AVII 500 with dual <sup>13</sup>C(<sup>1</sup>H) cryoprobe (500 MHz) or a Bruker AVIIIHD 500 (500 MHz) spectrometer with the stated solvents as a reference for the internal deuterium lock. Chemical shifts are reported as δH in parts per million (ppm) relative to tetramethylsilane (TMS) where δH (TMS) = 0.00 ppm. The



spectra are calibrated using the solvent peak with the data provided by Fulmer *et al.*<sup>409</sup> The multiplicity of each signal is indicated by: s (singlet), br s (broad singlet), d (doublet), t (triplet), q (quartet), sept (septet), m (multiplet) or combinations thereof. The number of protons (n) for a given resonance signal is indicated by nH. The shift values of resonances are quoted to 2 decimal places unless peaks have similar chemical shifts, in which case 3 decimal places are used. Where appropriate, coupling constants (*J*) are quoted in Hz. Identical proton coupling constants are averaged in each spectrum and reported to the nearest 0.1 Hz. The coupling constants were determined by analysis using Bruker TopSpin software (versions 3.2 and 4.0). <sup>1</sup>H spectra were assigned using 2D NMR experiments including COSY, HSQC, <sup>13</sup>C-<sup>1</sup>H HMBC and <sup>29</sup>Si-<sup>1</sup>H HMBC.

**<sup>13</sup>C NMR spectra** were recorded on a Bruker AVIIIHD 400 (101 MHz) or a Bruker AVII 500 with dual <sup>13</sup>C(<sup>1</sup>H) cryoprobe (126 MHz) spectrometer in the stated solvents with broadband proton decoupling and an internal deuterium lock. Chemical shifts are reported as  $\delta$ C in parts per million (ppm) relative to tetramethylsilane (TMS) where  $\delta$ C (TMS) = 0.00 ppm. The spectra are calibrated using the solvent peak with the data provided by Fulmer *et al.*<sup>409</sup> The shift values of resonances are quoted to 1 decimal place unless peaks have similar chemical shifts, in which case 2 decimal places are used. <sup>13</sup>C spectra were assigned using 2D NMR experiments including HSQC and <sup>13</sup>C-<sup>1</sup>H HMBC.

## Mass Spectrometry

**Electrospray ionisation (ESI) mass spectra** were acquired using an Agilent 6120 Quadrupole spectrometer or Waters LCT Premier spectrometer, operating in positive or negative mode, as indicated, from solutions of MeOH or MeCN. **Chemical ionisation (CI) mass spectra** were acquired using a Waters GCT spectrometer. MS data was processed using MestReNova. *m/z* values are reported in Daltons and followed by their percentage abundance in parentheses. **Accurate mass spectra** were obtained using Bruker  $\mu$ TOF spectrometer. *m/z* values are reported in Daltons. When a compound was not observed by LRMS, only HRMS is quoted.

## Melting Points

Melting points were determined using a Leica Galen III hot stage microscope and are uncorrected.

The solvent of crystallisation is shown in parentheses.

## Infrared Spectra

Infrared (IR) spectra were obtained either from neat samples, either as liquids or solids, or as a thin film using a diamond ATR module. The spectra were recorded on a Bruker Tensor 27 spectrometer. Absorption maxima are reported in wavenumbers ( $\text{cm}^{-1}$ ) and reported as s (strong), m (medium), w (weak) or br (broad). Only the main, relevant peaks have been assigned.

## Specific Optical Rotations

Specific optical rotations were measured using a Schmidt + Haensch UniPol L2000 polarimeter, in cells with a path length of 1 dm at 25 °, using a sodium lamp at 589 nm. The concentration (*c*) is expressed in g/100 mL. Specific rotations are denoted  $[\alpha]_{\text{D}}^{\text{T}}$  values are reported in implied units of  $10^{-1} \text{ }^{\circ} \text{ cm}^2 \text{ g}^{-1}$  at the temperature (T) stated.

## Compound Purity

Compound purity was determined by **analytical high-performance liquid chromatography** (HPLC) on a PerkinElmer Flexar system with a Binary LC Pump and UV/Vis LC Detector. For determination of compound purity on reversed phase (RP) a Dionex Acclaim<sup>®</sup> 120 column (C18, 5  $\mu\text{m}$ , 120 Å, 4.6  $\times$  150 mm) was employed with water as eluent A and acetonitrile as eluent B. Samples were injected in methanol, water or acetonitrile. For determination of compound purity on normal phase (NP) a Hypersil GOLD<sup>™</sup> Silica LC column (5  $\mu\text{m}$ , 175 Å, 4.6  $\times$  150 mm) was employed with hexane as eluent A and isopropanol as eluent B. Samples were injected in dichloromethane. For each compound, one of four methods was used, as described below (Table 6.1). Compounds which did not contain a chromophore could not be analysed by analytical HPLC, and therefore their purity was not determined *via* this method.

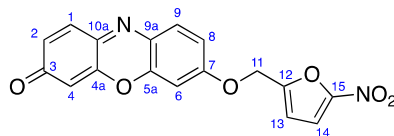
**Table 6.1:** Summary of methods used for HPLC analysis of compound purity

Method	Flow Rate mL/min	Start Time min	End Time min	%B Start	%B End
<b>1</b>	1.0	0	1	5	5
		1	11	5	95
		11	14	95	95
		14	15	95	5
		15	20	5	5
<b>2</b>	1.5	0	10	5	95
		10	15	95	95
<b>3</b>	1.5	0	10	5	95
		10	20	95	95
<b>4</b>	1.5	0	20	5	95
		20	25	95	95

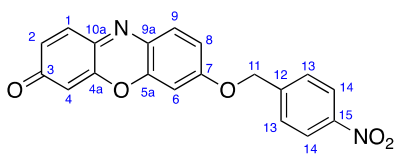
## 6.2. Synthetic Methods

### 6.2.1. Synthesis of Resorufin-Based Probes

#### 7-[(5-Nitrofuran-2-yl)methoxy]-3*H*-phenoxazin-3-one, **63**

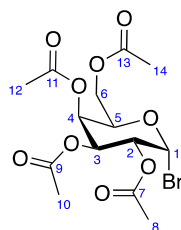


To a solution of resorufin sodium salt **64** (0.245 g, 1.04 mmol, 1.0 eq) and  $K_2CO_3$  (0.220 g, 1.59 mmol, 1.5 eq) in DMF (10 mL), stirred at 40 °C for 10 min, was added dropwise 2-bromomethyl-5-nitrofuran **78** (0.218 g, 1.06 mmol, 1.0 eq) in DMF (2 mL). The solution was stirred at 40 °C for 2 h, diluted with  $CH_2Cl_2$  (50 mL) and washed with water ( $3 \times 500$  mL). The aqueous layer was extracted with  $CH_2Cl_2$  ( $5 \times 200$  mL). The organic layers were combined, dried over  $MgSO_4$ , filtered, and concentrated *in vacuo*. The crude residue was purified by silica gel chromatography (70% ethyl acetate in hexanes) to yield 7-[(5-nitrofuran-2-yl)methoxy]-3*H*-phenoxazin-3-one **63** (0.177 g, 51%) as an orange solid:  $R_f$  0.19 (1:1 hexanes:ethyl acetate); mp 238–242 °C (ethyl acetate);  $\bar{\nu}_{max}$  (neat)/ $cm^{-1}$ : 3137 (w, aromatic C–H), 2360 (w), 1623 (m), 1570 (m), 1537 (s, N=O), 1505 (s), 1447 (m), 1401 (w), 1377 (w), 1350 (s, N=O), 1322 (m), 1290 (m), 1261 (s, C–O), 1213 (m, C–N), 1109 (w), 1013 (s), 971 (w), 950 (m), 883 (m), 862 (s), 824 (s), 809 (s);  $^1H$  NMR (500 MHz,  $CDCl_3$ )  $\delta$  7.76 (1H, d,  $J$  8.9,  $C^9$ -H), 7.43 (1H, d,  $J$  9.8,  $C^1$ -H), 7.33 (1H, d,  $J$  3.7,  $C^{14}$ -H), 7.00 (1H, dd,  $J$  8.9, 2.7,  $C^8$ -H), 6.89 (1H, d,  $J$  2.7,  $C^6$ -H), 6.85 (1H, dd,  $J$  9.8, 2.0,  $C^2$ -H), 6.73 (1H, d,  $J$  3.7,  $C^{13}$ -H), 6.34 (1H, d,  $J$  2.0,  $C^4$ -H), 5.18 (2H, s,  $C^{11}$ -H<sub>2</sub>);  $^{13}C$  NMR (126 MHz,  $CDCl_3$ )  $\delta$  186.4 ( $C^3$ ), 161.2 ( $C^7$ ), 151.9 ( $C^{12}$ ), 149.7 ( $C^{4a}$ ), 146.7 ( $C^{10a}$ ), 145.6 ( $C^{5a}$ ), 134.9 ( $C^1$ ), 134.7 ( $C^2$ ), 132.0 ( $C^9$ ), 129.1 ( $C^{9a}$ ), 113.7 ( $C^8$ ), 113.3 ( $C^{13}$ ), 112.1 ( $C^{14}$ ), 107.2 ( $C^4$ ), 101.3 ( $C^6$ ), 62.7 ( $C^{11}$ ); HRMS  $m/z$  (ESI<sup>+</sup>) [Found (M+H)<sup>+</sup> 339.06118  $C_{17}H_{11}N_2O_6$  requires M<sup>+</sup> 339.06116]; LRMS  $m/z$  (ES<sup>+</sup>) 339 ([M+H]<sup>+</sup>, 100%), 340 ([M+H]<sup>+</sup>, 29%); Analytical NP-HPLC (Method 1, 254 nm) Ret. time = 9.2 min, Purity = >99.9%. The data are in good agreement with the literature.<sup>201</sup>

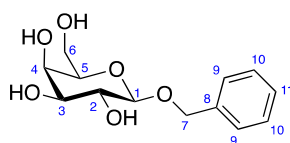
**7-[(4-Nitrobenzyl)oxy]-3*H*-phenoxazin-3-one, **79****

To a solution of resorufin sodium salt **64** (0.235 g, 1.00 mmol, 1.0 eq) and  $K_2CO_3$  (0.215 g, 1.56 mmol, 1.5 eq) in DMF (3 mL), stirred at 100 °C for 15 min, was added dropwise 4-nitrobenzyl bromide **80** (0.870 g, 4.03 mmol, 4.0 eq) in DMF (2 mL). The solution was stirred at 100 °C for 17 h and concentrated *in vacuo* at 60 °C. The residue was diluted with  $CH_2Cl_2$  (200 mL) and washed with water ( $3 \times 100$  mL). The aqueous layer was extracted with  $CH_2Cl_2$  ( $3 \times 100$  mL). The organic layers were combined, dried over  $MgSO_4$ , filtered, and concentrated *in vacuo*. The crude residue was crystallised from  $CH_2Cl_2$  to yield 7-[(4-nitrobenzyl)oxy]-3*H*-phenoxazin-3-one **79** (0.119 g, 34%) as a red solid:  $R_f$  0.23 (1:1 hexanes:ethyl acetate); mp 289–292 °C ( $CH_2Cl_2$ );  $\bar{\nu}_{max}$  (neat)/ $cm^{-1}$  2360 (w), 2342 (w), 1613 (s), 1563 (m), 1523 (s, N=O), 1506 (w, aromatic C–C), 1489 (w), 1348 (s, N=O), 1265 (s, C–O), 1210, (m, C–N), 1165 (w), 1121 (w), 1105 (m), 1037 (w), 1017 (w), 856 (s), 830 (m), 734 (w);  $^1H$  NMR (500 MHz,  $CDCl_3$ )  $\delta$  8.33–8.27 (2H, m,  $C^{14}$ -H), 7.75 (1H, d,  $J$  8.9,  $C^9$ -H), 7.66–7.60 (2H, m,  $C^{13}$ -H), 7.43 (1H, d,  $J$  9.8,  $C^1$ -H), 7.02 (1H, dd,  $J$  8.9, 2.7,  $C^8$ -H), 6.87 (1H, d,  $J$  2.7,  $C^6$ -H), 6.85 (1H, dd,  $J$  9.8, 2.0,  $C^2$ -H), 6.32 (1H, d,  $J$  2.0,  $C^4$ -H), 5.29 (2H, s,  $C^{11}$ -H<sub>2</sub>);  $^{13}C$  NMR (126 MHz,  $CDCl_3$ )  $\delta$  186.4 ( $C^3$ ), 161.8 ( $C^7$ ), 149.8 ( $C^{4a}$ ), 148.1 ( $C^{15}$ ), 146.4 ( $C^{10a}$ ), 145.7 ( $C^{5a}$ ), 142.8 ( $C^{12}$ ), 134.9 ( $C^1$ ), 134.6 ( $C^2$ ), 132.0 ( $C^9$ ), 128.9 ( $C^{9a}$ ), 127.9 ( $C^{13}$ ), 124.2 ( $C^{14}$ ), 114.0 ( $C^8$ ), 107.1 ( $C^4$ ), 101.3 ( $C^6$ ), 69.5 ( $C^{11}$ ); HRMS  $m/z$  (ESI<sup>+</sup>) [Found (M+H)<sup>+</sup> 349.08190  $C_{19}H_{13}N_2O_5$  requires M<sup>+</sup> 349.08194]; LRMS  $m/z$  (ES<sup>+</sup>) 349 ([M+H]<sup>+</sup>, 100%), 350 ([M+H]<sup>+</sup>, 35%); Analytical NP-HPLC (Method 1, 254 nm) Ret. time = 8.1 min, Purity = 96.7%.

## 6.2.2. Synthesis of UV-Active Inducers

2,3,4,6-Tetra-*O*-acetyl- $\alpha$ -D-galactopyranosyl bromide, **117**

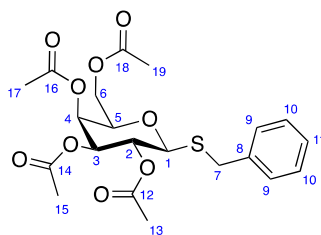
To  $\beta$ -D-galactose pentaacetate **116** (5.00 g, 12.8 mmol, 1.0 eq), cooled to 0 °C, was added HBr (33 wt.% in acetic acid, 11.3 mL, 64.5 mmol, 5.0 eq). The solution was warmed to room temperature and stirred for 2.5 h. The reaction solution was diluted with CH<sub>2</sub>Cl<sub>2</sub> (100 mL) and washed with sat. aq. NaHCO<sub>3</sub> (3  $\times$  75 mL) and brine (3  $\times$  50 mL). The organic layers were combined, dried over MgSO<sub>4</sub>, filtered, and concentrated *in vacuo*. The crude residue was purified by gradient silica gel chromatography (0–30% ethyl acetate in petroleum ether) to yield 2,3,4,6-tetra-*O*-acetyl- $\alpha$ -D-galactopyranosyl bromide **117** (5.07 g, 96%) as a colourless solid: *R*<sub>f</sub> 0.18 (1:4 ethyl acetate:petroleum ether);  $[\alpha]_D^{25} = +223.5$  (*c* 1.0, CHCl<sub>3</sub>) [lit.<sup>410</sup>  $[\alpha]_D^{25} = +217$  (*c* 1.2, CHCl<sub>3</sub>)]; mp 83–84 °C (ethyl acetate) [lit.<sup>410</sup> 84–85 °C]; <sup>1</sup>H NMR (400 MHz, CDCl<sub>3</sub>)  $\delta$  6.70 (1H, d, *J* 4.0, C<sup>1</sup>-*H*), 5.52 (1H, dd, *J* 3.3, 1.2, C<sup>4</sup>-*H*), 5.40 (1H, dd, *J* 10.6, 3.3, C<sup>3</sup>-*H*), 5.05 (1H, dd, *J* 10.6, 4.0, C<sup>2</sup>-*H*), 4.49 (1H, dd, *J*<sub>AX</sub> 6.7, *J*<sub>BX</sub> 6.5, C<sup>5</sup>-*H*<sub>X</sub>), 4.19 (1H, dd, *J*<sub>AB</sub> 11.4, *J*<sub>BX</sub> 6.5, C<sup>6</sup>-*H*<sub>B</sub>), 4.11 (1H, dd, *J*<sub>AB</sub> 11.4, *J*<sub>AX</sub> 6.7, C<sup>6</sup>-*H*<sub>A</sub>), 2.15 (3H, s, C<sup>8</sup>-*H*<sub>3</sub> or C<sup>10</sup>-*H*<sub>3</sub> or C<sup>12</sup>-*H*<sub>3</sub> or C<sup>14</sup>-*H*<sub>3</sub>), 2.12 (3H, s, C<sup>8</sup>-*H*<sub>3</sub> or C<sup>10</sup>-*H*<sub>3</sub> or C<sup>12</sup>-*H*<sub>3</sub> or C<sup>14</sup>-*H*<sub>3</sub>), 2.06 (3H, s, C<sup>8</sup>-*H*<sub>3</sub> or C<sup>10</sup>-*H*<sub>3</sub> or C<sup>12</sup>-*H*<sub>3</sub> or C<sup>14</sup>-*H*<sub>3</sub>), 2.01 (3H, s, C<sup>8</sup>-*H*<sub>3</sub> or C<sup>10</sup>-*H*<sub>3</sub> or C<sup>12</sup>-*H*<sub>3</sub> or C<sup>14</sup>-*H*<sub>3</sub>); LRMS *m/z* (ES<sup>+</sup>) 433 ([M<sup>79</sup>Br+Na]<sup>+</sup>, 100%), 434 ([M<sup>79</sup>Br+Na]<sup>+</sup>, 16%), 435 ([M<sup>81</sup>Br+Na]<sup>+</sup>, 96%), 436 ([M<sup>81</sup>Br+Na]<sup>+</sup>, 16%). The data are in good agreement with the literature.<sup>410,411</sup>

Benzyl  $\beta$ -D-galactopyranoside, **103**

To a suspension of benzyl alcohol (8.90 mL, 86.0 mmol, 7.0 eq) and silver carbonate (6.76 g, 24.5 mmol, 2.0 eq) in CH<sub>2</sub>Cl<sub>2</sub> (20 mL), pre-stirred over 4 Å molecular sieves for 30 min, was

added dropwise over 15 min a solution of **117** (5.05 g, 12.3 mmol, 1.0 eq) in CH<sub>2</sub>Cl<sub>2</sub> (20 mL), pre-stirred over 4 Å molecular sieves for 30 min. The solution was shielded from light and stirred at room temperature for 24 h. The reaction mixture was filtered through Celite® and concentrated *in vacuo* to afford a mixture of benzyl alcohol and benzyl 2,3,4,6-tetra-*O*-acetyl-β-D-galactopyranoside **118** as a colourless liquid. To a solution of this liquid in methanol (40 mL) was added sodium methoxide (0.277 g, 5.13 mmol, 0.4 eq). The solution was stirred at room temperature for 1 h, adjusted to pH 7 with Amberlite® IR120 resin (H<sup>+</sup>-form), filtered, and concentrated *in vacuo*. The crude residue was purified by gradient silica gel chromatography (50–100% ethyl acetate in petroleum ether to 0–5% methanol in ethyl acetate) to yield benzyl β-D-galactopyranoside **103** (2.77 g, 84%, 2 steps) as a colourless solid: *R*<sub>f</sub> 0.22 (1:9 methanol:ethyl acetate); [α]<sub>D</sub><sup>25</sup> = −39.1 (*c* 1.0, MeOH) [lit.<sup>277</sup> [α]<sub>D</sub><sup>25</sup> = −31.4 (*c* 0.14, MeOH)]; mp 103–105 °C (ethyl acetate) [lit.<sup>412</sup> 106–108 °C]; <sup>1</sup>H NMR (400 MHz, CD<sub>3</sub>OD) δ 7.43–7.41 (2H, m, C<sup>9</sup>-*H*), 7.34–7.30 (2H, m, C<sup>10</sup>-*H*), 7.28–7.24 (1H, m, C<sup>11</sup>-*H*), 4.93 (1H, d, *J*<sub>AB</sub> 11.8, C<sup>7</sup>-*H*<sub>A</sub>), 4.67 (1H, d, *J*<sub>AB</sub> 11.8, C<sup>7</sup>-*H*<sub>B</sub>), 4.31 (1H, d, *J* 7.7, C<sup>1</sup>-*H*), 3.83 (1H, d, *J* 3.4, 1.0, C<sup>4</sup>-*H*), 3.80 (1H, dd, *J*<sub>AB</sub> 11.3, *J*<sub>AX</sub> 6.9, C<sup>6</sup>-*H*<sub>A</sub>), 3.74 (1H, dd, *J*<sub>AB</sub> 11.3, *J*<sub>BX</sub> 5.3, C<sup>6</sup>-*H*<sub>B</sub>), 3.58 (1H, dd, *J* 9.7, 7.7, C<sup>2</sup>-*H*), 3.52–3.49 (1H, ddd, *J*<sub>AX</sub> 6.9, *J*<sub>BX</sub> 5.3, *J* 1.0, C<sup>5</sup>-*H*<sub>X</sub>), 3.45 (1H, dd, *J* 9.7, 3.4, C<sup>3</sup>-*H*); LRMS *m/z* (ES<sup>+</sup>) 293 ([M+Na]<sup>+</sup>, 100%), 294 ([M+Na]<sup>+</sup>, 15%), 295 ([M+Na]<sup>+</sup>, 3%). The data are in good agreement with the literature.<sup>277,412,413</sup>

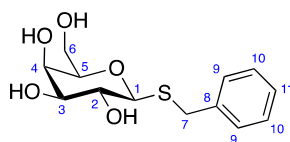
### Benzyl 2,3,4,6-tetra-*O*-acetyl-1-thio-β-D-galactopyranoside, **122**



To a solution of β-D-galactose pentaacetate **116** (5.00 g, 12.8 mmol, 1.0 eq) in CH<sub>2</sub>Cl<sub>2</sub> (20 mL) was added benzyl mercaptan (2.30 mL, 19.6 mmol, 1.5 eq). The solution was stirred at −78 °C for 5 min and BF<sub>3</sub>·Et<sub>2</sub>O (3.20 mL, 25.9 mmol, 2.0 eq) was added dropwise. The solution was warmed to room temperature and stirred for 6 h. The solution was diluted with CH<sub>2</sub>Cl<sub>2</sub> (50 mL)

and washed with sat. aq.  $\text{NaHCO}_3$  ( $5 \times 50$  mL). The organic layers were combined, dried over  $\text{MgSO}_4$ , filtered, and concentrated *in vacuo*. The crude residue was purified by crystallisation ( $\text{CH}_2\text{Cl}_2$ /hexane) to yield benzyl 2,3,4,6-tetra-*O*-acetyl-1-thio- $\beta$ -D-galactopyranoside **122** (3.59 g, 62%) as colourless crystals:  $R_f$  0.54 (1:3 ethyl acetate:petroleum ether);  $[\alpha]_D^{25} = -80.0$  ( $c$  1.0,  $\text{CHCl}_3$ ) [lit.<sup>414</sup>  $[\alpha]_D = -80.3$  ( $c$  1.02,  $\text{CHCl}_3$ )]; mp 96–98 °C ( $\text{CH}_2\text{Cl}_2$ /hexanes) [lit.<sup>415</sup> 97 °C];  $\bar{\nu}_{\text{max}}$  (neat)/ $\text{cm}^{-1}$  1746 (s, C=O), 1368 (m, C–O) 1219 (s, C–O), 1082 (m), 1051 (m), 918 (w), 705 (w, C–S);  $^1\text{H}$  NMR (400 MHz,  $\text{CDCl}_3$ )  $\delta$  7.36–7.24 (5H, m,  $\text{C}^9\text{-H}$ ,  $\text{C}^{10}\text{-H}$ ,  $\text{C}^{11}\text{-H}$ ), 5.41 (1H, dd,  $J$  3.4, 1.1,  $\text{C}^4\text{-H}$ ), 5.28 (1H, dd,  $J$  10.0, 10.0,  $\text{C}^2\text{-H}$ ), 4.96 (1H, dd,  $J$  10.0, 3.4,  $\text{C}^3\text{-H}$ ), 4.28 (1H, d,  $J$  10.0,  $\text{C}^1\text{-H}$ ), 4.16 (1H, dd,  $J_{\text{AB}}$  11.4,  $J_{\text{AX}}$  6.8,  $\text{C}^6\text{-H}_A$ ), 4.11 (1H, dd,  $J_{\text{AB}}$  11.4,  $J_{\text{BX}}$  6.4,  $\text{C}^6\text{-H}_B$ ), 3.96 (1H, d,  $J_{\text{AB}}$  12.9,  $\text{C}^7\text{-H}_A$ ), 3.84 (1H, d,  $J_{\text{AB}}$  12.9,  $\text{C}^7\text{-H}_B$ ), 3.85–3.81 (1H, m,  $\text{C}^5\text{-H}_X$ ), 2.16 (3H, s,  $\text{C}^{13}\text{-H}_3$  or  $\text{C}^{15}\text{-H}_3$  or  $\text{C}^{17}\text{-H}_3$  or  $\text{C}^{19}\text{-H}_3$ ), 2.08 (3H, s,  $\text{C}^{13}\text{-H}_3$  or  $\text{C}^{15}\text{-H}_3$  or  $\text{C}^{17}\text{-H}_3$  or  $\text{C}^{19}\text{-H}_3$ ), 2.02 (3H, s,  $\text{C}^{13}\text{-H}_3$  or  $\text{C}^{15}\text{-H}_3$  or  $\text{C}^{17}\text{-H}_3$  or  $\text{C}^{19}\text{-H}_3$ ), 1.97 (3H, s,  $\text{C}^{13}\text{-H}_3$  or  $\text{C}^{15}\text{-H}_3$  or  $\text{C}^{17}\text{-H}_3$  or  $\text{C}^{19}\text{-H}_3$ );  $^{13}\text{C}$  NMR (101 MHz,  $\text{CDCl}_3$ )  $\delta$  170.5 ( $\text{C}^{12}$  or  $\text{C}^{14}$  or  $\text{C}^{16}$  or  $\text{C}^{18}$ ), 170.4 ( $\text{C}^{12}$  or  $\text{C}^{14}$  or  $\text{C}^{16}$  or  $\text{C}^{18}$ ), 170.2 ( $\text{C}^{12}$  or  $\text{C}^{14}$  or  $\text{C}^{16}$  or  $\text{C}^{18}$ ), 169.8 ( $\text{C}^{12}$  or  $\text{C}^{14}$  or  $\text{C}^{16}$  or  $\text{C}^{18}$ ), 137.1 ( $\text{C}^8$ ), 129.2 ( $\text{C}^9$  or  $\text{C}^{10}$ ), 128.7 ( $\text{C}^9$  or  $\text{C}^{10}$ ), 127.5 ( $\text{C}^{11}$ ), 82.6 ( $\text{C}^1$ ), 74.6 ( $\text{C}^5$ ), 71.9 ( $\text{C}^3$ ), 67.4 ( $\text{C}^4$ ), 67.2 ( $\text{C}^2$ ), 61.7 ( $\text{C}^6$ ), 34.0 ( $\text{C}^7$ ), 20.93 ( $\text{C}^{13}$  or  $\text{C}^{15}$  or  $\text{C}^{17}$  or  $\text{C}^{19}$ ), 20.88 ( $\text{C}^{13}$  or  $\text{C}^{15}$  or  $\text{C}^{17}$  or  $\text{C}^{19}$ ), 20.86 ( $\text{C}^{13}$  or  $\text{C}^{15}$  or  $\text{C}^{17}$  or  $\text{C}^{19}$ ), 20.7 ( $\text{C}^{13}$  or  $\text{C}^{15}$  or  $\text{C}^{17}$  or  $\text{C}^{19}$ ); LRMS  $m/z$  ( $\text{ES}^+$ ) 477 ( $[\text{M}+\text{Na}]^+$ , 100%), 478 ( $[\text{M}+\text{Na}]^+$ , 23%), 479 ( $[\text{M}+\text{Na}]^+$ , 8%); Analytical RP-HPLC (Method 1, 254 nm) Ret. time = 12.8 min, Purity = 99.8%. The data are in good agreement with the literature.<sup>414,415</sup>

### Benzyl 1-thio- $\beta$ -D-galactopyranoside, **104**

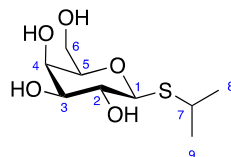


To a solution of **122** (1.8 g, 4.0 mmol, 1.0 eq) in methanol (40 mL) was added sodium methoxide (95 mg, 1.8 mmol, 0.4 eq). The solution was stirred at room temperature for 18 h, adjusted to pH 7 with Amberlite® IR120 resin ( $\text{H}^+$ -form), filtered, and concentrated *in vacuo*. The crude residue was purified by silica gel chromatography (10% methanol in ethyl acetate) to yield benzyl 1-thio- $\beta$ -D-galactopyranoside **104** (1.1 g, 93%) as a colourless solid:  $R_f$  0.34 (1:9 methanol:ethyl



acetate);  $[\alpha]_D^{25} = +154.0$  ( $c$  1.0, MeOH),  $-119.4$  ( $c$  1.0, H<sub>2</sub>O) [lit.<sup>416</sup>  $[\alpha]_D = -125$  ( $c$  3.0, H<sub>2</sub>O)]; mp 114–116 °C (ethyl acetate) [lit.<sup>416</sup> 114–116 °C];  $\bar{\nu}_{\max}$  (neat)/cm<sup>-1</sup> 3442 (br, O–H), 2882 (w), 1494 (w), 1455 (w), 1406 (w), 1285 (w), 1121 (m), 1085 (m, C–O), 1015 (s, C–O), 868 (m), 701 (s, C–S); <sup>1</sup>H NMR (400 MHz, CD<sub>3</sub>OD)  $\delta$  7.39–7.34 (2H, m, C<sup>9</sup>-H), 7.32–7.26 (2H, m, C<sup>10</sup>-H), 7.24–7.18 (1H, m, C<sup>11</sup>-H), 4.14 (1H, d,  $J$  9.7, C<sup>1</sup>-H), 4.03 (1H, d,  $J_{AB}$  12.9, C<sup>7</sup>-H<sub>A</sub>), 3.86 (1H, dd,  $J$  3.5, 1.0, C<sup>4</sup>-H), 3.85 (1H, d,  $J_{AB}$  12.9, C<sup>7</sup>-H<sub>B</sub>), 3.79 (1H, dd,  $J_{AB}$  11.5,  $J_{AX}$  7.1, C<sup>6</sup>-H<sub>A</sub>), 3.70 (1H, dd,  $J_{AB}$  11.5,  $J_{BX}$  5.1, C<sup>6</sup>-H<sub>B</sub>), 3.58 (1H, dd,  $J$  9.7, 9.4, C<sup>2</sup>-H), 3.44 (1H, ddd,  $J_{AX}$  7.1,  $J_{BX}$  5.1,  $J$  1.0, C<sup>5</sup>-H<sub>X</sub>), 3.37 (1H, dd,  $J$  9.4, 3.5, C<sup>3</sup>-H); <sup>13</sup>C NMR (101 MHz, CD<sub>3</sub>OD)  $\delta$  139.5 (C<sup>8</sup>), 130.3 (C<sup>9</sup>), 129.4 (C<sup>10</sup>), 127.9 (C<sup>11</sup>), 85.7 (C<sup>1</sup>), 80.7 (C<sup>5</sup>), 76.3 (C<sup>3</sup>), 71.4 (C<sup>2</sup>), 70.6 (C<sup>4</sup>), 62.8 (C<sup>6</sup>), 34.3 (C<sup>7</sup>); HRMS  $m/z$  (ESI<sup>+</sup>) [Found (M+Na)<sup>+</sup> 309.07672 C<sub>13</sub>H<sub>18</sub>O<sub>5</sub>SNa requires M<sup>+</sup> 309.07670]; LRMS  $m/z$  (ES<sup>+</sup>) 309 ([M+Na]<sup>+</sup>, 100%), 310 ([M+Na]<sup>+</sup>, 15%), 311 ([M+Na]<sup>+</sup>, 6%); Analytical RP-HPLC (Method 1, 254 nm) Ret. time = 8.0 min, Purity = >99.9%. The data are in good agreement with the literature.<sup>416</sup>

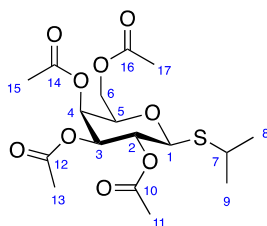
### Isopropyl 1-thio- $\beta$ -D-galactopyranoside, **76**



To a solution of  $\beta$ -D-galactose pentaacetate **116** (10.0 g, 25.6 mmol, 1.0 eq) in CH<sub>2</sub>Cl<sub>2</sub> (40 mL), pre-stirred over 4 Å molecular sieves at room temperature for 15 min, was added 2-propanethiol (3.70 mL, 39.8 mmol, 1.6 eq). The solution was cooled to  $-78$  °C and BF<sub>3</sub>·Et<sub>2</sub>O (6.33 mL, 51.3 mmol, 2.0 eq) was added dropwise. The solution was warmed to room temperature and stirred for 5 h. The solution was filtered through Celite®, diluted with CH<sub>2</sub>Cl<sub>2</sub> (50 mL), and washed with sat. aq. NaHCO<sub>3</sub> (3 × 50 mL). The aqueous phase was back extracted with CH<sub>2</sub>Cl<sub>2</sub> (3 × 50 mL). The organic layers were combined, dried over MgSO<sub>4</sub>, filtered, and concentrated *in vacuo* to yield crude isopropyl 2,3,4,6-tetra-*O*-acetyl-1-thio- $\beta$ -D-galactopyranoside **307** as a yellow oil.

To a solution of crude isopropyl 2,3,4,6-tetra-*O*-acetyl-1-thio- $\beta$ -D-galactopyranoside in methanol (40 mL) was added sodium methoxide (720 mg, 13.3 mmol, 0.5 eq). The solution was stirred at room temperature for 3 h, neutralised with Amberlite® IR120 resin ( $H^+$  form), filtered, and concentrated *in vacuo*. The crude residue was purified by gradient silica gel chromatography (0–10% methanol in ethyl acetate) to yield isopropyl 1-thio- $\beta$ -D-galactopyranoside **76** (4.35 g, 71%, 2 steps) as a colourless solid:  $R_f$  0.17 (1:9 methanol:ethyl acetate);  $[\alpha]_D^{25} -22.2$  ( $c$  1.0,  $H_2O$ ) [lit.<sup>417</sup>  $[\alpha]_D^{25} = -31.4$  ( $c$  1.0,  $H_2O$ )]; mp 111.5–112.4 °C (1,4-dioxane) [lit.<sup>417</sup> 109–110 °C];  $^1H$  NMR (400 MHz,  $CD_3OD$ )  $\delta$  4.40 (1H, d,  $J$  9.2,  $C^1-H$ ), 3.88 (1H, dd,  $J$  3.2, 0.9,  $C^4-H$ ), 3.73 (1H, dd,  $J_{AB}$  11.4,  $J_{AX}$  6.8,  $C^6-H_A$ ), 3.68 (1H, dd,  $J_{AB}$  11.4,  $J_{BX}$  5.4,  $C^6-H_B$ ), 3.53–3.50 (2H, m,  $C^2-H$ ,  $C^5-H_X$ ), 3.46 (1H, dd,  $J$  9.2, 3.2,  $C^3-H$ ), 3.24 (1H, sept,  $J$  6.6,  $C^7-H$ ), 1.32 (3H, d,  $J$  6.6,  $C^7-H_3$  or  $C^8-H_3$ ), 1.30 (3H, d,  $J$  6.6,  $C^7-H_3$  or  $C^8-H_3$ ); LRMS  $m/z$  ( $ES^+$ ) 261 ( $[M+Na]^+$ , 100%), 262 ( $[M+Na]^+$ , 12%), 263 ( $[M+Na]^+$ , 6%). The data are in good agreement with the literature.<sup>417</sup>

#### Isopropyl 2,3,4,6-tetra-*O*-acetyl-1-thio- $\beta$ -D-galactopyranoside, **307**

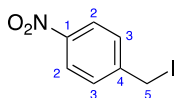


To a solution of isopropyl 1-thio- $\beta$ -D-galactopyranoside **76** (509 mg, 2.14 mmol, 1.0 eq) in pyridine (5 mL) was added acetic anhydride (5 mL). The solution was stirred at room temperature for 3 h and concentrated *in vacuo*. The crude residue was purified by gradient silica gel chromatography (0–40% ethyl acetate in petroleum ether) to yield isopropyl 2,3,4,6-tetra-*O*-acetyl-1-thio- $\beta$ -D-galactopyranoside **307** (777 mg, 90%) as a colourless oil:  $R_f$  0.23 (3:7 ethyl acetate:petroleum ether);  $[\alpha]_D^{25} = -6.35$  ( $c$  1.0,  $CHCl_3$ );  $\bar{\nu}_{max}$  (thin film)/ $cm^{-1}$  2967 (w), 1748 (s,  $C=O$ ), 1436 (w), 1370 (m), 1222 (s,  $C-O$ ), 1154 (w), 1083 (w), 1053 (m), 950 (w), 918 (w);  $^1H$  NMR (500 MHz,  $CDCl_3$ )  $\delta$  5.43 (1H, dd,  $J$  3.4, 0.9,  $C^4-H$ ), 5.21 (1H, dd,  $J$  10.0, 10.0,  $C^2-H$ ), 5.05 (1H, d,  $J$  10.0, 3.4,  $C^3-H$ ), 4.57 (1H, d,  $J$  10.0,  $C^1-H$ ), 4.17 (1H, dd,  $J_{AB}$  11.3,  $J_{AX}$  6.8,  $C^6-H_A$ ), 4.10 (1H, dd,  $J_{AB}$  11.3,  $J_{BX}$  6.6,  $C^6-H_B$ ), 3.92 (1H, ddd,  $J_{AX}$  6.8,  $J_{BX}$  6.6,  $J$  0.9,  $C^5-H_X$ ), 3.18 (1H,

sept,  $J$  6.8,  $C^7$ -H), 2.15 (3H, s,  $C^{15}$ -H<sub>3</sub>), 2.06 (3H, s,  $C^{11}$ -H<sub>3</sub>), 2.04 (3H, s,  $C^{17}$ -H<sub>3</sub>), 1.98 (3H, s,  $C^{13}$ -H<sub>3</sub>), 1.314 (3H, d,  $J$  6.8,  $C^8$ -H<sub>3</sub> or  $C^9$ -H<sub>3</sub>), 1.306 (3H, d,  $J$  6.8,  $C^8$ -H<sub>3</sub> or  $C^9$ -H<sub>3</sub>);  $^{13}\text{C}$  NMR (126 MHz,  $\text{CDCl}_3$ )  $\delta$  170.5 ( $C^{14}$  or  $C^{16}$ ), 170.4 ( $C^{14}$  or  $C^{16}$ ), 170.3 ( $C^{12}$ ), 169.7 ( $C^{10}$ ), 84.0 ( $C^1$ ), 74.5 ( $C^5$ ), 72.1 ( $C^3$ ), 67.6 ( $C^2$ ), 67.4 ( $C^4$ ), 61.7 ( $C^6$ ), 35.8 ( $C^7$ ), 24.1 ( $C^8$  or  $C^9$ ), 23.9 ( $C^8$  or  $C^9$ ), 21.0 ( $C^{11}$ ), 20.8 ( $C^{13}$  or  $C^{15}$  or  $C^{17}$ ), 20.8 ( $C^{13}$  or  $C^{15}$  or  $C^{17}$ ), 20.7 ( $C^{13}$  or  $C^{15}$  or  $C^{17}$ ); HRMS  $m/z$  (ESI<sup>+</sup>) [Found (M+Na)<sup>+</sup> 429.11864  $\text{C}_{17}\text{H}_{26}\text{O}_9\text{SNa}$  requires  $\text{M}^+$  429.11897]; LRMS  $m/z$  (ES<sup>+</sup>) 429 ([M+Na]<sup>+</sup>, 100%), 430 ([M+Na]<sup>+</sup>, 46%), 431 ([M+Na]<sup>+</sup>, 23%). The data are in good agreement with the literature.<sup>418</sup>

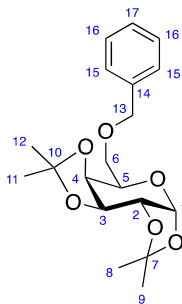
### 6.2.3. Optimisation of 4-Nitrobenzyl Alkylation Reaction

#### 4-Nitrobenzyl iodide, **133**



To a suspension of 4-nitrobenzyl chloride (1.027 g, 5.986 mmol, 1.0 eq) in acetone (15 mL) was added sodium iodide (4.449 g, 29.68 mmol, 5.0 eq). The suspension was stirred under reflux for 4 h. The reaction mixture was cooled to room temperature and water (20 mL) was added. The resulting yellow precipitate was extracted with ethyl acetate (3 × 20 mL). The organic layers were washed with brine (3 × 20 mL), dried over Na<sub>2</sub>SO<sub>4</sub>, filtered, and concentrated *in vacuo* to yield 4-nitrobenzyl iodide **133** (1.545 g, 98%) as a yellow solid: *R<sub>f</sub>* 0.50 (1:9 ethyl acetate:petroleum ether); mp 126–128 °C (ethyl acetate) [lit.<sup>419</sup> 120–122 °C]; <sup>1</sup>H NMR (400 MHz, CDCl<sub>3</sub>) δ 8.16 (2H, d, *J* 8.8, C<sup>2</sup>-*H*), 7.52 (2H, d, *J* 8.8, C<sup>3</sup>-*H*), 4.48 (2H, s, C<sup>5</sup>-*H*<sub>2</sub>); LRMS *m/z* (CI) 281 ([M+NH<sub>4</sub>]<sup>+</sup>, 100%), 282 ([M+NH<sub>4</sub>]<sup>+</sup>, 7%). The data are in good agreement with the literature.<sup>419,420</sup>

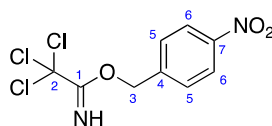
#### 1,2:3,4-di-*O*-isopropylidene-6-*O*-benzyl-α-D-galactopyranoside, **148**



To a solution of 1,2:3,4-di-*O*-isopropylidene-α-D-galactopyranoside **129** (300 mg, 1.15 mmol, 1.0 eq) in cyclohexane:CH<sub>2</sub>Cl<sub>2</sub> (2:1, 6 mL) was added benzyl 2,2,2-trichloroacetimidate **145** (428 μL, 2.30 mmol, 2.0 eq) and triflic acid (31 μL, 0.35 mmol, 0.3 eq). A colourless precipitate formed immediately. The suspension was stirred at room temperature for 1 h. The resulting dark orange solution was filtered through Celite®, washed with sat. aq. NaHCO<sub>3</sub> (20 mL), and extracted with CH<sub>2</sub>Cl<sub>2</sub> (3 × 15 mL). The organic layers were combined, dried over MgSO<sub>4</sub>, filtered, and concentrated *in vacuo*. The crude residue was purified by gradient silica gel

chromatography (0–20% diethyl ether in petroleum ether) to yield 6-*O*-benzyl-1,2:3,4-di-*O*-isopropylidene- $\alpha$ -D-galactopyranoside **148** (207 mg, 51%) as a yellow oil:  $R_f$  0.23 (1:4 diethyl ether:petroleum ether);  $[\alpha]_D^{25} = -61.9$  ( $c$  1.0,  $\text{CHCl}_3$ ) [lit.<sup>421</sup>  $[\alpha]_D = -68$  ( $c$  6.7,  $\text{CHCl}_3$ )];  $\bar{\nu}_{\text{max}}$  (thin film)/ $\text{cm}^{-1}$  2988 (w), 2935 (w), 1382 (m), 1211 (m), 1104 (m), 1070 (s), 1005 (m), 891 (w), 698 (w);  $^1\text{H}$  NMR (500 MHz,  $\text{CDCl}_3$ )  $\delta$  7.38–7.27 (5H, m,  $\text{C}^{15}\text{-H}$ ,  $\text{C}^{16}\text{-H}$ ,  $\text{C}^{17}\text{-H}$ ), 5.55 (1H, d,  $J$  5.0,  $\text{C}^1\text{-H}$ ), 4.62 (1H, d,  $J_{\text{AB}}$  12.1,  $\text{C}^{13}\text{-H}_A$ ), 4.60 (1H, dd,  $J$  8.0, 2.4,  $\text{C}^3\text{-H}$ ), 4.56 (1H, d,  $J_{\text{AB}}$  12.1,  $\text{C}^{13}\text{-H}_B$ ), 4.31 (1H, dd,  $J$  5.0, 2.4,  $\text{C}^2\text{-H}$ ), 4.28 (1H, dd,  $J$  8.0, 1.8,  $\text{C}^4\text{-H}$ ), 4.01 (1H, ddd,  $J_{\text{AX}}$  6.5,  $J_{\text{BX}}$  6.1,  $J$  1.8,  $\text{C}^5\text{-H}_X$ ), 3.70 (1H, dd,  $J$  10.1, 6.1,  $\text{C}^6\text{-H}_B$ ), 3.64 (1H, dd,  $J$  10.1, 6.5,  $\text{C}^6\text{-H}_A$ ), 1.54 (3H, s,  $\text{C}^8\text{-H}_3$  or  $\text{C}^9\text{-H}_3$ ), 1.44 (3H, s,  $\text{C}^{11}\text{-H}_3$  or  $\text{C}^{12}\text{-H}_3$ ), 1.34 (3H, s,  $\text{C}^{11}\text{-H}_3$  or  $\text{C}^{12}\text{-H}_3$ ), 1.33 (3H, s,  $\text{C}^8\text{-H}_3$  or  $\text{C}^9\text{-H}_3$ );  $^{13}\text{C}$  NMR (126 MHz,  $\text{CDCl}_3$ )  $\delta$  138.5 ( $\text{C}^{14}$ ), 128.5 ( $\text{C}^{16}$ ), 127.9 ( $\text{C}^{15}$ ), 127.7 ( $\text{C}^{17}$ ), 109.4 ( $\text{C}^{10}$ ), 108.7 ( $\text{C}^7$ ), 96.5 ( $\text{C}^1$ ), 73.5 ( $\text{C}^{13}$ ), 71.3 ( $\text{C}^4$ ), 70.8 ( $\text{C}^3$ ), 70.7 ( $\text{C}^2$ ), 69.0 ( $\text{C}^6$ ), 67.0 ( $\text{C}^5$ ), 26.2 ( $\text{C}^8$  or  $\text{C}^9$ ), 26.1 ( $\text{C}^{11}$  or  $\text{C}^{12}$ ), 25.1 ( $\text{C}^8$  or  $\text{C}^9$ ), 24.6 ( $\text{C}^{11}$  or  $\text{C}^{12}$ ); LRMS  $m/z$  ( $\text{ES}^+$ ) 351 ( $[\text{M}+\text{H}]^+$ , 67%), 352 ( $[\text{M}+\text{H}]^+$ , 15%), 373 ( $[\text{M}+\text{Na}]^+$ , 100%), 374 ( $[\text{M}+\text{Na}]^+$ , 21%), 375 ( $[\text{M}+\text{Na}]^+$ , 4%). The data are in good agreement with the literature.<sup>421,422</sup>

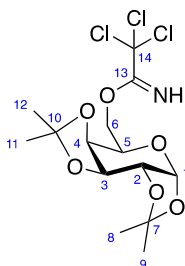
#### 4-Nitrobenzyl-2,2,2-trichloroacetimidate, **151**



To a suspension of 4-nitrobenzyl alcohol **149** (2.004 g, 13.09 mmol, 1.0 eq) in  $\text{CH}_2\text{Cl}_2$  (13 mL) was added trichloroacetonitrile **150** (13 mL, 20 mmol, 1.5 eq) and DBU (391  $\mu\text{L}$ , 2.61 mmol, 0.2 eq). The resulting dark red solution was stirred at room temperature for 15 min and concentrated *in vacuo*. The crude residue was purified by gradient silica gel chromatography (20–30% diethyl ether in petroleum ether) to yield 4-nitrobenzyl-2,2,2-trichloroacetimidate **151** as a pale yellow solid (3.710 g, 95%):  $R_f$  0.32 (1:4 diethyl ether:petroleum ether); mp 76–78  $^{\circ}\text{C}$  (diethyl ether) [lit.<sup>423</sup> 81–83  $^{\circ}\text{C}$ ];  $\bar{\nu}_{\text{max}}$  (neat)/ $\text{cm}^{-1}$  1662 (m), 1602 (w), 1512 (s,  $\text{N}=\text{O}$ ), 1342 (s,  $\text{N}=\text{O}$ ), 1295 (m), 1022 (s), 1012 (m), 831 (m), 798 (s), 736 (s), 647 (s);  $^1\text{H}$  NMR (400 MHz,  $\text{CDCl}_3$ )  $\delta$  8.48 (1H, br s,  $\text{C}^1\text{-NH}$ ), 8.25 (2H, d,  $J$  8.4,  $\text{C}^6\text{-H}$ ), 7.60 (2H, d,  $J$  8.4,  $\text{C}^5\text{-H}$ ), 5.44 (2H, s,  $\text{C}^3\text{-H}_2$ );  $^{13}\text{C}$  NMR (101 MHz,  $\text{CDCl}_3$ )  $\delta$  162.3 ( $\text{C}^1$ ), 147.9 ( $\text{C}^7$ ), 142.9 ( $\text{C}^4$ ), 128.1 ( $\text{C}^5$ ),

124.0 ( $C^6$ ), 91.1 ( $C^2$ ), 69.2 ( $C^3$ ); HRMS  $m/z$  (CI) [Found ( $M+H$ ) $^+$  296.9601  $C_9H_8Cl_3N_2O_3$  requires  $M^+$  296.9595]; LRMS  $m/z$  (CI) 297 ( $[M+H]^+$ , 100%), 298 ( $[M+H]^+$ , 9%), 299 ( $[M+H]^+$ , 95%), 300 ( $[M+H]^+$ , 9%), 301 ( $[M+H]^+$ , 30%); Analytical NP-HPLC (Method 1, 254 nm) Ret. time = 2.9 min, Purity = 98.9%. The data are in good agreement with the literature.<sup>423</sup>

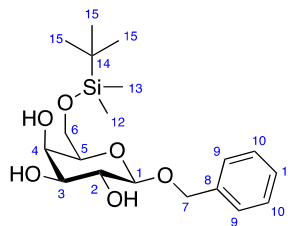
### 1,2:3,4-di-*O*-isopropylidene- $\alpha$ -D-galactopyranoside 2,2,2-trichloroacetimidate, **152**



To a solution of 1,2:3,4-di-*O*-isopropylidene- $\alpha$ -D-galactopyranoside **129** (0.196 g, 0.753 mmol, 1.0 eq) in  $CH_2Cl_2$  (1 mL) was added trichloroacetonitrile **150** (0.755 mL, 7.53 mmol, 10.0 eq) and DBU (20  $\mu$ L, 0.13 mmol, 0.2 eq). The resulting red solution was stirred at room temperature for 30 min and concentrated *in vacuo*. The crude residue was purified by 2 $\times$  silica gel chromatography (1: 10% diethyl ether; 2: 0.5% triethylamine in petroleum ether) to yield 1,2:3,4-di-*O*-isopropylidene- $\alpha$ -D-galactopyranoside 2,2,2-trichloroacetimidate **152** (0.272 mg, 89%) as a colourless solid:  $R_f$  0.29 (1:4 diethyl ether:petroleum ether); mp 82–85  $^{\circ}C$  (diethyl ether);  $\bar{\nu}_{max}$  (neat)/ $cm^{-1}$  2989 (w), 2937 (w), 1667 (w), 1383 (m), 1255 (m), 1212 (m), 1070 (s), 1004 (m), 800 (m);  $^1H$  NMR (400 MHz,  $CDCl_3$ )  $\delta$  8.35 (1H, s,  $C^{13}N-H$ ), 5.55 (1H, d,  $J$  4.9,  $C^1-H$ ), 4.64 (1H, dd,  $J$  7.9, 2.5,  $C^3-H$ ), 4.55 (1H, dd,  $J_{AB}$  11.2,  $J_{BX}$  5.0,  $C^6-H_B$ ), 4.41 (1H, dd,  $J_{AB}$  11.2,  $J_{AX}$  7.1,  $C^6-H_A$ ), 4.33 (1H, dd,  $J$  4.9, 2.5,  $C^2-H$ ), 4.31 (1H, dd,  $J$  7.9, 1.8,  $C^4-H$ ), 4.22 (1H, ddd,  $J_{AX}$  7.1,  $J_{BX}$  5.0,  $J$  1.8,  $C^5-H_X$ ), 1.50 (3H, s,  $C^8-H_3$  or  $C^9-H_3$ ), 1.46 (3H, s,  $C^{11}-H_3$  or  $C^{12}-H_3$ ), 1.34 (3H, s,  $C^{11}-H_3$  or  $C^{12}-H_3$ ), 1.33 (3H, s,  $C^8-H_3$  or  $C^9-H_3$ ); HRMS  $m/z$  (ESI $^+$ ) [Found ( $M^{35}Cl_3+H$ ) $^+$  404.04278 and ( $M^{35}Cl_2^{37}Cl+H$ ) $^+$  406.03982  $C_{14}H_{21}Cl_3NO_6$  requires  $M^{35}Cl_3^+$  404.04290 and  $M^{35}Cl_2^{37}Cl^+$  406.03995]; LRMS  $m/z$  (ES $^+$ ) 404 ( $[M+H]^+$ , 64%), 405 ( $[M+H]^+$ , 11%), 406 ( $[M+H]^+$ , 64%), 421 ( $[M+NH_4]^+$ , 100%), 422 ( $[M+NH_4]^+$ , 19%), 423 ( $[M+NH_4]^+$ , 97%).

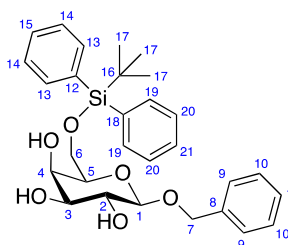
### 6.2.4. Synthesis of 2-Protected Galactopyranosides

#### Benzyl 6-*O*-(*tert*-butyldimethylsilyl)- $\beta$ -D-galactopyranoside, **154**



To a solution of **103** (209 mg, 0.773 mmol, 1.0 eq) in pyridine (4 mL) was added TBDMSCl (178 mg, 1.18 mmol, 1.5 eq). The solution was stirred at room temperature for 3 h, concentrated *in vacuo*, and co-evaporated with toluene ( $\times 3$ ) to remove traces of pyridine. The residue was purified by silica gel chromatography (66% ethyl acetate in petroleum ether) to yield benzyl 6-*O*-(*tert*-butyldimethylsilyl)- $\beta$ -D-galactopyranoside **154** (108 mg, 36%) as a colourless foam:  $R_f$  0.20 (1:2 petroleum ether:ethyl acetate);  $[\alpha]_D^{25} = -40.1$  ( $c$  0.15,  $\text{CHCl}_3$ ) [lit.<sup>277</sup>  $[\alpha]_D^{25} = -38.6$  ( $c$  0.05,  $\text{CHCl}_3$ )];  $\bar{\nu}_{\text{max}}$  (thin film)/ $\text{cm}^{-1}$  3397 (br, O–H), 2953 (w), 2928 (w), 2883 (w), 2856 (w), 1461 (w), 1253 (m, C–O), 1131 (m, Si–O), 1067 (s), 836 (s);  $^1\text{H}$  NMR (500 MHz,  $\text{CD}_3\text{OD}$ ): 7.41–7.39 (2H, m,  $\text{C}^9\text{-H}$ ), 7.34–7.30 (2H, m,  $\text{C}^{10}\text{-H}$ ), 7.28–7.25 (1H, m,  $\text{C}^{11}\text{-H}$ ), 4.89 (1H, d,  $J_{\text{AB}}$  11.7,  $\text{C}^7\text{-H}_A$ ), 4.65 (1H, d,  $J_{\text{AB}}$  11.7,  $\text{C}^7\text{-H}_B$ ), 4.30 (1H, d,  $J$  7.7,  $\text{C}^1\text{-H}$ ), 3.87 (1H, dd,  $J_{\text{AB}}$  10.4,  $J_{\text{BX}}$  6.1,  $\text{C}^6\text{-H}_B$ ), 3.84 (1H, dd,  $J_{\text{AB}}$  10.4,  $J_{\text{AX}}$  6.3,  $\text{C}^6\text{-H}_A$ ), 3.84 (1H, dd,  $J$  3.2, 1.0,  $\text{C}^4\text{-H}$ ), 3.59 (1H, d,  $J$  9.7, 7.7,  $\text{C}^2\text{-H}$ ), 3.50 (1H, ddd,  $J_{\text{AX}}$  6.3,  $J_{\text{BX}}$  6.1,  $J$  1.0,  $\text{C}^5\text{-H}_X$ ), 3.45 (1H, dd,  $J$  9.7, 3.2,  $\text{C}^3\text{-H}$ ), 0.93 (9H, s,  $\text{C}^{15}\text{-H}_3$ ), 0.12 (6H, s,  $\text{C}^{12}\text{-H}_3$ ,  $\text{C}^{13}\text{-H}_3$ ); LRMS  $m/z$  ( $\text{ES}^+$ ) 407 ( $[\text{M}+\text{Na}]^+$ , 100%), 408 ( $[\text{M}+\text{Na}]^+$ , 15%), 409 ( $[\text{M}+\text{Na}]^+$ , 3%). The data are in good agreement with the literature.<sup>277</sup>

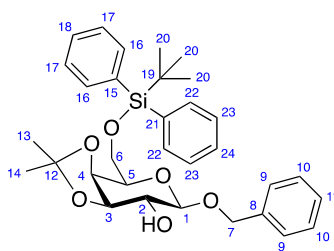
#### Benzyl 6-*O*-(*tert*-butyldiphenylsilyl)- $\beta$ -D-galactopyranoside, **156**



To a solution of **103** (1.00 g, 3.71 mmol, 1.0 eq) in DMF (5 mL) was added TBDPSCl (1.40 mL, 5.38 mmol, 1.5 eq) and imidazole (0.628 g, 9.23 mmol, 2.5 eq). The solution was stirred at room

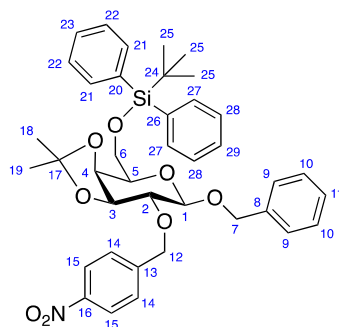
temperature for 4 h. The reaction was quenched with sat. aq.  $\text{NaHCO}_3$  (5 mL) and diluted with ethyl acetate (15 mL). The organic layer was washed with water ( $5 \times 15$  mL) and aq. 0.5 M lithium chloride ( $3 \times 20$  mL). The aqueous layers were back extracted with ethyl acetate ( $3 \times 30$  mL). The organic layers were combined, dried over  $\text{MgSO}_4$ , filtered, and concentrated *in vacuo*. The crude residue was purified by gradient silica gel chromatography (66–100% ethyl acetate in petroleum ether) to yield benzyl 6-*O*-(*tert*-butyldiphenylsilyl)- $\beta$ -D-galactopyranoside **156** (0.996 g, 53%) as a colourless foam:  $R_f$  0.20 (1:2 petroleum ether:ethyl acetate);  $[\alpha]_D^{25} = -34.5$  ( $c$  1.0,  $\text{CHCl}_3$ ),  $-36.7$  ( $c$  1.0, MeOH) [lit.<sup>424</sup>  $[\alpha]_D = -27$  ( $c$  2.15, MeOH)];  $\bar{\nu}_{\text{max}}$  (neat)/ $\text{cm}^{-1}$  3372 (br, O–H), 2929 (w), 2856 (w), 1427 (m), 1361 (w), 1112 (s, Si–C), 1069 (s), 825 (s), 772 (s), 739 (s);  $^1\text{H}$  NMR (500 MHz,  $\text{CDCl}_3$ )  $\delta$  7.72–7.68 (4H, m,  $\text{C}^{13}\text{-H}$ ,  $\text{C}^{19}\text{-H}$ ), 7.46–7.36 (6H, m,  $\text{C}^{14}\text{-H}$ ,  $\text{C}^{15}\text{-H}$ ,  $\text{C}^{20}\text{-H}$ ,  $\text{C}^{21}\text{-H}$ ), 7.35–7.28 (5H, m,  $\text{C}^9\text{-H}$ ,  $\text{C}^{10}\text{-H}$ ,  $\text{C}^{11}\text{-H}$ ), 4.91 (1H, d,  $J_{\text{AB}}$  11.6,  $\text{C}^7\text{-H}_A$ ), 4.58 (1H, d,  $J_{\text{AB}}$  11.6,  $\text{C}^7\text{-H}_B$ ), 4.30 (1H, d,  $J$  8.2,  $\text{C}^1\text{-H}$ ), 4.09–4.06 (1H, m,  $\text{C}^4\text{-H}$ ), 3.98 (1H, dd,  $J_{\text{AB}}$  10.6,  $J_{\text{AX}}$  5.9,  $\text{C}^6\text{-H}_A$ ), 3.94 (1H, dd,  $J_{\text{AB}}$  10.6,  $J_{\text{BX}}$  5.5,  $\text{C}^6\text{-H}_B$ ), 3.70 (1H, dd,  $J$  8.7, 8.2,  $\text{C}^2\text{-H}$ ), 3.58–3.55 (1H, m,  $\text{C}^3\text{-H}$ ), 3.53 (1H, dd,  $J_{\text{AX}}$  5.9,  $J_{\text{BX}}$  5.5,  $\text{C}^5\text{-H}_X$ ), 2.70 (1H, d,  $J$  5.1,  $\text{C}^3\text{-OH}$ ), 2.67 (1H, d,  $J$  3.5,  $\text{C}^4\text{-OH}$ ), 2.50 (1H, s,  $\text{C}^2\text{-OH}$ ), 1.07 (9H, s,  $\text{C}^{17}\text{-H}_3$ );  $^{13}\text{C}$  NMR (126 MHz,  $\text{CDCl}_3$ )  $\delta$  137.1 ( $\text{C}^8$ ), 135.8 ( $\text{C}^{13}$  or  $\text{C}^{19}$ ), 135.7 ( $\text{C}^{13}$  or  $\text{C}^{19}$ ), 133.2 ( $\text{C}^{12}$  or  $\text{C}^{18}$ ), 133.0 ( $\text{C}^{12}$  or  $\text{C}^{18}$ ), 130.04 ( $\text{C}^{15}$  or  $\text{C}^{21}$ ), 130.03 ( $\text{C}^{15}$  or  $\text{C}^{21}$ ), 128.6 ( $\text{C}^9$  or  $\text{C}^{10}$ ), 128.3 ( $\text{C}^9$  or  $\text{C}^{10}$ ), 128.2 ( $\text{C}^{11}$ ), 127.96 ( $\text{C}^{14}$  or  $\text{C}^{20}$ ), 127.95 ( $\text{C}^{14}$  or  $\text{C}^{20}$ ), 101.8 ( $\text{C}^1$ ), 74.6 ( $\text{C}^5$ ), 73.8 ( $\text{C}^3$ ), 72.4 ( $\text{C}^2$ ), 70.9 ( $\text{C}^7$ ), 69.0 ( $\text{C}^4$ ), 63.3 ( $\text{C}^6$ ), 26.9 ( $\text{C}^{17}$ ), 19.33 ( $\text{C}^{16}$ ); HRMS  $m/z$  ( $\text{ESI}^+$ ) [Found ( $\text{M}+\text{H}$ ) $^+$  509.23512  $\text{C}_{29}\text{H}_{37}\text{O}_6^{28}\text{Si}$  requires  $\text{M}^+$  509.23539]; LRMS  $m/z$  ( $\text{ES}^+$ ) 531 ( $[\text{M}+\text{Na}]^+$ , 100%), 533 ( $[\text{M}+\text{Na}]^+$ , 38%), 534 ( $[\text{M}+\text{Na}]^+$ , 11%); Analytical RP-HPLC (Method 1, 254 nm) Ret. time = 14.9 min, Purity = 99.0%. The data are in good agreement with the literature.<sup>277,424</sup>



**Benzyl 6-*O*-(*tert*-butyldiphenylsilyl)-3,4-*O*-isopropylidene- $\beta$ -D-galactopyranoside, **128****

To a solution of **156** (0.938 g, 1.8 mmol, 1.0 eq) in acetone (9.5 mL) was added 4-TsOH·H<sub>2</sub>O (17 mg, 0.089 mmol, 0.05 eq) and 2,2-dimethoxypropane (0.70 mL, 5.7 mmol, 3.1 eq). The solution was stirred at 40 °C for 2 h. The reaction was quenched with triethylamine (20  $\mu$ L) and concentrated *in vacuo*. The crude residue was purified by gradient silica gel chromatography (20–40% ethyl acetate in petroleum ether) to yield benzyl 6-*O*-(*tert*-butyldiphenylsilyl)-3,4-*O*-isopropylidene- $\beta$ -D-galactopyranoside **128** (1.01 g, 99%) as a colourless foam:  $R_f$  0.20 (1:4 ethyl acetate:petroleum ether);  $[\alpha]_D^{25} = -16.2$  ( $c$  1.0, CHCl<sub>3</sub>) [lit.<sup>277</sup>  $[\alpha]_D^{24} = -12.9$  ( $c$  0.14, CHCl<sub>3</sub>)];  $\bar{\nu}_{\max}$  (neat)/cm<sup>-1</sup> 3430 (br, O–H), 2933 (m), 2857 (m), 2364 (w), 2161 (w), 1428 (m), 1218 (m, C–O), 1112 (s, Si–C), 1079 (s), 1037 (s), 873 (m), 741 (m), 701 (s), 610 (m); <sup>1</sup>H NMR (500 MHz, CDCl<sub>3</sub>)  $\delta$  7.73–7.71 (4H, m, C<sup>16</sup>-H, C<sup>22</sup>-H), 7.46–7.36 (6H, m, C<sup>17</sup>-H, C<sup>18</sup>-H, C<sup>23</sup>-H, C<sup>24</sup>-H), 7.35–7.29 (5H, m, C<sup>9</sup>-H, C<sup>10</sup>-H, C<sup>11</sup>-H), 4.90 (1H, d,  $J_{AB}$  11.6, C<sup>7</sup>-H<sub>A</sub>), 4.59 (1H, d,  $J_{AB}$  11.6, C<sup>7</sup>-H<sub>B</sub>), 4.25 (1H, dd,  $J$  5.5, 2.1, C<sup>4</sup>-H), 4.23 (1H, d,  $J$  8.3, C<sup>1</sup>-H), 4.05 (1H, dd,  $J$  7.5, 5.5, C<sup>3</sup>-H), 4.01 (1H, dd,  $J_{AB}$  10.0,  $J_{AX}$  6.9, C<sup>6</sup>-H<sub>A</sub>), 3.97 (1H, dd,  $J_{AB}$  10.0,  $J_{BX}$  6.3, C<sup>6</sup>-H<sub>B</sub>), 3.86 (1H, ddd,  $J_{AX}$  6.9,  $J_{BX}$  6.3,  $J$  2.1, C<sup>5</sup>-H<sub>X</sub>), 3.61 (1H, dd,  $J$  8.3, 7.5, C<sup>2</sup>-H), 2.32 (1H, br s, C<sup>2</sup>-OH), 1.51 (3H, s, C<sup>13</sup>-H<sub>3</sub> or C<sup>14</sup>-H<sub>3</sub>), 1.34 (3H, s, C<sup>13</sup>-H<sub>3</sub> or C<sup>14</sup>-H<sub>3</sub>), 1.08 (9H, s, C<sup>20</sup>-H<sub>3</sub>); HRMS  $m/z$  (ESI<sup>+</sup>) [Found (M+Na)<sup>+</sup> 571.24797 C<sub>19</sub>H<sub>32</sub>O<sub>6</sub><sup>28</sup>SiNa requires M<sup>+</sup> 571.24864]; LRMS  $m/z$  (ES<sup>+</sup>) 571 ([M+Na]<sup>+</sup>, 100%), 572 ([M+Na]<sup>+</sup>, 39%), 573 ([M+Na]<sup>+</sup>, 12%). The data are in good agreement with the literature.<sup>277</sup>

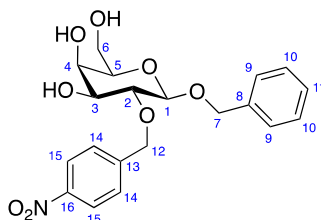
**Benzyl 6-*O*-(*tert*-butyldiphenylsilyl)-3,4-*O*-isopropylidene-2-*O*-(4-nitrobenzyl)- $\beta$ -D-galactopyranoside, **131****



To a solution of **128** (199 mg, 0.363 mmol, 1.0 eq) in cyclohexane (2 mL) was added silver oxide (133 mg, 0.574 mmol, 1.6 eq), 4-nitrobenzyl bromide **80** (118 mg, 0.546 mmol, 1.5 eq), and 4 Å molecular sieves. The suspension was shielded from light and stirred under reflux for 16 h. The reaction mixture was filtered through Celite® and concentrated *in vacuo*. The crude residue was purified by gradient silica gel chromatography (0–20% diethyl ether in petroleum ether) to yield benzyl 6-*O*-(*tert*-butyldiphenylsilyl)-3,4-*O*-isopropylidene-2-*O*-(4-nitrobenzyl)- $\beta$ -D-galactopyranoside **131** (226 mg, 91%) as a colourless foam:  $R_f$  0.38 (1:2 ethyl acetate:petroleum ether);  $[\alpha]_D^{25} = +20.3$  ( $c$  1.0,  $\text{CHCl}_3$ );  $\bar{\nu}_{\text{max}}$  (thin film)/ $\text{cm}^{-1}$  3070 (w), 2933 (m), 2858 (m), 1606 (w), 1521 (s, N=O), 1472 (w), 1345 (s, N=O), 1112 (s, Si–C), 1046 (m), 702 (s);  $^1\text{H}$  NMR (500 MHz,  $\text{CDCl}_3$ )  $\delta$  8.16–8.13 (2H, m,  $\text{C}^{15}\text{-H}$ ), 7.72–7.70 (4H, m,  $\text{C}^{21}\text{-H}$ ,  $\text{C}^{27}\text{-H}$ ), 7.52–7.48 (2H, m,  $\text{C}^{14}\text{-H}$ ), 7.47–7.35 (6H, m,  $\text{C}^{22}\text{-H}$ ,  $\text{C}^{23}\text{-H}$ ,  $\text{C}^{28}\text{-H}$ ,  $\text{C}^{29}$ ), 7.33–7.30 (5H, m,  $\text{C}^9\text{-H}$ ,  $\text{C}^{10}\text{-H}$ ,  $\text{C}^{11}\text{-H}$ ), 4.94 (1H, d,  $J_{\text{AB}}$  13.5,  $\text{C}^{12}\text{-H}_A$ ), 4.91 (1H, d,  $J_{\text{AB}}$  11.9,  $\text{C}^7\text{-H}_A$ ), 4.90 (1H, d,  $J_{\text{AB}}$  13.5,  $\text{C}^{12}\text{-H}_B$ ), 4.61 (1H, d,  $J_{\text{AB}}$  11.9,  $\text{C}^7\text{-H}_B$ ), 4.37 (1H, d,  $J$  8.1,  $\text{C}^1\text{-H}$ ), 4.25 (1H, dd,  $J$  5.5, 2.1,  $\text{C}^4\text{-H}$ ), 4.14 (1H, dd,  $J$  7.1, 5.5,  $\text{C}^3\text{-H}$ ), 3.98 (1H, dd,  $J_{\text{AB}}$  10.1,  $J_{\text{AX}}$  7.0,  $\text{C}^6\text{-H}_A$ ), 3.95 (1H, dd,  $J_{\text{AB}}$  10.1,  $J_{\text{BX}}$  6.2,  $\text{C}^6\text{-H}_B$ ), 3.84 (1H, ddd,  $J_{\text{AX}}$  7.0,  $J_{\text{BX}}$  6.2,  $J$  2.1,  $\text{C}^5\text{-H}_X$ ), 3.42 (1H, dd,  $J$  8.1, 7.1,  $\text{C}^2\text{-H}$ ), 1.38 (3H, s,  $\text{C}^{18}\text{-H}_3$  or  $\text{C}^{19}\text{-H}_3$ ), 1.33 (3H, s,  $\text{C}^{18}\text{-H}_3$  or  $\text{C}^{19}\text{-H}_3$ ), 1.07 (9H, s,  $\text{C}^{25}\text{-H}_3$ );  $^{13}\text{C}$  NMR (126 MHz,  $\text{CDCl}_3$ )  $\delta$  147.4 ( $\text{C}^{16}$ ), 146.4 ( $\text{C}^{14}$ ), 137.3 ( $\text{C}^8$ ), 135.8 ( $\text{C}^{21}$  or  $\text{C}^{27}$ ), 135.7 ( $\text{C}^{21}$  or  $\text{C}^{27}$ ), 133.5 ( $\text{C}^{20}$  or  $\text{C}^{26}$ ), 133.4 ( $\text{C}^{20}$  or  $\text{C}^{26}$ ), 129.9 ( $\text{C}^{23}$  or  $\text{C}^{29}$ ), 128.6 ( $\text{C}^{10}$ ), 128.2 ( $\text{C}^9$ ), 128.14 ( $\text{C}^{14}$ ), 128.09 ( $\text{C}^{11}$ ), 127.9 ( $\text{C}^{22}$  or  $\text{C}^{28}$ ), 127.8 ( $\text{C}^{22}$  or  $\text{C}^{28}$ ), 123.5 ( $\text{C}^{15}$ ), 110.1 ( $\text{C}^{17}$ ), 101.4 ( $\text{C}^1$ ), 80.9 ( $\text{C}^2$ ), 79.1 ( $\text{C}^3$ ), 73.6 ( $\text{C}^4$ ,  $\text{C}^5$ ), 72.4 ( $\text{C}^{12}$ ), 70.7 ( $\text{C}^7$ ), 62.8 ( $\text{C}^6$ ), 28.1 ( $\text{C}^{18}$  or  $\text{C}^{19}$ ), 26.4 ( $\text{C}^{18}$  or  $\text{C}^{19}$ ), 26.9 ( $\text{C}^{25}$ ), 19.4 ( $\text{C}^{24}$ );

HRMS  $m/z$  (ESI<sup>+</sup>) [Found (M+Na)<sup>+</sup> 706.28038 C<sub>39</sub>H<sub>45</sub>NO<sub>8</sub><sup>28</sup>SiNa requires M<sup>+</sup> 706.28067]; LRMS  $m/z$  (ES<sup>+</sup>) 706 ([M+Na]<sup>+</sup>, 100%), 707 ([M+Na]<sup>+</sup>, 49%), 708 ([M+Na]<sup>+</sup>, 19%); Analytical NP-HPLC (Method 1, 254 nm) Ret. time = 2.7 min, Purity = >99.9%.

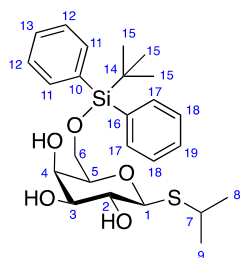
### Benzyl 2-*O*-(4-nitrobenzyl)-β-D-galactopyranoside, **123**



To a solution of **131** (150 mg, 0.22 mmol, 1.0 eq) in methanol (650 μL) was added acetyl chloride (1 M in methanol, 22 μL, 0.022 mmol, 0.1 eq). The solution was stirred at room temperature for 18 h and concentrated *in vacuo*. The crude residue was purified by gradient silica gel chromatography (60–100% ethyl acetate in petroleum ether) to yield benzyl 2-*O*-(4-nitrobenzyl)-β-D-galactopyranoside **123** (42 mg, 42%) and unreacted starting material **131** and intermediates (50 mg). To a solution of the unreacted **131** and intermediates in methanol (500 μL) was added acetyl chloride (3 μL). The solution was stirred at room temperature for 15 h and concentrated *in vacuo*. The crude residue was purified by gradient silica gel chromatography to yield additional benzyl 2-*O*-(4-nitrobenzyl)-β-D-galactopyranoside **123** (15 mg, 17%). The batches were combined to yield benzyl 2-*O*-(4-nitrobenzyl)-β-D-galactopyranoside **123** (57 mg, 59%) as a colourless solid:  $R_f$  0.14 (ethyl acetate);  $[\alpha]_D^{25} = -11.7$  ( $c$  0.3, CHCl<sub>3</sub>); mp 142.5–143.9 °C (ethyl acetate);  $\bar{\nu}_{\max}$  (thin film)/cm<sup>-1</sup> 3422 (br, O–H), 2923 (w), 2359 (w), 1605 (w), 1519 (s, N=O), 1455 (w), 1347 (s, N=O), 1106 (m), 738 (m); <sup>1</sup>H NMR (500 MHz, CDCl<sub>3</sub>)  $\delta$  8.17–8.14 (2H, m, C<sup>15</sup>-H), 7.47–7.43 (2H, m, C<sup>14</sup>-H), 7.34–7.30 (5H, m, C<sup>9</sup>-H, C<sup>10</sup>-H, C<sup>11</sup>-H), 5.06 (1H, d,  $J_{AB}$  12.9, C<sup>12</sup>-H<sub>A</sub>), 4.95 (1H, d,  $J_{AB}$  11.8, C<sup>7</sup>-H<sub>A</sub>), 4.82 (1H, d,  $J_{AB}$  12.9, C<sup>12</sup>-H<sub>B</sub>), 4.65 (1H, d,  $J_{AB}$  11.8, C<sup>7</sup>-H<sub>B</sub>), 4.52 (1H, d,  $J$  7.6, C<sup>1</sup>-H), 4.05 (1H, ddd,  $J$  3.3, 3.1, 1.2, C<sup>4</sup>-H), 4.00 (1H, ddd,  $J_{AB}$  11.8,  $J_{AX}$  5.6,  $J$  5.4, C<sup>6</sup>-H<sub>A</sub>), 3.92 (1H, ddd,  $J_{AB}$  11.8,  $J$  7.4,  $J_{BX}$  4.4, C<sup>6</sup>-H<sub>B</sub>), 3.67 (1H, ddd,  $J$  9.4, 5.2, 3.3, C<sup>3</sup>-H), 3.58 (1H, dd,  $J$  9.4, 7.6, C<sup>2</sup>-H), 3.55 (1H, ddd,  $J_{AX}$  5.6,  $J_{BX}$  4.4,  $J$  1.2, C<sup>5</sup>-H<sub>X</sub>), 2.82 (1H, d,  $J$  3.1, C<sup>4</sup>-OH), 2.54 (1H, d,  $J$  5.2, C<sup>3</sup>-OH), 2.05 (1H, dd,  $J$  7.4, 5.4, C<sup>6</sup>-OH);

$^{13}\text{C}$  NMR (126 MHz,  $\text{CDCl}_3$ )  $\delta$  147.5 ( $\text{C}^{16}$ ), 146.0 ( $\text{C}^{13}$ ), 137.2 ( $\text{C}^8$ ), 128.7 ( $\text{C}^{10}$ ), 128.19 ( $\text{C}^9$ ), 128.25 ( $\text{C}^{11}$ ), 128.1 ( $\text{C}^{14}$ ), 123.7 ( $\text{C}^{15}$ ), 102.6 ( $\text{C}^1$ ), 80.0 ( $\text{C}^2$ ), 74.1 ( $\text{C}^5$ ), 73.5 ( $\text{C}^{12}$ ), 73.4 ( $\text{C}^3$ ), 71.6 ( $\text{C}^7$ ), 70.0 ( $\text{C}^4$ ), 63.1 ( $\text{C}^6$ ); HRMS  $m/z$  ( $\text{ESI}^+$ ) [Found ( $\text{M}+\text{Na}$ ) $^+$  428.13147  $\text{C}_{20}\text{H}_{23}\text{NO}_8\text{Na}$  requires  $\text{M}^+$  428.13159]; LRMS  $m/z$  ( $\text{ES}^+$ ) 428 ( $[\text{M}+\text{Na}]^+$ , 100%), 429 ( $[\text{M}+\text{Na}]^+$ , 29%), 430 ( $[\text{M}+\text{Na}]^+$ , 11%); Analytical RP-HPLC (Method 1, 254 nm) Ret. time = 10.6 min, Purity = 99.8%.

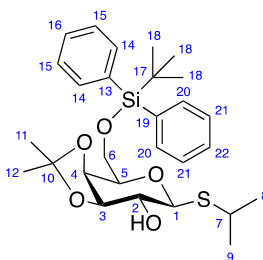
### Isopropyl 6-*O*-(*tert*-butyldiphenylsilyl)-1-thio- $\beta$ -D-galactopyranoside, **158**



To a solution of isopropyl 1-thio- $\beta$ -D-galactopyranoside **76** (1.00 g, 4.21 mmol, 1.0 eq) in DMF (5 mL) was added TBDPSCI (1.31 mL, 5.04 mmol, 1.2 eq) and imidazole (0.716 g, 10.5 mmol, 2.5 eq). The solution was stirred at room temperature for 7 h. The reaction was quenched with sat. aq.  $\text{NaHCO}_3$  (5 mL). The solution was diluted with ethyl acetate (40 mL) and washed with water ( $5 \times 40$  mL). The aqueous layers were back extracted with ethyl acetate ( $3 \times 100$  mL). The organic layers were combined, dried over  $\text{MgSO}_4$ , filtered, and concentrated *in vacuo*. The crude residue was purified by gradient silica gel chromatography (33–100% ethyl acetate in petroleum ether) to yield isopropyl 6-*O*-(*tert*-butyldiphenylsilyl)-1-thio- $\beta$ -D-galactopyranoside **OXF35** (1.19 g, 59%) as a colourless foam:  $R_f$  0.14 (1:1 ethyl acetate:petroleum ether);  $[\alpha]_{\text{D}}^{25} = -26.5$  (c 1.0,  $\text{CHCl}_3$ );  $\bar{\nu}_{\text{max}}$  (thin film)/ $\text{cm}^{-1}$  3435 (br, O–H), 2959 (m), 2930 (m), 2858 (m), 1428 (m), 1113 (s, Si–C), 1063 (m), 1030 (m), 703 (s), 614 (m);  $^1\text{H}$  NMR (500 MHz,  $\text{CDCl}_3$ )  $\delta$  7.71–7.66 (4H, m,  $\text{C}^{11}\text{-H}$ ,  $\text{C}^{17}\text{-H}$ ), 7.46–7.42 (2H, m,  $\text{C}^{13}\text{-H}$ ,  $\text{C}^{19}\text{-H}$ ), 7.41–7.37 (4H, m,  $\text{C}^{12}\text{-H}$ ,  $\text{C}^{18}\text{-H}$ ), 4.35 (1H, d,  $J$  9.4,  $\text{C}^1\text{-H}$ ), 4.12 (1H, d,  $J$  2.8,  $\text{C}^4\text{-H}$ ), 3.91 (1H, dd,  $J_{\text{AB}}$  10.6,  $J_{\text{AX}}$  6.1,  $\text{C}^6\text{-H}_A$ ), 3.88 (1H, dd,  $J_{\text{AB}}$  10.6,  $J_{\text{BX}}$  5.3,  $\text{C}^6\text{-H}_B$ ), 3.64 (1H, dd,  $J$  9.4, 9.1,  $\text{C}^2\text{-H}$ ), 3.58 (1H, dd,  $J$  9.1, 2.8,  $\text{C}^3\text{-H}$ ), 3.54 (1H, ddd,  $J_{\text{AX}}$  6.1,  $J_{\text{BX}}$  5.3,  $J$  1.0,  $\text{C}^5\text{-H}_X$ ), 3.19 (1H, sept,  $J$  6.8,  $\text{C}^7\text{-H}$ ), 2.86 (1H, br s,  $\text{C}^3\text{-OH}$ ), 2.69 (1H, br s,  $\text{C}^4\text{-OH}$ ), 2.58 (1H, br s,  $\text{C}^2\text{-OH}$ ), 1.32 (3H, d,  $J$  6.8,  $\text{C}^8\text{-H}_3$  or  $\text{C}^9\text{-H}_3$ ), 1.31 (3H, d,  $J$  6.8,

$C^8-H_3$  or  $C^9-H_3$ ), 1.05 (9H, s,  $C^{15}-H_3$ );  $^{13}C$  NMR (126 MHz,  $CDCl_3$ )  $\delta$  135.8 ( $C^{11}$  or  $C^{17}$ ), 135.7 ( $C^{11}$  or  $C^{17}$ ), 133.1 ( $C^{10}$  or  $C^{16}$ ), 132.9 ( $C^{10}$  or  $C^{16}$ ), 130.04 ( $C^{13}$  or  $C^{19}$ ), 130.02 ( $C^{13}$  or  $C^{19}$ ), 127.9 ( $C^{12}$ ,  $C^{18}$ ), 86.0 ( $C^1$ ), 78.3 ( $C^5$ ), 75.1 ( $C^3$ ), 70.9 ( $C^2$ ), 69.2 ( $C^4$ ), 63.4 ( $C^6$ ), 35.6 ( $C^7$ ), 26.9 ( $C^{15}$ ), 24.4 ( $C^8$  or  $C^9$ ), 24.2 ( $C^8$  or  $C^9$ ), 19.3 ( $C^{14}$ ); HRMS  $m/z$  (ESI $^+$ ) [Found ( $M+Na$ ) $^+$  499.19440  $C_{25}H_{36}O_5S^{28}SiNa$  requires  $M^+$  499.19449]; LRMS  $m/z$  (ES $^+$ ) 499 ( $[M+Na]^+$ , 100%), 500 ( $[M+Na]^+$ , 34%), 501 ( $[M+Na]^+$ , 14%); Analytical NP-HPLC (Method 1, 254 nm), Ret. time = 14.7 min, Purity = >99.9%.

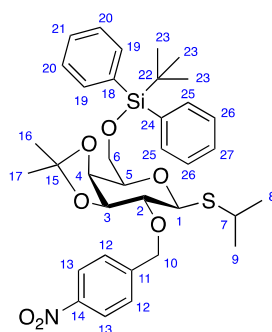
**Isopropyl 6-*O*-(*tert*-butyldiphenylsilyl)-3,4-*O*-isopropylidene-1-thio- $\beta$ -D-galactopyranoside, **159****



To a solution of **158** (1.1 g, 2.3 mmol, 1.0 eq) in acetone (11 mL) was added 4-TsOH $\cdot$ H $_2$ O (22 mg, 0.12 mmol, 0.05 eq) and 2,2-dimethoxypropane (0.86 mL, 7.0 mmol, 3.0 eq). The solution was stirred at room temperature for 2 h, quenched with triethylamine (22  $\mu$ L), and concentrated *in vacuo*. The crude residue was purified by gradient silica gel chromatography (0–30% ethyl acetate in petroleum ether) to yield isopropyl 6-*O*-(*tert*-butyldiphenylsilyl)-3,4-*O*-isopropylidene-1-thio- $\beta$ -D-galactopyranoside **159** (1.1 g, 93%) as a colourless foam:  $R_f$  0.22 (2:8 ethyl acetate:petroleum ether);  $[\alpha]_D^{25} = -10.9$  ( $c$  1.0,  $CHCl_3$ );  $\bar{\nu}_{max}$  (thin film)/ $cm^{-1}$  3452 (br, O–H), 2959 (m), 2931 (m), 2858 (m), 1473 (w), 1243 (m), 1152 (s, C–O), 1112 (s, Si–C), 873 (m), 703 (s);  $^1H$  NMR (500 MHz,  $CDCl_3$ )  $\delta$  7.70–7.68 (4H, m,  $C^{14}-H$ ,  $C^{20}-H$ ), 7.45–7.41 (2H, m,  $C^{16}-H$ ,  $C^{22}-H$ ), 7.40–7.35 (4H, m,  $C^{15}-H$ ,  $C^{21}-H$ ), 4.295 (1H, d,  $J$  10.3,  $C^1-H$ ), 4.294 (1H, dd,  $J$  5.4, 2.2,  $C^4-H$ ), 4.05 (1H, dd,  $J$  7.1, 5.4,  $C^3-H$ ), 3.93 (1H, dd,  $J_{AB}$  10.0,  $J_{AX}$  7.2,  $C^6-H_A$ ), 3.91 (1H, dd,  $J_{AB}$  10.0,  $J_{BX}$  5.9,  $C^6-H_B$ ), 3.85 (1H, ddd,  $J_{AX}$  7.2,  $J_{BX}$  5.9,  $J$  2.2,  $C^5-H_X$ ), 3.52 (1H, dd,  $J$  10.3, 7.1,  $C^2-H$ ), 3.18 (1H, sept,  $J$  6.7,  $C^7-H$ ), 2.37 (1H, br s,  $C^2-OH$ ), 1.50 (3H, s,  $C^{11}-H_3$  or  $C^{12}-H_3$ ), 1.34 (3H, s,  $C^{11}-H_3$  or  $C^{12}-H_3$ ), 1.32 (3H, s,  $C^8-H_3$  or  $C^9-H_3$ ), 1.31 (3H, s,  $C^8-H_3$  or  $C^9-H_3$ ), 1.05 (9H, s,

$C^{18}$ - $H_3$ );  $^{13}C$  NMR (126 MHz,  $CDCl_3$ )  $\delta$  135.79 ( $C^{14}$  or  $C^{20}$ ), 135.75 ( $C^{14}$  or  $C^{20}$ ), 133.5 ( $C^{13}$  or  $C^{19}$ ), 133.4 ( $C^{13}$  or  $C^{19}$ ), 129.9, ( $C^{16}$ ,  $C^{22}$ ), 127.84 ( $C^{15}$  or  $C^{21}$ ), 127.78 ( $C^{15}$  or  $C^{21}$ ), 110.2 ( $C^{10}$ ), 85.4 ( $C^1$ ), 79.0 ( $C^3$ ), 77.16 ( $C^5$ ), 73.5 ( $C^4$ ), 72.6 ( $C^2$ ), 63.0 ( $C^6$ ), 35.8 ( $C^7$ ), 28.4 ( $C^{11}$  or  $C^{12}$ ), 26.4 ( $C^{11}$  or  $C^{12}$ ), 26.9 ( $C^{18}$ ), 24.4 ( $C^8$  or  $C^9$ ), 24.1 ( $C^8$  or  $C^9$ ), 19.3 ( $C^{17}$ ); HRMS  $m/z$  ( $ESI^+$ ) [Found ( $M+Na$ ) $^+$  539.22517  $C_{28}H_{40}O_5S^{28}SiNa$  requires  $M^+$  539.22579]; LRMS  $m/z$  ( $ES^+$ ) 539 ( $[M+Na]^+$ , 100%), 540 ( $[M+Na]^+$ , 38%), 541 ( $[M+Na]^+$ , 16%); Analytical NP-HPLC (Method 1, 254 nm) Ret. time = 6.3 min, Purity = 97.3%.

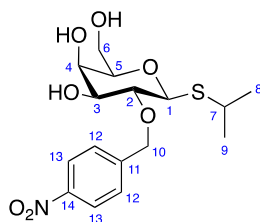
**Isopropyl 6-*O*-(*tert*-butyldiphenylsilyl)-3,4-*O*-isopropylidene-2-*O*-(4-nitrobenzyl)-1-thio- $\beta$ -D-galactopyranoside, **160****



To a solution of **159** (272 mg, 0.526 mmol, 1.0 eq) in cyclohexane (2.9 mL) was added 4 Å molecular sieves, 4-nitrobenzyl bromide **80** (170 mg, 0.787 mmol, 1.5 eq), and silver oxide (186 mg, 0.803 mmol, 1.5 eq). The resulting suspension was shielded from light and stirred under reflux for 17.5 h. The reaction mixture was filtered through Celite® and concentrated *in vacuo*. The crude residue was purified by gradient silica gel chromatography (0–15% diethyl ether in petroleum ether) to yield isopropyl 6-*O*-(*tert*-butyldiphenylsilyl)-3,4-*O*-isopropylidene-2-*O*-(4-nitrobenzyl)-1-thio- $\beta$ -D-galactopyranoside **160** (296 mg, 87%) as a colourless foam:  $R_f$  0.13 (1:9 diethyl ether:petroleum ether);  $[\alpha]_D^{25} = -18.2$  ( $c$  0.5,  $CHCl_3$ ),  $\bar{\nu}_{max}$  (thin film)/ $cm^{-1}$  3071 (w), 2959 (m), 2932 (m), 2859 (m), 1522 (s, N=O), 1346 (s, N=O), 1109 (s, Si–C), 705 (s);  $^1H$  NMR (400 MHz,  $CDCl_3$ )  $\delta$  8.22–8.17 (2H, m,  $C^{13}$ - $H$ ), 7.72–7.66 (4H, m,  $C^{19}$ - $H$ ,  $C^{25}$ - $H$ ), 7.61–7.56 (2H, m,  $C^{12}$ - $H$ ), 7.47–7.34 (6H,  $C^{20}$ - $H$ ,  $C^{21}$ - $H$ ,  $C^{26}$ - $H$ ,  $C^{27}$ - $H$ ), 4.93 (1H, d,  $J_{AB}$  12.9,  $C^{10}$ - $H_A$ ), 4.86 (1H, d,  $J_{AB}$  12.9,  $C^{10}$ - $H_B$ ), 4.47 (1H, d,  $J$  9.7,  $C^1$ - $H$ ), 4.29 (1H, dd,  $J$  5.6, 2.0,  $C^4$ - $H$ ), 4.19 (1H, dd,  $J$  6.7, 5.6,  $C^3$ - $H$ ), 3.93 (1H, dd,  $J_{AB}$  10.3,  $J_{AX}$  7.0,  $C^6$ - $H_A$ ), 3.90 (1H, dd,  $J_{AB}$  10.3,  $J_{BX}$  6.0,  $C^6$ - $H_B$ ), 3.82

(1H, ddd,  $J_{AX}$  7.0,  $J_{BX}$  6.0,  $J$  2.0,  $C^5-H_X$ ), 3.41 (1H, dd,  $J$  9.7, 6.7,  $C^2-H$ ), 3.26 (1H, sept,  $J$  6.8,  $C^7-H$ ), 1.41 (3H, s,  $C^{16}-H_3$  or  $C^{17}-H_3$ ), 1.33 (3H, s,  $C^{16}-H_3$  or  $C^{17}-H_3$ ), 1.32 (3H, d,  $J$  6.8,  $C^8-H_3$  or  $C^9-H_3$ ), 1.30 (3H, d,  $J$  6.8,  $C^8-H_3$  or  $C^9-H_3$ ), 1.05 (9H, s,  $C^{23}-H_3$ );  $^{13}C$  NMR (126 MHz,  $CDCl_3$ )  $\delta$  147.5 ( $C^{14}$ ), 145.9 ( $C^{11}$ ), 135.8 ( $C^{19}$  or  $C^{25}$ ), 135.7 ( $C^{19}$  or  $C^{25}$ ), 133.5 ( $C^{18}$  or  $C^{24}$ ), 133.4 ( $C^{18}$  or  $C^{24}$ ), 129.9 ( $C^{21}$ ,  $C^{27}$ ), 128.4 ( $C^{12}$ ), 127.9 ( $C^{20}$  or  $C^{26}$ ), 127.8 ( $C^{20}$  or  $C^{26}$ ), 123.6 ( $C^{13}$ ), 110.1 ( $C^{15}$ ), 82.7 ( $C^1$ ), 80.5 ( $C^2$ ), 79.7 ( $C^3$ ), 77.1 ( $C^5$ ), 73.7 ( $C^4$ ), 72.5 ( $C^{10}$ ), 63.0 ( $C^6$ ), 34.7 ( $C^7$ ), 28.2 ( $C^{16}$  or  $C^{17}$ ), 26.9 ( $C^{23}$ ), 26.5 ( $C^{16}$  or  $C^{17}$ ), 23.9 ( $C^8$  or  $C^9$ ), 23.8 ( $C^8$  or  $C^9$ ), 19.3 ( $C^{22}$ ); HRMS  $m/z$  ( $ESI^+$ ) [Found ( $M+Na$ ) $^+$  674.25770  $C_{35}H_{45}NO_7S^{28}SiNa$  requires  $M^+$  674.25782]; LRMS  $m/z$  ( $ES^+$ ) 674 ( $[M+Na]^+$ , 100%), 675 ( $[M+Na]^+$ , 44%), 676 ( $[M+Na]^+$ , 19%); Analytical HPLC – despite multiple elution conditions it was not possible to retain the compound on the column sufficiently to obtain reliable purity data by this method.

#### Isopropyl 2-*O*-(4-nitrobenzyl)-1-thio- $\beta$ -D-galactopyranoside, **86**



To a solution of **160** (240 mg, 0.368 mmol, 1.0 eq) in  $CH_2Cl_2$ :MeOH (2:1, 4.8 mL) was added acetyl chloride (16  $\mu$ L, 0.22 mmol, 0.6 eq). The solution was stirred at room temperature for 15 h and concentrated *in vacuo*. The crude residue was purified by gradient silica gel chromatography (50–100% ethyl acetate in petroleum ether) to yield isopropyl 2-*O*-(4-nitrobenzyl)-1-thio- $\beta$ -D-galactopyranoside **86** (117 mg, 85%) as a colourless solid:  $R_f$  0.17 (ethyl acetate); mp 138–139 °C (ethyl acetate);  $[\alpha]_D^{25} = +3.2$  ( $c$  0.5,  $CHCl_3$ );  $\bar{\nu}_{max}$  (thin film)/ $cm^{-1}$  3407 (br, O–H), 2961 (w), 2922 (w), 2866 (w), 1604 (w), 1519 (s, N=O), 1456 (w), 1347 (s, N=O), 1109 (m), 1075 (m), 817 (w);  $^1H$  NMR (500 MHz,  $CDCl_3$ )  $\delta$  8.22–8.20 (2H, m,  $C^{13}-H$ ), 7.59–7.57 (2H, m,  $C^{12}-H$ ), 5.03 (1H, d,  $J_{AB}$  12.3,  $C^{10}-H_A$ ), 4.88 (1H, d,  $J$  12.3,  $C^{10}-H_B$ ), 4.52 (1H, d,  $J$  9.5,  $C^1-H$ ), 4.08 (1H, d,  $J$  2.9,  $C^4-H$ ), 3.95 (1H, dd,  $J_{AB}$  11.9,  $J_{AX}$  5.4,  $C^6-H_A$ ), 3.90 (1H, dd,  $J_{AB}$  11.9,  $J_{BX}$  4.1,  $C^6-H_B$ ), 3.70–3.69 (1H, m,  $C^3-H$ ), 3.54 (1H, ddd,  $J_{AX}$  5.4,  $J_{BX}$  4.1,  $J$  1.2,  $C^5-H_X$ ), 3.51 (1H, dd,  $J$  9.5, 9.3,  $C^2-H$ ), 3.25 (1H,

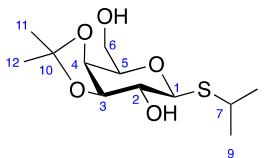
## Chapter 6

sept,  $J$  6.7,  $C^7$ -H), 3.02 (1H, br s,  $C^4$ -OH), 2.65 (1H, br s,  $C^3$ -OH), 2.20 (1H, br s,  $C^6$ -OH), 1.35 (3H, d,  $J$  6.7,  $C^8$ -H<sub>3</sub> or  $C^9$ -H<sub>3</sub>), 1.34 (3H, d,  $J$  6.7,  $C^8$ -H<sub>3</sub> or  $C^9$ -H<sub>3</sub>);  $^{13}\text{C}$  NMR (126 MHz,  $\text{CDCl}_3$ )  $\delta$  147.6 ( $C^{14}$ ), 145.8 ( $C^{11}$ ), 128.3 ( $C^{12}$ ), 123.7 ( $C^{13}$ ), 84.7 ( $C^1$ ), 80.0 ( $C^2$ ), 77.7 ( $C^5$ ), 75.3 ( $C^3$ ), 74.3 ( $C^{10}$ ), 70.5 ( $C^4$ ), 63.4 ( $C^6$ ), 35.9 ( $C^7$ ), 24.0 ( $C^8$ ,  $C^9$ ); HRMS  $m/z$  ( $\text{ESI}^+$ ) [Found ( $\text{M}+\text{Na}$ ) $^+$  396.10841  $\text{C}_{16}\text{H}_{23}\text{NO}_7\text{SNa}$  requires  $\text{M}^+$  396.10874]; LRMS  $m/z$  ( $\text{ES}^+$ ) 396 ( $[\text{M}+\text{Na}]^+$ , 100%), 397 ( $[\text{M}+\text{Na}]^+$ , 23%), 398 ( $[\text{M}+\text{Na}]^+$ , 10%); Analytical RP-HPLC (Method 1, 254 nm) Ret. time = 10.4 min, Purity = >99.9%.

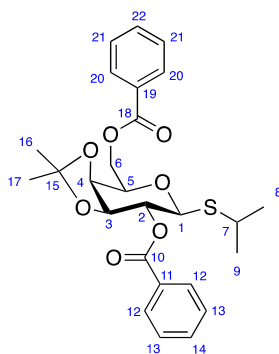


### 6.2.5. Synthesis of 3-Protected Galactopyranosides

#### Isopropyl 3,4-*O*-isopropylidene-1-thio- $\beta$ -D-galactopyranoside, **164**



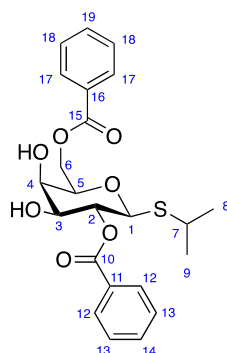
To a suspension of isopropyl 1-thio- $\beta$ -D-galactopyranoside **76** (3.00 g, 12.6 mmol, 1.0 eq) in acetone (30 mL) was added 4-TsOH·H<sub>2</sub>O (123 mg, 0.647 mmol, 0.05 eq) and 2,2-dimethoxypropane (9.50 mL, 77.3 mmol, 6.1 eq). The resulting solution was stirred at room temperature for 2.5 days, quenched with triethylamine (130  $\mu$ L), and concentrated *in vacuo*. The residue was dissolved in methanol:water (10:1, 110 mL), stirred under reflux for 24 h, and concentrated *in vacuo*. The crude residue was purified by gradient silica gel chromatography (0–56% ethyl acetate in petroleum ether) to yield isopropyl 3,4-*O*-isopropylidene-1-thio- $\beta$ -D-galactopyranoside **164** (1.73 g, 49%) as a colourless solid:  $R_f$  0.49 (ethyl acetate);  $[\alpha]_D^{25} = +1.1$  ( $c$  1.0, CHCl<sub>3</sub>); mp 87–88 °C (ethyl acetate);  $\bar{\nu}_{\max}$  (thin film)/cm<sup>−1</sup> 3422 (br, O–H), 2983 (m), 2932 (m), 2869 (m), 2362 (w), 1457 (w), 1378 (s), 1243 (s), 1220 (s, C–O), 1141 (m), 1078 (s), 1025 (s), 873 (s), 841 (w); <sup>1</sup>H NMR (500 MHz, CDCl<sub>3</sub>)  $\delta$  4.33 (1H, d,  $J$  10.3, C<sup>1</sup>-H), 4.20 (1H, dd,  $J$  5.6, 2.3, C<sup>4</sup>-H), 4.09 (1H, dd,  $J$  7.0, 5.6, C<sup>3</sup>-H), 3.97 (1H, ddd,  $J_{AB}$  11.7,  $J_{AX}$  7.5,  $J$  3.7, C<sup>6</sup>-H<sub>A</sub>), 3.87 (1H, ddd,  $J_{AX}$  7.5,  $J_{BX}$  4.0,  $J$  2.3, C<sup>5</sup>-H<sub>X</sub>), 3.79 (1H, ddd,  $J_{AB}$  11.7,  $J$  9.5,  $J_{BX}$  4.0, C<sup>6</sup>-H<sub>B</sub>), 3.53 (1H, ddd,  $J$  10.3, 7.0, 2.0, C<sup>2</sup>-H), 3.21 (1H, sept,  $J$  6.7, C<sup>7</sup>-H), 2.44 (1H, d,  $J$  2.0, C<sup>2</sup>-OH), 2.08 (1H, dd,  $J$  9.5, 3.7, C<sup>6</sup>-OH), 1.51 (3H, s, C<sup>11</sup>-H<sub>3</sub> or C<sup>12</sup>-H<sub>3</sub>), 1.36 (3H, s, C<sup>8</sup>-H<sub>3</sub> or C<sup>9</sup>-H<sub>3</sub>), 1.35 (3H, s, C<sup>11</sup>-H<sub>3</sub> or C<sup>12</sup>-H<sub>3</sub>), 1.34 (3H, s, C<sup>8</sup>-H<sub>3</sub> or C<sup>9</sup>-H<sub>3</sub>); <sup>13</sup>C NMR (126 MHz, CDCl<sub>3</sub>)  $\delta$  110.6 (C<sup>10</sup>), 85.4 (C<sup>1</sup>), 79.1 (C<sup>3</sup>), 77.2 (C<sup>5</sup>), 74.0 (C<sup>4</sup>), 72.4 (C<sup>2</sup>), 62.8 (C<sup>6</sup>), 36.1 (C<sup>7</sup>), 28.3, 26.5 (C<sup>11</sup>, C<sup>12</sup>), 24.4, 24.1 (C<sup>8</sup>, C<sup>9</sup>); HRMS  $m/z$  (ESI<sup>+</sup>) [Found (M+Na)<sup>+</sup> 301.10812 C<sub>12</sub>H<sub>22</sub>O<sub>5</sub>SNa requires M<sup>+</sup> 301.10802]; LRMS  $m/z$  (ES<sup>+</sup>) 301 ([M+Na]<sup>+</sup>, 100%), 302 ([M+Na]<sup>+</sup>, 14%), 303 ([M+Na]<sup>+</sup>, 6%).

Isopropyl 2,6-di-*O*-benzoyl-3,4-*O*-isopropylidene-1-thio- $\beta$ -D-galactopyranoside, **165**

To a solution of **164** (502 mg, 1.80 mmol, 1.0 eq) in pyridine (5 mL) was added 4-DMAP (22 mg, 0.18 mmol, 0.1 eq). The solution was cooled to 0 °C and benzoyl chloride (626  $\mu$ L, 5.39 mmol, 3.0 eq) was added dropwise over 5 min. A colourless precipitate formed immediately. The suspension was stirred at 0 °C for 1 h, warmed to room temperature and stirred for a further 4 h. The reaction was quenched with ice and diluted with ethyl acetate (20 mL). The organic layer was washed with water (3  $\times$  20 mL) and sat. aq. NaHCO<sub>3</sub> (3  $\times$  20 mL). The aqueous layers were back extracted with ethyl acetate (2  $\times$  50 mL). The organic layers were combined, washed with brine (40 mL), dried over MgSO<sub>4</sub>, filtered, and concentrated *in vacuo*. The crude residue was purified by gradient silica gel chromatography (0–100% ethyl acetate in petroleum ether) to yield isopropyl 2,6-di-*O*-benzoyl-3,4-*O*-isopropylidene-1-thio- $\beta$ -D-galactopyranoside **165** (837 mg, 98%) as a colourless solid:  $R_f$  0.33 (1:4 ethyl acetate: petroleum ether);  $[\alpha]_D^{25} = +50.5$  ( $c$  1.0, CHCl<sub>3</sub>); mp 166–168 °C (ethyl acetate);  $\bar{\nu}_{\max}$  (thin film)/cm<sup>-1</sup> 2979 (m), 2901 (w), 1722 (s, C=O), 1450 (m), 1379 (m), 1313 (m), 1262 (s, C–O), 1221 (m), 1109 (s), 1076 (s), 1044 (m), 876 (w), 705 (s); <sup>1</sup>H NMR (500 MHz, CDCl<sub>3</sub>)  $\delta$  8.08–8.03 (4H, m, C<sup>12</sup>-*H*, C<sup>20</sup>-*H*), 7.63–7.53 (2H, m, C<sup>14</sup>-*H*, C<sup>22</sup>-*H*), 7.49–7.41 (4H, m, C<sup>13</sup>-*H*, C<sup>21</sup>-*H*) 5.28 (1H, dd,  $J$  10.0, 7.0, C<sup>2</sup>-*H*), 4.70 (1H, dd,  $J_{AB}$  11.8,  $J_{BX}$  4.2, C<sup>6</sup>-*H*<sub>B</sub>), 4.66 (1H, d,  $J$  10.0, C<sup>1</sup>-*H*), 4.61 (1H, d,  $J_{AB}$  11.8,  $J_{AX}$  7.9, C<sup>6</sup>-*H*<sub>A</sub>), 4.40 (1H, dd,  $J$  7.0, 5.5, C<sup>3</sup>-*H*), 4.35 (1H, dd,  $J$  5.5, 2.1, C<sup>4</sup>-*H*), 4.21 (1H, ddd,  $J_{AX}$  7.9,  $J_{BX}$  4.2,  $J$  2.1, C<sup>5</sup>-*H*<sub>X</sub>), 3.14 (1H, sept,  $J$  6.8, C<sup>7</sup>-*H*), 1.63 (3H, s, C<sup>16</sup>-*H*<sub>3</sub> or C<sup>17</sup>-*H*<sub>3</sub>), 1.37 (3H, s, C<sup>16</sup>-*H*<sub>3</sub> or C<sup>17</sup>-*H*<sub>3</sub>), 1.26 (3H, d,  $J$  6.8, C<sup>8</sup>-*H*<sub>3</sub> or C<sup>9</sup>-*H*<sub>3</sub>), 1.23 (3H, d,  $J$  6.8, C<sup>8</sup>-*H*<sub>3</sub> or C<sup>9</sup>-*H*<sub>3</sub>); <sup>13</sup>C NMR (126 MHz, CDCl<sub>3</sub>)  $\delta$  166.5 (C<sup>18</sup>), 165.6 (C<sup>10</sup>), 133.35 (C<sup>14</sup> or C<sup>22</sup>), 133.28 (C<sup>14</sup> or C<sup>22</sup>), 130.1 (C<sup>12</sup> or C<sup>20</sup>), 129.99 (C<sup>11</sup> or C<sup>19</sup>), 129.97 (C<sup>11</sup> or C<sup>19</sup>), 129.8 (C<sup>12</sup> or C<sup>20</sup>), 128.55 (C<sup>13</sup> or C<sup>21</sup>), 128.47 (C<sup>13</sup> or

$C^{21}$ ), 111.1 ( $C^{15}$ ), 82.7 ( $C^1$ ), 77.4 ( $C^3$ ), 74.5 ( $C^5$ ), 73.9 ( $C^4$ ), 72.5 ( $C^2$ ), 64.2 ( $C^6$ ), 35.7 ( $C^7$ ), 27.9 ( $C^{18}$  or  $C^{19}$ ), 26.5 ( $C^{18}$  or  $C^{19}$ ), 24.1 ( $C^8$  or  $C^9$ ), 23.9 ( $C^8$  or  $C^9$ ); HRMS  $m/z$  (ESI<sup>+</sup>) [Found (M+Na)<sup>+</sup> 509.15894 C<sub>26</sub>H<sub>30</sub>O<sub>7</sub>SNa requires M<sup>+</sup> 509.16045]; LRMS  $m/z$  (ES<sup>+</sup>) 509 ([M+Na]<sup>+</sup>, 100%), 510 ([M+Na]<sup>+</sup>, 30%), 511 ([M+Na]<sup>+</sup>, 11%); Analytical RP-HPLC (Method 2, 254 nm) Ret. time = 12.2 min, Purity = >99.9%.

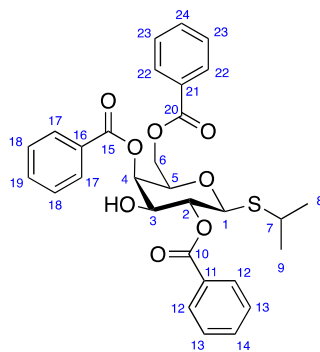
### Isopropyl 2,6-di-*O*-benzoyl-1-thio-β-D-galactopyranoside, **166**



To a solution of **165** (850 mg, 1.75 mmol, 1.0 eq) in methanol (100 mL) was added Dowex 50WX8 (50–100 mesh, 1.60 g) and the reaction mixture was stirred at room temperature for 3 h. Additional Dowex 50WX8 (50–100 mesh, 1.60 g) was added and the reaction mixture was stirred at room temperature for a further 24 h. 1 M aq. HCl (5.00 mL, 5.00 mmol, 2.9 eq) was added and the reaction mixture was stirred at room temperature for a further 15 h. The reaction mixture was filtered, and the filtrate was concentrated *in vacuo*. The residue was diluted with ethyl acetate (50 mL) and washed with water (3 × 50 mL), sat. aq. NaHCO<sub>3</sub> (3 × 50 mL). The aqueous layers were back extracted with ethyl acetate (3 × 80 mL). The organic layers were combined, washed with brine (150 mL), dried over MgSO<sub>4</sub>, filtered, and concentrated *in vacuo*. The crude residue was crystallised from CH<sub>2</sub>Cl<sub>2</sub>:hexanes to yield isopropyl 2,6-di-*O*-benzoyl-1-thio-β-D-galactopyranoside **166** (688 mg, 88%) as colourless crystals:  $R_f$  0.14 (1:2 ethyl acetate:petroleum ether);  $[\alpha]_D^{25} = +6.6$  ( $c$  1.0, CHCl<sub>3</sub>); mp 122–124 °C (CH<sub>2</sub>Cl<sub>2</sub>:hexanes);  $\bar{\nu}_{\max}$  (thin film)/cm<sup>-1</sup> 3453 (br, O–H), 1718 (s, C=O), 1602 (w), 1451 (w), 1270 (s, C–O), 1073 (m), 710 (s); <sup>1</sup>H NMR (400 MHz, CDCl<sub>3</sub>)  $\delta$  8.06–8.01 (4H, m, C<sup>12</sup>-H, C<sup>17</sup>-H) 7.59–7.52 (2H, m, C<sup>14</sup>-H, C<sup>19</sup>-H), 7.46–7.38 (4H, m, C<sup>13</sup>-H, C<sup>18</sup>-H), 5.28 (1H, dd,  $J$  9.8, 9.7, C<sup>2</sup>-H), 4.68 (1H, d,  $J$  9.8, C<sup>1</sup>-H), 4.66 (1H, dd,  $J_{AB}$  11.6,  $J_{BX}$  6.1, C<sup>6</sup>-H<sub>B</sub>), 4.57 (1H, dd,  $J_{AB}$  11.6,  $J_{AX}$  6.9, C<sup>6</sup>-H<sub>A</sub>), 4.10 (1H, br s, C<sup>4</sup>-H), 3.90

(1H, dd,  $J_{AX}$  6.9,  $J_{BX}$  6.1,  $C^5-H_X$ ), 3.86 (1H, br s,  $C^3-H$ ), 3.65 (1H, br s,  $C^3-OH$ ), 3.44 (1H, br s,  $C^4-OH$ ), 3.18 (1H, sept,  $J$  6.7,  $C^7-H$ ), 1.25 (3H, d,  $J$  6.7,  $C^8-H_3$  or  $C^9-H_3$ ), 1.24 (3H, d,  $J$  6.7,  $C^8-H_3$  or  $C^9-H_3$ );  $^{13}C$  NMR (126 MHz,  $CDCl_3$ )  $\delta$  166.9 ( $C^{10}$ ), 166.7 ( $C^{15}$ ), 133.43 ( $C^{14}$  or  $C^{19}$ ), 133.39 ( $C^{14}$  or  $C^{19}$ ), 130.1 ( $C^{12}$  or  $C^{17}$ ), 129.8 ( $C^{12}$  or  $C^{17}$ ), 129.72 ( $C^{11}$  or  $C^{16}$ ), 129.66 ( $C^{11}$  or  $C^{16}$ ), 128.51 ( $C^{13}$  or  $C^{18}$ ), 128.48 ( $C^{13}$  or  $C^{18}$ ), 83.2 ( $C^1$ ), 76.3 ( $C^5$ ), 73.7 ( $C^3$ ), 72.5 ( $C^2$ ), 69.1 ( $C^4$ ), 63.5 ( $C^6$ ), 35.4 ( $C^7$ ), 24.1 ( $C^8$  or  $C^9$ ), 23.9 ( $C^8$  or  $C^9$ ); HRMS  $m/z$  (ESI $^+$ ) [Found (M+Na) $^+$  469.12786  $C_{23}H_{26}O_7SNa$  requires M $^+$  469.12914]; LRMS  $m/z$  (ES $^+$ ) 469 ([M+Na] $^+$ , 100%), 470 ([M+Na] $^+$ , 29%), 471 ([M+Na] $^+$ , 9%); Analytical RP-HPLC (Method 2, 254 nm) Ret. time = 10.1 min, Purity = 94.7%.

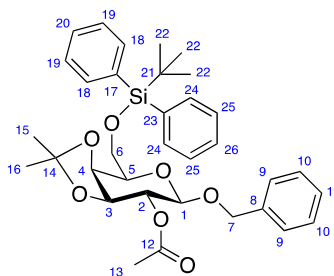
### Isopropyl 2,4,6-tri-*O*-benzoyl-1-thio- $\beta$ -D-galactopyranoside, **163**



To a solution of **166** (558 mg, 1.25 mmol, 1.0 eq) in  $CH_2Cl_2$  (2 mL) were added camphor-10-sulfonic acid (34 mg, 0.15 mmol, 0.1 eq) and trimethyl orthobenzoate (300  $\mu$ L, 1.75 mmol, 1.4 eq). The reaction solution was stirred at room temperature for 30 min, quenched with triethylamine (30  $\mu$ L), and concentrated *in vacuo*. The residue was dissolved in acetic acid (90% in water, 10 mL), stirred at room temperature for 2 h, and concentrated *in vacuo*. The crude residue was purified by gradient silica gel chromatography (10–35% ethyl acetate in petroleum ether) to yield isopropyl 2,4,6-tri-*O*-benzoyl-1-thio- $\beta$ -D-galactopyranoside **163** (582 mg, 79%) as a colourless solid:  $R_f$  0.31 (3:7 petroleum ether:ethyl acetate);  $[\alpha]_D^{25} = +10.0$  ( $c$  1.;0,  $CHCl_3$ ); mp 72–73  $^{\circ}C$  (ethyl acetate);  $\bar{\nu}_{max}$  (thin film)/ $cm^{-1}$  3485 (br, O–H), 3066 (w), 2963 (w), 2361 (w), 1723 (s, C=O), 1602 (w), 1452 (w), 1267 (s, C–O), 1112 (m), 1052 (m), 1027 (w), 710 (s);  $^1H$  NMR (400 MHz,  $CDCl_3$ )  $\delta$  8.14–8.12 and 8.08–8.00 (6H, m,  $C^{12}-H$ ,  $C^{17}-H$ ,  $C^{22}-H$ ), 7.65–7.54 (3H, m,  $C^{14}-H$ ,  $C^{19}-H$ ,  $C^{24}-H$ ), 7.52–7.41 (6H, m,  $C^{13}-H$ ,  $C^{18}-H$ ,  $C^{23}-H$ ), 5.80 (1H, dd,  $J$  3.5, 0.9,

$C^4-H$ ), 5.39 (1H, dd,  $J$  9.9, 9.9,  $C^2-H$ ), 4.83 (1H, d,  $J$  9.9,  $C^1-H$ ), 4.56 (1H, dd,  $J_{AB}$  11.5,  $J_{AX}$  7.3,  $C^6-H_A$ ), 4.43 (1H, dd,  $J_{AB}$  11.5,  $J_{BX}$  5.6,  $C^6-H_B$ ), 4.22–4.14 (2H, m,  $C^3-H$ ,  $C^5-H_X$ ), 3.25 (1H, sept,  $J$  6.8,  $C^7-H$ ), 2.76 ( $C^3-OH$ ), 1.31 (3H, d,  $J$  6.8,  $C^8-H_3$  or  $C^9-H_3$ ), 1.30 (3H, d,  $J$  6.8,  $C^8-H_3$  or  $C^9-H_3$ );  $^{13}C$  NMR (101 MHz,  $CDCl_3$ )  $\delta$  166.8 ( $C^{10}$  or  $C^{15}$  or  $C^{20}$ ), 166.5 ( $C^{10}$  or  $C^{15}$  or  $C^{20}$ ), 166.2 ( $C^{10}$  or  $C^{15}$  or  $C^{20}$ ), 133.8 ( $C^{14}$  or  $C^{19}$  or  $C^{24}$ ), 133.6 ( $C^{14}$  or  $C^{19}$  or  $C^{24}$ ), 133.4 ( $C^{14}$  or  $C^{19}$  or  $C^{24}$ ), 130.3 ( $C^{12}$  or  $C^{17}$  or  $C^{22}$ ), 130.1 ( $C^{12}$  or  $C^{17}$  or  $C^{22}$ ), 129.9 ( $C^{12}$  or  $C^{17}$  or  $C^{22}$ ), 129.7 ( $C^{11}$  or  $C^{16}$  or  $C^{21}$ ), 129.6 ( $C^{11}$  or  $C^{16}$  or  $C^{21}$ ), 129.1 ( $C^{11}$  or  $C^{16}$  or  $C^{21}$ ), 128.8 ( $C^{13}$  or  $C^{18}$  or  $C^{23}$ ), 128.59 ( $C^{13}$  or  $C^{18}$  or  $C^{23}$ ), 128.55 ( $C^{13}$  or  $C^{18}$  or  $C^{23}$ ), 83.6 ( $C^1$ ), 75.3 ( $C^3$  or  $C^5$ ), 73.1 ( $C^3$  or  $C^5$ ), 72.3 ( $C^2$ ), 70.9 ( $C^4$ ), 62.9 ( $C^6$ ), 35.7 ( $C^7$ ), 24.1 ( $C^8$  or  $C^9$ ), 23.9 ( $C^8$  or  $C^9$ ); HRMS  $m/z$  (ESI<sup>+</sup>) [Found (M+Na)<sup>+</sup> 573.15515  $C_{30}H_{30}O_8SNa$  requires M<sup>+</sup> 573.15536]; LRMS  $m/z$  (ES<sup>+</sup>) 573 ([M+Na]<sup>+</sup>, 100%), 574 ([M+Na]<sup>+</sup>, 41%), 575 ([M+Na]<sup>+</sup>, 17%); Analytical RP-HPLC (Purity Short Run, 254 nm) Ret. time = 11.8 min, Purity = 98.6%.

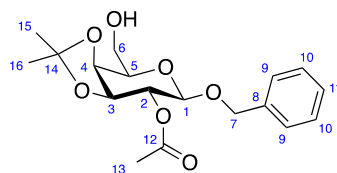
**Benzyl 2-*O*-acetyl-6-*O*-(*tert*-butyldiphenylsilyl)-3,4-*O*-isopropylidene- $\beta$ -D-galactopyranoside, **184****



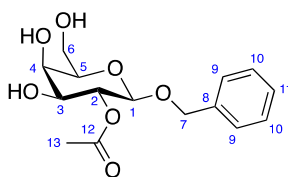
To a solution of **128** (0.500 g, 0.911 mmol, 1.0 eq) in pyridine (1.0 mL) was added acetic anhydride (1.0 mL). The solution was stirred at room temperature for 15 h and concentrated *in vacuo*. The crude residue was purified by gradient silica gel chromatography (10–20% diethyl ether in petroleum ether) to yield benzyl 2-*O*-acetyl-6-*O*-(*tert*-butyldiphenylsilyl)-3,4-*O*-isopropylidene- $\beta$ -D-galactopyranoside **184** (0.537 g, 99%) as a colourless foam:  $R_f$  0.72 (3:7 ethyl acetate:petroleum ether);  $[\alpha]_D^{25} = -14.3$  ( $c$  1.0,  $CHCl_3$ ) [lit.<sup>277</sup>  $[\alpha]_D^{24} = -14.5$  ( $c$  0.05,  $CHCl_3$ )];  $\bar{\nu}_{max}$  (thin film)/ $cm^{-1}$  3071 (w), 2933 (w), 2858 (w), 1750 (s, C=O), 1428 (w), 1372 (m), 1222 (s), 1113 (s), 1076 (s), 702 (s);  $^1H$  NMR (400 MHz,  $CDCl_3$ )  $\delta$  7.72–7.69 (4H, m,  $C^{18}-H$ ,  $C^{24}-H$ ), 7.43–7.24 (11H, m,  $C^9-H$ ,  $C^{10}-H$ ,  $C^{11}-H$ ,  $C^{19}-H$ ,  $C^{20}-H$ ,  $C^{25}-H$ ,  $C^{26}-H$ ), 5.03 (1H, dd,  $J$  8.1, 7.7,  $C^2-H$ ), 4.84

(1H, d,  $J_{AB}$  12.4, C<sup>7</sup>-H<sub>A</sub>), 4.58 (1H, d,  $J_{AB}$  12.4, C<sup>7</sup>-H<sub>B</sub>), 4.32 (1H, d,  $J$  8.1, C<sup>1</sup>-H), 4.25 (1H, dd,  $J$  5.3, 2.0, C<sup>4</sup>-H), 4.12 (1H, dd,  $J$  7.7, 5.3, C<sup>3</sup>-H), 3.99 (1H, dd,  $J_{AB}$  10.0,  $J_{AX}$  7.0, C<sup>6</sup>-H<sub>A</sub>), 3.96 (1H, dd,  $J_{AB}$  10.0,  $J_{BX}$  6.3, C<sup>6</sup>-H<sub>B</sub>), 3.84 (1H, ddd,  $J_{AX}$  7.0,  $J_{BX}$  6.3,  $J$  2.0, C<sup>5</sup>-H<sub>X</sub>), 2.07 (3H, s, C<sup>13</sup>-H<sub>3</sub>), 1.55 (3H, s, C<sup>15</sup>-H<sub>3</sub> or C<sup>16</sup>-H<sub>3</sub>), 1.32 (3H, s, C<sup>15</sup>-H<sub>3</sub> or C<sup>16</sup>-H<sub>3</sub>), 1.06 (9H, s, C<sup>22</sup>-H<sub>3</sub>); LRMS  $m/z$  (ES<sup>+</sup>) 613 ([M+Na]<sup>+</sup>, 100%), 614 ([M+Na]<sup>+</sup>, 40%), 615 ([M+Na]<sup>+</sup>, 13%). The data are in good agreement with the literature.<sup>277</sup>

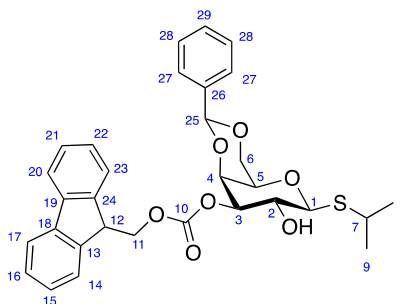
### Benzyl 2-*O*-acetyl-3,4-*O*-isopropylidene-β-D-galactopyranoside, **185**



To a solution of **184** (0.277 g, 0.469 mmol, 1.0 eq) in THF (1 mL) was added TBAF (1 M in THF, 0.930 μL, 0.930 mmol, 2.0 eq) and the solution was stirred at room temperature for 1 h. The reaction was quenched with CH<sub>2</sub>Cl<sub>2</sub> and concentrated *in vacuo*. The crude residue was purified by gradient silica gel chromatography (20–45% ethyl acetate in petroleum ether) to yield benzyl 2-*O*-acetyl-3,4-*O*-isopropylidene-β-D-galactopyranoside **185** (0.115 g, 70%) as a colourless solid:  $R_f$  0.29 (1:1 ethyl acetate:petroleum ether);  $[\alpha]_D^{25} = +0.31$  ( $c$  1.0, CHCl<sub>3</sub>) [lit.<sup>277</sup>  $[\alpha]_D^{24} = -0.83$  ( $c$  0.06, CHCl<sub>3</sub>)]; mp 91–92 °C (ethyl acetate) [lit.<sup>345</sup> 105–107 °C];  $\bar{\nu}_{\max}$  (thin film)/cm<sup>-1</sup> 3331 (br), 2933 (w), 1746 (m, C=O), 1371 (m), 1233 (m), 1133 (m), 1078 (s), 1040 (s), 870 (m), 735 (s); <sup>1</sup>H NMR (400 MHz, CDCl<sub>3</sub>)  $\delta$  7.37–7.27 (5H, m, C<sup>9</sup>-H, C<sup>10</sup>-H, C<sup>11</sup>-H), 5.05 (1H, dd,  $J$  8.1, 7.0, C<sup>2</sup>-H), 4.87 (1H, d,  $J_{AB}$  12.5, C<sup>7</sup>-H<sub>A</sub>), 4.66 (1H, d,  $J_{AB}$  12.5, C<sup>7</sup>-H<sub>B</sub>), 4.40 (1H, d,  $J$  8.1, C<sup>1</sup>-H), 4.19–4.14 (2H, m, C<sup>3</sup>-H, C<sup>4</sup>-H), 4.00 (1H, ddd,  $J_{AB}$  12.7,  $J$  9.0,  $J_{AX}$  3.8, C<sup>6</sup>-H<sub>A</sub>), 3.87–3.79 (2H, m, C<sup>5</sup>-H<sub>X</sub>, C<sup>6</sup>-H<sub>B</sub>), 2.08 (3H, s, C<sup>15</sup>-H<sub>3</sub>), 1.99 (1H, dd,  $J$  9.0, 3.6, C<sup>6</sup>-OH), 1.57 (3H, s, C<sup>15</sup>-H<sub>3</sub> or C<sup>16</sup>-H<sub>3</sub>), 1.33 (3H, s, C<sup>15</sup>-H<sub>3</sub> or C<sup>16</sup>-H<sub>3</sub>); LRMS  $m/z$  (ES<sup>+</sup>) 375 ([M+Na]<sup>+</sup>, 100%), 376 ([M+Na]<sup>+</sup>, 20%), 377 ([M+Na]<sup>+</sup>, 4%). The data are in good agreement with the literature.<sup>277,345</sup>

**Benzyl 2-*O*-acetyl- $\beta$ -D-galactopyranoside, **186****

To a solution of **185** (22 mg, 0.062 mmol, 1.0 eq) in methanol (4.6 mL) was added Dowex 50WX8 (105 mg). The suspension was stirred at room temperature for 17.5 h, filtered, and concentrated *in vacuo*. The crude residue was purified by silica gel chromatography (100% ethyl acetate) to yield benzyl 2-*O*-acetyl- $\beta$ -D-galactopyranoside **186** (15 mg, 79%) as a colourless solid:  $R_f$  0.17 (ethyl acetate);  $[\alpha]_D^{25} = -10.1$  ( $c$  0.5, MeOH) [lit.<sup>277</sup>  $[\alpha]_D^{23} = -10.4$  ( $c$  0.02, MeOH)]; mp 136–139 °C (ethyl acetate);  $\bar{\nu}_{\max}$  (neat)/ $\text{cm}^{-1}$  3431 (br, O–H), 2361 (w), 1744 (s), 1371 (s), 1242 (m), 1060 (s);  $^1\text{H}$  NMR (400 MHz,  $\text{CD}_3\text{OD}$ )  $\delta$  7.36–7.25 (5H, m,  $\text{C}^9\text{-H}$ ,  $\text{C}^{10}\text{-H}$ ,  $\text{C}^{11}\text{-H}$ ), 5.08 (1H, dd,  $J$  9.9, 8.0,  $\text{C}^2\text{-H}$ ), 4.87 (1H, d,  $J_{\text{AB}}$  12.2,  $\text{C}^7\text{-H}_A$ ), 4.62 (1H, d,  $J_{\text{AB}}$  12.2,  $\text{C}^7\text{-H}_B$ ), 4.46 (1H, d,  $J$  8.0,  $\text{C}^1\text{-H}$ ), 3.88 (1H, d,  $J$  3.3,  $\text{C}^4\text{-H}$ ), 3.82 (1H, dd,  $J_{\text{AB}}$  11.4,  $J_{\text{AX}}$  6.5,  $\text{C}^6\text{-H}_A$ ), 3.75 (1H, dd,  $J_{\text{AB}}$  11.4,  $J_{\text{BX}}$  5.6,  $\text{C}^6\text{-H}_B$ ), 3.63 (1H, dd,  $J$  9.9, 3.3,  $\text{C}^3\text{-H}$ ), 3.55 (1H, dd,  $J_{\text{AX}}$  6.5,  $J_{\text{BX}}$  5.6,  $\text{C}^5\text{-H}_X$ ), 2.03 (3H, s,  $\text{C}^{13}\text{-H}_3$ ); LRMS  $m/z$  ( $\text{ES}^+$ ) 335 ( $[\text{M}+\text{Na}]^+$ , 100%), 336 ( $[\text{M}+\text{Na}]^+$ , 17%), 337 ( $[\text{M}+\text{Na}]^+$ , 3%). The data are in good agreement with the literature.<sup>277</sup>

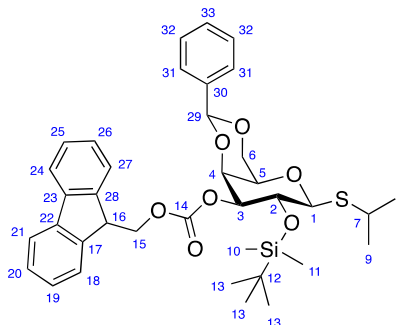
**Isopropyl 4,6-*O*-benzylidene-3-*O*-fluorenylmethoxycarbonyl-1-thio- $\beta$ -D-galactopyranoside, **188****

To a solution of **187** (2.01 g, 6.16 mmol, 1.0 eq) in pyridine (10 mL) was added 4-DMAP (152 mg, 1.24 mmol, 0.2 eq). The solution was cooled to 0 °C and FmocCl (3.10 g, 12.0 mmol, 1.9 eq) was added portionwise. The solution was stirred at 0 °C for 2 h, warmed to room temperature and stirred for a further 14 h. The reaction was quenched with ice and extracted with

ethyl acetate (20 mL). The separated organic layer was washed with water ( $3 \times 20$  mL), 1 M aq. HCl ( $3 \times 20$  mL), and sat. aq.  $\text{NaHCO}_3$  ( $3 \times 20$  mL). The aqueous layers were back extracted with ethyl acetate ( $3 \times 50$  mL). The organic layers were combined, dried over  $\text{MgSO}_4$ , filtered, and concentrated *in vacuo*. The crude residue was purified by gradient silica gel chromatography (0–30% ethyl acetate in petroleum ether) to yield isopropyl 4,6-*O*-benzylidene-3-*O*-fluorenylmethoxycarbonyl-1-thio- $\beta$ -D-galactopyranoside **188** (1.87 g, 55%) as a colourless solid:  $R_f$  0.26 (1:2 ethyl acetate:petroleum ether);  $[\alpha]_D^{25} = +19.2$  ( $c$  1.0,  $\text{CHCl}_3$ ) [lit.<sup>296</sup>  $[\alpha]_D^{25} = +31$  ( $c$  1.8,  $\text{CHCl}_3$ )]; mp 71–73 °C (ethyl acetate);  $\bar{\nu}_{\text{max}}$  (thin film)/ $\text{cm}^{-1}$  3476 (br, OH), 1744 (s, C=O), 1450 (m), 1389 (w), 1270 (s, C–O), 1171 (w), 1087 (m), 1043 (m), 998 (m), 759 (m), 741 (m);  $^1\text{H}$  NMR (400 MHz,  $\text{CDCl}_3$ )  $\delta$  7.76–7.73 (2H, m,  $\text{C}^{17}\text{-H}$ ,  $\text{C}^{20}\text{-H}$ ), 7.63–7.58 (2H, m,  $\text{C}^{14}\text{-H}$ ,  $\text{C}^{23}\text{-H}$ ), 7.53–7.50 (2H, m,  $\text{C}^{27}\text{-H}$ ), 7.41–7.36 (5H, m,  $\text{C}^{16}\text{-H}$ ,  $\text{C}^{21}\text{-H}$ ,  $\text{C}^{28}\text{-H}$ ,  $\text{C}^{29}\text{-H}$ ), 7.28–7.21 (2H, m,  $\text{C}^{15}\text{-H}$ ,  $\text{C}^{22}\text{-H}$ ), 5.51 (1H, s,  $\text{C}^{25}\text{-H}$ ), 4.77 (1H, dd,  $J$  9.7, 3.6,  $\text{C}^3\text{-H}$ ), 4.49 (1H, d,  $J$  9.7,  $\text{C}^1\text{-H}$ ), 4.46 (1H, dd,  $J$  3.6, 1.2,  $\text{C}^4\text{-H}$ ), 4.44 (2H, d,  $J$  7.5,  $\text{C}^{11}\text{-H}_2$ ), 4.34 (1H, dd,  $J_{\text{AB}}$  12.5,  $J_{\text{BX}}$  1.5,  $\text{C}^6\text{-H}_B$ ), 4.29 (1H, t,  $J$  7.5,  $\text{C}^{12}\text{-H}$ ), 4.13 (1H, ddd,  $J$  9.7, 9.7, 1.8,  $\text{C}^2\text{-H}$ ), 4.03 (1H, dd,  $J_{\text{AB}}$  12.5,  $J_{\text{AX}}$  1.6,  $\text{C}^6\text{-H}_A$ ), 3.54 (1H, ddd,  $J_{\text{AX}}$  1.6,  $J_{\text{BX}}$  1.5,  $J$  1.2,  $\text{C}^5\text{-H}_X$ ), 3.31 (1H, sept,  $J$  6.7,  $\text{C}^7\text{-H}$ ), 2.51 (1H, br s,  $\text{C}^2\text{-OH}$ ), 1.40 (3H, d,  $J$  6.7,  $\text{C}^8\text{-H}_3$  or  $\text{C}^9\text{-H}_3$ ), 1.36 (3H, d,  $J$  6.7,  $\text{C}^8\text{-H}_3$  or  $\text{C}^9\text{-H}_3$ );  $^{13}\text{C}$  NMR (101 MHz,  $\text{CDCl}_3$ )  $\delta$  154.8 ( $\text{C}^{10}$ ), 143.5 ( $\text{C}^{13}$  or  $\text{C}^{24}$ ), 143.2 ( $\text{C}^{13}$  or  $\text{C}^{24}$ ), 141.4 ( $\text{C}^{18}$ ,  $\text{C}^{19}$ ), 137.7 ( $\text{C}^{26}$ ), 129.2 ( $\text{C}^{29}$ ), 128.3 ( $\text{C}^{28}$ ), 128.0 ( $\text{C}^{16}$ ,  $\text{C}^{21}$ ), 127.32 ( $\text{C}^{15}$  or  $\text{C}^{22}$ ), 127.27 ( $\text{C}^{15}$  or  $\text{C}^{22}$ ), 126.5 ( $\text{C}^{27}$ ), 125.4 ( $\text{C}^{14}$ ,  $\text{C}^{23}$ ), 120.2 ( $\text{C}^{17}$ ,  $\text{C}^{20}$ ), 101.1 ( $\text{C}^{25}$ ), 86.1 ( $\text{C}^1$ ), 78.6 ( $\text{C}^3$ ), 73.6 ( $\text{C}^4$ ), 70.3 ( $\text{C}^{11}$ ), 69.9 ( $\text{C}^5$ ), 69.3 ( $\text{C}^6$ ), 66.9 ( $\text{C}^2$ ), 46.7 ( $\text{C}^{12}$ ), 35.2 ( $\text{C}^7$ ), 24.6 ( $\text{C}^8$  or  $\text{C}^9$ ), 24.2 ( $\text{C}^8$  or  $\text{C}^9$ ); HRMS  $m/z$  ( $\text{ESI}^+$ ) [Found ( $\text{M}+\text{Na})^+$  571.17598  $\text{C}_{31}\text{H}_{32}\text{O}_7\text{SNa}$  requires  $\text{M}^+$  571.17610]; LRMS  $m/z$  ( $\text{ES}^+$ ) 571 ( $[\text{M}+\text{Na}]^+$ , 100%), 572 ( $[\text{M}+\text{Na}]^+$ , 36%), 573 ( $[\text{M}+\text{Na}]^+$ , 12%). The data are in good agreement with the literature.<sup>296</sup>



**Isopropyl 4,6-*O*-benzylidene-2-*O*-(*tert*-butyldimethylsilyl)-3-*O*-fluorenylmethoxycarbonyl-1-thio- $\beta$ -D-galactopyranoside, **189****

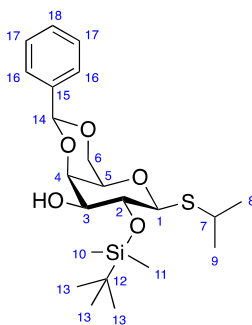


To a solution of **188** (1.39 g, 2.53 mmol, 1.0 eq) in  $\text{CH}_2\text{Cl}_2$  (27 mL) was added 2,6-lutidine (900  $\mu\text{L}$ , 7.72 mmol, 3.1 eq) and TBDMSOTf (1.28 mL, 5.57 mmol, 2.2 eq). The solution was stirred at room temperature for 4.5 h. Additional TBDMSOTf (100  $\mu\text{L}$ , 0.860 mmol, 0.3 eq) was added and the solution was stirred at room temperature for a further 15 h. The reaction was quenched with water (10 mL) and diluted with  $\text{CH}_2\text{Cl}_2$  (20 mL). The separated organic layer was washed with water ( $3 \times 50$  mL) and sat. aq.  $\text{NaHCO}_3$  ( $3 \times 50$  mL). The aqueous layers were back extracted with  $\text{CH}_2\text{Cl}_2$  ( $3 \times 100$  mL). The organic layers were combined, dried over  $\text{MgSO}_4$ , filtered, and concentrated *in vacuo*. The crude residue was purified by gradient silica gel chromatography (0–20% ethyl acetate in petroleum ether) to yield isopropyl 4,6-*O*-benzylidene-2-*O*-(*tert*-butyldimethylsilyl)-3-*O*-fluorenylmethoxycarbonyl-1-thio- $\beta$ -D-galactopyranoside **189** (1.44 g, 86%) as a colourless foam:  $R_f$  0.29 (3:7 ethyl acetate:petroleum ether);  $[\alpha]_D^{25} = +14.2$  ( $c$  1.0,  $\text{CHCl}_3$ );  $\bar{\nu}_{\text{max}}$  (thin film)/ $\text{cm}^{-1}$  2962 (w), 2930 (w), 2891 (w), 2858 (w), 1745 (w), C=O, 1451 (w), 1387 (w), 1369 (w), 1261 (s, C–O), 1138 (w), 1088 (w), 1049 (w), 1001 (w), 865 (w), 839 (w), 818 (w), 758 (w);  $^1\text{H}$  NMR (500 MHz,  $\text{CDCl}_3$ )  $\delta$  7.77–7.73 (2H, m,  $\text{C}^{21}\text{-H}$ ,  $\text{C}^{24}\text{-H}$ ), 7.64–7.59 (2H, m,  $\text{C}^{18}\text{-H}$ ,  $\text{C}^{27}\text{-H}$ ), 7.55–7.50 (2H, m,  $\text{C}^{31}\text{-H}$ ), 7.43–7.35 (5H, m,  $\text{C}^{20}\text{-H}$ ,  $\text{C}^{25}\text{-H}$ ,  $\text{C}^{32}\text{-H}$ ,  $\text{C}^{33}\text{-H}$ ), 7.27–7.22 (2H, m,  $\text{C}^{19}\text{-H}$ ,  $\text{C}^{26}\text{-H}$ ), 5.49 (1H, s,  $\text{C}^{29}\text{-H}$ ), 4.63 (1H, dd,  $J$  9.2, 3.7,  $\text{C}^3\text{-H}$ ), 4.50 (1H, dd,  $J_{\text{AB}}$  10.3,  $J_{\text{BX}}$  7.3,  $\text{C}^{15}\text{-H}_A$ ), 4.454 (1H, d,  $J$  9.3,  $\text{C}^1\text{-H}$ ), 4.448 (1H, dd,  $J$  3.7, 1.0,  $\text{C}^4\text{-H}$ ), 4.34 (1H, dd,  $J_{\text{AB}}$  10.3,  $J_{\text{AX}}$  7.5,  $\text{C}^{15}\text{-H}_B$ ), 4.33 (1H, dd,  $J_{\text{AB}}$  12.4,  $J_{\text{BX}}$  1.5,  $\text{C}^6\text{-H}_B$ ), 4.26 (1H, dd,  $J_{\text{AX}}$  7.5,  $J_{\text{BX}}$  7.3,  $\text{C}^{16}\text{-H}_X$ ), 4.06 (1H, dd,  $J$   $\text{C}^2\text{-H}$ ), 4.01 (1H, dd,  $J_{\text{AB}}$  12.4,  $J_{\text{AX}}$  1.8,  $\text{C}^6\text{-H}_A$ ), 3.49 (1H, ddd,  $J_{\text{AX}}$  1.8,  $J_{\text{BX}}$  1.5,  $J$  1.0,  $\text{C}^5\text{-H}_X$ ), 3.23 (1H, sept,  $J$  6.7,  $\text{C}^7\text{-H}$ ), 1.35 (3H, d,  $J$  6.7,  $\text{C}^8\text{-H}_3$  or

$C^9-H_3$ ), 1.33 (3H, d,  $J$  6.7,  $C^8-H_3$  or  $C^9-H_3$ ), 0.88 (9H, s,  $C^{13}-H_3$ ), 0.22 (3H, s,  $C^{10}-H_3$  or  $C^{11}-H_3$ ), 0.13 (3H, s,  $C^{10}-H_3$  or  $C^{11}-H_3$ );  $^{13}C$  NMR (126 MHz,  $CDCl_3$ )  $\delta$  154.8 ( $C^{14}$ ), 143.41 ( $C^{17}$  or  $C^{28}$ ), 143.38 ( $C^{17}$  or  $C^{28}$ ), 141.44 ( $C^{22}$  or  $C^{23}$ ), 141.36 ( $C^{22}$  or  $C^{23}$ ), 137.9 ( $C^{30}$ ), 129.1 ( $C^{33}$ ), 128.3 ( $C^{32}$ ), 128.02 ( $C^{20}$  or  $C^{25}$ ), 127.99 ( $C^{20}$  or  $C^{25}$ ), 127.3 ( $C^{19}$ ,  $C^{26}$ ), 126.5 ( $C^{31}$ ), 125.5 ( $C^{18}$  or  $C^{27}$ ), 125.3 ( $C^{18}$  or  $C^{27}$ ), 120.2 ( $C^{21}$  or  $C^{24}$ ), 120.1 ( $C^{21}$  or  $C^{24}$ ), 101.2 ( $C^{29}$ ), 86.1 ( $C^1$ ), 80.3 ( $C^3$ ), 73.7 ( $C^4$ ), 70.2 ( $C^{15}$ ), 69.5 ( $C^5$ ), 69.4 ( $C^6$ ), 68.5 ( $C^2$ ), 46.8 ( $C^{16}$ ), 35.0 ( $C^7$ ), 26.1 ( $C^{13}$ ), 24.1 ( $C^8$  or  $C^9$ ), 23.8 ( $C^8$  or  $C^9$ ), 18.4 ( $C^{12}$ ), -3.9 ( $C^{10}$  or  $C^{11}$ ), -4.0 ( $C^{10}$  or  $C^{11}$ ); HRMS  $m/z$  (ESI $^+$ ) [Found (M+Na) $^+$  685.26226  $C_{37}H_{46}O_7SSiNa$  requires  $M^{++}$  685.26257]; LRMS  $m/z$  (ES $^+$ ) 685 ([M+Na] $^+$ , 100%), 686 ([M+Na] $^+$ , 44%), 687 ([M+Na] $^+$ , 19%); Analytical RP-HPLC (Method 3, 254 nm) Ret. time = 16.4 min, Purity = 91.3%.

### Isopropyl 4,6-*O*-benzylidene-2-*O*-(*tert*-butyldimethylsilyl)-1-thio- $\beta$ -D-galactopyranoside,

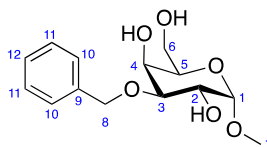
**190**



To a solution of **189** (1.38 g, 2.07 mmol, 1.0 eq) in  $CH_2Cl_2$  (30 mL) was added triethylamine (2.80 mL, 20.1 mmol, 9.7 eq). The reaction solution was stirred at room temperature for 11 h and concentrated *in vacuo*. The crude residue was purified by gradient silica gel chromatography (0–18% ethyl acetate in petroleum ether) to yield isopropyl 4,6-*O*-benzylidene-2-*O*-(*tert*-butyldimethylsilyl)-1-thio- $\beta$ -D-galactopyranoside **190** (764 mg, 84%) as a colourless foam:  $R_f$  0.23 (1:4 ethyl acetate:petroleum ether);  $[\alpha]_D^{25} = -69.4$  ( $c$  1.0,  $CHCl_3$ );  $\bar{\nu}_{max}$  (thin film)/ $cm^{-1}$  3570 (br, OH), 2957 (m), 2929 (m), 2857 (m), 1458 (m), 1401 (m), 1362 (m), 1246 (s, C–O), 1134 (s, Si–C), 1096 (s), 1048 (m), 997 (s), 901 (m), 865 (m), 838 (s), 779 (s), 705 (m);  $^1H$  NMR (500 MHz,  $CDCl_3$ )  $\delta$  7.53–7.48 (2H, m,  $C^{16}-H$ ), 7.41 (3H, m,  $C^{17}-H$ ,  $C^{18}-H$ ), 5.53 (1H, s,  $C^{14}-H$ ), 4.36 (1H, d,  $J$  9.1,  $C^1-H$ ), 4.33 (1H, dd,  $J_{AB}$  12.5,  $J_{BX}$  1.5,  $C^6-H_B$ ), 4.22 (1H, dd,  $J$  3.9, 1.0,  $C^4-H$ ),

4.02 (1H, dd,  $J_{AB}$  12.5,  $J_{AX}$  1.8,  $C^6-H_A$ ), 3.67 (1H, dd,  $J$  9.1, 8.8,  $C^2-H$ ), 3.57 (1H, ddd,  $J$  9.9, 8.8, 3.9,  $C^3-H$ ), 3.45 (1H, ddd,  $J_{AX}$  1.8,  $J_{BX}$  1.5,  $J$  1.1,  $C^5-H_X$ ), 3.21 (1H, sept,  $J$  6.7,  $C^7-H$ ), 2.39 (1H, d,  $J$  9.9,  $C^3-OH$ ), 1.34 (3H, d,  $J$  6.7,  $C^8-H$  or  $C^9-H$ ), 1.31 (3H, d,  $J$  6.7,  $C^8-H$  or  $C^9-H$ ), 0.92 (9H, s,  $C^{13}-H_3$ ), 0.15 (3H, s,  $C^{10}-H_3$  or  $C^{11}-H_3$ ), 0.14 (3H, s,  $C^{10}-H_3$  or  $C^{11}-H_3$ );  $^{13}C$  NMR (126 MHz,  $CDCl_3$ )  $\delta$  137.8 ( $C^{15}$ ), 129.4 ( $C^{18}$ ), 128.4 ( $C^{17}$ ), 126.7 ( $C^{16}$ ), 101.7 ( $C^{14}$ ), 85.8 ( $C^1$ ), 76.2 ( $C^4$ ), 75.2 ( $C^3$ ), 72.6 ( $C^2$ ), 69.9 ( $C^5$ ), 69.5 ( $C^6$ ), 34.7 ( $C^7$ ), 26.2 ( $C^{13}$ ), 24.1 ( $C^8$  or  $C^9$ ), 23.8 ( $C^8$  or  $C^9$ ), 18.6 ( $C^{12}$ ),  $-3.7$  ( $C^{10}$  or  $C^{11}$ ),  $-4.1$  ( $C^{10}$  or  $C^{11}$ ); HRMS  $m/z$  (ESI $^+$ ) [Found ( $M+Na$ ) $^+$  463.19357  $C_{22}H_{36}O_5S^{28}SiNa$  requires  $M^+$  463.19449]; LRMS  $m/z$  (ES $^+$ ) 463 ( $[M+Na]^+$ , 100%), 464 ( $[M+Na]^+$ , 34%), 465 ( $[M+Na]^+$ , 19%); Analytical RP-HPLC (Method 3, 254 nm) Ret. time = 13.0 min, Purity = 95.5%.

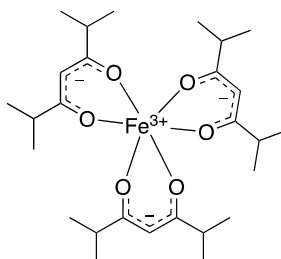
### Methyl 3-*O*-benzyl- $\alpha$ -D-galactopyranoside, **195**



To a solution of methyl  $\alpha$ -D-galactopyranoside (50 mg, 0.26 mmol, 1.0 eq) in toluene (7 mL) was added dibutyl tin oxide (7 mg, 0.03 mmol, 0.1 eq). The solution was stirred under reflux *via* a Soxhlet thimble filled with 3 Å molecular sieves for 19 h. The reaction solution was cooled to room temperature and concentrated *in vacuo* to yield a colourless film. To a solution of this film in DMF:acetonitrile (1:10, 1.1 mL) was added  $K_2CO_3$  (53 mg, 0.38 mmol, 1.5 eq), tetrabutylammonium bromide (9 mg, 0.03 mmol, 0.1 eq) and benzyl bromide **130** (61  $\mu$ L, 0.51 mmol, 2.0 eq). The solution was stirred under reflux for 2.5 h and concentrated *in vacuo*. The crude residue was purified by gradient silica gel chromatography (0–100% ethyl acetate in petroleum ether) to yield methyl 3-*O*-benzyl- $\alpha$ -D-galactopyranoside **195** (29 mg, 40%) as a colourless solid:  $R_f$  0.14 (ethyl acetate);  $[\alpha]_D^{25} = +115.9$  ( $c$  3.0,  $CHCl_3$ ) [lit.<sup>425</sup>  $[\alpha]_D^{20} = +141.43$  ( $c$  3.21,  $CHCl_3$ )]; mp 143–145 °C (ethyl acetate) [lit.<sup>426</sup> 146–147 °C];  $\bar{\nu}_{max}$  (thin film)/ $cm^{-1}$  3418 (br, O–H), 2924 (m), 2361 (w), 1454 (m), 1350 (m), 1194 (m), 1144 (s), 1050 (s), 962 (m), 700 (m);  $^1H$  NMR (400 MHz,  $CDCl_3$ )  $\delta$  7.40–7.30 (5H, m,  $C^{10}-H$ ,  $C^{11}-H$ ,  $C^{12}-H$ ), 4.88 (1H, d,  $J$  3.9,  $C^1-H$ ), 4.76 (1H,  $J_{AB}$  11.7,  $C^8-H_A$ ), 4.72 (1H,  $J_{AB}$  11.7,  $C^8-H_B$ ), 4.08 (1H, d,  $J$  3.3,  $C^4-H$ ), 4.00 (1H, ddd,

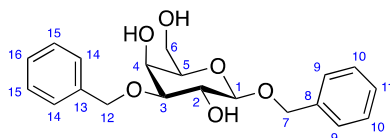
$J$  9.6, 8.1, 3.9,  $C^2-H$ ), 3.98–3.93 (1H, m,  $C^6-H_A$ ), 3.86–3.76 (2H, m,  $C^6-H_B$ ,  $C^5-H_X$ ), 3.65 (1H, dd,  $J$  9.6, 3.3,  $C^3-H$ ), 3.46 (3H, s,  $C^7-H_3$ ), 2.58 (1H, br s,  $C^4-OH$ ), 2.25 (1H, dd,  $J$  8.5, 3.7,  $C^6-OH$ ), 2.07 (1H, d,  $J$  8.1,  $C^2-OH$ ); LRMS  $m/z$  ( $ES^+$ ) 307 ( $[M+Na]^+$ , 100%), 308 ( $[M+Na]^+$ , 16%), 309 ( $[M+Na]^+$ , 3%). The data are in good agreement with the literature.<sup>425,426</sup>

### Iron(III) diisobutyrylmethane (Fe[dibm]<sub>3</sub>), **196**



To a bright yellow suspension of 2,6-dimethylheptane-2,5-dione (1.10 mL, 6.40 mmol, 3.0 eq) and sodium acetate trihydrate (874 mg, 6.42 mmol, 3.0 eq) in water:ethanol (1:1, 18 mL) was added iron (III) chloride hexahydrate (577 mg, 2.13 mmol, 1.0 eq). The resulting deep red suspension was stirred under reflux for 1 h, cooled to 0 °C, filtered, and washed with water. The orange powder was recrystallised from water:ethanol (1:9) to yield iron (III) diisobutyrylmethane (Fe[dibm]<sub>3</sub>) **196** (860 mg, 78%) as a red crystalline solid: mp 100–101 °C (water:ethanol) [lit.<sup>311</sup> 99.2–99.5 °C];  $\bar{\nu}_{\max}$  (neat)/cm<sup>-1</sup> 2966 (m), 2930 (m), 2871 (m), 1563 (s), 1501 (s), 1407 (s), 1357 (w), 1300 (s), 1239 (w), 1218 (w), 1180 (2), 1160 (m), 1093 (s), 961 (w), 923 (s), 790 (m), 758 (m), 690 (w). The data are in good agreement with the literature.<sup>311</sup>

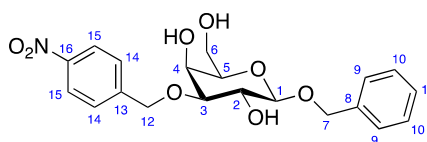
### Benzyl 3-*O*-benzyl- $\beta$ -D-galactopyranoside, **197**



To a solution of **103** (50 mg, 0.19 mmol, 1.0 eq) in DMF:acetonitrile (1:9, 1 mL) was added K<sub>2</sub>CO<sub>3</sub> (38 mg, 0.28 mmol, 1.5 eq), [Fe(dibm)<sub>3</sub>] **196** (9 mg, 0.02 mmol, 0.1 eq) and benzyl bromide **130** (33  $\mu$ L, 0.28 mmol, 1.5 eq). The solution was heated to 80 °C for 15 h and concentrated *in vacuo*. The crude residue was purified by gradient silica gel chromatography (30–80% ethyl acetate in petroleum ether) to yield benzyl 3-*O*-benzyl- $\beta$ -D-galactopyranoside **197**

(30 mg, 45%) as a colourless solid:  $R_f$  0.48 (ethyl acetate);  $[\alpha]_D^{25} = -19.3$  ( $c$  1.0,  $\text{CH}_2\text{Cl}_2$ ) [lit.<sup>427</sup>  $[\alpha]_D^{25} = -20$  ( $c$  2.0,  $\text{CH}_2\text{Cl}_2$ ); mp 101–103 °C (ethyl acetate) [lit.<sup>427</sup> 105 °C (diethyl ether)];  $\bar{\nu}_{\text{max}}$  (thin film)/ $\text{cm}^{-1}$  3445 (br, O–H), 2921 (w), 2883 (w), 2360 (w), 2338 (w), 1455 (w), 1367 (w), 1153 (w), 1075 (m), 742 (w), 699 (w);  $^1\text{H}$  NMR (500 MHz,  $\text{CDCl}_3$ )  $\delta$  7.41–7.28 (10H, m,  $\text{C}^9\text{-H}$ ,  $\text{C}^{10}\text{-H}$ ,  $\text{C}^{11}\text{-H}$ ,  $\text{C}^{14}\text{-H}$ ,  $\text{C}^{15}\text{-H}$ ,  $\text{C}^{16}\text{-H}$ ), 4.92 (1H, d,  $J_{\text{AB}}$  11.9,  $\text{C}^7\text{-H}_A$ ), 4.75 (1H, d,  $J_{\text{AB}}$  12.9,  $\text{C}^{12}\text{-H}_A$ ), 4.73 (1H, d,  $J_{\text{AB}}$  12.9,  $\text{C}^{12}\text{-H}_B$ ), 4.67 (1H, d,  $J_{\text{AB}}$  11.9,  $\text{C}^7\text{-H}_B$ ), 4.35 (1H, d,  $J$  7.8,  $\text{C}^1\text{-H}$ ), 3.99 (1H, dd,  $J$  3.2, 1.1,  $\text{C}^4\text{-H}$ ), 3.96 (1H, dd,  $J_{\text{AB}}$  11.7,  $J_{\text{AX}}$  6.7,  $\text{C}^6\text{-H}_A$ ), 3.86 (1H, dd,  $J$  9.4, 7.8,  $\text{C}^2\text{-H}$ ), 3.81 (1H, dd,  $J_{\text{AB}}$  11.8,  $J_{\text{BX}}$  4.6,  $\text{C}^6\text{-H}_B$ ), 3.47 (1H, ddd,  $J_{\text{AX}}$  6.7,  $J_{\text{BX}}$  4.6,  $J$  1.1,  $\text{C}^5\text{-H}_X$ ), 3.42 (1H, dd,  $J$  9.4, 3.2,  $\text{C}^3\text{-H}$ ), 2.65 (1H, br s,  $\text{C}^4\text{-OH}$ ), 2.43 (1H, br s,  $\text{C}^2\text{-OH}$ ), 2.17 (1H, br s,  $\text{C}^6\text{-OH}$ );  $^{13}\text{C}$  NMR (126 MHz,  $\text{CDCl}_3$ )  $\delta$  137.7 ( $\text{C}^{13}$ ), 137.2 ( $\text{C}^8$ ), 128.8 ( $\text{C}^{10}$  or  $\text{C}^{15}$ ), 128.7 ( $\text{C}^{10}$  or  $\text{C}^{15}$ ), 128.32 ( $\text{C}^9$ ), 128.28 ( $\text{C}^{11}$  or  $\text{C}^{16}$ ), 128.2 ( $\text{C}^{11}$  or  $\text{C}^{16}$ ), 128.1 ( $\text{C}^{14}$ ), 102.2 ( $\text{C}^1$ ), 80.2 ( $\text{C}^3$ ), 74.5 ( $\text{C}^5$ ), 72.4 ( $\text{C}^{12}$ ), 71.4 ( $\text{C}^7$ ), 71.2 ( $\text{C}^2$ ), 67.3 ( $\text{C}^4$ ), 62.6 ( $\text{C}^6$ ); HRMS  $m/z$  ( $\text{ESI}^+$ ) [Found ( $\text{M}+\text{Na}$ ) $^+$  383.14652  $\text{C}_{20}\text{H}_{24}\text{O}_6\text{Na}$  requires  $\text{M}^+$  383.14651]; LRMS  $m/z$  ( $\text{ES}^+$ ) 383 ( $[\text{M}+\text{Na}]^+$ , 100%), 384 ( $[\text{M}+\text{Na}]^+$ , 22%), 385 ( $[\text{M}+\text{Na}]^+$ , 6%); Analytical RP-HPLC (Method 2, 254 nm) Ret. time = 7.1 min, Purity = 97.9%. The data are in good agreement with the literature.<sup>427</sup>

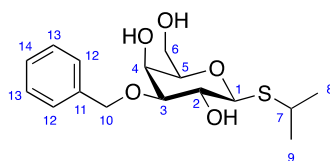
### Benzyl 3-*O*-(4-nitrobenzyl)- $\beta$ -D-galactopyranoside, **124**



To a solution of **103** (300 mg, 1.11 mmol, 1.0 eq) in MeCN:DMF (9:1, 6 mL) was added 4-nitrobenzyl bromide **80** (360 mg, 1.67 mmol, 1.5 eq),  $\text{K}_2\text{CO}_3$  (230 mg, 1.67 mmol, 1.5 eq), and  $\text{Fe}[(\text{dibm})_3]$  **196** (288 mg, 0.555 mmol, 0.5 eq). The solution was heated to 80 °C and stirred for 17.5 h. The reaction solution was concentrated *in vacuo*, filtered through an Isolute<sup>®</sup> SCX-2 cartridge (methanol), and concentrated *in vacuo*. The crude residue was purified by gradient silica gel chromatography (0–85% ethyl acetate in petroleum ether) to yield benzyl 3-*O*-(4-nitrobenzyl)- $\beta$ -D-galactopyranoside **124** (127 mg, 28%) as a pale yellow solid:  $R_f$  0.51 (1:19 methanol:ethyl acetate); mp 135–137 °C (ethyl acetate);  $[\alpha]_D^{25} = -12.1$  ( $c$  0.5,  $\text{CHCl}_3$ );  $\bar{\nu}_{\text{max}}$  (thin film)/ $\text{cm}^{-1}$  3419 (br, O–H), 2881 (w), 2362 (w), 1604 (w), 1519 (s, N=O), 1456 (w), 1346 (s,

N=O), 1153 (w), 1077 (s), 743 (m);  $^1\text{H}$  NMR (500 MHz,  $\text{CDCl}_3$ )  $\delta$  8.23–8.20 (2H, m,  $\text{C}^{15}\text{-H}$ ), 7.57–7.53 (2H, m,  $\text{C}^{14}\text{-H}$ ), 7.39–7.30 (5H, m,  $\text{C}^9\text{-H}$ ,  $\text{C}^{10}\text{-H}$ ,  $\text{C}^{11}\text{-H}$ ), 4.94 (1H, d,  $J_{\text{AB}}$  11.8,  $\text{C}^7\text{-H}_A$ ), 4.88 (2H, s,  $\text{C}^{12}\text{-H}_2$ ), 4.66 (1H, d,  $J_{\text{AB}}$  11.8,  $\text{C}^7\text{-H}_B$ ), 4.35 (1H, d,  $J$  7.7,  $\text{C}^1\text{-H}$ ), 4.09–4.07 (1H, m,  $\text{C}^4\text{-H}$ ), 3.99 (1H, ddd,  $J_{\text{AB}}$  11.8,  $J_{\text{AX}}$  6.0,  $J$  4.4,  $\text{C}^6\text{-H}_A$ ), 3.91 (1H, ddd,  $J$  9.5, 7.7, 2.2,  $\text{C}^2\text{-H}$ ), 3.87 (1H, ddd,  $J_{\text{AB}}$  11.8,  $J$  8.3,  $J_{\text{BX}}$  5.1,  $\text{C}^6\text{-H}_B$ ), 3.51 (1H, dd,  $J_{\text{AX}}$  6.0,  $J_{\text{BX}}$  5.1,  $\text{C}^5\text{-H}_X$ ), 3.44 (1H, dd,  $J$  9.5, 3.5,  $\text{C}^3\text{-H}$ ), 2.64 (1H, d,  $J$  1.4,  $\text{C}^4\text{-OH}$ ), 2.40 (1H, d,  $J$  2.2,  $\text{C}^2\text{-OH}$ ), 2.06 (1H, dd,  $J$  8.3, 4.4,  $\text{C}^6\text{-OH}$ );  $^{13}\text{C}$  NMR (126 MHz,  $\text{CDCl}_3$ )  $\delta$  147.7 ( $\text{C}^{16}$ ), 145.4 ( $\text{C}^{13}$ ), 137.0 ( $\text{C}^8$ ), 128.7 ( $\text{C}^{10}$ ), 128.4 ( $\text{C}^9$ ), 128.3 ( $\text{C}^{11}$ ), 128.1 ( $\text{C}^{14}$ ), 123.9 ( $\text{C}^{15}$ ), 102.3 ( $\text{C}^1$ ), 80.7 ( $\text{C}^3$ ), 74.4 ( $\text{C}^5$ ), 71.5 ( $\text{C}^7$ ,  $\text{C}^2$ ), 71.2 ( $\text{C}^{12}$ ), 67.7 ( $\text{C}^4$ ), 62.7 ( $\text{C}^6$ ); HRMS  $m/z$  ( $\text{ESI}^+$ ) [Found ( $\text{M}+\text{Na}$ ) $^+$  428.13124  $\text{C}_{20}\text{H}_{23}\text{NO}_8\text{Na}$  requires  $\text{M}^+$  428.13159]; LRMS  $m/z$  ( $\text{ES}^+$ ) 450 ( $[\text{M}+\text{HCOOH}]^+$ , 100%), 451 ( $[\text{M}+\text{HCOOH}]^+$ , 24%), 452 ( $[\text{M}+\text{HCOOH}]^+$ , 5%); Analytical RP-HPLC (Method 2, 220/254/300/365 nm) Ret. time = 7.4 min, Purity = 98.3%.

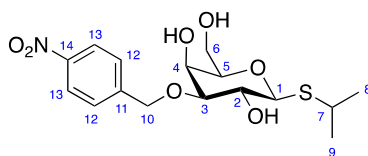
### Isopropyl 3-*O*-benzyl-1-thio- $\beta$ -D-galactopyranoside, **198**



To a solution of isopropyl 1-thio- $\beta$ -D-galactopyranoside **76** (50 mg, 0.21 mmol, 1.0 eq) in DMF:acetonitrile (1:9, 1.0 mL) was added  $\text{K}_2\text{CO}_3$  (45 mg, 0.32 mmol, 1.5 eq),  $[\text{Fe}(\text{dibm})_3]$  **196** (11 mg, 0.020 mmol, 0.1 eq) and benzyl bromide **130** (37  $\mu\text{L}$ , 0.32 mmol, 1.5 eq). The solution was heated to 80  $^\circ\text{C}$  for 22 h and concentrated *in vacuo*. The crude residue was purified by gradient silica gel chromatography (30–66% ethyl acetate in petroleum ether) to yield isopropyl 3-*O*-benzyl-1-thio- $\beta$ -D-galactopyranoside **198** (30 mg, 43%) as a colourless solid:  $R_f$  0.49 (ethyl acetate);  $[\alpha]_{\text{D}}^{25} = -3.4$  ( $c$  1.0,  $\text{CHCl}_3$ ) [lit.<sup>428</sup>  $[\alpha]_{\text{D}}^{25} = -7$  ( $c$  0.2,  $\text{CHCl}_3$ )]; mp 175–177  $^\circ\text{C}$  (ethyl acetate);  $\bar{\nu}_{\text{max}}$  (thin film)/ $\text{cm}^{-1}$  3374 (br, O–H), 2918 (w), 1449 (w), 1373 (w), 1151 (w), 1072 (m), 1051 (m), 986 (w), 751 (w), 663 (w);  $^1\text{H}$  NMR (500 MHz,  $\text{CDCl}_3$ )  $\delta$  7.41–7.29 (5H, m,  $\text{C}^{12}\text{-H}$ ,  $\text{C}^{13}\text{-H}$ ,  $\text{C}^{14}\text{-H}$ ), 4.79 (1H, d,  $J_{\text{AB}}$  11.9,  $\text{C}^{10}\text{-H}_A$ ), 4.76 (1H, d,  $J_{\text{AB}}$  11.9,  $\text{C}^{10}\text{-H}_B$ ), 4.38 (1H, d,  $J$  9.8,  $\text{C}^1\text{-H}$ ), 4.04 (1H, d,  $J$  3.1,  $\text{C}^4\text{-H}$ ), 3.96 (1H, dd,  $J_{\text{AB}}$  11.7,  $J_{\text{AX}}$  6.9,  $\text{C}^6\text{-H}_A$ ), 3.83–3.74 (2H, m,  $\text{C}^2\text{-H}$ ,

$C^6-H_B$ ), 3.53 (1H, dd,  $J_{AX}$  6.9,  $J_{BX}$  4.4,  $C^5-H_X$ ), 3.45 (1H, dd,  $J$  8.9, 3.1,  $C^3-H$ ), 3.22 (1H, sept,  $J$  6.8,  $C^7-H$ ), 2.57 (1H, s,  $C^4-OH$ ), 2.44 (1H, s,  $C^2-OH$ ), 2.09 (1H, br s,  $C^6-OH$ ), 1.343 (3H, d,  $J$  6.8,  $C^8-H_3$  or  $C^9-H_3$ ), 1.339 (3H, d,  $J$  6.8,  $C^8-H_3$  or  $C^9-H_3$ );  $^{13}C$  NMR (126 MHz,  $CDCl_3$ )  $\delta$  137.8 ( $C^{11}$ ), 128.8 ( $C^{13}$ ), 128.3 ( $C^{14}$ ), 128.1 ( $C^{12}$ ), 86.3 ( $C^1$ ), 81.3 ( $C^3$ ), 78.4 ( $C^5$ ), 72.4 ( $C^{10}$ ), 69.8 ( $C^2$ ), 67.6 ( $C^4$ ), 62.9 ( $C^6$ ), 35.7 ( $C^7$ ), 24.3 ( $C^8$  or  $C^9$ ), 24.2 ( $C^8$  or  $C^9$ ); HRMS  $m/z$  (ESI $^+$ ) [Found (M+Na) $^+$  351.12366  $C_{16}H_{24}O_5SNa$  requires  $M^+$  351.12367]; LRMS  $m/z$  (ES $^+$ ) 351 ([M+Na] $^+$ , 100%), 352 ([M+Na] $^+$ , 20%), 353 ([M+Na] $^+$ , 7%); Analytical RP-HPLC (Purity Short Run, 254 nm) Ret. time = 6.4 min, Purity = 99.0%. The data are in good agreement with the literature.<sup>428</sup>

### Isopropyl 3-*O*-(4-nitrobenzyl)-1-thio- $\beta$ -D-galactopyranoside, **87**



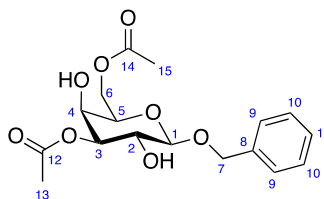
To a solution of isopropyl 1-thio- $\beta$ -D-galactopyranoside **76** (300 mg, 1.26 mmol, 1.0 eq) in DMF:acetonitrile (1:9) was added  $K_2CO_3$  (261 mg, 1.89 mmol, 1.5 eq),  $[Fe(dibm)_3]$  **196** (132 mg, 0.255 mmol, 0.2 eq) and 4-nitrobenzyl bromide **80** (409 mg, 1.89 mmol, 1.5 eq). The resulting deep red solution was heated at 80 °C for 24 h and concentrated *in vacuo*. The crude residue was purified by gradient silica gel chromatography (30–60% ethyl acetate in petroleum ether) and then recrystallised ( $CH_2Cl_2$ :hexanes) to yield isopropyl 3-*O*-(4-nitrobenzyl)-1-thio- $\beta$ -D-galactopyranoside **87** (180 mg, 38%) as a pale yellow solid:  $R_f$  0.34 (ethyl acetate);  $[\alpha]_D^{25} = -21.5$  ( $c$  1.0,  $CHCl_3$ ); mp 126–129 °C (ethyl acetate);  $\bar{\nu}_{max}$  (thin film)/ $cm^{-1}$  3449 (br, O–H), 2962 (w), 2922 (w), 2868 (w), 1604 (w), 1519 (s, N=O), 1457 (w), 1346 (s, N=O), 1243 (w), 1095 (m), 1062 (m), 860 (w), 741 (w);  $^1H$  NMR (500 MHz,  $CDCl_3$ )  $\delta$  8.23–8.17 (2H, m,  $C^{13}-H$ ), 7.56–7.52 (2H, m,  $C^{12}-H$ ), 4.93 (1H, d,  $J_{AB}$  13.2,  $C^{10}-H_A$ ), 4.90 (1H, d,  $J_{AB}$  13.2,  $C^{10}-H_B$ ), 4.38 (1H, d,  $J$  9.8,  $C^1-H$ ), 4.13 (1H, ddd,  $J$  3.1, 2.7, 1.1,  $C^4-H$ ), 3.96 (1H, ddd,  $J_{AB}$  11.8,  $J_{AX}$  6.6,  $J$  4.6,  $C^6-H_A$ ), 3.84 (1H, ddd,  $J$  9.8, 8.9, 1.8,  $C^2-H$ ), 3.82 (1H, ddd,  $J_{AB}$  11.8,  $J$  8.2,  $J_{BX}$  4.5,  $C^6-H_B$ ), 3.55 (1H, dddd,  $J_{AX}$  6.6,  $J_{BX}$  4.5,  $J$  1.1, 1.0,  $C^5-H_X$ ), 3.46 (1H, dd,  $J$  8.9, 3.1,  $C^3-H$ ), 3.23 (1H, sept,  $J$  6.8,  $C^7-H$ ), 2.65 (1H, dd,  $J$  2.7, 1.0,  $C^4-OH$ ), 2.50 (1H, d,  $J$  1.8,  $C^2-OH$ ), 2.13 (1H, dd,  $J$  8.2, 4.6,  $C^6-OH$ ),

1.353 (3H, d,  $J$  6.8, C<sup>8</sup>-H<sub>3</sub> or C<sup>9</sup>-H<sub>3</sub>), 1.346 (3H, d,  $J$  6.8, C<sup>8</sup>-H<sub>3</sub> or C<sup>9</sup>-H<sub>3</sub>); <sup>13</sup>C NMR (126 MHz, CDCl<sub>3</sub>)  $\delta$  147.7 (C<sup>11</sup>), 145.5 (C<sup>14</sup>), 128.1 (C<sup>12</sup>), 123.9 (C<sup>13</sup>), 86.6 (C<sup>1</sup>), 81.8 (C<sup>3</sup>), 78.4 (C<sup>5</sup>), 71.2 (C<sup>10</sup>), 70.0 (C<sup>2</sup>), 68.0 (C<sup>4</sup>), 62.9 (C<sup>6</sup>), 36.0 (C<sup>7</sup>), 24.4 (C<sup>8</sup> or C<sup>9</sup>), 24.3 (C<sup>8</sup> or C<sup>9</sup>); HRMS  $m/z$  (ESI<sup>+</sup>) [Found (M+Na)<sup>+</sup> 396.10773 C<sub>16</sub>H<sub>23</sub>NO<sub>7</sub>Na requires M<sup>+</sup> 396.10874]; LRMS  $m/z$  (ES<sup>+</sup>) 396 ([M+Na]<sup>+</sup>, 100%), 397 ([M+Na]<sup>+</sup>, 19%), 398 ([M+Na]<sup>+</sup>, 7%); Analytical RP-HPLC (Method 2, 220/254/300/365 nm) Ret. time = 6.6 min, Purity = 96.8%.

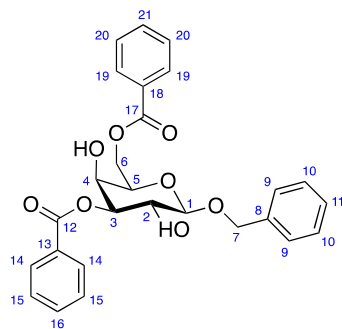


### 6.2.6. Synthesis of 4-Protected Galactopyranosides

#### Benzyl 3,6-di-*O*-acetyl- $\beta$ -D-galactopyranoside, **212**



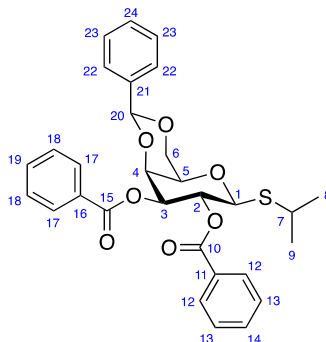
To a solution of **103** (200 mg, 0.762 mmol, 1.0 eq) in methanol (23 mL) was added dibutyl tin oxide (628 mg, 2.52 mmol, 3.3 eq). The resulting suspension was stirred under reflux for 2 h, cooled, concentrated *in vacuo*, and co-evaporated with toluene ( $2 \times 10$  mL) to yield a yellow oil. To a suspension of this yellow oil in toluene (8 mL), cooled to 0 °C, was added dropwise a solution of acetic anhydride (231  $\mu$ L, 2.44 mmol, 3.2 eq) in toluene (2 mL) over 5 min. The solution was stirred at 0 °C for 1 h, warmed to room temperature, and stirred at room temperature for 22 h. The reaction mixture was concentrated *in vacuo* and the crude residue was purified by gradient silica gel chromatography (0–50% ethyl acetate in petroleum ether) to yield benzyl 3,6-di-*O*-acetyl- $\beta$ -D-galactopyranoside **212** (118 mg, 44%) as colourless crystals:  $R_f$  0.26 (1:1 ethyl acetate:petroleum ether);  $[\alpha]_D^{25} = -14.3$  ( $c$  1.0,  $\text{CHCl}_3$ ); mp 105–108 °C (ethyl acetate/hexane);  $\bar{\nu}_{\text{max}}$  (thin film)/ $\text{cm}^{-1}$  3483 (br, O–H), 1739 (s, C=O), 1369 (m), 1245 (s, C–O), 1153 (m), 1128 (m), 1076 (s), 1042 (s), 702 (w);  $^1\text{H}$  NMR (500 MHz,  $\text{CDCl}_3$ )  $\delta$  7.39–7.29 (5H, m,  $\text{C}^9\text{-H}$ ,  $\text{C}^{10}\text{-H}$ ,  $\text{C}^{11}\text{-H}$ ), 4.94 (1H, d,  $J_{\text{AB}}$  11.7,  $\text{C}^7\text{-H}_A$ ), 4.83 (1H, dd,  $J$  10.2, 3.4,  $\text{C}^3\text{-H}$ ), 4.64 (1H, d,  $J_{\text{AB}}$  11.7,  $\text{C}^7\text{-H}_B$ ), 4.40 (1H, d,  $J$  7.7,  $\text{C}^1\text{-H}$ ), 4.34 (1H, dd,  $J_{\text{AB}}$  11.6,  $J_{\text{AX}}$  6.5,  $\text{C}^6\text{-H}_A$ ), 4.31 (1H, dd,  $J_{\text{AB}}$  11.6,  $J_{\text{BX}}$  6.5,  $\text{C}^6\text{-H}_B$ ), 4.02 (1H, dd,  $J$  5.3, 3.4,  $\text{C}^4\text{-H}$ ), 3.89 (1H, ddd,  $J$  10.2, 7.7, 2.7,  $\text{C}^2\text{-H}$ ), 3.72 (1H, dd,  $J_{\text{AX}}$  6.5,  $J_{\text{BX}}$  6.5,  $\text{C}^5\text{-H}_X$ ), 2.42 (1H, d,  $J$  2.7,  $\text{C}^2\text{-OH}$ ), 2.38 (1H, d,  $J$  5.3,  $\text{C}^4\text{-OH}$ ), 2.16 (3H, s,  $\text{C}^{15}\text{-H}_3$ ), 2.09 (3H, s,  $\text{C}^{13}\text{-H}_3$ );  $^{13}\text{C}$  NMR (126 MHz,  $\text{CDCl}_3$ )  $\delta$  171.1 ( $\text{C}^{14}$ ), 170.7 ( $\text{C}^{12}$ ), 136.8 ( $\text{C}^8$ ), 128.7 ( $\text{C}^{10}$ ), 128.4 ( $\text{C}^9$ ), 128.3 ( $\text{C}^{11}$ ), 102.2 ( $\text{C}^1$ ), 74.8 ( $\text{C}^3$ ), 72.3 ( $\text{C}^5$ ), 71.3 ( $\text{C}^7$ ), 69.3 ( $\text{C}^2$ ), 67.2 ( $\text{C}^4$ ), 62.4 ( $\text{C}^6$ ), 21.2 ( $\text{C}^{15}$ ), 21.0 ( $\text{C}^{13}$ ); HRMS  $m/z$  ( $\text{ESI}^+$ ) [Found ( $\text{M}+\text{Na}$ ) $^+$  377.12010  $\text{C}_{17}\text{H}_{22}\text{O}_8\text{Na}$  requires  $\text{M}^+$  377.12069]; LRMS  $m/z$  ( $\text{ES}^+$ ) 377 ( $[\text{M}+\text{Na}]^+$ , 100%), 378 ( $[\text{M}+\text{Na}]^+$ , 20%), 379 ( $[\text{M}+\text{Na}]^+$ , 4%); Analytical RP-HPLC (Method 1, 254 nm) Ret. time = 11.1 min, Purity = 97.8%.

**Benzyl 3,6-di-*O*-benzoyl- $\beta$ -D-galactopyranoside, 215**

To a solution of **103** (0.310 g, 1.15 mmol, 1.0 eq) in methanol (40 mL) was added dibutyl tin oxide (0.995 g, 4.00 mmol, 3.5 eq). The resulting suspension was stirred under reflux for 2 h, cooled, and concentrated *in vacuo* to yield a yellow foam. To a solution of this yellow foam in toluene (15 mL), cooled to 0 °C, was added dropwise benzoyl chloride (0.425 mL, 3.37 mmol, 3.0 eq) over 5 min. The solution was stirred at 0 °C for 2 h, quenched with ethyl acetate, and concentrated *in vacuo*. The crude residue was purified by gradient silica gel chromatography (0–20% ethyl acetate in petroleum ether) to yield benzyl 3,6-di-*O*-benzoyl- $\beta$ -D-galactopyranoside **215** (0.451 g, 82%) as a colourless solid:  $R_f$  0.43 (1:1 ethyl acetate:petroleum ether);  $[\alpha]_D^{25} = -18.3$  ( $c$  2.0,  $\text{CHCl}_3$ ); mp 149–152 °C (ethyl acetate:hexanes);  $\bar{\nu}_{\text{max}}$  (neat)/ $\text{cm}^{-1}$  3511 (br, O–H), 1714 (s, C=O), 1452 (w), 1316 (w), 1274 (s, C–O), 1113 (m), 1071 (m), 1027 (m), 711 (s), 605 (w);  $^1\text{H}$  NMR (500 MHz,  $\text{CDCl}_3$ )  $\delta$  8.10–8.02 (4H, m,  $\text{C}^{14}\text{-H}$ ,  $\text{C}^{19}\text{-H}$ ), 7.60–7.53 (2H,  $\text{C}^{16}\text{-H}$ ,  $\text{C}^{21}\text{-H}$ ), 7.48–7.39 (4H, m,  $\text{C}^{15}\text{-H}$ ,  $\text{C}^{20}\text{-H}$ ), 7.37–7.27 (5H,  $\text{C}^9\text{-H}$ ,  $\text{C}^{10}\text{-H}$ ,  $\text{C}^{11}\text{-H}$ ), 5.12 (1H, dd,  $J$  10.2, 3.5,  $\text{C}^3\text{-H}$ ), 4.96 (1H, d,  $J_{\text{AB}}$  11.7,  $\text{C}^7\text{-H}_A$ ), 4.67 (1H, d,  $J_{\text{AB}}$  11.7,  $\text{C}^7\text{-H}_B$ ), 4.65 (1H, d,  $J_{\text{AB}}$  11.5,  $J_{\text{BX}}$  6.3,  $\text{C}^6\text{-H}_B$ ), 4.58 (1H, dd,  $J_{\text{AB}}$  11.5,  $J_{\text{AX}}$  6.6,  $\text{C}^6\text{-H}_A$ ), 4.49 (1H, d,  $J$  7.7,  $\text{C}^1\text{-H}$ ), 4.22 (1H, dd,  $J$  5.2, 3.5,  $\text{C}^4\text{-H}$ ), 4.11 (1H, dd,  $J$  10.2, 7.7, 2.9,  $\text{C}^2\text{-H}$ ), 3.94 (1H, ddd,  $J_{\text{AX}}$  6.6,  $J_{\text{BX}}$  6.3,  $J$  0.8  $\text{C}^5\text{-H}_X$ ), 2.61 (1H, d,  $J$  5.2,  $\text{C}^4\text{-OH}$ ), 2.53 (1H, d,  $J$  2.9,  $\text{C}^2\text{-OH}$ );  $^{13}\text{C}$  NMR (126 MHz,  $\text{CDCl}_3$ )  $\delta$  166.6 ( $\text{C}^{17}$ ), 166.2 ( $\text{C}^{12}$ ), 136.7 ( $\text{C}^8$ ), 133.54 ( $\text{C}^{16}$  or  $\text{C}^{21}$ ), 133.47 ( $\text{C}^{16}$  or  $\text{C}^{21}$ ), 130.0 ( $\text{C}^{14}$  or  $\text{C}^{19}$ ), 129.9 ( $\text{C}^{14}$  or  $\text{C}^{19}$ ), 129.7 ( $\text{C}^{13}$ ,  $\text{C}^{18}$ ), 128.7 ( $\text{C}^{10}$ ), 128.60 ( $\text{C}^{15}$  or  $\text{C}^{20}$ ), 128.58 ( $\text{C}^{15}$  or  $\text{C}^{20}$ ), 128.4 ( $\text{C}^9$ ), 128.3 ( $\text{C}^{11}$ ), 102.0 ( $\text{C}^1$ ), 75.4 ( $\text{C}^3$ ), 72.5 ( $\text{C}^5$ ), 71.2 ( $\text{C}^7$ ), 69.5 ( $\text{C}^2$ ), 67.4 ( $\text{C}^4$ ), 63.0 ( $\text{C}^6$ ); HRMS  $m/z$  (ESI<sup>+</sup>) [Found ( $\text{M}+\text{Na}$ )<sup>+</sup> 501.15168  $\text{C}_{27}\text{H}_{26}\text{O}_8\text{Na}$  requires  $\text{M}^+$  501.15199]; LRMS  $m/z$  (ES<sup>+</sup>) 501

( $[M+Na]^+$ , 100%), 502 ( $[M+Na]^+$ , 30%), 503 ( $[M+Na]^+$ , 7%); Analytical RP-HPLC (Method 1, 254 nm) Ret. time = 13.0 min, Purity = 99.6%.

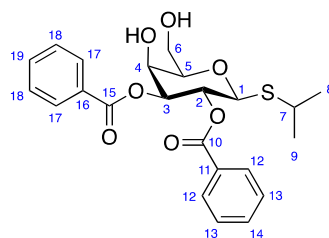
### Isopropyl 2,3-di-*O*-benzoyl-4,6-*O*-benzylidene-1-thio- $\beta$ -D-galactopyranoside, **224**



To a solution of **187** (1.00 g, 3.06 mmol, 1.0 eq) in pyridine (10 mL) was added 4-DMAP (39 mg, 0.32 mmol, 0.1 eq). The solution was cooled to 0 °C and benzoyl chloride (1.07 mL, 9.19 mmol, 3.0 eq) in pyridine (5 mL) was added dropwise over 5 min. The solution was stirred at 0 °C for 30 min, then warmed to room temperature, and stirred for a further 1.5 h. The reaction was quenched with ice and diluted with CH<sub>2</sub>Cl<sub>2</sub> (50 mL). The separated organic layer was washed with sat. aq. NaHCO<sub>3</sub> (3 × 50 mL) and water (3 × 50 mL). The aqueous layers were back extracted with CH<sub>2</sub>Cl<sub>2</sub> (3 × 80 mL). The organic layers were dried over MgSO<sub>4</sub>, filtered, and concentrated *in vacuo*. The crude residue was purified by gradient silica gel chromatography (0–50% ethyl acetate in petroleum ether) to yield isopropyl 2,3-di-*O*-benzoyl-4,6-*O*-benzylidene-1-thio- $\beta$ -D-galactopyranoside **224** (1.40 g, 85%) as a colourless solid:  $R_f$  0.30 (1:2 ethyl acetate:petroleum ether);  $[\alpha]_D^{25} = +114.4$  ( $c$  1.0, CHCl<sub>3</sub>); mp 225–227 °C (ethyl acetate);  $\bar{\nu}_{\max}$  (thin film)/cm<sup>−1</sup> 3066 (w), 2966 (w), 2867 (w), 1717 (s, C=O), 1452 (m), 1279 (s, C–O), 1176 (m), 1106 (s), 1026 (s), 709 (s); <sup>1</sup>H NMR (500 MHz, CDCl<sub>3</sub>)  $\delta$  7.98–7.96 (4H, m, C<sup>12</sup>-*H*, C<sup>17</sup>-*H*), 7.52–7.47 (4H, m, C<sup>14</sup>-*H*, C<sup>19</sup>-*H*, C<sup>21</sup>-*H*), 7.40–7.33 (7H, m, C<sup>13</sup>-*H*, C<sup>18</sup>-*H*, C<sup>23</sup>-*H*, C<sup>24</sup>-*H*), 5.94 (1H, dd,  $J$  10.0, 9.9, C<sup>2</sup>-*H*), 5.54 (1H, s, C<sup>20</sup>-*H*), 5.39 (1H, dd,  $J$  9.9, 3.5, C<sup>3</sup>-*H*), 4.81 (1H, d,  $J$  10.0, C<sup>1</sup>-*H*), 4.62 (1H,  $J$  3.5, 1.1, C<sup>4</sup>-*H*), 4.41 (1H, dd,  $J_{AB}$  12.4,  $J_{BX}$  1.6, C<sup>6</sup>-*H*<sub>B</sub>), 4.09 (1H, dd,  $J_{AB}$  12.4,  $J_{AX}$  1.7, C<sup>6</sup>-*H*<sub>A</sub>), 3.70 (1H, ddd,  $J_{AX}$  1.7,  $J_{BX}$  1.6,  $J$  1.1, C<sup>5</sup>-*H*<sub>X</sub>), 3.38 (1H, sept,  $J$  6.8, C<sup>7</sup>-*H*), 1.39 (3H, d,  $J$  6.8, C<sup>8</sup>-*H*<sub>3</sub> or C<sup>9</sup>-*H*<sub>3</sub>), 1.27 (3H, d,  $J$  6.8, C<sup>8</sup>-*H*<sub>3</sub> or C<sup>9</sup>-*H*<sub>3</sub>); <sup>13</sup>C NMR (126 MHz, CDCl<sub>3</sub>)  $\delta$  166.3 (C<sup>15</sup>), 166.4 (C<sup>10</sup>), 137.7 (C<sup>21</sup>), 133.5 (C<sup>14</sup> or C<sup>19</sup>), 133.2 (C<sup>14</sup> or C<sup>19</sup>), 130.1 (C<sup>12</sup> or C<sup>17</sup>),

129.9 ( $C^{12}$  or  $C^{17}$ ), 129.8 ( $C^{11}$  or  $C^{16}$ ), 129.3 ( $C^{11}$  or  $C^{16}$ ), 129.1 ( $C^{24}$ ), 128.5 ( $C^{13}$  or  $C^{18}$  or  $C^{23}$ ), 128.4 ( $C^{13}$  or  $C^{18}$  or  $C^{23}$ ), 128.3 ( $C^{13}$  or  $C^{18}$  or  $C^{23}$ ), 126.5 ( $C^{22}$ ), 101.2 ( $C^{20}$ ), 83.4 ( $C^1$ ), 74.1 ( $C^3$ ), 74.0 ( $C^4$ ), 70.0 ( $C^5$ ), 69.4 ( $C^6$ ), 67.7 ( $C^2$ ), 34.8 ( $C^7$ ), 25.0 ( $C^8$  or  $C^9$ ), 23.7 ( $C^8$  or  $C^9$ ); HRMS  $m/z$  (CI) [Found ( $M+NH_4$ )<sup>+</sup> 552.2050  $C_{30}H_{34}O_7SN$  requires  $M^+$  552.2050]; LRMS  $m/z$  (CI) 552 ( $[M+NH_4]^+$ , 100%), 553 ( $[M+NH_4]^+$ , 26%), 554 ( $[M+NH_4]^+$ , 7%); Analytical RP-HPLC (Method 2, 254 nm) Ret. time = 12.2 min, Purity = 98.8%.

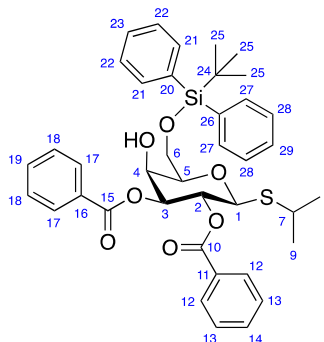
### Isopropyl 2,3-di-*O*-benzoyl-1-thio- $\beta$ -D-galactopyranoside, **225**



A solution of **224** (1.32 g, 2.48 mmol, 1.0 eq) in acetic acid (80% in water, 46 mL) was stirred at 60 °C for 48 h. The reaction solution was concentrated *in vacuo* and the crude residue was purified by gradient silica gel chromatography (20–80% ethyl acetate in petroleum ether) to yield isopropyl 2,3-di-*O*-benzoyl-1-thio- $\beta$ -D-galactopyranoside **225** (0.959 g, 87%) as a colourless solid:  $R_f$  0.23 (1:1 petroleum ether:ethyl acetate);  $[\alpha]_D^{25} = +99.6$  ( $c$  1.0,  $CHCl_3$ ); mp 155–157 °C (ethyl acetate/hexanes);  $\bar{\nu}_{max}$  (thin film)/ $cm^{-1}$  2278 (br, O–H), 2975 (m), 2982 (m), 1724 (s, C=O), 1451 (m), 1275 (s, C–O), 1110 (m), 1064 (s), 708 (s);  $^1H$  NMR (500 MHz,  $CDCl_3$ )  $\delta$  7.98–7.95 (4H, m,  $C^{12}$ -H,  $C^{17}$ -H), 7.52–7.49 (2H, m,  $C^{14}$ -H,  $C^{19}$ -H), 7.39–7.35 (4H, m,  $C^{13}$ -H,  $C^{18}$ -H), 5.79 (1H, dd,  $J$  10.0, 9.9,  $C^2$ -H), 5.35 (1H, dd,  $J$  9.9, 2.9,  $C^3$ -H), 4.82 (1H, d,  $J$  10.0,  $C^1$ -H), 4.43 (1H, d,  $J$  2.9,  $C^4$ -H), 4.02 (1H, dd,  $J_{AB}$  12.0,  $J_{AX}$  5.9,  $C^6$ -H<sub>A</sub>), 3.92 (1H, dd,  $J_{AB}$  12.0,  $J_{BX}$  4.3,  $C^6$ -H<sub>B</sub>), 3.80 (1H, ddd,  $J_{AX}$  5.9,  $J_{BX}$  4.3,  $J$  1.1,  $C^5$ -H<sub>X</sub>), 3.26 (1H, sept,  $J$  6.8,  $C^7$ -H), 2.77 (1H, br s,  $C^4$ -OH), 2.18 (1H, br s,  $C^6$ -OH), 1.31 (3H, d,  $J$  6.8,  $C^8$ -H<sub>3</sub> or  $C^9$ -H<sub>3</sub>), 1.29 (3H, d,  $J$  6.8,  $C^8$ -H<sub>3</sub> or  $C^9$ -H<sub>3</sub>);  $^{13}C$  NMR (126 MHz,  $CDCl_3$ )  $\delta$  166.0 ( $C^{15}$ ), 165.5 ( $C^{10}$ ), 133.6 ( $C^{14}$  or  $C^{19}$ ), 133.3 ( $C^{14}$  or  $C^{19}$ ), 130.0 ( $C^{12}$  or  $C^{17}$ ), 129.9 ( $C^{12}$  or  $C^{17}$ ), 129.6 ( $C^{11}$  or  $C^{16}$ ), 129.2 ( $C^{11}$  or  $C^{16}$ ), 128.6 ( $C^{13}$  or  $C^{18}$ ), 128.4 ( $C^{13}$  or  $C^{18}$ ), 84.0 ( $C^1$ ), 78.2 ( $C^5$ ), 75.6 ( $C^3$ ), 68.8 ( $C^4$ ), 68.3 ( $C^2$ ), 63.1 ( $C^6$ ), 35.6 ( $C^7$ ), 24.4 ( $C^8$  or  $C^9$ ), 23.9 ( $C^8$  or  $C^9$ ); HRMS  $m/z$  (ESI<sup>+</sup>) [Found ( $M+Na$ )<sup>+</sup> 469.12902  $C_{23}H_{26}O_7SNa$  requires

$M^+$  469.12914]; LRMS  $m/z$  ( $ES^+$ ) 469 ( $[M+Na]^+$ , 100%), 470 ( $[M+Na]^+$ , 27%), 471 ( $[M+Na]^+$ , 9%); Analytical RP-HPLC (Method 1, 254 nm) Ret. time = 12.5 min, Purity = 98.9%.

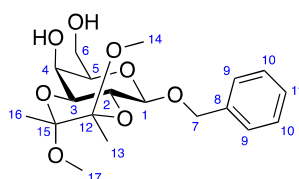
**Isopropyl 2,3-di-*O*-benzoyl-6-*O*-(*tert*-butyldiphenylsilyl)-1-thio- $\beta$ -D-galactopyranoside, **226****



To a solution of **225** (50 mg, 0.11 mmol, 1.0 eq) in pyridine (700  $\mu$ L) was added 4-DMAP (5 mg, 0.04 mmol, 0.4 eq) and TBDPSCl (66  $\mu$ L, 0.25 mmol, 2.2 eq). The solution was heated to 50  $^{\circ}$ C and stirred for 30 min. The reaction was quenched with water (1 mL) and concentrated *in vacuo*. The residue was diluted with ethyl acetate (2 mL) and washed with sat. aq.  $NaHCO_3$  ( $3 \times 1$  mL) and water ( $3 \times 1$  mL). The aqueous layers were back extracted with ethyl acetate ( $3 \times 2$  mL). The organic layers were combined, dried over  $MgSO_4$ , filtered, and concentrated *in vacuo*. The crude residue was purified by gradient silica gel chromatography (0–40% diethyl ether in petroleum ether) to yield isopropyl 2,3-di-*O*-benzoyl-6-*O*-(*tert*-butyldiphenylsilyl)-1-thio- $\beta$ -D-galactopyranoside **226** (61 mg, 79%) as a colourless foam:  $R_f$  0.27 (3:7 diethyl ether:petroleum ether);  $[\alpha]_D^{25} = +57.5$  ( $c$  1.0,  $CHCl_3$ );  $\bar{\nu}_{max}$  (thin film)/ $cm^{-1}$  3484 (br, O–H), 2959 (w), 2931 (w), 2860 (w), 1724 (s, C=O), 1453 (w), 1280 (s, C–O), 1110 (s, Si–C), 1071 (m), 707 (s);  $^1H$  NMR (500 MHz,  $CDCl_3$ )  $\delta$  8.00–7.98 (2H, m,  $C^{17}$ -H), 7.97–7.95 (2H, m,  $C^{12}$ -H), 7.73–7.71 (2H, m,  $C^{21}$ -H or  $C^{27}$ -H), 7.70–7.68 (2H, m,  $C^{21}$ -H or  $C^{27}$ -H), 7.52–7.48 (2H, m,  $C^{14}$ -H,  $C^{19}$ -H), 7.47–7.42 (2H, m,  $C^{23}$ -H,  $C^{29}$ -H), 7.42–7.35 (8H, m,  $C^{13}$ -H,  $C^{18}$ -H,  $C^{22}$ -H,  $C^{28}$ -H), 5.82 (1H, dd,  $J$  10.0, 9.9,  $C^2$ -H), 5.34 (1H, dd,  $J$  9.9, 3.3,  $C^3$ -H), 4.76 (1H, d,  $J$  10.0,  $C^1$ -H), 4.48 (1H, dd,  $J$  4.0, 3.3,  $C^4$ -H), 4.00 (1H, dd,  $J$  10.7, 5.4,  $C^6$ - $H_A$ ), 3.94 (1H, dd,  $J$  10.7, 5.0,  $C^6$ - $H_B$ ), 3.75 (1H, dd,  $J_{AX}$  5.4,  $J_{BX}$  5.0,  $C^5$ - $H_X$ ), 3.26 (1H, sept,  $J$  6.8,  $C^7$ -H), 2.79 (1H, d,  $J$  4.0,  $C^4$ -OH), 1.30 (3H, d,  $J$  6.8,  $C^8$ - $H_3$  or  $C^9$ - $H_3$ ), 1.26 (3H, d,  $J$  6.8,  $C^8$ - $H_3$  or  $C^9$ - $H_3$ ), 1.06 (9H, s,  $C^{25}$ -H);  $^{13}C$  NMR (126 MHz,  $CDCl_3$ )  $\delta$  166.1 ( $C^{15}$ ), 165.5 ( $C^{10}$ ), 135.8 ( $C^{21}$  or  $C^{27}$ ), 135.7 ( $C^{21}$  or  $C^{27}$ ), 133.5 ( $C^{19}$ ), 133.2 ( $C^{14}$ ), 133.0

( $C^{20}$  or  $C^{26}$ ), 132.7 ( $C^{20}$  or  $C^{26}$ ), 130.07 ( $C^{23}$ ,  $C^{29}$ ), 130.05 ( $C^{12}$  or  $C^{17}$ ), 129.9 ( $C^{12}$  or  $C^{17}$ ), 129.8 ( $C^{11}$  or  $C^{16}$ ), 129.4 ( $C^{11}$  or  $C^{16}$ ), 128.6 ( $C^{13}$  or  $C^{18}$ ), 128.4 ( $C^{13}$  or  $C^{18}$ ), 127.99 ( $C^{22}$  or  $C^{28}$ ), 127.96 ( $C^{22}$  or  $C^{28}$ ), 83.8 ( $C^1$ ), 78.1 ( $C^5$ ), 75.8 ( $C^3$ ), 68.49 ( $C^2$  or  $C^4$ ), 68.47 ( $C^2$  or  $C^4$ ), 63.7 ( $C^6$ ), 35.1 ( $C^7$ ), 26.9 ( $C^{25}$ ), 24.6 ( $C^8$  or  $C^9$ ), 23.9 ( $C^8$  or  $C^9$ ), 19.3 ( $C^{24}$ ); HRMS  $m/z$  (ESI<sup>+</sup>) [Found (M+Na)<sup>+</sup> 707.24659 C<sub>39</sub>H<sub>44</sub>O<sub>7</sub>S<sup>28</sup>SiNa requires M<sup>+</sup> 707.24692]; LRMS  $m/z$  (ES<sup>+</sup>) 707 ([M+Na]<sup>+</sup>, 100%), 708 ([M+Na]<sup>+</sup>, 55%), 709 ([M+Na]<sup>+</sup>, 10%); Analytical RP-HPLC (Method 3, 254 nm) Ret. time = 15.3 min, Purity = 97.6%.

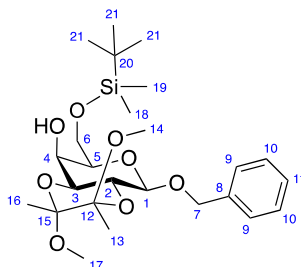
### Benzyl 2,3-di-*O*-(2',3'-dimethoxybutane-2',3'-diyl)-β-D-galactopyranoside, **235**



To a solution of **103** (0.927 g, 3.43 mmol, 1.0 eq) in methanol (13 mL) was added DL-camphor-10-sulfonic acid (88 mg, 0.38 mmol, 0.1 eq), trimethylorthoformate (1.35 mL, 12.3 mmol, 3.6 eq) and 2,3-butanedione (360 μL, 4.10 mmol, 1.2 eq). The resulting yellow solution was stirred under reflux for 15.5 h, quenched with triethylamine (5.6 μL), and concentrated *in vacuo*. The crude residue was purified by gradient silica gel chromatography (25–100% ethyl acetate in petroleum ether) to yield benzyl 2,3-di-*O*-(2',3'-dimethoxybutane-2',3'-diyl)-β-D-galactopyranoside **235** (820 mg, 62%) as a colourless solid:  $R_f$  0.40 (ethyl acetate);  $[\alpha]_D^{25} = -131.4$  ( $c$  1.0, CHCl<sub>3</sub>); mp 87–88 °C (ethyl acetate);  $\bar{\nu}_{\max}$  (thin film)/cm<sup>-1</sup> 3449 (br, O–H), 2994 (w), 2947 (w), 2896 (w), 2835 (w), 1456 (w), 1375 (w), 1212 (w), 1138 (s, C–O), 1118 (s), 1078 (s), 1036 (s), 927 (w), 752 (w); <sup>1</sup>H NMR (400 MHz, CDCl<sub>3</sub>) δ 7.41–7.24 (5H, m, C<sup>9</sup>-H, C<sup>10</sup>-H, C<sup>11</sup>-H), 4.91 (1H, d,  $J_{AB}$  12.3, C<sup>7</sup>-H<sub>A</sub>), 4.72 (1H, d,  $J_{AB}$  12.3, C<sup>7</sup>-H<sub>B</sub>), 4.61 (1H, d,  $J$  8.0, C<sup>1</sup>-H), 3.99 (1H, dd,  $J$  10.3, 8.0, C<sup>2</sup>-H), 3.97–3.91 (2H, m, C<sup>4</sup>-H, C<sup>6</sup>-H<sub>A</sub>), 3.81 (1H, ddd,  $J_{AB}$  11.8,  $J$  8.4,  $J_{BX}$  5.1, C<sup>6</sup>-H<sub>B</sub>), 3.74 (1H, dd,  $J$  10.3, 3.1, C<sup>3</sup>-H), 3.57 (1H, dd,  $J_{AX}$  6.1,  $J_{BX}$  5.1, C<sup>5</sup>-H<sub>X</sub>), 3.29 (3H, s, C<sup>14</sup>-H<sub>3</sub> or C<sup>17</sup>-H<sub>3</sub>), 3.26 (3H, s, C<sup>14</sup>-H<sub>3</sub> or C<sup>17</sup>-H<sub>3</sub>), 2.60–2.56 (1H, m, C<sup>4</sup>-OH), 2.1 (1H, dd,  $J$  8.4, 4.2, C<sup>6</sup>-OH), 1.33 (3H, s, C<sup>13</sup>-H<sub>3</sub> or C<sup>16</sup>-H<sub>3</sub>), 1.32 (3H, s, C<sup>13</sup>-H<sub>3</sub> or C<sup>16</sup>-H<sub>3</sub>); HRMS  $m/z$  (ESI<sup>+</sup>) [Found (M+Na)<sup>+</sup> 407.16711 C<sub>19</sub>H<sub>28</sub>O<sub>8</sub>Na requires M<sup>+</sup> 407.16764]; LRMS  $m/z$  (ES<sup>+</sup>)

407 ( $[M+Na]^+$ , 100%), 408 ( $[M+Na]^+$ , 22%), 409 ( $[M+Na]^+$ , 4%). The data are in good agreement with the literature.<sup>429</sup>

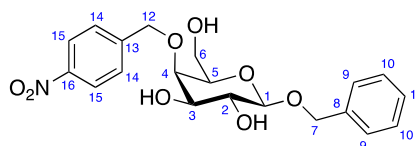
**Benzyl 6-*O*-(*tert*-butyldimethylsilyl)-2,3-di-*O*-(2',3'-dimethoxybutane-2',3'-diyl)- $\beta$ -D-galactopyranoside, **236****



To a solution of **235** (772 mg, 2.01 mmol, 1.0 eq) in pyridine (35 mL), cooled to 0 °C, was added 4-DMAP (62 mg, 0.51 mmol, 0.3 eq) and TBDMSCl (462 mg, 3.07 mmol, 1.5 eq). The reaction solution was warmed to room temperature and stirred for 3.5 h. Additional TBDMSCl (50 mg, 0.33 mmol, 0.2 eq) was added and the reaction solution was stirred at room temperature for a further 1 h. The reaction was quenched with water (30 mL) and diluted with ethyl acetate (50 mL). The separated organic layer was washed with 1 M aq. HCl (50 mL), sat. aq. NaHCO<sub>3</sub> (50 mL) and brine (50 mL). The organic layer was dried over MgSO<sub>4</sub>, filtered, and concentrated *in vacuo*. The crude residue was purified by gradient silica gel chromatography (×2) (0–25% diethyl ether in petroleum ether) to yield benzyl 6-*O*-(*tert*-butyldimethylsilyl)-2,3-di-*O*-(2',3'-dimethoxybutane-2',3'-diyl)- $\beta$ -D-galactopyranoside **236** (813 mg, 81%) as a colourless foam:  $R_f$  0.23 (1:4 ethyl acetate:petroleum ether);  $[\alpha]_D^{25} = -132.9$  ( $c$  1.0, CHCl<sub>3</sub>);  $\bar{\nu}_{\max}$  (thin film)/cm<sup>-1</sup> 3461 (br, O–H), 2951 (m), 2889 (m), 2857 (m), 1464 (w), 1374 (w), 1254 (w), 1118 (s, Si–C), 1069 (m), 1042 (m), 840 (m), 780 (m), 737 (w); <sup>1</sup>H NMR (500 MHz, CDCl<sub>3</sub>)  $\delta$  7.39–7.36 (2H, m, C<sup>9</sup>-H), 7.34–7.29 (2H, m, C<sup>10</sup>-H), 7.28–7.24 (1H, m, C<sup>11</sup>-H), 4.92 (1H, d,  $J_{AB}$  12.2, C<sup>7</sup>-H<sub>A</sub>), 4.66 (1H, d,  $J_{AB}$  12.2, C<sup>7</sup>-H<sub>B</sub>), 4.57 (1H, d,  $J$  8.0, C<sup>1</sup>-H), 4.01 (1H, dd,  $J$  10.3, 8.0, C<sup>2</sup>-H), 3.99–3.97 (1H, m, C<sup>4</sup>-H), 3.93 (1H, dd,  $J_{AB}$  10.3,  $J_{AX}$  6.2, C<sup>6</sup>-H<sub>A</sub>), 3.84 (1H, dd,  $J_{AB}$  10.3,  $J_{BX}$  5.7, C<sup>6</sup>-H<sub>B</sub>), 3.71 (1H, dd,  $J$  10.3, 3.0, C<sup>3</sup>-H), 3.53 (1H, dd,  $J_{AX}$  6.2,  $J_{BX}$  5.7, C<sup>5</sup>-H<sub>X</sub>), 3.28 (3H, s, C<sup>14</sup>-H<sub>3</sub>), 3.26 (3H, s, C<sup>17</sup>-H<sub>3</sub>), 2.35 (1H, d,  $J$  2.4, C<sup>4</sup>-OH), 1.33 (3H, s, C<sup>16</sup>-H<sub>3</sub>), 1.31 (3H, s, C<sup>13</sup>-H<sub>3</sub>), 0.91 (9H, s, C<sup>21</sup>-H<sub>3</sub>), 0.10 (6H, s, C<sup>18</sup>-H<sub>3</sub>, C<sup>19</sup>-H<sub>3</sub>); <sup>13</sup>C NMR (126 MHz, CDCl<sub>3</sub>)  $\delta$  138.0 (C<sup>8</sup>), 128.3 (C<sup>10</sup>),

127.6 ( $C^9$ ), 127.5 ( $C^{11}$ ), 100.40 ( $C^1$ ), 100.35 ( $C^{15}$ ), 99.8 ( $C^{12}$ ), 75.4 ( $C^5$ ), 70.6 ( $C^3$ ), 70.5 ( $C^7$ ), 67.5 ( $C^4$ ), 67.1 ( $C^2$ ), 62.4 ( $C^6$ ), 48.2 ( $C^{14}$  or  $C^{17}$ ), 48.0 ( $C^{14}$  or  $C^{17}$ ), 26.0 ( $C^{21}$ ), 18.5 ( $C^{20}$ ), 17.9 ( $C^{13}$  or  $C^{16}$ ), 17.8 ( $C^{13}$  or  $C^{16}$ ), -5.25 ( $C^{18}$  or  $C^{19}$ ), -5.27 ( $C^{18}$  or  $C^{19}$ ); HRMS  $m/z$  ( $ESI^+$ ) [Found ( $M+Na$ ) $^+$  521.25371  $C_{25}H_{42}O_8^{28}SiNa$  requires  $M^+$  521.25412]; LRMS  $m/z$  ( $ES^+$ ) 521 ( $[M+Na]^+$ , 100%), 522 ( $[M+Na]^+$ , 35%), 523 ( $[M+Na]^+$ , 10%); Analytical RP-HPLC (Method 2, 254 nm) Ret. time = 12.8 min, Purity = 98.3%.

### Benzyl 4-*O*-(4-nitrobenzyl)- $\beta$ -D-galactopyranoside, **125**



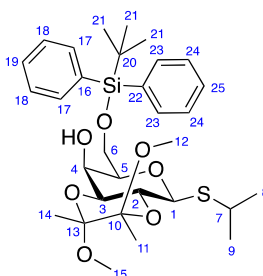
To a solution of **236** (0.616 g, 1.24 mmol, 1.0 eq) in cyclohexane (6 mL) was added silver oxide (1.24 g, 5.34 mmol, 4.3 eq), 4-nitrobenzyl bromide **80** (0.577 g, 2.67 mmol, 2.2 eq) and 3 Å molecular sieves and the reaction mixture stirred under reflux for 17 h. The reaction mixture was resuspended in  $CH_2Cl_2$  (6 mL) and additional 4-nitrobenzyl bromide **80** (300 mg, 1.39 mmol, 1.1 eq) was added. The reaction mixture was stirred under reflux for a further 51 h, filtered through Celite<sup>®</sup>, and concentrated *in vacuo*. The crude residue was purified by gradient silica gel chromatography (0–10% ethyl acetate in petroleum ether) to yield benzyl 6-*O*-(*tert*-butyldimethylsilyl)-2,3-*O*-(2',3'-dimethoxybutane-2',3'-diyl)-4-*O*-(4-nitrobenzyl)- $\beta$ -D-galactopyranoside **237** (637 mg) as a yellow oil in a 3:1 ratio with an unknown impurity as determined by  $^1H$  NMR.

The residue was dissolved in AcOH (80% in water) and heated at 80 °C for 1 h. Then the reaction solution was heated to 100 °C and stirred for a further 1 h. The reaction solution was concentrated *in vacuo*. The crude residue was purified by gradient silica gel chromatography (50–100% ethyl acetate in petroleum ether) to yield benzyl 4-*O*-(4-nitrobenzyl)- $\beta$ -D-galactopyranoside **125** (137 mg, 28%, 2 steps) as a colourless solid:  $R_f$  0.23 (ethyl acetate);  $[\alpha]_D^{25} = -32.4$  ( $c$  0.5,  $CHCl_3$ ); mp 137–138 °C (ethyl acetate);  $\bar{\nu}_{max}$  (thin film)/ $cm^{-1}$  3425 (br, O–H), 2880 (w), 2362 (w), 1604 (w), 1519 (s, N=O), 1457 (w), 1346 (s, N=O), 1211 (w), 1144 (w), 1078 (s), 854 (w), 741 (m),



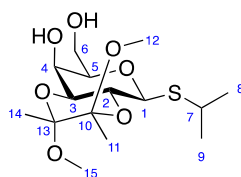
700 (w);  $^1\text{H}$  NMR (500 MHz,  $\text{CDCl}_3$ )  $\delta$  8.22–8.18 (2H, m,  $\text{C}^{15}\text{-H}$ ), 7.56–7.51 (2H, m,  $\text{C}^{14}\text{-H}$ ), 7.40–7.30 (5H, m,  $\text{C}^9\text{-H}$ ,  $\text{C}^{10}\text{-H}$ ,  $\text{C}^{11}\text{-H}$ ), 5.03 (1H, d,  $J_{\text{AB}}$  12.8,  $\text{C}^{12}\text{-H}_A$ ), 4.94 (1H, d,  $J_{\text{AB}}$  11.7,  $\text{C}^7\text{-H}_A$ ), 4.78 (1H, d,  $J_{\text{AB}}$  12.8,  $\text{C}^{12}\text{-H}_B$ ), 4.65 (1H, d,  $J_{\text{AB}}$  11.7,  $\text{C}^7\text{-H}_B$ ), 4.36 (1H, d,  $J$  7.6,  $\text{C}^1\text{-H}$ ), 3.94 (1H, ddd,  $J_{\text{AB}}$  11.0,  $J_{\text{AX}}$  7.2,  $J$  3.6,  $\text{C}^6\text{-H}_B$ ), 3.85 (1H, d,  $J$  2.6,  $\text{C}^4\text{-H}$ ), 3.81 (1H, ddd,  $J$  9.8, 7.6, 2.2,  $\text{C}^2\text{-H}$ ), 3.75–3.68 (2H, m,  $\text{C}^3\text{-H}$ ,  $\text{C}^6\text{-H}_A$ ), 3.59 (ddd,  $J_{\text{AX}}$  7.2,  $J_{\text{BX}}$  5.2,  $J$  1.3,  $\text{C}^5\text{-H}_X$ ), 2.52 (1H, d,  $J$  4.1,  $\text{C}^3\text{-OH}$ ), 2.46 (1H, d,  $J$  2.2,  $\text{C}^2\text{-OH}$ ), 1.75 (1H, dd,  $J$  8.6, 3.6,  $\text{C}^6\text{-OH}$ );  $^{13}\text{C}$  NMR (126 MHz,  $\text{CDCl}_3$ )  $\delta$  147.5 ( $\text{C}^{16}$ ), 145.8 ( $\text{C}^{13}$ ), 137.1 ( $\text{C}^8$ ), 128.7 ( $\text{C}^{10}$ ), 128.37 ( $\text{C}^9$ ), 128.35 ( $\text{C}^{11}$ ), 128.2 ( $\text{C}^{14}$ ), 123.8 ( $\text{C}^{15}$ ), 102.3 ( $\text{C}^1$ ), 76.6 ( $\text{C}^4$ ), 75.3 ( $\text{C}^5$ ), 74.6 ( $\text{C}^3$ ), 74.0 ( $\text{C}^{12}$ ), 72.4 ( $\text{C}^2$ ), 71.7 ( $\text{C}^7$ ), 62.2 ( $\text{C}^6$ ); HRMS  $m/z$  ( $\text{ESI}^+$ ) [Found ( $\text{M}+\text{Na}$ ) $^+$  428.13152  $\text{C}_{20}\text{H}_{23}\text{NO}_8\text{Na}$  requires  $\text{M}^+$  428.13159]; LRMS  $m/z$  ( $\text{ES}^+$ ) 428 ( $[\text{M}+\text{Na}]^+$ , 100%), 429 ( $[\text{M}+\text{Na}]^+$ , 24%), 430 ( $[\text{M}+\text{Na}]^+$ , 5%); Analytical RP-HPLC (Method 2, 220/254/300/365 nm) Ret. time = 7.5 min, Purity = 99.7%.

**Isopropyl 6-*O*-(*tert*-butyldiphenylsilyl)-2,3-*O*-(2',3'-dimethoxybutane-2',3'-diyl)-1-thio- $\beta$ -D-galactopyranoside, **230****



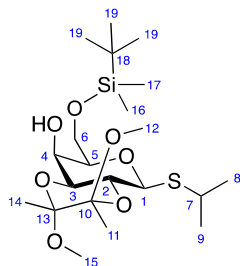
To a solution of isopropyl 1-thio- $\beta$ -D-galactopyranoside **76** (5.00 g, 21.0 mmol, 1.0 eq) in methanol (250 mL) was added 2,3-butanedione (3.69 mL, 42.2 mmol, 2.0 eq), trimethylorthoformate (11.5 mL, 105 mmol, 5.0 eq), and DL-camphor-10-sulfonic acid (490 mg, 2.11 mmol, 0.1 eq). The solution was stirred under reflux for 17.5 h, quenched with triethylamine (300  $\mu\text{L}$ ), and concentrated *in vacuo*. The crude residue was purified by gradient silica gel chromatography (5–100% ethyl acetate in petroleum ether) to yield a mixture of isopropyl 2,3-*O*-(2',3'-dimethoxybutane-2',3'-diyl)-1-thio- $\beta$ -D-galactopyranoside **229** and an unknown, inseparable side product (6.63 g).

To a solution of this mixture in pyridine (100 mL) was added 4-DMAP (462 mg, 3.78 mmol, 0.2 eq) and TBDPSCl (7.50 mL, 28.8 mmol, 1.5 eq). The reaction solution was heated to 50 °C, stirred for 7 h, quenched with ice-cold water (50 mL), and diluted with ethyl acetate (100 mL). The organic layer was washed with water (3 × 100 mL) and sat. aq. NaHCO<sub>3</sub> (3 × 100 mL). The aqueous layers were back extracted with ethyl acetate (3 × 100 mL). The organic layers were combined, dried over MgSO<sub>4</sub>, filtered, and concentrated *in vacuo*. The crude residue was purified by crystallisation (hexane) to yield isopropyl 6-*O*-(*tert*-butyldiphenylsilyl)-2,3-*O*-(2',3'-dimethoxybutane-2',3'-diyl)-1-thio-β-D-galactopyranoside **230** (5.63 g, 45%, 2 steps) as colourless crystals: *R*<sub>f</sub> 0.28 (1:4 ethyl acetate:petroleum ether);  $[\alpha]_{\text{D}}^{25} = -121.6$  (*c* 1.0, CHCl<sub>3</sub>); mp 150–152 °C (hexane);  $\bar{\nu}_{\text{max}}$  (thin film)/cm<sup>-1</sup> 3479 (br, O–H), 2958 (m), 2859 (m), 1463 (w), 1428 (w), 1378 (w), 1112 (s, Si–C), 1036 (m), 931 (m), 885 (w), 851 (w), 823 (w), 743 (w), 705 (s); <sup>1</sup>H NMR (500 MHz, CDCl<sub>3</sub>) δ 7.72–7.65 (4H, m, C<sup>17</sup>-*H*, C<sup>23</sup>-*H*), 7.46–7.40 (2H, m, C<sup>19</sup>-*H*, C<sup>25</sup>-*H*), 7.40–7.34 (4H, m, C<sup>18</sup>-*H*, C<sup>24</sup>-*H*), 4.61 (1H, d, *J* 9.9, C<sup>1</sup>-*H*), 4.05 (1H, br s, C<sup>4</sup>-*H*), 3.94 (1H, dd, *J* 9.9, 9.9, C<sup>2</sup>-*H*), 3.93 (1H, dd, *J*<sub>AB</sub> 10.5, *J*<sub>AX</sub> 6.0, C<sup>6</sup>-*H*<sub>A</sub>), 3.86 (1H, dd, *J*<sub>AB</sub> 10.5, *J*<sub>BX</sub> 5.8, C<sup>6</sup>-*H*<sub>B</sub>), 3.73 (1H, dd, *J* 9.9, 3.0, C<sup>3</sup>-*H*), 3.55 (1H, ddd, *J*<sub>AX</sub> 6.0, *J*<sub>BX</sub> 5.8, *J* 1.0, C<sup>5</sup>-*H*<sub>X</sub>), 3.28 (3H, s, C<sup>12</sup>-*H*<sub>3</sub> or C<sup>15</sup>-*H*<sub>3</sub>), 3.27 (3H, s, C<sup>12</sup>-*H*<sub>3</sub> or C<sup>15</sup>-*H*<sub>3</sub>), 3.23 (1H, sept, *J* 6.8, C<sup>7</sup>-*H*), 2.47 (1H, br s, C<sup>4</sup>-OH), 1.34 (3H, s, C<sup>14</sup>-*H*<sub>3</sub>), 1.31 (3H, s, C<sup>11</sup>-*H*<sub>3</sub>), 1.29 (3H, d, *J* 6.8, C<sup>8</sup>-*H*<sub>3</sub> or C<sup>9</sup>-*H*<sub>3</sub>), 1.28 (3H, d, *J* 6.8, C<sup>8</sup>-*H*<sub>3</sub> or C<sup>9</sup>-*H*<sub>3</sub>), 1.05 (9H, s, C<sup>21</sup>-*H*<sub>3</sub>); <sup>13</sup>C NMR (126 MHz, CDCl<sub>3</sub>) δ 135.7 (C<sup>17</sup> or C<sup>23</sup>), 135.6 (C<sup>17</sup> or C<sup>23</sup>), 133.2 (C<sup>16</sup> or C<sup>22</sup>), 133.0, (C<sup>16</sup> or C<sup>22</sup>), 129.8 (C<sup>19</sup>, C<sup>25</sup>), 127.8 (C<sup>18</sup> or C<sup>24</sup>), 127.7 (C<sup>18</sup> or C<sup>24</sup>), 100.3 (C<sup>10</sup> or C<sup>13</sup>), 100.2 (C<sup>10</sup> or C<sup>13</sup>), 82.1 (C<sup>1</sup>), 78.8 (C<sup>5</sup>), 71.9 (C<sup>3</sup>), 67.8 (C<sup>4</sup>), 66.3 (C<sup>2</sup>), 63.1, (C<sup>6</sup>), 48.10 (C<sup>12</sup> or C<sup>15</sup>), 48.09 (C<sup>12</sup> or C<sup>15</sup>), 34.2 (C<sup>7</sup>), 26.8 (C<sup>21</sup>), 23.8 (C<sup>8</sup> or C<sup>9</sup>), 23.7 (C<sup>8</sup> or C<sup>9</sup>), 19.2 (C<sup>20</sup>), 17.8 (C<sup>11</sup>), 17.7 (C<sup>14</sup>); HRMS *m/z* (ESI<sup>+</sup>) [Found (M+Na)<sup>+</sup> 613.26218 C<sub>31</sub>H<sub>46</sub>O<sub>7</sub>S<sup>28</sup>SiNa requires M<sup>+</sup> 613.26257]; LRMS *m/z* (ES<sup>+</sup>) 613 ([M+Na]<sup>+</sup>, 100%), 614 ([M+Na]<sup>+</sup>, 35%), 615 ([M+Na]<sup>+</sup>, 12%); Analytical RP-HPLC (Method 3, 254 nm) Ret. time = 14.1 min, Purity = 95.1%.

Isopropyl 2,3-*O*-(2',3'-dimethoxybutane-2',3'-diyl)-1-thio- $\beta$ -D-galactopyranoside, **229**

To a solution of **230** (708 mg, 1.20 mmol, 1.0 eq) in THF (7 mL) was added TBAF (1 M in THF, 2.40 mL, 2.40 mmol, 2.0 eq). The reaction solution was stirred at room temperature for 2 h and concentrated *in vacuo*. The crude residue was purified by gradient silica gel chromatography (50–100% ethyl acetate in petroleum ether) to yield isopropyl 2,3-*O*-(2',3'-dimethoxybutane-2',3'-diyl)-1-thio- $\beta$ -D-galactopyranoside **229** (354 mg, 84%) as a colourless foam:  $R_f$  0.31 (ethyl acetate);  $[\alpha]_D^{25} = -138.7$  ( $c$  1.0,  $\text{CHCl}_3$ );  $\bar{\nu}_{\text{max}}$  (thin film)/ $\text{cm}^{-1}$  3454 (br, O–H), 2957 (m), 1456 (w), 1378 (m), 1207 (w), 1130 (s), 1035 (s), 930 (s), 857 (m), 755 (m);  $^1\text{H}$  NMR (500 MHz,  $\text{CDCl}_3$ )  $\delta$  4.62 (1H, d,  $J$  9.9,  $\text{C}^1\text{-H}$ ), 3.99–3.97 (1H, m,  $\text{C}^4\text{-H}$ ), 3.92–3.87 (1H, m,  $\text{C}^6\text{-H}_A$ ), 3.88 (1H, dd,  $J$  9.9, 9.9,  $\text{C}^2\text{-H}$ ), 3.78 (1H, dd,  $J_{AB}$  11.8,  $J$  7.8,  $J_{BX}$  5.4,  $\text{C}^6\text{-H}_B$ ), 3.73 (1H, dd,  $J$  9.9, 3.1,  $\text{C}^3\text{-H}$ ), 3.58 (1H, dd,  $J_{AX}$  5.8,  $J_{BX}$  5.4,  $\text{C}^5\text{-H}_X$ ), 3.25 (3H, s,  $\text{C}^{12}\text{-H}_3$  or  $\text{C}^{15}\text{-H}_3$ ), 3.246 (3H, s,  $\text{C}^{12}\text{-H}_3$  or  $\text{C}^{15}\text{-H}_3$ ), 3.22 (1H, sept,  $J$  6.7,  $\text{C}^7\text{-H}$ ), 2.82 (1H, d,  $J$  1.7,  $\text{C}^4\text{-OH}$ ), 2.48 (1H, dd,  $J$  7.8, 4.6,  $\text{C}^6\text{-OH}$ ), 1.31 (3H, s,  $\text{C}^{11}\text{-H}_3$  or  $\text{C}^{14}\text{-H}_3$ ), 1.31 (3H, d,  $J$  6.7,  $\text{C}^8\text{-H}_3$  or  $\text{C}^9\text{-H}_3$ ), 1.30 (3H, d,  $J$  6.7,  $\text{C}^8\text{-H}_3$  or  $\text{C}^9\text{-H}_3$ ), 1.28 (3H, s,  $\text{C}^{11}\text{-H}_3$  or  $\text{C}^{14}\text{-H}_3$ );  $^{13}\text{C}$  NMR (126 MHz,  $\text{CDCl}_3$ )  $\delta$  100.41 ( $\text{C}^{10}$  or  $\text{C}^{13}$ ), 100.36 ( $\text{C}^{10}$  or  $\text{C}^{13}$ ), 82.5 ( $\text{C}^1$ ), 78.7 ( $\text{C}^5$ ), 71.8 ( $\text{C}^3$ ), 68.2 ( $\text{C}^4$ ), 66.3 ( $\text{C}^2$ ), 62.4 ( $\text{C}^6$ ), 48.17 ( $\text{C}^{12}$  or  $\text{C}^{15}$ ), 48.16 ( $\text{C}^{12}$  or  $\text{C}^{15}$ ), 34.7 ( $\text{C}^7$ ), 24.0 ( $\text{C}^8$  or  $\text{C}^9$ ), 23.8 ( $\text{C}^8$  or  $\text{C}^9$ ), 17.8 ( $\text{C}^{11}$  or  $\text{C}^{14}$ ), 17.6 ( $\text{C}^{11}$  or  $\text{C}^{14}$ ); HRMS  $m/z$  ( $\text{ESI}^+$ ) [Found ( $\text{M}+\text{Na}$ ) $^+$  375.14476  $\text{C}_{15}\text{H}_{28}\text{O}_7\text{SNa}$  requires  $\text{M}^+$  375.14480]; LRMS  $m/z$  ( $\text{ES}^+$ ) 375 ( $[\text{M}+\text{Na}]^+$ , 100%), 376 ( $[\text{M}+\text{Na}]^+$ , 18%), 377 ( $[\text{M}+\text{Na}]^+$ , 8%).

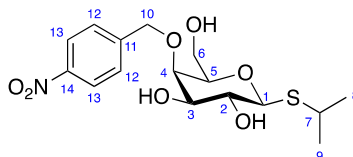
**Isopropyl 6-*O*-(*tert*-butyldimethylsilyl)-2,3-*O*-(2',3'-dimethoxybutane-2',3'-diyl)-1-thio- $\beta$ -D-galactopyranoside, **232****



To a solution of **229** (296 mg, 0.840 mmol, 1.0 eq) and 4-DMAP (26 mg, 0.21 mmol, 0.3 eq) in pyridine (10 mL), cooled to 0 °C, was added a solution of TBDMSCl (152 mg, 1.01 mmol, 1.2 eq) in pyridine (5 mL) dropwise over 5 min. The reaction solution was warmed to room temperature and stirred for 25 h, after which time additional TBDMSCl (152 mg, 1.01 mmol, 1.2 eq) was added. The reaction solution was stirred at room temperature for 18.5 h, quenched with water (15 mL) and diluted with ethyl acetate (20 mL). The organic components were washed with 1 M aq. HCl (20 mL), sat. aq. NaHCO<sub>3</sub> (20 mL) and brine (20 mL), combined, dried over MgSO<sub>4</sub>, filtered, and concentrated *in vacuo*. The crude residue was purified by silica gel chromatography (0–10% ethyl acetate in petroleum ether) to yield isopropyl 6-*O*-(*tert*-butyldimethylsilyl)-2,3-*O*-(2',3'-dimethoxybutane-2',3'-diyl)-1-thio- $\beta$ -D-galactopyranoside **232** (377 mg, 99%) as a colourless foam:  $R_f$  0.43 (1:4 ethyl acetate:petroleum ether);  $[\alpha]_D^{25} = -141.5$  ( $c$  1.0, CHCl<sub>3</sub>);  $\bar{\nu}_{\max}$  (thin film)/cm<sup>-1</sup> 3471 (br, O–H), 2955 (m), 2931 (m), 2859 (m), 1466 (w), 1378 (w), 1253 (w), 1210 (w), 1116 (s), 1038 (s), 840 (s), 778 (m); <sup>1</sup>H NMR (500 MHz, CDCl<sub>3</sub>)  $\delta$  4.62 (1H, d,  $J$  9.9, C<sup>1</sup>-H), 4.01 (1H, ddd,  $J$  3.0, 2.6, 1.1, C<sup>4</sup>-H), 3.93 (1H, dd,  $J$  9.9, 9.9, C<sup>2</sup>-H), 3.88 (1H, dd,  $J_{AB}$  10.3,  $J_{AX}$  6.4, C<sup>6</sup>-H<sub>A</sub>), 3.80 (1H, dd,  $J_{AB}$  10.3,  $J_{BX}$  5.5, C<sup>6</sup>-H<sub>B</sub>), 3.74 (1H, dd,  $J$  9.9, 3.0, C<sup>3</sup>-H), 3.53 (1H, dd,  $J_{AX}$  6.4,  $J_{BX}$  5.5, C<sup>5</sup>-H<sub>X</sub>), 3.27 (3H, s, C<sup>12</sup>-H<sub>3</sub> or C<sup>15</sup>-H<sub>3</sub>), 3.26 (3H, s, C<sup>12</sup>-H<sub>3</sub> or C<sup>15</sup>-H<sub>3</sub>), 3.24 (1H, sept,  $J$  6.8, C<sup>7</sup>-H), 2.44 (1H, d,  $J$  2.6, C<sup>4</sup>-OH), 1.33 (3H, s, C<sup>11</sup>-H<sub>3</sub> or C<sup>14</sup>-H<sub>3</sub>), 1.31 (3H, s, C<sup>11</sup>-H<sub>3</sub> or C<sup>14</sup>-H<sub>3</sub>), 1.30 (3H, d,  $J$  6.8, C<sup>8</sup>-H<sub>3</sub> or C<sup>9</sup>-H<sub>3</sub>), 1.29 (3H, d,  $J$  6.8, C<sup>8</sup>-H<sub>3</sub> or C<sup>9</sup>-H<sub>3</sub>), 0.89 (9H, s, C<sup>19</sup>-H<sub>3</sub>), 0.08 (3H, s, C<sup>16</sup>-H<sub>3</sub> or C<sup>17</sup>-H<sub>3</sub>), 0.07 (3H, s, C<sup>16</sup>-H<sub>3</sub> or C<sup>17</sup>-H<sub>3</sub>); <sup>13</sup>C NMR (126 MHz, CDCl<sub>3</sub>)  $\delta$  100.44 (C<sup>10</sup> or C<sup>13</sup>), 100.35 (C<sup>10</sup> or C<sup>13</sup>), 82.3 (C<sup>1</sup>), 79.0 (C<sup>5</sup>), 72.0 (C<sup>3</sup>), 67.7 (C<sup>4</sup>), 66.5 (C<sup>2</sup>), 62.5 (C<sup>6</sup>), 48.2 (C<sup>12</sup>, C<sup>15</sup>), 34.5 (C<sup>7</sup>), 26.0 (C<sup>19</sup>), 24.0 (C<sup>8</sup> or

$C^9$ ), 23.9 ( $C^8$  or  $C^9$ ), 18.4 ( $C^{18}$ ), 17.9 ( $C^{11}$  or  $C^{14}$ ), 17.8 ( $C^{11}$  or  $C^{14}$ ),  $-5.32$  ( $C^{16}$  or  $C^{17}$ ),  $-5.33$  ( $C^{16}$  or  $C^{17}$ ); HRMS  $m/z$  (ESI<sup>+</sup>) [Found (M+Na)<sup>+</sup> 489.23091 C<sub>21</sub>H<sub>42</sub>O<sub>7</sub>S<sup>28</sup>SiNa requires M<sup>+</sup> 489.23127]; LRMS  $m/z$  (ES<sup>+</sup>) 489 ([M+Na]<sup>+</sup>, 100%), 490 ([M+Na]<sup>+</sup>, 32%), 491 ([M+Na]<sup>+</sup>, 15%).

### Isopropyl 6-*O*-(4-nitrobenzyl)-1-thio- $\beta$ -D-galactopyranoside, **88**



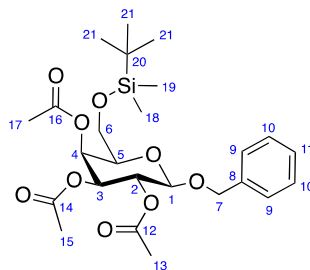
To a solution of **232** (375 mg, 0.804 mmol, 1.0 eq) in cyclohexane (4 mL) was added 4-nitrobenzyl bromide **80** (260 mg, 1.21 mmol, 1.5 eq), silver oxide (279 mg, 1.21 mmol, 1.5 eq) and 4 Å molecular sieves and the suspension was stirred under reflux for 20.5 h. Additional 4-nitrobenzyl bromide **80** (85 mg, 0.39 mmol, 0.5 eq) and silver oxide (93 mg, 0.40 mmol, 0.5 eq) were added and the suspension was stirred under reflux for a further 18.5 h. The reaction mixture was filtered through Celite® and concentrated *in vacuo*. The crude residue was purified by gradient silica gel chromatography (0–20% ethyl acetate in petroleum ether) to yield a mixture of isopropyl 6-*O*-(*tert*-butyldimethylsilyl)-2,3-*O*-(2',3'-dimethoxybutane-2',3'-diyl)-4-*O*-(4-nitrobenzyl)-1-thio- $\beta$ -D-galactopyranoside **233** and an unidentified side product (168 mg) in a ratio of 7.5:1 as determined by <sup>1</sup>H NMR.

A solution of this mixture in AcOH (80% in water, 3.5 mL) was stirred under reflux for 2.5 h and concentrated *in vacuo*. The crude residue was purified by gradient silica gel chromatography (50–100% ethyl acetate in petroleum ether) to yield isopropyl 6-*O*-(4-nitrobenzyl)-1-thio- $\beta$ -D-galactopyranoside **88** (56 mg, 19%, 2 steps) as a colourless solid:  $R_f$  0.20 (ethyl acetate);  $[\alpha]_D^{25} = -39.1$  ( $c$  0.5, CHCl<sub>3</sub>); mp 139–141 °C (ethyl acetate);  $\bar{\nu}_{\max}$  (thin film)/cm<sup>−1</sup> 3427 (br, O–H), 2962 (w), 2922 (w), 2867 (w), 2362 (w), 1519 (s, N=O), 1458 (w), 1356 (s, N=O), 1242 (w), 1060 (m), 860 (w), 737 (w); <sup>1</sup>H NMR (500 MHz, CDCl<sub>3</sub>)  $\delta$  8.22–8.17 (2H, m, C<sup>13</sup>-H), 7.54–7.50 (2H, m, C<sup>12</sup>-H), 5.04 (1H, d,  $J_{AB}$  12.9, C<sup>10</sup>-H<sub>A</sub>), 4.77 (1H, d,  $J_{AB}$  12.9, C<sup>10</sup>-H<sub>B</sub>), 4.39 (1H, d,  $J$  9.2, C<sup>1</sup>-H), 3.95–3.90 (1H, m, C<sup>6</sup>-H), 3.89 (1H, d,  $J$  2.1, C<sup>4</sup>-H), 3.79–3.71 (2H, m, C<sup>2</sup>-H, C<sup>3</sup>-H), 3.70–3.65 (1H, m, C<sup>6</sup>-H), 3.65–3.62 (1H, m, C<sup>5</sup>-H), 3.22 (1H, sept,  $J$  6.8, C<sup>7</sup>-H), 2.62 (1H, s,

$C^3$ -OH), 2.48 (1H, s,  $C^2$ -OH), 1.82 (1H, dd,  $J$  8.4, 3.5,  $C^6$ -OH), 1.35 (3H, d,  $J$  6.8,  $C^8$ - $H_3$  or  $C^9$ - $H_3$ ), 1.34 (3H, d,  $J$  6.8,  $C^8$ - $H_3$  or  $C^9$ - $H_3$ );  $^{13}\text{C}$  NMR (126 MHz,  $\text{CDCl}_3$ )  $\delta$  147.5 ( $C^{14}$ ), 145.9 ( $C^{11}$ ), 128.0 ( $C^{12}$ ), 123.7 ( $C^{13}$ ), 86.5 ( $C^1$ ), 79.2 ( $C^5$ ), 76.7 ( $C^4$ ), 76.1 ( $C^3$ ), 73.9 ( $C^{10}$ ), 70.9 ( $C^2$ ), 62.4 ( $C^6$ ), 36.2 ( $C^7$ ), 24.4 ( $C^8$  or  $C^9$ ), 24.2 ( $C^8$  or  $C^9$ ); HRMS  $m/z$  ( $\text{ESI}^+$ ) [Found ( $\text{M}+\text{Na}$ ) $^+$  396.10878  $\text{C}_{16}\text{H}_{23}\text{NO}_7\text{SNa}$  requires  $\text{M}^+$  396.10874]; LRMS  $m/z$  ( $\text{ES}^+$ ) 396 ( $[\text{M}+\text{Na}]^+$ , 100%), 397 ( $[\text{M}+\text{Na}]^+$ , 20%), 398 ( $[\text{M}+\text{Na}]^+$ , 10%); Analytical RP-HPLC (Method 2, 220/254/300/365 nm) Ret. time = 7.1 min, Purity = >99.9%.

### 6.2.7. Synthesis of 6-Protected Galactopyranosides

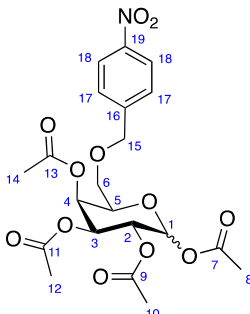
#### Benzyl 2,3,4-tri-*O*-acetyl-6-*O*-(*tert*-butyldimethylsilyl)- $\beta$ -D-galactopyranoside, **242**



To a solution of **103** (209 mg, 0.773 mmol, 1.0 eq) in pyridine (5 mL) was added TBDMSCl (175 mg, 1.16 mmol, 1.5 eq) and the solution was stirred at room temperature for 3.5 h. Acetic anhydride (1.45 mL, 15.3 mmol, 19.8 eq) was added and the solution was stirred at room temperature for a further 2 h. The reaction solution was concentrated *in vacuo* and diluted with ethyl acetate (10 mL). The organic layer was washed with water (2 × 10 mL), 1 M aq. HCl (2 × 10 mL), sat. aq. NaHCO<sub>3</sub> (2 × 10 mL), and brine (10 mL). The organic layer was dried over MgSO<sub>4</sub>, filtered, and concentrated *in vacuo*. The crude residue was purified by gradient silica gel chromatography (0–15% ethyl acetate in petroleum ether) to yield benzyl 2,3,4-tri-*O*-acetyl-6-*O*-(*tert*-butyldimethylsilyl)- $\beta$ -D-galactopyranoside **242** (316 mg, 80%) as a colourless solid: *R<sub>f</sub>* 0.43 (1:4 ethyl acetate:petroleum ether);  $[\alpha]_{\text{D}}^{25} = -48.4$  (*c* 1.0, CHCl<sub>3</sub>); mp 125–126 °C (ethyl acetate);  $\bar{\nu}_{\text{max}}$  (thin film)/cm<sup>-1</sup> 2954 (w), 2932 (w), 2885 (w), 2858 (w), 1752 (s, C=O), 1369 (w), 1249 (m), 1220 (s, C–O), 1072 (m), 842 (m), 779 (w); <sup>1</sup>H NMR (500 MHz, CDCl<sub>3</sub>)  $\delta$  7.36–7.26 (5H, m, C<sup>9</sup>-H, C<sup>10</sup>-H, C<sup>11</sup>-H), 5.46 (1H, dd, *J* 3.4, 0.8, C<sup>4</sup>-H), 5.26 (1H, dd *J* 10.4, 8.0, C<sup>2</sup>-H), 5.00 (1H, dd, *J* 10.0, 3.4, C<sup>3</sup>-H), 4.91 (1H, d, *J*<sub>AB</sub> 12.4, C<sup>7</sup>-H<sub>A</sub>), 4.62 (1H, d, *J*<sub>AB</sub> 12.4, C<sup>7</sup>-H<sub>B</sub>), 4.50 (1H, d, *J* 8.0, C<sup>1</sup>-H), 3.75 (1H, dd, *J*<sub>AB</sub> 8.8, *J*<sub>BX</sub> 5.6, C<sup>6</sup>-H<sub>B</sub>), 3.71 (1H, ddd, *J*<sub>AX</sub> 6.9, *J*<sub>BX</sub> 5.6, *J* 0.8, C<sup>5</sup>-H<sub>X</sub>), 3.65 (1H, dd, *J*<sub>AB</sub> 8.8, *J*<sub>AX</sub> 6.9, C<sup>6</sup>-H<sub>A</sub>), 2.14 (3H, s, C<sup>17</sup>-H<sub>3</sub>), 2.00 (3H, s, C<sup>13</sup>-H<sub>3</sub>), 1.97 (3H, s, C<sup>15</sup>-H<sub>3</sub>), 0.87 (9H, s, C<sup>21</sup>-H<sub>3</sub>), 0.05 (3H, s, C<sup>18</sup>-H<sub>3</sub> or C<sup>19</sup>-H<sub>3</sub>), 0.03 (3H, s, C<sup>18</sup>-H<sub>3</sub> or C<sup>19</sup>-H<sub>3</sub>); <sup>13</sup>C NMR (126 MHz, CDCl<sub>3</sub>)  $\delta$  170.32 (C<sup>14</sup> or C<sup>16</sup>), 170.25 (C<sup>14</sup> or C<sup>16</sup>), 169.7 (C<sup>12</sup>), 137.0 (C<sup>8</sup>), 128.6 (C<sup>10</sup>), 128.1 (C<sup>11</sup>), 127.9 (C<sup>9</sup>), 99.9 (C<sup>1</sup>), 73.7 (C<sup>5</sup>), 71.4 (C<sup>3</sup>), 70.7 (C<sup>7</sup>), 69.4 (C<sup>2</sup>), 67.3 (C<sup>4</sup>), 60.8 (C<sup>6</sup>), 25.9 (C<sup>21</sup>), 20.92 (C<sup>13</sup> or C<sup>17</sup>), 20.89 (C<sup>13</sup> or C<sup>17</sup>), 20.8 (C<sup>15</sup>), 18.3 (C<sup>20</sup>), -5.4 (C<sup>18</sup> or C<sup>19</sup>), -5.5 (C<sup>18</sup> or C<sup>19</sup>); HRMS *m/z* (ESI<sup>+</sup>) [Found (M+Na)<sup>+</sup> 533.21757 C<sub>25</sub>H<sub>38</sub>O<sub>9</sub>SiNa requires M<sup>+</sup>

533.21773]; LRMS  $m/z$  ( $\text{ES}^+$ ) 533 ( $[\text{M}+\text{Na}]^+$ , 100%), 534 ( $[\text{M}+\text{Na}]^+$ , 30%), 535 ( $[\text{M}+??]^+$ , 9%); Analytical RP-HPLC (Method 3, 254 nm) Ret. time = 12.6 min, Purity = 98.1%.

### 1,2,3,4-Tetra-*O*-acetyl-6-*O*-(4-nitrobenzyl)- $\alpha,\beta$ -D-galactopyranoside, **245**



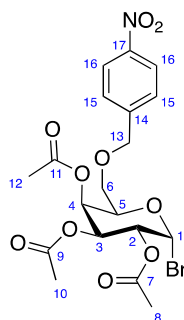
To a solution of 1,2:3,4-di-*O*-isopropylidene- $\alpha$ -D-galactopyranoside **129** (0.685 g, 2.63 mmol, 1.0 eq) in cyclohexane (5 mL) was added silver oxide (0.926 g, 4.00 mmol, 1.5 eq), 4-nitrobenzyl bromide **80** (0.856 g, 3.96 mmol, 1.5 eq), and 4 Å molecular sieves. The resulting suspension was shielded from light and stirred under reflux for 15 h. The reaction mixture was filtered through Celite® and concentrated *in vacuo*. Excess 4-nitrobenzyl bromide **80** was removed by gradient silica gel chromatography (0–15% ethyl acetate in petroleum ether) to yield crude 1,2:3,4-di-*O*-isopropylidene-6-*O*-(4-nitrobenzyl)- $\alpha$ -D-galactopyranoside **132** (1.03 g), which was used without further purification.

The residue was dissolved in trifluoroacetic acid (80% in water, 5 mL) and stirred at room temperature for 30 min. The reaction solution was concentrated *in vacuo*, filtered through silica (20% water, 40% IPA in ethyl acetate), and concentrated *in vacuo* to yield crude 6-*O*-(4-nitrobenzyl)- $\alpha,\beta$ -D-galactopyranoside **244** (0.638 g), which was used without further purification.

To a solution of this crude 6-*O*-(4-nitrobenzyl)- $\alpha,\beta$ -D-galactopyranoside **244** in pyridine (10 mL) was added acetic anhydride (10 mL). The solution was stirred at room temperature for 21 h and concentrated *in vacuo*. The crude residue was purified by gradient silica gel chromatography (33–66% ethyl acetate in petroleum ether) to yield 1,2,3,4-tetra-*O*-acetyl-6-*O*-(4-nitrobenzyl)- $\alpha,\beta$ -D-galactopyranoside **245** (0.861 g, 68%, 3 steps) as a colourless foam in a 2:1 ( $\alpha$ : $\beta$ ) ratio as determined by  $^1\text{H}$  NMR:  $R_f$  0.14 (1:2 ethyl acetate:petroleum ether);  $\bar{\nu}_{\text{max}}$  (thin



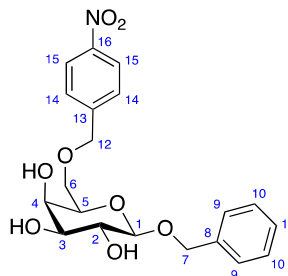
film)/cm<sup>-1</sup> 2875 (w), 1749 (s, C=O), 1607 (w), 1522 (m, N=O), 1370 (m), 1347 (m, N=O), 1216 (s), 1067 (m), 739 (w); <sup>1</sup>H NMR (500 MHz, CDCl<sub>3</sub>) δ 8.21–8.18 (2H<sub>α</sub> and 2H<sub>β</sub>, m, αC<sup>18</sup>-H and βC<sup>18</sup>-H), 7.45–7.43 (2H<sub>α</sub> and 2H<sub>β</sub>, m, αC<sup>17</sup>-H and βC<sup>17</sup>-H), 6.37 (1H<sub>α</sub>, d, *J* 3.1, αC<sup>1</sup>-H), 5.69 (1H<sub>β</sub>, d, *J* 8.3, βC<sup>1</sup>-H), 5.60–5.58 (1H<sub>α</sub>, m, αC<sup>4</sup>-H), 5.52 (1H<sub>β</sub>, dd, *J* 3.4, 0.9, βC<sup>4</sup>-H), 5.37–5.31 (2H<sub>α</sub> and 1H<sub>β</sub>, m, αC<sup>2</sup>-H, αC<sup>3</sup>-H and βC<sup>2</sup>-H), 5.09 (1H<sub>β</sub>, dd, *J* 10.4, 3.4, βC<sup>3</sup>-H), 4.62 (1H<sub>α</sub> and 1H<sub>β</sub>, d, *J*<sub>AB</sub> 13.1, αC<sup>15</sup>-H<sub>A</sub> and βC<sup>15</sup>-H<sub>A</sub>), 4.53 (1H<sub>α</sub> and 1H<sub>β</sub>, d, *J*<sub>AB</sub> 13.1, αC<sup>15</sup>-H<sub>B</sub> and βC<sup>15</sup>-H<sub>B</sub>), 4.33 (1H<sub>α</sub>, ddd, *J*<sub>AX</sub> 6.4, *J*<sub>BX</sub> 6.2, *J* 0.8, αC<sup>5</sup>-H<sub>X</sub>), 4.05–4.02 (1H<sub>β</sub>, m, βC<sup>5</sup>-H<sub>X</sub>), 3.63 (1H<sub>β</sub>, dd, *J*<sub>AB</sub> 9.8, *J*<sub>AX</sub> 6.0, βC<sup>6</sup>-H<sub>A</sub>), 3.57 (1H<sub>α</sub>, dd, *J*<sub>AB</sub> 9.7, *J*<sub>BX</sub> 6.2, αC<sup>6</sup>-H<sub>B</sub>), 3.55 (1H<sub>β</sub>, dd, *J*<sub>AB</sub> 9.8, *J*<sub>BX</sub> 6.6, βC<sup>6</sup>-H<sub>B</sub>), 3.50 (1H<sub>α</sub>, dd, *J*<sub>AB</sub> 9.7, *J*<sub>AX</sub> 6.4, αC<sup>6</sup>-H<sub>A</sub>), 2.15 (3H<sub>α</sub>, s, αC<sup>8</sup>-H<sub>3</sub>), 2.11 (6H<sub>β</sub>, s, βC<sup>8</sup>-H<sub>3</sub>, βC<sup>14</sup>-H<sub>3</sub>), 2.10 (3H<sub>α</sub>, s, αC<sup>14</sup>-H<sub>3</sub>), 2.04 (3H<sub>β</sub>, s, βC<sup>10</sup>-H<sub>3</sub>), 2.02 (3H<sub>α</sub>, s, αC<sup>10</sup>-H<sub>3</sub>), 2.00 (3H<sub>α</sub>, s, αC<sup>12</sup>-H<sub>3</sub>), 1.99 (3H<sub>β</sub>, s, βC<sup>12</sup>-H<sub>3</sub>); <sup>13</sup>C NMR (126 MHz, CDCl<sub>3</sub>) δ 170.23 (αC<sup>13</sup>), 170.20 (βC<sup>13</sup>), 170.1 (αC<sup>11</sup> and βC<sup>11</sup>), 169.5 (αC<sup>9</sup> and βC<sup>9</sup>), 169.17 (βC<sup>7</sup>), 169.15 (αC<sup>7</sup>), 147.6 (αC<sup>19</sup> and βC<sup>19</sup>), 145.15 (αC<sup>16</sup>), 145.12 (βC<sup>16</sup>), 128.0 (βC<sup>17</sup>), 127.9 (αC<sup>17</sup>), 123.83 (αC<sup>18</sup>), 123.81 (βC<sup>18</sup>), 92.4 (βC<sup>1</sup>), 89.9 (αC<sup>1</sup>), 73.0 (βC<sup>5</sup>), 72.5 (αC<sup>15</sup>), 72.4 (βC<sup>15</sup>), 71.1 (βC<sup>3</sup>), 70.2 (αC<sup>5</sup>), 68.5 (αC<sup>6</sup>), 68.2 (βC<sup>6</sup>), 68.1 (βC<sup>2</sup>), 68.0 (αC<sup>4</sup>), 67.6 (αC<sup>3</sup>), 67.4 (βC<sup>4</sup>), 66.7 (αC<sup>2</sup>), 21.0 (αC<sup>8</sup>), 20.9 (αC<sup>10</sup> or αC<sup>12</sup> or αC<sup>14</sup> or βC<sup>8</sup> or βC<sup>10</sup> or βC<sup>12</sup> or βC<sup>14</sup>), 20.79 (αC<sup>10</sup> or αC<sup>12</sup> or αC<sup>14</sup> or βC<sup>8</sup> or βC<sup>10</sup> or βC<sup>12</sup> or βC<sup>14</sup>), 20.76 (αC<sup>10</sup> or αC<sup>12</sup> or αC<sup>14</sup> or βC<sup>8</sup> or βC<sup>10</sup> or βC<sup>12</sup> or βC<sup>14</sup>), 20.7 (αC<sup>10</sup> or αC<sup>12</sup> or αC<sup>14</sup> or βC<sup>8</sup> or βC<sup>10</sup> or βC<sup>12</sup> or βC<sup>14</sup>); HRMS *m/z* (ESI<sup>+</sup>) [Found (M+Na)<sup>+</sup> 506.12678 C<sub>21</sub>H<sub>25</sub>NO<sub>12</sub>Na requires M<sup>+</sup> 506.12690]; LRMS *m/z* (ES<sup>+</sup>) 506 ([M+Na]<sup>+</sup>, 100%), 507 ([M+Na]<sup>+</sup>, 22%), 508 ([M+Na]<sup>+</sup>, 5%); Analytical RP-HPLC (Method 1, 254 nm) Ret. time = 12.5 min, Purity = 27.5% (β) and Ret. time 12.6 min, Purity = 71.1% (α).

**2,3,4-Tri-*O*-acetyl-6-*O*-(4-nitrobenzyl)- $\alpha$ -D-galactopyranosyl bromide, **246****

A solution of **245** (0.800 g, 1.66 mmol, 1.0 eq) in HBr (33% wt. in acetic acid, 1.20 mL, 6.85 mmol, 4.1 eq) was stirred at room temperature for 2 h and concentrated *in vacuo*. The reaction solution was diluted with CH<sub>2</sub>Cl<sub>2</sub> (40 mL), and the organic layer washed with sat. aq. NaHCO<sub>3</sub> (3 × 40 mL) and water (3 × 40 mL). The aqueous layers were back extracted with CH<sub>2</sub>Cl<sub>2</sub> (3 × 40 mL). The organic layers were combined, dried over MgSO<sub>4</sub>, filtered, and concentrated *in vacuo*. The crude residue was purified by gradient silica gel chromatography (0–25% ethyl acetate in petroleum ether) to yield 2,3,4-tri-*O*-acetyl-6-*O*-(4-nitrobenzyl)- $\alpha$ -D-galactopyranosyl bromide **246** (0.395 g, 78%) as a colourless foam: 0.57 (1:1 ethyl acetate:petroleum ether);  $[\alpha]_D^{25} = +63.0$  (*c* 1.0, CHCl<sub>3</sub>);  $\bar{\nu}_{\max}$  (thin film)/cm<sup>−1</sup> 1742 (s, C=O), 1520 (s, N=O), 1347 (s, N=O), 1240 (s), 1070 (s), 738 (m), 617 (s); <sup>1</sup>H NMR (500 MHz, CDCl<sub>3</sub>)  $\delta$  8.22–8.18 (2H, m, C<sup>16</sup>-*H*), 7.47–7.43 (2H, m, C<sup>15</sup>-*H*), 6.71 (1H, d, *J* 4.0, C<sup>1</sup>-*H*), 5.60 (1H, dd, *J* 3.3, 1.2, C<sup>4</sup>-*H*), 5.41 (1H, dd, *J* 10.6, 3.3, C<sup>3</sup>-*H*), 5.05 (1H, dd, *J* 10.6, 4.0, C<sup>2</sup>-*H*), 4.63 (1H, d, *J*<sub>AB</sub> 13.1, C<sup>13</sup>-*H*<sub>A</sub>), 4.55 (1H, d, *J*<sub>AB</sub> 13.1, C<sup>13</sup>-*H*<sub>B</sub>), 4.50 (1H, dd, *J*<sub>AX</sub> 6.3, *J*<sub>BX</sub> 6.3, C<sup>5</sup>-*H*<sub>X</sub>), 3.63 (1H, dd, *J*<sub>AB</sub> 10.0, *J*<sub>AX</sub> 6.3, C<sup>6</sup>-*H*<sub>A</sub>), 3.56 (1H, dd, *J*<sub>AB</sub> 10.0, *J*<sub>BX</sub> 6.3, C<sup>6</sup>-*H*<sub>B</sub>), 2.11 (3H, s, C<sup>8</sup>-*H*<sub>3</sub>), 2.10 (3H, s, C<sup>12</sup>-*H*<sub>3</sub>), 2.01 (3H, s, C<sup>10</sup>-*H*<sub>3</sub>); <sup>13</sup>C NMR (126 MHz, CDCl<sub>3</sub>)  $\delta$  170.3 (C<sup>7</sup>), 170.0 (C<sup>11</sup>), 169.9 (C<sup>9</sup>), 147.7 (C<sup>17</sup>), 145.0 (C<sup>14</sup>), 127.9 (C<sup>15</sup>), 123.8 (C<sup>16</sup>), 88.6 (C<sup>1</sup>), 72.4 (C<sup>13</sup>), 72.2 (C<sup>5</sup>), 68.2 (C<sup>3</sup>), 68.04 (C<sup>2</sup> or C<sup>6</sup>), 68.03 (C<sup>2</sup> or C<sup>6</sup>), 67.6 (C<sup>4</sup>), 20.9 (C<sup>8</sup>), 20.73 (C<sup>10</sup> or C<sup>12</sup>), 20.71 (C<sup>10</sup> or C<sup>12</sup>); HRMS *m/z* (ESI<sup>+</sup>) [Found (M<sup>79</sup>Br+Na)<sup>+</sup> 526.03193 and (M<sup>81</sup>Br+Na)<sup>+</sup> 528.02977 C<sub>19</sub>H<sub>22</sub><sup>79</sup>BrNO<sub>10</sub>Na requires M<sup>+</sup> 526.03193 and C<sub>19</sub>H<sub>22</sub><sup>81</sup>BrNO<sub>10</sub>Na M<sup>+</sup> 528.02988]; LRMS *m/z* (ES<sup>+</sup>) 526 ([M<sup>79</sup>Br+Na]<sup>+</sup>, 100%), 527 ([M<sup>79</sup>Br+Na]<sup>+</sup>, 24%), 528 ([M<sup>81</sup>Br+Na]<sup>+</sup>, 96%), 529

( $[M^{81}Br+Na]^+$ , 22%); Analytical NP-HPLC (Method 1, 254 nm) Ret. time = 6.9 min, Purity = 97.0%.

### Benzyl 6-*O*-(4-nitrobenzyl)- $\beta$ -D-galactopyranoside, **126**

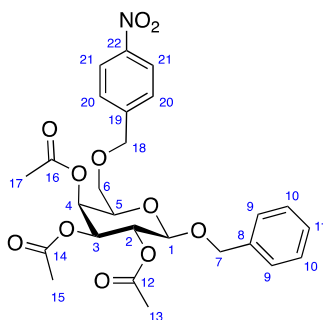


To a solution of benzyl alcohol (0.600 mL, 5.80 mmol, 7.9 eq) and silver carbonate (0.408 g, 1.48 mmol, 2.0 eq) in  $CH_2Cl_2$  (4 mL), pre-stirred over 4 Å molecular sieves at room temperature for 30 min, was added dropwise over 5 min a solution of **246** (0.369 g, 0.732 mmol, 1.0 eq) in  $CH_2Cl_2$  (3 mL), also pre-stirred over 4 Å molecular sieves at room temperature for 30 min. The solution was shielded from light and stirred at room temperature for 9 h. The reaction mixture was filtered through Celite® and concentrated *in vacuo* to yield a yellow liquid.

To a solution of this liquid in methanol (5 mL) was added sodium methoxide (29 mg, 0.54 mmol, 0.7 eq). The solution was stirred at room temperature for 19.5 h, filtered, and concentrated *in vacuo*. The crude residue was purified by gradient silica gel chromatography (50% ethyl acetate in petroleum ether to 5% methanol in ethyl acetate) to yield benzyl 6-*O*-(4-nitrobenzyl)- $\beta$ -D-galactopyranoside **126** (0.227 g, 76%, 2 steps) as a colourless solid:  $R_f$  0.23 (ethyl acetate);  $[\alpha]_D^{25} = -50.6$  ( $c$  0.5,  $CHCl_3$ ); mp 102–104 °C (ethyl acetate);  $\bar{\nu}_{max}$  (thin film)/ $cm^{-1}$  3420 (br, O–H), 2929 (w), 1605, (w), 1519 (s, N=O), 1346 (s, N=O), 1071 (s), 738 (m);  $^1H$  NMR (400 MHz,  $CDCl_3$ )  $\delta$  8.22–8.18 (2H, m,  $C^{15}$ -H), 7.52–7.48 (2H, m,  $C^{14}$ -H), 7.38–7.28 (5H, m,  $C^9$ -H,  $C^{10}$ -H,  $C^{11}$ -H), 4.93 (1H, d,  $J_{AB}$  11.6,  $C^7$ - $H_A$ ), 4.69 (2H, s,  $C^{12}$ - $H_2$ ), 4.62 (1H, d,  $J_{AB}$  11.6,  $C^7$ - $H_B$ ), 4.34 (1H, d,  $J$  7.7,  $C^1$ -H), 3.98 (1H, dd,  $J$  3.3, 3.3,  $C^4$ -H), 3.84 (1H, dd,  $J_{AB}$  10.1,  $J_{AX}$  5.6,  $C^6$ - $H_A$ ), 3.80 (1H, dd,  $J_{AB}$  10.1,  $J_{BX}$  5.8,  $C^6$ - $H_B$ ), 3.72 (1H, ddd,  $J$  9.5, 7.7, 2.6,  $C^2$ -H), 3.67 (1H, dd,  $J_{AX}$  5.6,  $J_{BX}$  5.8,  $C^5$ - $H_X$ ), 3.59 (1H, ddd,  $J$  9.5, 4.8, 3.3,  $C^3$ -H), 3.01 (1H, d,  $J$  4.8,  $C^3$ -OH), 2.80 (1H, d,  $J$  2.6,  $C^2$ -OH), 2.78 (1H, d,  $J$  3.3,  $C^4$ -OH);  $^{13}C$  NMR (126 MHz,  $CDCl_3$ )  $\delta$  147.6 ( $C^{16}$ ), 145.7

( $C^{13}$ ), 137.0 ( $C^8$ ), 128.7 ( $C^{10}$ ), 128.32 ( $C^9$ ), 128.28 ( $C^{11}$ ), 127.8 ( $C^{14}$ ), 123.8 ( $C^{15}$ ), 102.0 ( $C^1$ ), 73.8 ( $C^5$ ), 73.5 ( $C^3$ ), 72.5 ( $C^{12}$ ), 72.1 ( $C^2$ ), 71.3 ( $C^7$ ), 70.1 ( $C^6$ ), 69.1 ( $C^4$ ); HRMS  $m/z$  (ESI<sup>+</sup>) [Found ( $M+Na$ )<sup>+</sup> 428.13140  $C_{20}H_{23}NO_8Na$  requires  $M^+$  428.13159]; LRMS  $m/z$  (ES<sup>+</sup>) 428 ([ $M+Na$ ]<sup>+</sup>, 100%), 429 ([ $M+Na$ ]<sup>+</sup>, 23%), 430 ([ $M+Na$ ]<sup>+</sup>, 5%); Analytical RP-HPLC (Method 1, 254 nm) Ret. time = 10.5 min, Purity = 98.7%.

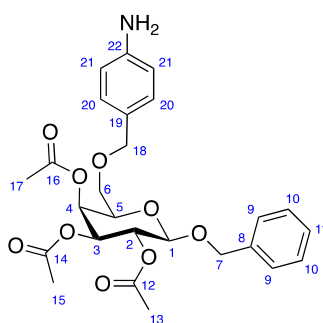
### Benzyl 2,3,4-tri-*O*-acetyl-6-*O*-(4-nitrobenzyl)-β-D-galactopyranoside, **247**



To a solution of benzyl alcohol (660  $\mu$ L, 6.38 mmol, 4.0 eq) and silver carbonate (875 mg, 3.17 mmol, 2.0 eq) in  $CH_2Cl_2$  (5 mL), pre-stirred over 4 Å molecular sieves at room temperature for 30 min, was added dropwise over 10 min a solution of **246** (800 mg, 1.59 mmol, 1.0 eq) in  $CH_2Cl_2$  (4 mL), also pre-stirred over 4 Å molecular sieves at room temperature for 30 min. The suspension was shielded from light and stirred at room temperature for 20 h, filtered through Celite®, and concentrated *in vacuo*. The crude residue was purified by gradient silica gel chromatography (0–30% ethyl acetate in petroleum ether) to yield benzyl 2,3,4-tri-*O*-acetyl-6-*O*-(4-nitrobenzyl)-β-D-galactopyranoside **247** (762 mg, 90%) as a colourless foam:  $R_f$  0.23 (1:2 ethyl acetate:petroleum ether);  $[\alpha]_D^{25} = -57.4$  ( $c$  1.0,  $CHCl_3$ );  $\bar{\nu}_{max}$  (thin film)/ $cm^{-1}$  2875 (w), 1749 (s, C=O), 1605 (w), 1522 (m, N=O), 1430 (w), 1369 (m), 1347 (m, N=O), 1247 (m), 1221 (s, C–O), 1070 (m), 953 (w), 740 (w);  $^1H$  NMR (500 MHz,  $CDCl_3$ )  $\delta$  8.24–8.18 (2H, m,  $C^{21}$ -H), 7.50–7.45 (2H, m,  $C^{20}$ -H), 7.37–7.26 (5H, m,  $C^9$ -H,  $C^{10}$ -H,  $C^{11}$ -H), 5.48 (1H, dd,  $J$  3.5, 1.1,  $C^4$ -H), 5.29 (1H, dd,  $J$  10.4, 8.0,  $C^2$ -H), 5.01 (1H, dd,  $J$  10.4, 3.5,  $C^3$ -H), 4.91 (1H, d,  $J_{AB}$  12.4,  $C^7$ - $H_A$ ), 4.65 (1H, d,  $J_{AB}$  13.1,  $C^{18}$ - $H_A$ ), 4.63 (1H, d,  $J_{AB}$  12.4,  $C^7$ - $H_B$ ), 4.58 (1H, d,  $J_{AB}$  13.1,  $C^{18}$ - $H_B$ ), 4.54 (1H, d,  $J$  8.0,  $C^1$ -H), 3.89 (1H, ddd,  $J_{AX}$  6.3,  $J_{BX}$  6.2,  $J$  1.1,  $C^5$ - $H_X$ ), 3.67 (1H, dd,  $J_{AB}$  9.7,  $J_{BX}$  6.2,  $C^6$ - $H_B$ ), 3.59 (1H, dd,  $J_{AB}$  9.7,  $J_{AX}$  6.3,  $C^6$ - $H_A$ ), 2.11 (3H, s,  $C^{17}$ - $H_3$ ), 2.01

(3H, s,  $C^{13}$ - $H_3$ ), 1.98 (3H, s,  $C^{15}$ - $H_3$ );  $^{13}\text{C}$  NMR (126 MHz,  $\text{CDCl}_3$ )  $\delta$  170.4 ( $C^{16}$ ), 170.3 ( $C^{14}$ ), 169.6 ( $C^{12}$ ), 147.7 ( $C^{22}$ ), 145.3 ( $C^{19}$ ), 136.9 ( $C^8$ ), 128.6 ( $C^{10}$ ), 128.1 ( $C^{11}$ ), 127.9 ( $C^{20}$ ), 127.8 ( $C^9$ ), 123.9 ( $C^{21}$ ), 100.1 ( $C^1$ ), 72.5 ( $C^{18}$ ), 72.3 ( $C^5$ ), 71.2 ( $C^3$ ), 70.9 ( $C^7$ ), 69.1 ( $C^2$ ), 68.7 ( $C^6$ ), 67.8 ( $C^4$ ), 20.89 ( $C^{13}$  or  $C^{17}$ ), 20.85 ( $C^{13}$  or  $C^{17}$ ), 20.7 ( $C^{15}$ ); HRMS  $m/z$  ( $\text{ESI}^+$ ) [Found ( $\text{M}+\text{Na}$ ) $^+$  554.16319  $\text{C}_{26}\text{H}_{29}\text{NO}_{11}\text{Na}$  requires  $\text{M}^+$  554.16328]; LRMS  $m/z$  ( $\text{ES}^+$ ) 554 ( $[\text{M}+\text{Na}]^+$ , 100%), 555 ( $[\text{M}+\text{Na}]^+$ , 29%), 556 ( $[\text{M}+\text{Na}]^+$ , 6%); Analytical RP-HPLC (Method 2, 254 nm) Ret. time = 10.9 min, Purity = >99.9%.

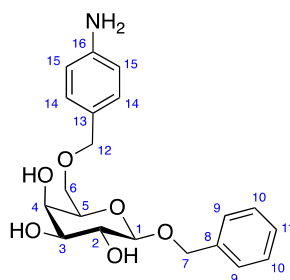
### Benzyl 2,3,4,-tri-*O*-acetyl-6-*O*-(4-aminobenzyl)- $\beta$ -D-galactopyranoside, **306**



To a solution of **247** (400 mg, 0.753 mmol, 1.0 eq) in ethyl acetate (10 mL), under  $\text{N}_{2(g)}$ , was added Pd/C (40 mg, 10% w/w, 0.038 mmol, 0.05 eq). The  $\text{N}_{2(g)}$  was evacuated and replaced with  $\text{H}_{2(g)}$  by purging the flask with 2 balloons of  $\text{H}_{2(g)}$ . The suspension was stirred at room temperature for 2.5 h, filtered through Celite<sup>®</sup>, and concentrated *in vacuo* to yield benzyl 2,3,4,-tri-*O*-acetyl-6-*O*-(4-aminobenzyl)- $\beta$ -D-galactopyranoside **306** (376 mg, 99%) as a colourless oil:  $R_f$  0.34 (1:1 ethyl acetate:petroleum ether);  $[\alpha]_D^{25} = -61.4$  ( $c$  1.0,  $\text{CHCl}_3$ );  $\bar{\nu}_{\text{max}}$  (thin film)/ $\text{cm}^{-1}$  3465 (w, N–H), 3276 (w, N–H), 3031 (w), 2870 (w), 2362 (w), 1747 (s, C=O), 1627 (w), 1519 (w), 1369 (m), 1249 (m), 1222 (s, C–O), 1068 (s), 830 (w), 742 (w);  $^1\text{H}$  NMR (500 MHz,  $\text{CDCl}_3$ )  $\delta$  7.37–7.26 (5H, m,  $C^9$ - $H$ ,  $C^{10}$ - $H$ ,  $C^{11}$ - $H$ ), 7.11–7.06 (2H, m,  $C^{20}$ - $H$ ), 6.67–6.62 (2H, m,  $C^{21}$ - $H$ ), 5.43 (1H, dd,  $J$  3.5, 1.0,  $C^4$ - $H$ ), 5.25 (1H, dd,  $J$  10.4, 8.0,  $C^2$ - $H$ ), 4.97 (1H, dd,  $J$  10.4, 3.5,  $C^3$ - $H$ ), 4.91 (1H, d,  $J_{AB}$  12.4,  $C^7$ - $H_A$ ), 4.62 (1H, d,  $J_{AB}$  12.4,  $C^7$ - $H_B$ ), 4.49 (1H, d,  $J$  8.0,  $C^1$ - $H$ ), 4.44 (1H, d,  $J_{AB}$  11.5,  $C^{18}$ - $H_A$ ), 4.32 (1H, d,  $J_{AB}$  11.5,  $C^{18}$ - $H_B$ ), 3.80 (1H, ddd,  $J_{AX}$  6.7,  $J_{BX}$  6.2,  $J$  1.0,  $C^5$ - $H_X$ ), 3.67 (2H, br s,  $C^{22}$ - $\text{NH}_2$ ), 3.56 (1H, dd,  $J_{AB}$  9.6,  $J_{BX}$  6.2,  $C^6$ - $H_B$ ), 3.48 (1H, dd,  $J_{AB}$  9.6,  $J_{AX}$  6.7,  $C^6$ - $H_A$ ), 2.07 (3H, s,  $C^{17}$ - $H_3$ ), 1.99 (3H, s,  $C^{13}$ - $H_3$ ), 1.96 (3H, s,  $C^{15}$ - $H_3$ );  $^{13}\text{C}$  NMR (126 MHz,  $\text{CDCl}_3$ )  $\delta$  170.4

( $C^{16}$ ), 170.2 ( $C^{14}$ ), 169.6 ( $C^{12}$ ), 146.4 ( $C^{22}$ ), 137.0 ( $C^8$ ), 129.8 ( $C^{20}$ ), 128.6 ( $C^{10}$ ), 128.0 ( $C^{11}$ ), 127.8 ( $C^9$ ), 127.5 ( $C^{19}$ ), 115.1 ( $C^{21}$ ), 100.0 ( $C^1$ ), 73.6 ( $C^{18}$ ), 72.4 ( $C^5$ ), 71.3 ( $C^3$ ), 70.8 ( $C^7$ ), 69.3 ( $C^2$ ), 67.8 ( $C^4$ ), 67.1 ( $C^6$ ), 20.9 ( $C^{13}$  or  $C^{15}$  or  $C^{17}$ ), 20.82 ( $C^{13}$  or  $C^{15}$  or  $C^{17}$ ), 20.75 ( $C^{13}$  or  $C^{15}$  or  $C^{17}$ ); HRMS  $m/z$  (ESI<sup>+</sup>) [Found (M+Na)<sup>+</sup> 524.18895 C<sub>26</sub>H<sub>31</sub>NO<sub>9</sub>Na requires M<sup>+</sup> 524.18910]; LRMS  $m/z$  (ES<sup>+</sup>) 524 ([M+Na]<sup>+</sup>, 100%), 525 ([M+Na]<sup>+</sup>, 29%), 526 ([M+Na]<sup>+</sup>, 5%); Analytical RP-HPLC (Method 2, 254 nm) Ret. time = 9.8 min, Purity = >99.9%.

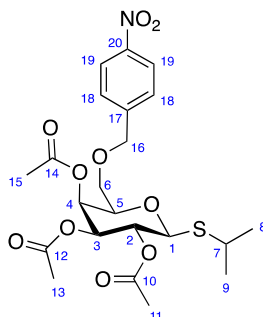
### Benzyl 6-*O*-(4-aminobenzyl)-β-D-galactopyranoside, **304**



To a solution of **306** (356 mg, 0.710 mmol, 1.0 eq) in methanol (7 mL) was added sodium methoxide (19 mg, 0.36 mmol, 0.5 eq). The solution was stirred at room temperature for 3 h, adjusted to pH 7 with Amberlite® IR120 resin (H<sup>+</sup> form), filtered, and concentrated *in vacuo*. The crude residue was purified four times by silica gel chromatography (1: 0–5% methanol in ethyl acetate; 2: isocratic 100% ethyl acetate; 3: 0–5% methanol in dichloromethane; 4: isocratic 5% methanol in dichloromethane) to yield benzyl 6-*O*-(4-aminobenzyl)-β-D-galactopyranoside **304** (78 mg, 29%) as a colourless foam:  $R_f$  0.30 (1:9 methanol:dichloromethane);  $[\alpha]_D^{25} = -24.8$  ( $c$  1.0, MeOH);  $\bar{\nu}_{\max}$  (thin film)/cm<sup>-1</sup> 3364 (br, O–H), 2915 (w, N–H), 2870 (w, N–H), 2361 (w), 2338 (w), 1621 (m), 1518 (m, N=O), 1454 (w), 1367 (m, N=O), 1285 (w), 1214 (w), 1069 (m), 912 (w), 828 (w), 745 (w), 700 (w); <sup>1</sup>H NMR (400 MHz, CD<sub>3</sub>OD)  $\delta$  7.42–7.38 (2H, m, C<sup>9</sup>-H), 7.34–7.23 (3H, m, C<sup>10</sup>-H, C<sup>11</sup>-H), 7.13–7.08 (2H, m, C<sup>14</sup>-H), 6.73–6.67 (2H, m, C<sup>15</sup>-H), 4.89 (1H, d,  $J_{AB}$  11.8, C<sup>7</sup>-H<sub>A</sub>), 4.65 (1H, d,  $J_{AB}$  11.8, C<sup>7</sup>-H<sub>B</sub>), 4.44 (2H, s, C<sup>12</sup>-H<sub>2</sub>), 4.30 (1H, d,  $J$  7.7, C<sup>1</sup>-H), 3.80 (1H, dd,  $J$  3.4, 1.0, C<sup>4</sup>-H), 3.71–3.67 (2H, m, C<sup>6</sup>-H<sub>2</sub>), 3.62 (1H, ddd,  $J$  6.5, 5.3, 1.0, C<sup>5</sup>-H), 3.58 (1H, dd,  $J$  9.7, 7.7, C<sup>2</sup>-H), 3.44 (1H, dd,  $J$  9.7, 3.4, C<sup>3</sup>-H); <sup>13</sup>C NMR (101 MHz, CD<sub>3</sub>OD)  $\delta$  148.6 (C<sup>16</sup>), 139.1 (C<sup>8</sup>), 130.5 (C<sup>14</sup>), 129.24 (C<sup>9</sup> or C<sup>10</sup>), 129.21 (C<sup>9</sup> or C<sup>10</sup>), 128.7 (C<sup>13</sup>), 128.6 (C<sup>11</sup>), 116.3 (C<sup>15</sup>), 103.9 (C<sup>1</sup>), 75.1 (C<sup>5</sup>), 74.9 (C<sup>3</sup>), 74.6 (C<sup>12</sup>), 72.5 (C<sup>2</sup>), 71.8 (C<sup>7</sup>), 70.6 (C<sup>4</sup>), 70.3

( $C^6$ ); HRMS  $m/z$  (ESI $^+$ ) [Found (M+Na) $^+$  398.15727  $C_{20}H_{25}NO_6$  requires M $^+$  398.15741]; LRMS  $m/z$  (ES $^+$ ) 106 ([M- $C_{13}H_{17}O_6$ )+H] $^+$ , 100%), 398 ([M+Na] $^+$ , 76%), 541 ([2(M- $C_7H_8N$ )+H] $^+$ , 14%); Analytical RP-HPLC (Method 2, 220/254/300 nm) Ret. time = 6.5 min, Purity = 95.7%.

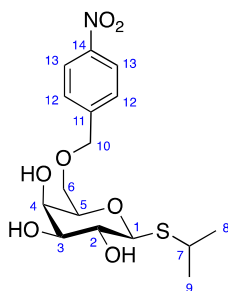
#### Isopropyl 2,3,4-tri-*O*-acetyl-6-*O*-(4-nitrobenzyl)-1-thio- $\beta$ -D-galactopyranoside, **248**



To a solution of **245** (880 mg, 1.82 mmol, 1.0 eq) and in  $CH_2Cl_2$  (9 mL) was added 2-propanethiol (340  $\mu$ L, 3.66 mmol, 2.0 eq) and 4 Å molecular sieves. The resulting suspension was stirred at room temperature for 20 min, cooled to  $-78^\circ C$ , and  $BF_3 \cdot Et_2O$  (450  $\mu$ L, 3.65 mmol, 2.0 eq) was added dropwise over 5 min. The solution was warmed to room temperature and stirred for 48 h. The reaction was quenched with triethylamine (1.5 mL), filtered through Celite $^{\text{®}}$ , and concentrated *in vacuo*. The crude residue was purified by gradient silica gel chromatography (0–30% ethyl acetate in petroleum ether) to yield isopropyl 2,3,4-tri-*O*-acetyl-6-*O*-(4-nitrobenzyl)-1-thio- $\beta$ -D-galactopyranoside **248** (397 mg, 44%) as a colourless oil:  $R_f$  0.26 (1:1 ethyl acetate:petroleum ether);  $[\alpha]_D^{25} = -14.8$  ( $c$  1.0,  $CHCl_3$ );  $\bar{\nu}_{max}$  (thin film)/ $cm^{-1}$  2964 (w), 2927 (w), 2869 (w), 1749 (s, C=O), 1522 (m, N=O), 1370 (m), 1347 (m, N=O), 1244 (s), 1221 (s), 1084 (m), 1054 (m);  $^1H$  NMR (500 MHz,  $CDCl_3$ )  $\delta$  8.20–8.17 (2H, m,  $C^{19}$ -H), 7.46–7.43 (2H, m,  $C^{18}$ -H), 5.51 (1H, dd,  $J$  3.4, 0.8,  $C^4$ -H), 5.21 (1H, dd,  $J$  10.0, 10.0,  $C^2$ -H), 5.07 (1H, dd,  $J$  10.0, 3.4,  $C^3$ -H), 4.62 (1H, d,  $J_{AB}$  13.1,  $C^{16}$ - $H_A$ ), 4.58 (1H, d,  $J$  10.0,  $C^1$ -H), 4.55 (1H, d,  $J_{AB}$  13.1,  $C^{16}$ - $H_B$ ), 3.91 (1H, ddd,  $J_{AX}$  6.3,  $J_{BX}$  6.2,  $J$  0.8,  $C^5$ - $H_X$ ), 3.63 (1H, dd,  $J_{AB}$  9.7,  $J_{AX}$  6.3,  $C^6$ - $H_A$ ), 3.53 (1H, dd,  $J_{AB}$  9.7,  $J_{BX}$  6.2,  $C^6$ - $H_B$ ), 3.17 (1H, sept,  $J$  6.7,  $C^7$ -H), 2.10 (3H, s,  $C^{11}$ - $H_3$ ), 2.05 (3H, s,  $C^{15}$ - $H_3$ ), 1.98 (3H, s,  $C^{13}$ - $H_3$ ), 1.31 (3H, d,  $J$  6.7,  $C^8$ - $H_3$  or  $C^9$ - $H_3$ ), 1.30 (3H, d,  $J$  6.7,  $C^8$ - $H_3$  or  $C^9$ - $H_3$ );  $^{13}C$  NMR (126 MHz,  $CDCl_3$ )  $\delta$  170.4 ( $C^{14}$ ), 170.2 ( $C^{12}$ ), 169.7 ( $C^{10}$ ), 147.6 ( $C^{20}$ ), 145.3 ( $C^{17}$ ), 127.9 ( $C^{18}$ ), 123.8 ( $C^{19}$ ), 84.0 ( $C^1$ ), 75.9 ( $C^5$ ), 72.4 ( $C^{16}$ ), 72.2 ( $C^3$ ), 68.9 ( $C^6$ ), 67.9 ( $C^2$ ),

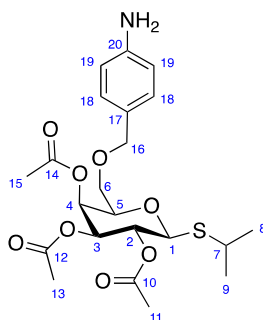
67.7 ( $C^4$ ), 35.8 ( $C^7$ ), 24.1 ( $C^8$  or  $C^9$ ), 23.9 ( $C^8$  or  $C^9$ ), 21.0 ( $C^{15}$ ), 20.8 ( $C^{11}$ ), 20.7 ( $C^{13}$ ); HRMS  $m/z$  ( $ESI^+$ ) [Found ( $M+Na$ ) $^+$  428.14044  $C_{22}H_{29}NO_{10}SNa$  requires  $M^+$  522.14044]; LRMS  $m/z$  ( $ES^+$ ) 522 ( $[M+Na]^+$ , 100%), 523 ( $[M+Na]^+$ , 21%), 524 ( $[M+Na]^+$ , 8%); Analytical RP-HPLC (Method 1, 254 nm) Ret. time = 13.4 min, Purity = 95.5%.

### Isopropyl 6-*O*-(4-nitrobenzyl)-1-thio- $\beta$ -D-galactopyranoside, **89**

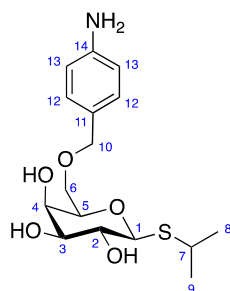


To a solution of **248** (85 mg, 0.17 mmol, 1.0 eq) in methanol (2 mL) was added sodium methoxide (12 mg, 0.20 mmol, 1.2 eq). The solution was stirred at room temperature for 16 h, neutralised with Amberlite<sup>®</sup> IR120 resin ( $H^+$  form), filtered, and concentrated *in vacuo*. The crude residue was purified by silica gel chromatography (100% ethyl acetate) to yield isopropyl 6-*O*-(4-nitrobenzyl)-1-thio- $\beta$ -D-galactopyranoside **89** (50 mg, 79%) as a colourless solid:  $R_f$  0.43 (1:9 methanol:ethyl acetate); mp 132–133 °C (ethyl acetate);  $[\alpha]_D^{25} = -34.8$  ( $c$  0.5,  $CHCl_3$ );  $\bar{\nu}_{max}$  (thin film)/ $cm^{-1}$  3422 (br, O–H), 2962 (w), 2920 (w), 2867 (w), 1605 (w), 1520 (s, N=O), 1456 (w), 1347 (s, N=O), 1095 (w), 1060 (m), 866 (w), 740 (w);  $^1H$  NMR (500 MHz,  $CDCl_3$ )  $\delta$  8.18 (2H, m,  $C^{13}$ -H), 7.48 (2H, m,  $C^{12}$ -H), 4.66 (2H, s,  $C^{10}$ - $H_2$ ), 4.41 (1H, d,  $J$  9.1,  $C^1$ -H), 4.05 (1H, dd,  $J$  3.0, 0.8,  $C^4$ -H), 3.78 (1H, dd,  $J_{AB}$  10.1,  $J_{BX}$  5.6,  $C^6$ - $H_B$ ), 3.75 (1H, dd,  $J_{AB}$  10.1,  $J_{AX}$  5.8,  $C^6$ - $H_A$ ), 3.71 (1H, ddd,  $J_{AX}$  5.8,  $J_{BX}$  5.6,  $J$  0.8,  $C^5$ - $H_X$ ), 3.67 (1H, dd,  $J$  9.1, 9.1,  $C^2$ -H), 3.63 (1H, dd,  $J$  9.1, 3.0,  $C^3$ -H), 3.20 (1H, sept,  $J$  6.8,  $C^7$ -H), 1.33 (3H, d,  $J$  6.8,  $C^8$ - $H_3$  or  $C^9$ - $H_3$ ), 1.31 (3H, d,  $J$  6.8,  $C^8$ - $H_3$  or  $C^9$ - $H_3$ );  $^{13}C$  NMR (126 MHz,  $CDCl_3$ )  $\delta$  147.5 ( $C^{14}$ ), 145.7 ( $C^{11}$ ), 127.8 ( $C^{12}$ ), 123.8 ( $C^{13}$ ), 86.1 ( $C^1$ ), 77.4 ( $C^5$ ), 74.9 ( $C^3$ ), 72.4 ( $C^{10}$ ), 70.5 ( $C^2$ ), 70.2 ( $C^6$ ), 69.4 ( $C^4$ ), 36.0 ( $C^7$ ), 24.4 ( $C^8$  or  $C^9$ ), 24.1 ( $C^8$  or  $C^9$ ); HRMS  $m/z$  ( $ESI^+$ ) [Found ( $M+Na$ ) $^+$  396.10861  $C_{16}H_{23}NO_7SNa$  requires  $M^+$  396.10874]; LRMS  $m/z$  ( $ES^+$ ) 396 ( $[M+Na]^+$ , 100%), 397 ( $[M+Na]^+$ , 17%), 398 ( $[M+Na]^+$ , 7%); Analytical RP-HPLC (Method 1, 254 nm) Ret. time = 10.1 min, Purity = >99.9%.



Isopropyl 2,3,4-tri-*O*-acetyl-6-*O*-(4-aminobenzyl)-1-thio- $\beta$ -D-galactopyranoside, **305**

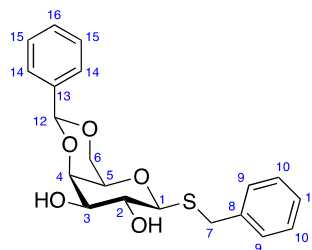
To a solution of **248** (189 mg, 0.378 mmol, 1.0 eq) in ethyl acetate (6 mL), under  $N_{2(g)}$ , was added a suspension of Pd/C (19 mg, 10% w/w, 0.018 mmol, 0.05 eq) in ethyl acetate (500  $\mu$ L). The  $N_{2(g)}$  was evacuated and replaced with  $H_{2(g)}$  by purging the flask with 3 balloons of  $H_{2(g)}$ . The suspension was stirred at room temperature for 1.5 h, filtered through Celite<sup>®</sup>, and concentrated *in vacuo*. The crude residue was purified by silica gel chromatography (50% ethyl acetate in petroleum ether) to afford **305** (165 mg, 93%) as a colourless oil:  $R_f$  0.34 (1:1 ethyl acetate:petroleum ether);  $[\alpha]_D^{25}$   $-33.3$  ( $c$  1.0,  $CHCl_3$ );  $\bar{\nu}_{max}$  (thin film)/ $cm^{-1}$  3466 (w, N–H), 3374 (w, N–H), 2965 (w), 2928 (w), 2867 (w), 1746 (s, C=O), 1627 (w), 1519 (w), 1370 (m), 1222 (s), 1083 (m), 1054 (m), 920 (w);  $^1H$  NMR (400 MHz,  $CDCl_3$ )  $\delta$  7.09–7.00 (2H, m,  $C^{18}$ -H), 6.66–6.56 (2H, m,  $C^{19}$ -H), 5.46 (1H, d,  $J$  3.1,  $C^4$ -H), 5.16 (1H, dd,  $J$  10.0, 10.0,  $C^2$ -H), 5.02 (1H, dd,  $J$  10.0, 3.1,  $C^3$ -H), 4.54 (1H, d,  $J$  10.0,  $C^1$ -H), 4.39 (1H, d,  $J_{AB}$  11.4,  $C^{16}$ - $H_A$ ), 4.26 (1H, d,  $J_{AB}$  11.4,  $C^{16}$ - $H_B$ ), 3.81 (1H, dd,  $J_{AX}$  6.7,  $J_{BX}$  6.2,  $C^5$ - $H_X$ ), 3.68 (2H, br s,  $C^{20}$ - $NH_2$ ), 3.50 (1H, dd,  $J_{AB}$  9.5,  $J_{BX}$  6.2,  $C^6$ - $H_B$ ), 3.41 (1H, dd,  $J_{AB}$  9.5,  $J_{AX}$  6.7,  $C^6$ - $H_A$ ), 3.16 (1H, sept,  $J$  6.8,  $C^7$ -H), 2.034 (3H, s,  $C^{15}$ - $H_3$ ), 2.029 (3H, s,  $C^{11}$ - $H_3$ ), 1.95 (3H, s,  $C^{13}$ - $H_3$ ), 1.29 (3H, d,  $J$  6.8,  $C^8$ - $H_3$  or  $C^9$ - $H_3$ ), 1.28 (3H, d,  $J$  6.8,  $C^8$ - $H_3$  or  $C^9$ - $H_3$ );  $^{13}C$  NMR (101 MHz,  $CDCl_3$ )  $\delta$  170.3 ( $C^{14}$ ), 170.1 ( $C^{12}$ ), 169.7 ( $C^{10}$ ), 146.4 ( $C^{20}$ ), 129.8 ( $C^{18}$ ), 127.3 ( $C^{17}$ ), 114.9 ( $C^{19}$ ), 83.8 ( $C^1$ ), 75.9 ( $C^5$ ), 73.5 ( $C^{16}$ ), 72.2 ( $C^3$ ), 67.84 ( $C^2$  or  $C^4$ ), 67.81 ( $C^2$  or  $C^4$ ), 67.0 ( $C^6$ ), 35.5 ( $C^7$ ), 24.1 ( $C^8$  or  $C^9$ ), 23.8 ( $C^8$  or  $C^9$ ), 20.9 ( $C^{11}$  or  $C^{15}$ ), 20.74 ( $C^{11}$  or  $C^{15}$ ), 20.69 ( $C^{13}$ ); HRMS  $m/z$  (ESI<sup>+</sup>) [Found ( $M+Na$ )<sup>+</sup> 492.16583  $C_{22}H_{31}NO_8SNa$  requires  $M^+$  492.16626]; LRMS  $m/z$  (ES<sup>+</sup>) 492 ( $[M+Na]^+$ , 100%), 493 ( $[M+Na]^+$ , 26%), 494 ( $[M+Na]^+$ , 9%); Analytical RP-HPLC (Method 4, 254 nm) Ret. time = 14.8 min, Purity = 95.5%.

**Isopropyl 6-*O*-(4-aminobenzyl)-1-thio- $\beta$ -D-galactopyranoside, **303****

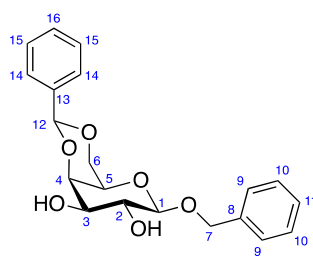
To a suspension of **303** (165 mg, 0.351 mmol, 1.0 eq) in methanol (3 mL) was added sodium methoxide (9 mg, 0.2 mmol, 0.5 eq). The resulting solution was stirred at room temperature for 1 h, neutralised with Amberlite® IR120 resin ( $H^+$ -form), filtered, and concentrated *in vacuo*. The crude residue was purified by gradient silica gel chromatography (75–100% ethyl acetate in petroleum ether) to yield isopropyl 6-*O*-(4-aminobenzyl)-1-thio- $\beta$ -D-galactopyranoside **303** (98 mg, 82%) as a colourless solid:  $R_f$  0.20 (ethyl acetate);  $[\alpha]_D^{25} = -22.9$  ( $c$  0.5, MeOH); mp 108–109 °C (ethyl acetate);  $\bar{\nu}_{max}$  (thin film)/ $cm^{-1}$  3359 (br, O–H), 2977 (w, N–H), 2888 (w, N–H), 1617 (w), 1518 (w), 1459 (w), 1386 (w), 1252 (w), 1151 (w), 1087 (w), 953 (w), 743 (w);  $^1H$  NMR (400 MHz,  $CDCl_3$ )  $\delta$  7.15–7.08 (2H, m,  $C^{12}$ -H), 6.68–6.62 (2H, m,  $C^{13}$ -H), 4.44 (2H, s,  $C^{10}$ - $H_2$ ), 4.36 (1H, d,  $J$  9.5,  $C^1$ -H), 4.03 (1H, d,  $J$  2.9,  $C^4$ -H), 3.77–3.64 (4H, m,  $C^6$ - $H_2$ ,  $C^{14}$ - $NH_2$ ), 3.63–3.59 (2H, m,  $C^2$ -H,  $C^5$ -H), 3.55 (1H, dd,  $J$  9.0,  $C^3$ -H), 3.21 (1H, sept,  $J$  6.6,  $C^7$ -H), 2.90 (1H, br s,  $C^2$ -OH or  $C^3$ -OH), 2.83 (1H, br s,  $C^4$ -OH), 2.62 (3H, br s,  $C^2$ -OH or  $C^3$ -OH), 1.34 (3H, d,  $J$  6.6,  $C^8$ - $H_3$  or  $C^9$ - $H_3$ ), 1.33 (3H, d,  $J$  6.6,  $C^8$ - $H_3$  or  $C^9$ - $H_3$ );  $^{13}C$  NMR (101 MHz,  $CDCl_3$ )  $\delta$  146.4 ( $C^{14}$ ), 129.7 ( $C^{12}$ ), 127.7 ( $C^{11}$ ), 115.2 ( $C^{13}$ ), 86.1 ( $C^1$ ), 77.4 ( $C^2$ ), 74.9 ( $C^3$ ), 73.8 ( $C^{10}$ ), 70.9 ( $C^5$ ), 69.5 ( $C^4$ ), 69.1 ( $C^6$ ), 35.8 ( $C^7$ ), 24.4 ( $C^8$  or  $C^9$ ), 24.2 ( $C^8$  or  $C^9$ ); HRMS  $m/z$  (ESI $^+$ ) [Found ( $M+Na$ ) $^+$  366.13450  $C_{16}H_{25}NO_5SNa$  requires  $M^+$  366.13456]; LRMS  $m/z$  (ES $^+$ ) 366 ( $[M+Na]^+$ , 100%), 367 ( $[M+Na]^+$ , 19%), 368 ( $[M+Na]^+$ , 7%); Analytical RP-HPLC (Method 2, 254 nm) Ret. time = 5.9 min, Purity = 96.7%.

### 6.2.8. Synthesis of 4,6-Acetal Protected Galactopyranosides

#### Benzyl 4,6-*O*-benzylidene-1-thio- $\beta$ -D-galactopyranoside, **256**



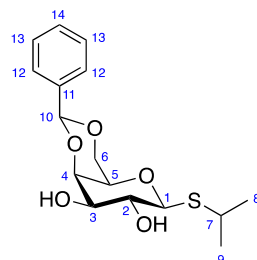
To a stirred suspension of **104** (199 mg, 0.695 mmol, 1.0 eq) in acetonitrile (10 mL) was added 4-TsOH·H<sub>2</sub>O (50 mg, 0.26 mmol, 0.4 eq) and benzaldehyde dimethyl acetal (130  $\mu$ L, 0.866 mmol, 1.2 eq). The suspension immediately turned clear and the solution was stirred at room temperature for 1 h. The reaction was quenched with triethylamine (500  $\mu$ L) and concentrated *in vacuo*. The crude residue was purified by silica gel chromatography (1:4 ethyl acetate:petroleum ether) to yield benzyl 4,6-*O*-benzylidene-1-thio- $\beta$ -D-galactopyranoside **256** (210 mg, 81%) as a colourless solid:  $R_f$  0.26 (1:4 ethyl acetate:petroleum ether);  $[\alpha]_D^{25} = -94.3$  ( $c$  1.0, CHCl<sub>3</sub>); mp 158–159 °C (ethyl acetate);  $\bar{\nu}_{\max}$  (neat)/cm<sup>-1</sup> 3316 (br, O–H), 2924 (w), 1656 (w, C–C stretch), 1451 (w), 1402 (w), 1166 (w), 1099 (m), 1068 (m), 1042 (m), 998 (m), 817 (m), 695 (s); <sup>1</sup>H NMR (400 MHz, CDCl<sub>3</sub>)  $\delta$  7.52–7.50 (2H, m, C<sup>14</sup>-H), 7.40–7.35 (5H, m, C<sup>9</sup>-H, C<sup>15</sup>-H, C<sup>16</sup>-H), 7.31–7.24 (3H, m, C<sup>10</sup>-H, C<sup>11</sup>-H), 5.56 (1H, s, C<sup>12</sup>-H), 4.36 (1H, dd,  $J_{AB}$  12.6,  $J_{BX}$  1.5, C<sup>6</sup>-H<sub>B</sub>), 4.25 (1H, d,  $J$  3.8, 1.2, C<sup>4</sup>-H), 4.24 (1H, d,  $J$  9.4, C<sup>1</sup>-H), 4.06 (1H, dd,  $J_{AB}$  12.6,  $J_{AX}$  1.6, C<sup>6</sup>-H<sub>A</sub>), 4.00 (1H, d,  $J_{AB}$  14.5, C<sup>7</sup>-H<sub>A</sub>), 3.97 (1H, d,  $J_{AB}$  14.5, C<sup>7</sup>-H<sub>B</sub>), 3.78 (1H, ddd,  $J$  9.4, 9.2, 1.6, C<sup>2</sup>-H), 3.61 (1H, ddd,  $J$  9.2, 9.1, 3.8, C<sup>3</sup>-H), 3.47 (1H, ddd,  $J_{AX}$  1.6,  $J_{BX}$  1.5,  $J$  1.2, C<sup>5</sup>-H<sub>X</sub>), 2.51 (1H, d,  $J$  9.1, C<sup>3</sup>-OH), 2.40 (1H, d,  $J$  1.6, C<sup>2</sup>-OH); <sup>13</sup>C NMR (101 MHz, CDCl<sub>3</sub>)  $\delta$  137.9 (C<sup>8</sup> or C<sup>13</sup>), 137.7 (C<sup>8</sup> or C<sup>13</sup>), 129.4 (C<sup>16</sup>), 129.2 (C<sup>9</sup>), 128.8 (C<sup>10</sup>), 128.4 (C<sup>15</sup>), 127.4 (C<sup>11</sup>), 126.5 (C<sup>14</sup>), 101.6 (C<sup>12</sup>), 84.2 (C<sup>4</sup>), 75.6 (C<sup>1</sup>), 74.0 (C<sup>3</sup>), 70.3 (C<sup>5</sup>), 70.1 (C<sup>2</sup>), 69.4 (C<sup>6</sup>), 33.2 (C<sup>7</sup>); HRMS  $m/z$  (ESI<sup>+</sup>) [Found (M+H)<sup>+</sup> 375.12604 C<sub>20</sub>H<sub>23</sub>O<sub>5</sub>S requires M<sup>+</sup> 375.12607]; LRMS  $m/z$  (ES<sup>+</sup>) 397 ([M+Na]<sup>+</sup>, 100%), 398 ([M+Na]<sup>+</sup>, 24%), 399 ([M+Na]<sup>+</sup>, 8%); Analytical RP-HPLC (Method 1, 254 nm) Ret. time = 11.2 min, 99.6%.

**Benzyl 4,6-*O*-benzylidene- $\beta$ -D-galactopyranoside, **255****

To a stirred suspension of **103** (500 g, 1.85 mmol, 1.0 eq) in acetonitrile (10 mL) was added 4-TsOH·H<sub>2</sub>O (70 mg, 0.37 mmol, 0.2 eq) and benzaldehyde dimethyl acetal (350  $\mu$ L, 2.33 mmol, 1.3 eq). A clear solution immediately formed followed by formation of a colourless precipitate after 5 min. The precipitate was collected and washed with methanol. The methanol filtrate was concentrated *in vacuo*. To a suspension of this residue in acetonitrile (10 mL) was added 4-TsOH (45 mg, 0.24 mmol, 0.1 eq) and benzaldehyde dimethyl acetal (250  $\mu$ L, 1.67 mmol, 0.9 eq). The suspension was stirred at room temperature for 1 h and concentrated *in vacuo*. The crude residue was purified by gradient silica gel chromatography (0–100% ethyl acetate in petroleum ether). This was combined with the precipitate to yield benzyl 4,6-*O*-benzylidene- $\beta$ -D-galactopyranoside **255** (394 mg, 59%) as a colourless solid:  $R_f$  0.13 (1:2 petroleum ether:ethyl acetate);  $[\alpha]_D^{25} = -71.9$  ( $c$  0.5, CHCl<sub>3</sub>) [lit.<sup>430</sup>  $[\alpha]_D^{24} = -62.0$  ( $c$  0.65, CHCl<sub>3</sub>)]; mp 215–216 °C (ethyl acetate) [lit.<sup>430</sup> 213–215 °C];  $\bar{\nu}_{\max}$  (neat)/cm<sup>−1</sup> 2987 (br, O–H), 1453 (w), 1366 (w), 1249 (m), 1172 (m), 1076 (s), 1054 (s), 734 (s), 697 (s); <sup>1</sup>H NMR (400 MHz, CDCl<sub>3</sub>)  $\delta$  7.53–7.50 (2H, m, C<sup>14</sup>-H), 5.41–7.31 (8H, m, C<sup>9</sup>-H, C<sup>10</sup>-H, C<sup>11</sup>-H, C<sup>15</sup>-H, C<sup>16</sup>-H), 5.57 (1H, s, C<sup>12</sup>-H), 5.01 (1H, d,  $J_{AB}$  11.7, C<sup>7</sup>-H<sub>A</sub>), 4.64 (1H, d,  $J_{AB}$  11.7, C<sup>7</sup>-H<sub>B</sub>), 4.39 (1H, d,  $J$  7.7, C<sup>1</sup>-H), 4.38 (1H, dd,  $J_{AB}$  12.5,  $J_{BX}$  1.6, C<sup>6</sup>-H<sub>B</sub>), 4.22 (1H, dd,  $J$  3.9, 1.3, C<sup>4</sup>-H), 4.11 (1H, dd,  $J_{AB}$  12.5,  $J_{AX}$  1.8, C<sup>6</sup>-H<sub>A</sub>), 3.83 (1H, dd,  $J$  9.7, 7.7, 1.9, C<sup>2</sup>-H), 3.69 (1H, dd,  $J$  9.4, 9.2, 3.9, C<sup>3</sup>-H), 3.50 (1H, ddd,  $J_{AX}$  1.8,  $J_{BX}$  1.6,  $J$  1.3, C<sup>5</sup>-H<sub>X</sub>), 2.54 (1H, d,  $J$  9.2, C<sup>3</sup>-OH), 2.52 (1H, d,  $J$  1.9, C<sup>2</sup>-OH); <sup>13</sup>C NMR (101 MHz, CDCl<sub>3</sub>)  $\delta$  137.6 (C<sup>8</sup> or C<sup>13</sup>), 137.2 (C<sup>8</sup> or C<sup>13</sup>), 129.4 (C<sup>16</sup>), 128.7 (C<sup>9</sup> or C<sup>10</sup> or C<sup>15</sup>), 128.4 (C<sup>9</sup> or C<sup>10</sup> or C<sup>15</sup>), 128.3 (C<sup>9</sup> or C<sup>10</sup> or C<sup>15</sup>), 128.2 (C<sup>11</sup>), 126.5 (C<sup>14</sup>), 101.7 (C<sup>12</sup>), 101.6 (C<sup>1</sup>), 75.4 (C<sup>4</sup>), 72.8 (C<sup>3</sup>), 72.0 (C<sup>2</sup>), 71.1 (C<sup>7</sup>), 69.3 (C<sup>6</sup>), 66.9 (C<sup>5</sup>); HRMS  $m/z$  (ESI<sup>+</sup>) [Found (M+Na)<sup>+</sup> 381.13094 C<sub>20</sub>H<sub>22</sub>O<sub>6</sub>Na requires M<sup>+</sup> 381.13086]; LRMS  $m/z$  (ES<sup>+</sup>) 381

( $[M+Na]^+$ , 100%), 382 ( $[M+Na]^+$ , 22%), 383 ( $[M+Na]^+$ , 4%); Analytical RP-HPLC (Method 1, 254 nm) Ret. time = 10.9 min, >99.9%. The data are in good agreement with the literature.<sup>430</sup>

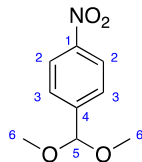
### Isopropyl 4,6-*O*-benzylidene-1-thio- $\beta$ -D-galactopyranoside, **187**



To a suspension of isopropyl 1-thio- $\beta$ -D-galactopyranoside **76** (4.99 g, 20.9 mmol, 1.0 eq) in  $CH_2Cl_2$  (50 mL) was added 4-TsOH·H<sub>2</sub>O (200 mg, 1.05 mmol, 0.05 eq) and benzaldehyde dimethyl acetal (1.30 mL, 29.2 mmol, 1.4 eq). The suspension was stirred at room temperature for 1 h. The resulting solution was quenched with triethylamine (200  $\mu$ L) and concentrated *in vacuo*. The crude residue was purified by crystallisation ( $CH_2Cl_2$ ) to yield isopropyl 4,6-*O*-benzylidene-1-thio- $\beta$ -D-galactopyranoside **187** (6.89 g, 95%) as colourless crystals:  $R_f$  0.37 (ethyl acetate);  $[\alpha]_D^{25} = -85.3$  ( $c$  1.0,  $CHCl_3$ ) [lit.<sup>298</sup>  $[\alpha]_D^{25} = -89.9$  ( $c$  1.0,  $CHCl_3$ )]; mp 180–181 °C ( $CH_2Cl_2$ ) [lit.<sup>298</sup> 176–178 °C];  $\bar{\nu}_{max}$  (thin film)/ $cm^{-1}$  3388 (br, O–H), 2963 (m), 2923 (m), 2867 (m), 1450 (m), 1403 (m), 1364 (m), 1244 (m), 1166 (m), 1100 (s), 1052 (s), 997 (m), 897 (w), 761 (w), 698 (w);  $^1H$  NMR (400 MHz,  $CDCl_3$ )  $\delta$  7.51–7.46 (2H, m,  $C^{12}$ -H), 7.39–7.34 (3H,  $C^{13}$ -H,  $C^{14}$ -H), 5.53 (1H, s,  $C^{10}$ -H), 4.40 (1H, d,  $J$  9.4,  $C^1$ -H), 4.33 (1H, dd,  $J_{AB}$  12.5,  $J_{BX}$  1.5,  $C^6$ - $H_B$ ), 4.25 (1H, dd,  $J$  3.7, 1.2,  $C^4$ -H), 4.03 (1H, dd,  $J_{AB}$  12.5,  $J_{AX}$  1.7,  $C^6$ - $H_A$ ), 3.77 (1H, dd,  $J$  9.4, 9.3,  $C^2$ -H), 3.72–3.65 (1H, m,  $C^3$ -H), 3.49 (1H, ddd,  $J_{AX}$  1.7,  $J_{BX}$  1.5,  $J$  1.2,  $C^5$ - $H_X$ ), 3.28 (1H, sept,  $J$  6.7,  $C^7$ -H), 2.67 (1H, br s,  $C^3$ -OH), 2.65 (1H, br s,  $C^2$ -OH), 1.38 (3H, d,  $J$  6.7,  $C^8$ - $H_3$  or  $C^9$ - $H_3$ ), 1.35 (3H, d,  $J$  6.7,  $C^8$ - $H_3$  or  $C^9$ - $H_3$ );  $^{13}C$  NMR (101 MHz,  $CDCl_3$ )  $\delta$  137.7 ( $C^{11}$ ), 129.4 ( $C^{14}$ ), 128.4 ( $C^{13}$ ), 126.6 ( $C^{12}$ ), 101.7 ( $C^{10}$ ), 85.6 ( $C^1$ ), 75.7 ( $C^4$ ), 74.1 ( $C^3$ ), 70.21 ( $C^2$  or  $C^5$ ), 70.17 ( $C^2$  or  $C^5$ ), 69.5 ( $C^6$ ), 35.1 ( $C^7$ ), 24.5 ( $C^8$  or  $C^9$ ), 24.2 ( $C^8$  or  $C^9$ ); HRMS  $m/z$  (ESI<sup>+</sup>) [Found ( $M+Na$ )<sup>+</sup> 349.10814  $C_{16}H_{22}O_5SNa$  requires  $M^+$  349.10802]; LRMS  $m/z$  (ES<sup>+</sup>) 349 ( $[M+Na]^+$ , 100%), 350

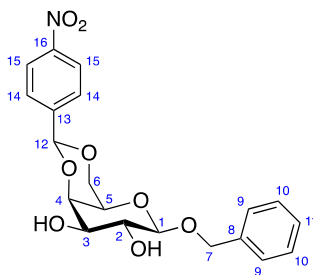
( $[M+N]^+$ , 18%), 351 ( $[M+Na]^+$ , 10%); Analytical RP-HPLC (Method 4, 254 nm) Ret. time = 10.5 min, 98.5%. The data are in good agreement with the literature.<sup>298</sup>

#### 4-Nitrobenzaldehyde dimethyl acetal, **257**



To a suspension of 4-nitrobenzaldehyde (5.04 g, 33.3 mmol, 1.0 eq) in methanol (20 mL) was added trimethylorthoformate (3.80 mL, 34.7 mmol, 1.1 eq) and 4-TsOH·H<sub>2</sub>O (320 mg, 1.68 mmol, 0.05 eq). The resulting solution was stirred under reflux for 5.5 h. The reaction was quenched with triethylamine (320  $\mu$ L) and concentrated *in vacuo*. The crude residue was purified by gradient silica gel chromatography (0–6% diethyl ether in petroleum ether) to yield 4-nitrobenzaldehyde dimethyl acetal **257** (6.57 g, 99%) as a pale yellow liquid: 0.37 (1:19 diethyl ether:petroleum ether);  $\bar{\nu}_{\text{max}}$  (thin film)/cm<sup>-1</sup> 2939 (w), 2833 (w), 1523 (s, N=O), 1344 (s, N=O), 1205 (m), 1101 (s), 1056 (s), 854 (m); <sup>1</sup>H NMR (400 MHz, CDCl<sub>3</sub>)  $\delta$  8.26–8.18 (2H, m, C<sup>2</sup>-H), 7.68–7.60 (2H, m, C<sup>3</sup>-H), 5.47 (1H, s, C<sup>5</sup>-H), 3.33 (6H, s, C<sup>6</sup>-H<sub>3</sub>); LRMS  $m/z$  (ES<sup>+</sup>) 220 ( $[M+Na]^+$ , 100%), 221 ( $[M+Na]^+$ , 15%), 222 ( $[M+Na]^+$ , 9%). The data are in good agreement with the literature.<sup>357</sup>

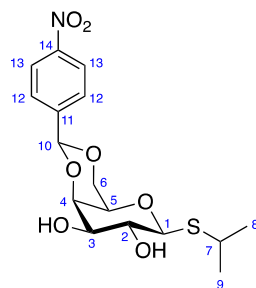
#### Benzyl 4,6-O-(4-nitrobenzylidene)- $\beta$ -D-galactopyranoside, **127**



To a suspension of **103** (150 mg, 1.85 mmol, 1.0 eq) in 4-nitrobenzaldehyde dimethyl acetal **257** (1.40 mL, 8.33 mmol, 4.5 eq) was added indium triflate (76 mg, 0.14 mmol, 0.07 eq). The suspension was stirred at room temperature for 17.5 h. The reaction mixture was directly purified by gradient silica gel chromatography (0–100% ethyl acetate in petroleum ether) to yield benzyl

4,6-*O*-(4-nitrobenzylidene)- $\beta$ -D-galactopyranoside **127** (85 mg, 38%) as a colourless solid:  $R_f$  0.37 (ethyl acetate); mp 196–198 °C (ethyl acetate);  $[\alpha]_D^{25} = -24.0$  ( $c$  1.0, MeOH);  $\bar{\nu}_{\max}$  (thin film)/ $\text{cm}^{-1}$  3520 (w, O–H), 2870 (w), 1607 (w), 1526 (s, N=O), 1497 (w), 1351 (s, N=O), 1156 (m), 1087 (s, C–O), 1050 (s), 1013 (s), 860 (m), 741 (s), 700 (s);  $^1\text{H}$  NMR (500 MHz,  $\text{CDCl}_3$ )  $\delta$  8.25–8.20 (2H, m,  $\text{C}^{15}\text{-H}$ ), 7.73–7.69 (2H, m,  $\text{C}^{14}\text{-H}$ ), 7.39–7.30 (5H, m,  $\text{C}^9\text{-H}$ ,  $\text{C}^{10}\text{-H}$ ,  $\text{C}^{11}\text{-H}$ ), 5.65 (1H, s,  $\text{C}^{12}\text{-H}$ ), 5.00 (1H, d,  $J_{\text{AB}}$  11.7,  $\text{C}^7\text{-H}_A$ ), 4.63 (1H, d,  $J_{\text{AB}}$  11.7,  $\text{C}^7\text{-H}_B$ ), 4.41 (1H, dd,  $J_{\text{AB}}$  12.5,  $J_{\text{BX}}$  1.5,  $\text{C}^6\text{-H}_B$ ), 4.39 (1H, d,  $J$  7.6,  $\text{C}^1\text{-H}$ ), 4.27 (1H, dd,  $J$  3.8, 1.1,  $\text{C}^4\text{-H}$ ), 4.14 (1H, dd,  $J_{\text{AB}}$  12.5,  $J_{\text{AX}}$  1.8,  $\text{C}^6\text{-H}_A$ ), 3.81 (1H, ddd,  $J$  9.7, 7.6, 2.1,  $\text{C}^2\text{-H}$ ), 3.72 (1H, ddd,  $J$  9.7, 7.6, 3.8,  $\text{C}^3\text{-H}$ ), 3.52 (1H, ddd,  $J_{\text{AX}}$  1.8,  $J_{\text{BX}}$  1.5,  $J$  1.1,  $\text{C}^5\text{-H}_X$ ), 2.52 (1H, d,  $J$  2.1,  $\text{C}^2\text{-OH}$ ), 2.50 (1H, d,  $J$  7.6,  $\text{C}^3\text{-OH}$ );  $^{13}\text{C}$  NMR (126 MHz,  $\text{CDCl}_3$ )  $\delta$  148.5 ( $\text{C}^{16}$ ), 143.9 ( $\text{C}^{13}$ ), 137.0 ( $\text{C}^8$ ), 128.7 ( $\text{C}^{10}$ ), 128.32 ( $\text{C}^9$ ), 128.27 ( $\text{C}^{11}$ ), 127.7 ( $\text{C}^{14}$ ), 123.6 ( $\text{C}^{15}$ ), 101.8 ( $\text{C}^1$ ), 99.9 ( $\text{C}^{12}$ ), 75.6 ( $\text{C}^4$ ), 72.6 ( $\text{C}^3$ ), 71.8 ( $\text{C}^2$ ), 71.2 ( $\text{C}^7$ ), 69.4 ( $\text{C}^6$ ), 66.7 ( $\text{C}^5$ ); HRMS  $m/z$  ( $\text{ESI}^+$ ) [Found ( $\text{M}+\text{Na}$ ) $^+$  426.11564  $\text{C}_{20}\text{H}_{21}\text{NO}_8\text{Na}$  requires  $\text{M}^+$  426.11594]; LRMS  $m/z$  ( $\text{ES}^+$ ) 426 ( $[\text{M}+\text{Na}]^+$ , 100%), 427 ( $[\text{M}+\text{Na}]^+$ , 20%), 428 ( $[\text{M}+\text{Na}]^+$ , 4%); Analytical RP-HPLC (Method 1, 254 nm) Ret. time = 11.3 min, Purity = 99.2%.

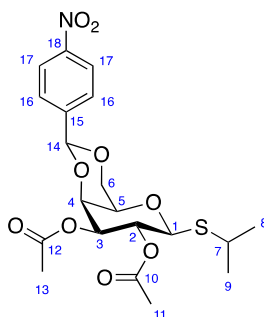
#### Isopropyl 4,6-*O*-(4-nitrobenzylidene)-1-thio- $\beta$ -D-galactopyranoside, **94**



To a suspension of isopropyl 1-thio- $\beta$ -D-galactopyranoside **76** (199 mg, 0.835 mmol, 1.0 eq) in  $\text{CH}_2\text{Cl}_2$  (2 mL) was added 4-TsOH $\cdot$ H $_2\text{O}$  (6 mg, 0.03 mmol, 0.04 eq) and 4-nitrobenzaldehyde dimethyl acetal **257** (234  $\mu\text{L}$ , 281 mg, 1.43 mmol, 1.7 eq). The reaction mixture was stirred at room temperature for 23 h, quenched with triethylamine (15  $\mu\text{L}$ ), and concentrated *in vacuo*. The crude residue was purified by gradient silica gel chromatography (50–100% ethyl acetate in petroleum ether) to yield isopropyl 4,6-*O*-(4-nitrobenzylidene)-1-thio- $\beta$ -D-galactopyranoside **94**

(182 mg, 59%) as a colourless solid:  $R_f$  0.49 (ethyl acetate);  $[\alpha]_D^{25} = -82.7$  ( $c$  1.0,  $\text{CHCl}_3$ ); mp 139–140 °C (methanol);  $\bar{\nu}_{\text{max}}$  (thin film)/ $\text{cm}^{-1}$  3377 (br, O–H), 2959 (w), 2922 (w), 2866 (w), 1609 (w), 1526 (s, N=O), 1423 (w), 1348 (s, N=O), 1242 (w), 1167 (m), 1101 (s), 1050 (s), 853 (m), 814 (w), 738 (w), 703 (w);  $^1\text{H}$  NMR (500 MHz,  $\text{CDCl}_3$ )  $\delta$  8.23–8.21 (2H, m,  $\text{C}^{13}\text{-H}$ ), 7.70–7.67 (2H, m,  $\text{C}^{12}\text{-H}$ ), 5.63 (1H, s,  $\text{C}^{10}\text{-H}$ ), 4.42 (1H, d,  $J$  9.3,  $\text{C}^1\text{-H}$ ), 4.36 (1H, dd,  $J_{\text{AB}}$  12.5,  $J_{\text{BX}}$  1.4,  $\text{C}^6\text{-H}_B$ ), 4.31 (1H, dd,  $J$  3.1, 1.2,  $\text{C}^4\text{-H}$ ), 4.07 (1H, dd,  $J_{\text{AB}}$  12.5,  $J_{\text{AX}}$  1.7,  $\text{C}^6\text{-H}_A$ ), 3.76–3.72 (2H, m,  $\text{C}^2\text{-H}$ ,  $\text{C}^3\text{-H}$ ), 3.54 (1H, ddd,  $J_{\text{AX}}$  1.7,  $J_{\text{BX}}$  1.4,  $J$  1.2,  $\text{C}^5\text{-H}_X$ ), 3.26 (1H, sept,  $J$  6.8,  $\text{C}^7\text{-H}$ ), 2.61 (2H, br s,  $\text{C}^2\text{-OH}$ ,  $\text{C}^3\text{-OH}$ ), 1.37 (3H, d,  $J$  6.8,  $\text{C}^8\text{-H}$  or  $\text{C}^9\text{-H}$ ), 1.35 (3H, d,  $J$  6.8,  $\text{C}^8\text{-H}$  or  $\text{C}^9\text{-H}$ );  $^{13}\text{C}$  NMR (126 MHz,  $\text{CDCl}_3$ )  $\delta$  148.5 ( $\text{C}^{14}$ ), 143.9 ( $\text{C}^{11}$ ), 127.7 ( $\text{C}^{12}$ ), 123.6 ( $\text{C}^{13}$ ), 99.9 ( $\text{C}^{10}$ ), 85.8 ( $\text{C}^1$ ), 75.8 ( $\text{C}^4$ ), 73.9 ( $\text{C}^2$  or  $\text{C}^3$ ), 70.1 ( $\text{C}^2$  or  $\text{C}^3$ ), 70.0 ( $\text{C}^5$ ), 69.5 ( $\text{C}^6$ ), 35.5 ( $\text{C}^7$ ), 24.4 ( $\text{C}^8$  or  $\text{C}^9$ ), 24.1 ( $\text{C}^8$  or  $\text{C}^9$ ); HRMS  $m/z$  (ESI $^+$ ) [Found ( $\text{M}+\text{Na}$ ) $^+$  394.09196  $\text{C}_{16}\text{H}_{21}\text{NO}_7\text{SNa}$  requires  $\text{M}^+$  394.09309]; LRMS  $m/z$  (ES $^+$ ) 394 ( $[\text{M}+\text{Na}]^+$ , 100%), 395 ( $[\text{M}+\text{Na}]^+$ , 19%), 396 ( $[\text{M}+\text{Na}]^+$ , 5%); Analytical RP-HPLC (Method 1, 254 nm) Ret. time = 10.7 min, Purity = 99.6%.

#### Isopropyl 2,3-di-*O*-acetyl-4,6-*O*-(4-nitrobenzylidene)-1-thio- $\beta$ -D-galactopyranoside, **308**

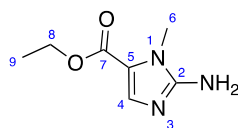


To a solution of **94** (205 mg, 0.552 mmol, 1.0 eq) in pyridine (2 mL) was added acetic anhydride (2 mL). The solution was stirred at room temperature for 3 h and concentrated *in vacuo*. The crude residue was purified by gradient silica gel chromatography (Biotage, 0–50% ethyl acetate in heptane) to yield isopropyl 2,3-di-*O*-acetyl-4,6-*O*-(4-nitrobenzylidene)-1-thio- $\beta$ -D-galactopyranoside **308** (251 mg, >99%) as a colourless solid:  $R_f$  0.33 (1:1: ethyl acetate:heptane);  $[\alpha]_D^{25} = +40.1$  ( $c$  1.0,  $\text{CHCl}_3$ ); mp 92–94 °C (chloroform);  $\bar{\nu}_{\text{max}}$  (thin film)/ $\text{cm}^{-1}$  2964 (w), 2926 (w), 2866 (w), 2362 (w), 1750 (s, C=O), 1609 (w), 1525 (s, N=O), 1447 (w), 1349 (s, N=O), 1239 (s, C–O), 1173 (w), 1097 (m), 1054 (s), 929 (w), 853 (w), 738 (w);  $^1\text{H}$  NMR (500 MHz,  $\text{CDCl}_3$ )



$\delta$  8.26–8.22 (2H, m, C<sup>17</sup>-H), 7.71–7.66 (2H, m, C<sup>16</sup>-H), 5.58 (1H, s, C<sup>14</sup>-H), 5.40 (1H, dd,  $J$  10.0, 10.0, C<sup>2</sup>-H), 5.01 (1H, dd,  $J$  10.0, 3.6, C<sup>3</sup>-H), 4.56 (1H, d,  $J$  10.0, C<sup>1</sup>-H), 4.45 (1H, dd,  $J$  3.6, 1.1, C<sup>4</sup>-H), 4.36 (1H, dd,  $J_{AB}$  12.5,  $J_{BX}$  1.6, C<sup>6</sup>-H<sub>B</sub>), 4.04 (1H, dd,  $J_{AB}$  12.5,  $J_{AX}$  1.7, C<sup>6</sup>-H<sub>A</sub>), 3.57 (1H, ddd,  $J_{AX}$  1.7,  $J_{BX}$  1.6,  $J$  1.1, C<sup>5</sup>-H<sub>X</sub>), 3.26 (1H, sept,  $J$  6.7, C<sup>7</sup>-H), 2.09 (3H, s, C<sup>13</sup>-H<sub>3</sub>), 2.07 (3H, s, C<sup>11</sup>-H<sub>3</sub>), 1.35 (2H, d,  $J$  6.7, C<sup>8</sup>-H<sub>3</sub> or C<sup>9</sup>-H<sub>3</sub>), 1.27 (3H, d,  $J$  6.7, C<sup>8</sup>-H<sub>3</sub> or C<sup>9</sup>-H<sub>3</sub>); <sup>13</sup>C NMR (126 MHz, CDCl<sub>3</sub>)  $\delta$  170.8 (C<sup>12</sup>), 169.6 (C<sup>10</sup>), 148.5 (C<sup>18</sup>), 143.9 (C<sup>15</sup>), 127.7 (C<sup>16</sup>), 123.6 (C<sup>17</sup>), 99.6 (C<sup>14</sup>), 83.4 (C<sup>1</sup>), 73.9 (C<sup>4</sup>), 73.1 (C<sup>3</sup>), 69.6 (C<sup>5</sup>), 69.3 (C<sup>6</sup>), 67.0 (C<sup>2</sup>), 35.0 (C<sup>7</sup>), 24.8 (C<sup>8</sup> or C<sup>9</sup>), 23.6 (C<sup>8</sup> or C<sup>9</sup>), 21.0 (C<sup>11</sup>, C<sup>13</sup>); HRMS  $m/z$  (ESI<sup>+</sup>) [Found (M+Na)<sup>+</sup> 478.11416 C<sub>20</sub>H<sub>25</sub>NO<sub>9</sub>SNa requires M<sup>+</sup> 478.11422]; LRMS  $m/z$  (ES<sup>+</sup>) 478 ([M+Na]<sup>+</sup>, 100%), 479 ([M+Na]<sup>+</sup>, 21%), 480 ([M+Na]<sup>+</sup>, 8%); Analytical RP-HPLC (Method 2, 220/254/300/365 nm) Ret. time = 10.3 min, Purity = 99.4%.

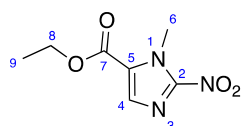
#### Ethyl-2-amino-1-methyl-1H-imidazole-5-carboxylate, **264**



To a suspension of sarcosine ethyl ester hydrochloride **261** (3.327 g, 21.66 mmol, 1.0 eq) in ethyl formate (60 mL) and THF (60 mL) was added sodium hydride (60% dispersion in mineral oil, 5.975 g, 149.4 mmol, 6.9 eq) slowly, portionwise at room temperature. The suspension was stirred at room temperature for 3 h, until the reaction had become a pale-yellow suspension, and concentrated *in vacuo*. The residue was triturated with hexane (3 × 120 mL) and excess hexane removed *in vacuo*. The residue was suspended in ethanol (60 mL) and conc. aq. HCl (12 mL) and stirred under reflux for 2 h. The reaction mixture was filtered and the colourless solid washed with hot ethanol (3 × 100 mL). The filtrate was concentrated *in vacuo* and the residue suspended in ethanol (75 mL) and water (35 mL). The solution was adjusted to pH 3 with 2 M aq. NaOH. Cyanamide (1.833 g, 43.60 mmol, 2.0 eq) was added and the solution was stirred under reflux for 1.5 h, cooled to room temperature, and concentrated *in vacuo* to approximately  $\frac{1}{8}$  of the original volume. The solution was adjusted to pH 8 using solid K<sub>2</sub>CO<sub>3</sub>. The resulting precipitate was filtered, washed with 1 M K<sub>2</sub>CO<sub>3</sub>, and dried *in vacuo* to yield ethyl-2-amino-1-methyl-1H-

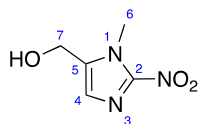
imidazole-5-carboxylate **264** (1.833 g, 50%) as a pale yellow solid:  $R_f$  0.14 (ethyl acetate); mp 144–146 °C (water) [lit. 130–133 °C];  $^1\text{H}$  NMR (400 MHz,  $\text{CDCl}_3$ )  $\delta$  7.44 (1H, s,  $\text{C}^4\text{-H}$ ), 4.26 (2H, q,  $J$  7.1,  $\text{C}^8\text{-H}_2$ ), 4.22 (2H, br s,  $\text{C}^2\text{-NH}_2$ ), 3.67 (3H, s,  $\text{C}^6\text{-H}_3$ ), 1.33 (3H, t,  $J$  7.1,  $\text{C}^9\text{-H}_3$ ); LRMS  $m/z$  ( $\text{ES}^+$ ) 170 ( $[\text{M}+\text{H}]^+$ , 100%), 171 ( $[\text{M}+\text{H}]^+$ , 9%), 172 ( $[\text{M}+\text{H}]^+$ , 1%). The data are in good agreement with the literature.<sup>233</sup>

### Ethyl-2-nitro-1-methyl-1*H*-imidazole-5-carboxylate, **265**



To a solution of sodium nitrite (13.65 g, 197.8 mmol, 10.0 eq) in water (17 mL) at 0 °C was added dropwise over 30 min a solution of **264** (3.346 g, 19.78 mmol, 1.0 eq) in acetic acid (34 mL). The solution was warmed to room temperature and stirred for 6 h. The reaction solution was diluted with  $\text{CH}_2\text{Cl}_2$  (100 mL) and washed with brine (40 mL). The aqueous layer was back extracted with  $\text{CH}_2\text{Cl}_2$  ( $2 \times 30$  mL). The organic layers were combined, dried over  $\text{MgSO}_4$ , filtered, and concentrated *in vacuo*. The crude residue was purified by silica gel chromatography ( $\text{CH}_2\text{Cl}_2$ ) to yield ethyl-2-nitro-1-methyl-1*H*-imidazole-5-carboxylate **265** (2.324 g, 59%) as a pale yellow solid:  $R_f$  0.45 (1:2 ethyl acetate:petroleum ether); mp 58–60 °C ( $\text{CH}_2\text{Cl}_2$ ) [lit. 56–58 °C];  $^1\text{H}$  NMR (400 MHz,  $\text{CDCl}_3$ )  $\delta$  7.73 (1H, s,  $\text{C}^4\text{-H}$ ), 4.39 (2H, q,  $J$  7.1,  $\text{C}^8\text{-H}_2$ ), 4.34 (3H, s,  $\text{C}^6\text{-H}_3$ ), 1.40 (3H, t,  $J$  7.1,  $\text{C}^9\text{-H}_3$ ); LRMS  $m/z$  ( $\text{ES}^+$ ) 200 ( $[\text{M}+\text{H}]^+$ , 100%), 201 ( $[\text{M}+\text{H}]^+$ , 10%), 222 ( $[\text{M}+\text{Na}]^+$ , 75%). The data are in good agreement with the literature.<sup>233</sup>

### (1-Methyl-2-nitro-1*H*-imidazol-5-yl)methanol, **266**



To a solution of **265** (2.320 g, 11.65 mmol, 1.0 eq) in THF (60 mL) and methanol (5 mL) at –10 °C was added sodium borohydride (1.300 g, 34.46 mmol, 2.9 eq) portionwise over 15 min. The reaction mixture was stirred at 0 °C for 45 min. The reaction solution was warmed to room temperature and stirred for a further 3 h. The reaction mixture was cooled to 0 °C, quenched with

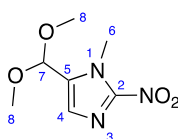
the addition of ice, and the solution adjusted to pH 7 with 1 M aq. HCl. The aqueous mixture was saturated with solid sodium chloride and the organic components extracted with ethyl acetate ( $4 \times 100$  mL). The organic layers were combined, dried over  $\text{MgSO}_4$ , filtered, and concentrated *in vacuo*. The crude residue was purified by silica gel chromatography (100% ethyl acetate) to yield (1-methyl-2-nitro-1*H*-imidazol-5-yl)methanol **266** (1.677 g, 92%) as a yellow solid:  $R_f$  0.31 (ethyl acetate); mp 145–147 °C (ethyl acetate) [lit. 141–145 °C];  $^1\text{H}$  NMR (400 MHz,  $\text{DMSO}-d_6$ )  $\delta$  7.11 (1H, s,  $\text{C}^4\text{-H}$ ), 5.49 (1H, t,  $J$  5.4,  $\text{C}^7\text{-OH}$ ), 4.54 (2H, d,  $J$  5.4,  $\text{C}^7\text{-H}_2$ ), 3.91 (3H, s,  $\text{C}^6\text{-H}_3$ ); LRMS  $m/z$  ( $\text{ES}^+$ ) 180 ( $[\text{M}+\text{Na}]^+$ , 100%), 181 ( $[\text{M}+\text{Na}]^+$ , 7%). The data are in good agreement with the literature.<sup>233</sup>

#### 1-Methyl-2-nitro-1*H*-imidazole-5-carbaldehyde, **267**



To a suspension of **266** (360 mg, 2.29 mmol, 1.0 eq) in chloroform (10 mL) was added manganese dioxide (1.303 g, 14.99 mmol, 6.5 eq). The reaction mixture was stirred under reflux for 16 h, filtered through Celite<sup>®</sup> and concentrated *in vacuo*. The crude residue was purified by silica gel chromatography (50% ethyl acetate in petroleum ether) to yield 1-methyl-2-nitro-1*H*-imidazole-5-carbaldehyde **267** (280 mg, 79%) as a pale yellow solid:  $R_f$  0.33 (1:1 petroleum ether: ethyl acetate); mp 112–114 °C (ethyl acetate) [lit. 113–115 °C];  $^1\text{H}$  NMR (500 MHz,  $\text{CDCl}_3$ )  $\delta$  9.93 (1H, s,  $\text{C}^7\text{-H}$ ), 7.81 (1H, s,  $\text{C}^4\text{-H}$ ), 4.36 (3H, s,  $\text{C}^6\text{-H}_3$ ); LRMS  $m/z$  ( $\text{ES}^+$ ) 210 ( $[\text{M}+\text{MeOH}+\text{Na}]^+$ , 100%), 211 ( $[\text{M}+\text{MeOH}+\text{Na}]^+$ , 15%). The data are in good agreement with the literature.<sup>233</sup>

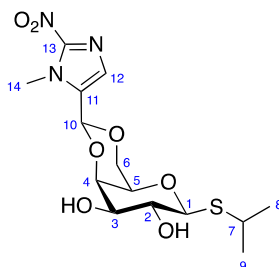
#### 5-(dimethoxymethyl)-1-methyl-2-nitro-1*H*-imidazole, **268**



To a suspension of **267** (275 mg, 1.77 mmol, 1.0 eq) in methanol (2 mL) was added 4-TsOH· $\text{H}_2\text{O}$  (17 mg, 0.089 mmol, 0.05 eq) and trimethyl orthoformate (215  $\mu\text{L}$ , 1.97 mmol, 1.1 eq). The

suspension was stirred under reflux for 14 h, after which time an orange solution had formed. The reaction was quenched with triethylamine (20  $\mu$ L) and concentrated *in vacuo*. The crude residue was purified by silica gel chromatography (50% ethyl acetate in petroleum ether) to yield 5-(dimethoxymethyl)-1-methyl-2-nitro-1*H*-imidazole **268** (302 mg, 85%) as a dark yellow solid:  $R_f$  0.34 (1:1 petroleum ether:ethyl acetate); mp 66–69 °C (ethyl acetate);  $\bar{\nu}_{\max}$  (neat)/ $\text{cm}^{-1}$  3132 (w), 2940 (w), 2837 (w), 1678 (w), 1527 (m, N=O), 1485 (m), 1361 (m, N=O), 1339 (m), 1272 (m), 1204 (m), 1178 (m), 1117 (m), 1097 (m, C–O), 1050 (s), 983 (s), 893 (m), 871 (m), 834 (s), 661 (w), 629 (w);  $^1\text{H}$  NMR (500 MHz,  $\text{CDCl}_3$ )  $\delta$  7.19 (1H, s,  $\text{C}^4\text{-H}$ ), 5.41 (1H, s,  $\text{C}^7\text{-H}$ ), 4.03 (3H, s,  $\text{C}^6\text{-H}_3$ ), 3.36 (6H, s,  $\text{C}^8\text{-H}_3$ );  $^{13}\text{C}$  NMR (126 MHz,  $\text{CDCl}_3$ )  $\delta$  146.4 ( $\text{C}^2$ ), 133.8 ( $\text{C}^5$ ), 128.5 ( $\text{C}^4$ ), 97.1 ( $\text{C}^7$ ), 53.5 ( $\text{C}^8$ ), 34.9 ( $\text{C}^6$ ); HRMS  $m/z$  ( $\text{ESI}^+$ ) [Found ( $\text{M}+\text{H}$ ) $^+$  202.08231  $\text{C}_7\text{H}_{12}\text{N}_3\text{O}_4$  requires  $\text{M}^+$  202.08223]; LRMS  $m/z$  ( $\text{ES}^+$ ) 224 ( $[\text{M}+\text{Na}]^+$ , 100%), 225 ( $[\text{M}+\text{Na}]^+$ , 8%), 226 ( $[\text{M}+\text{Na}]^+$ , 1%); Analytical RP-HPLC (Method 2, 254 nm) Ret. time = 6.5 min, Purity = 97.3%.

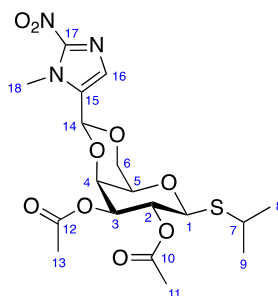
**Isopropyl 4,6-*O*-(1-methyl-2-nitro-1*H*-imidazol-5-yl(methylidene))-1-thio- $\beta$ -D-galactopyranoside, **253****



To a suspension of isopropyl 1-thio- $\beta$ -D-galactopyranoside **76** (155 mg, 0.650 mmol, 1.0 eq) in  $\text{CH}_2\text{Cl}_2$  (2 mL) was added 4-TsOH $\cdot\text{H}_2\text{O}$  (14 mg, 0.074 mmol, 0.1 eq) and **268** (200 mg, 0.994 mmol, 1.5 eq) and the reaction suspension stirred under reflux for 7.5 h. The reaction was quenched with triethylamine (20  $\mu$ L) and concentrated *in vacuo*. The crude residue was purified by gradient silica gel chromatography (50–100% ethyl acetate in petroleum ether to 1% methanol in ethyl acetate) to yield isopropyl 4,6-*O*-(1-methyl-2-nitro-1*H*-imidazol-5-yl(methylidene))-1-thio- $\beta$ -D-galactopyranoside **253** (179 mg, 73%) as a pale yellow solid:  $R_f$  0.31 (1:9 methanol:ethyl acetate);  $[\alpha]_{\text{D}}^{25} = -78.5$  ( $c$  1.0,  $\text{CHCl}_3$ ); mp 80–82 °C (ethyl acetate);  $\bar{\nu}_{\max}$  (thin film)/ $\text{cm}^{-1}$  3415 (br, O–H), 2964 (w), 2915 (w), 2867 (w), 1541 (m, N=O), 1495 (s), 1448 (m), 1335 (s, N=O),

1270 (w), 1243 (w), 1201 (w), 1160 (s, C–O), 1097 (s), 1069 (m), 1032 (s), 995 (m), 952 (w), 803 (w);  $^1\text{H}$  NMR (500 MHz,  $\text{CDCl}_3$ )  $\delta$  7.13 (1H, s,  $\text{C}^{12}\text{-H}$ ), 5.73 (1H, s,  $\text{C}^{10}\text{-H}$ ), 4.45 (1H, d,  $J$  9.3,  $\text{C}^1\text{-H}$ ), 4.31 (1H, dd,  $J_{\text{AB}}$  12.5,  $J_{\text{AX}}$  1.6,  $\text{C}^6\text{-H}_A$ ), 4.25 (1H, dd,  $J$  3.4, 1.2,  $\text{C}^4\text{-H}$ ), 4.19 (3H, s,  $\text{C}^{14}\text{-H}_3$ ), 4.00 (1H, dd,  $J_{\text{AB}}$  12.5,  $J_{\text{BX}}$  1.6,  $\text{C}^6\text{-H}_B$ ), 3.73 (1H, ddd,  $J$  9.4, 6.1, 3.4,  $\text{C}^3\text{-H}$ ), 3.68 (1H, ddd,  $J$  9.4, 9.3, 1.4,  $\text{C}^2\text{-H}$ ), 3.54 (1H, ddd,  $J_{\text{AX}}$  1.6,  $J_{\text{BX}}$  1.6,  $J$  1.2,  $\text{C}^5\text{-H}_X$ ), 3.24 (1H, sept,  $J$  6.8,  $\text{C}^7\text{-H}$ ), 2.87 (1H, d,  $J$  6.1,  $\text{C}^3\text{-OH}$ ), 2.72 (1H, d,  $J$  1.4,  $\text{C}^2\text{-OH}$ ), 1.358 (3H, d,  $J$  6.8,  $\text{C}^8\text{-H}_3$  or  $\text{C}^9\text{-H}_3$ ), 1.356 (3H, d,  $J$  6.8,  $\text{C}^8\text{-H}_3$  or  $\text{C}^9\text{-H}_3$ );  $^{13}\text{C}$  NMR (126 MHz,  $\text{CDCl}_3$ )  $\delta$  146.6 ( $\text{C}^{13}$ ), 132.7 ( $\text{C}^{11}$ ), 128.0 ( $\text{C}^{12}$ ), 94.6 ( $\text{C}^{10}$ ), 85.9 ( $\text{C}^1$ ), 75.9 ( $\text{C}^4$ ), 73.7 ( $\text{C}^3$ ), 70.3 ( $\text{C}^2$ ), 69.52 ( $\text{C}^5$  or  $\text{C}^6$ ), 69.47 ( $\text{C}^5$  or  $\text{C}^6$ ), 36.1 ( $\text{C}^{14}$ ), 35.7 ( $\text{C}^7$ ), 24.3 ( $\text{C}^8$  or  $\text{C}^9$ ), 24.2 ( $\text{C}^8$  or  $\text{C}^9$ ); HRMS  $m/z$  ( $\text{ESI}^+$ ) [Found ( $\text{M}+\text{H})^+$  376.11623  $\text{C}_{14}\text{H}_{22}\text{N}_3\text{O}_7\text{S}$  requires  $\text{M}^+$  376.11730]; LRMS  $m/z$  ( $\text{ES}^+$ ) 398 ( $[\text{M}+\text{Na}]^+$ , 100%), 399 ( $[\text{M}+\text{Na}]^+$ , 18%), 400 ( $[\text{M}+\text{Na}]^+$ , 9%); Analytical RP-HPLC (Method 1, 254 nm) Ret. time = 9.3 min, Purity = >99.9%.

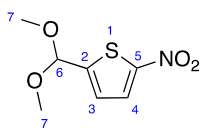
**Isopropyl 2,3-di-*O*-acetyl-4,6-*O*-(1-methyl-2-nitro-1*H*-imidazol-5-yl(methylidene))-1-thio- $\beta$ -D-galactopyranoside, **309****



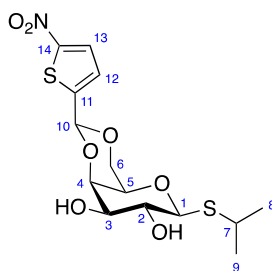
To a solution of **253** (100 mg, 0.266 mmol, 1.0 eq) in pyridine (1 mL) was added acetic anhydride (1 mL). The solution was stirred at room temperature for 15 h and concentrated *in vacuo*. The crude residue was purified by gradient silica gel chromatography (0–60% ethyl acetate in petroleum ether) to yield isopropyl 2,3-di-*O*-acetyl-4,6-*O*-(1-methyl-2-nitro-1*H*-imidazol-5-yl(methylidene))-1-thio- $\beta$ -D-galactopyranoside **309** (115 mg, 94%) as a pale-yellow foam: 0.14 (4:6 petroleum ether:ethyl acetate);  $[\alpha]_{\text{D}}^{25} = +57.6$  ( $c$  1.0,  $\text{CHCl}_3$ );  $\bar{\nu}_{\text{max}}$  (thin film)/ $\text{cm}^{-1}$  2967 (w), 2926 (w), 2867 (w), 1750 (s, C=O), 1542 (s, N=O), 1494 (m), 1371 (m), 1333 (m, N=O), 1239 (s, C–O), 1170 (w), 1094 (m), 1051 (s), 1001 (m), 927 (w), 836 (w), 753 (w);  $^1\text{H}$  NMR (500 MHz,

CDCl<sub>3</sub>)  $\delta$  7.15 (1H, s, C<sup>16</sup>-H), 5.69 (1H, s, C<sup>14</sup>-H), 5.28 (1H, dd,  $J$  1.0, 1.0, C<sup>2</sup>-H), 4.99 (1H, dd,  $J$  10.0, 3.4, C<sup>3</sup>-H), 4.60 (1H, d,  $J$  10.0, C<sup>1</sup>-H), 4.39 (1H, dd,  $J$  3.4, 1.0, C<sup>4</sup>-H), 4.33 (1H, dd,  $J_{AB}$  12.5,  $J_{AX}$  1.7, C<sup>6</sup>-H<sub>A</sub>), 4.25 (3H, s, C<sup>18</sup>-H<sub>3</sub>), 3.98 (1H, dd,  $J_{AB}$  12.5,  $J_{BX}$  1.7, C<sup>6</sup>-H<sub>B</sub>), 3.59 (1H, ddd,  $J_{AX}$  1.7,  $J_{BX}$  1.7,  $J$  1.0, C<sup>5</sup>-H<sub>X</sub>), 3.20 (1H, sept,  $J$  6.8, C<sup>7</sup>-H), 2.06 (3H, s, C<sup>11</sup>-H<sub>3</sub>), 2.05 (3H, s, C<sup>13</sup>-H<sub>3</sub>), 1.34 (3H, d,  $J$  6.8, C<sup>8</sup>-H<sub>3</sub> or C<sup>9</sup>-H<sub>3</sub>), 1.29 (3H, d,  $J$  6.8, C<sup>8</sup>-H<sub>3</sub> or C<sup>9</sup>-H<sub>3</sub>); <sup>13</sup>C NMR (126 MHz, CDCl<sub>3</sub>)  $\delta$  170.7 (C<sup>12</sup>), 169.5 (C<sup>10</sup>), 146.7 (C<sup>17</sup>), 132.6 (C<sup>15</sup>), 128.0 (C<sup>16</sup>), 94.6 (C<sup>14</sup>), 83.5 (C<sup>1</sup>), 74.0 (C<sup>4</sup>), 72.7 (C<sup>3</sup>), 69.2 (C<sup>5</sup>, C<sup>6</sup>), 66.9 (C<sup>2</sup>), 36.1 (C<sup>18</sup>), 35.2 (C<sup>7</sup>), 24.7 (C<sup>8</sup> or C<sup>9</sup>), 23.8 (C<sup>8</sup> or C<sup>9</sup>), 20.99 (C<sup>11</sup> or C<sup>13</sup>), 20.97 (C<sup>11</sup> or C<sup>13</sup>); HRMS  $m/z$  (ESI<sup>+</sup>) [Found (M+Na)<sup>+</sup> 482.12017 C<sub>18</sub>H<sub>25</sub>N<sub>3</sub>O<sub>9</sub>SNa requires M<sup>+</sup> 482.12037]; LRMS  $m/z$  (ES<sup>+</sup>) 482 ([M+Na]<sup>+</sup>, 100%), 483 ([M+Na]<sup>+</sup>, 20%), 484 ([M+Na]<sup>+</sup>, 8%); Analytical RP-HPLC (Method 2, 220/254/300/365 nm) Ret. time = 9.1 min, Purity = 99.1%.

## 2-(Dimethoxymethyl)-5-nitrothiophene, **270**



To a solution of 5-nitrothiophene-2-carboxaldehyde **269** (500 mg, 3.18 mmol, 1.0 eq) in methanol (5 mL) was added 4-TsOH·H<sub>2</sub>O (61 mg, 0.32 mmol, 0.1 eq) and trimethylorthoformate (390  $\mu$ L, 3.56 mmol, 1.1 eq). The reaction solution was stirred under reflux for 16 h, quenched with triethylamine, and concentrated *in vacuo*. The crude residue was purified by gradient silica gel chromatography (0–25% ethyl acetate in petroleum ether) to yield 2-(dimethoxymethyl)-5-nitrothiophene **270** (618 mg, 96%) as a brown liquid:  $R_f$  0.50 (1:3 ethyl acetate:petroleum ether);  $\bar{\nu}_{\max}$  (thin film)/cm<sup>-1</sup> 2939 (w), 2835 (w), 1541 (m, N=O), 1504 (s), 1441 (m), 1331 (s, N=O), 1174 (s), 1092 (s, C–O), 1057 (s), 976 (m), 901 (m), 815 (m), 734 (m), 675 (m); <sup>1</sup>H NMR (400 MHz, CDCl<sub>3</sub>)  $\delta$  7.84 (1H, d,  $J$  4.2, C<sup>4</sup>-H), 7.01 (1H, dd,  $J$  4.2, 1.0, C<sup>3</sup>-H), 5.61 (1H, d,  $J$  1.0, C<sup>6</sup>-H), 3.38 (6H, s, C<sup>7</sup>-H<sub>3</sub>); <sup>13</sup>C NMR (101 MHz, CDCl<sub>3</sub>)  $\delta$  128.5 (C<sup>4</sup>), 124.7 (C<sup>3</sup>), 98.9 (C<sup>6</sup>), 52.8 (C<sup>7</sup>); HRMS  $m/z$  (Methane CI) [Found (M+H)<sup>+</sup> 204.0328 C<sub>7</sub>H<sub>10</sub>NO<sub>4</sub>S requires M<sup>+</sup> 304.0325]; LRMS  $m/z$  (Methane CI) 204 ([M+H]<sup>+</sup>, 100%), 205 ([M+H]<sup>+</sup>, 8%), 206 ([M+H]<sup>+</sup>, 5%); Analytical RP-HPLC (Method 2, 254 nm) Ret. time = 9.4 min, Purity = >99.9%.

Isopropyl 4,6-*O*-(5-nitrothiophen-2-yl(methylidene))-1-thio- $\beta$ -D-galactopyranoside, **254**

To a solution of **270** (386 mg, 1.90 mmol, 1.5 eq) in  $\text{CH}_2\text{Cl}_2$  (3 mL) was added isopropyl 1-thio- $\beta$ -D-galactopyranoside **76** (300 mg, 1.26 mmol, 1.0 eq) and 4-TsOH $\cdot$ H $_2$ O (24 mg, 0.13 mmol, 0.1 eq) and the suspension was stirred under reflux for 22 h. The reaction was quenched with triethylamine and concentrated *in vacuo*. The crude residue was purified by crystallisation (methanol). The filtrate was further purified by gradient silica gel chromatography (50–100% ethyl acetate in petroleum ether) and combined with the crystals to yield isopropyl 4,6-*O*-(5-nitrothiophen-2-yl(methylidene))-1-thio- $\beta$ -D-galactopyranoside **254** (295 mg, 62%) as pale brown crystals:  $R_f$  0.14 (ethyl acetate);  $[\alpha]_D^{25} = -63.9$  ( $c$  1.0,  $\text{CHCl}_3$ ); mp 141–143 °C (methanol);  $\bar{\nu}_{\text{max}}$  (thin film)/ $\text{cm}^{-1}$  3383 (br, O–H), 2977 (m), 1546 (m, N=O), 1509 (w), 1456 (w), 1334 (s, N=O), 1242 (w), 1162 (m), 1098 (m), 1050 (s), 1025 (m), 997 (w), 962 (w), 895 (w), 848 (w), 815 (w), 734 (w);  $^1\text{H}$  NMR (500 MHz,  $\text{CDCl}_3$ )  $\delta$  7.80 (1H, d,  $J$  4.2,  $\text{C}^{13}\text{-H}$ ), 7.09 (1H, dd,  $J$  4.2, 0.6,  $\text{C}^{12}\text{-H}$ ), 5.76 (1H, s,  $\text{C}^{10}\text{-H}$ ), 4.40 (1H, d,  $J$  9.0,  $\text{C}^1\text{-H}$ ), 4.33 (1H, dd,  $J_{\text{AB}}$  12.6,  $J_{\text{BX}}$  1.5,  $\text{C}^6\text{-H}_B$ ), 4.29 (1H, dd,  $J$  3.3, 1.3,  $\text{C}^4\text{-H}$ ), 4.04 (1H, dd,  $J_{\text{AB}}$  12.6,  $J_{\text{AX}}$  1.7,  $\text{C}^6\text{-H}_A$ ), 3.76 (1H, dd,  $J$  9.1, 9.0,  $\text{C}^2\text{-H}$ ), 3.73 (1H, dd,  $J$  9.1, 3.3,  $\text{C}^3\text{-H}$ ), 3.53 (1H, ddd,  $J_{\text{AX}}$  1.7,  $J_{\text{BX}}$  1.5,  $J$  1.3,  $\text{C}^5\text{-H}_X$ ), 3.27 (1H, sept,  $J$  6.8,  $\text{C}^7\text{-H}$ ), 2.60 (2H, br s,  $\text{C}^2\text{-OH}$ ,  $\text{C}^3\text{-OH}$ ), 1.38 (3H, d,  $J$  6.8,  $\text{C}^8\text{-H}_3$  or  $\text{C}^9\text{-H}_3$ ), 1.35 (3H, d,  $J$  6.8,  $\text{C}^8\text{-H}_3$  or  $\text{C}^9\text{-H}_3$ );  $^{13}\text{C}$  NMR (126 MHz,  $\text{CDCl}_3$ )  $\delta$  152.3 ( $\text{C}^{14}$ ), 147.6 ( $\text{C}^{11}$ ), 128.0 ( $\text{C}^{13}$ ), 124.9 ( $\text{C}^{12}$ ), 96.8 ( $\text{C}^{10}$ ), 85.8 ( $\text{C}^1$ ), 75.8 ( $\text{C}^4$ ), 73.8 ( $\text{C}^3$ ), 69.8 ( $\text{C}^2$ ), 69.7 ( $\text{C}^5$ ), 69.5 ( $\text{C}^6$ ), 35.3 ( $\text{C}^7$ ), 24.6 ( $\text{C}^8$  or  $\text{C}^9$ ), 24.2 ( $\text{C}^8$  or  $\text{C}^9$ ); HRMS  $m/z$  ( $\text{ESI}^+$ ) [Found ( $\text{M}+\text{Na}$ ) $^+$  400.04943  $\text{C}_{14}\text{H}_{19}\text{NO}_7\text{S}_2\text{Na}$  requires  $\text{M}^+$  400.04951]; LRMS  $m/z$  ( $\text{ES}^+$ ) 400 ( $[\text{M}+\text{Na}]^+$ , 100%), 401 ( $[\text{M}+\text{Na}]^+$ , 19%), 402 ( $[\text{M}+\text{Na}]^+$ , 12%); Analytical RP-HPLC (Method 2, 220/254/300/365 nm) Ret. time = 7.8 min, Purity = 98.8%.

### 6.3. General Biological Methods

#### 6.3.1. Chemicals and Cell Culture Reagents

All cell culture media was supplied by Sigma-Aldrich. Laboratory plasticware was supplied by CoStar<sup>®</sup> and Corning<sup>®</sup>. In addition, the following reagents (Table 6.2) were used.

**Table 6.2:** General biological laboratory reagents.

Name	Supplier
Acetic Acid	Sigma-Aldrich
Acetonitrile	Sigma-Aldrich UK
Agarose	Sigma-Aldrich UK
Ammonium chloride	Sigma Aldrich
$\beta$ -mercaptoethanol	Fisher Scientific
Blocking Buffer LiCor	LiCor
Bromophenol blue	Fisher Scientific
Calcium chloride	Sigma-Aldrich
DMSO	Fisher Scientific
Ethanol	Fisher Scientific
Ethylenediaminetetraacetic acid (EDTA)	Sigma-Aldrich
FBS (foetal bovine serum)	Autogen Bioscience
Glycerol	Fisher Scientific
Glycine	Sigma-Aldrich
JetPrime	Polyplus-transfection <sup>®</sup> SA
Lipofectamine 2000	Invitrogen/Life Technologies
Lipofectamine 3000	Invitrogen/Life Technologies
Lipofectamine LTX	Invitrogen/Life Technologies
Luria Bertani (LB) Broth	Sigma-Aldrich
Luria Bertani LB Broth with Agar	Sigma-Aldrich
Paraformaldehyde	Fisher Scientific
PBS (phosphate-buffered saline)	Fisher Scientific
Ponceau S	Sigma-Aldrich
ProLong <sup>®</sup> Diamond	Invitrogen/Life Technologies
ProLong <sup>®</sup> Gold	Invitrogen/Life Technologies
SOC media	New England Biolabs (NEB)
Sodium chloride (NaCl)	Sigma-Aldrich
Sodium dodecyl sulphate (SDS)	Fisher Scientific



Name	Supplier
SYBR Safe™	Invitrogen/Life Technologies
Tris(2-carboxyethyl)phosphine hydrochloride (TCEP)	Sigma-Aldrich
Tris(hydroxymethyl)aminomethane hydrochloride (Tris-HCl)	Thermo Fisher Scientific
Trypsin 0.05% EDTA	Sigma-Aldrich UK
Tryptone	Sigma-Aldrich
Tween 20	Fisher Scientific
Urea	Fisher Scientific
Yeast Extract	Sigma-Aldrich
Zinc	Sigma-Aldrich

### 6.3.2. Bacterial Cell Culture

Standard sterile practices were followed throughout. Media and equipment were sterilised by autoclaving at 121 °C, 15 psi for 30 min.

**Incubation** of bacteria was performed in a New Brunswick G-25 or Innova-42 Shaker Incubator.

**Optical density at 600 nm** (OD<sub>600</sub>) was measured with a Novaspec III visible spectrophotometer or an Amersham Pharmacia biotech Ultrospec 2000. Where necessary, samples were diluted below OD<sub>600</sub> = 1.0.

*E. coli* DH5 $\alpha$ <sup>431,432</sup> cells were routinely used for cloning and propagation of plasmids. *E. coli* BL21 (DE3)<sup>245</sup> were used for all other experiments.

Cells were grown with vigorous shaking (225 rpm) at 37 °C in either **LB Broth** (Lennox, 10 g L<sup>-1</sup> Oxoid™ Tryptone, 5 g L<sup>-1</sup> Oxoid™ Yeast Extract, 5 g L<sup>-1</sup> NaCl), **2× YT** (16 g L<sup>-1</sup> Oxoid™ Tryptone, 10 g L<sup>-1</sup> Oxoid™ Yeast Extract, 5 g L<sup>-1</sup> NaCl), according to the experimental requirements. When solid medium was required, Bacto agar was added to a final concentration of 1.5% (w/v).

**Ampicillin** and **kanamycin** (Fisher Scientific) were prepared as stocks solutions in water of 100 mg/mL and 50 mg/mL, respectively. The final concentrations of ampicillin and kanamycin

were 100 µg/mL and 50 µg/mL, respectively. Solutions of antibiotics were sterilised by filtering through 0.22 µm filters (Millex®-GP, SLGP033RS).

### 6.3.3. Mammalian Cell Culture

In this study, the following human cell lines were used: HCT116 colorectal cancer cells and HepG2 hepatic cancer cells. All cell lines were originally obtained from ATCC. Cells were cultured in DMEM supplemented with 10% FBS in a standard humidified incubator for mammalian tissue culture maintained at 37 °C, 21% O<sub>2</sub> and 5% CO<sub>2</sub>. Experiments were carried out with cells at 65–75% confluence.

Cells were passaged 1–3 times per week (depending on the cell line). In each case, the medium was removed, and the cells washed with PBS. Cells were trypsinised with Trypsin-EDTA solution for 1–5 min until all cells had detached. Trypsin was inactivated by the addition of fresh media. The cell density was determined using a Neuenbauer haemocytometer chamber.

All cell lines were routinely tested for mycoplasma using the Plasmotest™ kit (InvivoGen), according to the manufacturer's instructions, and found to be negative.

### 6.3.4. Cryopreservation of Cell Lines

#### Preparation of bacterial glycerol stocks

A sterile tip was used to pick a single bacterial colony, which was grown in 2× YT (10 mL), containing the appropriate antibiotic, overnight. *E. coli* were diluted (1:100) into fresh 2× YT and grown to OD<sub>600</sub> = 0.4–0.5. A sample of this culture (500 µL) was added to glycerol (50% v/v in H<sub>2</sub>O, 500 µL) and stored at –80 °C.

#### Recovery of *E. coli* from the glycerol stock

A sterile loop was used to scrape frozen *E. coli* from the glycerol stock, inoculated into 2× YT (10 mL) and grown overnight. *E. coli* from the overnight colony were streaked onto Agar plates, grown at 37 °C overnight, and stored at 4 °C. *E. coli* were stored at 4 °C for a maximum of 1 month. During recovery, the glycerol stock was not allowed to thaw.

### **Cryopreservation of Mammalian Cell Lines**

Cells at 70–80% confluence were trypsinised, resuspended in fresh media and centrifuged ( $160 \times g$ , 5 min) at room temperature. The supernatant was removed, the cell pellet resuspended in 1 mL freezing media (10% DMSO, 90% FBS), and stored in a 1.5 mL cryovial (Thermo Scientific Nunc™, #5001-1020) for freezing. The vial was insulated by wrapping with tissue and placed at  $-80\text{ }^{\circ}\text{C}$  for 24 h before being stored in liquid nitrogen for long term storage.

### **Recovery of Mammalian Cell Lines**

When required, cells were removed from liquid nitrogen, rapidly thawed in a water bath at  $37\text{ }^{\circ}\text{C}$  and transferred to pre-warmed media. Cells were centrifuged ( $160 \times g$ , 5 min) at room temperature and resuspended in fresh media. The cell suspension was transferred to a  $75\text{ cm}^3$  flask and incubated under normal conditions.

### **6.3.5. Hypoxia Treatment**

#### **Enzyme Assays and Mammalian Cells**

Hypoxia treatments were carried out in a Bactron II Anaerobic Chamber (Shel Laboratories) or Bactron EZ anaerobic (Shel Laboratories). Although no oxygen is supplied to this chamber, a complete absence of oxygen cannot be guaranteed at all times due to potential leaks. The oxygen concentration is estimated to be  $<0.1\%$ . For experiments at  $<0.1\%$   $\text{O}_2$ , enzymatic assays were performed in glass vials and cells were plated on glass dishes. A Whitley H35 hypoxystation (Don Whitley Scientific®) was used for oxygen concentrations of 1–0.1%. The oxygen tensions of the chambers were routinely tested using an OxyLite probe (Oxford Optronix) or using the anaerobic paper indicator (BR0055B, Oxoid).

#### ***E. coli***

Anaerobic culture conditions were established by growing cells in air-tight sealed 2 mL Eppendorfs, completely filled with growth media. Anaerobic conditions were confirmed using an OxyLite probe (Figure 6.1).

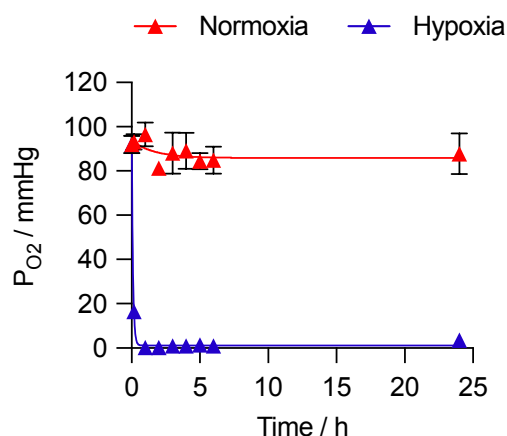


**Figure 6.1:** Measurement of oxygen tension when BL21 (DE3) *E.coli* were grown in 2 mL media in either a 50 mL Falcon tube (normoxia) or a 2 mL Eppendorf (hypoxia).

### 6.3.6. Cell lysis and SDS–PAGE Electrophoresis

For bacterial cell lysis, media was removed from the cells. The cells were washed with PBS, and pelleted by centrifugation ( $4,500 \times g$ , 2 min  $4^\circ\text{C}$ ). The cell pellet was lysed with lysis solution (20 mM Tris-HCl, 1 mM tris(2-carboxyethyl)phosphine (TCEP), 0.5 mM NaCl, pH 7.8), sonicated (20 s, rest on ice, 20 s) and centrifuged to remove cell debris ( $15,000 \times g$ , 15 min,  $4^\circ\text{C}$ ). The supernatant was transferred to a clean Eppendorf. Protein concentration was quantified with a Nanodrop™ spectrophotometer. Absorbance was detected at 280 nm, using lysis solution as a blank. The appropriate volume of sample (typically corresponding to 2–50  $\mu\text{g}$  of protein) was added to sample buffer (3.3% SDS, 6 M urea, 17 mM Tris-HCl (pH 7.5), 0.07 M  $\beta$ -mercaptoethanol, 0.01% bromophenol blue). Each sample was heated at  $100^\circ\text{C}$  for 10 min. The gels used were 4–20% pre-cast polyacrylamide Mini-PROTEAN TGX™ gels (Bio-Rad, #4561096) or 4–20% Criterion™TGX™ pre-cast midi protein gel (Bio-Rad, #5671094) and were electrophoresed for 60 min at 120 V in Tris-glycine running buffer (25 mM Tris base, 192 mM glycine, 0.1% (w/v) SDS). 5  $\mu\text{L}$  of Precision Plus Protein Kaleidoscope Standards (Bio-Rad, #1610375) was loaded to enable analysis of the molecular weight of bands.

### 6.3.7. Western blot

Proteins in the electrophoresed gels were transferred onto nitrocellulose membranes (Trans-Blot® Turbo™ Transfer Pack, Bio-Rad) by a Trans-Blot® Turbo™ transfer system. Transfers were run

for 7 min at 25 V. The membrane was blocked for 1 h using a 1:1 mixture of LiCor buffer and tris-buffered saline solution (TBS, 50 mM Tris-HCl, pH 7.6, 150 mM NaCl). Primary antibodies were diluted in a 1:1 mixture of LiCor buffer and TBS-Tween (TBS-T, 0.1% Tween). The membranes were treated with primary antibodies for 1 h at room temperature. The dilutions for each primary antibody used are given in Table 6.3. The membrane was washed with TBS-T ( $3 \times 5$  min), then treated with the appropriate secondary antibody, diluted in a 1:1 mixture of LiCor buffer:TBS-Tween, for 1 h at room temperature. The dilutions for each secondary antibody used are given in Table 6.4. The membrane was washed with TBS-T ( $2 \times 5$  min), TBS ( $1 \times 5$  min) and developed using an Odyssey infrared imaging system.

**Table 6.3:** Primary antibodies used for western blot.

Name	Species	Dilution	Supplier/Cat. No.
LacI	Mouse	1:1000	Abcam/ab33832
His <sub>6</sub> -Tag	Mouse	1:1000	ThermoFisher/MA1-21315

**Table 6.4:** Secondary antibody used for western blot.

Name	Dilution	Supplier/Cat. No.
IRDye 800CW donkey anti-mouse IgG	1:10,000	LiCor/926-32212

### 6.3.8. Fluorometric Analysis

Where appropriate, samples were diluted such that  $OD_{600} < 0.4$ .

#### Resorufin

Fluorescence spectra were obtained using a PerkinElmer LS 50B Luminescence Spectrometer. Samples (500  $\mu$ L) were evaluated in a 1 mL quartz cuvette. Samples were excited with light at 550 nm and the emission spectra measured from 550 nm to 700 nm ( $\lambda_{\text{max}} = 585$  nm). The excitation slit was 5 nm and the emission slit was 2 nm. Sample emission was scanned at a rate of 100 nm/min.

### **iLOV and creiLOV**

Fluorescence spectra were obtained using a PerkinElmer LS 50B Luminescence Spectrometer. Samples (500  $\mu$ L) were evaluated in a 1 mL quartz cuvette. Samples were excited with light at 450 nm and the emission spectra measured from 450 nm to 600 nm. The excitation slit was 7 nm and the emission slit was 20 nm. Sample emission was scanned at a rate of 100 nm/min.

Alternatively, fluorescence was measured using a POLARstar<sup>®</sup> Omega Plate Reader (BMG Labtech). Samples (200  $\mu$ L) were prepared in a 96 well plate (Corning Falcon, black, clear, flat bottom, #353219). Samples were excited with light at 485 nm and the emission was measured at 520 nm. The scan mode was orbital averaging with 10 flashes per well.

### **sfGFP**

Fluorescence was measured using a POLARstar<sup>®</sup> Omega Plate Reader (BMG Labtech). Samples (200  $\mu$ L) were prepared in a 96 well plate (Corning Falcon, black, clear, flat bottom, #353219). Samples were excited with light at 485 nm and the emission was measured at 520 nm. The scan mode was orbital averaging with 10 flashes per well.

### **6.3.9. HPLC-MS Analysis**

Aliquots taken from chemical and biological assays were evaluated on a Waters system (2695 pump/autosampler 2996 diode array detector and ZQ2000 mass spectrometer). The column was a Hichrom RPB, 5  $\mu$ m, 100  $\times$  3.2 mm at 35  $^{\circ}$ C. The flow rate was 0.5 mL/min. For each sample, UV spectra were collected between 192–800 nm, and mass spectra collected for  $m/z$  ratios from 200–900. These ranges were reduced where appropriate. The injection volume for each sample was 10  $\mu$ L. describes the methods of HPLC elution for each compound. The peak area for each compound was evaluated at the indicated wavelength ( $\lambda_{vis}$ ).

Concentrations of compounds in assay aliquots were determined by means of calibration curves. Calibration curves were obtained from solutions of each compound in DMSO and were diluted in MeCN:H<sub>2</sub>O (1:1). The peak area for each concentration was plotted against concentration and a line of best fit introduced, such that the intercept was 0.

**Table 6.5:** HPLC analysis method for each compound. Intermediates from reduction of **123–127** were visualised at 205 nm.

Compound	Eluent A	Eluent B	Gradient		$\lambda_{vis}$ nm
			Time / min	%B	
<b>63</b>	10 mM Formic acid	MeCN	0–5 5–7	20–95 95	470
<b>79</b>	10 mM Formic acid	MeCN	0–5 5–7	20–95 95	470
<b>103</b>	Water	MeCN	According to protected compound		205
<b>123</b>	Water	MeCN	0–6	5–95	270
<b>124</b>	Water	MeCN	0–6	5–95	270
<b>125</b>	Water	MeCN	0–6	5–95	270
<b>126</b>	Water	MeCN	0–6	5–95	270
<b>127</b>	Water	MeCN	0–1 1–3.5 3.5–7 7–8	5 5–50 50–95 95	270
<b>304</b>	Water	MeCN	1–3.5 3.5–7 7–8	5–50 50–95 95	205
<b>308</b>	Water	MeCN	1–5 5–6	45–95 95	270
<b>309</b>	Water	MeCN	1–1.5 1.5–3.5 3.5–4.5 4.5–6 6–8	5 5–65 65 65–95 95	270

### 6.3.10. Fluorescence Microscopy

#### Bacterial Cells

Bacterial cells were treated according to the experimental requirements. At the end of the experiment, cells were washed with PBS (500  $\mu$ L), centrifuged ( $4,500 \times g$ , 2 mins, 4 °C), and resuspended in PBS (1.5 mL). The appropriate volume of sample was diluted with PBS to obtain 100  $\mu$ L at  $OD_{600} = 5$  and centrifuged ( $4,500 \times g$ , 2 mins, 4 °C). The pellet was resuspended in DAPI solution (50  $\mu$ L, 0.1  $\mu$ g/mL, PBS), incubated at room temperature for 10 mins, and centrifuged ( $4,500 \times g$ , 2 mins, 4 °C). The pellet was washed with PBS ( $3 \times 50 \mu$ L) and

resuspended in 25  $\mu$ L PBS. Samples were mounted onto slides with ProLong<sup>®</sup> Diamond mounting medium (Invitrogen/Life technologies) and covered with a glass cover slip. The slides were left to dry for 24 h before analysis. Slides were imaged using a Nikon Ni-E upright microscope with a 100X Oil objective, using NIS Elements Advanced Research software. Images were processed using Fiji.<sup>433</sup>

### **Mammalian Cells**

$0.5\text{--}1 \times 10^6$  cells were seeded in 6 cm dishes containing cover slips and left to adhere for 16 h. Cells were treated according to the experimental requirements. At the end of the experiment, the media was removed, and the cells washed with PBS ( $\times 3$ ). The cells were fixed with 4% paraformaldehyde (PFA) solution (4% w/v paraformaldehyde, PBS) for 10 min at room temperature. The PFA solution was removed and the cells washed with PBS ( $\times 3$ ). The cells were treated with DAPI solution (0.1  $\mu$ g/mL, PBS) for 10 min at room temperature, followed by washing with PBS for 5 min, twice. The DAPI solution was removed and the cells washed with PBS ( $\times 3$ ). The cover slips were then carefully removed and mounted onto slides with ProLong<sup>®</sup> Gold mounting medium (Invitrogen/Life technologies). The slides were left to dry for 24 h before analysis. Slides were imaged using a Nikon Ni-E upright microscope with a 100X Oil objective, using NIS Elements Advanced Research software. Average pixel intensities were quantified using the “Measure” command in Fiji on manual ROIs containing cells.<sup>433</sup>

#### **6.3.11. DNA Transfection**

Cells were transfected with Lipofectamine LTX (Invitrogen), Lipofectamine 2000 (Invitrogen), Lipofectamine 3000 (Invitrogen) or JetPrime (Polyplus-transfection<sup>®</sup> SA), according to the manufacturer’s instructions.

#### **6.3.12. Statistical Analysis**

Statistical analyses were carried out using Microsoft Excel software. Error bars represent  $\pm$  SEM. The standard error (S.E.M) was calculated using the following formula:



$$\text{S.E.M.} = \frac{\text{S.D.}}{\sqrt{n}}$$

S.D is the standard deviation, and  $n$  is the number of samples. Statistical significance of differences between means of at least  $n = 3$  experiments was determined using Student's  $t$  test.

## 6.4. Molecular Biology

### 6.4.1. Primers

Oligonucleotide primers were supplied by Sigma-Aldrich Life Science as a dried pellet, resuspended in Millipore™ Water to a final primer concentration of 100  $\mu$ M, and stored at  $-20^{\circ}\text{C}$ . The primers used in this study are listed in Table 6.6 and Table 6.7. Melting temperatures ( $T_m$ ) for the regions of initial annealing to DNA templates are predicted by NEB  $T_m$  Calculator (<http://tmcalculator.neb.com/#!/main>) using the settings for Q5 High-Fidelity DNA Polymerase.

**Table 6.6:** Primers used for cloning. Regions for initial annealing to DNA templates are underlined.  $T_m$  refers to the melting temperature for these regions of DNA template annealing.

Primer Name	Direction	Sequence (5' to 3')	$T_m$ ( $^{\circ}\text{C}$ )
iLOV_f1	Forward	<u>AAGGAATGGTGCATG</u>	55
iLOV_r1	Reverse	CTAGCATATGATCTCCATGGA <u>AATTTCG</u> <u>CGGGATC</u>	55
PT5_f1	Forward	CATGGAAAAATTTATTTGCTTTGTGAG CGGATAACAATTATAATATGTGTGGA ATTGTGAGCGCTCACAATTCCACACA GGAAACAGACCA	79
PT5_r1	Reverse	TATGGTCTGTTTCCTGTGTGGAATTGT GAGCGCTCACAATTCCACACATATTAT AATTGTTATCCGCTCACAAAGCAAAT AAATTTTTC	79
sfGFP_p1	Forward	TTAACTTTAAGAAGGAGATATACATA <u>A</u> <u>TGGGTCATCACCAC</u>	55
sfGFP_p2	Reverse	CGGAGCTCGAATTCGGATCCT <u>CATTAT</u> <u>TACTTGTAGAGTTCGT</u>	56
F_GFP1	Forward	GGTATCGATAAGCTTGATATC <u>ATGGGT</u> <u>CATCACCAC</u>	55
R_GFP1	Reverse	CGCGGTGGCGCCGCTCATTATTACTT <u>GTAGAGTTTCG</u>	56
F_GFP2	Forward	CAACCAAGCTTGCGGCCGC <u>ATGGGTC</u> <u>ATCACCAC</u>	55
R_GFP2	Reverse	TTTCAGTTCTTAAGAATTGCGGCCGCT <u>CATTATTACTTGTAGAGTTCG</u>	56

**Table 6.7:** Primers used for sequencing.

Primer Name	Direction	Sequence (5' to 3')	T <sub>m</sub> (°C)
T7F	Forward	TAATACGACTCACTATAGGG	56
T7R	Reverse	GCTAGTTATTGCTCAGCGG	57
Seq_f4	Forward	AGCAGCCCAGTAG	56
Seq_T5f	Forward	GATGTCGGCGATATAG	55
Seq_N1	Forward	GCTCCTCAGGGAT	55
Seq_N2	Reverse	GCGGGTTCCTTC	55

### 6.4.2. Constructs

The plasmids used in this study are listed in Table 6.8. The pNIC28-Bsa4 expression vector was obtained from Opher Gileadi (Addgene plasmid #26103).<sup>262</sup> The pET-sfGFP construct was a kind gift from Prof. Andrew Baldwin (University of Oxford). pCMVLacI, pOPRSVI/MCS and pOPI3CAT were purchased from Stratagene, Agilent Technologies. Vector maps are available in Appendix B.

**Table 6.8:** Plasmids used in this study

Plasmid Name	Reference	Antibiotic Resistance
pET-sfGFP	Unknown	Ampicillin
pNIC28-Bsa4	Savitsky <i>et al.</i> <sup>262</sup>	Kanamycin
pNIC28-iLOV	Constructed in this work	Kanamycin
pNIC28-creiLOV	Constructed in this work	Kanamycin
pT5-iLOV	Constructed in this work	Kanamycin
pNIC28-sfGFP	Constructed in this work	Kanamycin
pCMV-LacI	Stratagene, Agilent Technologies <sup>223</sup>	Ampicillin
pOPRSVI/MCS	Stratagene, Agilent Technologies <sup>223</sup>	Ampicillin
pOPI3CAT	Stratagene, Agilent Technologies <sup>223</sup>	Ampicillin
pOPRSVI-sfGFP	Constructed in this work	Ampicillin
pOPI3-sfGFP	Constructed in this work	Ampicillin

### 6.4.3. Preparation of Competent *E. coli*

Competent *E. coli* were prepared using the CaCl<sub>2</sub> method.<sup>361</sup> Specifically, a sterile tip was used to inoculate a single colony into 10 mL 2 × YT, the culture incubated (37 °C, 225 rpm) overnight.

A portion of the overnight culture (50  $\mu\text{L}$ , 0.1%) was subcultured into fresh 2 $\times$  YT (50 mL) and the culture incubated (37  $^{\circ}\text{C}$ , 225 rpm) until  $\text{OD}_{600} = 0.5$ . The bacterial cells were harvested by centrifugation (4000  $\times g$ , 15 mins, 4  $^{\circ}\text{C}$ ), divided into two tubes and each tube resuspended in freshly autoclaved  $\text{CaCl}_2$  solution (12.5 mL, 60 mM  $\text{CaCl}_2$ , 15% glycerol (v/v), 4  $^{\circ}\text{C}$ ). The cells were placed on ice for 2–5 h, centrifuged (4000  $\times g$ , 15 mins, 4  $^{\circ}\text{C}$ ) and resuspended in  $\text{CaCl}_2$  solution (1.4 mL). Cells were stored in 100  $\mu\text{L}$  aliquots at  $-80^{\circ}\text{C}$ .

#### 6.4.4. Cloning

##### PCR

PCR amplification of gene inserts was carried out in a Labnet Multigene II Personal Thermal Cycler using Q5<sup>®</sup> High-Fidelity DNA Polymerase (NEB, #M0491). The composition for a typical PCR reaction is detailed in Table 6.9. An initial denaturation step 98  $^{\circ}\text{C}$  for 3 min was followed by 30 cycles of denaturing at 98  $^{\circ}\text{C}$  for 10 s, annealing at  $T^{\circ}\text{C}$  for 10 s, and extension at 72  $^{\circ}\text{C}$  for  $x$  s with a final extension of 2 min.  $T$  and  $x$  were determined according to the primer with the higher melting temperature ( $T = T_m + 3^{\circ}\text{C}$ ) and the length of PCR product (30 s/kb), respectively. A final extension at 72  $^{\circ}\text{C}$  for 2 mins ensured completion of any partially amplified products. The resulting samples were held at 4  $^{\circ}\text{C}$  before removal from the cycler and purification by agarose gel electrophoresis.

**Table 6.9:** Volumes for a typical 50  $\mu\text{L}$  PCR reaction with Q5<sup>®</sup> DNA polymerase

Component	Volume ( $\mu\text{L}$ )	Final Concentration
Q5 Reaction Buffer (5 $\times$ )	10	1 $\times$
dNTPs (10 mM)	1	200 $\mu\text{M}$
Forward Primer (10 $\mu\text{M}$ )	2.5	0.5 $\mu\text{M}$
Reverse Primer (10 $\mu\text{M}$ )	2.5	0.5 $\mu\text{M}$
Template DNA (50–100 ng/ $\mu\text{L}$ )	0.5	0.5–1 ng/ $\mu\text{L}$
Q5 High-Fidelity DNA Polymerase	0.5	0.02 U/ $\mu\text{L}$
Water	33	-

### Vector Inserts

Vector inserts were generated either by PCR or GeneArt Strings, or formed by annealing two primers. A summary of the techniques and appropriate primers used to generate each insert is shown in Table 6.10. GeneArt Strings were synthesised by ThermoFisher Scientific and supplied as a dried pellet, resuspended in Millipore™ Water to a final concentration of 20 ng/μL, and stored at –20 °C. The DNA sequences for iLOV and creiLOV inserts, synthesised by GeneArt Strings are given in Appendix A. For pT5, the two annealing primers were mixed (1:1), denatured (98 °C, 3 min), and annealed (79 °C, 3 min) before use in cloning.

**Table 6.10:** Vector inserts used for cloning of each construct used in this work.

Insert	Method	Forward Primer	Reverse Primer
iLOV	GeneArt Strings	-	-
creiLOV	GeneArt Srtrings	-	-
pNull	PCR	iLOV_f1	iLOV_r1
pT5	Annealing Primers	PT5_f1	PT5_r1
sfGFP1	PCR	sfGFP_p1	sfGFP_p2
sfGFP2	PCR	F_GFP1	R_GFP1
sfGFP3	PCR	F_GFP2	R_GFP2

### Vector Linearisation

Restriction enzymes were purchased from NEB: *Bam*HI-HF (#R3136), *Eco*RV-HF (#R3195), *Nde*I (#R0111), *Not*I-HF (#R3189). Vectors were digested using the appropriate restriction enzymes according to the manufacturer's instructions (NEB). The specific enzymes used for each cloning reaction are detailed in Table 6.11. Typically, 1–3 μg vector was digested in a 30 μL reaction (CutSmart®) at 37 °C for 4–16 h. After digestion, the linearised vectors were purified by agarose gel electrophoresis.

**Table 6.11:** Restriction enzymes used for linearisation of the vector in each cloning reaction

Initial Vector	Vector Insert	Plasmid Product	Restriction Enzymes
pNIC28-Bsa4	iLOV	pNIC28-iLOV	<i>NdeI</i> <i>BamHI</i> -HF
pNIC28-Bsa4	creiLOV	pNIC28-creiLOV	<i>NdeI</i> <i>BamHI</i> -HF
pNIC28-iLOV	pNull	pNull-iLOV	<i>NdeI</i> <i>SphI</i> -HF
pNull-iLOV	pT5	pT5-iLOV	<i>NdeI</i> <i>NcoI</i> -HF
pNIC28-Bsa4	sfGFP1	pNIC28-sfGFP	<i>NdeI</i> <i>BamHI</i> -HF
pOPRSVI/MCS	sfGFP2	pOPRSVI-sfGFP	<i>EcoRV</i> -HF <i>NotI</i> -HF
pOPI3CAT	sfGFP3	pOPI3-sfGFP	<i>NotI</i> -HF

### Gibson Assembly Ligation

For pNIC28-iLOV, pNIC28-iLOV, pNIC28-creiLOV, pOPRSVI/MCS, and pOPI3CAT, ligation was achieved using Gibson assembly.<sup>434</sup> Cloning was performed using NEBuilder® HiFi DNA Assembly Master Mix (NEB, #E2621), using 50–100 ng of vector in a molar ratio of 1:2 of vector:insert. Reactions were carried out at 50 °C for 1 h. The entire reaction mixture was used directly to transform competent DH5α cells, which were spread on 2× YT agar plates, containing the appropriate antibiotic, and incubated at 37 °C overnight.

### T4 DNA Ligase

For pNull-iLOV and pT5-iLOV, ligation was achieved using T4 DNA Ligase (NEB, #M0202). Ligation was performed using 50–100 ng of vector in a molar ratio of 1:3 of vector:insert. Reactions were carried out at room temperature for 1 h. The entire reaction mixture was used directly to transform competent DH5α cells, which were spread on 2× YT agar plates, containing the appropriate antibiotic, and incubated at 37 °C overnight.

### 6.4.5. Agarose Gel Electrophoresis

DNA samples were analysed and purified by gel electrophoresis of the DNA mixture. Agarose gels were prepared by dissolving agarose in TAE buffer (40 mM Tris, 20 mM acetic acid, 1mM

EDTA) to a final concentration of 1–2% agarose. SYBR Safe™ DNA gel stain (Invitrogen, #S33102) was used for staining of the DNA. Samples were loaded after mixing with 6× loading buffer (NEB, #B7024) and run in TAE buffer at a constant potential of 75 V until desired fragment separation was achieved. Gels were visualised using a Bio-Rad ChemiDoc™ MP transilluminator and the size of the fragments was referenced to 1 kb DNA Ladder (NEB, #N3232).

#### 6.4.6. Extraction of DNA from Agarose Gels

PCR products and digested DNA were purified by gel electrophoresis. DNA was extracted from the agarose gel using either GeneJET Gel Extraction Kit (Thermo Scientific, #K0691) or QIAQuick Gel Extraction Kit (Qiagen, #28704) according to the manufacturer's instructions.

#### 6.4.7. Transformation of Bacteria

Plasmid DNA was transformed into *E. coli* using the CaCl<sub>2</sub> method.<sup>361</sup> Specifically, 100 µL of competent cells were thawed on ice. 100–200 ng purified plasmid DNA or the entire volume of a cloning reaction was added. The bacteria and DNA were mixed by flicking the tube (×10). Bacterial cells were incubated on ice for 30 mins, heat shocked at 42 °C for 45 s and placed on ice for an additional 2 mins. 500 µL SOC medium was added and the cells incubated at 37 °C for 1 h. For ampicillin resistant cells, this SOC recovery step was omitted. Transformation reactions were spread onto 2× YT plates, supplemented with the appropriate antibiotic, and incubated at 37 °C overnight. Plates were stored at 4 °C.

#### 6.4.8. Extraction of Plasmid DNA from Bacterial Cells

##### MiniPrep

A sterile tip was used to inoculate a single colony into 10 mL 2 × YT, containing the appropriate antibiotic, and the culture incubated (37 °C, 225 rpm) for 12–16 h. Purification of plasmid DNA was performed using either GeneJET Plasmid Miniprep Kit (Thermo Scientific™, #K0503) or QIAprep Spin Miniprep Kit (Qiagen, # 27104) according to the manufacturer's instructions. Volume of culture processed was varied according to whether the plasmid was a high or low copy number vector (typically 3 mL for high copy plasmids and 10 mL for low copy plasmids).

### MaxiPrep

A sterile tip was used to inoculate a single colony into 5 mL LB medium, containing the appropriate antibiotic, and the culture incubated (37 °C, 225 rpm) for 8 h. The starter culture was diluted 1:500 into fresh LB medium and incubated (37 °C, 225 rpm) for 12–16 h. After this time, the bacterial culture was harvested by centrifugation (4000 × g, 15 min, 4 °C). Purification of plasmid DNA was performed using either HiSpeed® Plasmid Maxi Kit (Qiagen, #12663) or Plasmid *Plus* Maxi Kit (Qiagen, #12963) according to the manufacturer's instructions.

#### 6.4.9. Determination of DNA Concentration

DNA concentration was determined by measuring optical density (OD) at A<sub>260</sub> nm with 1 A<sub>260</sub> nm representing an equivalent of 50 µg of DNA in 1 ml distilled water. A ratio of absorbance of ≥1.8 at 260 nm and 280 nm indicated that DNA was pure and free from protein contamination.

#### 6.4.10. DNA Sequencing

Plasmid sequencing was performed by Source BioScience Sequencing facility in the Department of Biochemistry (University of Oxford). T7 promoter and terminator sequence primers were used unless otherwise stated, on a 3730xl DNA Analyser-Titania.



## 6.5. Procedures for Biological Evaluation of Compounds

### 6.5.1. Zinc Reduction

Zinc reduction was performed using zinc dust (Sigma-Aldrich), ammonium chloride (Fisher Scientific), and DMF (Sigma-Aldrich). T=0 refers to the aliquot taken before the addition of zinc dust. The general procedure was as follows.

To a stirred solution of compound and ammonium chloride in DMF was added zinc powder. The solution was stirred at room temperature for 1 h. Aliquots (100  $\mu$ L) were taken at designated times (where t = 0 refers to before the addition of zinc powder). The aliquots were diluted (10  $\mu$ L sample + 90  $\mu$ L MeCN) and analysed by HPLC-MS. 10  $\mu$ L of the t = 1 h aliquot was added to 90  $\mu$ L phosphate buffer and the solution analysed by HPLC-MS.

The concentration of compound and number of equivalents of ammonium chloride and zinc are detailed in Table 6.12.

**Table 6.12:** Concentration and number of equivalents of ammonium chloride and zinc powder used for reduction of each compound.

Compound	Concentration mM	NH <sub>4</sub> Cl eq.	Zinc eq.
<b>63</b>	1.5	10	5
<b>79</b>	1	10	5
<b>123</b>	2	20	40
<b>124</b>	2	20	40
<b>125</b>	2	20	40
<b>126</b>	2	20	40
<b>127</b>	2	20	40

### 6.5.2. Enzyme Assays

Purified bactosomal human NADPH-CYP reductase (cat. CYP004) was purchased from Cypex Limited (Dundee, UK), stored in aliquots at  $-80\text{ }^{\circ}\text{C}$ , and used as supplied.

An NADPH regenerating system was used in each assay. Solution A (20 $\times$ , Corning<sup>®</sup>, #451220) and Solution B (100 $\times$ , Corning<sup>®</sup>, #451200) were stored at  $-20\text{ }^{\circ}\text{C}$  and used as supplied. Solution A and Solution B comprise the following:

**Solution A:** 26 mM NADP<sup>+</sup>, 66 mM MgCl<sub>2</sub>, 66 mM glucose-6-phosphate in H<sub>2</sub>O

**Solution B:** 40 units/mL glucose-6-phosphate dehydrogenase in 5 mM sodium citrate

In all cases, Millipore<sup>™</sup> water and 0.5 M K<sub>2</sub>HPO<sub>4</sub> buffer (BD Gentest<sup>™</sup>) were used.

Each compound was prepared as a stock solution in DMSO. The stock concentration and final assay concentration for each compound are described in Table 6.13. The composition for a typical 1 mL assay with NADPH-CYP reductase is detailed in Table 6.14.

**Table 6.13:** Concentration of stock solutions (prepared in DMSO) and final assay concentration for each compound

Compound	[Stock] mM	[Final] $\mu\text{M}$
<b>63</b>	1	5
<b>79</b>	1	5
<b>123</b>	10	10
<b>124</b>	10	10
<b>125</b>	10	10
<b>126</b>	10	10
<b>127</b>	10	10
<b>127</b>	20	20

**Table 6.14:** Volumes for a typical 1 mL assay with NADPH-CYP reductase

Component	Volume $\mu\text{L}$	Final Concentration
0.5 M $\text{K}_2\text{HPO}_4$	200	100 mM
Solution A (20 $\times$ )	50	1 $\times$
Solution B (100 $\times$ )	10	1 $\times$
NADPH-CYP reductase	9.7	92 pmol/mL
Substrate (n mmol)	1	n $\mu\text{mol}$
Water	729.3	-

Vials were incubated at 37 °C either under atmospheric conditions (21%  $\text{O}_2$ ) or hypoxic conditions (<0.1%  $\text{O}_2$ ), as described above. Aliquots (50  $\mu\text{L}$ ), taken at designated times (where  $t = 0$  refers to immediately after the addition of enzyme), were added to acetonitrile (50  $\mu\text{L}$ ), centrifuged (17,000  $\times g$ , 10 min) and the supernatant analysed by HPLC-MS, as described above.

### 6.5.3. Cellular Analysis of **63** and **79**

**63** and **79** were prepared as 1 mM solutions in DMSO.

#### Bacterial Cells

A sterile tip was used to inoculate a single colony into 10 mL 2 $\times$  YT and the culture incubated (37 °C, 225 rpm) for 12–16 h. A portion of the overnight culture (1%) was subcultured into fresh 2 $\times$  YT and the culture incubated (37 °C, 225 rpm) until  $\text{OD}_{600} = 0.2$ . **63** or **79** was added to a final concentration of 5  $\mu\text{M}$  in 2 mL of culture and the cells incubated under either normoxic or hypoxic growth conditions (37 °C, 225 rpm), as described above. At designated times (where  $t = 0$  refers to the sample immediately after addition of compound), samples were removed, the optical density at 600 nm was measured and the samples analysed by fluorescence ( $\lambda_{\text{ex}} = 550 \text{ nm}$ ;  $\lambda_{\text{em}} = 585 \text{ nm}$ ).

#### Mammalian Cells

$0.5\text{--}1 \times 10^6$  cells were seeded in 6 cm dishes containing cover slips and left to adhere for 16 h. **63** or **79** was added to a final concentration of 5  $\mu\text{M}$  in 3 mL media and the cells were incubated

under either normoxic (21%) or hypoxic (<0.1%) growth conditions at 37 °C for 6–24 h. After this time, cells were harvested and analysed by fluorescence microscopy, as described above.

#### 6.5.4. Analysis of Alternative Inducers **103** and **104**

A sterile tip was used to inoculate a single colony into 10 mL 2× YT and the culture incubated (37 °C, 225 rpm) for 12–16 h. A portion of the overnight culture (1%) was subcultured into fresh 2× YT and the culture incubated until OD<sub>600</sub> = 0.8. DMSO, IPTG **76**, **103** or **104** was added to a final concentration as described in Table 6.15 in 2 mL of culture and the cells incubated under normoxic growth conditions (37 °C, 225 rpm). After 24 h, 1.5 mL of culture was centrifuged (4,500 × g, 2 min), the pellet washed with PBS (500 µL) and resuspended in 1.5 mL PBS. Samples were diluted as appropriate (such that OD<sub>600</sub> <0.4) and analysed by fluorescence (POLARstar® Omega Plate Reader: λ<sub>ex</sub> = 485 nm; λ<sub>em</sub> = 520).

**Table 6.15:** Concentration of stock solutions (prepared in H<sub>2</sub>O) and final assay concentration for each compound

Compound	[Stock] M	[Final] mM
DMSO	-	-
IPTG <b>76</b>	0.1	1
<b>103</b>	0.1	1
<b>103</b>	0.5	5
<b>103</b>	1.0	10
<b>103</b>	1.5	15
<b>104</b>	0.1	1
<b>104</b>	0.5	5
<b>104</b>	1.0	10
<b>104</b>	1.5	15

#### 6.5.5. GFP Fluorescence Recovery

A sterile tip was used to inoculate a single colony into 10 mL 2× YT and the culture incubated (37 °C, 225 rpm) for 12–16 h. A portion of the overnight culture (1%) was subcultured into fresh 2× YT and the culture incubated until OD<sub>600</sub> = 0.8. DMSO or IPTG **76** was added to a final

concentration of 1 mM in 2 mL of culture and the cells incubated under either normoxic or hypoxic growth conditions (37 °C, 225 rpm). After 24 h, samples were removed, transferred to 50 mL Falcon tubes and aerobically cultured (37 °C, 225 rpm) for a further 0–150 min. At the indicated time points (Section 4.3.5), 1.5 mL of culture was centrifuged ( $4,500 \times g$ , 2 min), the pellet washed with PBS (500  $\mu$ L) and resuspended in 1.5 mL PBS. Samples were analysed by fluorescence and western blot as described above.

#### 6.5.6. Procedure for Bacterial Hypoxia-Induced Gene Expression

IPTG **76**, **86–89**, **94**, **253**, and **254** were prepared as 0.1 M solutions in DMSO. A sterile tip was used to inoculate a single colony into 10 mL 2 $\times$  YT and the culture incubated (37 °C, 225 rpm) for 12–16 h. A portion of the overnight culture (1%) was subcultured into fresh 2 $\times$  YT and the culture incubated until OD<sub>600</sub> = 0.8. DMSO or compound was added to a final concentration of 1 mM in 2 mL of culture and the cells incubated under either normoxic or hypoxic growth conditions (37 °C, 225 rpm). After 24 h, samples were removed, transferred to 50 mL Falcon tubes and aerobically cultured (37 °C, 225 rpm) for a further 30 min. 1.5 mL of culture was centrifuged ( $4,500 \times g$ , 2 min), the pellet washed with PBS (500  $\mu$ L) and resuspended in 1.5 mL PBS. Samples were analysed by fluorescence and western blot as described above.

#### 6.5.7. Disc Assay Analysis of the Oxygen Dependency of **94**

Test discs were prepared by impregnating 20  $\mu$ L of DMSO, IPTG **76**, or **94** (10 mM) onto Whatman<sup>®</sup> antibiotic assay discs of 6 mm diameter (Cat. No: WHA2017006). *E. coli* was aerobically cultured overnight. A portion of the overnight culture (1%) was inoculated into fresh 2 $\times$  YT medium (50 mL). When the bacterial culture reached an optical density of 0.2 at 600 nm, bacteria were spread onto solid 2 $\times$  YT agar plates (20 mL solid media in a 10 cm diameter plate) using a sterile cotton swab. The compound discs were aseptically placed onto the plates and the plates incubated at the indicated oxygen concentration at 37 °C. After 24 h, the plates were removed, transferred to a 21% O<sub>2</sub> and incubated for a further 30 min. Plates were imaged using a Bio-Rad ChemiDoc<sup>™</sup> MP transilluminator, using the Alexa488 setting with an exposure time of 0.02 s.



---

# REFERENCES

---

- 1 G. L. Semenza, *Cell*, 2012, **148**, 399–408.
- 2 M. G. V. Heiden, L. C. Cantley and C. B. Thompson, *Science*, 2009, **324**, 1029–1033.
- 3 O. Warburg, *Science*, 1956, **123**, 309–314.
- 4 J. Zheng, *Oncol. Lett.*, 2012, **4**, 1151–1157.
- 5 J. Raymond and D. Segrè, *Science*, 2006, **311**, 1764–1767.
- 6 N. Lane and W. Martin, *Nature*, 2010, **467**, 929–934.
- 7 M. Höckel and P. Vaupel, *J. Natl. Cancer Inst.*, 2001, **93**, 266–276.
- 8 T. Rossignol, C. Ding, A. Guida, C. d’Enfert, D. G. Higgins and G. Butler, *Eukaryot. Cell*, 2009, **8**, 550–559.
- 9 J. T. van Dongen and F. Licausi, Eds., *Low-oxygen stress in plants: oxygen sensing and adaptive responses to hypoxia*, Springer Verlag, Wien ; New York, 2013.
- 10 E. B. Rankin and A. J. Giaccia, *Science*, 2016, **352**, 175–180.
- 11 C. Wigerup, S. Pählman and D. Bexell, *Pharmacol. Ther.*, 2016, **164**, 152–169.
- 12 A. R. David and M. R. Zimmerman, *Nat. Rev. Cancer*, 2010, **10**, 728–733.
- 13 J. Ferlay, I. Soerjomataram, M. Ervik, R. Dikshit, S. Eser, C. Mathers, M. Rebelo, D. M. Parkin, D. Forman and F. Bray, *Cancer Incidence and Mortality Worldwide: IARC CancerBase No. 11*, GLOBOCAN 2012 v1.0, Lyon, France: International Agency for Research on Cancer, 2013.
- 14 F. Bray, A. Jemal, N. Grey, J. Ferlay and D. Forman, *Lancet Oncol.*, 2012, **13**, 790–801.
- 15 D. Hanahan and R. A. Weinberg, *Cell*, 2000, **100**, 57–70.
- 16 M. R. Stratton, P. J. Campbell and P. A. Futreal, *Nature*, 2009, **458**, 719–724.

## References

- 17 L. B. Alexandrov, S. Nik-Zainal, D. C. Wedge, S. A. J. R. Aparicio, S. Behjati, A. V. Biankin, G. R. Bignell, N. Bolli, A. Borg, A.-L. Børresen-Dale, S. Boyault, B. Burkhardt, A. P. Butler, C. Caldas, H. R. Davies, C. Desmedt, R. Eils, J. E. Eyfjörd, J. A. Foekens, M. Greaves, F. Hosoda, B. Hutter, T. Ilicic, S. Imbeaud, M. Imielinski, N. Jäger, D. T. W. Jones, D. Jones, S. Knappskog, M. Kool, S. R. Lakhani, C. López-Otín, S. Martin, N. C. Munshi, H. Nakamura, P. A. Northcott, M. Pajic, E. Papaemmanuil, A. Paradiso, J. V. Pearson, X. S. Puente, K. Raine, M. Ramakrishna, A. L. Richardson, J. Richter, P. Rosenstiel, M. Schlesner, T. N. Schumacher, P. N. Span, J. W. Teague, Y. Totoki, A. N. J. Tutt, R. Valdés-Mas, M. M. van Buuren, L. van 't Veer, A. Vincent-Salomon, N. Waddell, L. R. Yates, A. P. C. G. Initiative, I. B. C. Consortium, I. M.-S. Consortium, I. PedBrain, J. Zucman-Rossi, P. A. Futreal, U. McDermott, P. Lichter, M. Meyerson, S. M. Grimmond, R. Siebert, E. Campo, T. Shibata, S. M. Pfister, P. J. Campbell and M. R. Stratton, *Nature*, 2013, **500**, 415–421.
- 18 D. Hanahan and R. A. Weinberg, *Cell*, 2011, **144**, 646–674.
- 19 M. Wang, J. Zhao, L. Zhang, F. Wei, Y. Lian, Y. Wu, Z. Gong, S. Zhang, J. Zhou, K. Cao, X. Li, W. Xiong, G. Li, Z. Zeng and C. Guo, *J. Cancer*, 2017, **8**, 761–773.
- 20 P. Vaupel and L. Harrison, *Oncologist*, 2004, **9**, 4–9.
- 21 J. M. Brown and W. R. Wilson, *Nat. Rev. Cancer*, 2004, **4**, 437–447.
- 22 R. G. Bristow and R. P. Hill, *Nat. Rev. Cancer*, 2008, **8**, 180–192.
- 23 P. Vaupel, *Oncologist*, 2008, **13** (Suppl. 3), 21–26.
- 24 P. Vaupel and L. Harrison, *Oncologist*, 2004, **9** (Suppl. 5), 4–9.
- 25 G. Bergers and L. E. Benjamin, *Nat. Rev. Cancer*, 2003, **3**, 401–410.
- 26 C. W. Pugh and P. J. Ratcliffe, *Nat. Med.*, 2003, **9**, 677–684.
- 27 J. M. Brown and A. J. Giaccia, *Cancer Res.*, 1998, **58**, 1408–1416.
- 28 S. Ramachandran, J. Ient, E.-L. Göttgens, A. Krieg and E. Hammond, *Genes*, 2015, **6**, 935–956.
- 29 R. H. Thomlinson and L. H. Gray, *Br. J. Cancer*, 1955, **9**, 539–549.
- 30 C. Bayer, K. Shi, S. T. Astner, C.-A. Maftai and P. Vaupel, *Int. J. Radiat. Oncol. Biol. Phys.*, 2011, **80**, 965–968.
- 31 J. M. Brown, *Br. J. Radiol.*, 1979, **52**, 650–656.
- 32 M. W. Dewhirst, *Radiat. Res.*, 2009, **172**, 653–665.
- 33 C. Michiels, C. Tellier and O. Feron, *Biochim. Biophys. Acta, Rev. Cancer*, 2016, **1866**, 76–86.
- 34 A. Carreau, B. E. Hafny-Rahbi, A. Matejuk, C. Grillon and C. Kieda, *J. Cell. Mol. Med.*, 2011, **15**, 1239–1253.
- 35 P. Vaupel, A. Mayer and M. Höckel, *Tumor Hypoxia and Malignant Progression in Methods in Enzymology*, Elsevier, 2004, vol. 381, 335–354.
- 36 B. Muz, P. de la Puente, F. Azab and A. K. Azab, *Hypoxia*, 2015, **3**, 83–92.



- 37 J. L. Tatum, *Int. J. Radiat. Biol.*, 2006, **82**, 699–757.
- 38 M. Höckel, K. Schlenger, B. Aral, M. Mitze, U. Schaffer and P. Vaupel, *Cancer Res.*, 1996, **56**, 4509–4515.
- 39 R. A. Gatenby, H. B. Kessler, J. S. Rosenblum, L. R. Coia, P. J. Moldofsky, W. H. Hartz and G. J. Broder, *Int. J. Radiat. Oncol. Biol. Phys.*, 1988, **14**, 831–838.
- 40 L. S. Mortensen, J. Johansen, J. Kallehauge, H. Primdahl, M. Busk, P. Lassen, J. Alsner, B. S. Sørensen, K. Toustrup, S. Jakobsen, J. Petersen, H. Petersen, J. Theil, M. Nordsmark and J. Overgaard, *Radiother. Oncol.*, 2012, **105**, 14–20.
- 41 M. Nordsmark, S. M. Bentzen, V. Rudat, D. Brizel, E. Lartigau, P. Stadler, A. Becker, M. Adam, M. Molls, J. Dunst, D. J. Terris and J. Overgaard, *Radiother. Oncol.*, 2005, **77**, 18–24.
- 42 D. M. Brizel, S. P. Scully, J. M. Harrelson, L. J. Layfield, J. M. Bean, L. R. Prosnitz and M. W. Dewhirst, *Cancer Res.*, 1996, **56**, 941–943.
- 43 M. Nordsmark, J. Alsner, J. Keller, O. S. Nielsen, O. M. Jensen, M. R. Horsman and J. Overgaard, *Br. J. Cancer*, 2001, **84**, 1070–1075.
- 44 S. Rockwell, I. T. Dobrucki, E. Y. Kim, S. T. Marrison and V. T. Vu, *Curr. Mol. Med.*, 2009, **9**, 442–458.
- 45 A. M. Shannon, D. J. Bouchier-Hayes, C. M. Condrón and D. Toomey, *Cancer Treat. Rev.*, 2003, **29**, 297–307.
- 46 Y. Kato, M. Yashiro, Y. Fuyuhiko, S. Kashiwagi, J. Matsuoka, T. Hirakawa, S. Noda, N. Aomatsu, T. Hasegawa, T. Matsuzaki, T. Sawada, M. Ohira and K. Hirakawa, *Anticancer Res.*, 2011, **31**, 3369–3375.
- 47 D. J. Chaplin, R. E. Durand and P. L. Olive, *Int. J. Radiat. Oncol. Biol. Phys.*, 1986, **12**, 1279–1282.
- 48 L. H. Gray, A. D. Conger, M. Ebert, S. Hornsey and O. C. A. Scott, *Br. J. Radiol.*, 1953, **26**, 638–648.
- 49 E. J. Hall and A. J. Giaccia, *Radiobiology for the Radiologist*, Wolters Kluwer Health, Philadelphia, USA, 2011.
- 50 D. R. Grimes and M. Partridge, *Biomed. Phys. Eng. Express*, 2015, **1**, 045209.
- 51 J. A. Bertout, S. A. Patel and M. C. Simon, *Nat. Rev. Cancer*, 2008, **8**, 967–975.
- 52 P. Howard-Flanders and D. Moore, *Radiat. Res.*, 1958, **9**, 422–437.
- 53 J. M. Brown, *Tumor Hypoxia in Cancer Therapy* in *Methods in Enzymology*, Academic Press, 2007, vol. 435, 295–321.
- 54 A. I. Minchinton and I. F. Tannock, *Nat. Rev. Cancer*, 2006, **6**, 583–592.
- 55 K. O. Hicks, F. B. Pruijn, T. W. Secomb, M. P. Hay, R. Hsu, J. M. Brown, W. A. Denny, M. W. Dewhirst and W. R. Wilson, *J. Natl. Cancer Inst.*, 2006, **98**, 1118–1128.
- 56 I. F. Tannock, *Br. J. Cancer*, 1968, **22**, 258–273.

## References

- 57 J. Overgaard, *J. Clin. Oncol.*, 2007, **25**, 4066–4074.
- 58 I. Moen and L. E. B. Stuhr, *Targ. Oncol.*, 2012, **7**, 233–242.
- 59 J. Overgaard, H. Sand Hansen, M. Overgaard, L. Bastholt, A. Berthelsen, L. Specht, B. Lindeløv and K. Jørgensen, *Radiother. Oncol.*, 1998, **46**, 135–146.
- 60 G. L. Semenza, *Nat. Rev. Cancer*, 2003, **3**, 721–732.
- 61 D. Bhattarai, X. Xu and K. Lee, *Med. Res. Rev.*, 2018, **38**, 1404–1442.
- 62 J. Zhang, V. Kale and M. Chen, *AAPS J.*, 2014, **17**, 102–110.
- 63 R. C. Wright, A. Khakhar, J. R. Eshleman and M. Ostermeier, *PLoS One*, 2014, **9**, e114032.
- 64 N. S. Forbes, *Nat. Rev. Cancer*, 2010, **10**, 785–794.
- 65 F. W. Hunter, B. G. Wouters and W. R. Wilson, *Br. J. Cancer*, 2016, **114**, 1071–1077.
- 66 L. Hall-Stoodley, J. W. Costerton and P. Stoodley, *Nat. Rev. Microbiol.*, 2004, **2**, 95–108.
- 67 R. M. Donlan, *Emerg. Infect. Dis.*, 2002, **8**, 881–890.
- 68 R. M. Donlan and J. W. Costerton, *Clin. Microbiol. Rev.*, 2002, **15**, 167–193.
- 69 B. Rasmussen, *Nature*, 2000, **405**, 676–679.
- 70 F. Westall, M. J. de Wit, J. Dann, S. van der Gaast, C. E. J. de Ronde and D. Gerneke, *Precambrian Res.*, 2001, **106**, 93–116.
- 71 S. Fanning and A. P. Mitchell, *PLoS Pathog.*, 2012, **8**, e1002585.
- 72 D. López, H. Vlamakis and R. Kolter, *Cold Spring Harbor Perspect. Biol.*, 2010, **2**, 1–11.
- 73 D. Davies, *Nat. Rev. Drug Discovery*, 2003, **2**, 114–122.
- 74 B. L. Pihlstrom, B. S. Michalowicz and N. W. Johnson, *Lancet*, 2005, **366**, 1809–1820.
- 75 G. A. James, E. Swogger, R. Wolcott, E. deLancey Pulcini, P. Secor, J. Sestrich, J. W. Costerton and P. S. Stewart, *Wound Repair Regen.*, 2008, **16**, 37–44.
- 76 T. Bjarnsholt, *APMIS*, 2013, **121**, 1–58.
- 77 J. Lam, R. Chan, K. Lam and J. W. Costerton, *Infect. Immun.*, 1980, **28**, 546–556.
- 78 D. Worlitzsch, R. Tarran, M. Ulrich, U. Schwab, A. Cekici, K. C. Meyer, P. Birrer, G. Bellon, J. Berger, T. Weiss, K. Botzenhart, J. R. Yankaskas, S. Randell, R. C. Boucher and G. Döring, *J. Clin. Invest.*, 2002, **109**, 317–325.
- 79 N. Høiby, *J. Cyst. Fibros.*, 2002, **1**, 249–254.
- 80 M. Gominet, F. Compain, C. Beloin and D. Lebeaux, *APMIS*, 2017, **125**, 365–375.
- 81 L. Passerini, K. Lam, J. W. Costerton and E. G. King, *Crit. Care Med.*, 1992, **20**, 665–673.
- 82 N. S. Morris, D. J. Stickler and R. J. McLean, *World J. Urol.*, 1999, **17**, 345–350.
- 83 A. G. Gristina, Y. Shibata, G. Giridhar, A. Kreger and Q. N. Myrvik, *Semin. Arthroplasty*, 1994, **5**, 160–170.
- 84 P.-Y. Litzler, L. Benard, N. Barbier-Frebourg, S. Vilain, T. Jouenne, E. Beucher, C. Bunel, J.-F. Lemeland and J.-P. Bessou, *J. Thorac. Cardiovasc. Surg.*, 2007, **134**, 1025–1032.
- 85 Carla C. C. R. de Carvalho, *Recent Pat. Biotechnol.*, 2007, **1**, 49–57.
- 86 R. D. Monds and G. A. O’Toole, *Trends Microbiol.*, 2009, **17**, 73–87.

- 87 M. Beitelshes, A. Hill, C. H. Jones and B. A. Pfeifer, *Materials (Basel)*, 2018, **11**, 1086.
- 88 J. R. Blankenship and A. P. Mitchell, *Curr. Opin. Microbiol.*, 2006, **9**, 588–594.
- 89 D. Monroe, *PLoS Biol.*, 2007, **5**, e307.
- 90 J. W. Costerton, Z. Lewandowski, D. E. Caldwell, D. R. Korber and H. M. Lappin-Scott, *Annu. Rev. Microbiol.*, 1995, **49**, 711–745.
- 91 T. R. Garrett, M. Bhakoo and Z. Zhang, *Prog. Nat. Sci.*, 2008, **18**, 1049–1056.
- 92 M. Kostakioti, M. Hadjifrangiskou and S. J. Hultgren, *Cold Spring Harbor Perspect. Med.*, 2013, **3**, a010306.
- 93 H.-C. Flemming and J. Wingender, *Nat. Rev. Microbiol.*, 2010, **8**, 623–633.
- 94 J. B. Kaplan, *J. Dent. Res.*, 2010, **89**, 205–218.
- 95 M. O. Elasri and R. V. Miller, *Appl. Environ. Microbiol.*, 1999, **65**, 2025–2031.
- 96 W.-S. Chang, M. van de Mortel, L. Nielsen, G. N. de Guzman, X. Li and L. J. Halverson, *J. Bacteriol.*, 2007, **189**, 8290–8299.
- 97 K. McNeill and I. R. Hamilton, *FEMS Microbiol. Lett.*, 2003, **221**, 25–30.
- 98 T.-F. C. Mah and G. A. O'Toole, *Trends Microbiol.*, 2001, **9**, 34–39.
- 99 P. S. Stewart and J. William Costerton, *Lancet*, 2001, **358**, 135–138.
- 100 N. Høiby, T. Bjarnsholt, M. Givskov, S. Molin and O. Ciofu, *Int. J. Antimicrob. Agents*, 2010, **35**, 322–332.
- 101 P. S. Stewart and M. J. Franklin, *Nat. Rev. Microbiol.*, 2008, **6**, 199–210.
- 102 T. C. Zhang, Y.-C. Fu and P. L. Bishop, *Water Environ. Res.*, 1995, **67**, 992–1003.
- 103 M. C. Walters, F. Roe, A. Bugnicourt, M. J. Franklin and P. S. Stewart, *Antimicrob. Agents Chemother.*, 2003, **47**, 317–323.
- 104 K. D. Xu, P. S. Stewart, F. Xia, C.-T. Huang and G. A. McFeters, *Appl. Environ. Microbiol.*, 1998, **64**, 4035–4039.
- 105 G. Borriello, E. Werner, F. Roe, A. M. Kim, G. D. Ehrlich and P. S. Stewart, *Antimicrob. Agents Chemother.*, 2004, **48**, 2659–2664.
- 106 S. E. Cramton, M. Ulrich, F. Götz and G. Döring, *Infect. Immun.*, 2001, **69**, 4079–4085.
- 107 A. A. Mashruwala, A. van de Guchte and J. M. Boyd, *eLife*, 2017, **6**, e23845.
- 108 J. T. van Dongen and F. Licausi, *Annu. Rev. Plant Biol.*, 2015, **66**, 345–367.
- 109 J. Peretó, *Oxygenic Photosynthesis in Encyclopedia of Astrobiology*, eds. M. Gargaud, R. Amils, J. C. Quintanilla, H. J. Cleaves, W. M. Irvine, D. L. Pinti and M. Viso, Springer, Berlin, Heidelberg, 2011, 1209–1209.
- 110 Q. T. Ho, P. Verboven, B. E. Verlinden, E. Herremans, M. Wevers, J. Carmeliet and B. M. Nicolaï, *Plant Physiol.*, 2011, **155**, 1158–1168.
- 111 J. T. van Dongen, U. Schurr, M. Pfister and P. Geigenberger, *Plant Physiology*, 2003, **131**, 1529–1543.
- 112 P. Perata and A. Alpi, *Plant Sci.*, 1993, **93**, 1–17.

## References

- 113 A. J. M. Smucker and R. R. Allmaras, *Whole plant responses to soil compaction in International Crop Science I*, Crop Science Society of America, Inc., USA, 1993, 727–737.
- 114 C. J. Andrews, *Ann. Bot.*, 1997, **79** (Suppl. 1), 87–91.
- 115 M. Sachs and B. Vartapetian, *Plant Stress*, 2007, **1**, 123–135.
- 116 J. Bailey-Serres and L. A. C. J. Voesenek, *Annu. Rev. Plant Biol.*, 2008, **59**, 313–339.
- 117 I. K. Kouadio, S. Aljunid, T. Kamigaki, K. Hammad and H. Oshitani, *Expert Rev. Anti. Infect. Ther.*, 2012, **10**, 95–104.
- 118 F. Ahmed, M. Y. Rafii, M. R. Ismail, A. S. Juraimi, H. A. Rahim, R. Asfaliza and M. A. Latif, *Biomed Res. Int.*, 2013, **2013**, 1–10.
- 119 A. A. Lone and M. Z. K. Warsi, *Bot. Res. Int*, 2009, **2**, 211–217.
- 120 T. L. Setter, I. Waters, S. K. Sharma, K. N. Singh, N. Kulshreshtha, N. P. S. Yaduvanshi, P. C. Ram, B. N. Singh, J. Rane, G. McDonald, H. Khabaz-Saberi, T. B. Biddulph, R. Wilson, I. Barclay, R. McLean and M. Cakir, *Ann. Bot.*, 2009, **103**, 221–235.
- 121 D. McFarlane and B. Wheaton, *The extent and cost of waterlogging*, Journal of the Department of Agriculture, Western Australia, Series 4, 1990.
- 122 T. L. Setter and I. Waters, *Plant Soil*, 2003, **253**, 1–34.
- 123 T. Fukao and J. Bailey-Serres, *Trends Plant Sci.*, 2004, **9**, 449–456.
- 124 J. Gibbs and H. Greenway, *Funct. Plant Biol.*, 2003, **30**, 353–353.
- 125 L. a. C. J. Voesenek, T. D. Colmer, R. Pierik, F. F. Millenaar and A. J. M. Peeters, *New Phytol.*, 2006, **170**, 213–226.
- 126 E. Loreti, H. van Veen and P. Perata, *Curr. Opin. Plant Biol.*, 2016, **33**, 64–71.
- 127 H. Takahashi, T. Yamauchi, T. D. Colmer and M. Nakazono, *Aerenchyma Formation in Plants in Low-Oxygen Stress in Plants: Oxygen Sensing and Adaptive Responses to Hypoxia*, eds. J. T. van Dongen and F. Licausi, Springer, Vienna, 2014, 247–265.
- 128 W. H. Vriezen, Z. Zhou and D. Van Der Straeten, *Ann. Bot.*, 2003, **91**, 263–270.
- 129 B. B. Vartapetian, Y. I. Dolgikh, L. I. Polyakova, N. V. Chichkova and A. B. Vartapetian, *Acta Naturae*, 2014, **6**, 19–30.
- 130 B. B. Vartapetian, I. N. Andreeva, G. I. Kozlova and L. P. Agapova, *Protoplasma*, 1977, **91**, 243–256.
- 131 W. R. Wilson and M. P. Hay, *Nat. Rev. Cancer*, 2011, **11**, 393–410.
- 132 L. J. O'Connor, C. Cazares-Körner, J. Saha, C. N. G. Evans, M. R. L. Stratford, E. M. Hammond and S. J. Conway, *Nat. Protoc.*, 2016, **11**, 781–794.
- 133 W. A. Denny, W. R. Wilson and M. P. Hay, *Br. J. Cancer*, 1996, **74** (Suppl. 27), 32–38.
- 134 C. P. Guise, A. M. Mowday, A. Ashoorzadeh, R. Yuan, W.-H. Lin, D.-H. Wu, J. B. Smaill, A. V. Patterson and K. Ding, *Chin. J. Cancer*, 2014, **33**, 80–86.
- 135 R. M. Phillips, *Cancer Chemother. Pharmacol.*, 2016, **77**, 441–457.

- 136 L. J. O'Connor, C. Cazares-Körner, J. Saha, C. N. G. Evans, M. R. L. Stratford, E. M. Hammond and S. J. Conway, *Nature Protocols*, 2016, **11**, 781–794.
- 137 L. H. Patterson and S. R. McKeown, *Br. J. Cancer*, 2000, **83**, 1589–1593.
- 138 S. R. McKeown, R. L. Cowen and K. J. Williams, *Clin. Oncol.*, 2007, **19**, 427–442.
- 139 A. Foehrenbacher, T. W. Secomb, W. R. Wilson and K. O. Hicks, *Front. Oncol.*, 2013, **3**, 314.
- 140 R. P. Mason and J. L. Holtzman, *Biochem. Biophys. Res. Commun.*, 1975, **67**, 1267–1274.
- 141 B. A. Moore, B. Palcic and L. D. Skarsgard, *Radiat. Res.*, 1976, **67**, 459–473.
- 142 R. S. Singleton, C. P. Guise, D. M. Ferry, S. M. Pullen, M. J. Dorie, J. M. Brown, A. V. Patterson and W. R. Wilson, *Cancer Res.*, 2009, **69**, 3884–3891.
- 143 R. M. Phillips, H. R. Hendriks, J. B. Sweeney, G. Reddy and G. J. Peters, *Expert Opin. Drug Metab. Toxicol.*, 2017, **13**, 783–791.
- 144 C. P. Guise, A. T. Wang, A. Theil, D. J. Bridewell, W. R. Wilson and A. V. Patterson, *Biochem. Pharmacol.*, 2007, **74**, 810–820.
- 145 F. W. Hunter, J. K. Jaiswal, D. G. Hurley, H. D. S. Liyanage, S. P. McManaway, Y. Gu, S. Richter, J. Wang, M. Tercel, C. G. Print, W. R. Wilson and F. B. Pruijn, *Biochem. Pharmacol.*, 2014, **89**, 224–235.
- 146 C. P. Guise, M. R. Abbattista, R. S. Singleton, S. D. Holford, J. Connolly, G. U. Dachs, S. B. Fox, R. Pollock, J. Harvey, P. Guilford, F. Doñate, W. R. Wilson and A. V. Patterson, *Cancer Res.*, 2010, **70**, 1573–1584.
- 147 G. K. Abou-Alfa, S. L. Chan, C.-C. Lin, E. G. Chiorean, R. F. Holcombe, M. F. Mulcahy, W. D. Carter, K. Patel, W. R. Wilson, T. J. Melink, J. C. Gutheil and C.-J. Tsao, *Cancer Chemother. Pharmacol.*, 2011, **68**, 539–545.
- 148 M. Konopleva, P. F. Thall, C. A. Yi, G. Borthakur, A. Coveler, C. Bueso-Ramos, J. Benito, S. Konoplev, Y. Gu, F. Ravandi, E. Jabbour, S. Faderl, D. Thomas, J. Cortes, T. Kadia, S. Kornblau, N. Daver, N. Pemmaraju, H. Q. Nguyen, J. Feliu, H. Lu, C. Wei, W. R. Wilson, T. J. Melink, J. C. Gutheil, M. Andreeff, E. H. Estey and H. Kantarjian, *Haematologica*, 2015, **100**, 927–934.
- 149 J.-X. Duan, H. Jiao, J. Kaizerman, T. Stanton, J. W. Evans, L. Lan, G. Lorente, M. Banica, D. Jung, J. Wang, H. Ma, X. Li, Z. Yang, R. M. Hoffman, W. S. Ammons, C. P. Hart and M. Matteucci, *J. Med. Chem.*, 2008, **51**, 2412–2420.
- 150 F. Meng, J. W. Evans, D. Bhupathi, M. Banica, L. Lan, G. Lorente, J.-X. Duan, X. Cai, A. M. Mowday, C. P. Guise, A. Maroz, R. F. Anderson, A. V. Patterson, G. C. Stachelek, P. M. Glazer, M. D. Matteucci and C. P. Hart, *Mol. Cancer Ther.*, 2012, **11**, 740–751.
- 151 G. J. Weiss, J. R. Infante, E. G. Chiorean, M. J. Borad, J. C. Bendell, J. R. Molina, R. Tibes, R. K. Ramanathan, K. Lewandowski, S. F. Jones, M. E. Lacouture, V. K. Langmuir, H. Lee, S. Kroll and H. A. Burris, *Clin. Cancer Res.*, 2011, **17**, 2997–3004.

## References

- 152 S. P. Chawla, L. D. Cranmer, B. A. Van Tine, D. R. Reed, S. H. Okuno, J. E. Butrynski, D. R. Adkins, A. E. Hendifar, S. Kroll and K. N. Ganjoo, *J. Clin. Oncol.*, 2014, **32**, 3299–3306.
- 153 M. J. Borad, S. G. Reddy, N. Bahary, H. E. Uronis, D. Sigal, A. L. Cohn, W. R. Schelman, J. Stephenson, E. G. Chiorean, P. J. Rosen, B. Ulrich, T. Dragovich, S. A. Del Prete, M. Rarick, C. Eng, S. Kroll and D. P. Ryan, *J. Clin. Oncol.*, 2015, **33**, 1475–1481.
- 154 W. Tap, Z. Papai, B. van Tine, S. Attia, K. Ganjoo, R. L. Jones, S. Schuetze, D. Reed, S. P. Chawla, R. Riedel, A. Krarup-Hansen, A. Italiano, P. Hohenberger, G. Grignani, L. Cranmer, T. Alcindor, A. Lopez-Pousa, T. Pearce, S. Kroll and P. Schoffski, *Ann. Oncol.*, 2016, **27** (Suppl. 6), vi483–vi492.
- 155 H. S. Schwartz, J. E. Sodergren and F. S. Philips, *Science*, 1963, **142**, 1181–1183.
- 156 V. N. Iyer and W. Szybalski, *Science*, 1964, **145**, 55–58.
- 157 K. A. Kennedy, S. Rockwell and A. C. Sartorelli, *Cancer Res.*, 1980, **40**, 2356–2360.
- 158 H. R. Hendriks, P. E. Pizao, D. P. Berger, K. L. Kooistra, M. C. Bibby, E. Boven, H. C. Dreef-van der Meulen, R. E. C. Henrar, H. H. Fiebig, J. A. Double, H. W. Hornstra, H. M. Pinedo, P. Workman and G. Schwartzmann, *Eur. J. Cancer*, 1993, **29**, 897–906.
- 159 R. M. Phillips, H. R. Hendriks and G. J. Peters, *Br. J. Pharmacol.*, 2013, **168**, 11–18.
- 160 E. M. Zeman, J. M. Brown, M. J. Lemmon, V. K. Hirst and W. W. Lee, *Int. J. Radiat. Oncol. Biol. Phys.*, 1986, **12**, 1239–1242.
- 161 S. S. Shinde, M. P. Hay, A. V. Patterson, W. A. Denny and R. F. Anderson, *J. Am. Chem. Soc.*, 2009, **131**, 14220–14221.
- 162 A. V. Patterson, N. Robertson, S. Houlbrook, M. A. Stephens, G. E. Adams, A. L. Harris, I. J. Stratford and J. Carmichael, *Int. J. Radiat. Oncol. Biol. Phys.*, 1994, **29**, 369–372.
- 163 J. M. Brown, *Br. J. Cancer*, 1993, **67**, 1163–1170.
- 164 S. K. Williamson, J. J. Crowley, P. N. Lara, J. McCoy, D. H. M. Lau, R. W. Tucker, G. M. Mills and D. R. Gandara, *J. Clin. Oncol.*, 2005, **23**, 9097–9104.
- 165 D. Rischin, L. J. Peters, B. O’Sullivan, J. Giralt, R. Fisher, K. Yuen, A. Trotti, J. Bernier, J. Bourhis, J. Ringash, M. Henke and L. Kenny, *J. Clin. Oncol.*, 2010, **28**, 2989–2995.
- 166 P. A. DiSilvestro, S. Ali, P. S. Craighead, J. A. Lucci, Y.-C. Lee, D. E. Cohn, N. M. Spirtos, K. S. Tewari, C. Muller, W. H. Gajewski, M. M. Steinhoff and B. J. Monk, *J. Clin. Oncol.*, 2014, **32**, 458–464.
- 167 K. O. Hicks, F. B. Pruijn, J. R. Sturman, W. A. Denny and W. R. Wilson, *Cancer Res.*, 2003, **63**, 5970–5977.
- 168 K. O. Hicks, B. G. Siim, J. K. Jaiswal, F. B. Pruijn, A. M. Fraser, R. Patel, A. Hogg, H. D. S. Liyanage, M. Jo Dorie, J. M. Brown, W. A. Denny, M. P. Hay and W. R. Wilson, *Clin. Cancer Res.*, 2010, **16**, 4946–4957.
- 169 C. R. Nishida, M. Lee and P. R. O. de Montellano, *Mol. Pharmacol.*, 2010, **78**, 497–502.
- 170 C. R. Nishida and P. R. Ortiz de Montellano, *J. Med. Chem.*, 2008, **51**, 5118–5120.

- 171 M. Mehibel, S. Singh, E. C. Chinje, R. L. Cowen and I. J. Stratford, *Mol. Cancer Ther.*, 2009, **8**, 1261–1269.
- 172 S. McKeown, M. Hejmadi, I. McIntyre, J. McAleer and L. Patterson, *Br. J. Cancer*, 1995, **72**, 76–81.
- 173 L. H. Patterson, S. R. McKeown, K. Ruparelia, J. A. Double, M. C. Bibby, S. Cole and I. J. Stratford, *Br. J. Cancer*, 2000, **82**, 1984–1990.
- 174 M. V. Hejmadi, S. R. McKeown, O. P. Friery, I. A. McIntyre, L. H. Patterson and D. G. Hirst, *Br. J. Cancer*, 1996, **73**, 499–505.
- 175 W. P. Steward, M. Middleton, A. Benghiat, P. M. Loadman, C. Hayward, S. Waller, S. Ford, G. Halbert, L. H. Patterson and D. Talbot, *Ann. Oncol.*, 2007, **18**, 1098–1103.
- 176 M. R. Albertella, P. M. Loadman, P. H. Jones, R. M. Phillips, R. Rampling, N. Burnet, C. Alcock, A. Anthoney, E. Vjaters, C. R. Dunk, P. A. Harris, A. Wong, A. S. Lalani and C. J. Twelves, *Clin. Cancer Res.*, 2008, **14**, 1096–1104.
- 177 S. Ogrodzinski, P. Smith, S. McKeown, L. Patterson and R.J. Errington, New compounds and uses thereof, United States, US20150307441A1, 2015.
- 178 I. N. Mistry, M. Thomas, E. D. D. Calder, S. J. Conway and E. M. Hammond, *Int. J. Radiat. Oncol. Biol. Phys.*, 2017, **98**, 1183–1196.
- 179 I. Parveen, D. P. Naughton, W. J. D. Wish and M. D. Threadgill, *Bioorg. Med. Chem. Lett.*, 1999, **9**, 2031–2036.
- 180 P. Thomson, M. A. Naylor, S. A. Everett, M. R. L. Stratford, G. Lewis, S. Hill, K. B. Patel, P. Wardman and P. D. Davis, *Mol. Cancer Ther.*, 2006, **5**, 2886–2894.
- 181 C. Granchi, T. Funaioli, J. T. Erler, A. J. Giaccia, M. Macchia and F. Minutolo, *ChemMedChem*, 2009, **4**, 1590–1594.
- 182 C. Cazares-Körner, I. M. Pires, I. D. Swallow, S. C. Grayer, L. J. O'Connor, M. M. Olcina, M. Christlieb, S. J. Conway and E. M. Hammond, *ACS Chem. Biol.*, 2013, **8**, 1451–1459.
- 183 K. E. Lindquist, J. D. Cran, K. Kordic, P. C. Chua, G. C. Winters, J. S. Tan, J. Lozada, A. H. Kyle, J. W. Evans and A. I. Minchinton, *Tumour Micronenviron. Ther.*, 2013, **1**, 46–55.
- 184 A. V. Patterson, J. Jaswail, S. P. Syddall, M. Abbattista, W. van Leeuwen, M. Puryer, A. Thompson, A. Hsu, S. Mehta, A. Pruijn, G. L. Lu, F. Doñate, W. A. Denny, W. R. Wilson and J. B. Smaill, *Mol. Cancer Ther.*, 2009, **8** (Suppl. 12), B76.
- 185 A. V. Patterson, J. Jaiswal, K. Carlin, M. R. Abbattista, C. P. Guise, S. Silva, H. Lee, G.-L. Lu, R. F. Anderson, T. J. Melink, J. C. Gutheil and J. B. Smaill, *Mol. Cancer Ther.*, 2013, **12** (Suppl. 11), B278.
- 186 G.-L. Lu, A. Ashoorzadeh, R. F. Anderson, A. V. Patterson and J. B. Smaill, *Tetrahedron*, 2013, **69**, 9130–9138.

## References

- 187 A. V. Patterson, S. Silva, C. Guise, M. Abbattista, M. Bull, H.-L. Hsu, C. Hart, J. Sun, A. Grey, A. Ashoorzadeh, R. Anderson and J. B. Smaill, *Cancer Res.*, 2015, **75 (Suppl. 15)**, 5358–5358.
- 188 A. V. Patterson, S. Silva, C. Guise, M. Bull, M. Abbattista, A. Hsu, J. D. Sun, C. P. Hart, T. E. Pearce and J. B. Smaill, *J. Clin. Oncol.*, 2015, **33 (Suppl. 15)**, e13548–e13548.
- 189 Study for Treatment of Patients With EGFR Mutant, T790M-negative NSCLC, <https://clinicaltrials.gov/ct2/show/NCT02454842>, (accessed 13 September 2018).
- 190 Study for Treatment of Patients With Recurrent or Metastatic SCCHN or SCCS, <https://clinicaltrials.gov/ct2/show/NCT02449681>, (accessed 13 September 2018).
- 191 G. da Cunha Santos, F. A. Shepherd and M. S. Tsao, *Annu. Rev. Pathol.-Mech. Dis.*, 2011, **6**, 49–69.
- 192 J. Liu, W. Bu and J. Shi, *Chem. Rev.*, 2017, **117**, 6160–6224.
- 193 E. Nakata, Y. Yukimachi, H. Kariyazono, S. Im, C. Abe, Y. Uto, H. Maezawa, T. Hashimoto, Y. Okamoto and H. Hori, *Bioorg. Med. Chem.*, 2009, **17**, 6952–6958.
- 194 A. C. Begg, E. L. Engelhardt, R. J. Hodgkiss, N. J. McNally, N. H. A. Terry and P. Wardman, *Br. J. Cancer*, 1983, **56**, 970–973.
- 195 P. Wardman, E. D. Clarke, R. J. Hodgkiss, R. W. Middleton, J. Parrick and M. R. L. Stratford, *Int. J. Radiat. Oncol. Biol. Phys.*, 1984, **10**, 1347–1351.
- 196 M. R. L. Stratford, E. D. Clarke, R. J. Hodgkiss, R. W. Middleton and P. Wardman, *Int. J. Radiat. Oncol. Biol. Phys.*, 1984, **10**, 1353–1356.
- 197 A. L. James, J. D. Perry and S. P. Stanforth, *J. Heterocycl. Chem.*, 2006, **43**, 515–517.
- 198 J. Xu, S. Sun, Q. Li, Y. Yue, Y. Li and S. Shao, *Analyst*, 2014, **140**, 574–581.
- 199 D. Yang, H. Y. Tian, T. N. Zang, M. Li, Y. Zhou and J. F. Zhang, *Sci. Rep.*, 2017, **7**, 9174.
- 200 L. Cui, Y. Zhong, W. Zhu, Y. Xu, Q. Du, X. Wang, X. Qian and Y. Xiao, *Org. Lett.*, 2011, **13**, 928–931.
- 201 Z. Li, X. Li, X. Gao, Y. Zhang, W. Shi and H. Ma, *Anal. Chem.*, 2013, **85**, 3926–3932.
- 202 Z. Li, X. Gao, W. Shi, X. Li and H. Ma, *Chem. Commun.*, 2013, **49**, 5859–5861.
- 203 H.-C. Huang, K.-L. Wang, S.-T. Huang, H.-Y. Lin and C.-M. Lin, *Biosens. Bioelectron.*, 2011, **26**, 3511–3516.
- 204 T. Guo, L. Cui, J. Shen, W. Zhu, Y. Xu and X. Qian, *Chem. Commun.*, 2013, **49**, 10820–10822.
- 205 Y. Shi, S. Zhang and X. Zhang, *Analyst*, 2013, **138**, 1952–1955.
- 206 Z. Li, X. He, Z. Wang, R. Yang, W. Shi and H. Ma, *Biosens. Bioelectron.*, 2015, **63**, 112–116.
- 207 C. Xue, Y. Lei, S. Zhang and Y. Sha, *Anal. Methods*, 2015, **7**, 10125–10128.
- 208 A. L. Vahrmeijer, M. Hutteman, J. R. van der Vorst, C. J. H. van de Velde and J. V. Frangioni, *Nat. Rev. Clin. Oncol.*, 2013, **10**, 507–518.



- 209 K. Itakura, T. Hirose, R. Crea, A. D. Riggs, H. L. Heyneker, F. Bolivar and H. W. Boyer, *Science*, 1977, **198**, 1056–1063.
- 210 G. L. Rosano and E. A. Ceccarelli, *Front. Microbiol.*, 2014, **5**, 172–189.
- 211 I. S. Johnson, *Science*, 1983, **219**, 632–637.
- 212 L. A. Palomares, S. Estrada-Moncada and O. T. Ramírez, *Production of Recombinant Proteins in Recombinant Gene Expression: Reviews and Protocols*, eds. P. Balbás and A. Lorence, Humana Press, Totowa, NJ, 2004, 15–51.
- 213 P. Balbas and A. Lorence, Eds., *Recombinant Gene Expression: Reviews and Protocols*, Humana Press, 2nd edn., 2004.
- 214 E. Saez, D. No, A. West and R. M. Evans, *Curr. Opin. Biotechnol.*, 1997, **8**, 608–616.
- 215 C. V. Rao, *Curr. Opin. Biotechnol.*, 2012, **23**, 689–694.
- 216 C. A. Voigt, *Curr. Opin. Biotechnol.*, 2006, **17**, 548–557.
- 217 M. B. Elowitz, A. J. Levine, E. D. Siggia and P. S. Swain, *Science*, 2002, **297**, 1183–1186.
- 218 W. Weber, M. Rimann, M. Spielmann, B. Keller, M. D.-E. Baba, D. Aubel, C. C. Weber and M. Fussenegger, *Nat. Biotechnol.*, 2004, **22**, 1440–1444.
- 219 S. Hartenbach, M. Daoud-El Baba, W. Weber and M. Fussenegger, *Nucleic Acids Res.*, 2007, **35**, e136.
- 220 W. Weber, C. Lienhart, M. Daoud-El Baba and M. Fussenegger, *Metab. Eng.*, 2009, **11**, 117–124.
- 221 A. Mullick, Y. Xu, R. Warren, M. Koutroumanis, C. Guilbault, S. Broussau, F. Malenfant, L. Bourget, L. Lamoureux, R. Lo, A. W. Caron, A. Pilotte and B. Massie, *BMC Biotechnol.*, 2006, **6**, 43.
- 222 W. Weber, C. Fux, M. D.-E. Baba, B. Keller, C. C. Weber, B. P. Kramer, C. Heinzen, D. Aubel, J. E. Bailey and M. Fussenegger, *Nat. Biotechnol.*, 2002, **20**, 901–907.
- 223 D. L. Wyborski, L. C. DuCoeur and J. M. Short, *Environ. Mol. Mutagen.*, 1996, **28**, 447–458.
- 224 L. Malphettes, C. C. Weber, M. D. El-Baba, R. G. Schoenmakers, D. Aubel, W. Weber and M. Fussenegger, *Nucleic Acids Res.*, 2005, **33**, e107.
- 225 S. Tascou, T.-K. Sorensen, V. Glénat, M. Wang, M. M. Lakich, R. Darteil, E. Vigne and V. Thuillier, *Mol. Ther.*, 2004, **9**, 637–649.
- 226 M. Gossen and H. Bujard, *Proc. Natl. Acad. Sci. U.S.A.*, 1992, **89**, 5547–5551.
- 227 C. Kemmer, M. Gitzinger, M. D.-E. Baba, V. Djonov, J. Stelling and M. Fussenegger, *Nat. Biotechnol.*, 2010, **28**, 355–360.
- 228 L. M. Guzman, D. Belin, M. J. Carson and J. Beckwith, *J. Bacteriol.*, 1995, **177**, 4121–4130.
- 229 R. Lutz and H. Bujard, *Nucleic Acids Res*, 1997, **25**, 1203–1210.
- 230 M. Lewis, *C. R. Biol.*, 2005, **328**, 521–548.
- 231 R. Bertram and W. Hillen, *Microb. Biotechnol.*, 2008, **1**, 2–16.

## References

- 232 U. Baron and H. Bujard, Tet repressor-based system for regulated gene expression in eukaryotic cells: Principles and advances in *Methods in Enzymology*, eds. J. Thorner, S. D. Emr and J. N. Abelson, Academic Press, 2000, vol. 327, 401–421.
- 233 L. J. O'Connor, C. Cazares-Körner, J. Saha, C. N. G. Evans, M. R. L. Stratford, E. M. Hammond and S. J. Conway, *Org. Chem. Front.*, 2015, **2**, 1026–1029.
- 234 L. J. O'Connor, I. N. Mistry, S. L. Collins, L. K. Folkes, G. Brown, S. J. Conway and E. M. Hammond, *ACS Cent. Sci.*, 2017, **3**, 20–30.
- 235 D. D. Young and A. Deiters, *Org. Biomol. Chem.*, 2007, **5**, 999–1005.
- 236 D. D. Young and A. Deiters, *Angew. Chem. Int. Ed.*, 2007, **46**, 4290–4292.
- 237 F. W. Hunter, R. J. Young, Z. Shalev, R. N. Vellanki, J. Wang, Y. Gu, N. Joshi, S. Sreebhavan, I. Weinreb, D. P. Goldstein, J. Moffat, T. Ketela, K. R. Brown, M. Koritzinsky, B. Solomon, D. Rischin, W. R. Wilson and B. G. Wouters, *Cancer Res.*, 2015, **75**, 4211–4223.
- 238 J. Wang, C. P. Guise, G. U. Dachs, Y. Phung, A. H.-L. Hsu, N. K. Lambie, A. V. Patterson and W. R. Wilson, *Biochem. Pharmacol.*, 2014, **91**, 436–446.
- 239 R. P. Gunsalus and S.-J. Park, *Res. Microbiol.*, 1994, **145**, 437–450.
- 240 P. J. Kiley and H. Beinert, *Curr. Opin. Microbiol.*, 2003, **6**, 181–185.
- 241 G. Sawers, *Curr. Opin. Microbiol.*, 1999, **2**, 181–187.
- 242 J. N. Copp, A. M. Mowday, E. M. Williams, C. P. Guise, A. Ashoorzadeh, A. V. Sharrock, J. U. Flanagan, J. B. Smaill, A. V. Patterson and D. F. Ackerley, *Cell Chem. Biol.*, 2017, **24**, 391–403.
- 243 M. D. Roldán, E. Pérez-Reinado, F. Castillo and C. Moreno-Vivián, *FEMS Microbiol. Rev.*, 2008, **32**, 474–500.
- 244 C. Cazares-Körner, I. M. Pires, I. D. Swallow, S. C. Grayer, L. J. O'Connor, M. M. Olcina, M. Christlieb, S. J. Conway and E. M. Hammond, *ACS Chemical Biology*, 2013, **8**, 1451–1459.
- 245 H. Jeong, V. Barbe, C. H. Lee, D. Vallenet, D. S. Yu, S.-H. Choi, A. Couloux, S.-W. Lee, S. H. Yoon, L. Cattolico, C.-G. Hur, H.-S. Park, B. Ségurens, S. C. Kim, T. K. Oh, R. E. Lenski, F. W. Studier, P. Daegelen and J. F. Kim, *J. Mol. Biol.*, 2009, **394**, 644–652.
- 246 E. W. P. Damen, T. J. Nevalainen, T. J. M. van den Bergh, F. M. H. de Groot and H. W. Scheeren, *Bioorg. Med. Chem.*, 2002, **10**, 71–77.
- 247 P. Wardman, *Environ. Health Perspect.*, 1985, **64**, 309–320.
- 248 R. Daber, S. Stayrook, A. Rosenberg and M. Lewis, *J. Mol. Biol.*, 2007, **370**, 609–619.
- 249 M. D. Barkley, A. D. Riggs, A. Jobe and S. Bourgeois, *Biochemistry*, 1975, **14**, 1700–1712.
- 250 A. D. Riggs, R. F. Newby and S. Bourgeois, *J. Mol. Biol.*, 1970, **51**, 303–314.
- 251 A. Jobe and S. Bourgeois, *J. Mol. Biol.*, 1972, **69**, 397–408.
- 252 J. Monod, G. Cohen-Bazire and M. Cohn, *Biochim. Biophys. Acta*, 1951, **7**, 585–599.

- 253 B. Müller-Hill, H. V. Rickenberg and K. Wallenfels, *J. Mol. Biol.*, 1964, **10**, 303–318.
- 254 W. Boos, P. Schaedel and K. Wallenfels, *Eur. J. Biochem.*, 1967, **1**, 382–394.
- 255 W. Koenigs and E. Knorr, *Ber. Dtsch. Chem. Ges.*, 1901, **34**, 957–981.
- 256 H. Paulsen, *Angew. Chem. Int. Ed.*, 1982, **21**, 155–173.
- 257 K. Toshima and K. Tatsuta, *Chem. Rev.*, 1993, **93**, 1503–1531.
- 258 T. Nukada, A. Berces, M. Z. Zgierski and D. M. Whitfield, *J. Am. Chem. Soc.*, 1998, **120**, 13291–13295.
- 259 Z. Wang, *Zemplén Deacetylation in Comprehensive Organic Name Reactions and Reagents*, Wiley, 2010, 3123–3128.
- 260 R. J. Ferrier and R. H. Furneaux, *Methods Carbohydr. Chem.*, 1980, **8**, 251–253.
- 261 J.-D. Pédelacq, S. Cabantous, T. Tran, T. C. Terwilliger and G. S. Waldo, *Nat. Biotechnol.*, 2006, **24**, 79–88.
- 262 P. Savitsky, J. Bray, C. D. O. Cooper, B. D. Marsden, P. Mahajan, N. A. Burgess-Brown and O. Gileadi, *J. Struct. Biol.*, 2010, **172**, 3–13.
- 263 Z. Wang, *Williamson Ether Synthesis in Comprehensive Organic Name Reactions and Reagents*, Wiley, 2010, 3026–3030.
- 264 P. G. M. Wuts, *Protection for the Hydroxyl Group, Including 1,2- and 1,3-Diols in Greene's Protective Groups in Organic Synthesis*, Wiley-Blackwell, 5th edn., 2014, 17–471.
- 265 S. Czernecki, C. Georgoulis and C. Provelenghiou, *Tetrahedron Lett.*, 1976, **17**, 3535–3536.
- 266 G. L. Closs and S. H. Goh, *J. Chem. Soc., Perkin Trans. 2*, 1972, 1473–1477.
- 267 M. Stanton-Humphreys, DPhil Thesis, University of Oxford, 2010.
- 268 D. J. Wardrop and C. L. Landrie, *p-Nitrobenzyl Bromide in Encyclopedia of Reagents for Organic Synthesis*, Wiley, 2003.
- 269 K. Fukase, H. Tanaka, S. Toriib and S. Kusumoto, *Tetrahedron Lett.*, 1990, **31**, 389–392.
- 270 J. M. Berry and L. D. Hall, *Carbohydr. Res.*, 1976, **47**, 307–310.
- 271 N. Nagashima and M. Ohno, *Chem. Lett.*, 1987, **16**, 141–144.
- 272 K. Fukase, S. Hase, T. Ikenaka and S. Kusumoto, *Bull. Chem. Soc. Jpn.*, 1992, **65**, 436–445.
- 273 P. J. Garegg, T. Iversen and S. Oscarson, *Carbohydr. Res.*, 1976, **50**, C12–C14.
- 274 T. Iversen and D. R. Bundle, *J. Chem. Soc., Chem. Commun.*, 1981, 1240–1241.
- 275 H.-P. Wessel, T. Iversen and D. R. Bundle, *J. Chem. Soc., Perkin Trans. 1*, 1985, 2247–2250.
- 276 L. Wang, Y. Hashidoko and M. Hashimoto, *J. Org. Chem.*, 2016, **81**, 4464–4474.
- 277 R. L. Lehtilä, J. O. Lehtilä, M. U. Roslund and R. Leino, *Tetrahedron*, 2004, **60**, 3653–3661.
- 278 J. S. Davies, C. L. Higginbotham, E. J. Tremeer, C. Brown and R. C. Treadgold, *J. Chem. Soc., Perkin Trans. 1*, 1992, 3043–3048.
- 279 J. W. Gillard, R. Fortin, H. E. Morton, C. Yoakim, C. A. Quesnelle, S. Daignault and Y. Guindon, *J. Org. Chem.*, 1988, **53**, 2602–2608.
- 280 E. J. Corey and A. Venkateswarlu, *J. Am. Chem. Soc.*, 1972, **94**, 6190–6191.

## References

- 281 C. S. Kraihanzel and J. E. Poist, *J. Organomet. Chem.*, 1967, **8**, 239–243.
- 282 J. H. Clark, *Chem. Rev.*, 1980, **80**, 429–452.
- 283 A. T. Khan and E. Mondal, *Synlett*, 2003, **5**, 694–698.
- 284 P. Peng, D.-C. Xiong and X.-S. Ye, *Carbohydr. Res.*, 2014, **384**, 1–8.
- 285 J. F. King and A. D. Allbutt, *Can. J. Chem.*, 1970, **48**, 1754–1769.
- 286 H. Dong, Y. Zhou, X. Pan, F. Cui, W. Liu, J. Liu and O. Ramström, *J. Org. Chem.*, 2012, **77**, 1457–1467.
- 287 P. Deslongchamps, *Stereoelectronic Effects in Organic Chemistry*, Pergamon Press, Oxford, 1st edn., 1983, vol. 1.
- 288 R. U. Lemieux and H. Driguez, *J. Am. Chem. Soc.*, 1975, **97**, 4069–4075.
- 289 L.-D. Lu, C.-R. Shie, S. S. Kulkarni, G.-R. Pan, X.-A. Lu and S.-C. Hung, *Org. Lett.*, 2006, **8**, 5995–5998.
- 290 Z. Khedri, Y. Li, S. Muthana, M. M. Muthana, C.-W. Hsiao, H. Yu and X. Chen, *Carbohydr. Res.*, 2014, **389**, 100–111.
- 291 S.-C. Hung, S. R. Thopate, F.-C. Chi, S.-W. Chang, J.-C. Lee, C.-C. Wang and Y.-S. Wen, *J. Am. Chem. Soc.*, 2001, **123**, 3153–3154.
- 292 C.-E. Yeom, S. Y. Lee, Y. J. Kim and B. M. Kim, *Synlett*, 2005, **2005**, 1527–1530.
- 293 J. Lawandi, S. Rocheleau and N. Moitessier, *Tetrahedron*, 2016, **72**, 6283–6319.
- 294 T. Kurahashi, T. Mizutani and J.-I. Yoshida, *J. Chem. Soc., Perkin Trans. 1*, 1999, 465–473.
- 295 F. Roussel, L. Knerr, M. Grathwohl and R. R. Schmidt, *Org. Lett.*, 2000, **2**, 3043–3046.
- 296 G. Gu, Y. Du and R. J. Linhardt, *J. Org. Chem.*, 2004, **69**, 5497–5500.
- 297 T. Angles d’Ortoli and G. Widmalm, *Tetrahedron*, 2016, **72**, 912–927.
- 298 L. Kong, A. Almond, H. Bayley and B. G. Davis, *Nat. Chem.*, 2016, **8**, 461–469.
- 299 T. Zhang, T. Wang and Z. Fang, *Synth. Commun.*, 2015, **45**, 2567–2575.
- 300 A. Joffrin, DPhil Thesis, University of Oxford, 2017.
- 301 P. J. Garegg, *Pure Appl. Chem.*, 1984, **56**, 845–858.
- 302 R. Eby, K. T. Webster and C. Schuerch, *Carbohydr. Res.*, 1984, **129**, 111–120.
- 303 H. M. I. Osborn, V. A. Brome, L. M. Harwood and W. G. Suthers, *Carbohydr. Res.*, 2001, **332**, 157–166.
- 304 Ru. Gangadharmath and A. V. Demchenko, *Synlett*, 2004, **12**, 2191–2193.
- 305 L. Chan and M. S. Taylor, *Org. Lett.*, 2011, **13**, 3090–3093.
- 306 S. David and S. Hanessian, *Tetrahedron*, 1985, **41**, 643–663.
- 307 I. J. Boyer, *Toxicology*, 1989, **55**, 253–298.
- 308 H. Xu, Y. Lu, Y. Zhou, B. Ren, Y. Pei, H. Dong and Z. Pei, *Adv. Synth. Catal.*, 2014, **356**, 1735–1740.
- 309 M. Giordano and A. Iadonisi, *J. Org. Chem.*, 2014, **79**, 213–222.
- 310 B. Ren, O. Ramström, Q. Zhang, J. Ge and H. Dong, *Chem. Eur. J.*, 2016, **22**, 2481–2486.

- 311 J. C. Lo, J. Gui, Y. Yabe, C.-M. Pan and P. S. Baran, *Nature*, 2014, **516**, 343–348.
- 312 M. Ohlin, R. Johnsson and U. Ellervik, *Carbohydr. Res.*, 2011, **346**, 1358–1370.
- 313 C.-H. Lai, H. S. Hahm, C.-F. Liang and P. H. Seeberger, *Beilstein J. Org. Chem.*, 2015, **11**, 617–621.
- 314 J. G. Taylor, X. Li, M. Oberthür, W. Zhu and D. E. Kahne, *J. Am. Chem. Soc.*, 2006, **128**, 15084–15085.
- 315 K. Kurimoto, H. Yamamura and A. Miyagawa, *Carbohydr. Res.*, 2015, **401**, 39–50.
- 316 S. Tani, S. Sawadi, M. Kojima, S. Akai and K. Sato, *Tetrahedron Lett.*, 2007, **48**, 3103–3104.
- 317 R. Johnsson, M. Ohlin and U. Ellervik, *J. Org. Chem.*, 2010, **75**, 8003–8011.
- 318 I. D. Swallow, DPhil Thesis, University of Oxford, 2014.
- 319 Y. Fukase, S.-Q. Zhang, K. Iseki, M. Oikawa, K. Fukase and S. Kusumoto, *Synlett*, 2001, **2001**, 1693–1698.
- 320 D. J. Jenkins and B. V. L. Potter, *Carbohydr. Res.*, 1994, **265**, 145–149.
- 321 F. Peri, L. Cipolla and F. Nicotra, *Tetrahedron Lett.*, 2000, **41**, 8587–8590.
- 322 K. Takeo and K. Shibata, *Carbohydr. Res.*, 1984, **133**, 147–151.
- 323 Z. Zhang and C.-H. Wong, *Tetrahedron*, 2002, **58**, 6513–6519.
- 324 H. Dong, Z. Pei, S. Byström and O. Ramström, *J. Org. Chem.*, 2007, **72**, 1499–1502.
- 325 S. V. Ley, D. K. Baeschlin, D. J. Dixon, A. C. Foster, S. J. Ince, H. W. M. Priepe and D. J. Reynolds, *Chem. Rev.*, 2001, **101**, 53–80.
- 326 S. V. Ley, H. W. M. Priepe and S. L. Warriner, *Angew. Chem. Int. Ed.*, 1994, **33**, 2290–2292.
- 327 A. Hense, S. V. Ley, H. M. I. Osborn, D. R. Owen, J.-F. Poisson, S. L. Warriner and K. E. Wesson, *J. Chem. Soc., Perkin Trans. 1*, 1997, 2023–2032.
- 328 J.-L. Montchamp, F. Tian, M. E. Hart and J. W. Frost, *J. Org. Chem.*, 1996, **61**, 3897–3899.
- 329 T. Buskas, Y. Li and G.-J. Boons, *Chem. Eur. J.*, 2005, **11**, 5457–5467.
- 330 D. Crich and P. Jayalath, *J. Org. Chem.*, 2005, **70**, 7252–7259.
- 331 R. Eskandari, K. Jones, D. R. Rose and B. M. Pinto, *Bioorg. Med. Chem. Lett.*, 2010, **20**, 5686–5689.
- 332 A. Hara, A. Imamura, H. Ando, H. Ishida and M. Kiso, *Molecules*, 2013, **19**, 414–437.
- 333 D. Liu, W. He, Z. Wang, L. Liu, C. Wang, C. Zhang, C. Wang, Y. Wang, G. Tanabe, O. Muraoka, X. Wu, L. Wu and W. Xie, *Eur. J. Med. Chem.*, 2016, **110**, 224–236.
- 334 K. M. Sureshan, A. M. Riley, M. P. Thomas, S. C. Tovey, C. W. Taylor and B. V. L. Potter, *J. Med. Chem.*, 2012, **55**, 1706–1720.
- 335 K. Ruda, J. Lindberg, P. J. Garegg, S. Oscarson and P. Konradsson, *J. Am. Chem. Soc.*, 2000, **122**, 11067–11072.
- 336 J.-F. Valdor and W. Mackie, *J. Carbohydr. Chem.*, 1997, **16**, 429–440.
- 337 E. Sasaki, C.-I. Lin, K.-Y. Lin and H. Liu, *J. Am. Chem. Soc.*, 2012, **134**, 17432–17435.

## References

- 338 D. J. Chambers, G. R. Evans and A. J. Fairbanks, *Tetrahedron*, 2005, **61**, 7184–7192.
- 339 S. Malik and K. P. R. Kartha, *Synlett*, 2009, **2009**, 1809–1811.
- 340 G. O. Aspinall, R. C. Carpenter and L. Khondo, *Carbohydr. Res.*, 1987, **165**, 281–298.
- 341 S. Yan, N. Ding, W. Zhang, P. Wang, Y. Li and M. Li, *Carbohydr. Res.*, 2012, **354**, 6–20.
- 342 M. J. Kiefel, B. Beisner, S. Bennett, I. D. Holmes and M. von Itzstein, *J. Med. Chem.*, 1996, **39**, 1314–1320.
- 343 S. Dasgupta, K. Pramanik and B. Mukhopadhyay, *Tetrahedron*, 2007, **63**, 12310–12316.
- 344 M. J. Marín, A. Rashid, M. Rejzek, S. A. Fairhurst, S. A. Wharton, S. R. Martin, J. W. McCauley, T. Wileman, R. A. Field and D. A. Russell, *Org. Biomol. Chem.*, 2013, **11**, 7101–7107.
- 345 P. L. Barili, G. Catelani, F. D’Andrea and E. Mastrorilli, *J. Carbohydr. Chem.*, 1997, **16**, 1001–1010.
- 346 A. K. Prasad, N. Kalra, Y. Yadav, S. K. Singh, S. K. Sharma, S. Patkar, L. Lange, C. E. Olsen, J. Wengel and V. S. Parmar, *Org. Biomol. Chem.*, 2007, **5**, 3524–3530.
- 347 E. Fischer, *Chem. Ber.*, **53**, 1621–1633.
- 348 H. Ohle, *Chem. Ber.*, **57**, 403–409.
- 349 M. L. Wolfrom, A. Thompson and M. Inatome, *J. Am. Chem. Soc.*, 1957, **79**, 3868–3871.
- 350 M. U. Roslund, O. Aitio, J. Wärmå, H. Maaheimo, D. Y. Murzin and R. Leino, *J. Am. Chem. Soc.*, 2008, **130**, 8769–8772.
- 351 K. B. Wiberg, W. F. Bailey, K. M. Lambert and Z. D. Stempel, *J. Org. Chem.*, 2018, **83**, 5242–5255.
- 352 D. M. Hall, *Carbohydr. Res.*, 1980, **86**, 158–160.
- 353 M. E. Evans, *Carbohydr. Res.*, 1972, **21**, 473–475.
- 354 U. Ellervik and G. Magnusson, *J. Org. Chem.*, 1998, **63**, 9314–9322.
- 355 G. Hirai, T. Watanabe, K. Yamaguchi, T. Miyagi and M. Sodeoka, *J. Am. Chem. Soc.*, 2007, **129**, 15420–15421.
- 356 J. Ohlsson and G. Magnusson, *Carbohydr. Res.*, 2000, **329**, 49–55.
- 357 B. M. Smith, T. M. Kubiczyk and A. E. Graham, *Tetrahedron*, 2012, **68**, 7775–7781.
- 358 R. Hevey, X. Chen and C.-C. Ling, *Carbohydr. Res.*, 2013, **376**, 37–48.
- 359 W. Frick, H. Glombik, S. Theis and R. Elvert, Novel aromatic fluoroglycoside derivatives, pharmaceuticals comprising said compounds, and the use thereof, World Intellectual Property Organization, WO2009100936A3, 2009.
- 360 J. Alam and J. L. Cook, *Anal. Biochem.*, 1990, **188**, 245–254.
- 361 J. Sambrook and D. W. Russell, *Molecular Cloning: A Laboratory Manual*, Cold Spring Harbor Laboratory Press, New York, 3rd ed., 2001.
- 362 S. J. Gould and S. Subramani, *Anal. Biochem.*, 1988, **175**, 5–13.

- 363 L. Tian, Y. Yang, L. M. Wysocki, A. C. Arnold, A. Hu, B. Ravichandran, S. M. Sternson, L. L. Looger and L. D. Lavis, *Proc. Natl. Acad. Sci. U.S.A.*, 2012, **109**, 4756–4761.
- 364 N. Shin, K. Hanaoka, W. Piao, T. Miyakawa, T. Fujisawa, S. Takeuchi, S. Takahashi, T. Komatsu, T. Ueno, T. Terai, T. Tahara, M. Tanokura, T. Nagano and Y. Urano, *ACS Chem. Biol.*, 2017, **12**, 558–563.
- 365 O. Shimomura, F. H. Johnson and Y. Saiga, *J. Cell. Comp. Physiol.*, 1962, **59**, 223–239.
- 366 R. Y. Tsien, *Annu. Rev. Biochem.*, 1998, **67**, 509–544.
- 367 G.-J. Kremers, S. G. Gilbert, P. J. Cranfill, M. W. Davidson and D. W. Piston, *J. Cell Sci.*, 2011, **124**, 157–160.
- 368 C. Coralli, M. Cemazar, C. Kanthou, G. M. Tozer and G. U. Dachs, *Cancer Res.*, 2001, **61**, 4784–4790.
- 369 R. Heim, D. C. Prasher and R. Y. Tsien, *Proc. Natl. Acad. Sci. U.S.A.*, 1994, **91**, 12501–12504.
- 370 B. G. Reid and G. C. Flynn, *Biochemistry*, 1997, **36**, 6786–6791.
- 371 J. Walter, S. Hausmann, T. Drepper, M. Puls, T. Eggert and M. Dihné, *PLoS One*, 2012, **7**, e43921.
- 372 A. M. Buckley, J. Petersen, A. J. Roe, G. R. Douce and J. M. Christie, *Curr. Opin. Chem. Biol.*, 2015, **27**, 39–45.
- 373 A. Mukherjee and C. M. Schroeder, *Curr. Opin. Biotechnol.*, 2015, **31**, 16–23.
- 374 A. Mukherjee, J. Walker, K. B. Weyant and C. M. Schroeder, *PLoS One*, 2013, **8**, e64753.
- 375 T. Drepper, T. Eggert, F. Circolone, A. Heck, U. Krauß, J.-K. Guterl, M. Wendorff, A. Losi, W. Gärtner and K.-E. Jaeger, *Nat. Biotechnol.*, 2007, **25**, 443–445.
- 376 S. Chapman, C. Faulkner, E. Kaiserli, C. Garcia-Mata, E. I. Savenkov, A. G. Roberts, K. J. Oparka and J. M. Christie, *Proc. Natl. Acad. Sci. U.S.A.*, 2008, **105**, 20038–20043.
- 377 A. Mukherjee, K. B. Weyant, U. Agrawal, J. Walker, I. K. O. Cann and C. M. Schroeder, *ACS Synth. Biol.*, 2015, **4**, 371–377.
- 378 S. Balzer, V. Kucharova, J. Megerle, R. Lale, T. Brautaset and S. Valla, *Microb. Cell Fact.*, 2013, **12**, 26–40.
- 379 H. Tegel, J. Ottosson and S. Hober, *FEBS J.*, 2011, **278**, 729–739.
- 380 M. Lanzer and H. Bujard, *Proc. Natl. Acad. Sci. U.S.A.*, 1988, **85**, 8973–8977.
- 381 S. Oehler, M. Amouyal, P. Kolkhof, B. von Wilcken-Bergmann and B. Müller-Hill, *EMBO J.*, 1994, **13**, 3348–3355.
- 382 J. R. Sadler, H. Sasmor and J. L. Betz, *Proc. Natl. Acad. Sci. U.S.A.*, 1983, **80**, 6785–6789.
- 383 P. Penumetcha, K. Lau, X. Zhu, K. Davis, T. T. Eckdahl and A. M. Campbell, *BIOS*, 2010, **81**, 7–15.
- 384 Y. Qu and J. C. Spain, *Environ. Microbiol.*, 2011, **13**, 1010–1017.
- 385 W. A. Denny, *Lancet Oncol.*, 2000, **1**, 25–29.

## References

- 386 Y. Chen and L. Hu, *Med. Res. Rev.*, 2009, **29**, 29–64.
- 387 M. C. T. Hu and N. Davidson, *Cell*, 1987, **48**, 555–566.
- 388 S.-J. Fan, C. Snell, H. Turley, J.-L. Li, R. McCormick, S. M. W. Perera, S. Heublein, S. Kazi, A. Azad, C. Wilson, A. L. Harris and D. C. I. Goberdhan, *Oncogene*, 2016, **35**, 3004–3015.
- 389 D. Chen, O. Tavana, B. Chu, L. Erber, Y. Chen, R. Baer and W. Gu, *Mol. Cell*, 2017, **68**, 224–232.
- 390 L. Caron, M. Prot, M. Rouleau, M. Rolando, F. Bost and B. Binétruy, *Cell. Mol. Life Sci.*, 2005, **62**, 1605–1612.
- 391 C. A. Cronin, W. Gluba and H. Scrable, *Genes Dev.*, 2001, **15**, 1506–1517.
- 392 H. Scrable, *Semin. Cell Dev. Biol.*, 2002, **13**, 109–119.
- 393 J. K. Rose, *Curr. Protoc. Cell Biol.*, 2003, **19**, 20.7.1–20.7.4.
- 394 N. J. Yang and M. J. Hinner, *Methods Mol. Biol.*, 2015, **1266**, 29–53.
- 395 M. Mueckler and B. Thorens, *Mol. Aspects Med.*, 2013, **34**, 121–138.
- 396 L. Di, E. H. Kerns, K. Fan, O. J. McConnell and G. T. Carter, *Eur. J. Med. Chem.*, 2003, **38**, 223–232.
- 397 C. Zhu, L. Jiang, T.-M. Chen and K.-K. Hwang, *Eur. J. Med. Chem.*, 2002, **37**, 399–407.
- 398 F. Wohnsland and B. Faller, *J. Med. Chem.*, 2001, **44**, 923–930.
- 399 M. Kansy, F. Senner and K. Gubernator, *J. Med. Chem.*, 1998, **41**, 1007–1010.
- 400 M. P. Murphy and R. A. J. Smith, *Annu. Rev. Pharmacol. Toxicol.*, 2007, **47**, 629–656.
- 401 M. F. Ross, T. Da Ros, F. H. Blaikie, T. A. Prime, C. M. Porteous, I. I. Severina, V. P. Skulachev, H. G. Kjaergaard, R. A. J. Smith and M. P. Murphy, *Biochem. J.*, 2006, **400**, 199–208.
- 402 H.-K. Han and G. L. Amidon, *AAPS PharmSci*, 2000, **2**, 48–58.
- 403 A. Abazari, L. G. Meimetis, G. Budin, S. S. Bale, R. Weissleder and M. Toner, *PLoS One*, 2015, **10**, e0130323.
- 404 G. E. Adams, I. J. Stratford, R. G. Wallace, P. Wardman and M. E. Watts, *J. Natl. Cancer Inst.*, 1980, **64**, 555–560.
- 405 B. A. Winn, Z. Shi, G. J. Carlson, Y. Wang, B. L. Nguyen, E. M. Kelly, R. D. Ross, E. Hamel, D. J. Chaplin, M. L. Trawick and K. G. Pinney, *Bioorg. Med. Chem. Lett.*, 2017, **27**, 636–641.
- 406 M. T. S. Mok and B. R. Henderson, *Cytometry A*, 2012, **81A**, 101–104.
- 407 A. Mullick, Y. Xu, R. Warren, M. Koutroumanis, C. Guilbault, S. Broussau, F. Malenfant, L. Bourget, L. Lamoureux, R. Lo, A. W. Caron, A. Pilotte and B. Massie, *BMC Biotechnology*, 2006, **6**, 43–61.
- 408 A. B. Pangborn, M. A. Giardello, R. H. Grubbs, R. K. Rosen and F. J. Timmers, *Organometallics*, 1996, **15**, 1518–1520.



- 409 G. R. Fulmer, A. J. M. Miller, N. H. Sherden, H. E. Gottlieb, A. Nudelman, B. M. Stoltz, J. E. Bercaw and K. I. Goldberg, *Organometallics*, 2010, **29**, 2176–2179.
- 410 W. T. Haskins, R. M. Hann and C. S. Hudson, *J. Am. Chem. Soc.*, 1942, **64**, 1852–1856.
- 411 B. J. Ayers, J. Hollinshead, A. W. Saville, S. Nakagawa, I. Adachi, A. Kato, K. Izumori, B. Bartholomew, G. W. J. Fleet and R. J. Nash, *Phytochemistry*, 2014, **100**, 126–131.
- 412 M. H. Clausen, M. R. Jorgensen, J. Thorsen and R. Madsen, *J. Chem. Soc., Perkin Trans. I*, 2001, 543–551.
- 413 Y. Guo, Y. Zhao, C. Zheng, Y. Meng and Y. Yang, *Chem. Pharm. Bull.*, 2010, **58**, 1627–1629.
- 414 S. Mandal and U. J. Nilsson, *Org. Biomol. Chem.*, 2014, **12**, 4816–4819.
- 415 M. Sakata, M. Haga and S. Tejima, *Carbohydr. Res.*, 1970, **13**, 379–390.
- 416 M. Černý, J. Staněk and J. Pacák, *Monatsh. Chem.*, 1963, **94**, 290–294.
- 417 B. Helferich and D. Türk, *Chem. Ber.*, 1956, **89**, 2215–2219.
- 418 Y. Du, M. Zhang, F. Yang and G. Gu, *J. Chem. Soc., Perkin Trans. I*, 2001, 3122–3127.
- 419 S. F. Andrade, C. S. Teixeira, J. P. Ramos, M. S. Lopes, R. M. Pádua, M. C. Oliveira, E. M. Souza-Fagundes and R. J. Alves, *MedChemComm*, 2014, **5**, 1693–1699.
- 420 S. Hayat, Atta-ur-Rahman, K. Mohammed Khan, M. Iqbal Choudhary, G. M. Maharvi, Zia-Ullah and E. Bayer, *Synth. Commun.*, 2003, **33**, 2531–2540.
- 421 B. Doboszewski and P. Herdewijn, *Tetrahedron Lett.*, 2012, **53**, 2253–2256.
- 422 T. Kurita, K. Hattori, S. Seki, T. Mizumoto, F. Aoki, Y. Yamada, K. Ikawa, T. Maegawa, Y. Monguchi and H. Sajiki, *Chem. Eur. J.*, 2008, **14**, 664–673.
- 423 A. A. Adhikari, L. Radal and J. D. Chisholm, *Synlett*, 2017, **28**, 2335–2339.
- 424 H. Redlich, W. Sudau, A. K. Szardenings and R. Vollerthun, *Carbohydr. Res.*, 1992, **226**, 57–78.
- 425 J. M. Aurrecoechea, J. H. Gil and B. López, *Tetrahedron*, 2003, **59**, 7111–7121.
- 426 R. Ruiz Contreras, J. P. Kamerling, J. Breg and J. F. G. Vliegthart, *Carbohydr. Res.*, 1988, **179**, 411–418.
- 427 S. David, A. Thieffry and A. Veyrieres, *J. Chem. Soc., Perkin Trans. I*, 1981, **0**, 1796–1801.
- 428 X. Geng, L. Wang, G. Gu and Z. Guo, *Carbohydr. Res.*, 2016, **427**, 13–20.
- 429 H. Liu, R. Nasi, K. Jayakanthan, L. Sim, H. Heipel, D. R. Rose and B. M. Pinto, *J. Org. Chem.*, 2007, **72**, 6562–6572.
- 430 Y. Kobayashi, M. Shiozaki and O. Ando, *J. Org. Chem.*, 1995, **60**, 2570–2580.
- 431 Bethesda Research Laboratories, *Focus*, 1986, **8**, 9.
- 432 J. Chen, Y. Li, K. Zhang and H. Wang, *Genome Announc.*, 2018, **6**, e00097-18.
- 433 J. Schindelin, I. Arganda-Carreras, E. Frise, V. Kaynig, M. Longair, T. Pietzsch, S. Preibisch, C. Rueden, S. Saalfeld, B. Schmid, J.-Y. Tinevez, D. J. White, V. Hartenstein, K. Eliceiri, P. Tomancak and A. Cardona, *Nat. Methods*, 2012, **9**, 676–682.

## *References*

- 434 D. G. Gibson, L. Young, R.-Y. Chuang, J. C. Venter, C. A. Hutchison and H. O. Smith, *Nat. Methods*, 2009, **6**, 343–345.

---

# APPENDICES

---

## A. DNA Sequences for Fluorescent Proteins

### A1. iLOV

5'-TTTAACTTTAAGAAGGAGATATACATATGCACCATCATCATCATCATATTGAAAA  
AAACTTTGTGATTACCGACCCGCGTCTGCCGGATAACCCGATCATTTTCGCGTCTGA  
TGGCTTCCTGGAAGTACTGAGTATAGCCGTGAAGAAATCCTGGGCCGCAATGCTC  
GTTTTCTGCAGGGCCCGGAGACCGATCAAGCTACCGTGCAGAAGATTCGTGATGCA  
ATTCGTGACCAGCGCGAAACGACTGTGCAGCTGATTAAGTATAACCAAGAGCGGTAA  
AAGATTCTGGAACCTGCTGCACCTGCAGCCGGTCCGTGATCAGAAAGGCGAGCTGC  
AGTATTTTCATCGGTGTTTCAGCTGGATGGTTCTGACCACGTATAATGAGGATCCGAAT  
TCGAGCTCC-3'

### A2. creiLOV

5'-TTTAACTTTAAGAAGGAGATATACATATGCACCATCACCATCACCATGCAGGTTT  
ACGTCATACATTCGTCTGTGGCAGACGCGACCCTGCCCCGACTGCCCCCTTGTGTACGC  
ATCGGAAGGATTCTACGCGATGACTGGGTATGGCCCTGATGAAGTTTTGGGACATA  
ACGCCCCGTTTCCTGCAAGGCGAAGGCACAGATCCTAAAGAGGTCCAAAAAATCCGC  
GATGCCATCAAGAAGGGGGAGGCGTGTAGCGTCCGCTTGTTAAATTACCGCAAGGA  
TGGTACACCTTTTTTGAATTTATTAACAGTTACTCCGATTAAAACGCCGGACGGGCG  
TGTGAGCAAATTCGTGGGCGTTCAAGTCGATGTTACCAGCAAGACTGAGGGTAAAG  
CGTTGGCTTAATGAGGATCCGAATTCGAGCTCC-3'

### A3. sfGFP

5'- ATGGGTCATCACCACCACCATCACGGTGGCGCTAGCAAAGGTGAAGAGCTGTTT  
ACGGGTGTAGTACCGATCTTAGTGGAATTAGACGGCGACGTGAACGGTCACAAATT  
TAGCGTGCGCGGCGAAGGCGAAGGTGACGCTACCAATGGTAAATTGACCCTGAAG

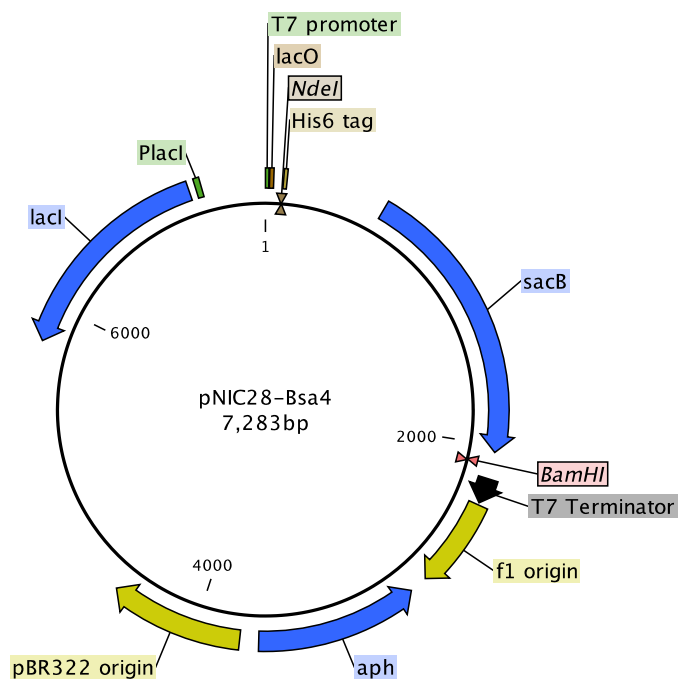
TTTATTTGCACAACAGGCAAATTACCCGTTCCGTGGCCCACCTTAGTGACCACCCTG  
ACCTATGGCGTTCAGTGCTTCAGTCGTTACCCAGATCATATGAAACAACACGATTTT  
TTCAAATCAGCCATGCCTGAAGGATATGTTCAAGAGCGTACAATCAGCTTCAAGGA  
CGATGGCACCTATAAAACGCGTGCGGAAGTGAAATTTGAAGGCGACACATTAGTA  
AACCGTATCGAACTGAAAGGTATCGACTTCAAAGAAGACGGCAACATTTTAGGCCA  
TAAGCTGGAATATAACTTTAATTCTCATAACGTGTATATTACGGCCGATAAACAGA  
AAAACGGTATCAAGGCAAATTTCAAAATTCGCCATAACGTGGAAGACGGCAGCGTT  
CAATTAGCGGATCATTATCAACAAAACACGCCGATTGGTGACGGGCCTGTACTGTT  
ACCTGACAACCACTACCTGAGCACCCAGTCAGCACTGAGCAAAGATCCGAACGAA  
AAACGCGATCACATGGTTCTGTTAGAATTCGTGACCGCTGCAGGCATTACTCACGG  
AATGGACGAACTCTACAAGTAATAATGA-3'

## B. Plasmid Maps

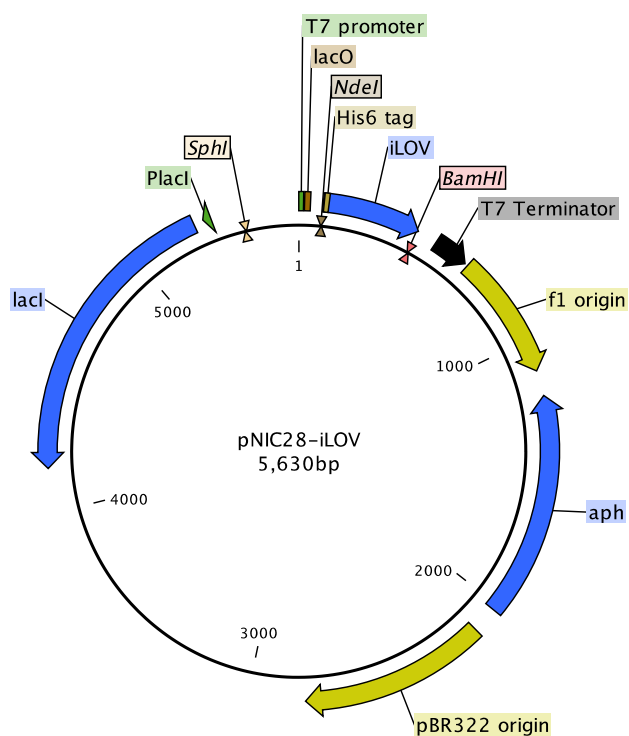
The plasmid maps shown below were generated and annotated by using CLC Main Workbench 7.9.2 and are drawn to scale. Where appropriate, the following features are indicated.

- Promoters (T7, T5, CMV, HSV-TK, RSV) for transcribing the target gene
- Terminators (T7, HSV-TK PolyA signal) for terminating gene transcription
- Restriction sites or multiple cloning site (MCS) region for linearizing the
- His6 tag for labelling proteins with a hexa-histidine tag
- Location of *lacO* (*lac* operator, the site bound by the LacI repressor)
- DNA replication origins, pBR322 or pUC (for double-stranded DNA replication of plasmid in *E. coli*) and f1 (for single stranded replication in presence of a helper phage)
- Kanamycin (*ahh*), ampicillin (*bla*), hygromycin (hygromycin B phosphotransferase), and G418 (neomycin) selectable marker genes
- SV40 nuclear localization sequence (NLS)

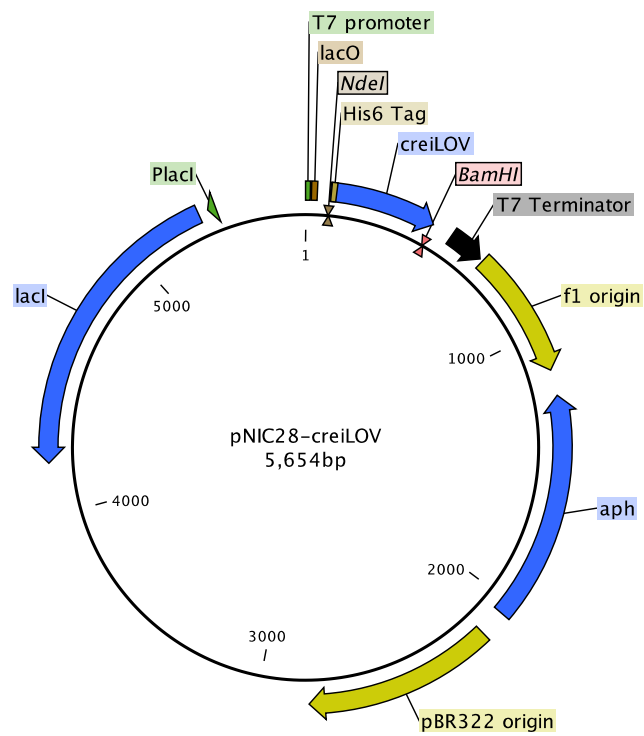
## B1. pNIC28-Bsa4



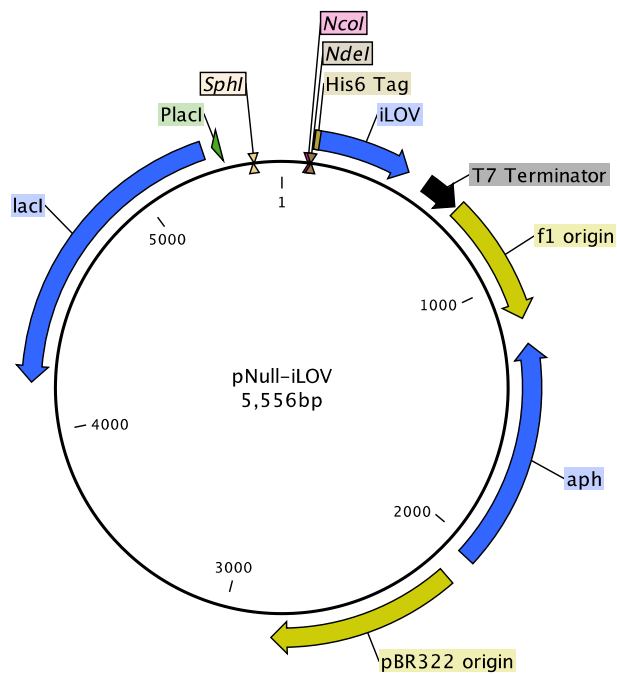
## B2. pNIC28-iLOV



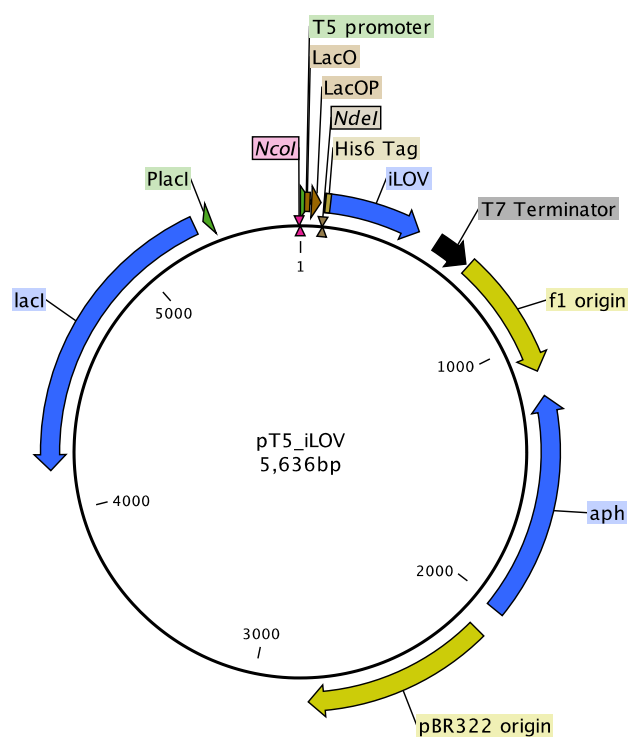
### B3. pNIC28-creiLOV



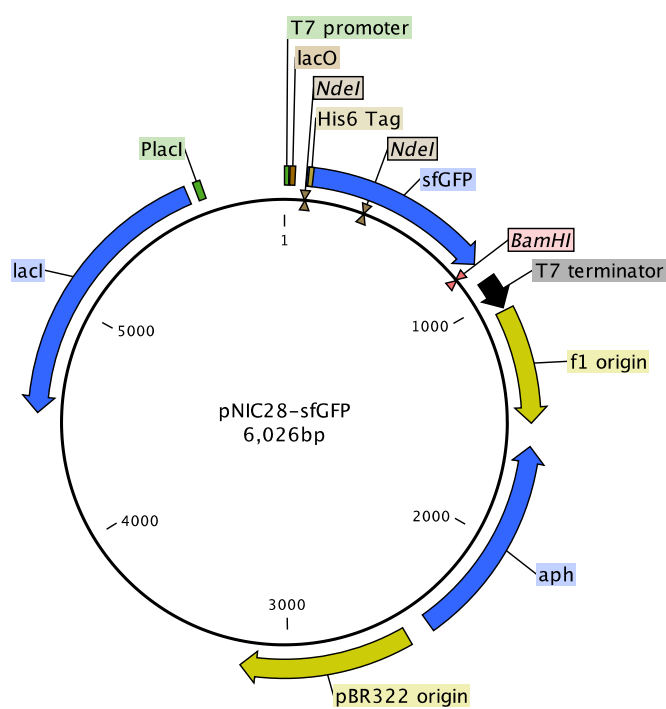
### B4. pNull-iLOV



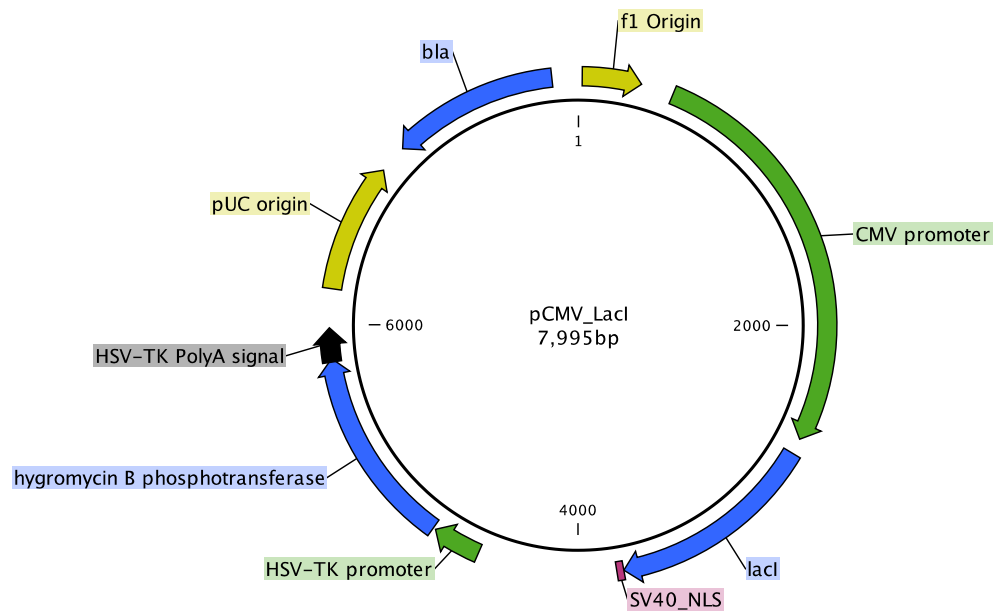
## B5. pT5-iLOV



## B6. pNIC28-sfGFP

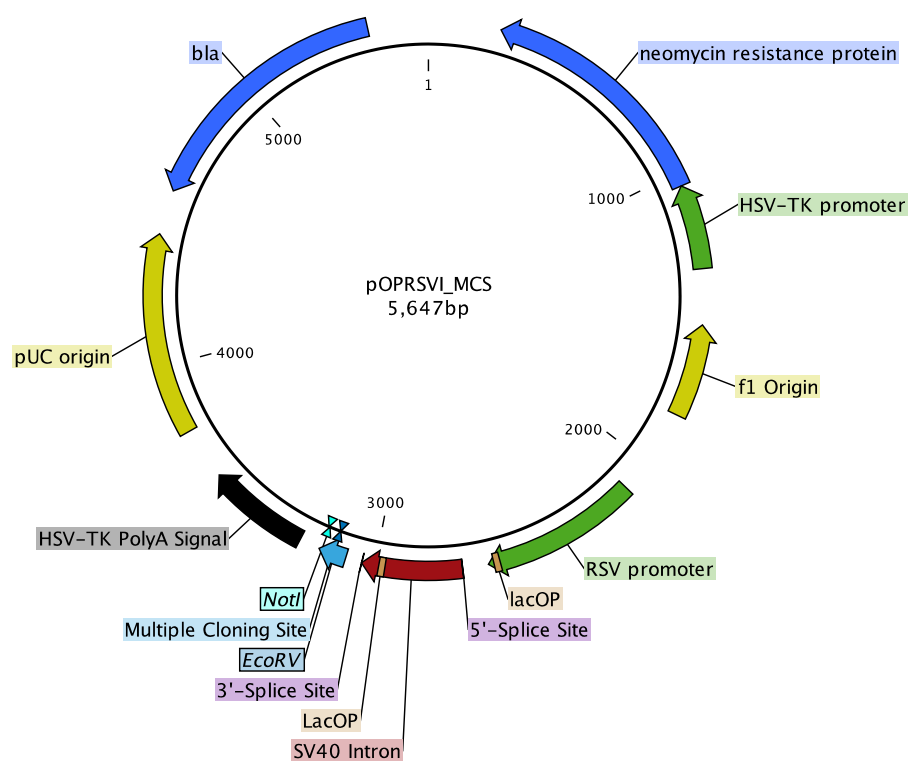
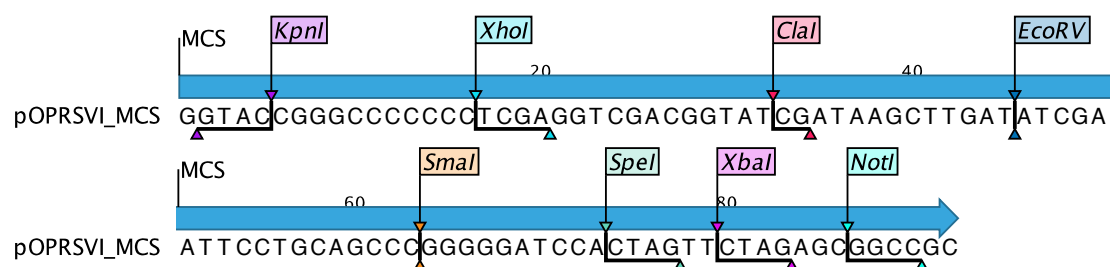


## B7. pCMVLacI



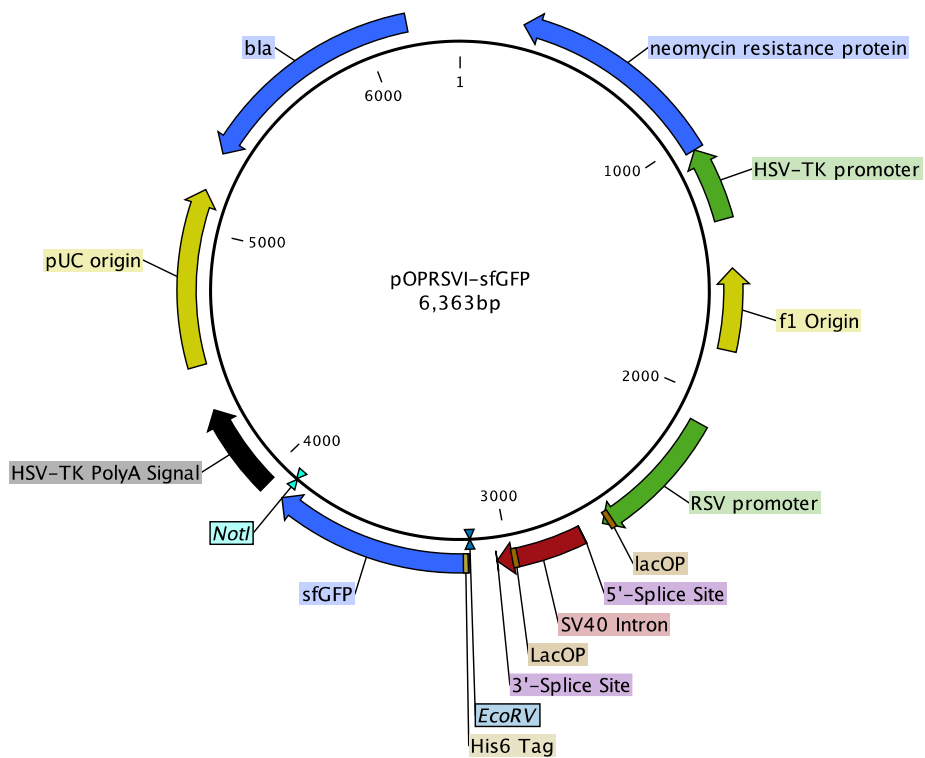
The complete nucleotide sequence and list of restriction sites is available from the GenBank<sup>®</sup> database (Accession #U64448).



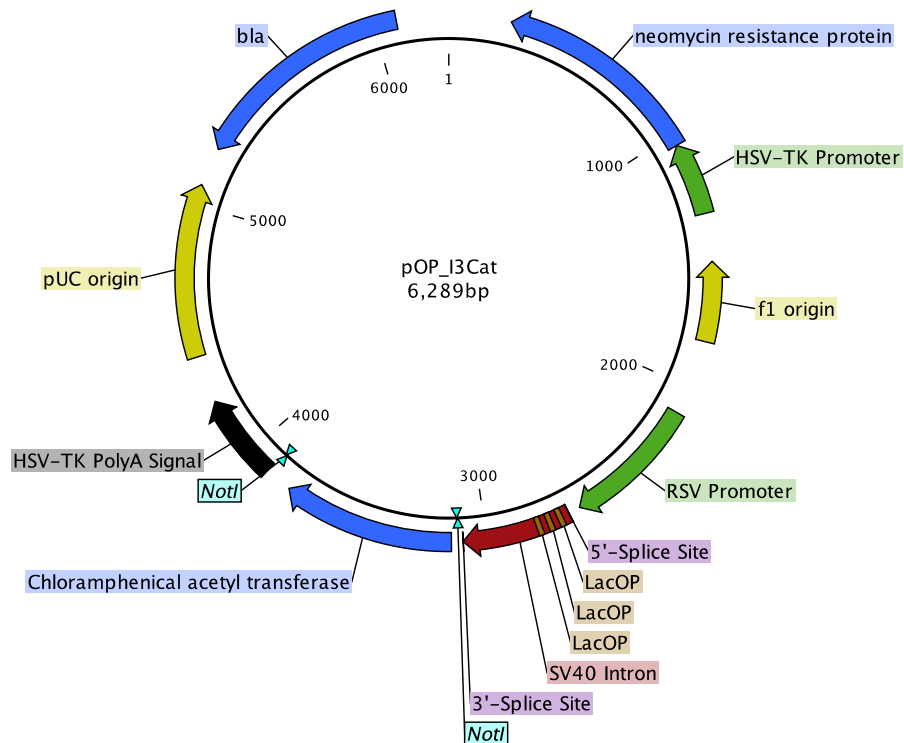
**B8. pOPRSVI/MCS****pOPRSVI/MCS Multiple Cloning Site Region**

The complete nucleotide sequence and list of restriction sites is available from the GenBank® database (Accession #U64449).

## B9. pOPRSVI-sfGFP

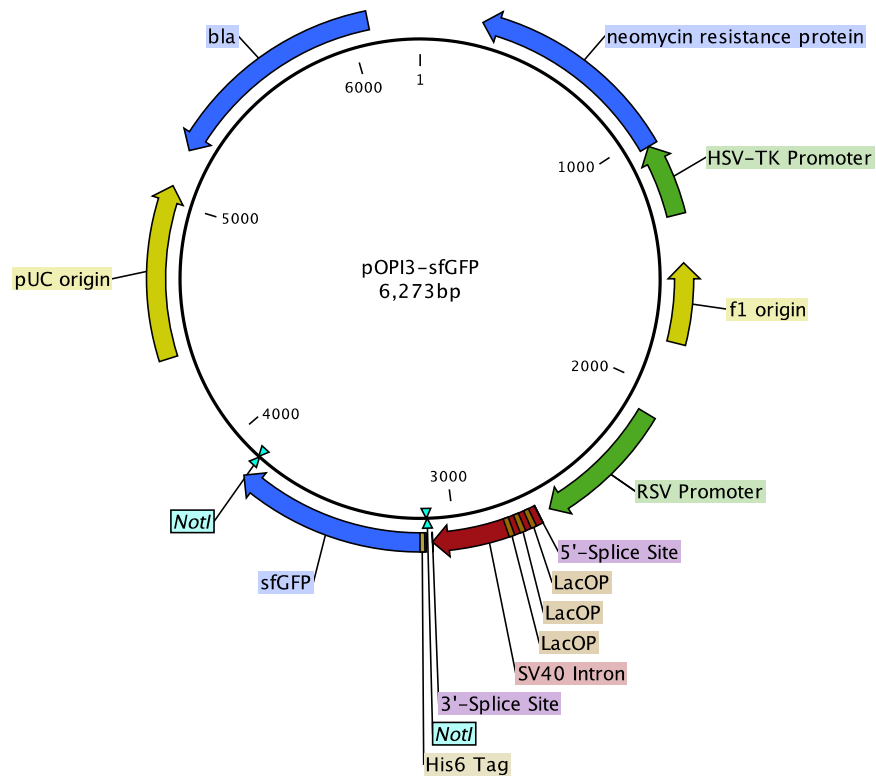


## B10. pOPI3CAT



The complete nucleotide sequence and list of restriction sites is available from [www.stratagene.com](http://www.stratagene.com) or from the GenBank® database (Accession #U42373).

# B11. pOPI3-sfGFP



### **C. Selected NMR Spectra**

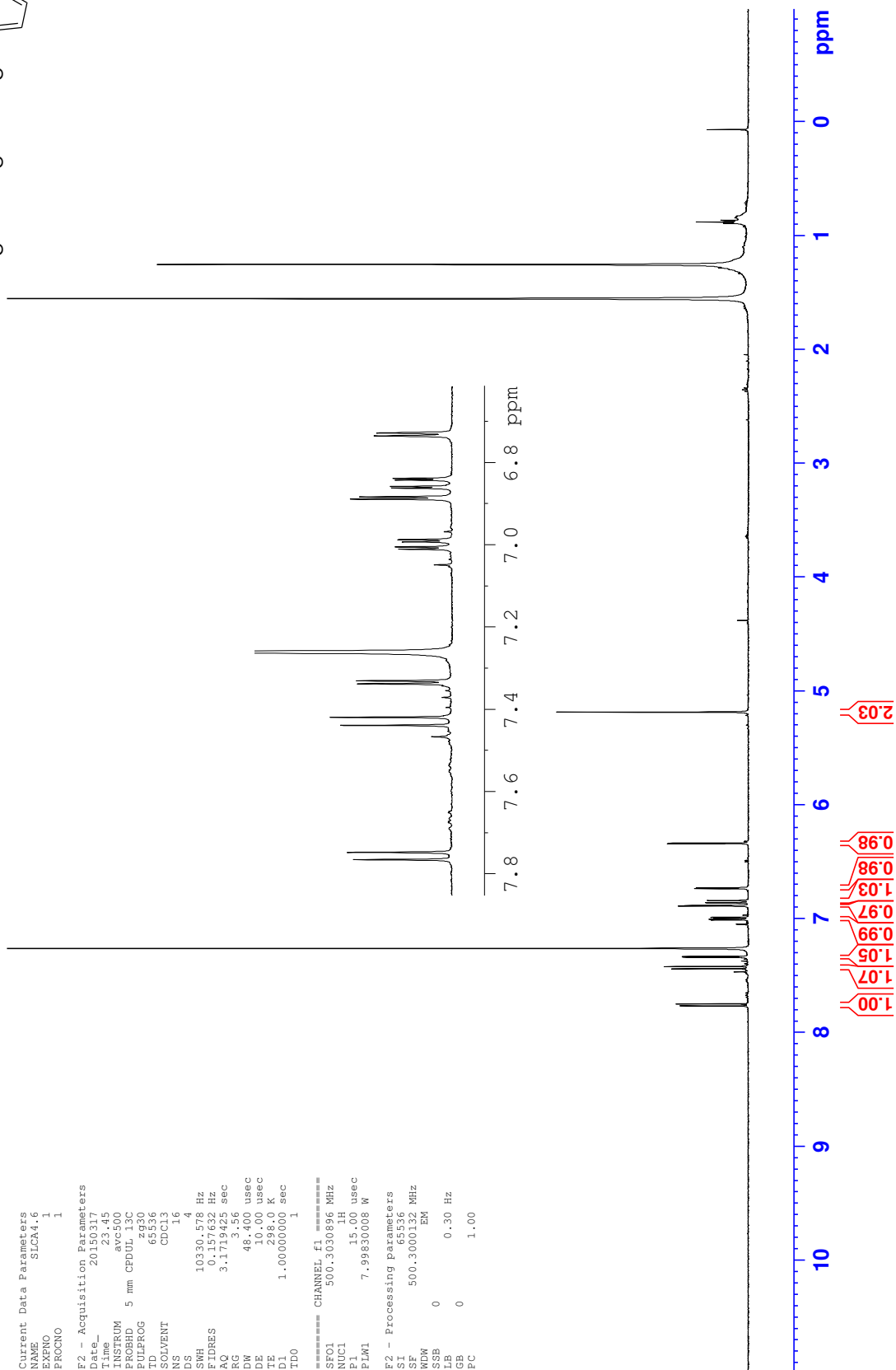
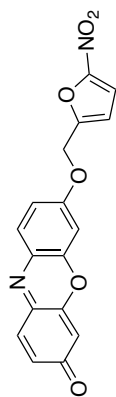
NMR spectra ( $^1\text{H}$ ,  $^{13}\text{C}$  and, where applicable,  $^1\text{H}$ - $^{29}\text{Si}$  HMBC) are reported for all novel and final compounds. Spectra are presented in the order in which the compounds appear in Chapter 6 (Experimental).

### **D. Image Permissions**

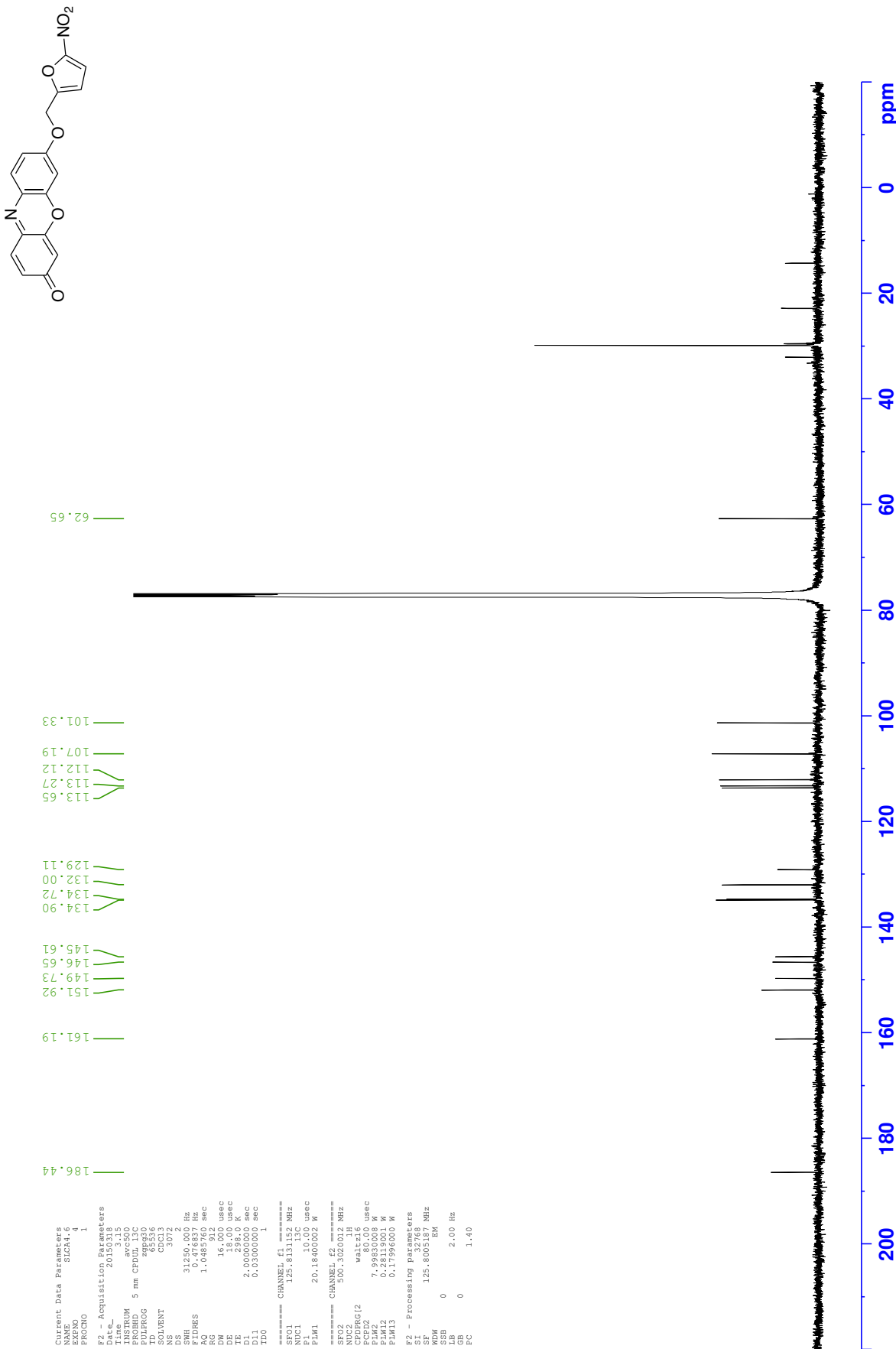
Permissions for the images featured in Chapter 1 of this dissertation can be found at the end of the appendices.



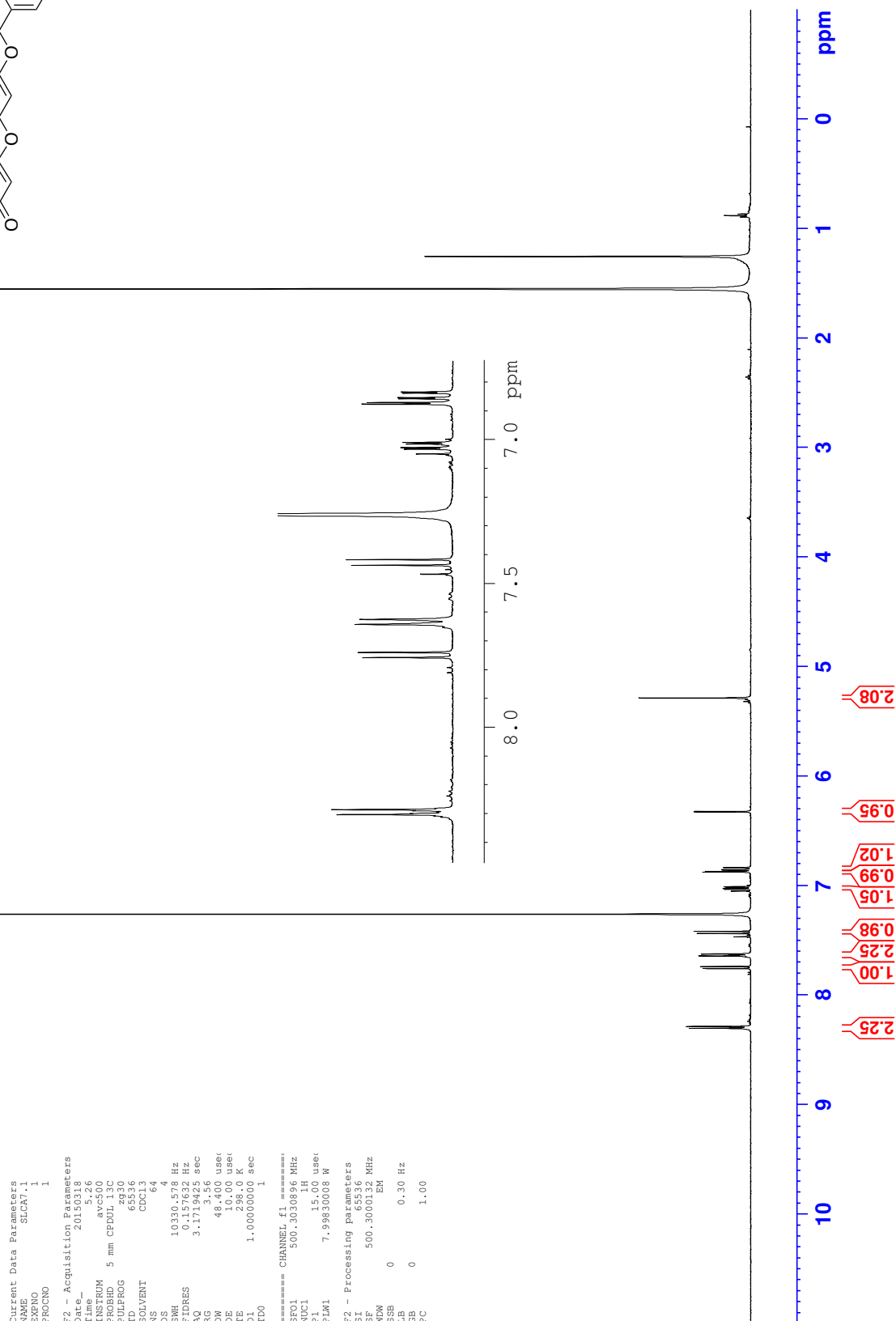
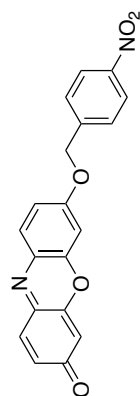
<sup>1</sup>H NMR - 7-[(5-Nitrofur-2-yl)methoxy]-3*H*-phenoxazin-3-one **63**



<sup>13</sup>C NMR - 7-[(5-Nitrofur-2-yl)methoxy]-3H-phenoxazin-3-one **63**

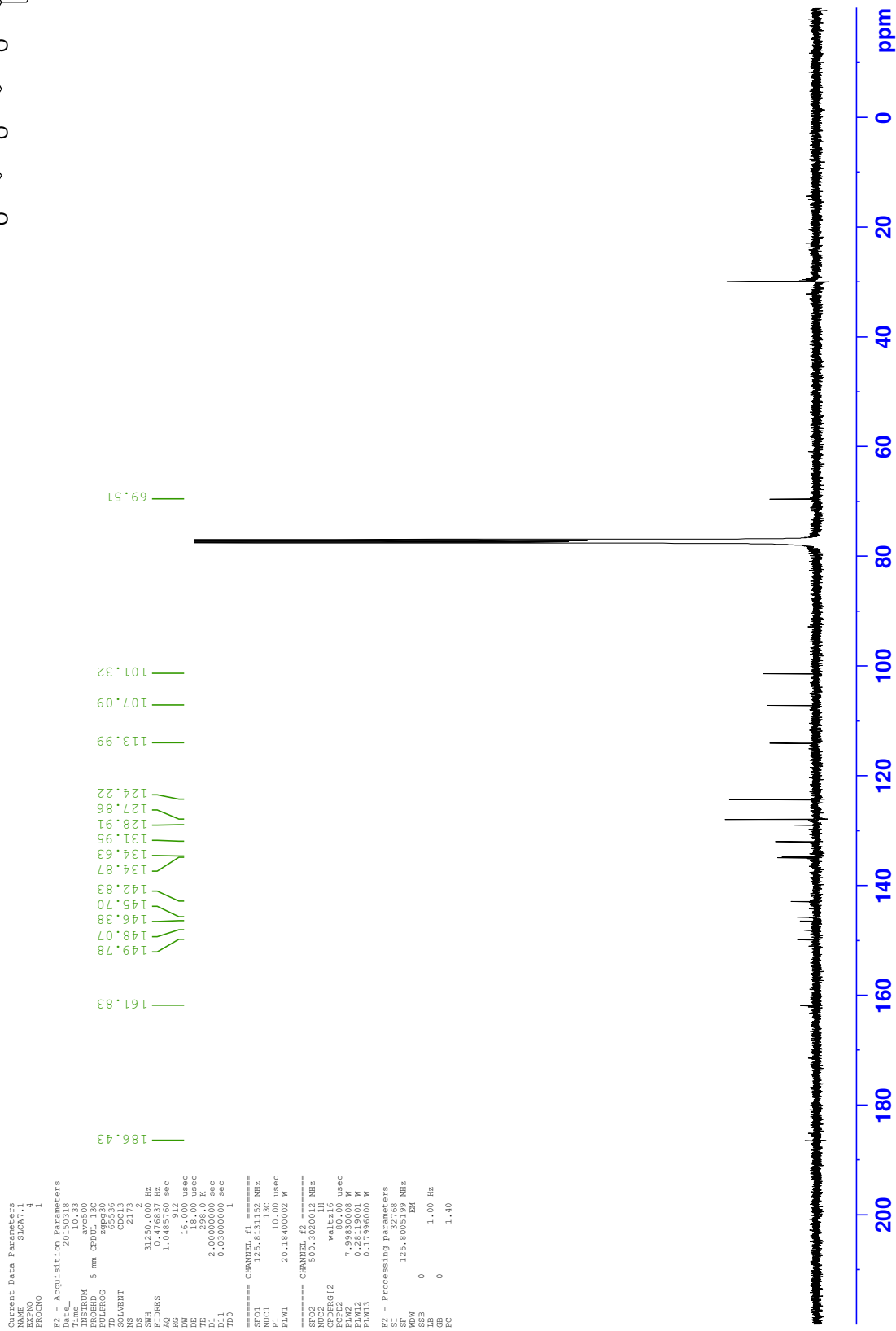
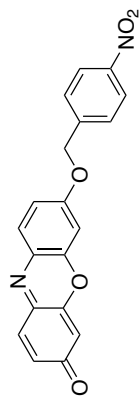


<sup>1</sup>H NMR - 7-[(4-Nitrobenzyl)oxy]-3H-phenoxazin-3-one 79

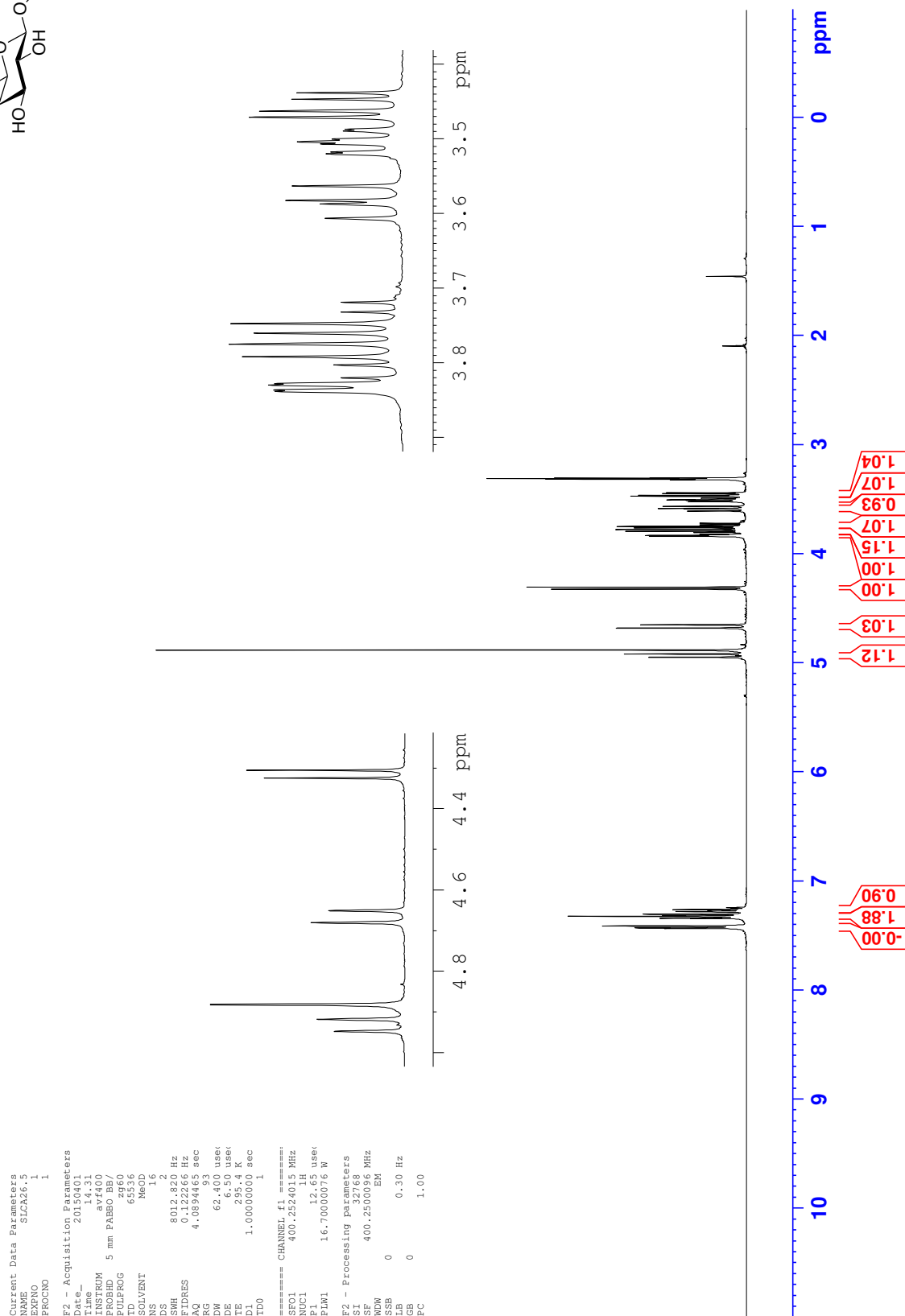
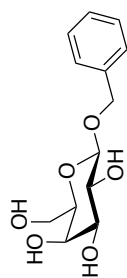


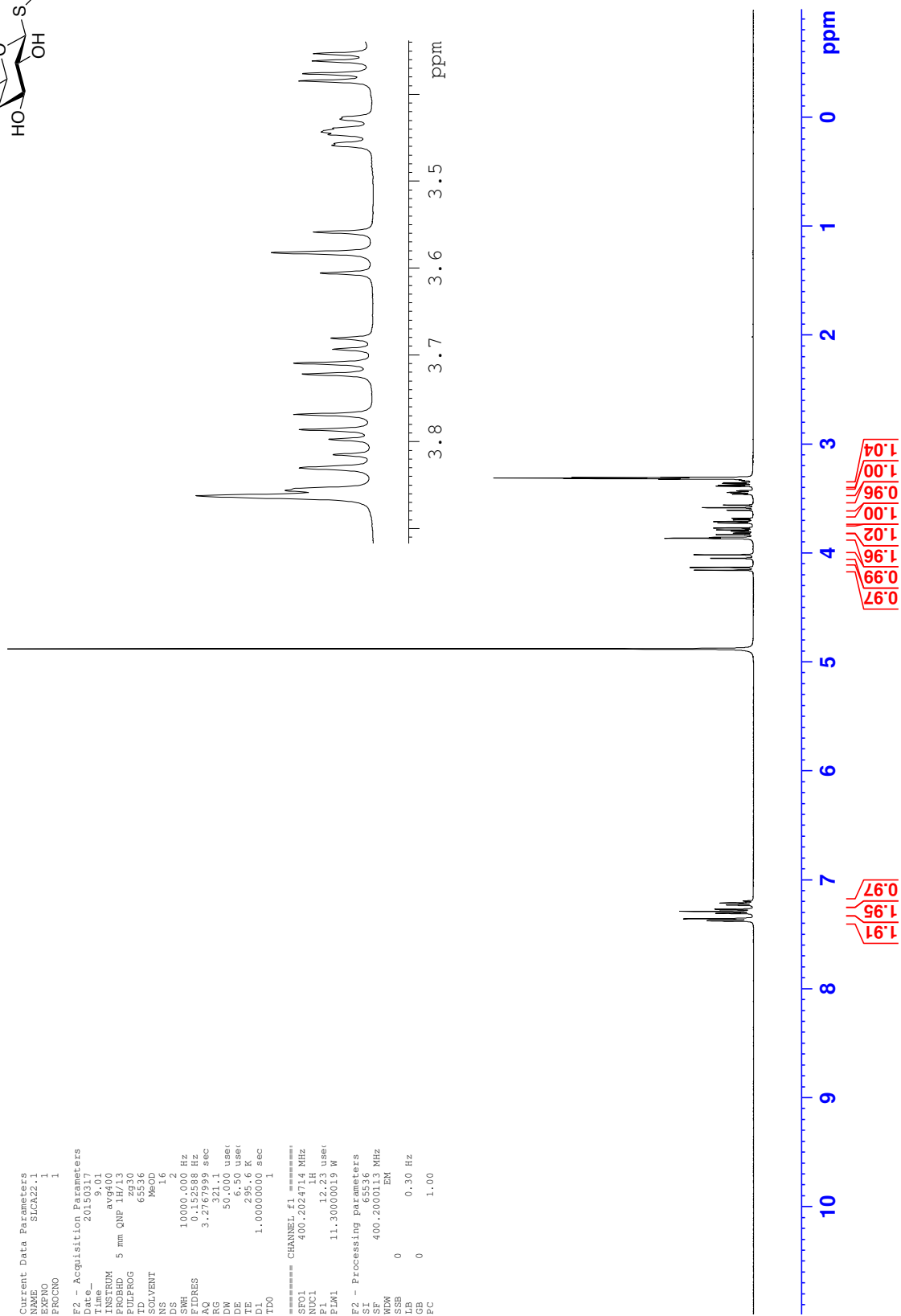
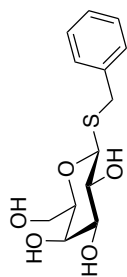


<sup>13</sup>C NMR - 7-[ (4-Nitrobenzyl)oxy] -3H-phenoxazin-3-one 79



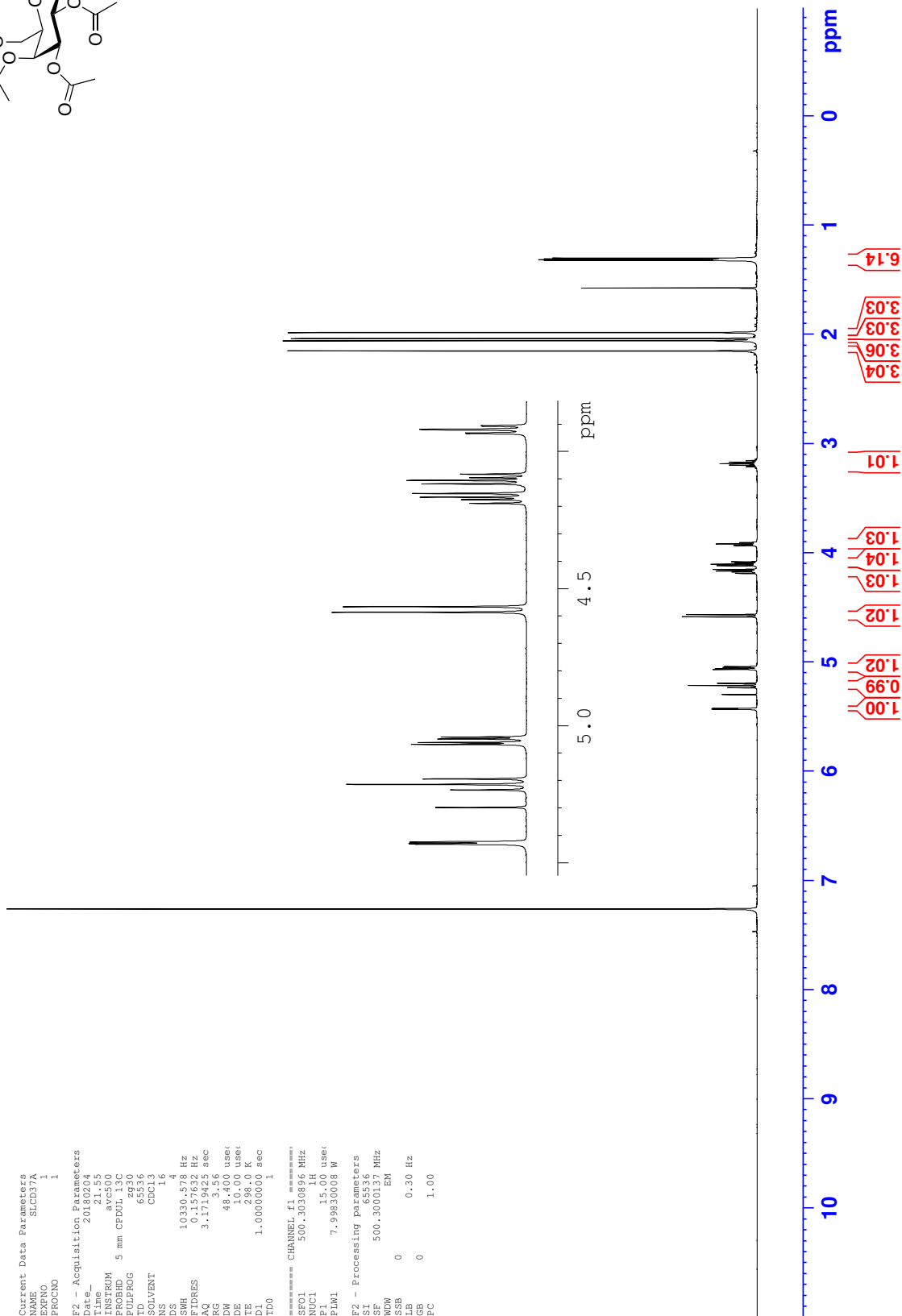
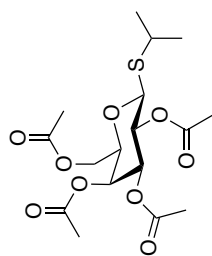
<sup>1</sup>H NMR - Benzyl β-D-galactopyranoside **103**



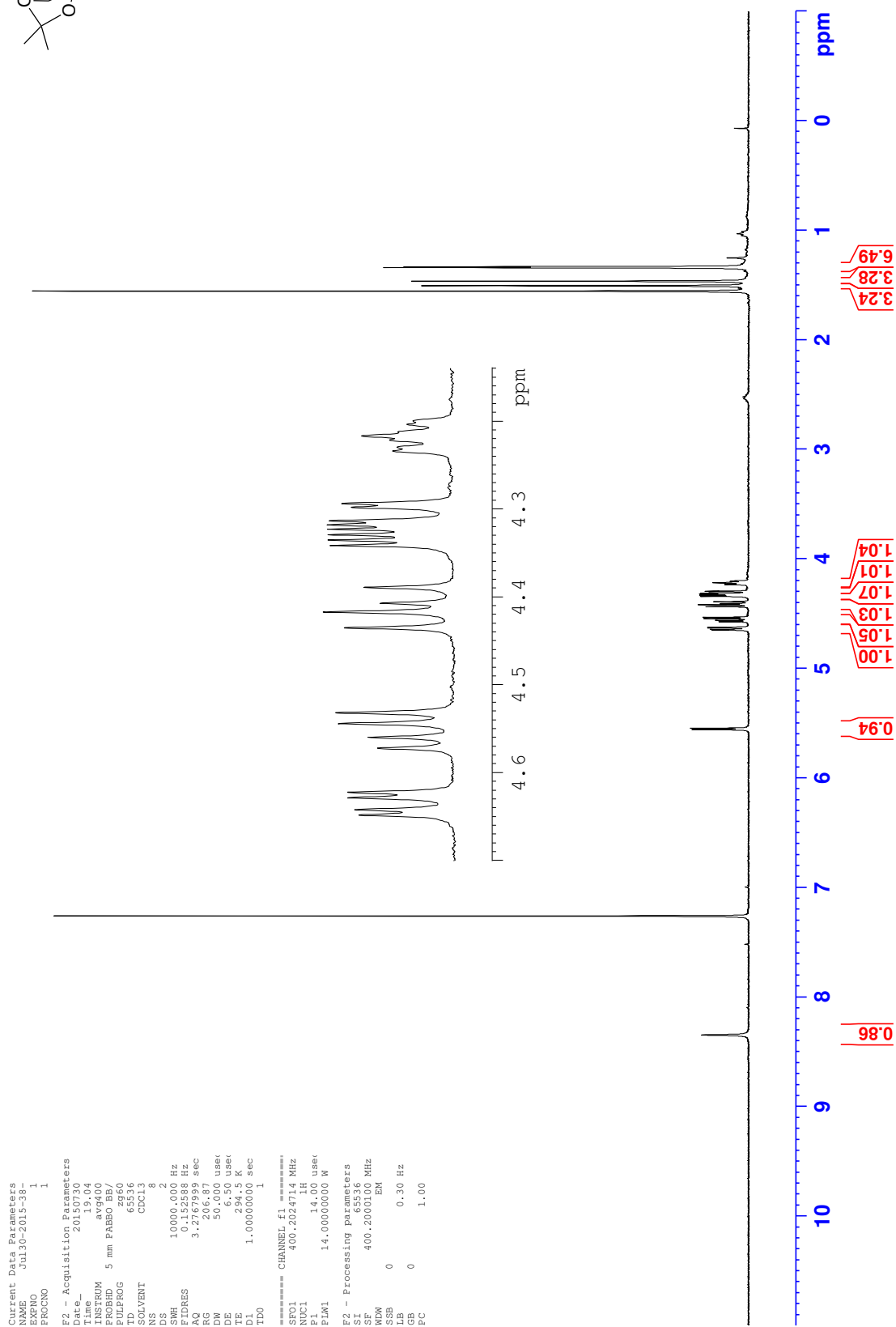
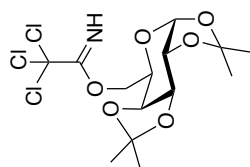
<sup>1</sup>H NMR - Benzyl 1-thio-β-D-galactopyranoside **104**



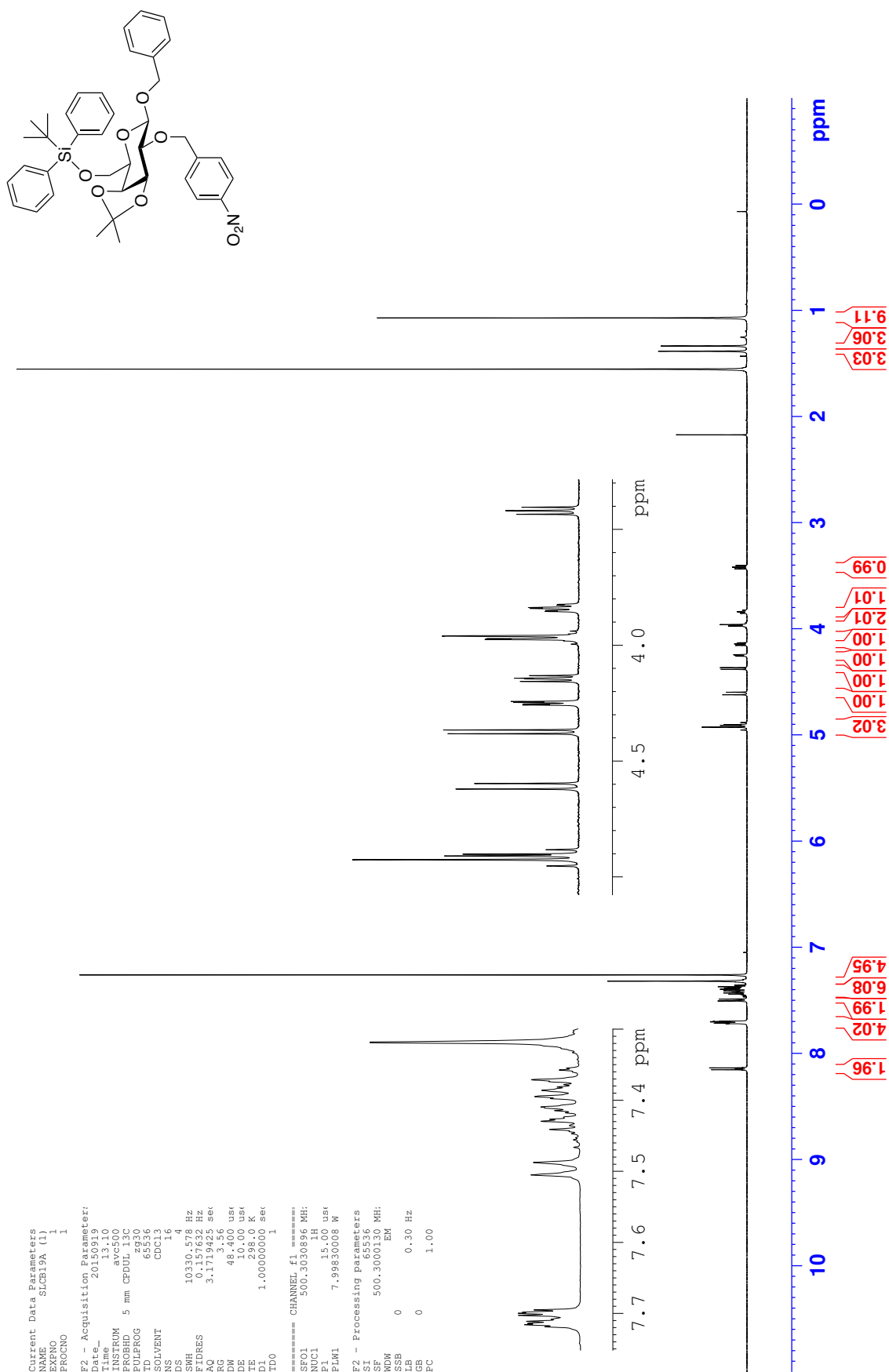
<sup>1</sup>H NMR - Isopropyl 2,3,4,6-tetra-*O*-acetyl-1-*l*-thio-β-D-galactopyranoside 307



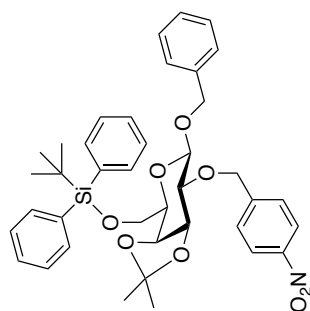


<sup>1</sup>H NMR - 1,2,3,4-di-*O*-isopropylidene- $\alpha$ -D-galactopyranoside 2,2,2-trichloroacetimidate **152**

<sup>1</sup>H NMR - Benzyl 6-*O*-(*tert*-butyldiphenylsilyl)-3,4-*O*-isopropylidene-2-*O*-(4-nitrobenzyl)-β-D-galactopyranoside **131**

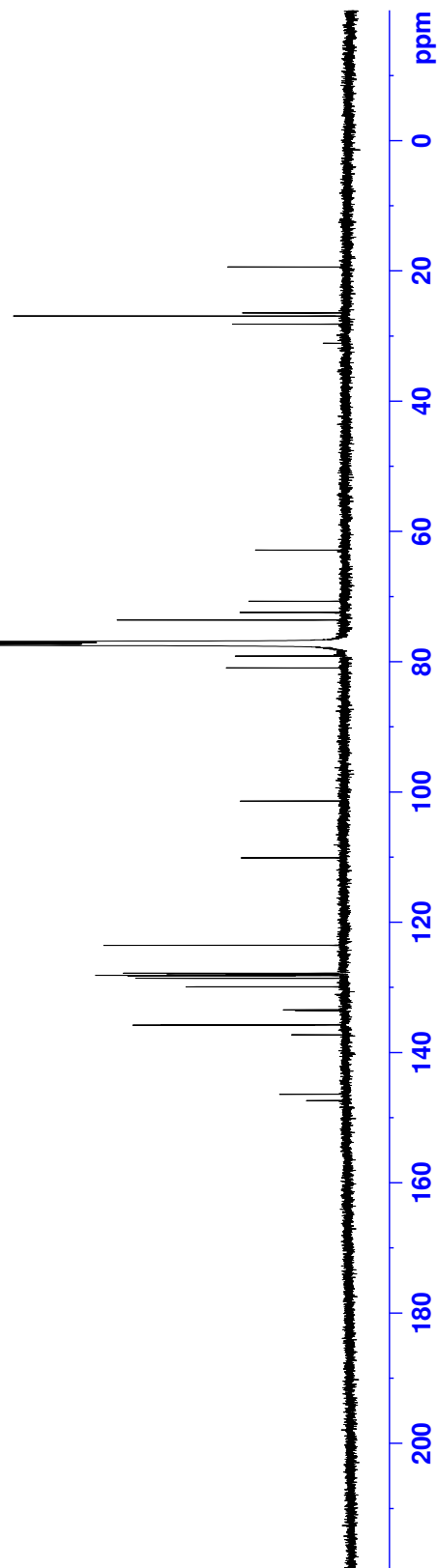




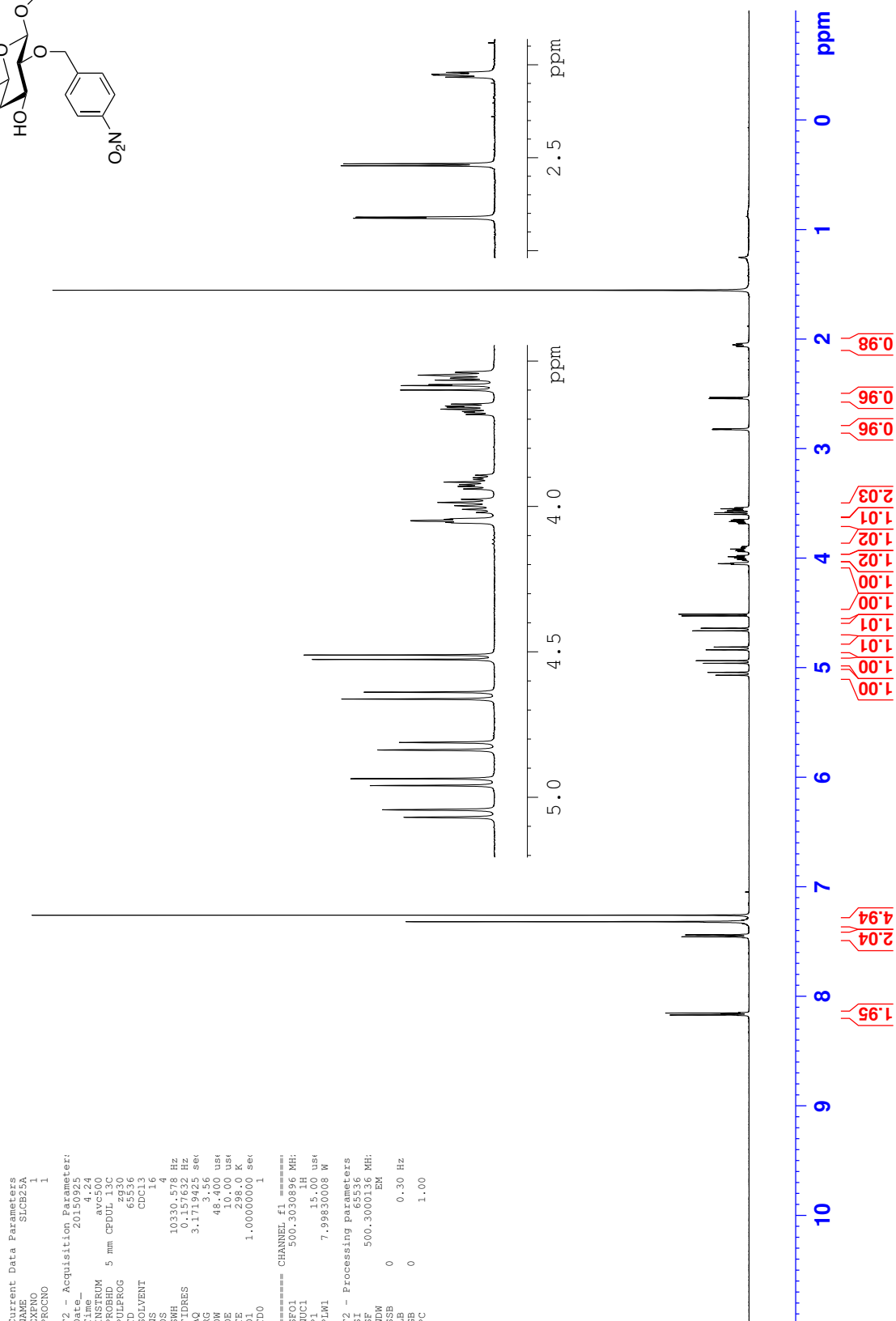
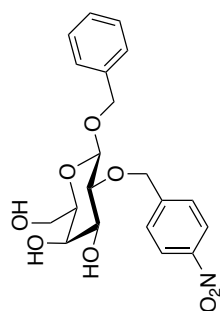
<sup>13</sup>C NMR - Benzyl 6-*O*-(*tert*-butyldiphenylsilyl)-3,4-*O*-isopropylidene-2-*O*-(4-nitrobenzyl)-β-D-galactopyranoside **131**

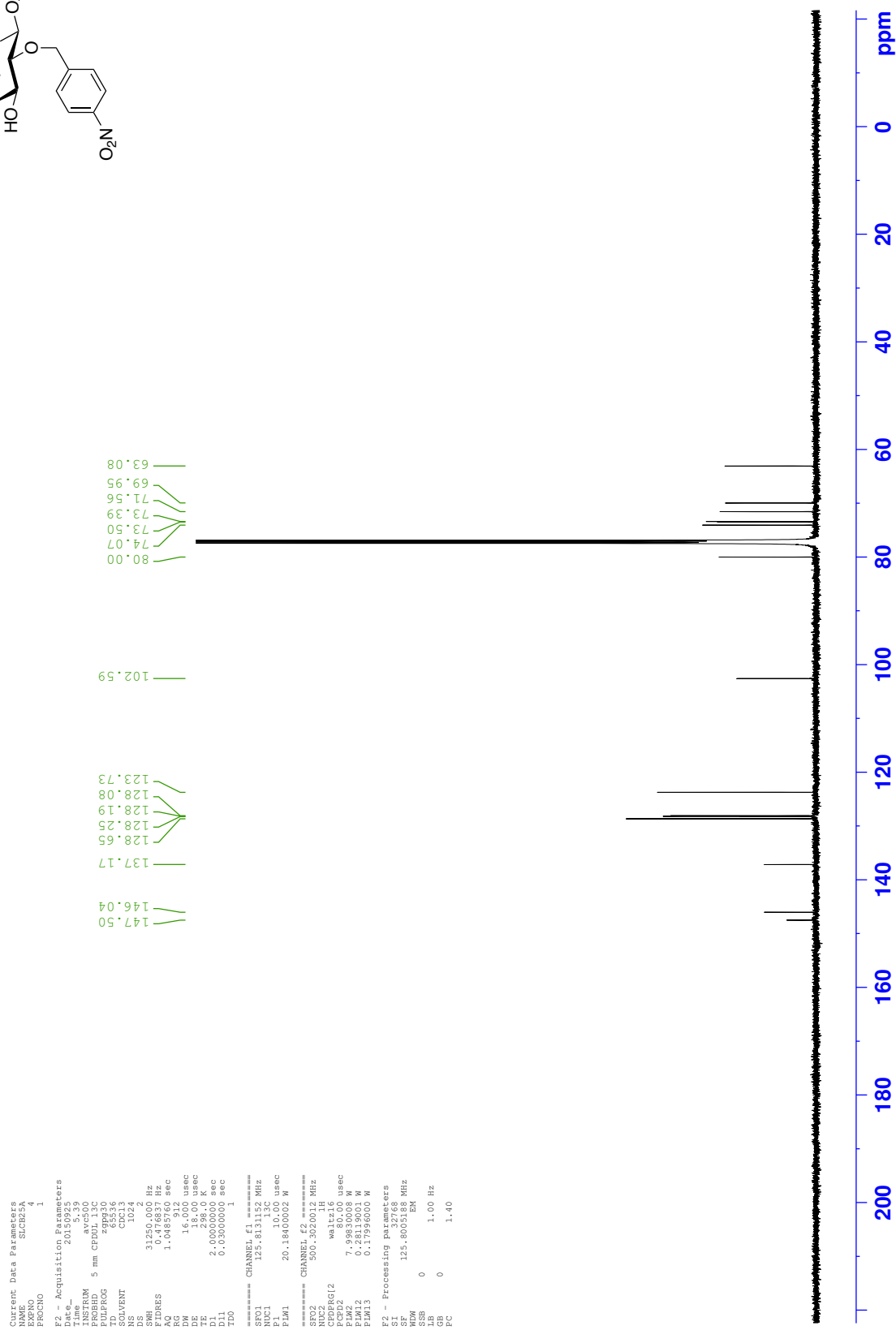
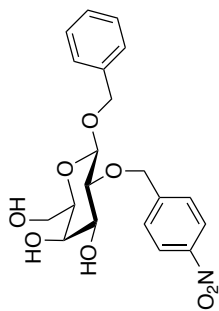
Current Data Parameters  
 NAME SLCE19A (1)  
 EXPNO 4  
 PROCNO 1  
 F2 - Acquisition Parameters  
 Date\_ 20151118  
 Time 20:15:18  
 INSTRUM avc500  
 PULPROG zgpg30  
 FIDRES 0.00130  
 TD 65536  
 SOLVENT CDCl3  
 CDCl3 200.13  
 DS 2  
 SH 31250.00 Hz  
 F2 200.1300000 MHz  
 AQ 0.0485760 sec  
 RG 912  
 DW 15.000 usec  
 DE 1.000 usec  
 TE 298.0 K  
 D1 2.00000000 sec  
 D11 0.05000000 sec  
 D2 1.00000000 sec  
 T2 1.00000000 sec  
 T20 1.00000000 sec  
 F2 - Processing parameters  
 SI 32768  
 SF 200.1300000 MHz  
 DS 2  
 SSB 0  
 LB 0  
 GB 0  
 PC 1.40

147.37  
146.40  
137.27  
135.77  
135.72  
133.54  
133.42  
129.90  
128.59  
128.18  
128.14  
128.09  
127.88  
127.81  
123.52  
110.10  
101.37  
80.93  
79.11  
73.58  
72.41  
70.69  
62.85  
31.09  
28.14  
26.90  
26.43  
19.38

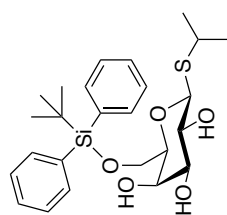


<sup>1</sup>H NMR - Benzyl 2-O-(4-nitrobenzyl)-β-D-galactopyranoside 123



<sup>13</sup>C NMR - Benzyl 2-*O*-(4-nitrobenzyl)-β-D-galactopyranoside **123**

<sup>1</sup>H NMR - Isopropyl 6-O-(*tert*-butyldiphenylsilyl)-1-thio-β-D-galactopyranoside **158**

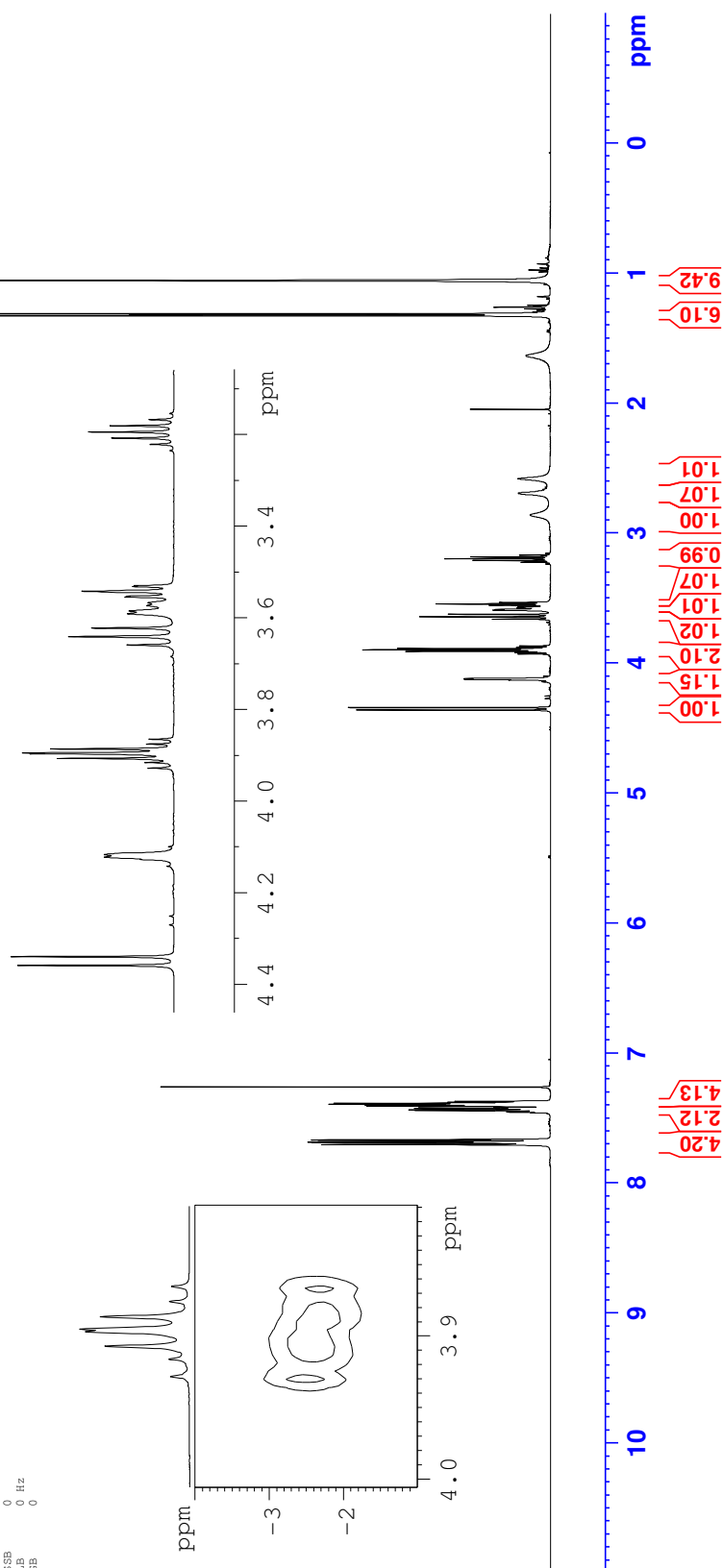


Current Data Parameters  
NAME SC54741312  
EXNO 2  
PROCNO 1

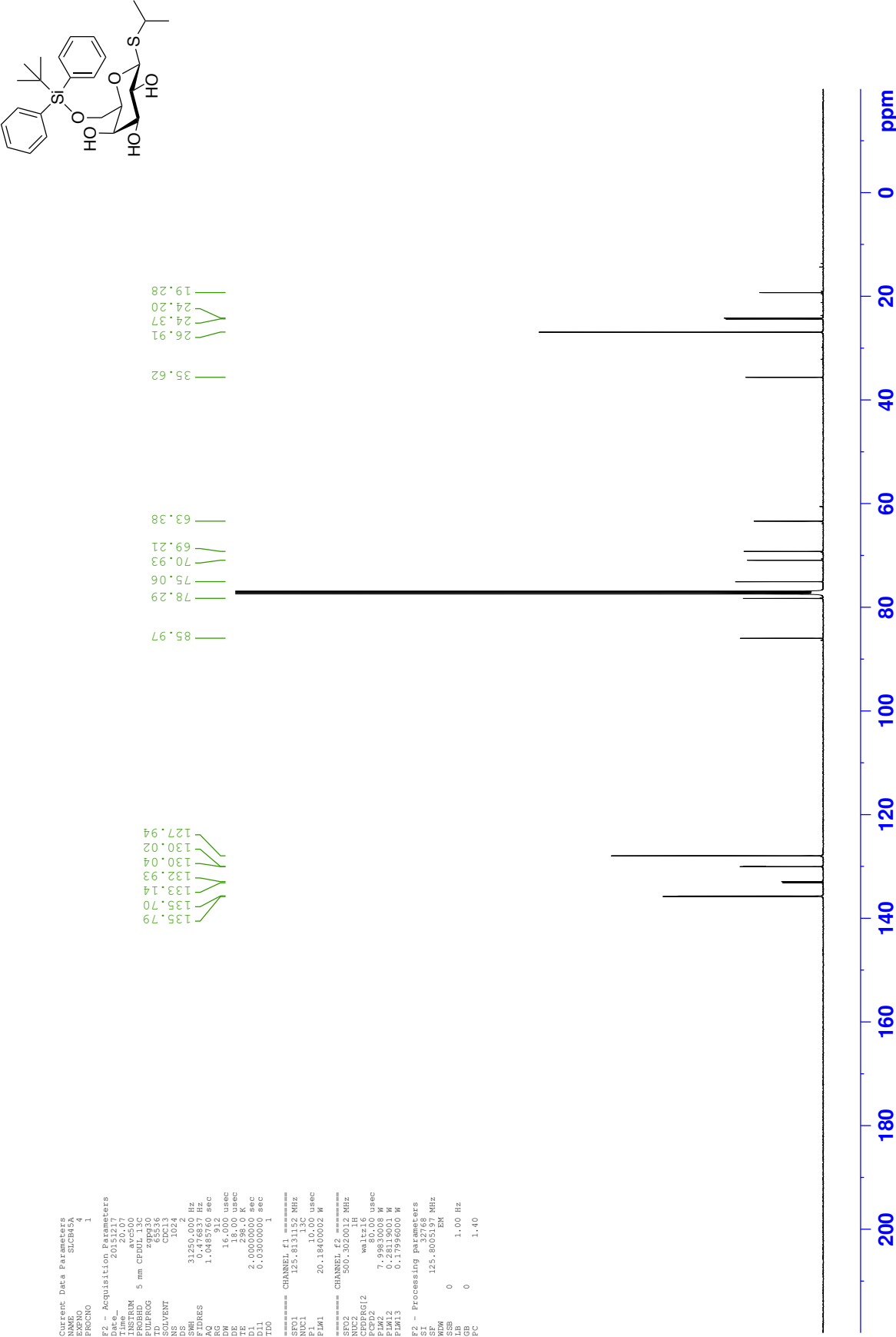
F1 - Acquisition Parameters  
TD 65536  
SFO 99.3128 MHz  
AQ 0.519042 Hz  
FIDRES 77.659042 Hz  
SW 100.042 PPM  
F1MODE QF

F2 - Processing parameters  
SI 32768  
SF 500.130019 MHz  
WDW SINE  
SSB 4  
LB 0 Hz  
GB 0  
PC 1.40

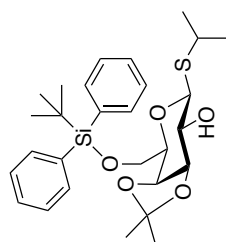
F1 - Processing parameters  
SI 1024  
MC2 QF  
SF 99.3617620 MHz  
WDW QSSINE  
SSB 0  
LB 0 Hz  
GB 0



<sup>13</sup>C NMR - Isopropyl 6-*O*-(*tert*-butyldiphenylsilyl)-1-thio-β-D-galactopyranoside **158**



<sup>1</sup>H NMR - Isopropyl 6-*O*-(*tert*-butyldiphenylsilyl)-3,4-*O*-isopropylidene-1-thio-β-D-galactopyranoside **159**

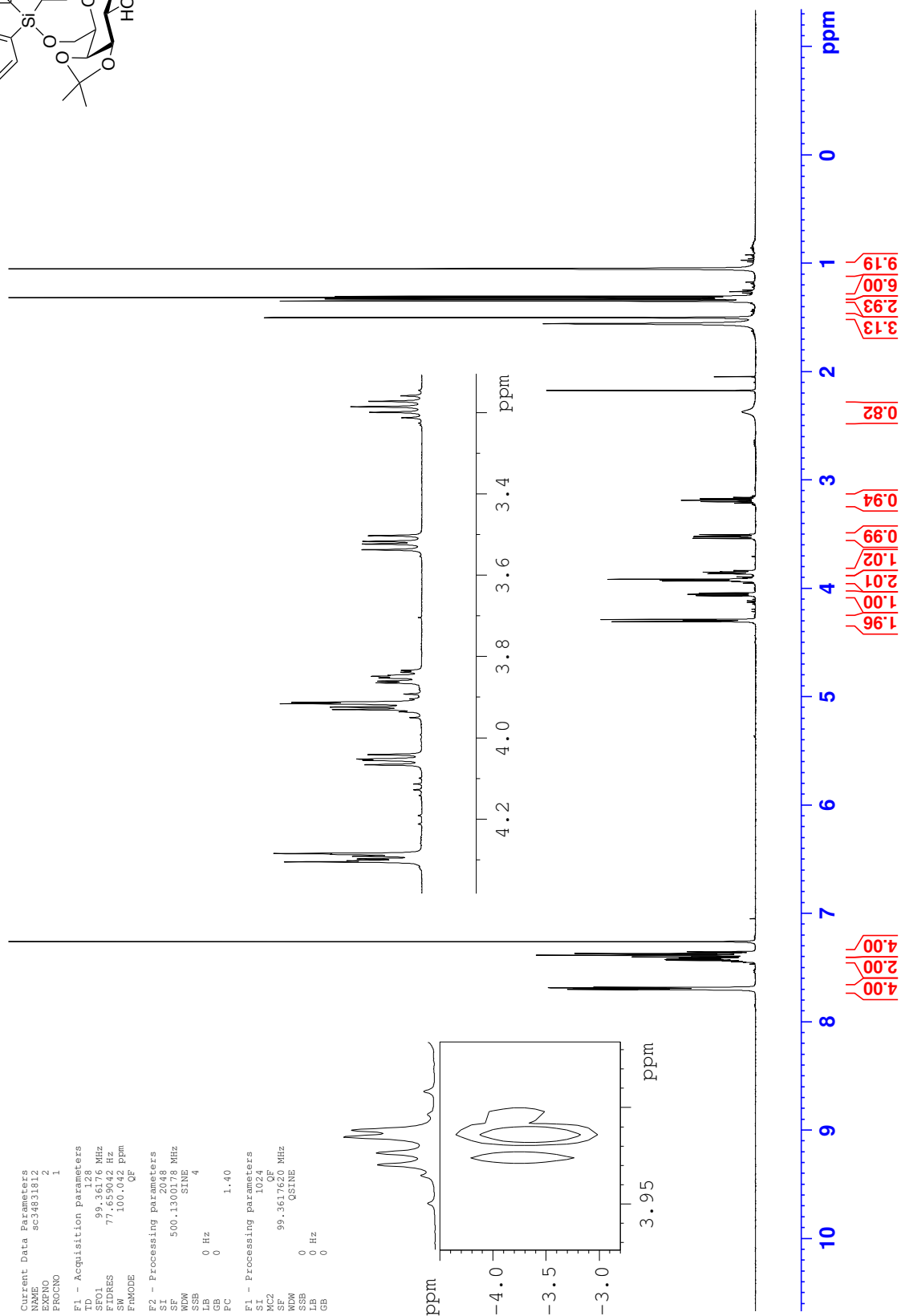


Current Data Parameters  
NAME SC54631312  
EXNO 2  
PROCNO 1

F1 - Acquisition Parameters  
TD 65536  
SFO1 99.36128 MHz  
AQ 0.519042 Hz  
FIDRES 77.659042 Hz  
SW 100.042 PPM  
F1MODE QF

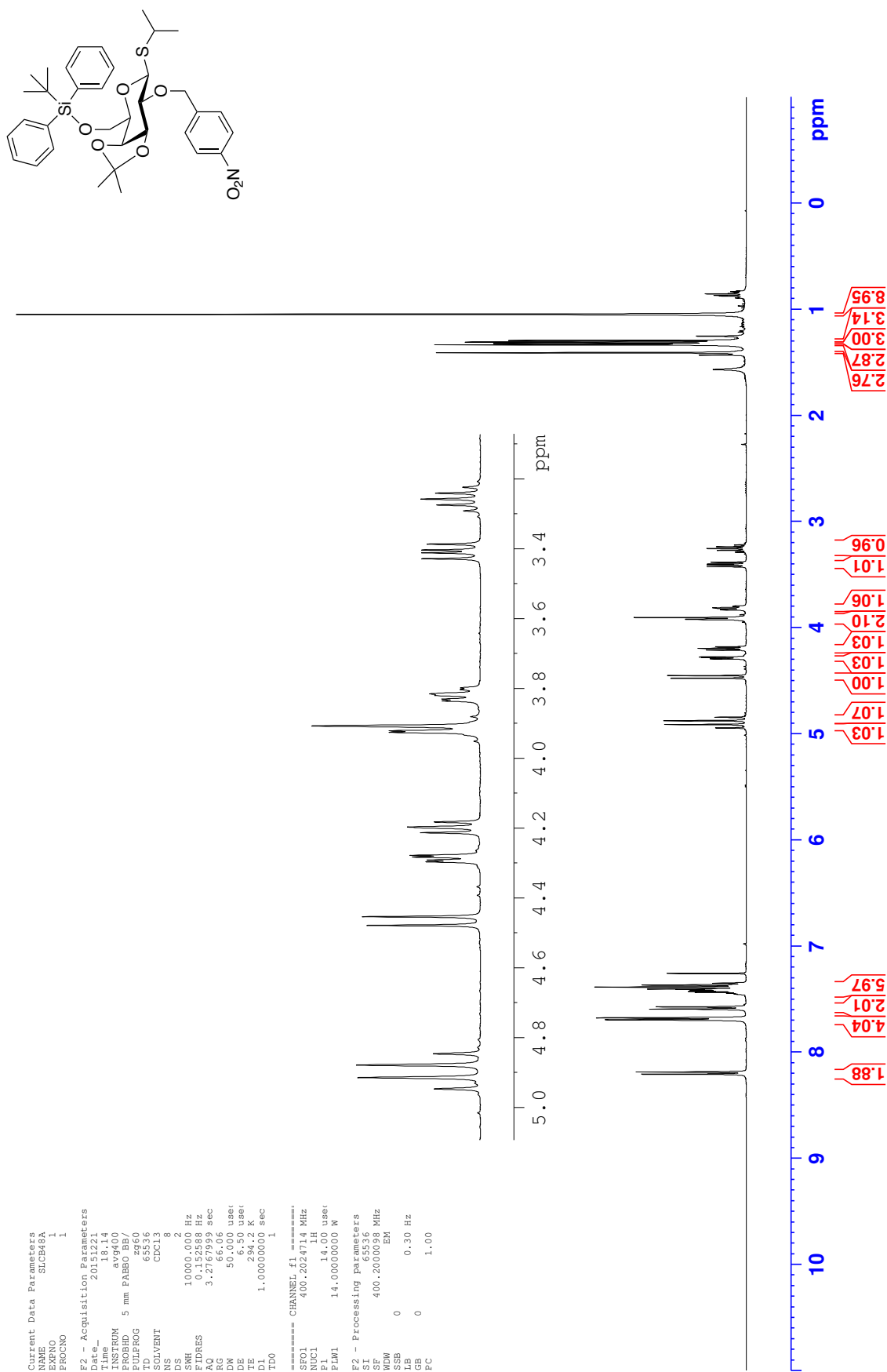
F2 - Processing Parameters  
SI 32768  
SF 500.130178 MHz  
WDW 4  
SSB 0 Hz  
LB 0  
GB 0  
FC 1.40

F1 - Processing Parameters  
SI 1024  
MC2 QF  
SF 99.3617620 MHz  
WDW 0  
SSB 0 Hz  
LB 0  
GB 0



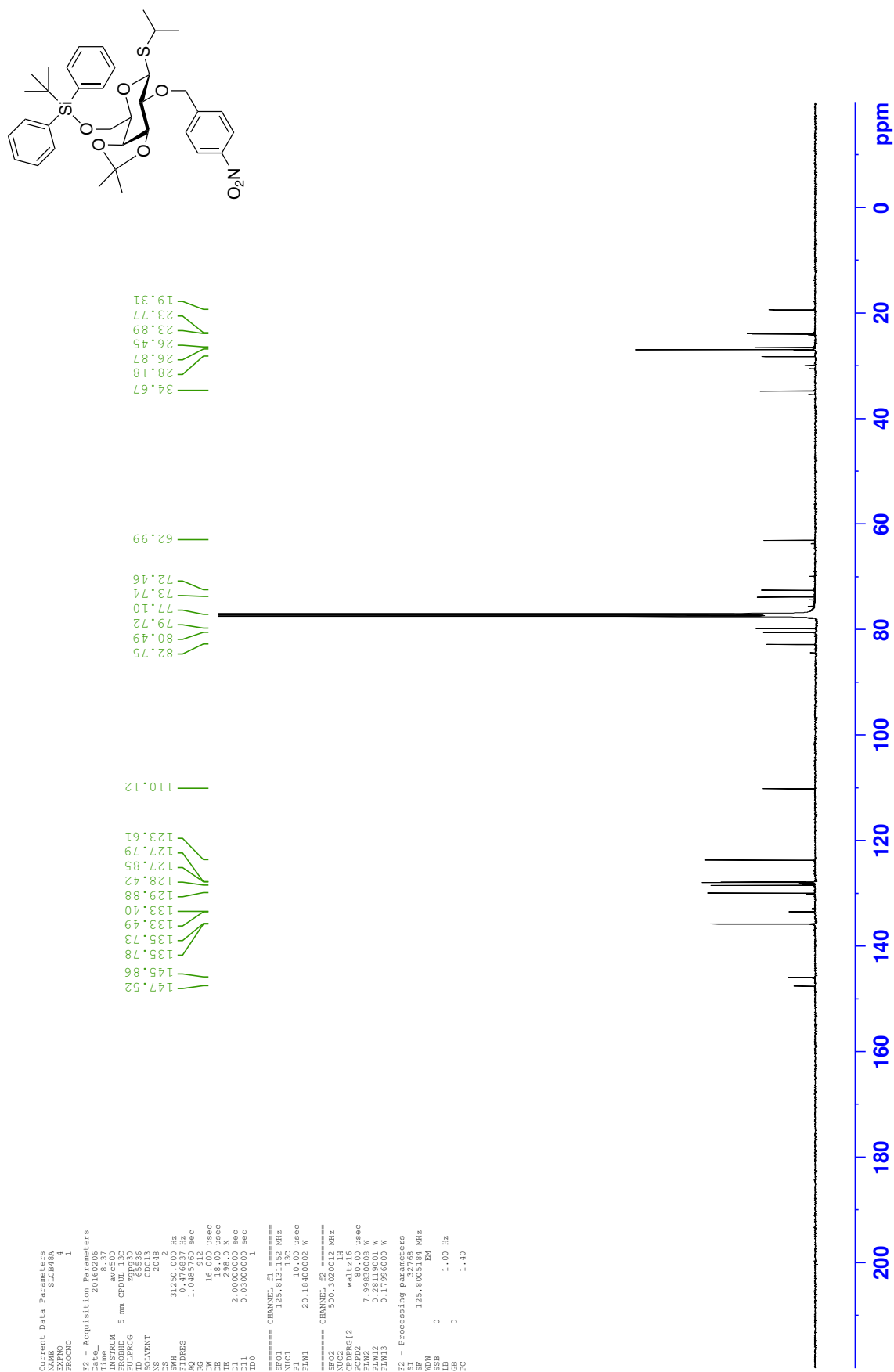


<sup>1</sup>H NMR - Isopropyl 6-*O*-(*tert*-butyldiphenylsilyl)-3,4-*O*-isopropylidene-2-*O*-(4-nitrobenzyl)-1-thio-β-D-galactopyranoside **160**

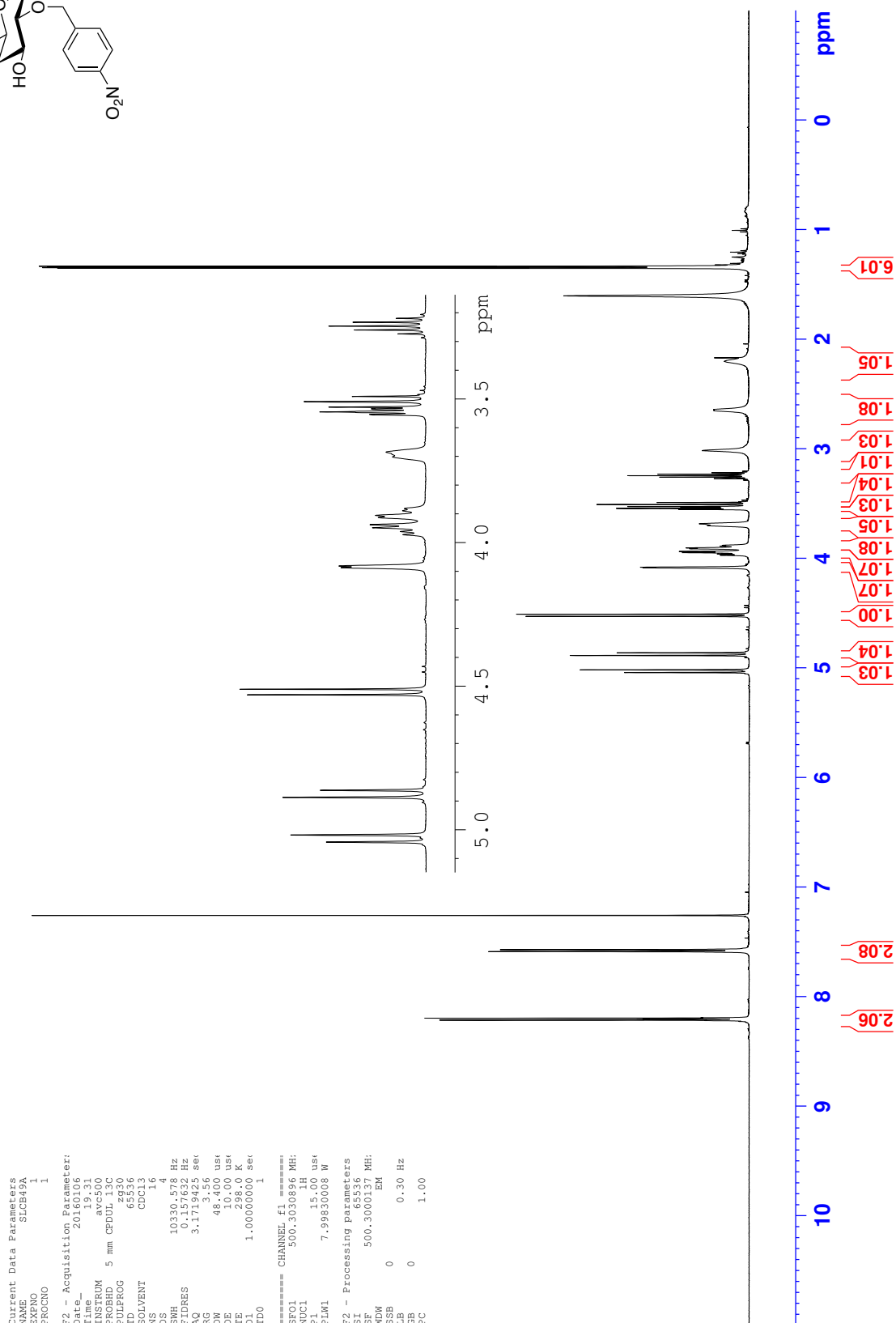
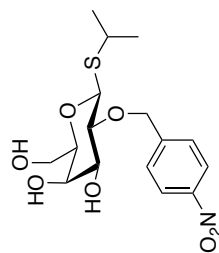




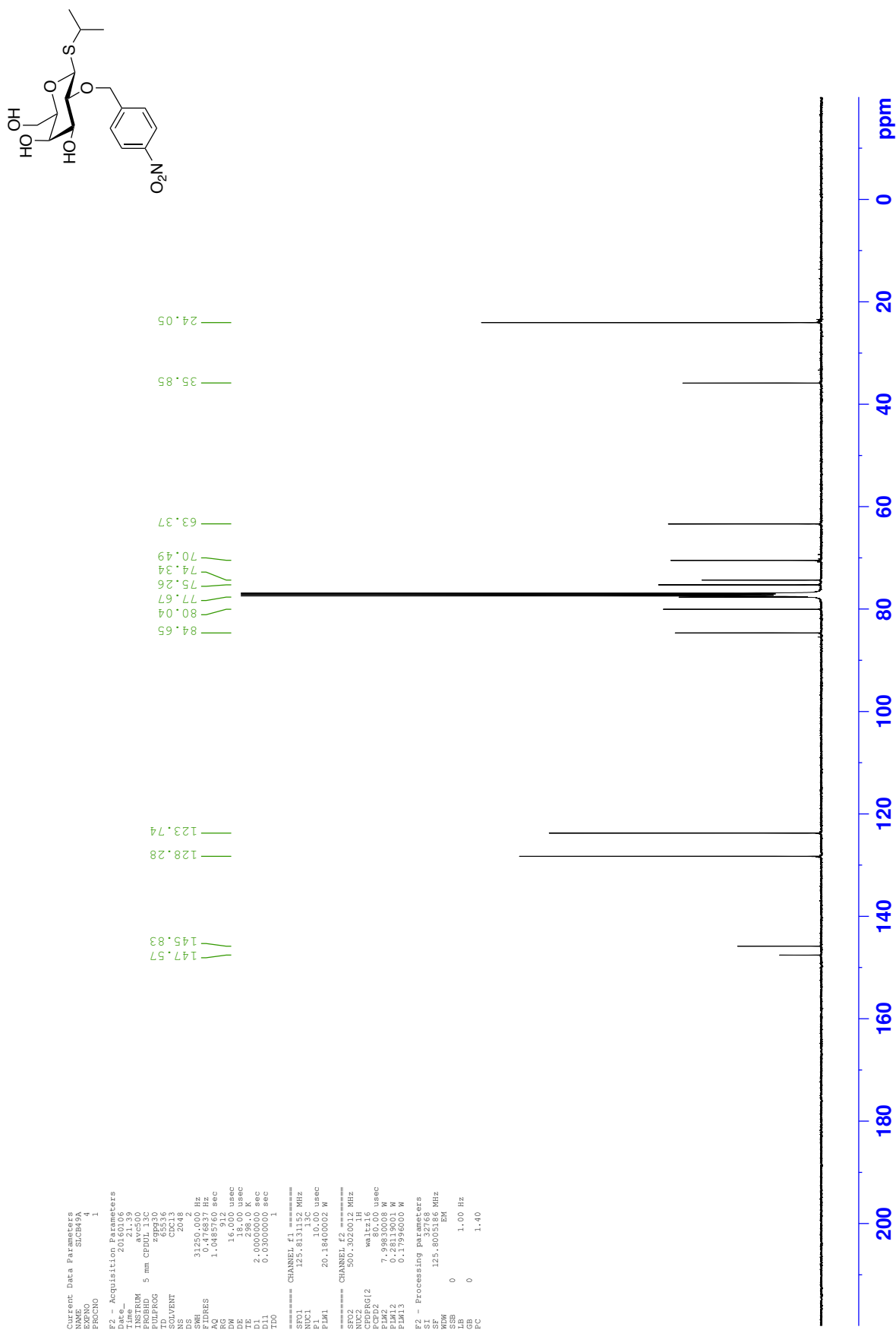
<sup>13</sup>C NMR - Isopropyl 6-*O*-(*tert*-butyldiphenylsilyl)-3,4-*O*-isopropylidene-2-*O*-(4-nitrobenzyl)-1-thio-β-D-galactopyranoside **160**



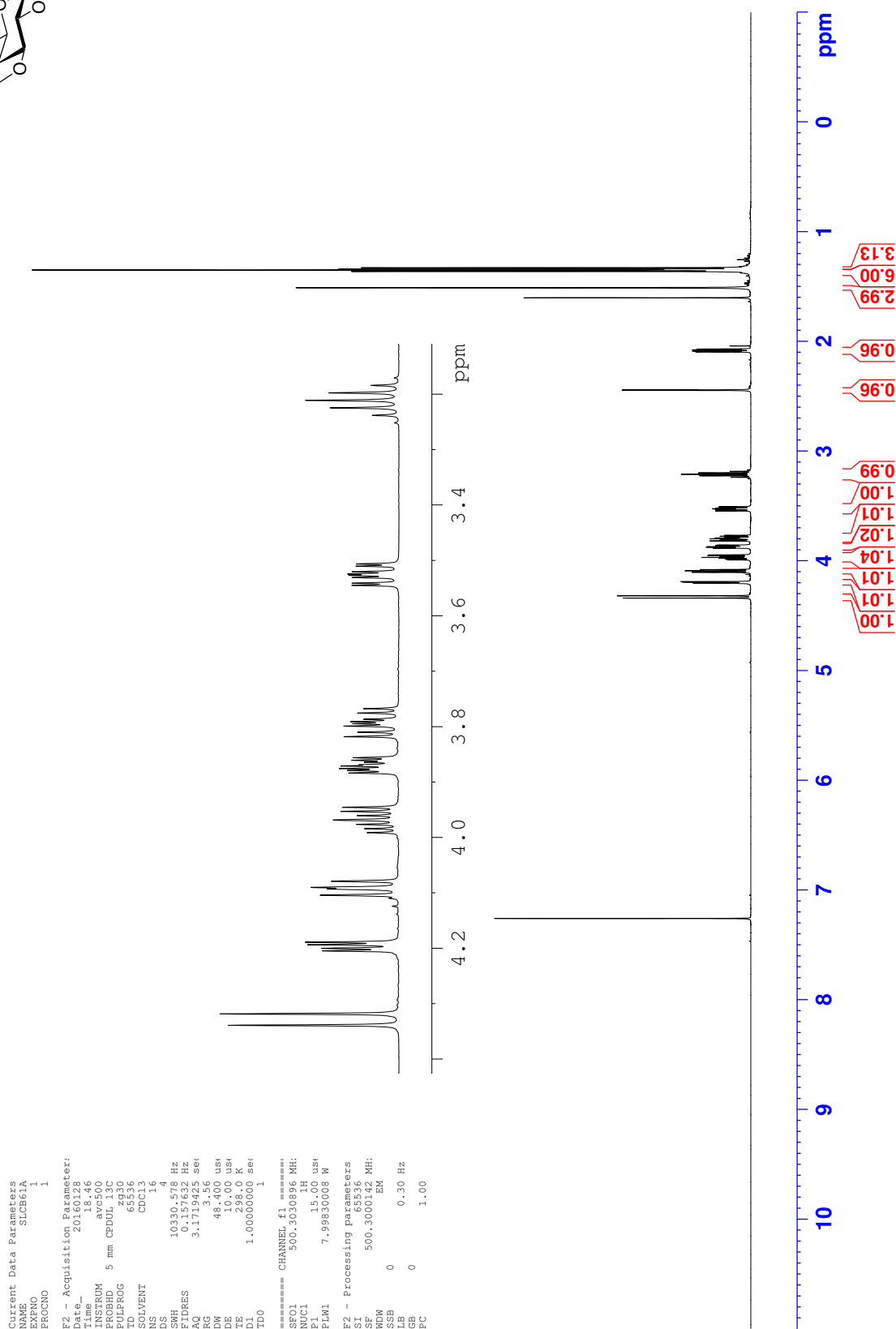
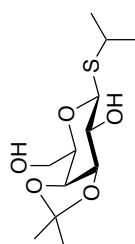
<sup>1</sup>H NMR - Isopropyl 2-O-(4-nitrobenzyl)-1-thio-β-D-galactopyranoside **86**

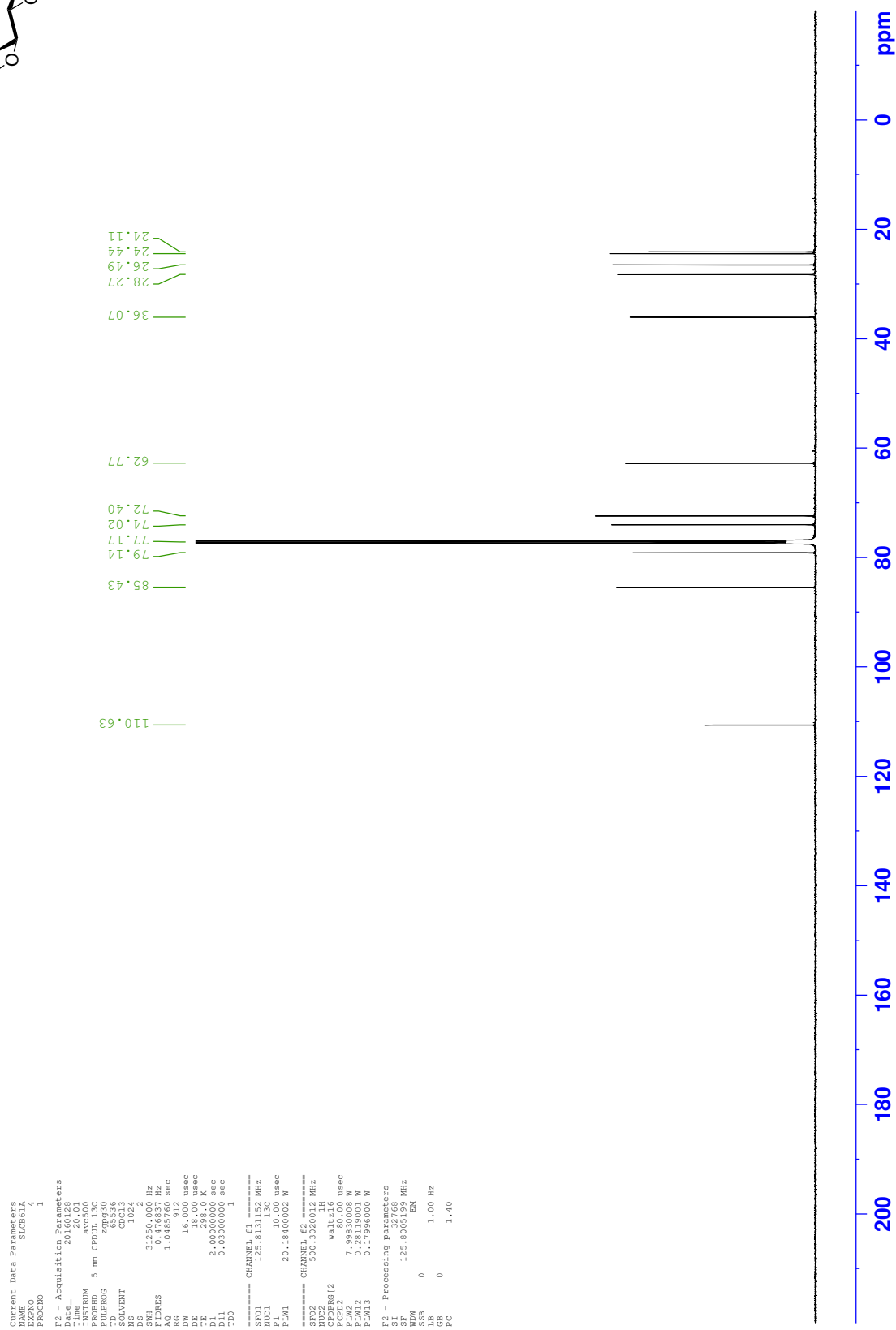
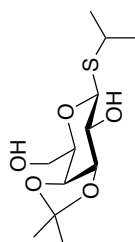


<sup>13</sup>C NMR - Isopropyl 2-*O*-(4-nitrobenzyl)-1-thio-β-D-galactopyranoside **86**

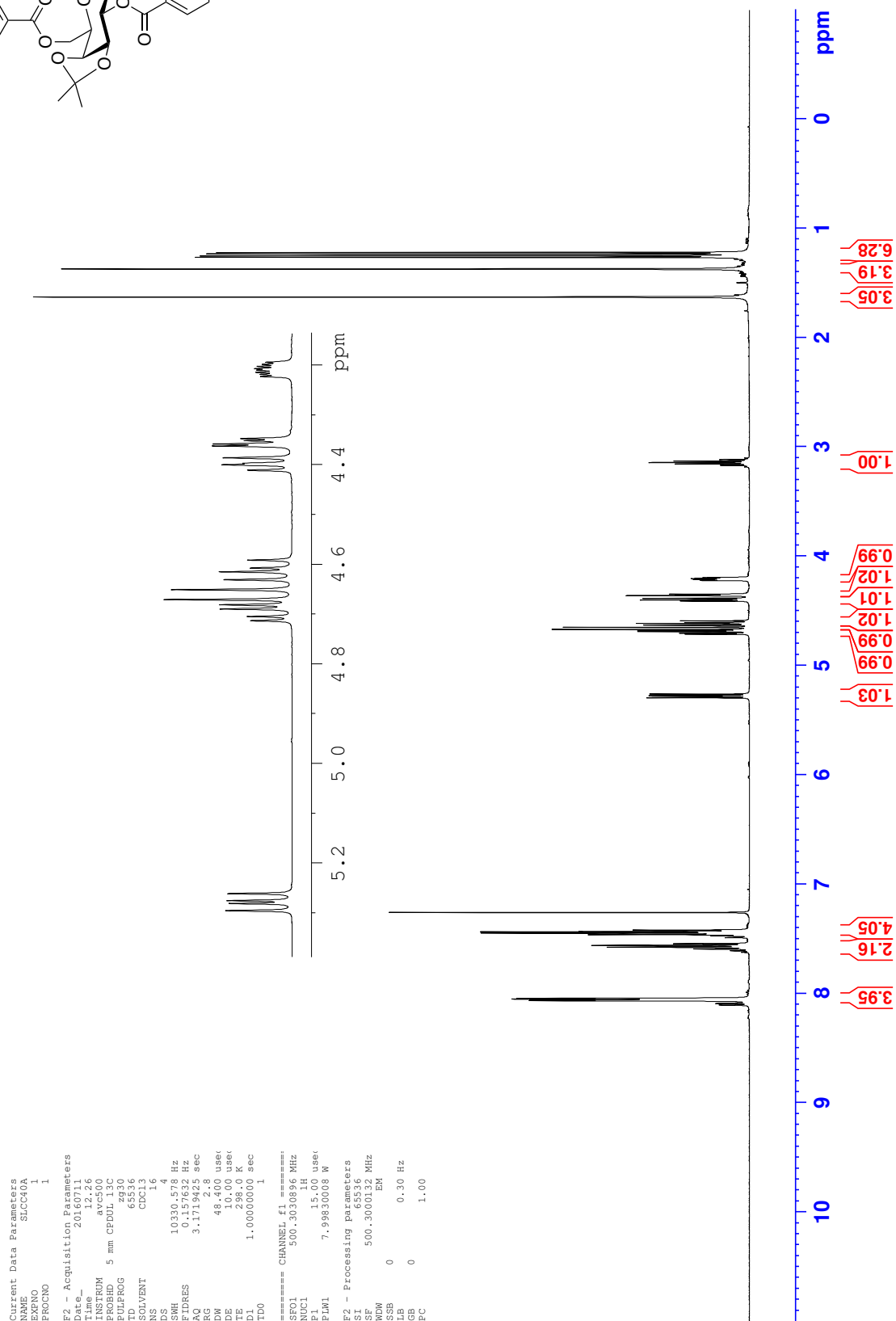
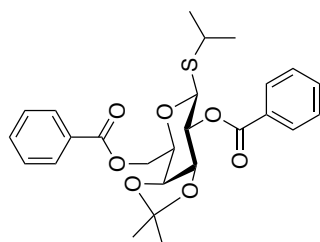


<sup>1</sup>H NMR - Isopropyl 3,4-*O*-isopropylidene-1-thio-β-D-galactopyranoside **164**

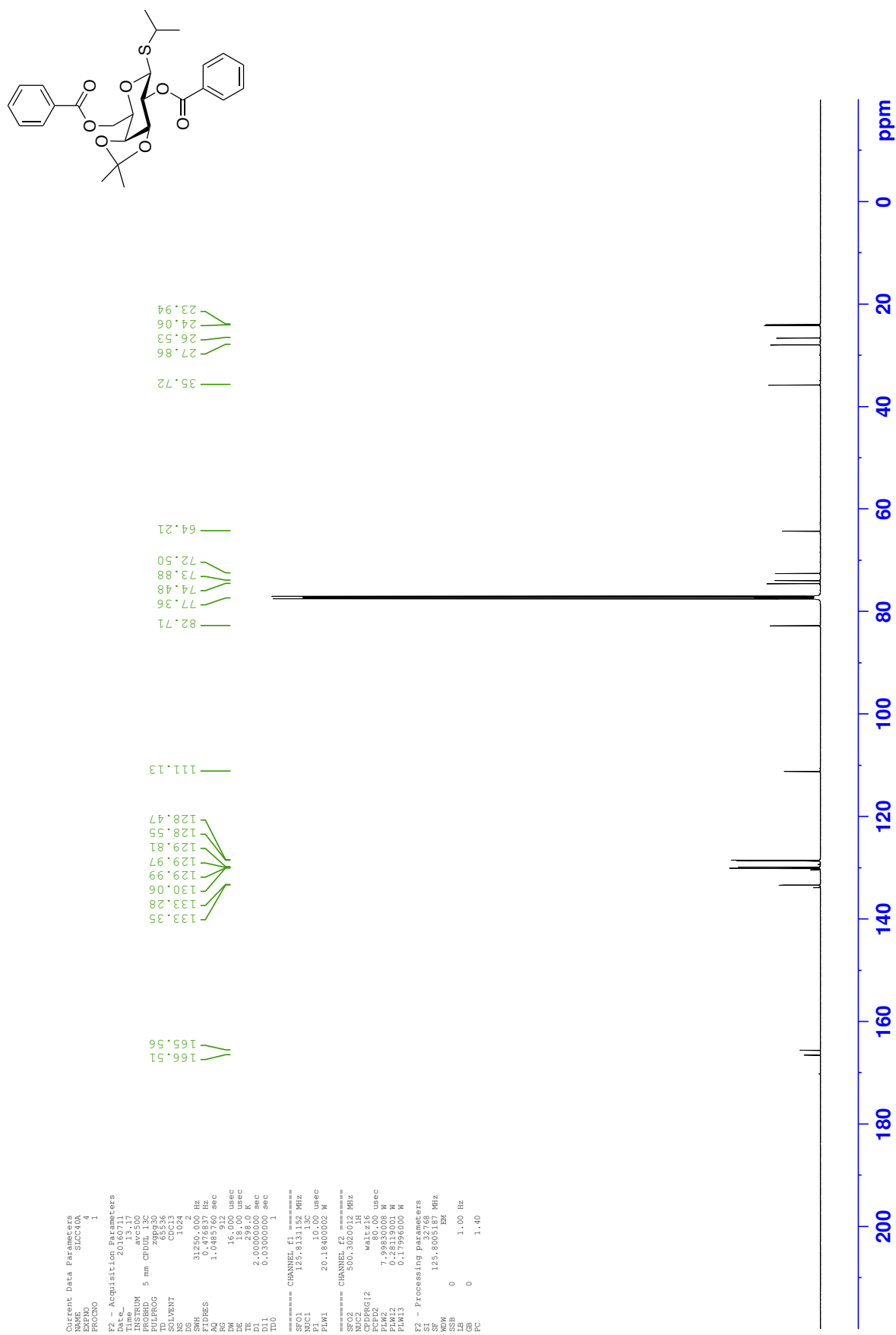




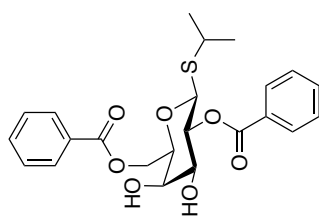
<sup>1</sup>H NMR - Isopropyl 2,6-di-*O*-benzoyl-3,4-*O*-isopropylidene-1-thio-β-D-galactopyranoside **165**



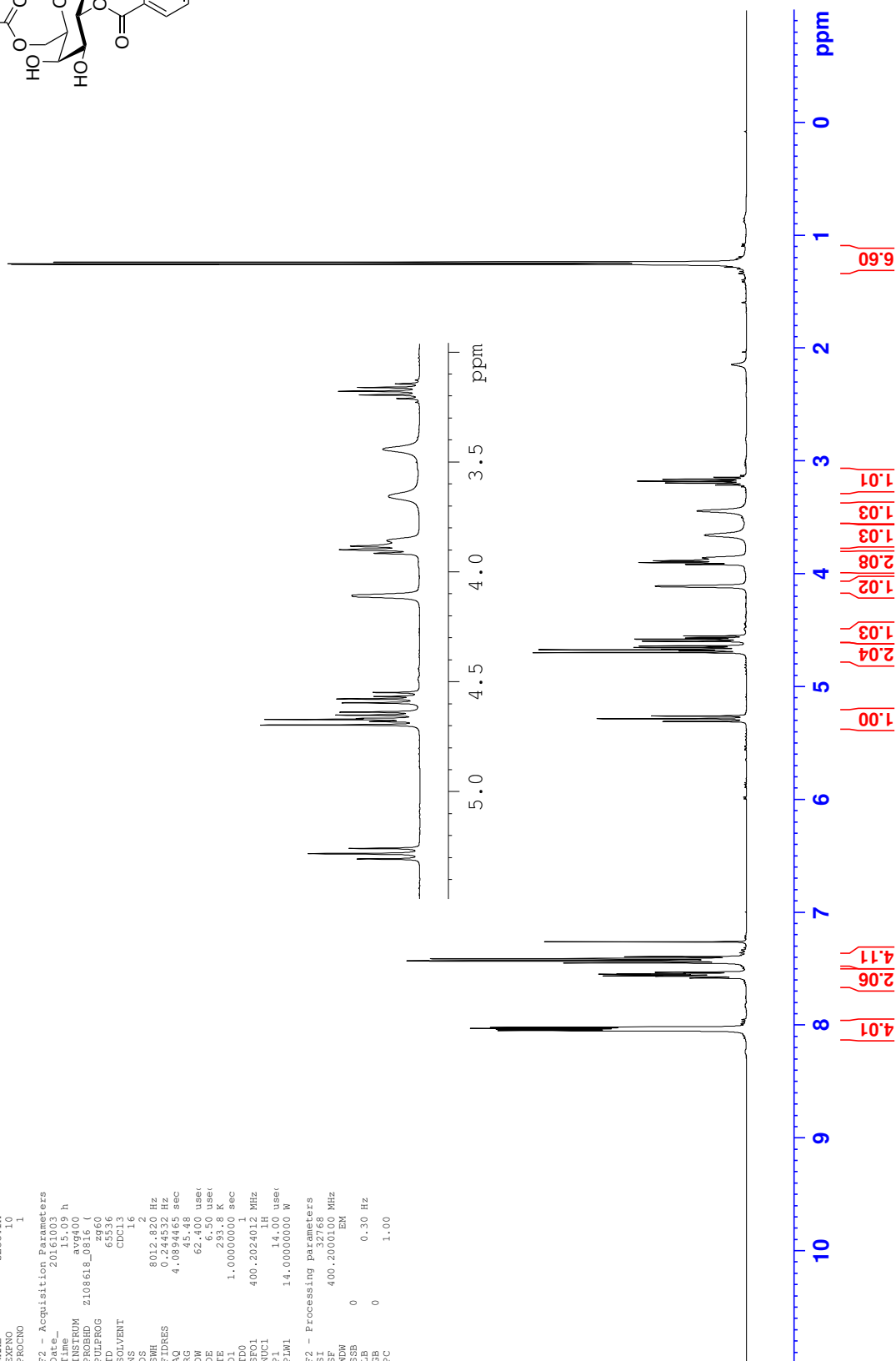
<sup>13</sup>C NMR - Isopropyl 2,6-di-*O*-benzoyl-3,4-*O*-isopropylidene-1-thio-β-D-galactopyranoside **165**



<sup>1</sup>H NMR - Isopropyl 2,6-di-*O*-benzoyl-1-thio-β-D-galactopyranoside **166**

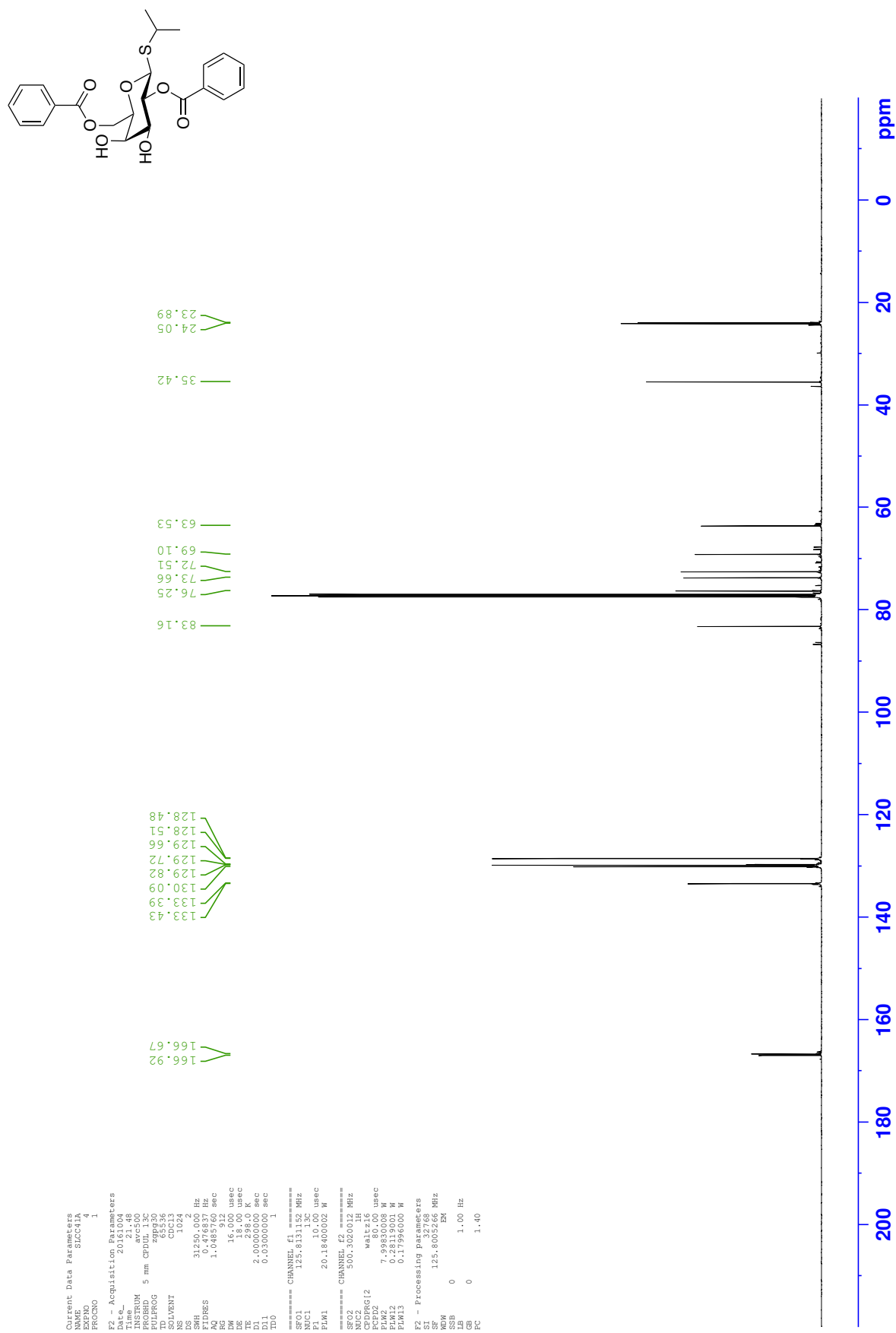


Current Data Parameters  
 NAME 166  
 EXNO 10  
 PROCNO 1  
 F2 - Acquisition Parameters  
 Date\_ 20161003  
 Time\_ 15:00  
 INSTRUM av400  
 PROBHD 2108618\_0816 (1  
 PULPROG zgpg30  
 TD 65536  
 SOLVENT CDCl3  
 NS 12  
 DS 2  
 SWH 8012.820 Hz  
 FIDRES 0.244532 Hz  
 AQ 4.0894465 sec  
 RG 45.48  
 DW 62.400 usec  
 DE 19.00 usec  
 TE 293.2 K  
 D1 1.00000000 sec  
 D11 1.00000000 sec  
 TD0 1  
 SFO1 400.2024012 MHz  
 NUC1 1H  
 P1 14.00 usec  
 PL1 0.00 dB  
 F1W1 14.00000000 MHz  
 F2 - Processing parameters  
 SI 32768  
 SF 400.2000100 MHz  
 WDW EM  
 SSB 0  
 LB 0.30 Hz  
 GB 0  
 PC 1.00

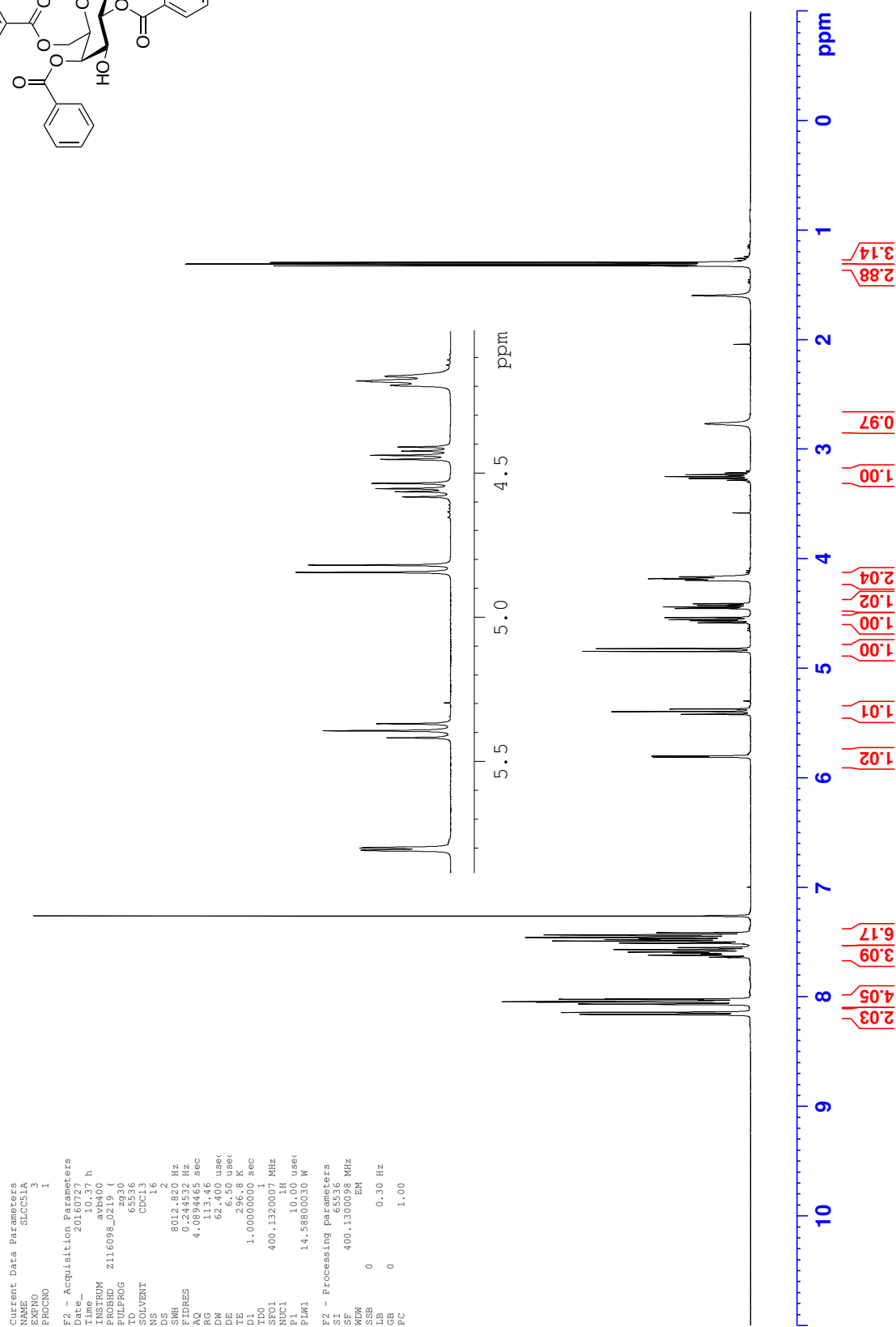
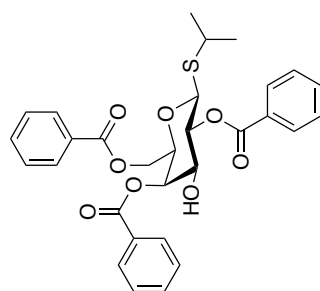




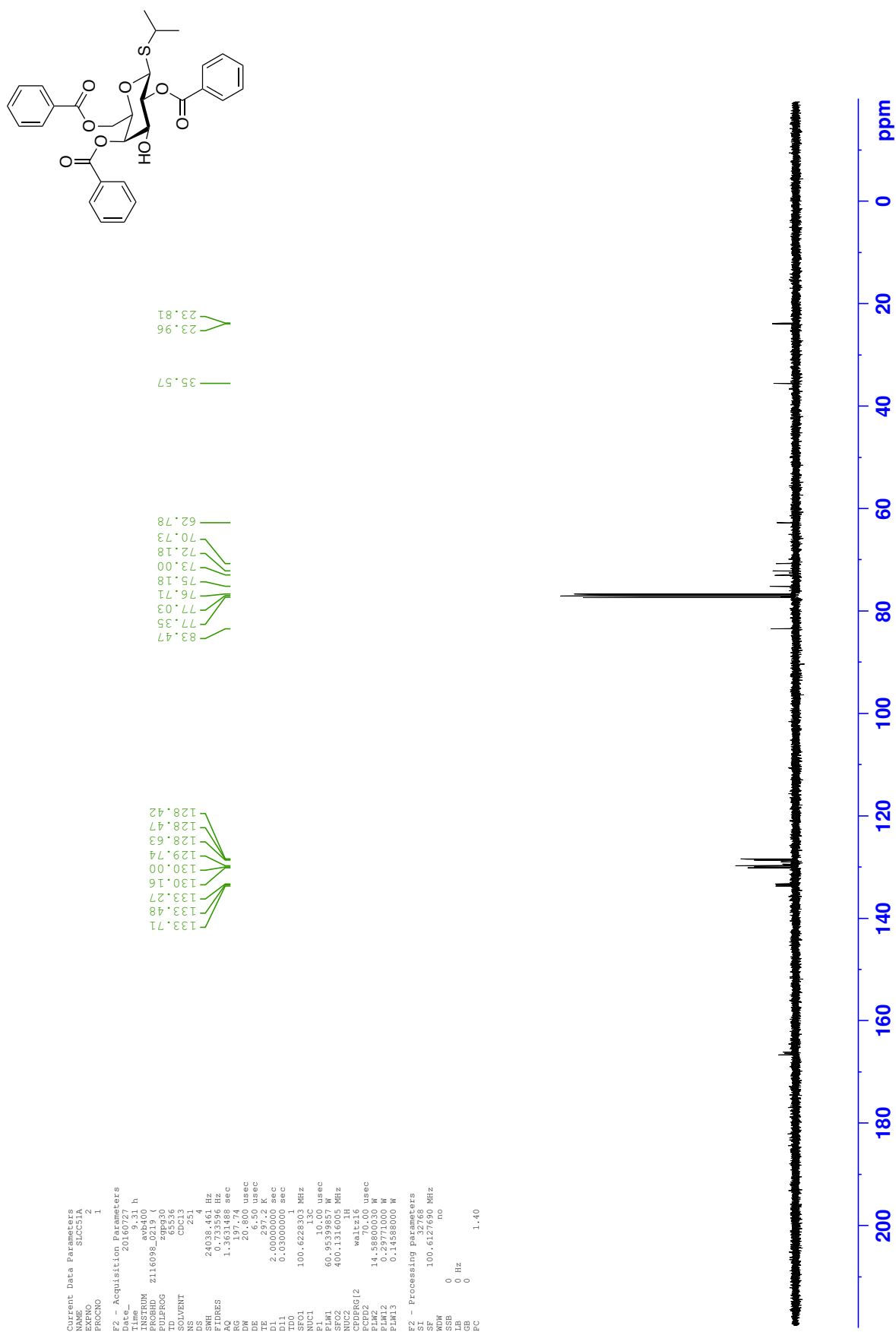
<sup>13</sup>C NMR - Isopropyl 2,6-di-*O*-benzoyl-1-thio-β-D-galactopyranoside 166



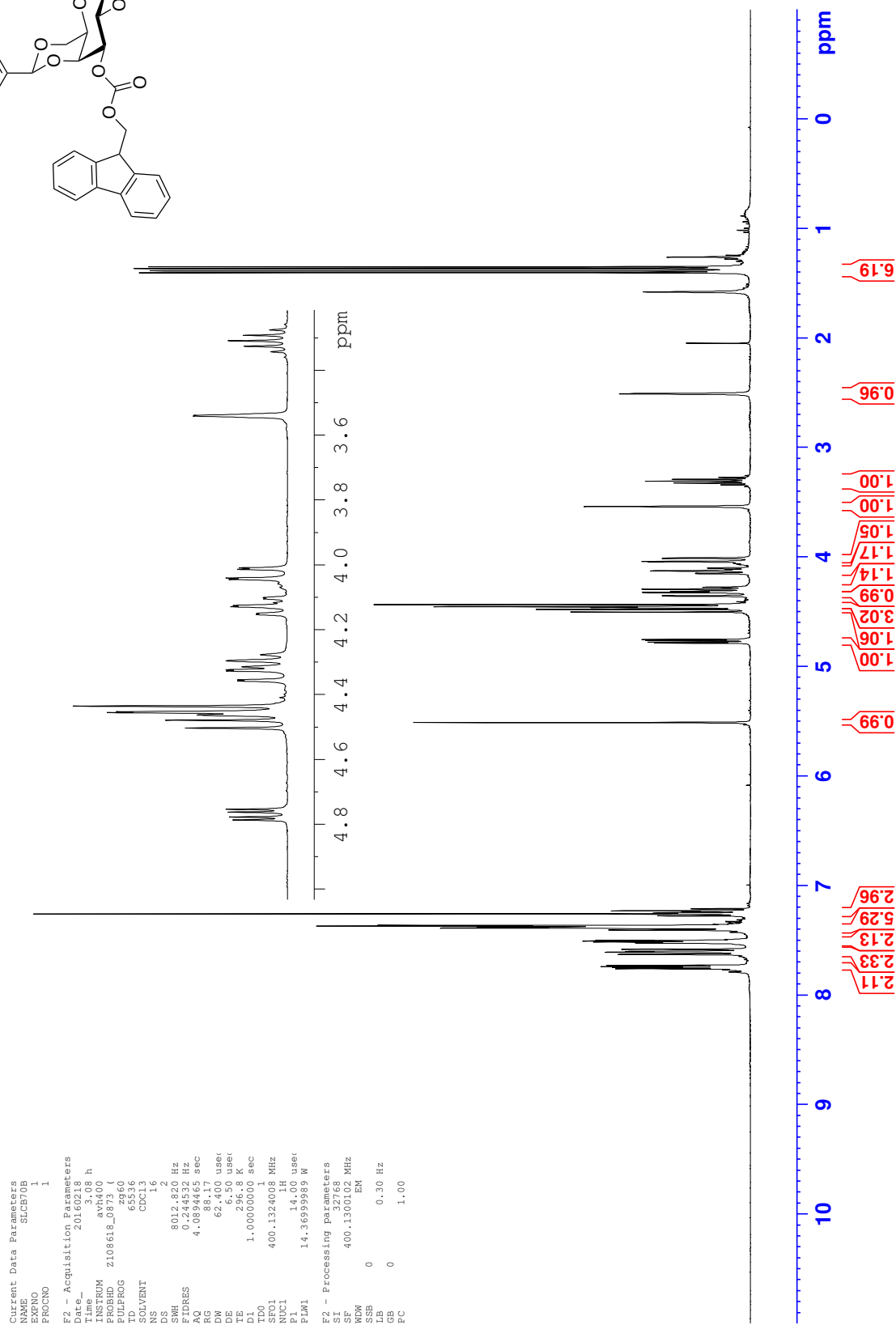
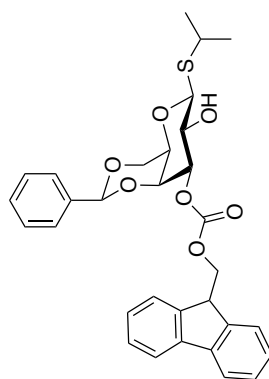
<sup>1</sup>H NMR - Isopropyl 2,4,6-tri-*O*-benzoyl-1-thio-β-D-galactopyranoside **163**

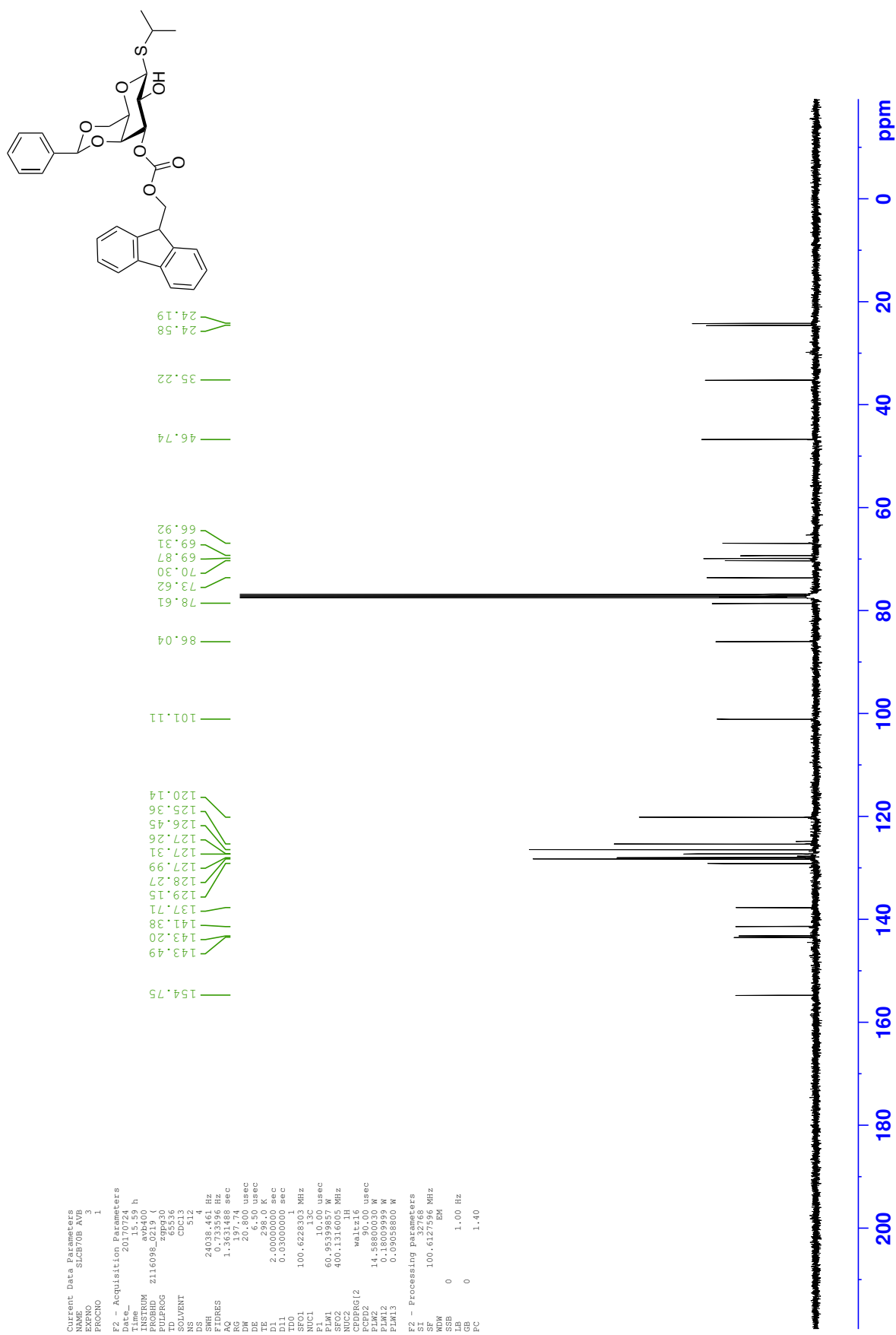


<sup>13</sup>C NMR - Isopropyl 2,4,6-tri-*O*-benzoyl-1-thio-β-D-galactopyranoside **163**

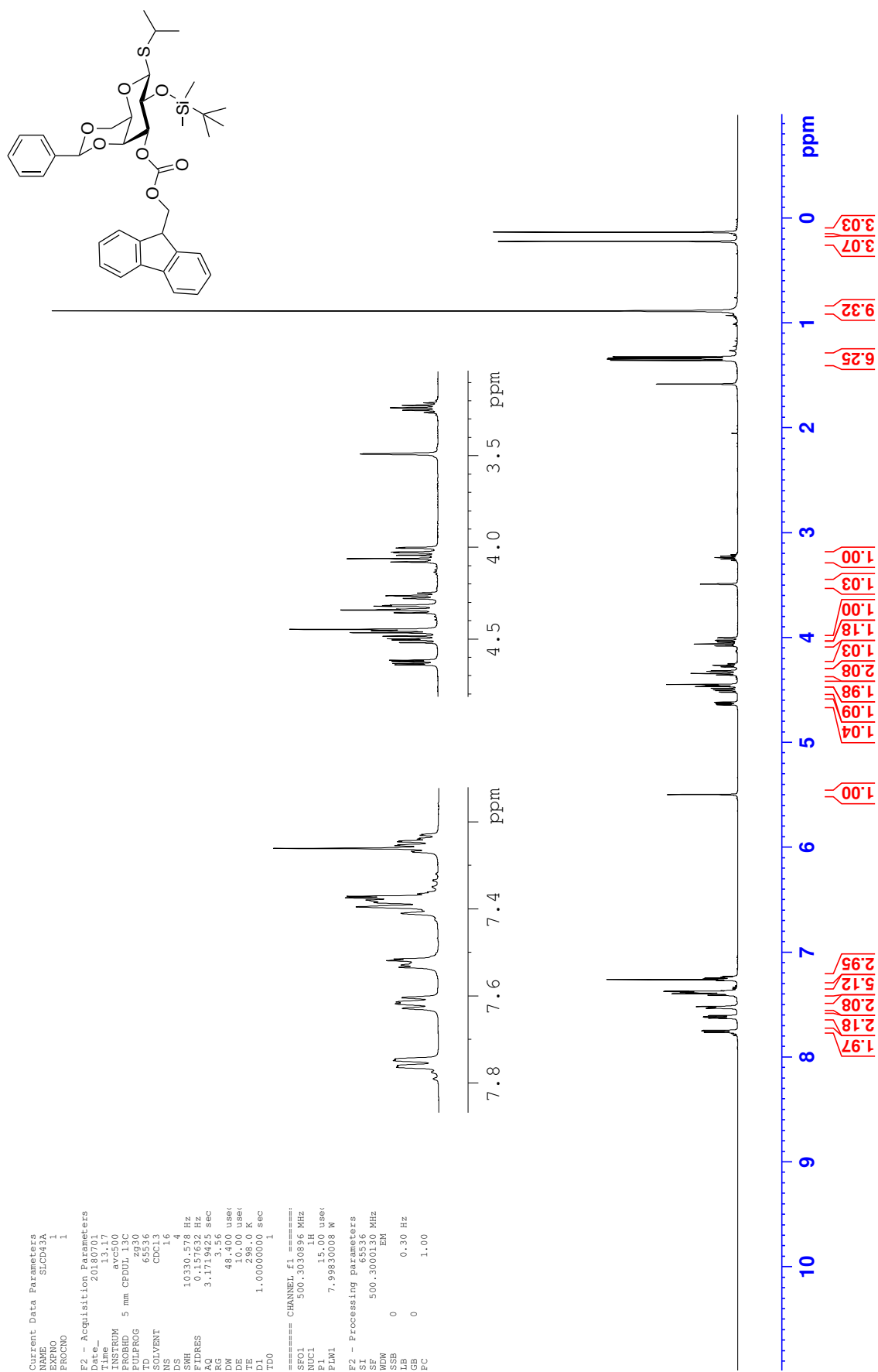


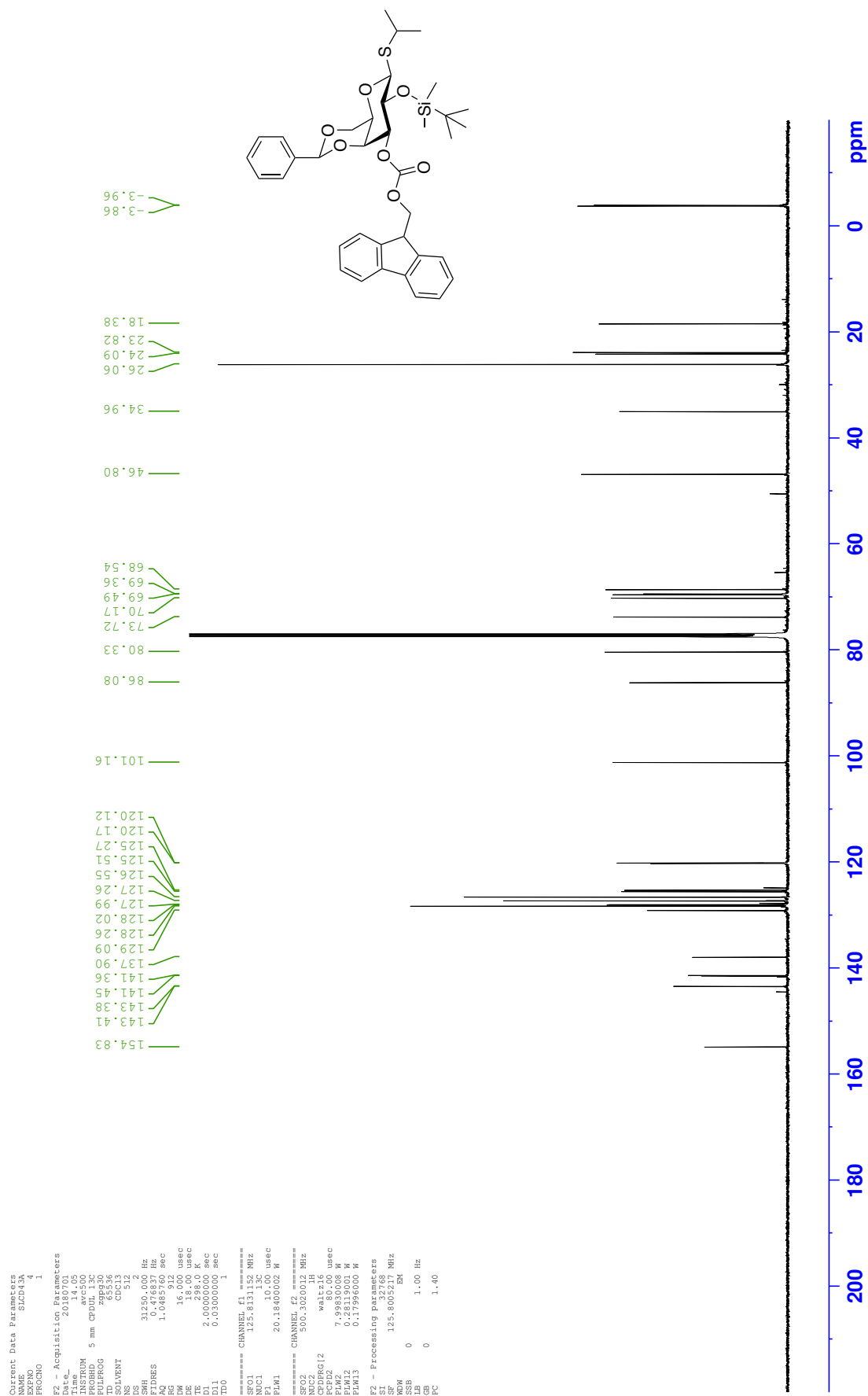
<sup>1</sup>H NMR - Isopropyl 4,6-*O*-benzylidene-3-*O*-fluorenylmethoxycarbonyl-1-thio-β-D-galactopyranoside **188**



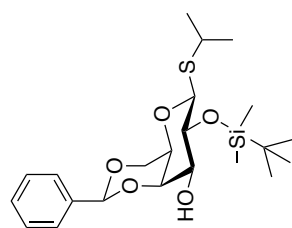
<sup>13</sup>C NMR - Isopropyl 4,6-*O*-benzylidene-3-*O*-fluorenylmethoxycarbonyl-1-thio-β-D-galactopyranoside **188**

<sup>1</sup>H NMR - Isopropyl 4,6-*O*-benzylidene-2-*O*-(*tert*-butyldimethylsilyl)-3-*O*-fluorenylmethoxycarbonyl-1-thio-β-D-galactopyranoside **189**

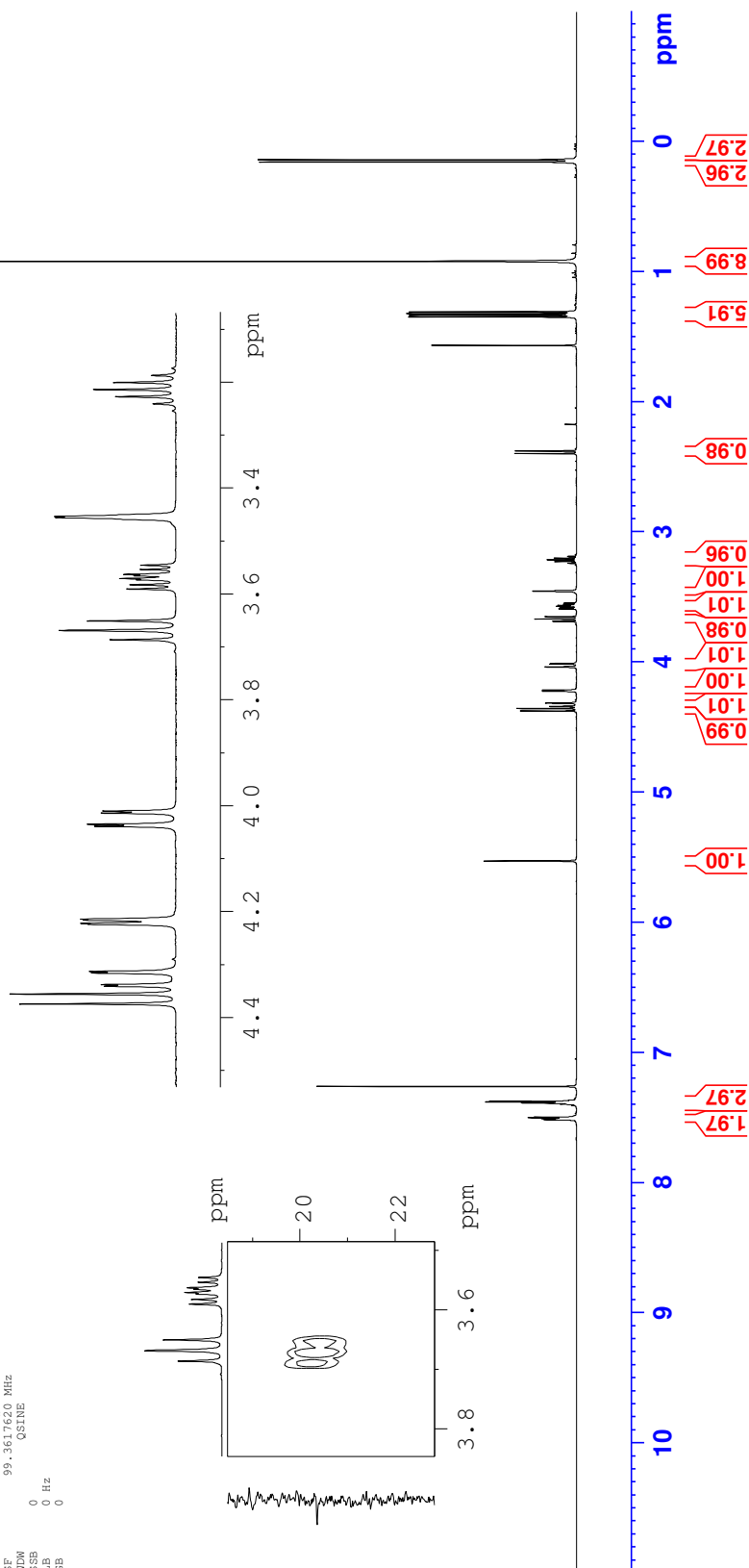


<sup>13</sup>C NMR - Isopropyl 4,6-*O*-benzylidene-2-*O*-(*tert*-butyldimethylsilyl)-3-*O*-fluorenylmethoxycarbonyl-1-thio-β-D-galactopyranoside **189**

<sup>1</sup>H NMR - Isopropyl 4,6-*O*-benzylidene-2-*O*-(*tert*-butyldimethylsilyl)-1-thio-β-D-galactopyranoside **190**

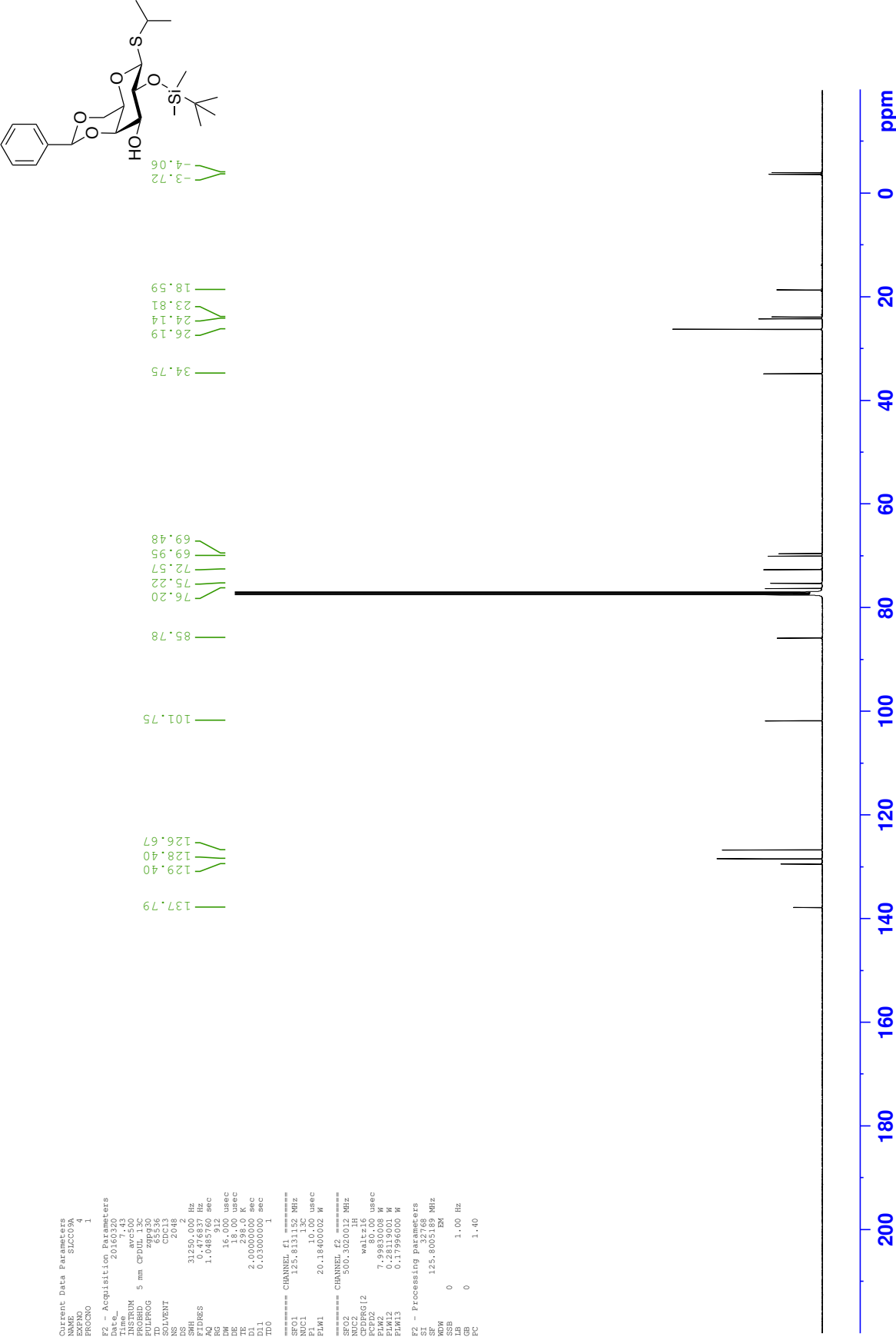


Current Data Parameters  
NAME SUCC09A.SI  
EXPNO 2  
PROCNO 1  
F1 - Acquisition Parameters  
TD 65536  
SFO 500.130112 MHz  
FIDRES 77.659042 Hz  
SW 100.042 PPM  
F2 - Processing parameters  
SI 32768  
SF 500.130112 MHz  
WDW 4  
SSB 0 Hz  
LB 0  
GB 0  
FC 1.40  
F1 - Processing parameters  
SI 1024  
MC2 QF  
SF 99.3617620 MHz  
WDW 0  
SSB 0 Hz  
LB 0  
GB 0

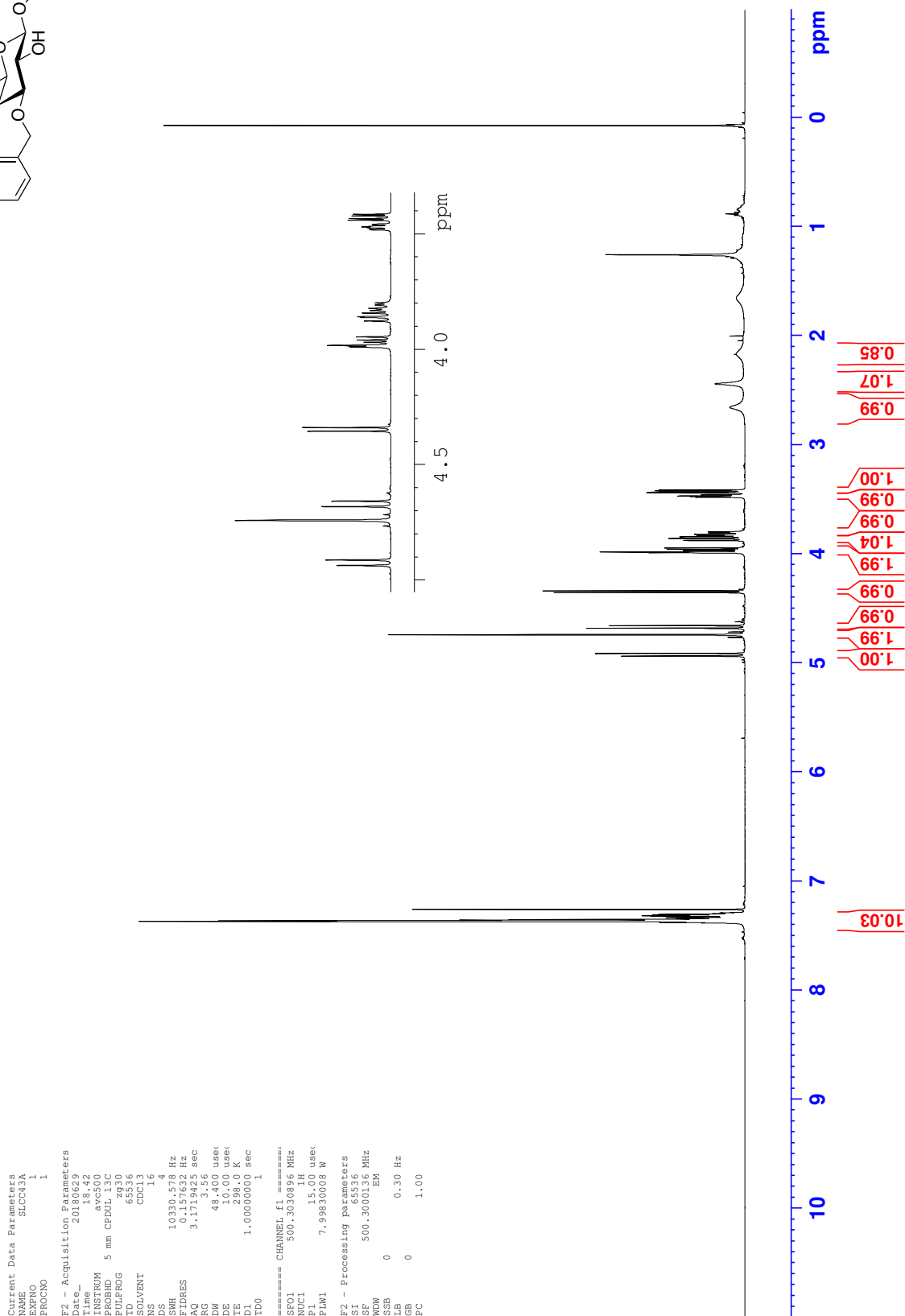
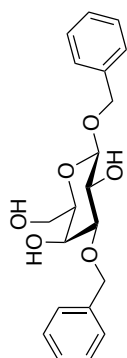




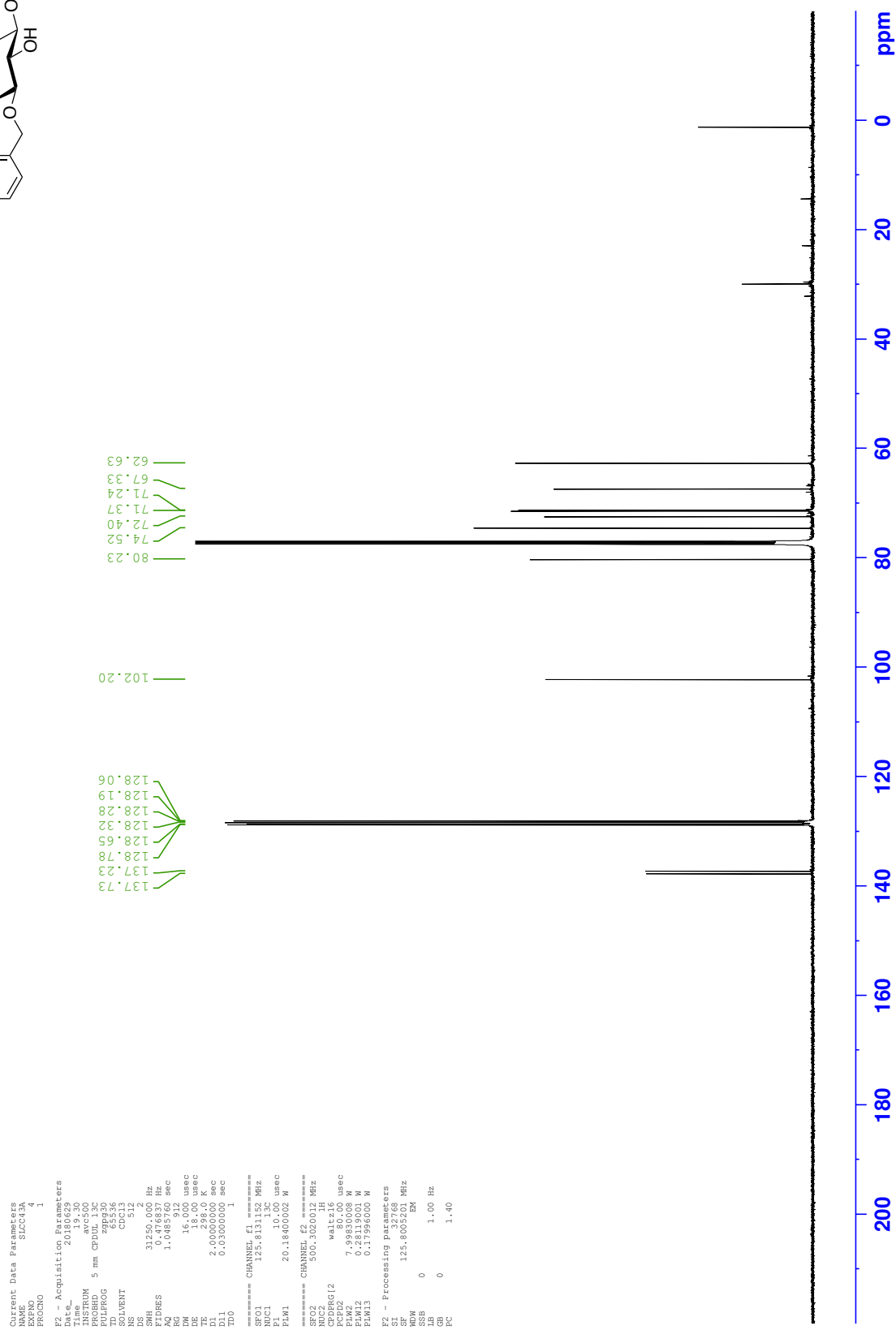
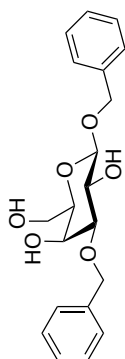
<sup>13</sup>C NMR - Isopropyl 4,6-O-benzylidene-2-O-(*tert*-butyldimethylsilyl)-1-thio-β-D-galactopyranoside **190**



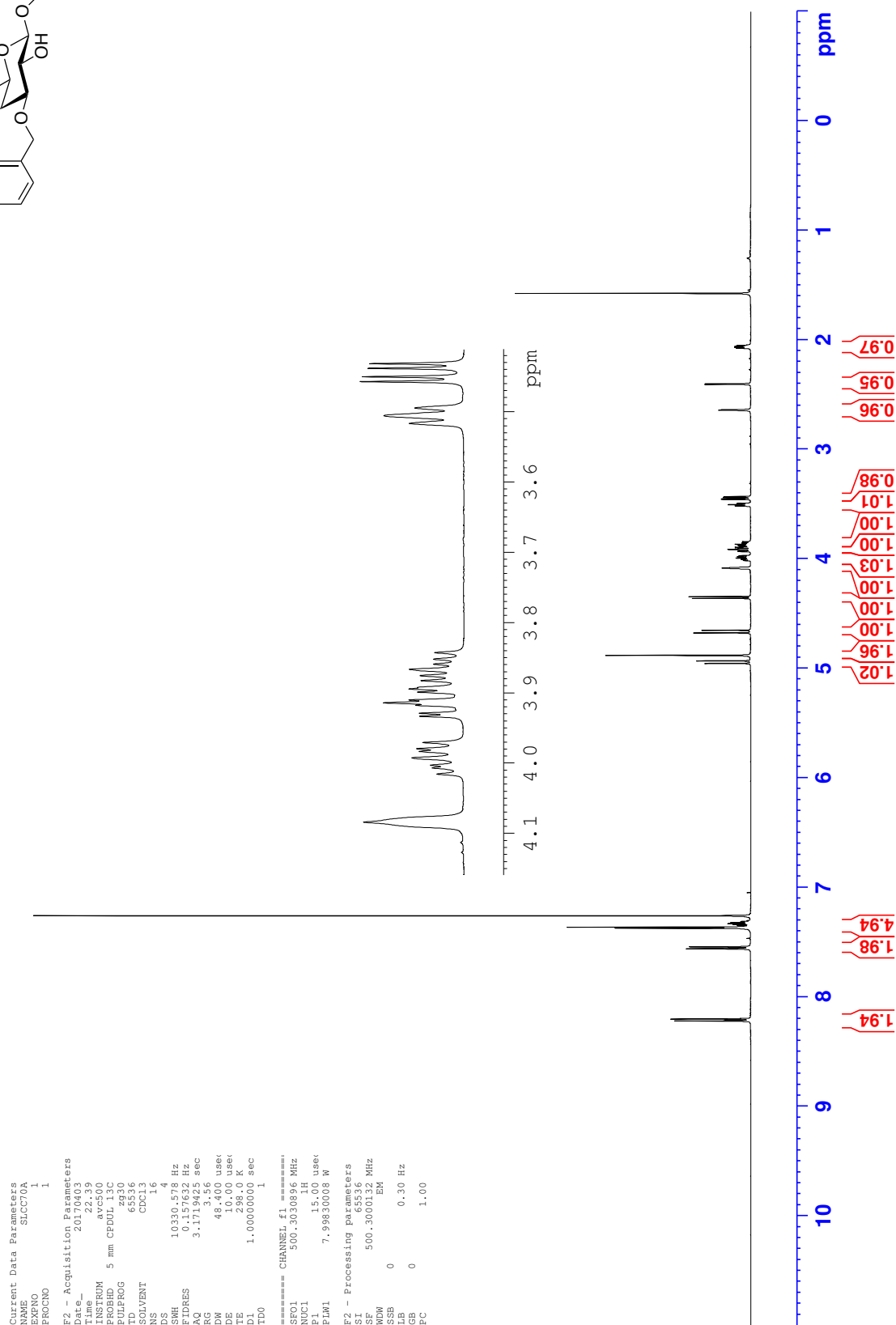
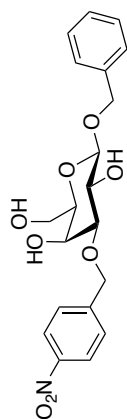
<sup>1</sup>H NMR - Benzyl 3-O-benzyl-β-D-galactopyranoside 197



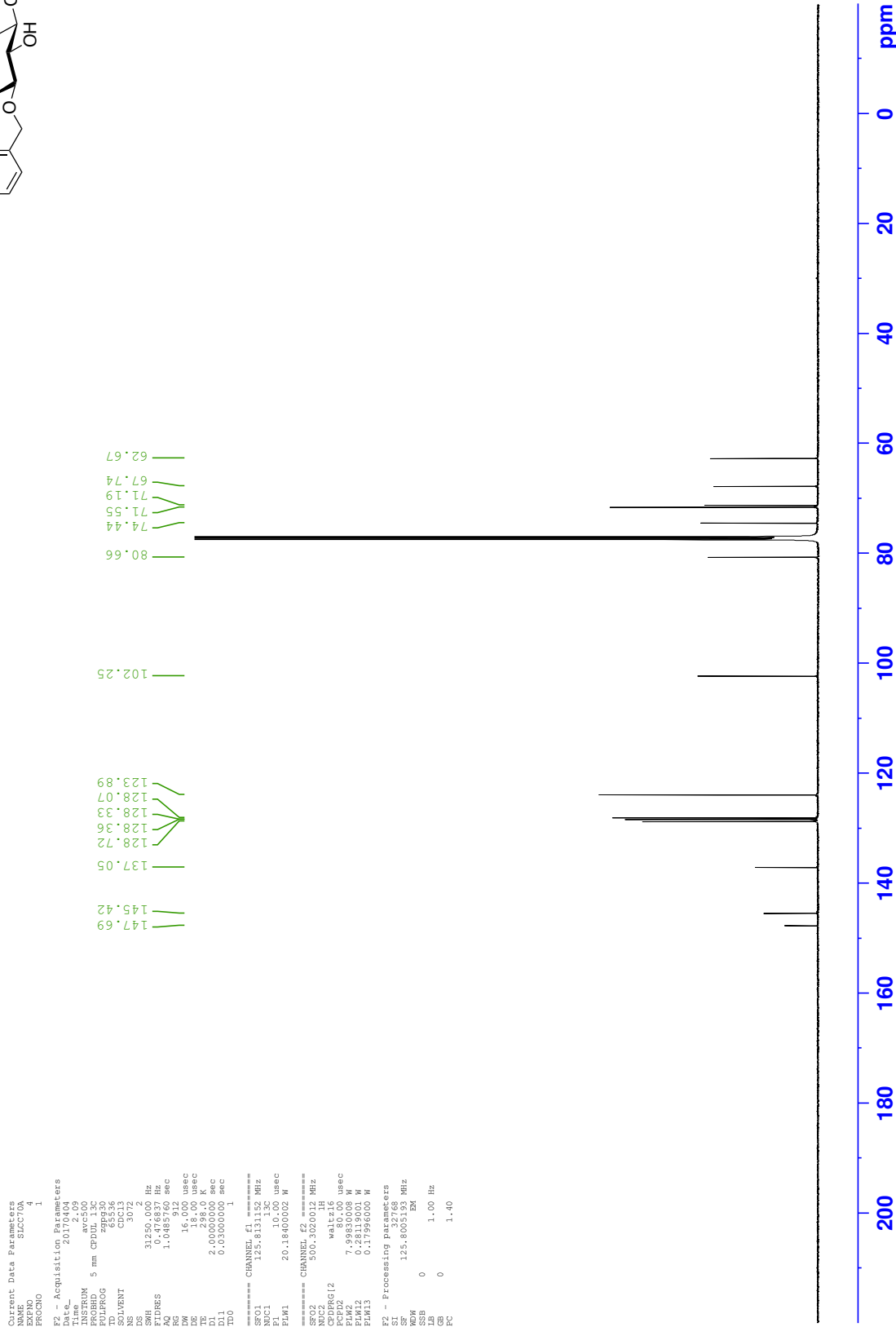
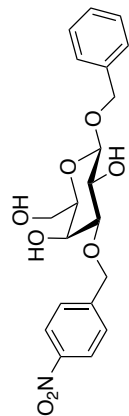
**<sup>13</sup>C NMR - Benzyl 3-*O*-benzyl-β-D-galactopyranoside 197**



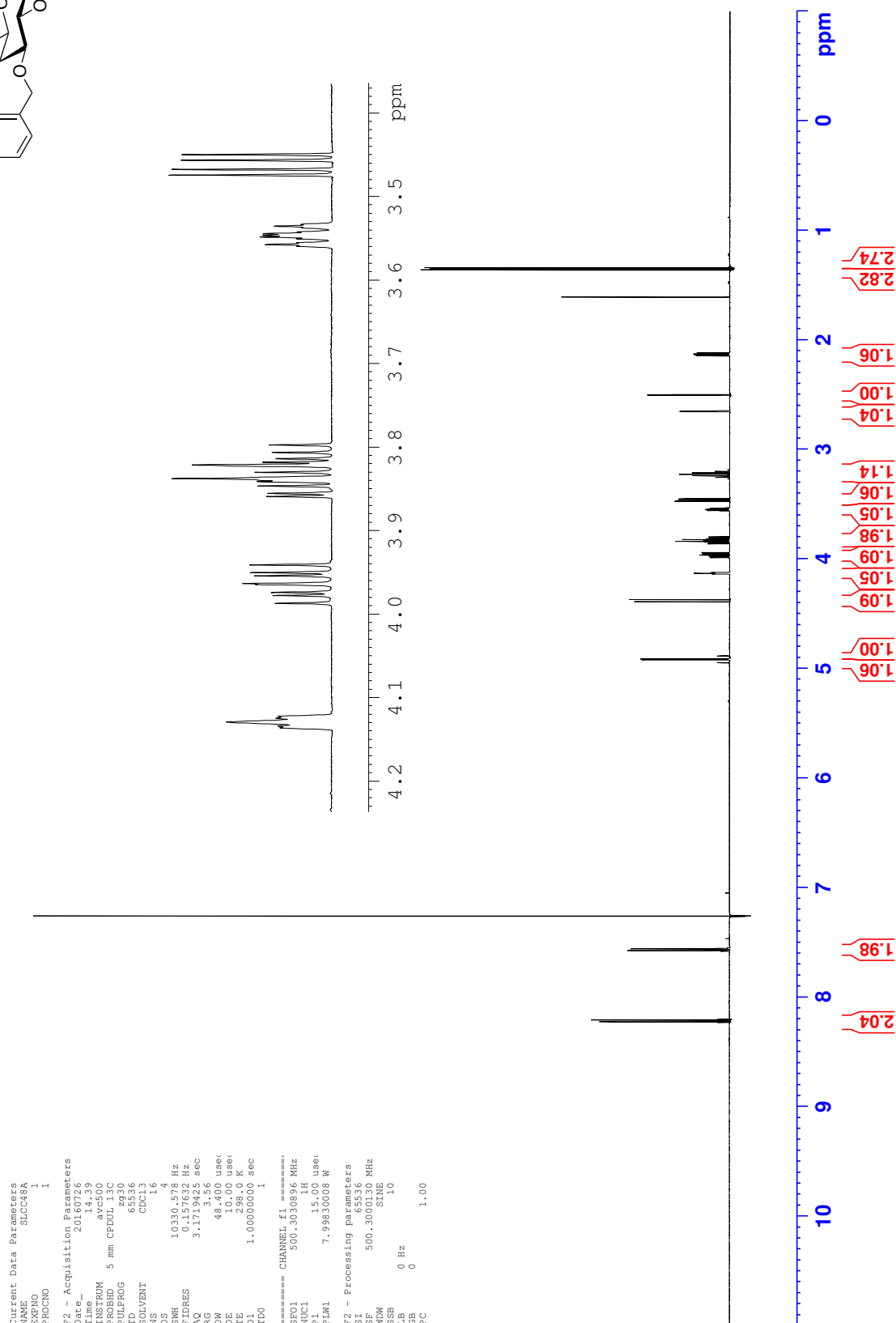
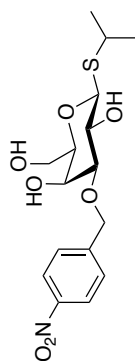
<sup>1</sup>H NMR - Benzyl 3-O-(4-nitrobenzyl)-β-D-galactopyranoside 124



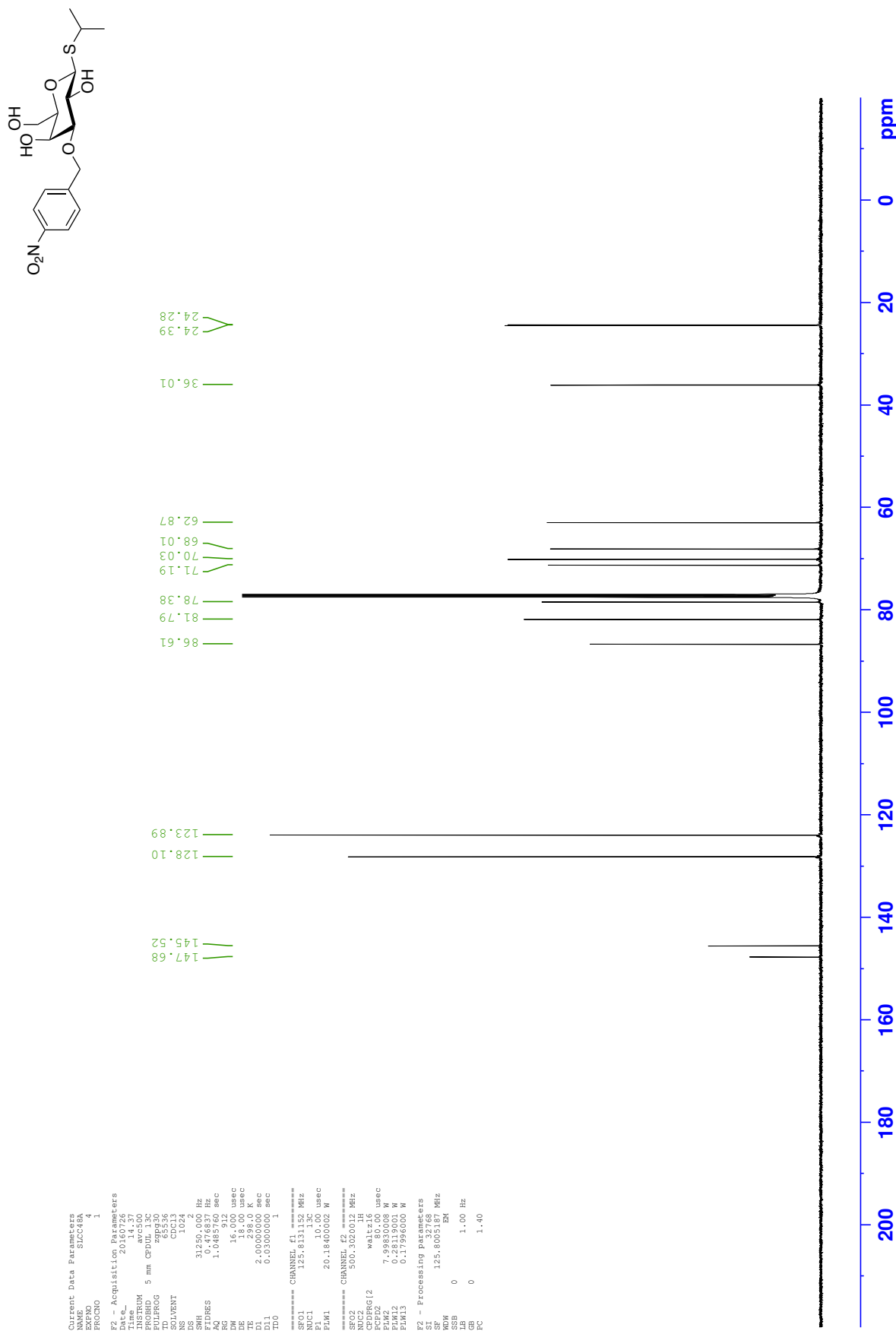
<sup>13</sup>C NMR - Benzyl 3-O-(4-nitrobenzyl)-β-D-galactopyranoside 124



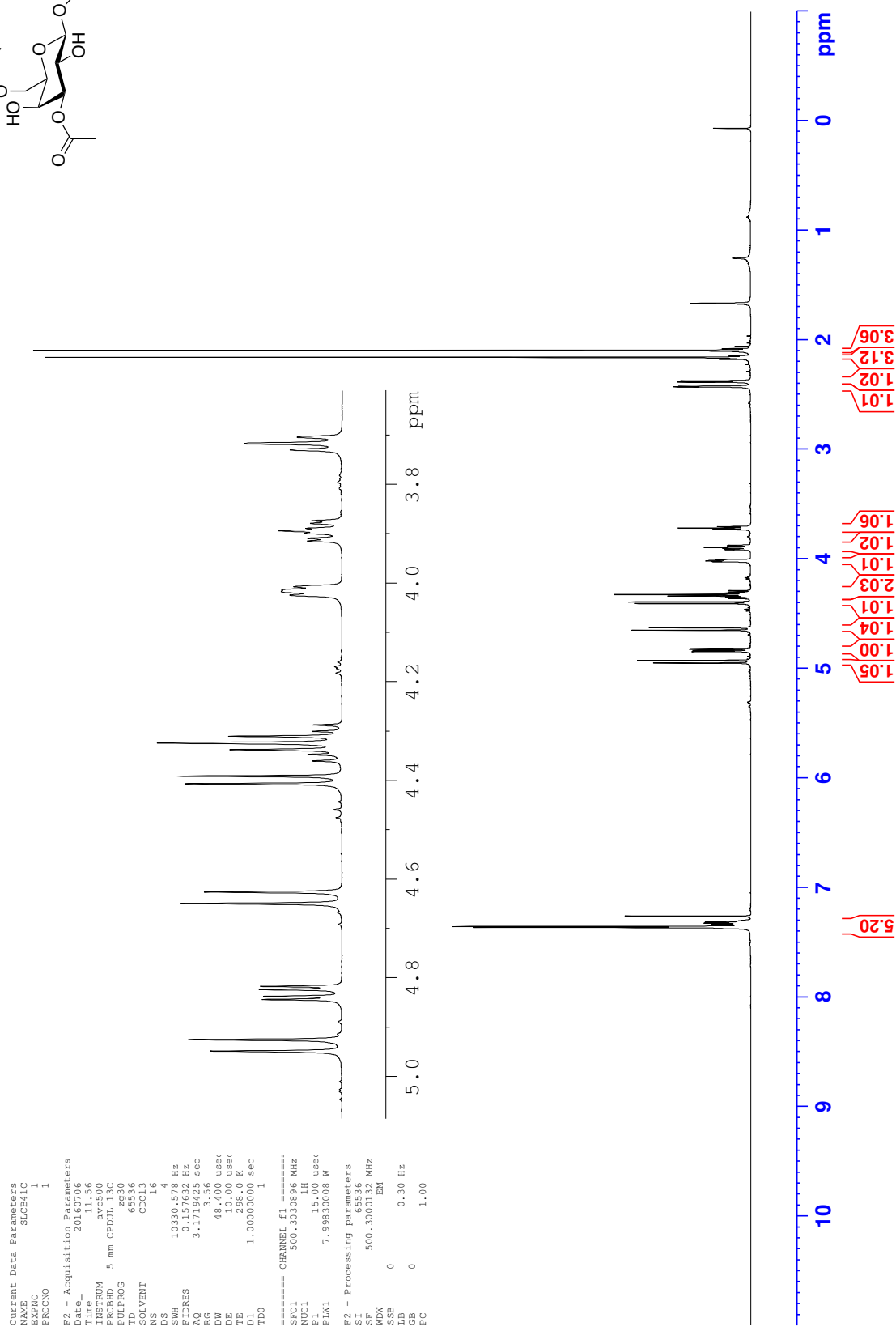
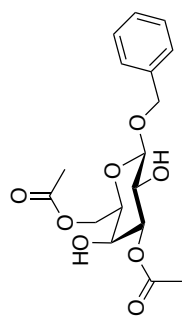
<sup>1</sup>H NMR - Isopropyl 3-O-(4-nitrobenzyl)-1-thio-β-D-galactopyranoside **87**



<sup>13</sup>C NMR - Isopropyl 3-O-(4-nitrobenzyl)-1-thio-β-D-galactopyranoside **87**

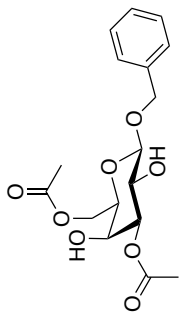


<sup>1</sup>H NMR - Benzyl 3,6-di-*O*-acetyl-β-D-galactopyranoside **212**

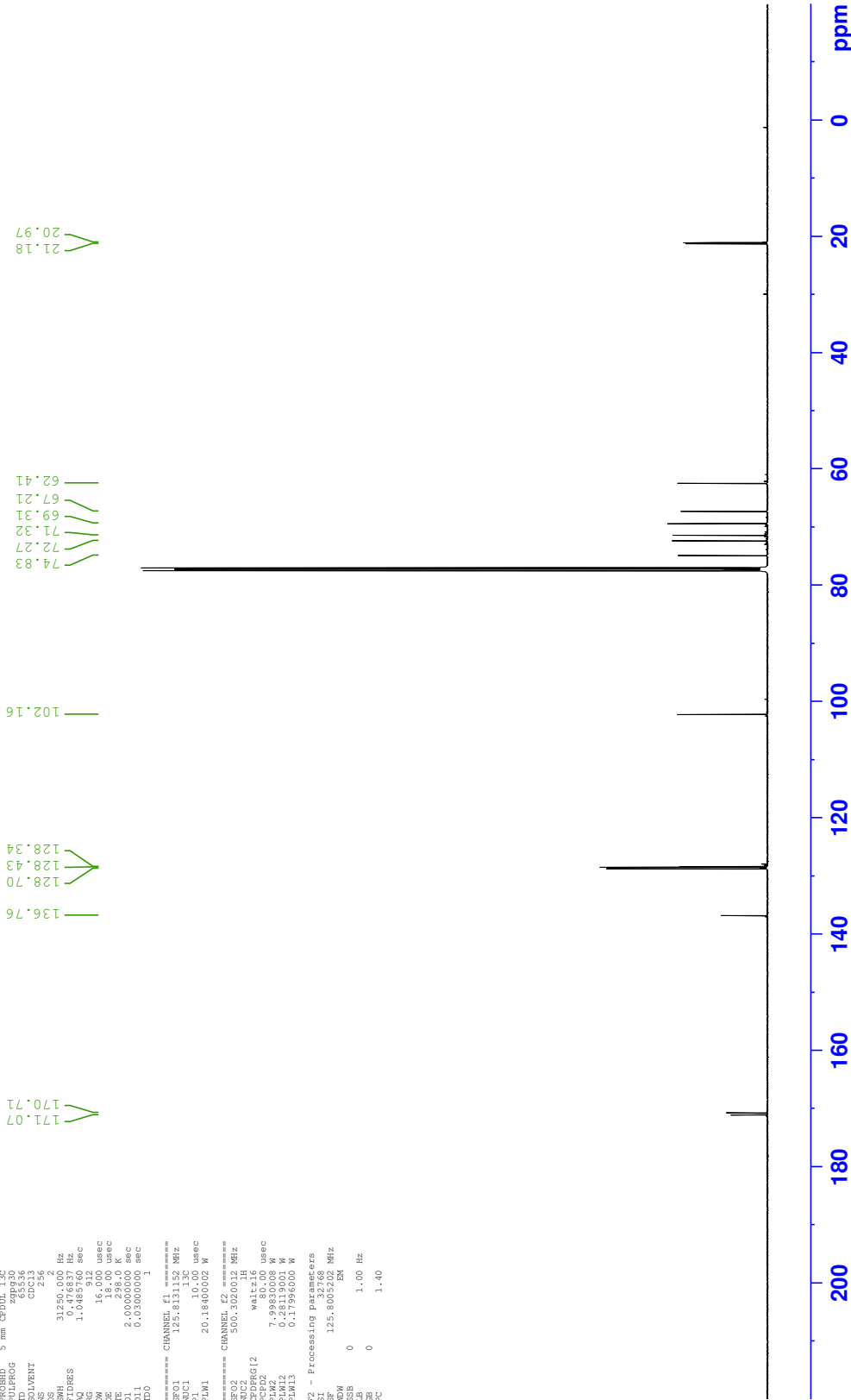




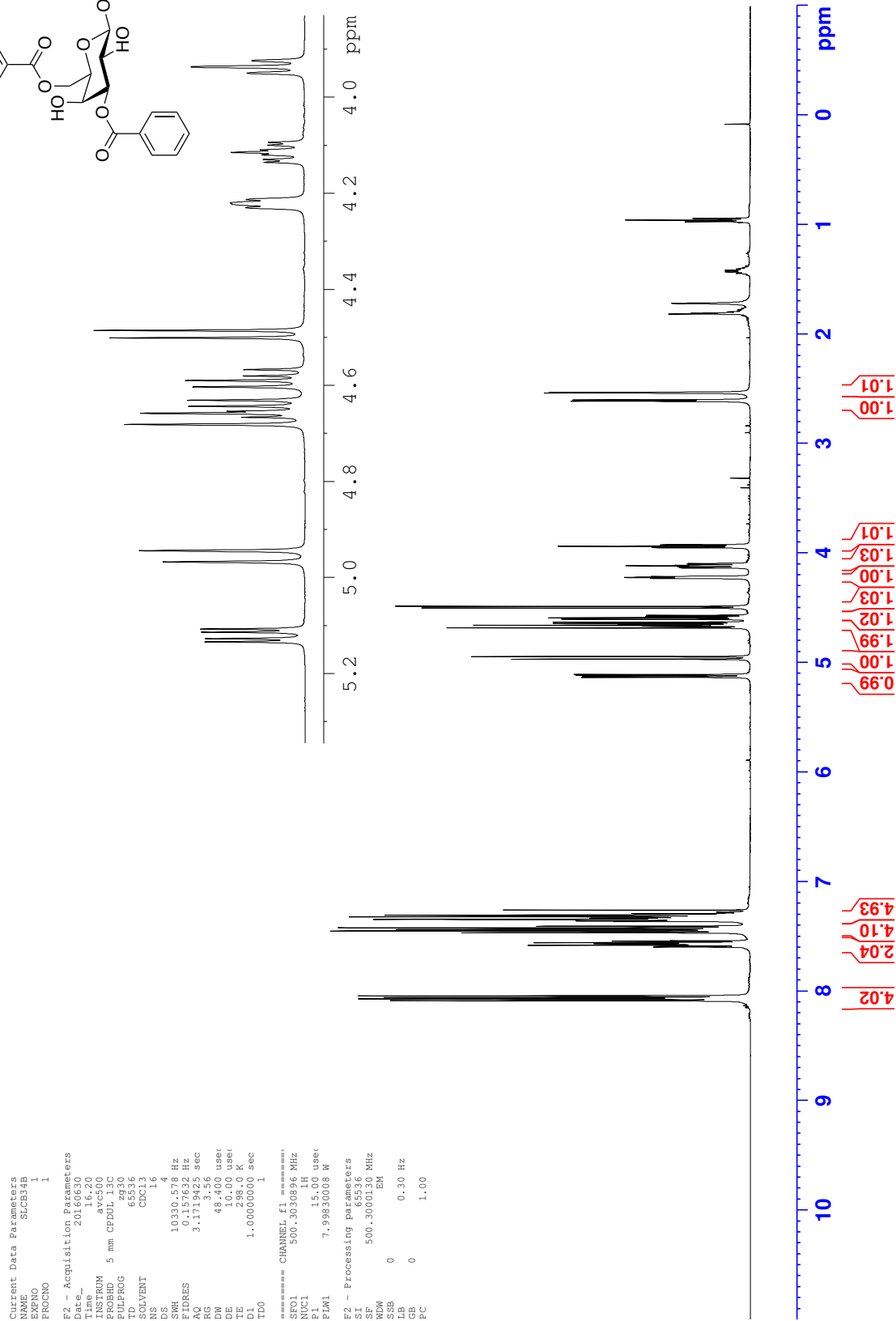
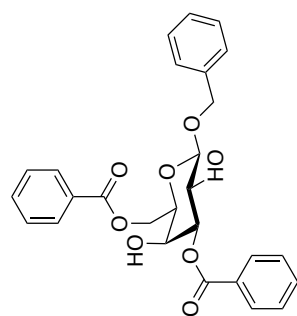
<sup>13</sup>C NMR - Benzyl 3,6-di-O-acetyl-β-D-galactopyranoside 212



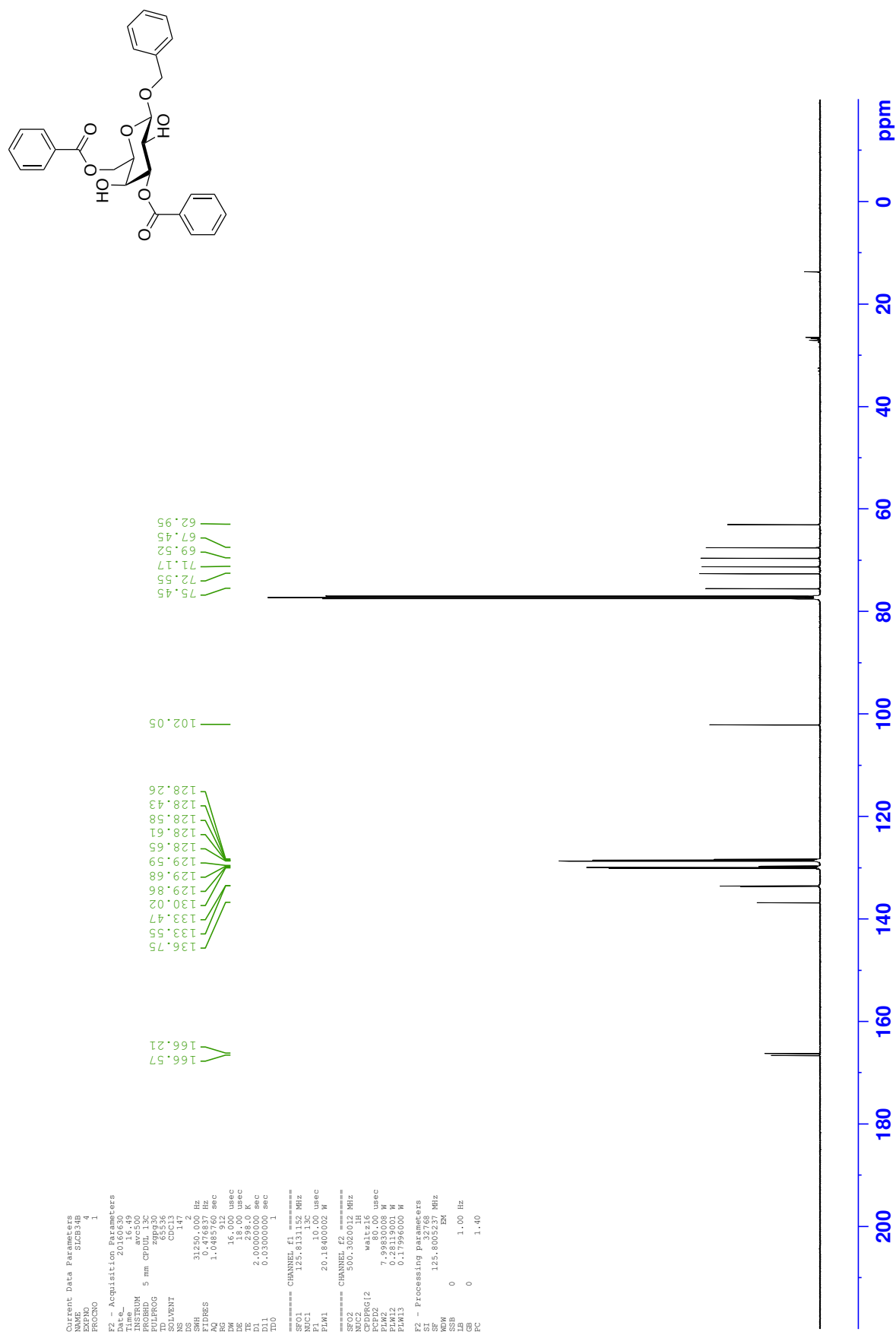
Current Data Parameters  
NAME: SJ2B41C  
EXPNO: 4  
PROCNO: 1  
F2 - Acquisition Parameters  
Date\_ : 20160705  
Time: 12.30  
INSTRUM: avc500  
PROBHD: 5 mm CPDPR 1H  
PULPROG: zgpg30  
TD: 65536  
SOLVENT: CDCl3  
DS: 2  
SWH: 31250.00 Hz  
FIDRES: 0.14777 Hz  
AQ: 1.00485760 sec  
RG: 912  
DW: 15.000 usec  
DE: 2.000 usec  
TE: 298.0 K  
D1: 2.00000000 sec  
d11: 0.03000000 sec  
TD0: 1  
===== CHANNEL f1 =====  
NUC1: 13C  
NUC1: 13C  
F1: 10.00 usec  
P1: 20.18400002 W  
===== CHANNEL f2 =====  
NUC2: 1H  
NUC2: 1H  
F2: 500.30200000 MHz  
P2: 12.00 usec  
P2PRG2: waltz16  
PCPD2: 50.00 usec  
PCPD2: 10.00 usec  
F1F2: 500.13619901 MHz  
F1F2: 0.28119001 W  
F1F2: 0.17996000 W  
F2 - Processing parameters  
SI: 32768  
SF: 125.8055232 MHz  
WDW: EM  
SSB: 0  
LB: 1.00 Hz  
GB: 0  
PC: 1.40



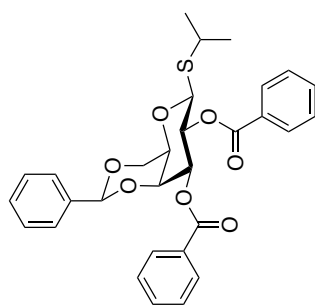
<sup>1</sup>H NMR - Benzyl 3,6-di-*O*-benzoyl-β-D-galactopyranoside **215**



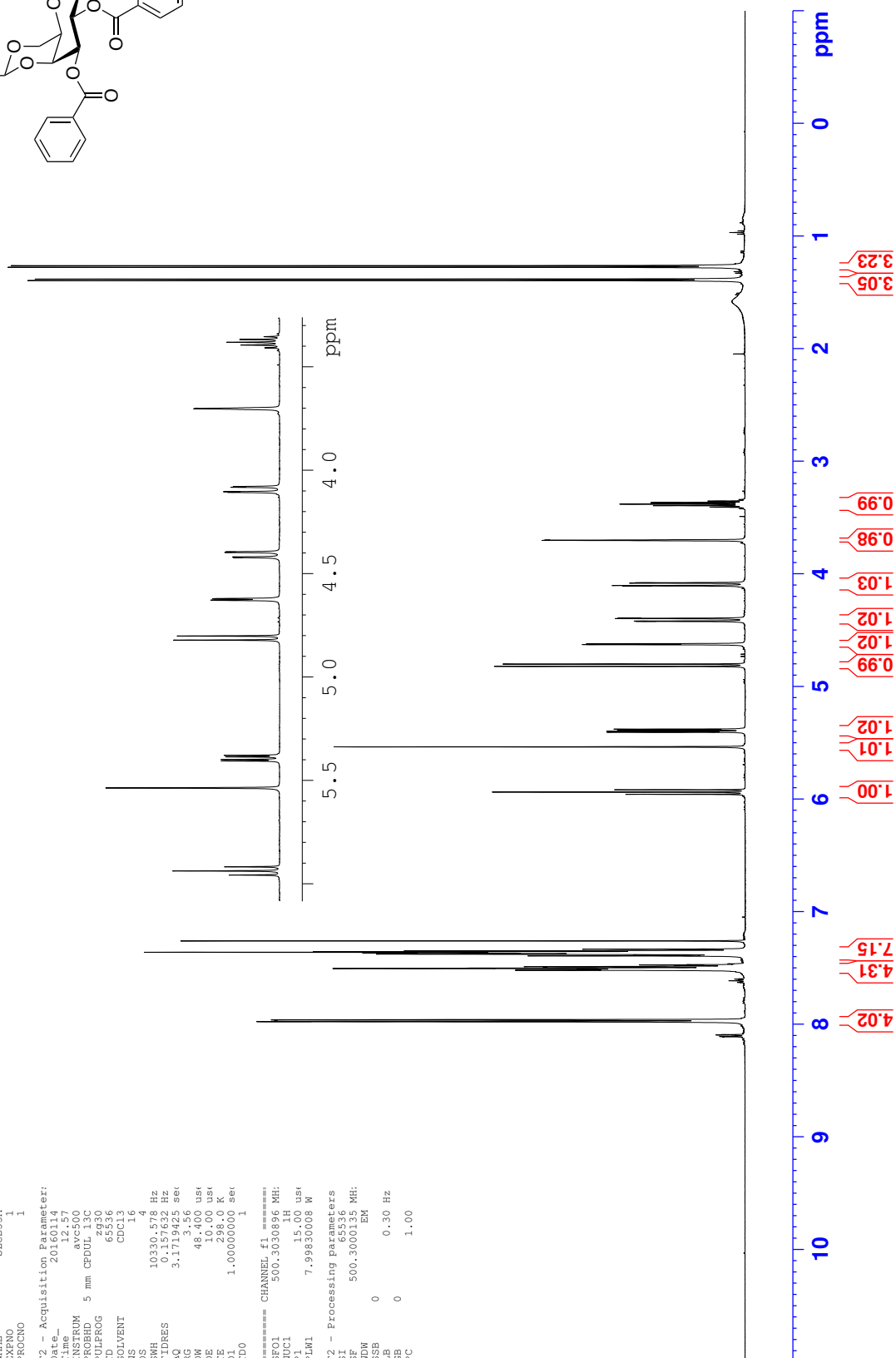
**<sup>13</sup>C NMR - Benzyl 3,6-di-*O*-benzoyl-β-D-galactopyranoside 215**



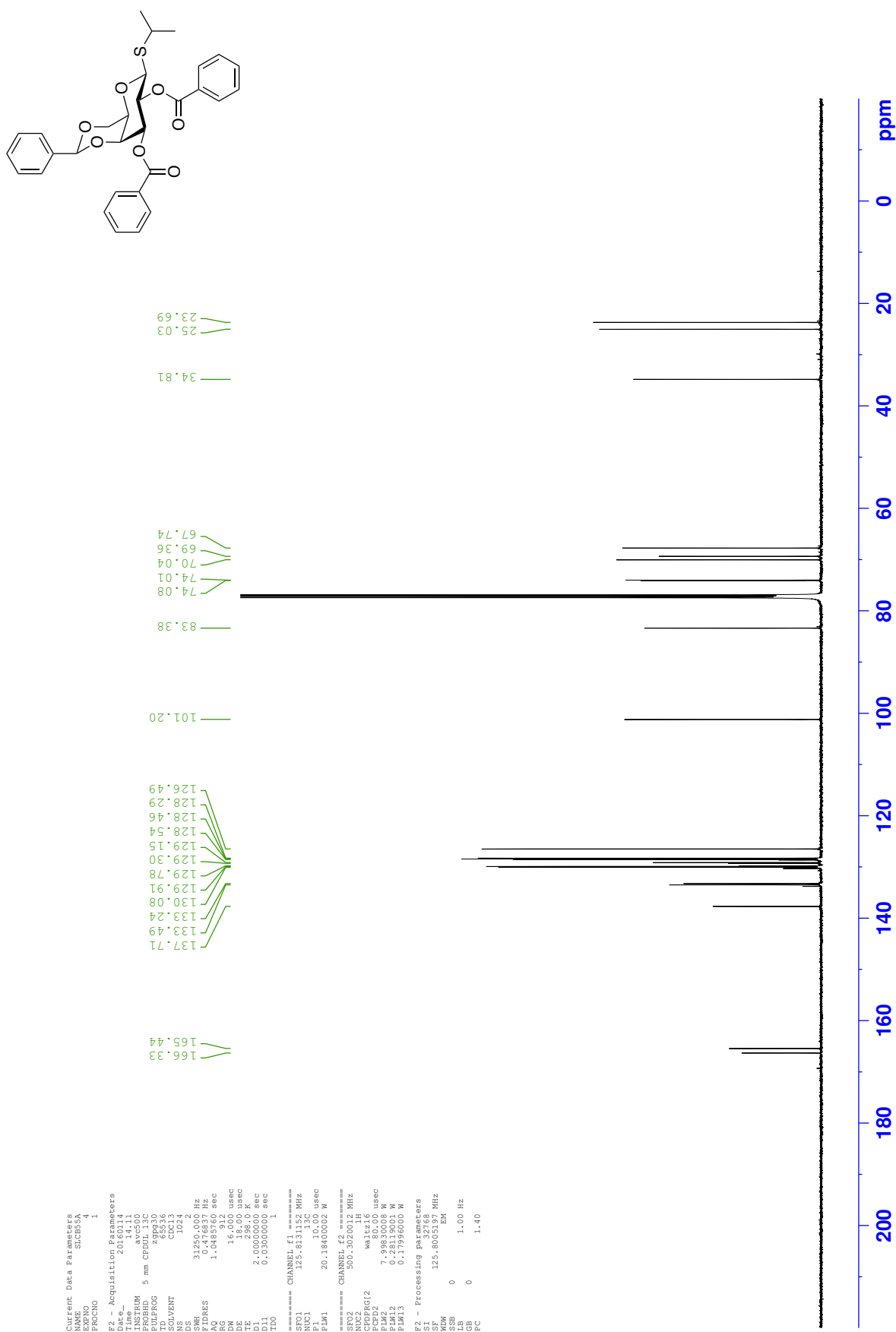
<sup>1</sup>H NMR - Isopropyl 2,3-di-*O*-benzoyl-4,6-*O*-benzylidene-1-thio-β-D-galactopyranoside 224



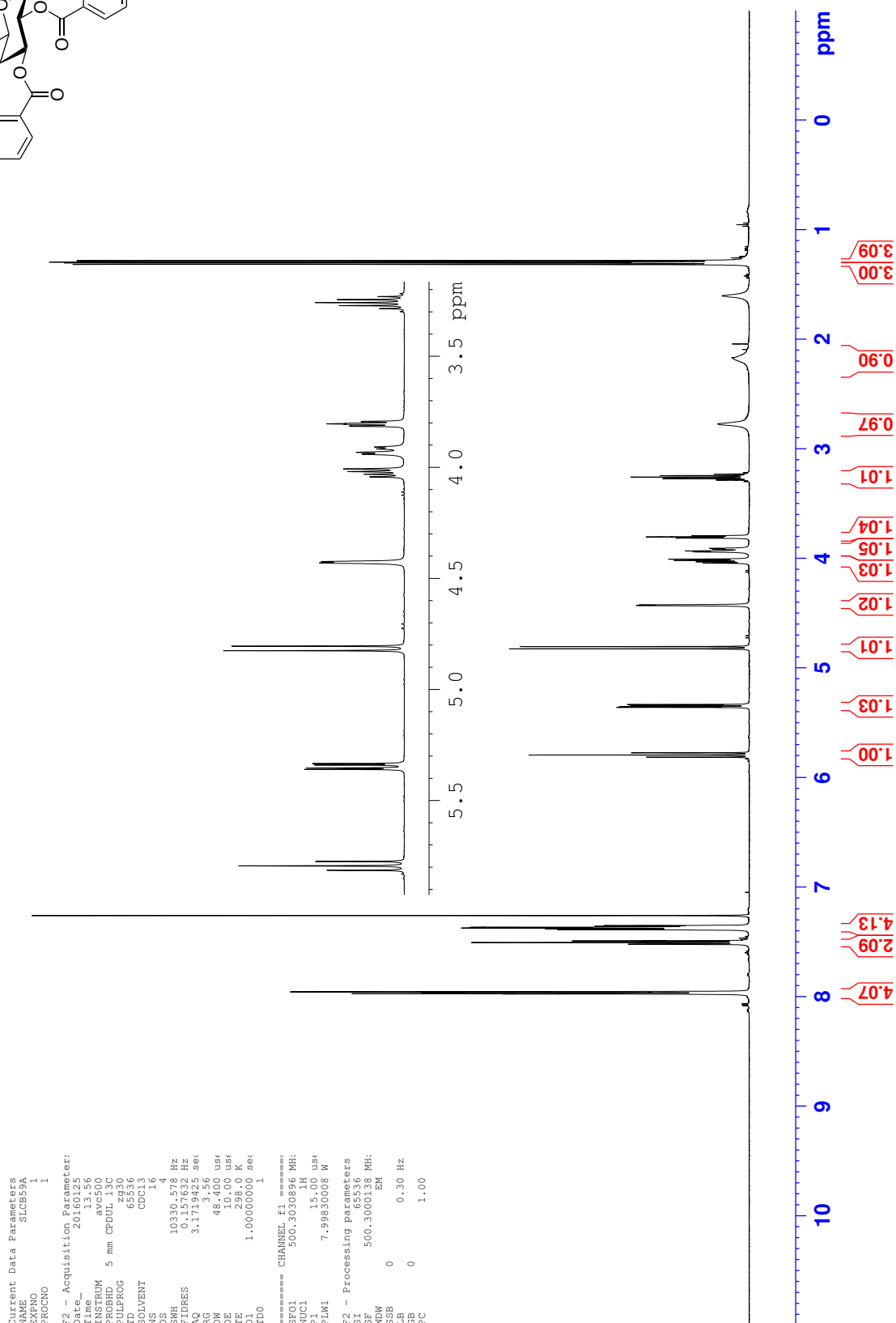
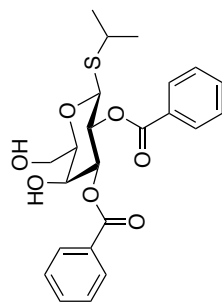
Current Data Parameters  
 NAME SUCBS3A  
 EXNO 1  
 PROCNO 1  
 F2 - Acquisition Parameters:  
 Date\_ 20160114  
 Time\_ 12:07  
 INSTRUM spect  
 PROBHD 5 mm CPDUL13C  
 PULPROG zgpg30  
 TD 65536  
 SOLVENT CDCl3  
 NS 16  
 DS 4  
 SWH 10330.578 Hz  
 FIDRES 0.157632 Hz  
 AQ 3.1719425 sec  
 RG 3.56  
 DW 48.400 usec  
 DE 15.00 usec  
 TE 298.0 K  
 D1 1.00000000 sec  
 TDO 1  
 CHANNEL f1  
 SFO1 500.303085 MHz  
 NUC1 1H  
 P1 15.00 usec  
 PLW1 7.99830008 W  
 F2 - Processing parameters  
 SF 500.3000135 MHz  
 WDW EM  
 SSB 0  
 LB 0.30 Hz  
 GB 0  
 PC 1.00



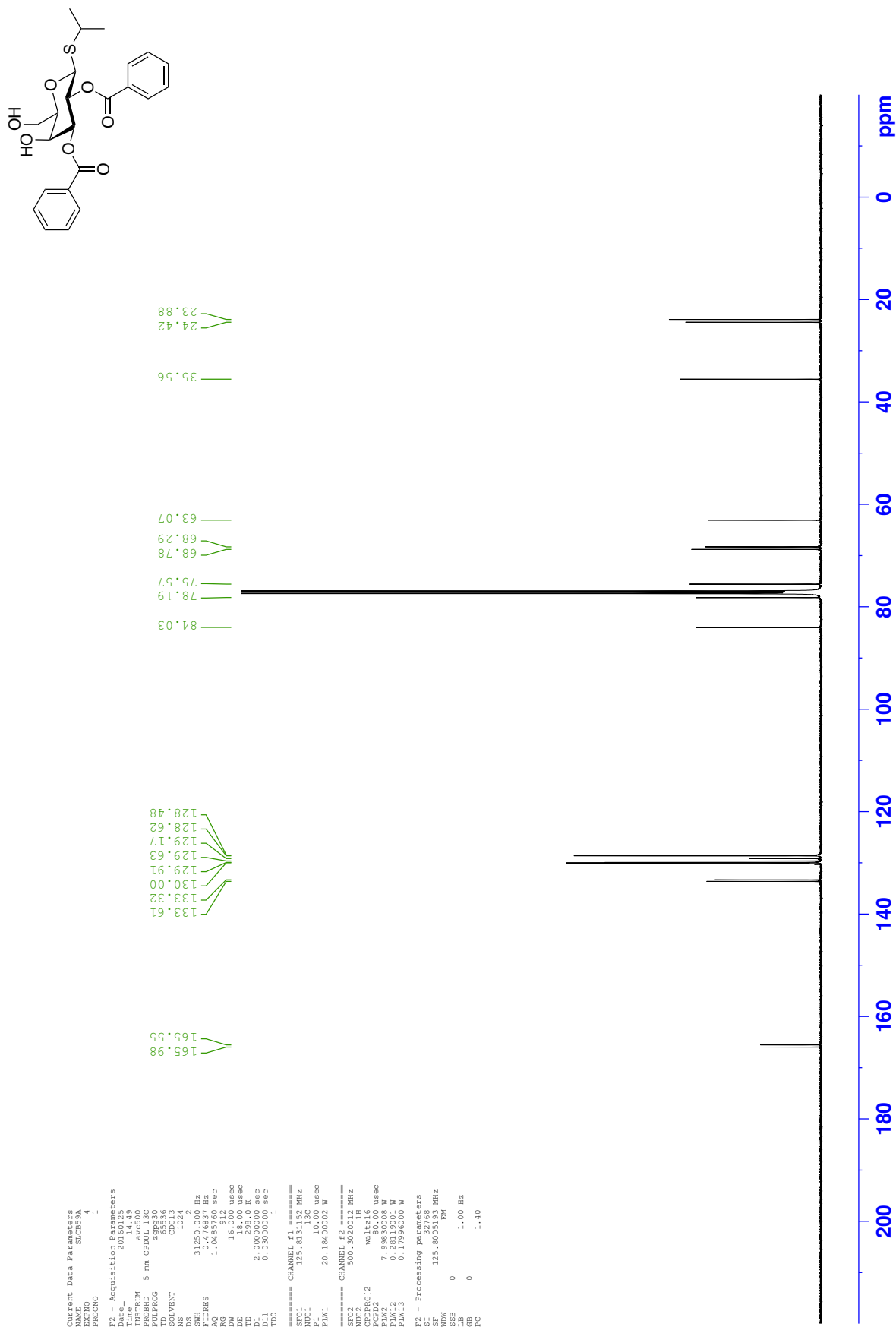
<sup>13</sup>C NMR - Isopropyl 2,3-di-*O*-benzoyl-4,6-*O*-benzylidene-1-thio-β-D-galactopyranoside **224**



<sup>1</sup>H NMR - Isopropyl 2,3-di-O-benzoyl-1-thio-β-D-galactopyranoside 225



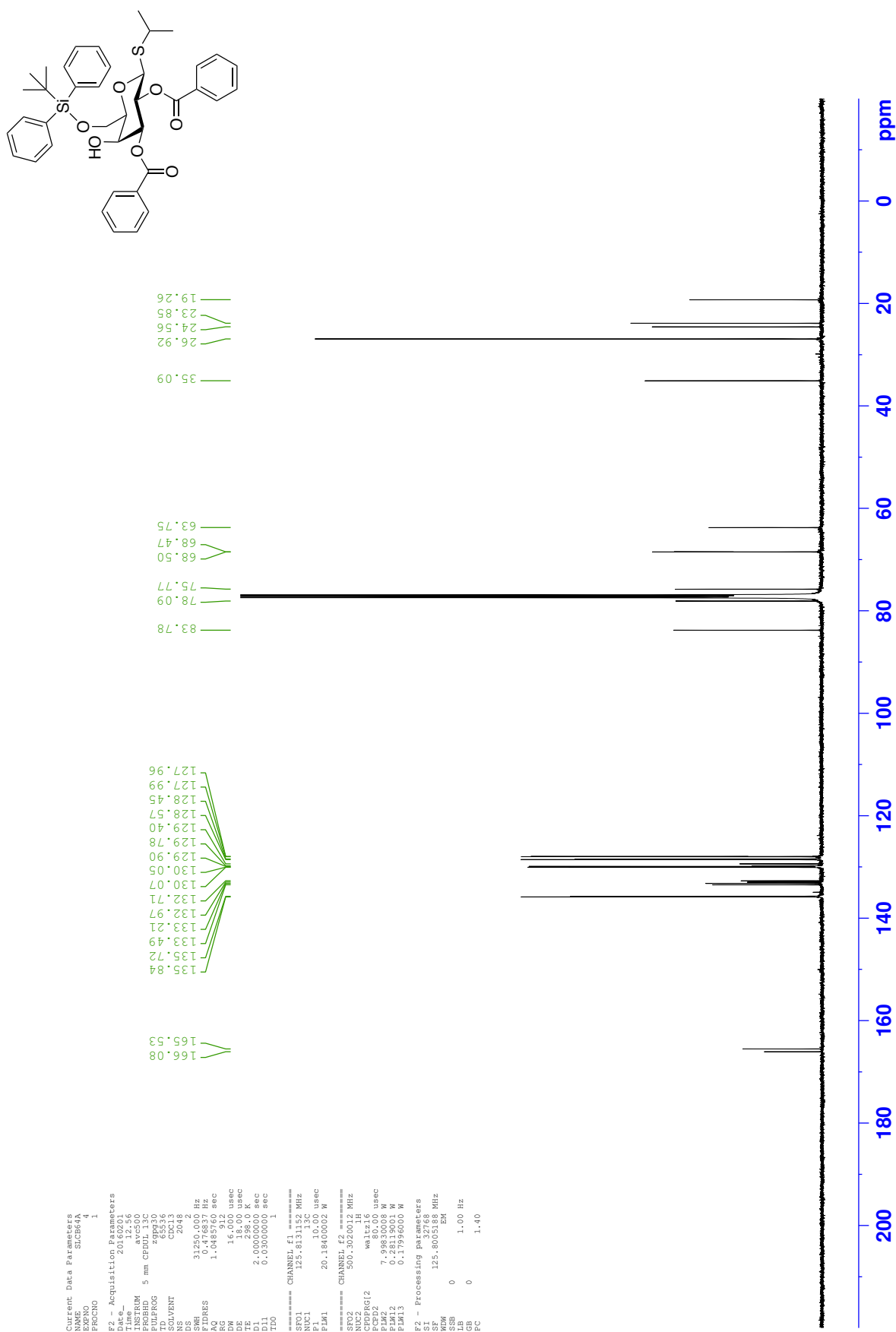
<sup>13</sup>C NMR - Isopropyl 2,3-di-*O*-benzoyl-1-thio-β-D-galactopyranoside **225**



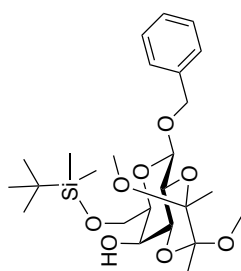




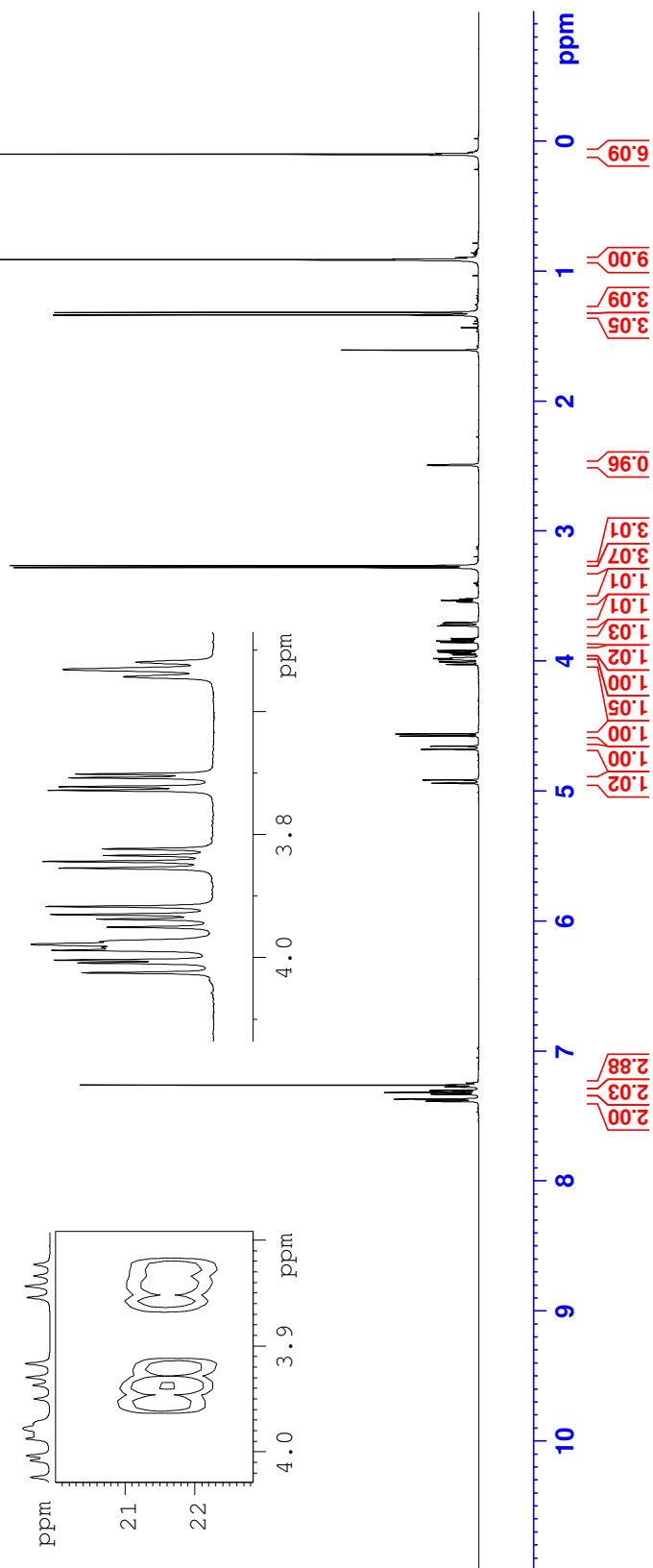
<sup>13</sup>C NMR - Isopropyl 2,3-di-*O*-benzoyl-6-*O*-(*tert*-butyldiphenylsilyl)-1-thio-β-D-galactopyranoside **226**



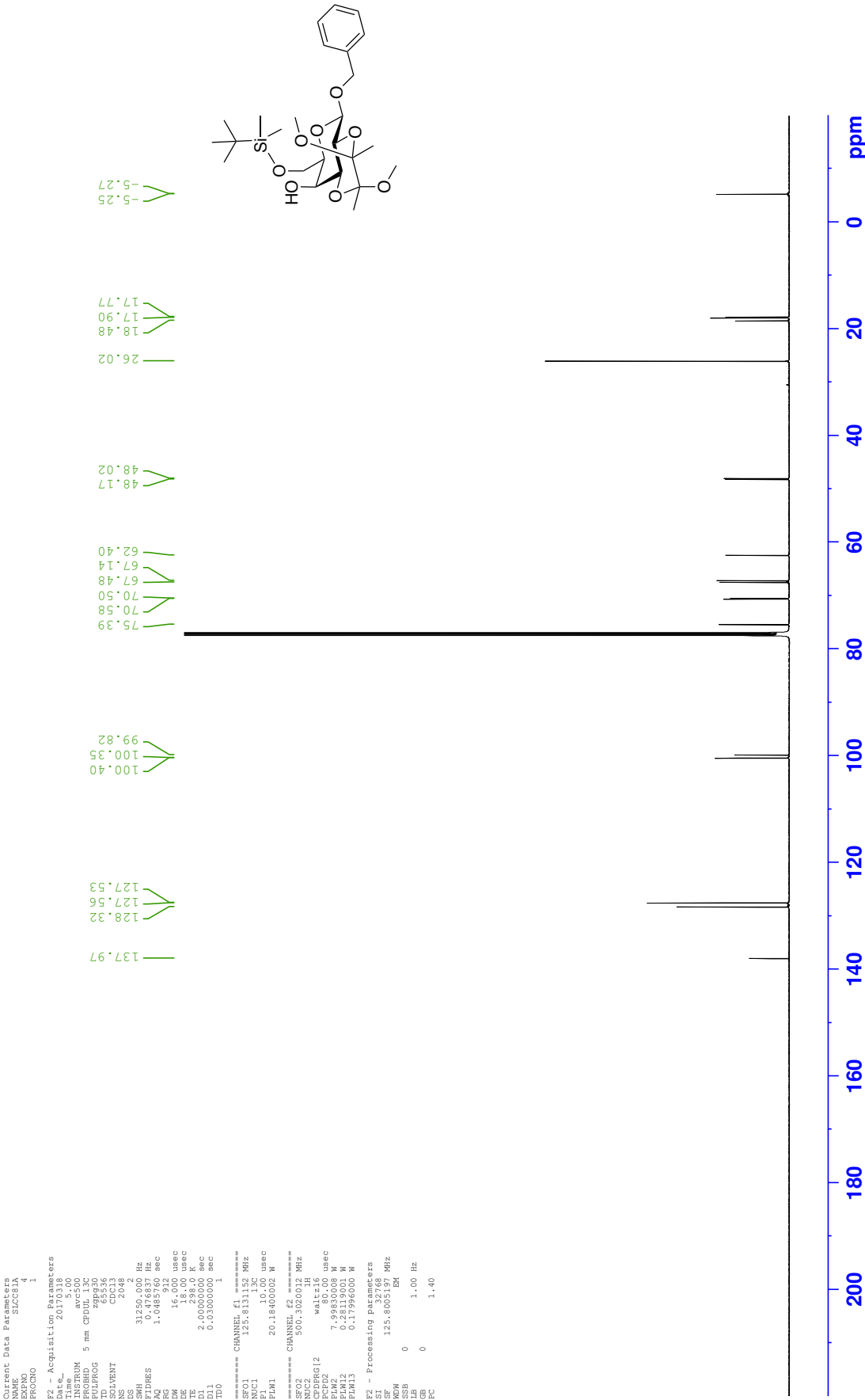
<sup>1</sup>H NMR - Benzyl 6-*O*-(*tert*-butyldimethylsilyl)-2,3-di-*O*-(2',3'-dimethoxybutane-2',3'-diyl)-β-D-galactopyranoside **236**



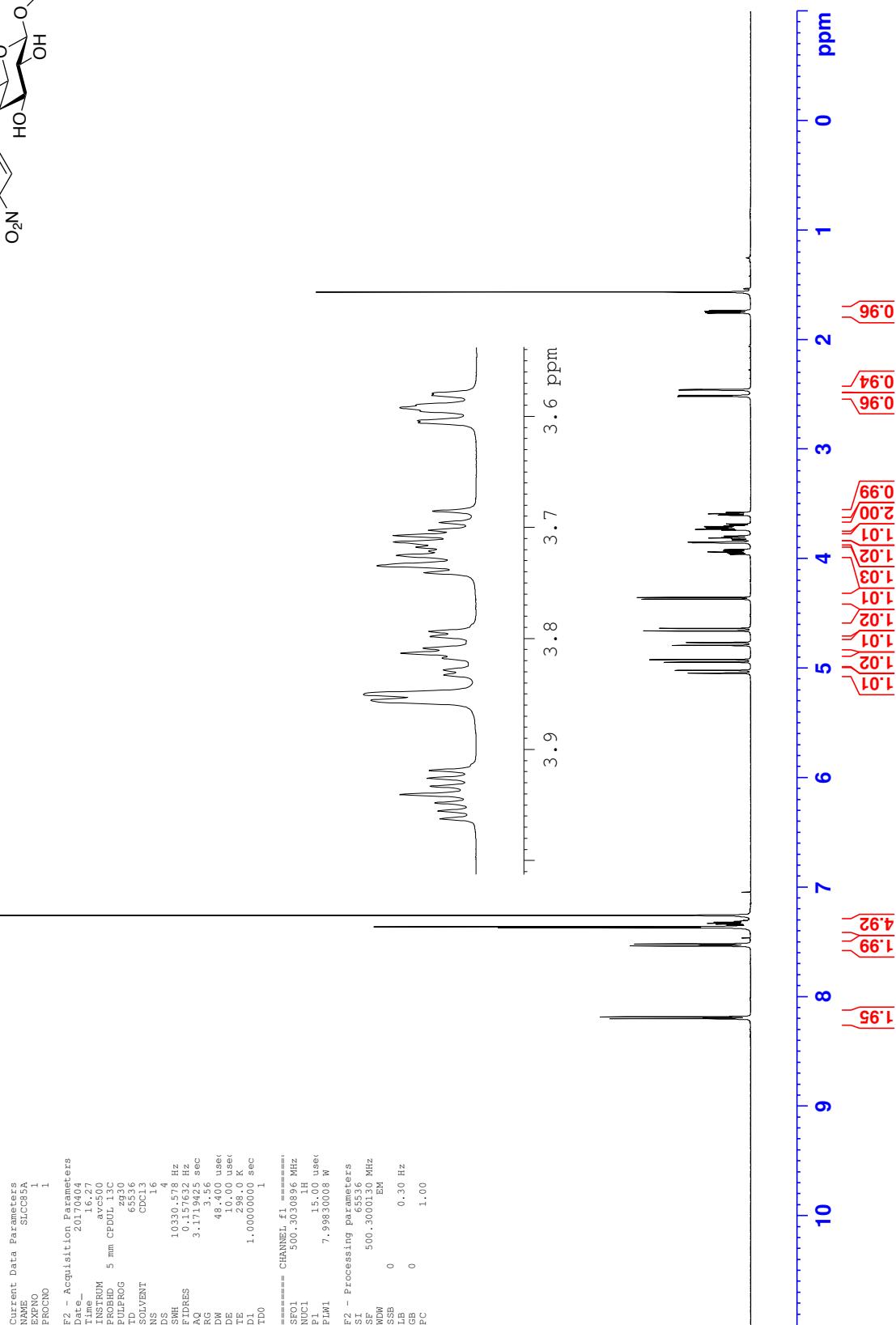
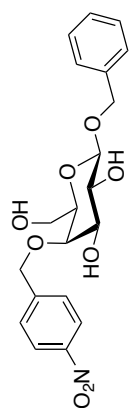
Current Data Parameters  
NAME SUCCIA\_2  
EXPNO 2  
PROCNO 1  
F1 - Acquisition Parameters  
TD 65536  
SFO 99.3128 MHz  
AQ 0.51964 s  
FIDRES 77.659042 Hz  
SW 100.042 PPM  
F2 - Processing parameters  
SI 32768  
SF 500.130110 MHz  
WDW 4  
SSB 0 Hz  
LB 0  
GB 0  
FC 1.40  
F1 - Processing parameters  
SI 1024  
MC2 QF  
SF 99.3617620 MHz  
WDW 4  
SSB 0 Hz  
LB 0  
GB 0



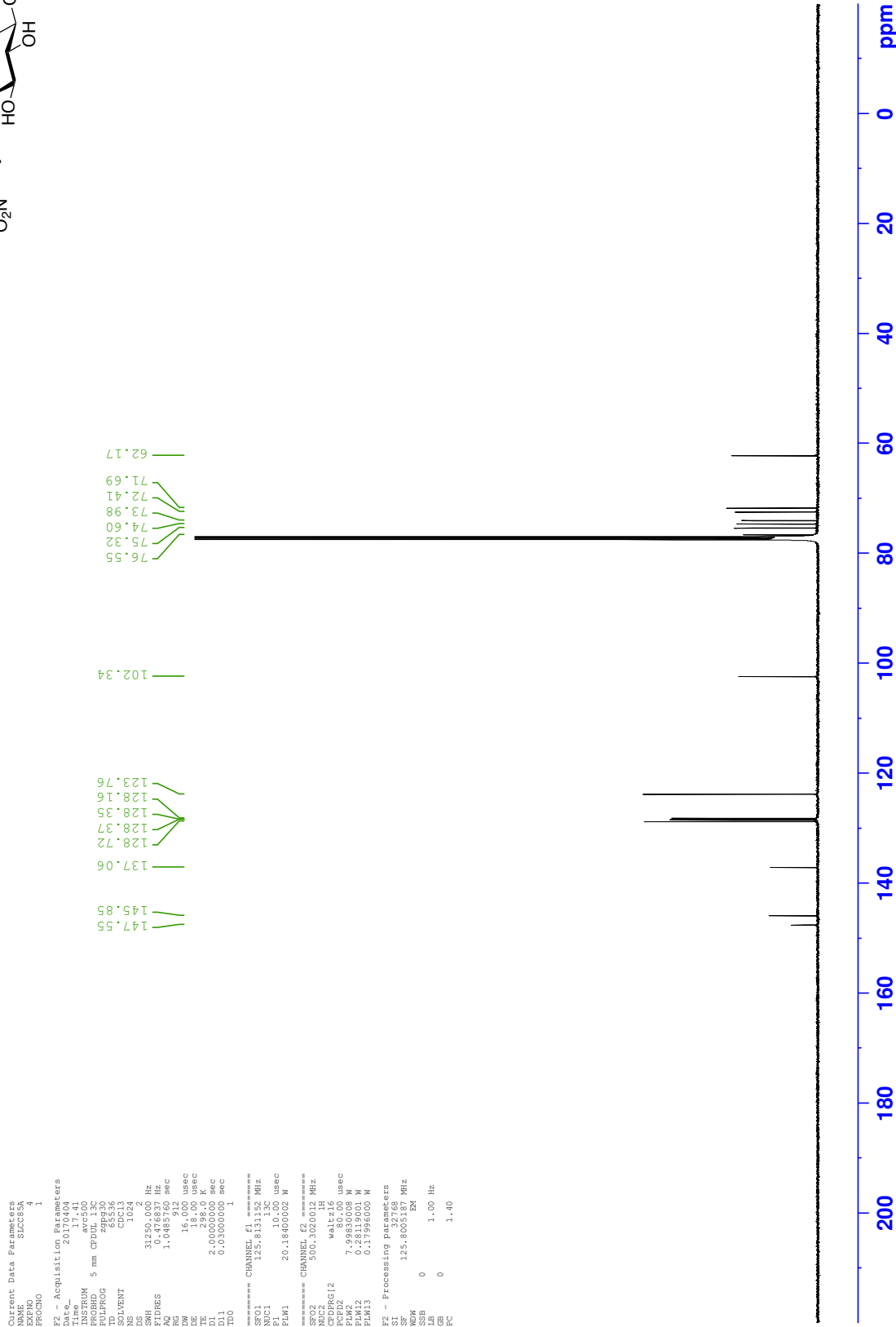
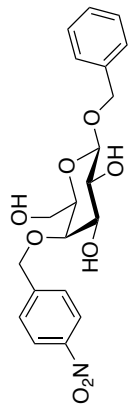
<sup>13</sup>C NMR - Benzyl 6-*O*-(*tert*-butyldimethylsilyl)-2,3-di-*O*-(2',3'-dimethoxybutane-2',3'-diyl)-β-D-galactopyranoside 236



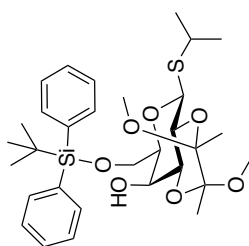
<sup>1</sup>H NMR - Benzyl 4-O-(4-nitrobenzyl)-β-D-galactopyranoside 125



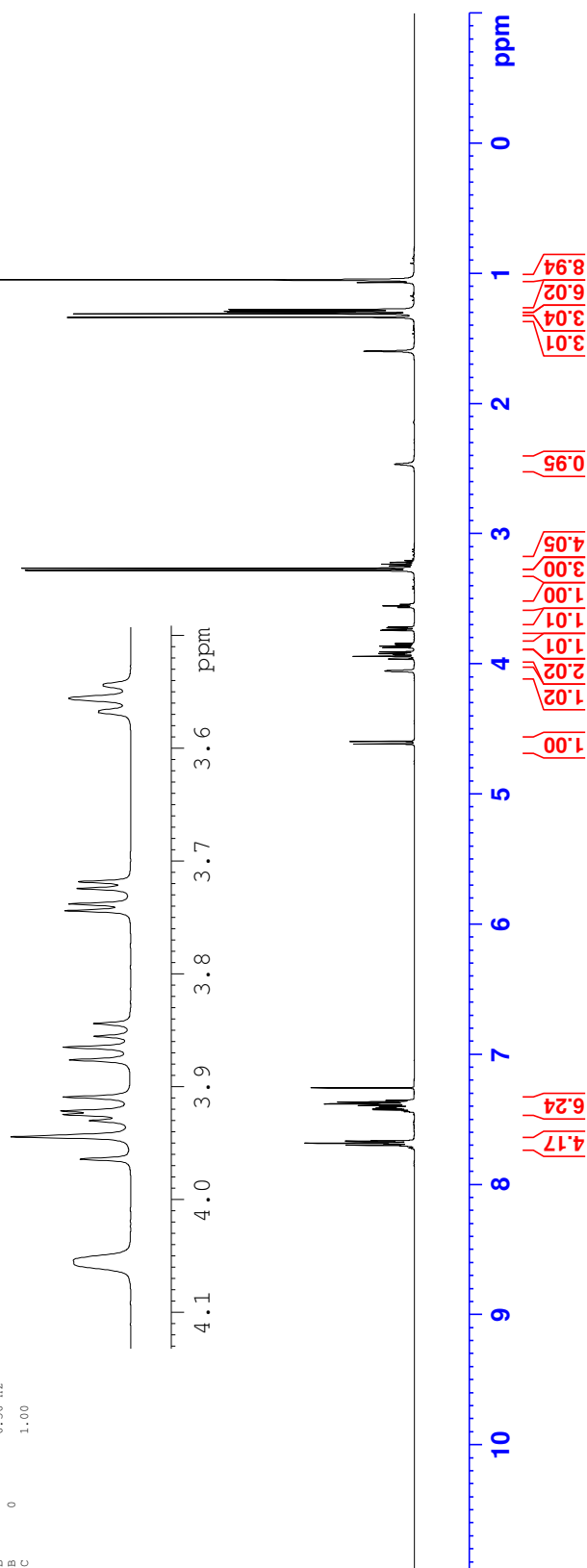
<sup>13</sup>C NMR - Benzyl 4-O-(4-nitrobenzyl)-β-D-galactopyranoside 125



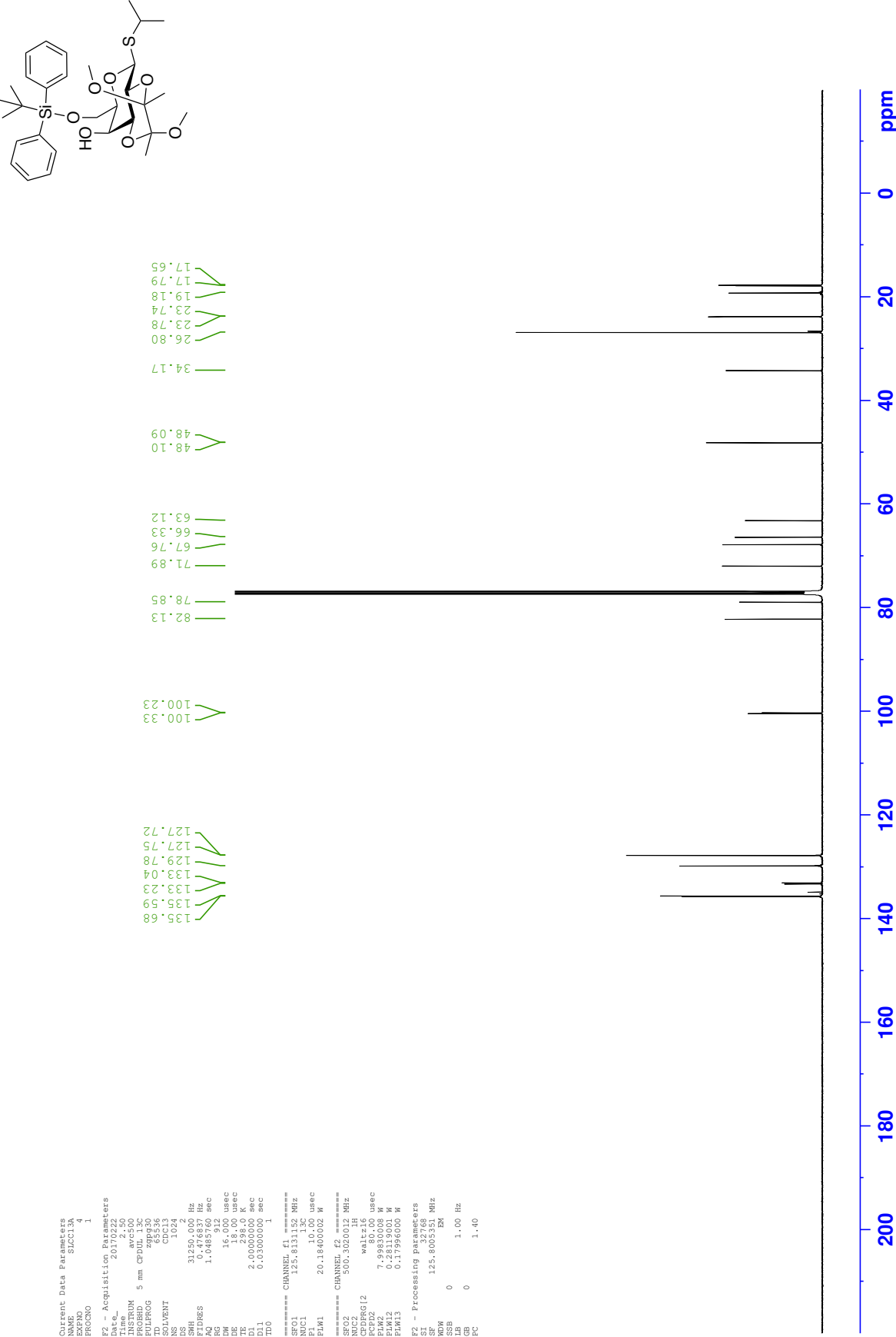
<sup>1</sup>H NMR - Isopropyl 6-O-(*tert*-butyldiphenylsilyl)-2,3-O-(2',3'-dimethoxybutane-2',3'-diyl)-1-thio-β-D-galactopyranoside **230**



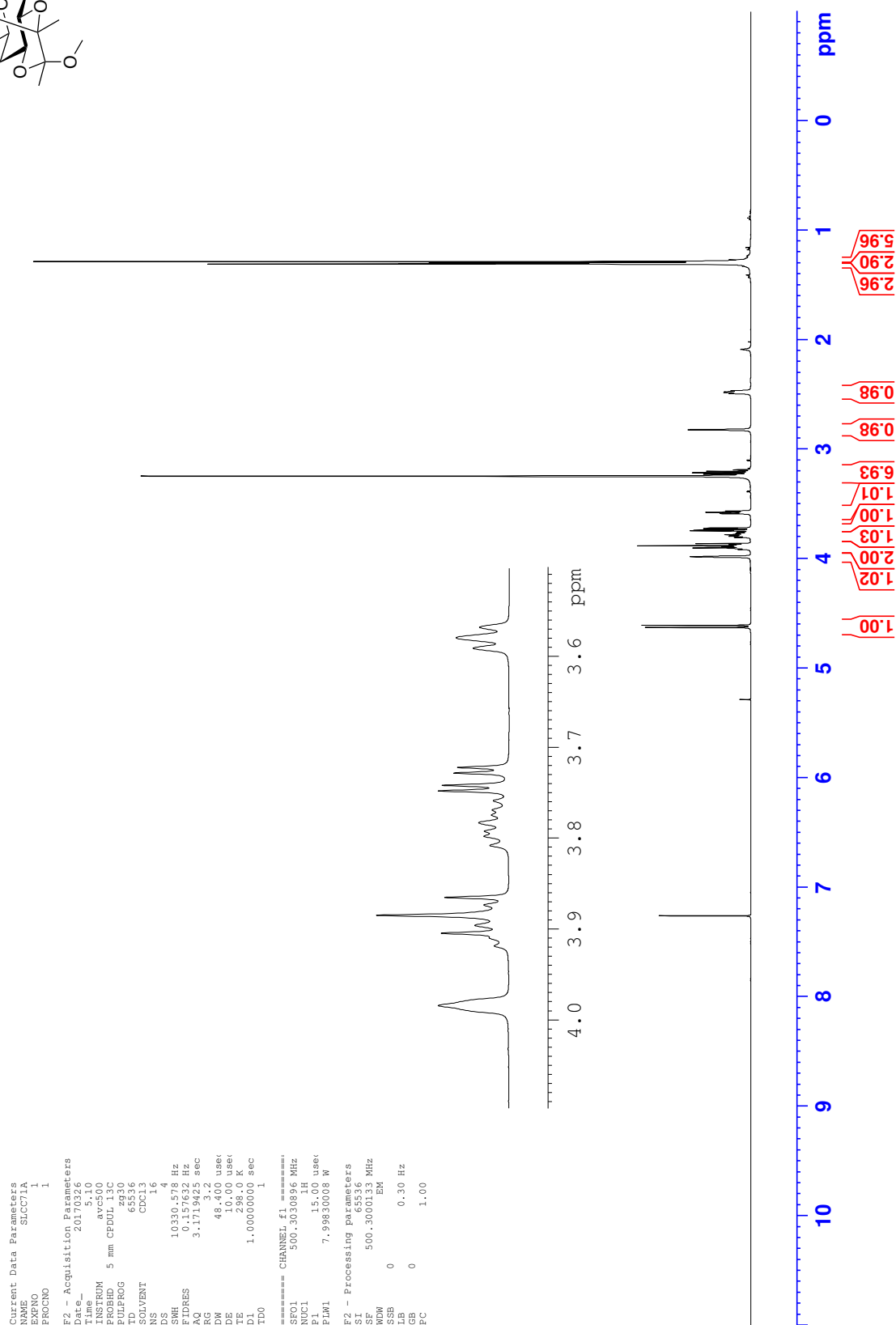
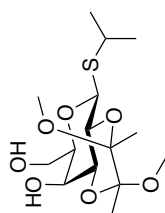
Current Data Parameters  
 NAME 230  
 EXNO 1  
 PROCNO 1  
 F2 - Acquisition Parameters  
 Date\_ 20170222  
 Time\_ 12:05:22  
 INSTRUM spect  
 PROBHD 5 mm CPDOL 13C  
 PULPROG zg30  
 TD 65536  
 SOLVENT CDCl3  
 NS 16  
 DS 4  
 SWH 10330.578 Hz  
 FIDRES 0.157632 Hz  
 AQ 3.1719425 sec  
 RG 3.56  
 DW 49.400 usec  
 DE 0.000 usec  
 TE 298.0 K  
 D1 1.00000000 sec  
 TD0 1  
 ===== CHANNEL f1 =====  
 SFO1 500.3030856 MHz  
 NUC1 13C  
 P1 15.00 usec  
 PLW1 7.99830008 W  
 F2 - Processing parameters  
 SI 32768  
 SF 500.3000130 MHz  
 WDW EM  
 SSB 0  
 LB 0.30 Hz  
 GB 0  
 FC 1.00



<sup>13</sup>C NMR - Isopropyl 6-O-(*tert*-butyldiphenylsilyl)-2,3-O-(2',3'-dimethoxybutane-2',3'-diyl)-1-thio-β-D-galactopyranoside **230**

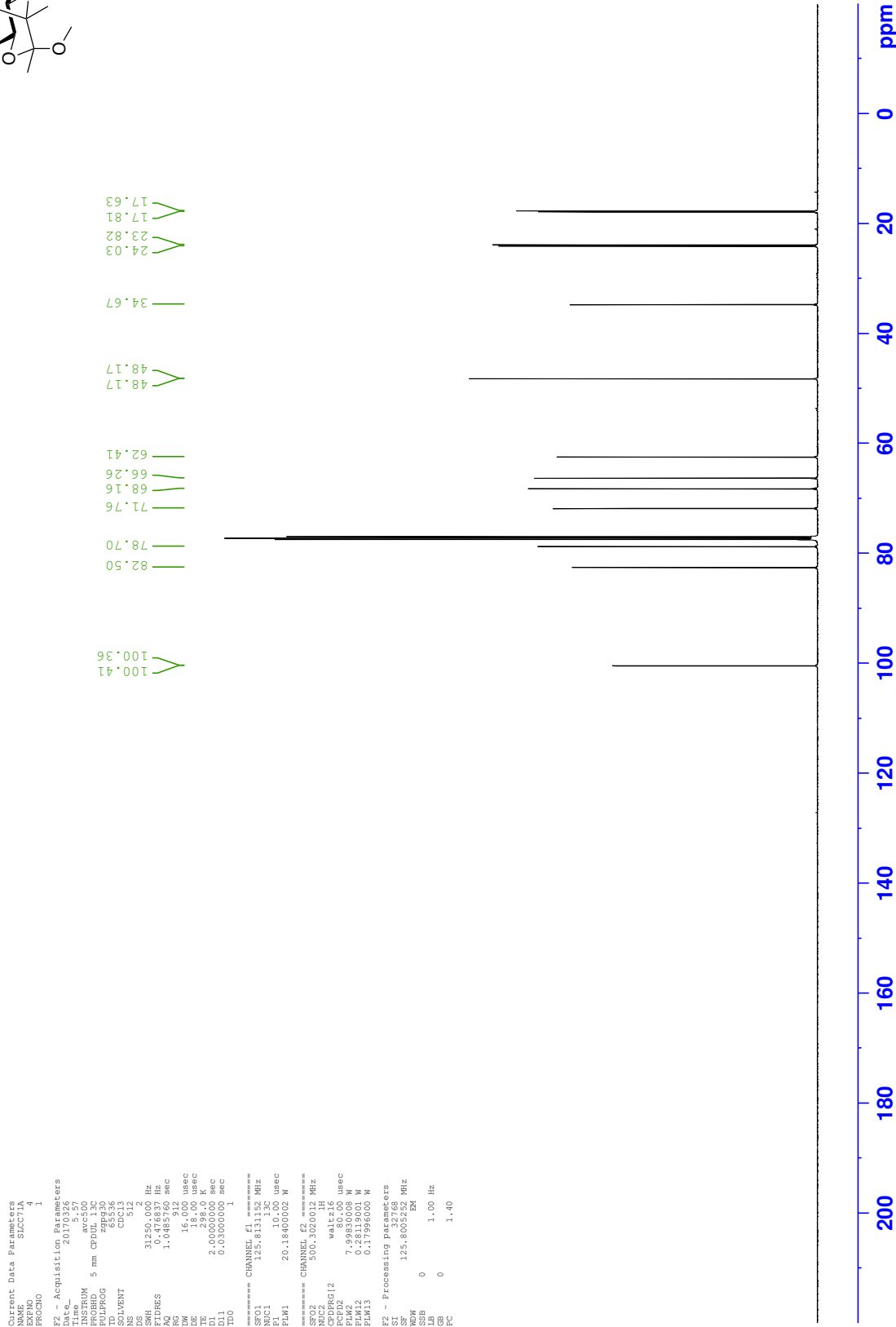
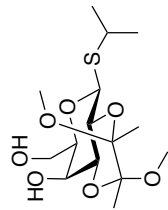


<sup>1</sup>H NMR - Isopropyl 2,3-O-(2',3'-dimethoxybutane-2',3'-diyl)-1-thio-β-D-galactopyranoside **229**

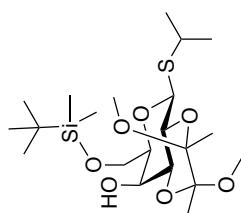




<sup>13</sup>C NMR - Isopropyl 2,3-O-(2',3'-dimethoxybutane-2',3'-diyl)-1-thio-β-D-galactopyranoside **229**



<sup>1</sup>H NMR - Isopropyl 6-O-(*tert*-butyldimethylsilyl)-2,3-O-(2',3'-dimethoxybutane-2',3'-diyl)-1-thio-β-D-galactopyranoside **232**

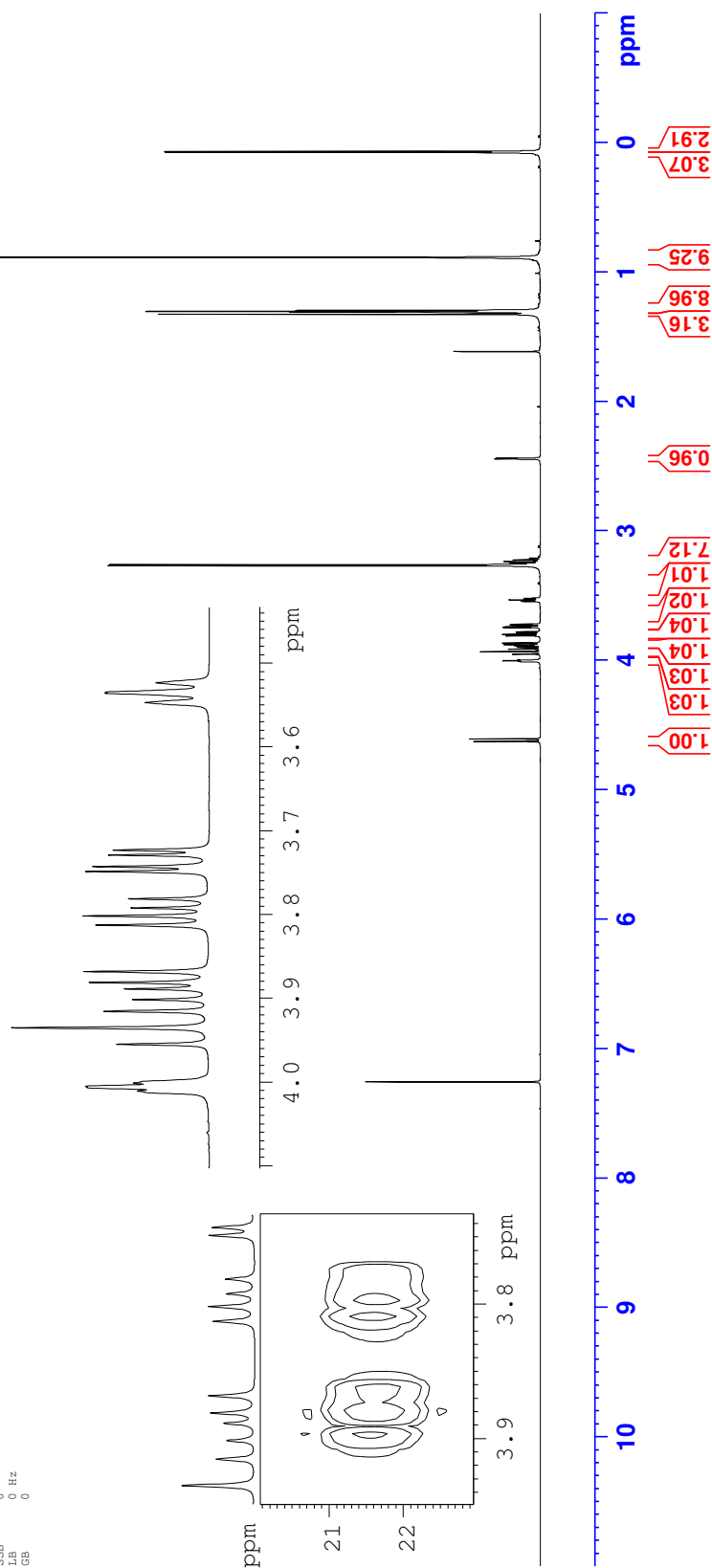


Current Data Parameters  
NAME SUCC73A.SI  
EXNO 2  
PROCNO 1

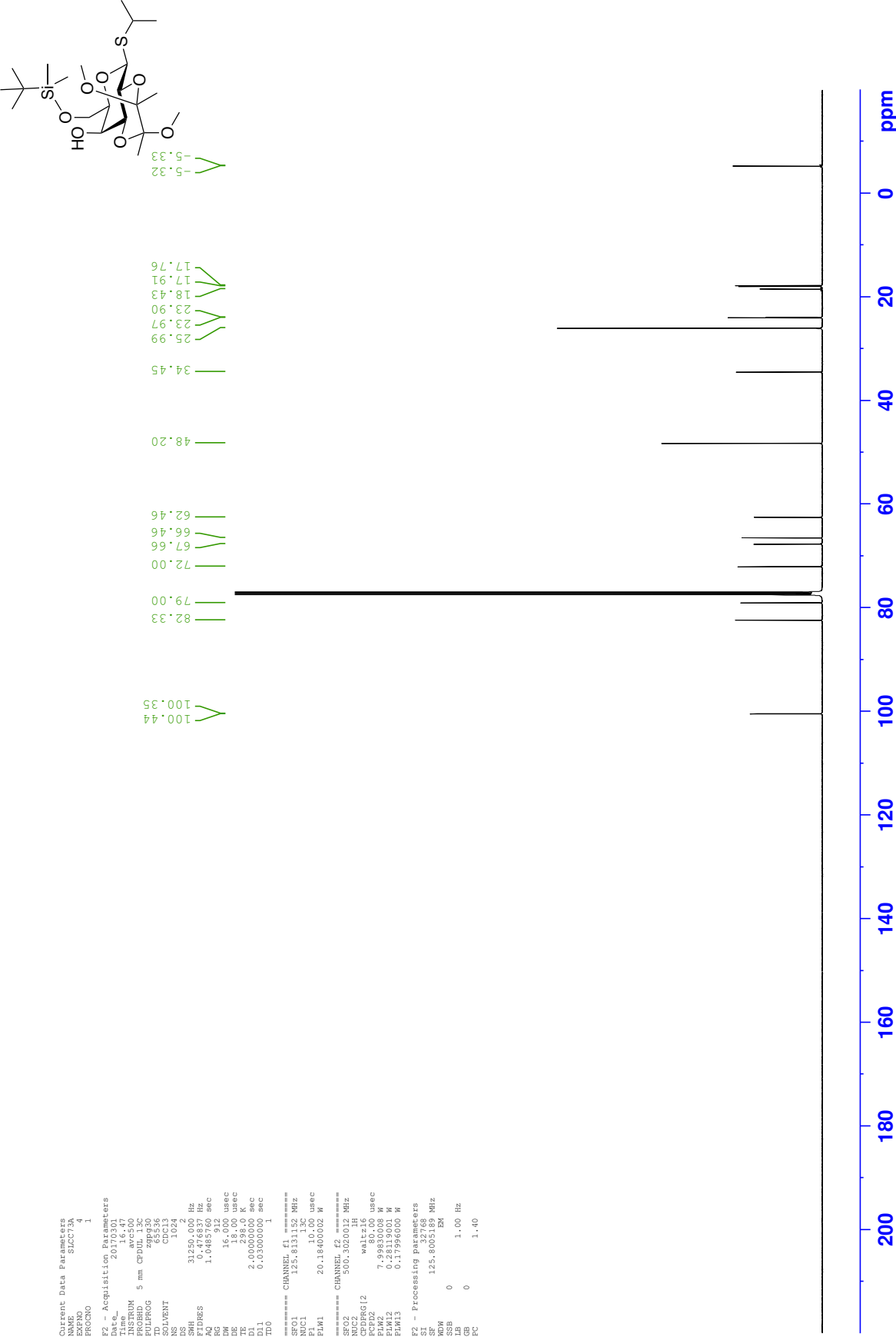
F1 - Acquisition Parameters  
TD 128  
SFO 99.361762 MHz  
AQ 0.180000  
FIDRES 77.659042 Hz  
SW 100.042 PPM  
F1MODE QF

F2 - Processing Parameters  
SI 2048  
SF 500.130012 MHz  
WDW 4  
SSB 0 Hz  
LB 0  
GB 0  
FC 1.40

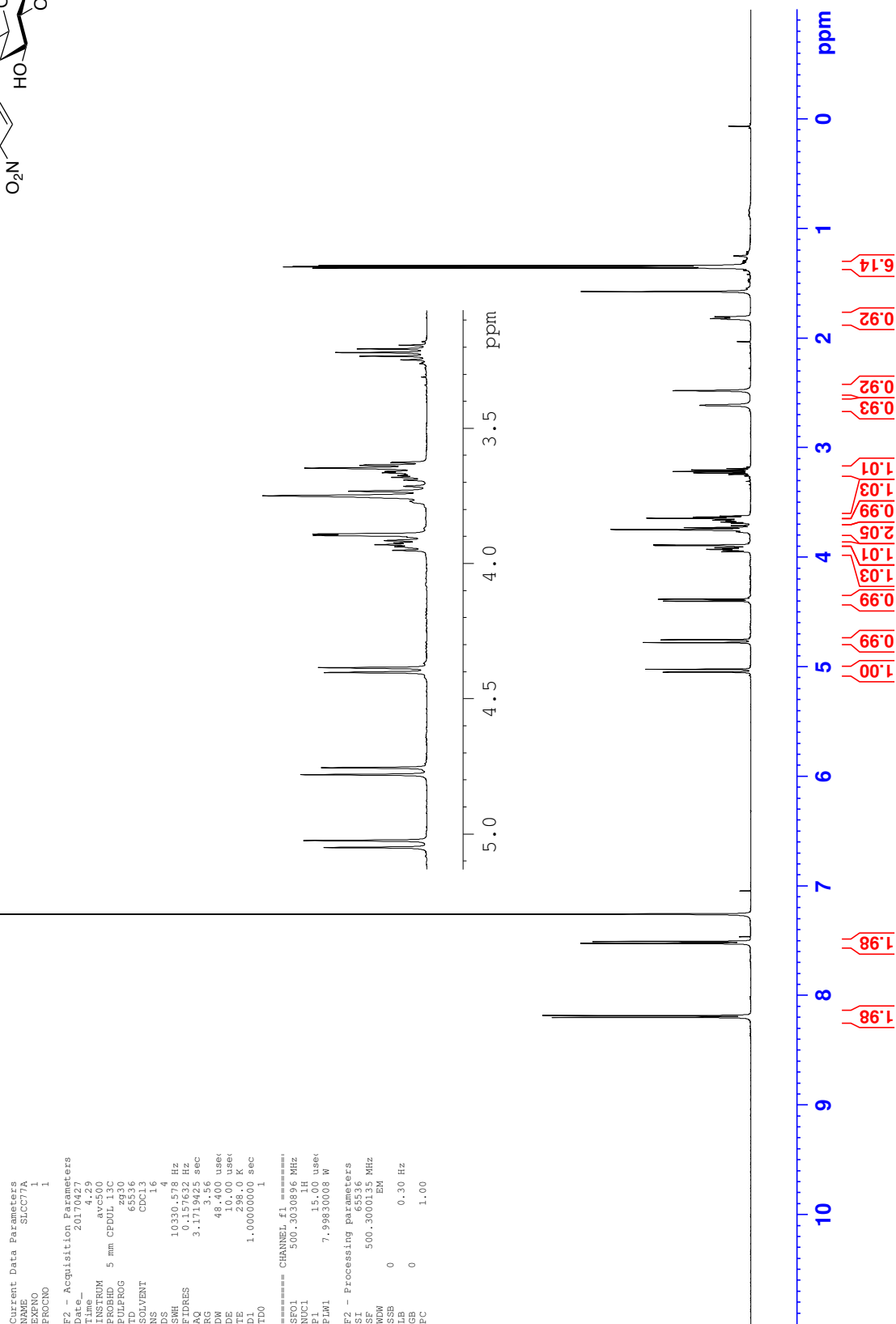
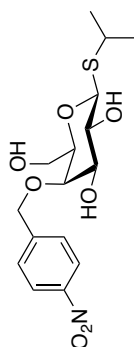
F1 - Processing Parameters  
SI 1024  
MC2 QF  
SF 99.3617620 MHz  
WDW 0  
SSB 0 Hz  
LB 0  
GB 0



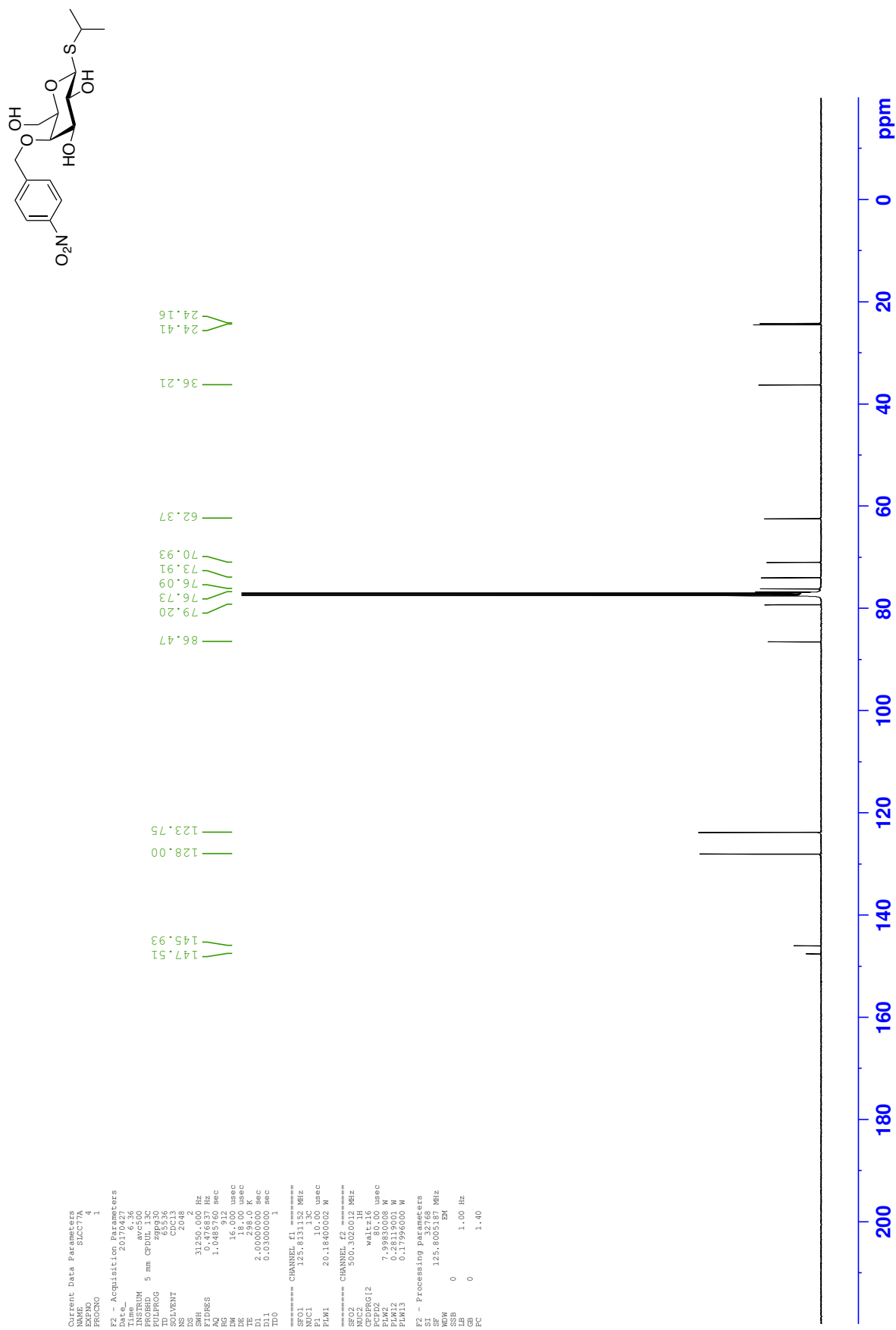
<sup>13</sup>C NMR - Isopropyl 6-*O*-(*tert*-butyldimethylsilyl)-2,3-*O*-(2',3'-dimethoxybutane-2',3'-diyl)-1-thio-β-D-galactopyranoside **232**



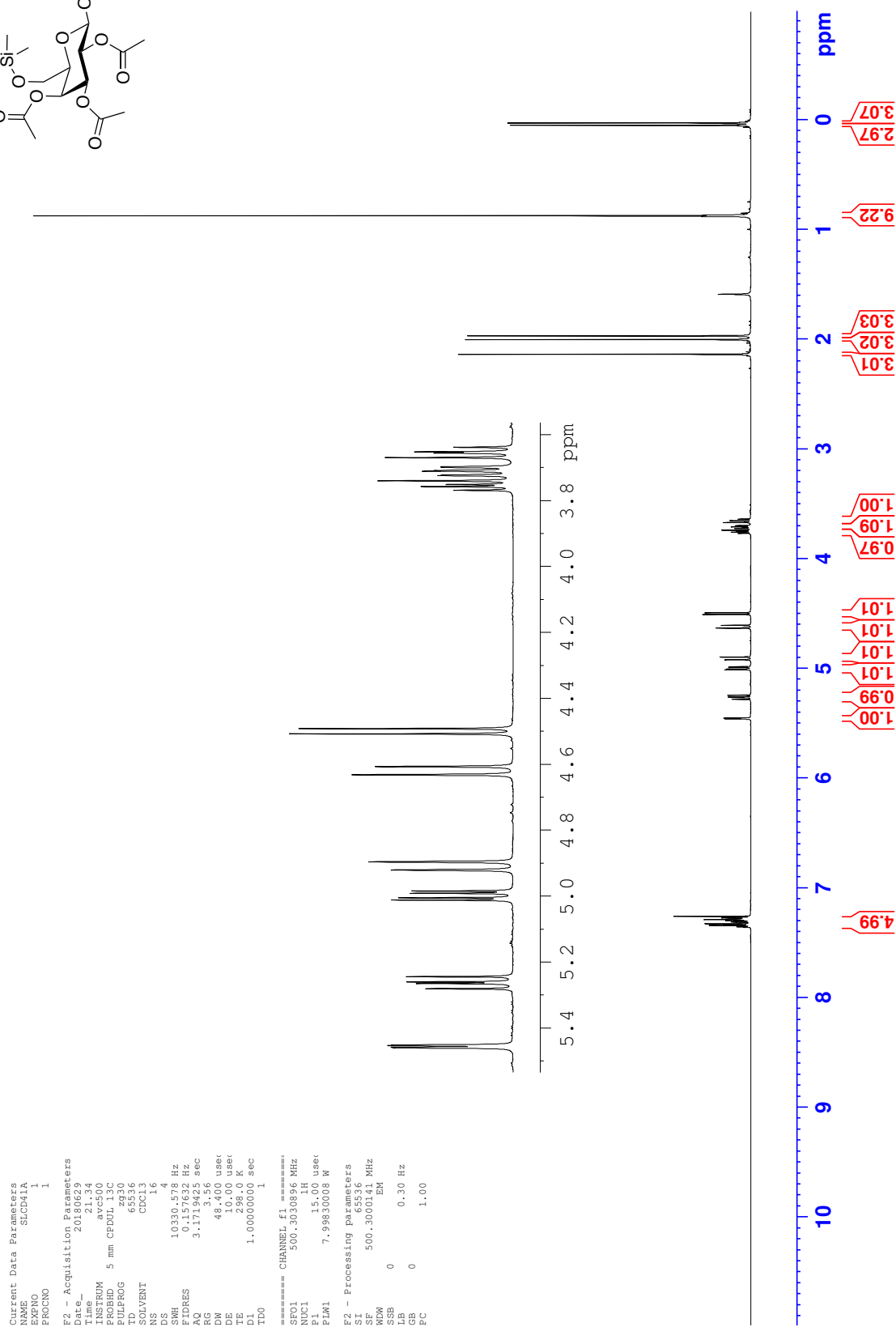
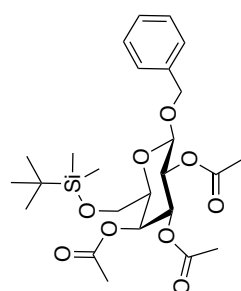
<sup>1</sup>H NMR - Isopropyl 6-O-(4-nitrobenzyl)-1-thio-β-D-galactopyranoside **88**



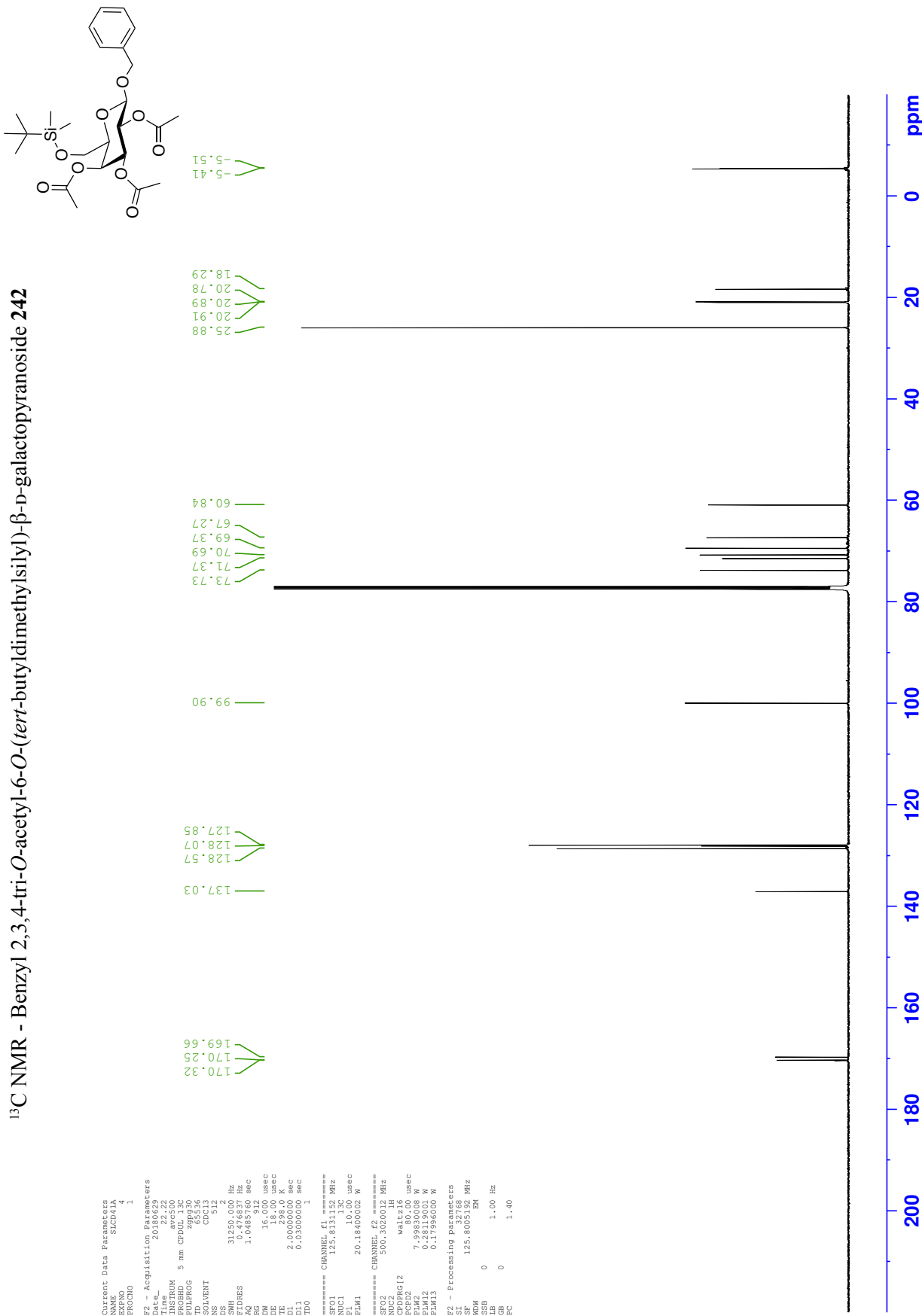
<sup>13</sup>C NMR - Isopropyl 6-*O*-(4-nitrobenzyl)-1-thio-β-D-galactopyranoside **88**



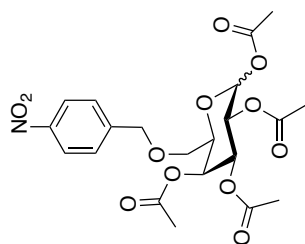
<sup>1</sup>H NMR - Benzyl 2,3,4-tri-*O*-acetyl-6-*O*-(*tert*-butyldimethylsilyl)-β-D-galactopyranoside **242**



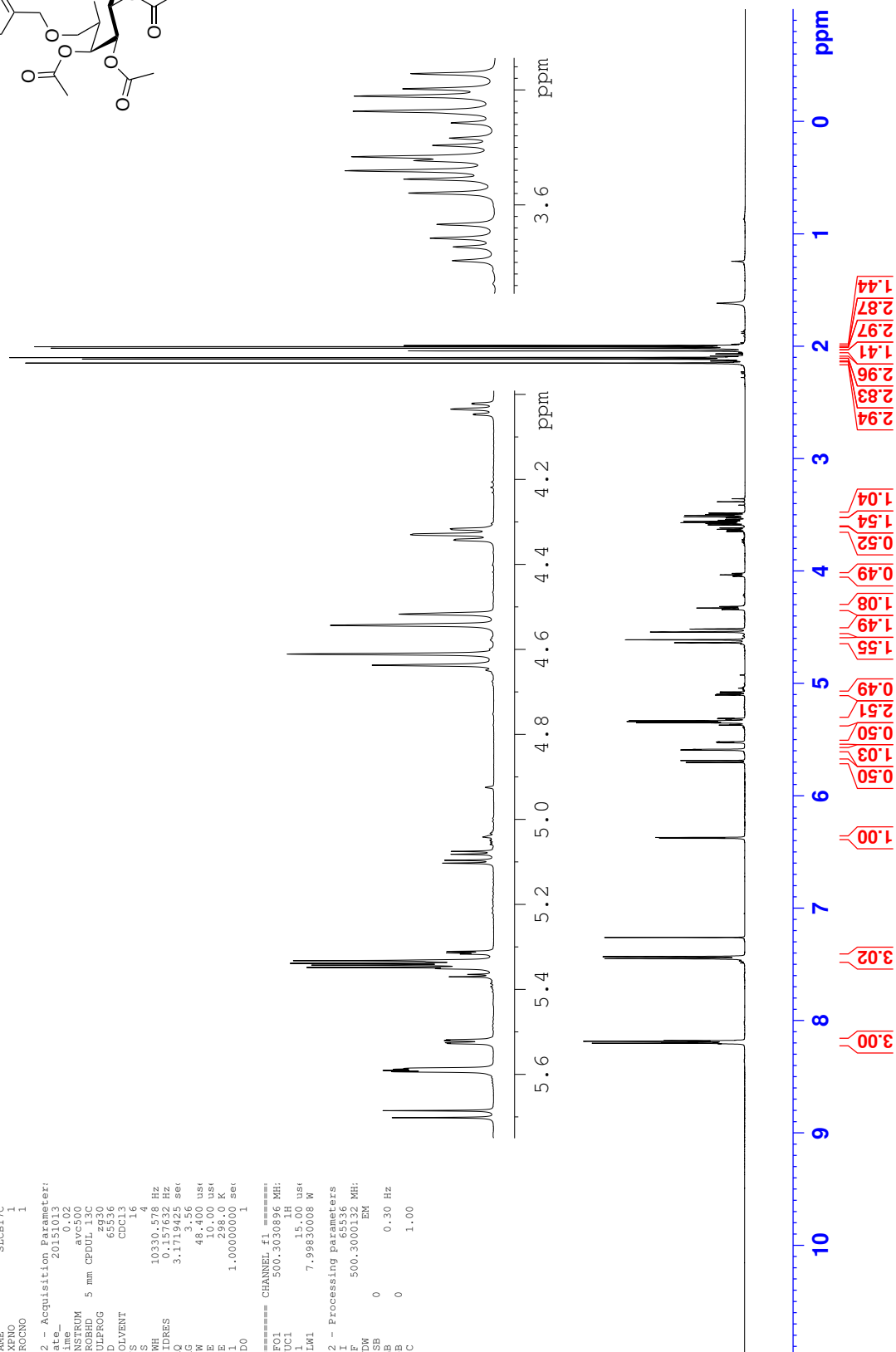
<sup>13</sup>C NMR - Benzyl 2,3,4-tri-O-acetyl-6-O-(*tert*-butyldimethylsilyl)-β-D-galactopyranoside **242**



<sup>1</sup>H NMR - 1,2,3,4-Tetra-*O*-acetyl-6-*O*-(4-nitrobenzyl)- $\alpha$ , $\beta$ -D-galactopyranoside **245**

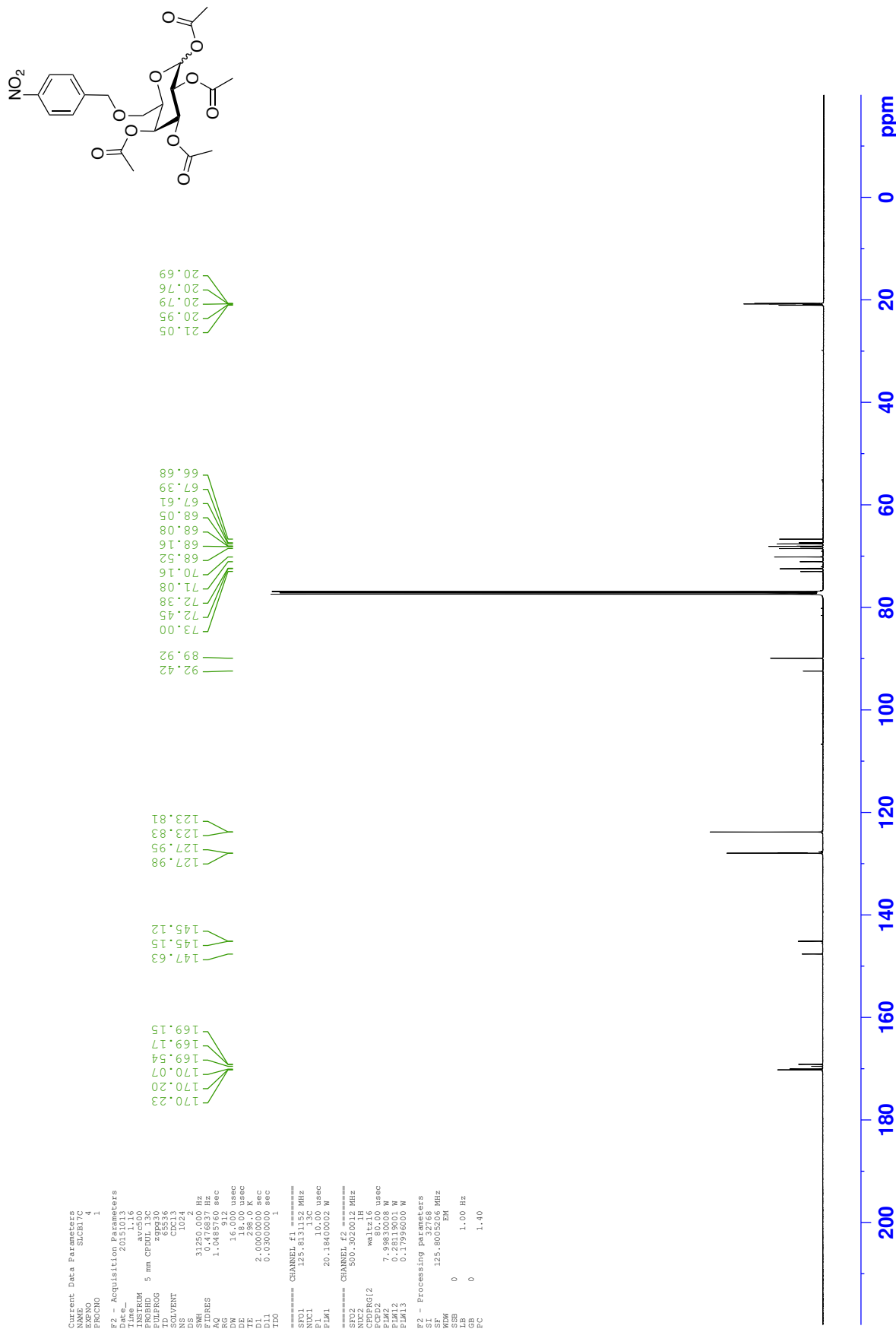


Current Data Parameters  
NAME SUCB11C  
EXPNO 1  
PROCNO 1  
F2 - Acquisition Parameters:  
Date\_ 20151013  
Time 05:02  
INSTRUM avo  
PROBHD 5 mm CPDUL 13C  
PULPROG zgpg30  
TD 65536  
SOLVENT CDCl3  
NS 16  
DS 4  
SWH 10330.578 Hz  
FIDRES 0.157632 Hz  
AQ 3.1719425 sec  
RG 3.56  
DW 48.400 usec  
DE 15.00 usec  
TE 298.0 K  
D1 1.00000000 sec  
TD0 1  
===== CHANNEL f1 =====  
NUC1 13C  
P1 15.00 usec  
PLW1 7.99830008 W  
F2 - Processing parameters  
SI 32768  
SF 500.3000132 MHz  
WDW 0  
SSB 0  
LB 0.30 Hz  
GB 0  
PC 1.00

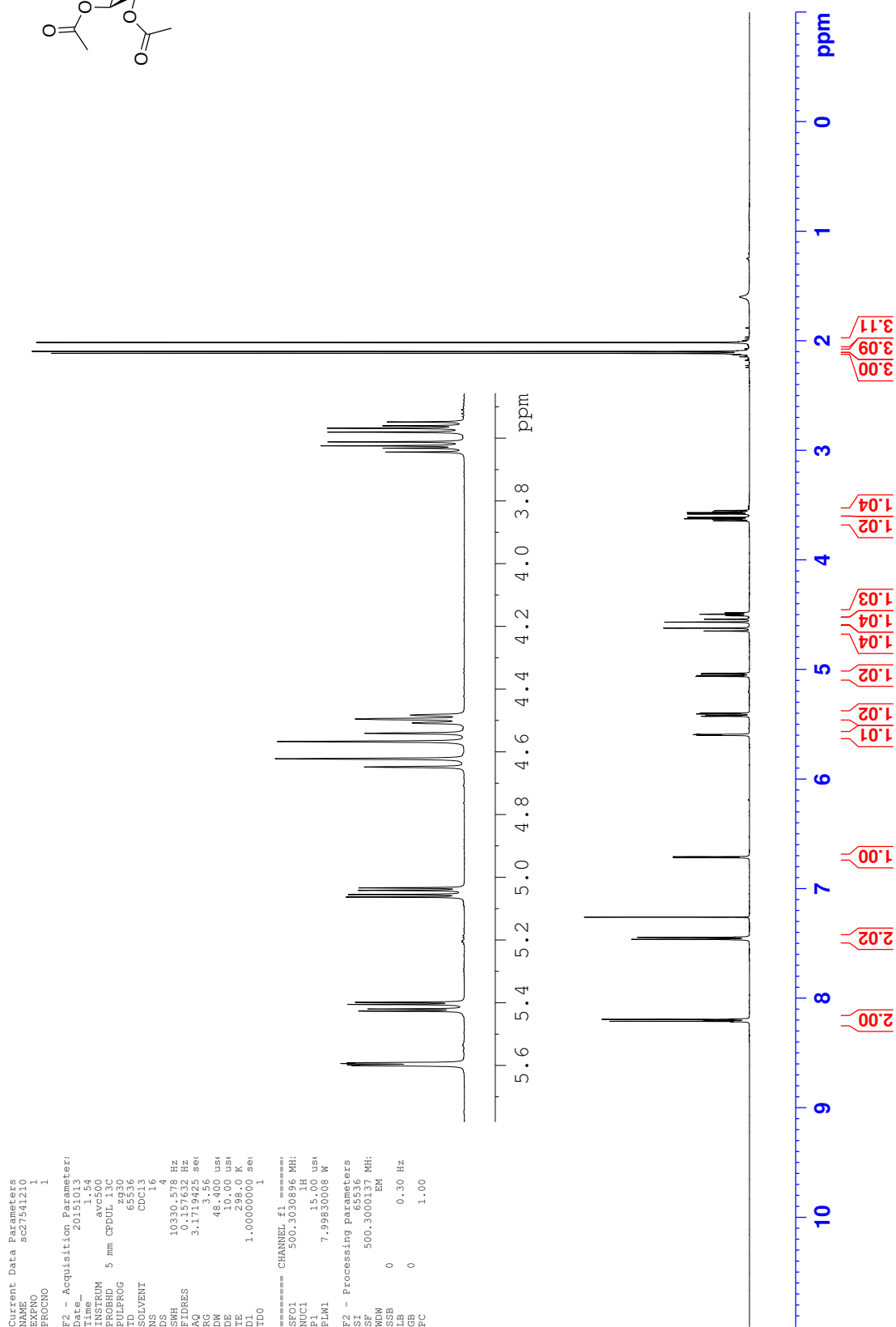
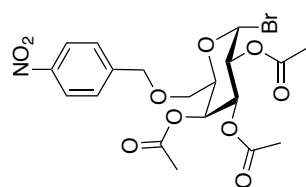




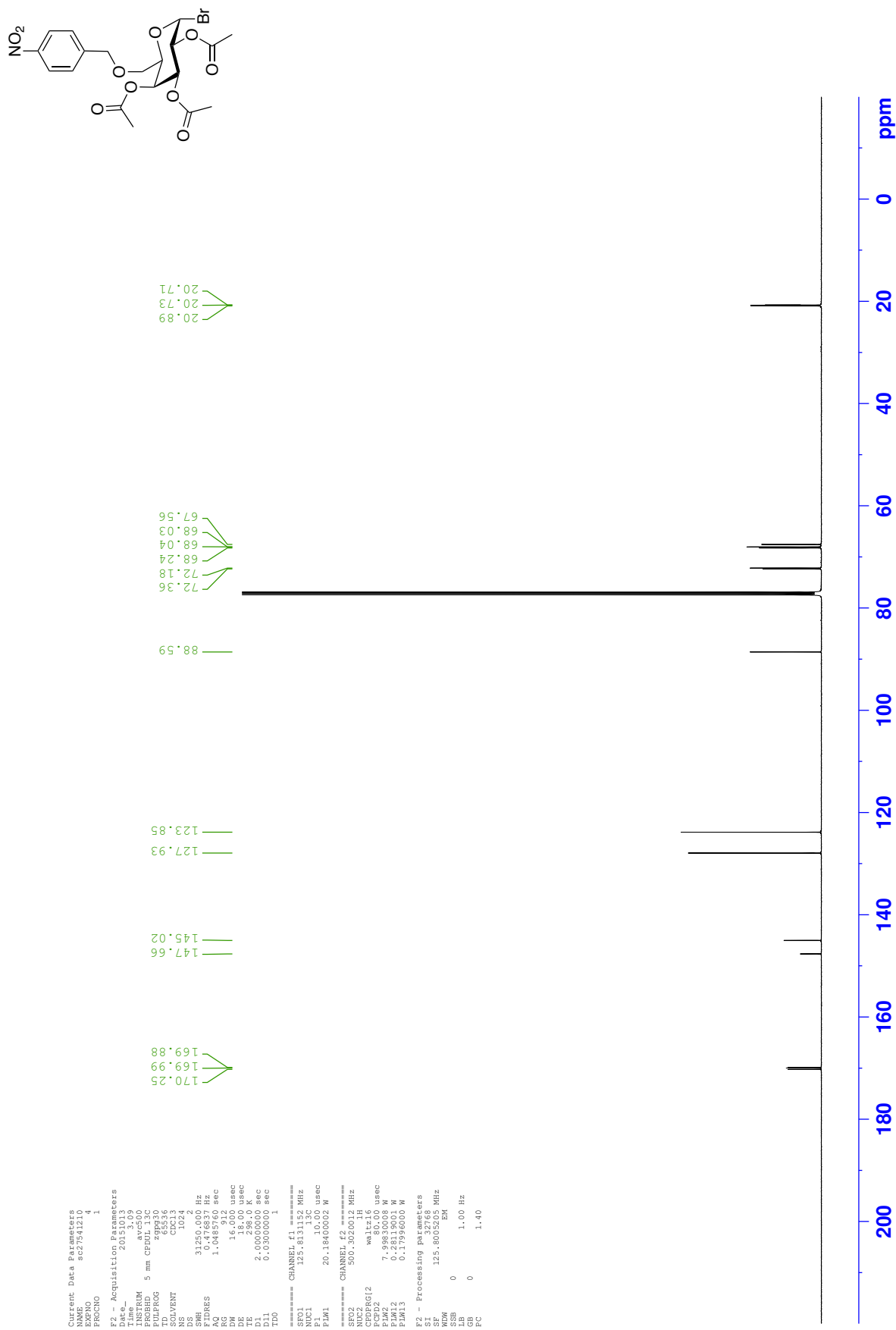
<sup>13</sup>C NMR - 1,2,3,4-Tetra-O-acetyl-6-O-(4-nitrobenzyl)-α,β-D-galactopyranoside **245**



<sup>1</sup>H NMR - 2,3,4-Tri-*O*-acetyl-6-*O*-(4-nitrobenzyl)-α-D-galactopyranosyl bromide **246**

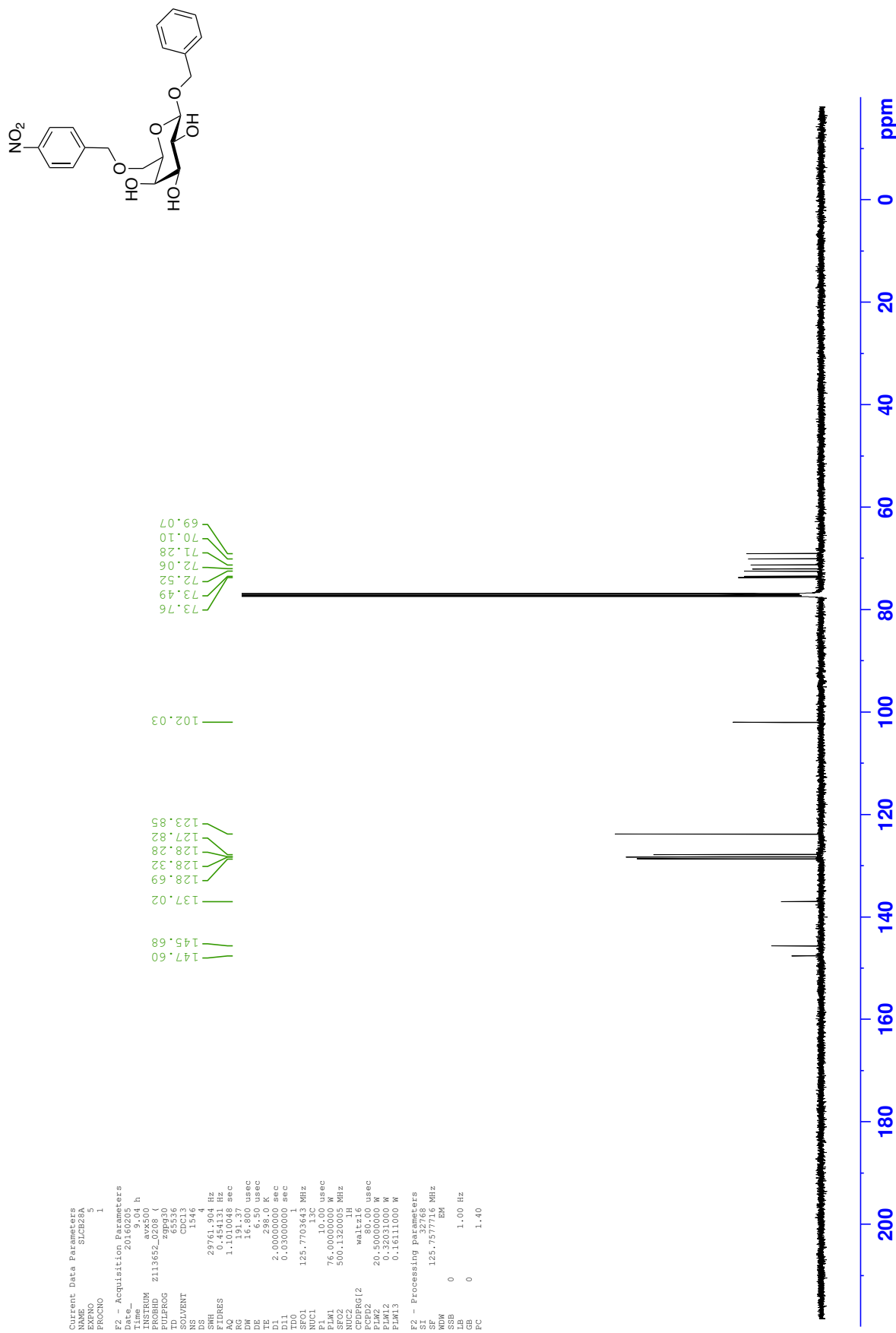


<sup>13</sup>C NMR - 2,3,4-Tri-*O*-acetyl-6-*O*-(4-nitrobenzyl)- $\alpha$ -D-galactopyranosyl bromide **246**

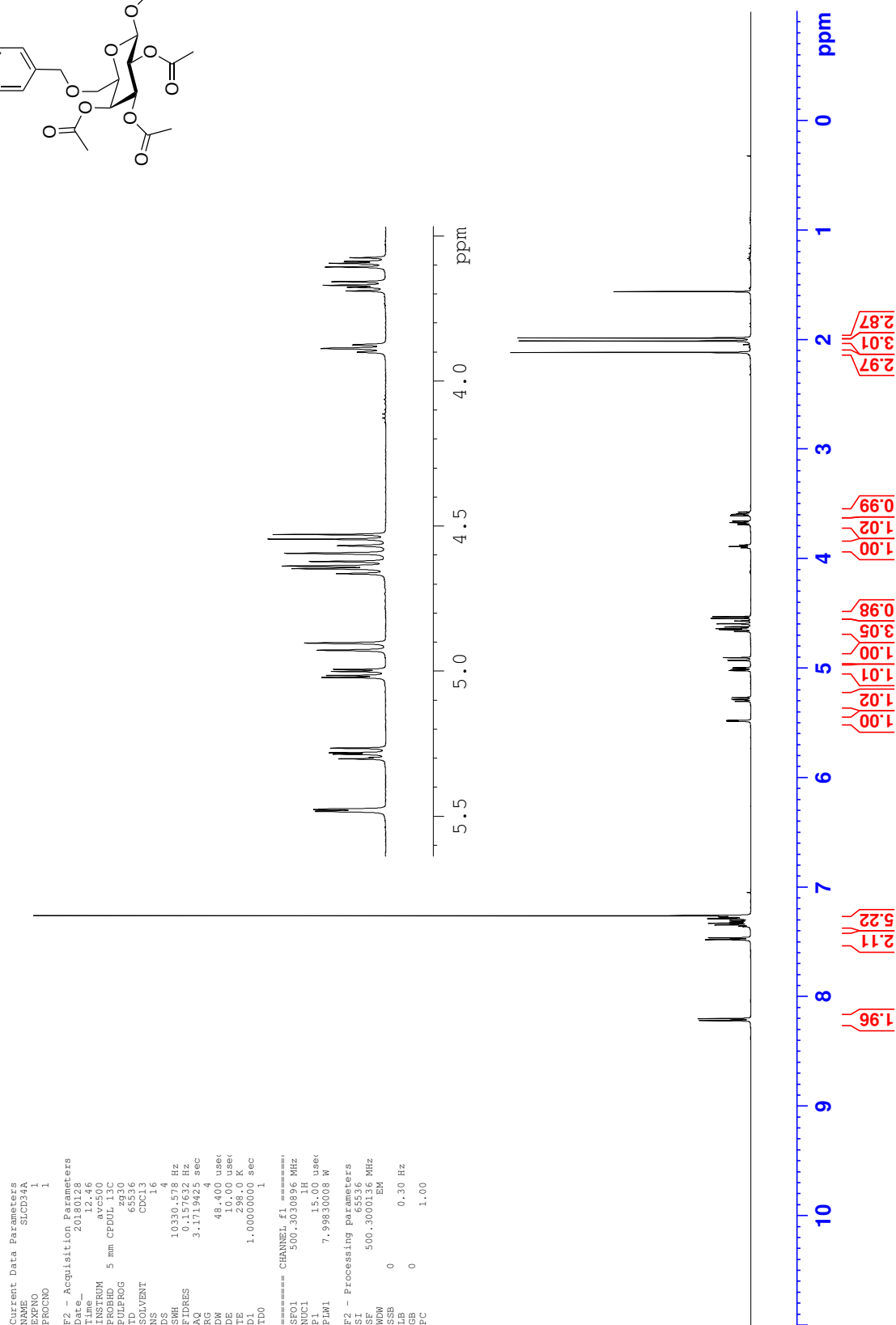
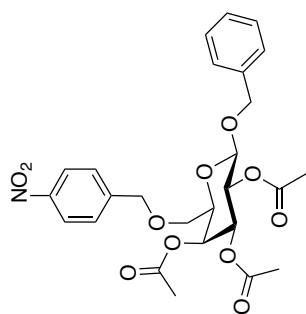




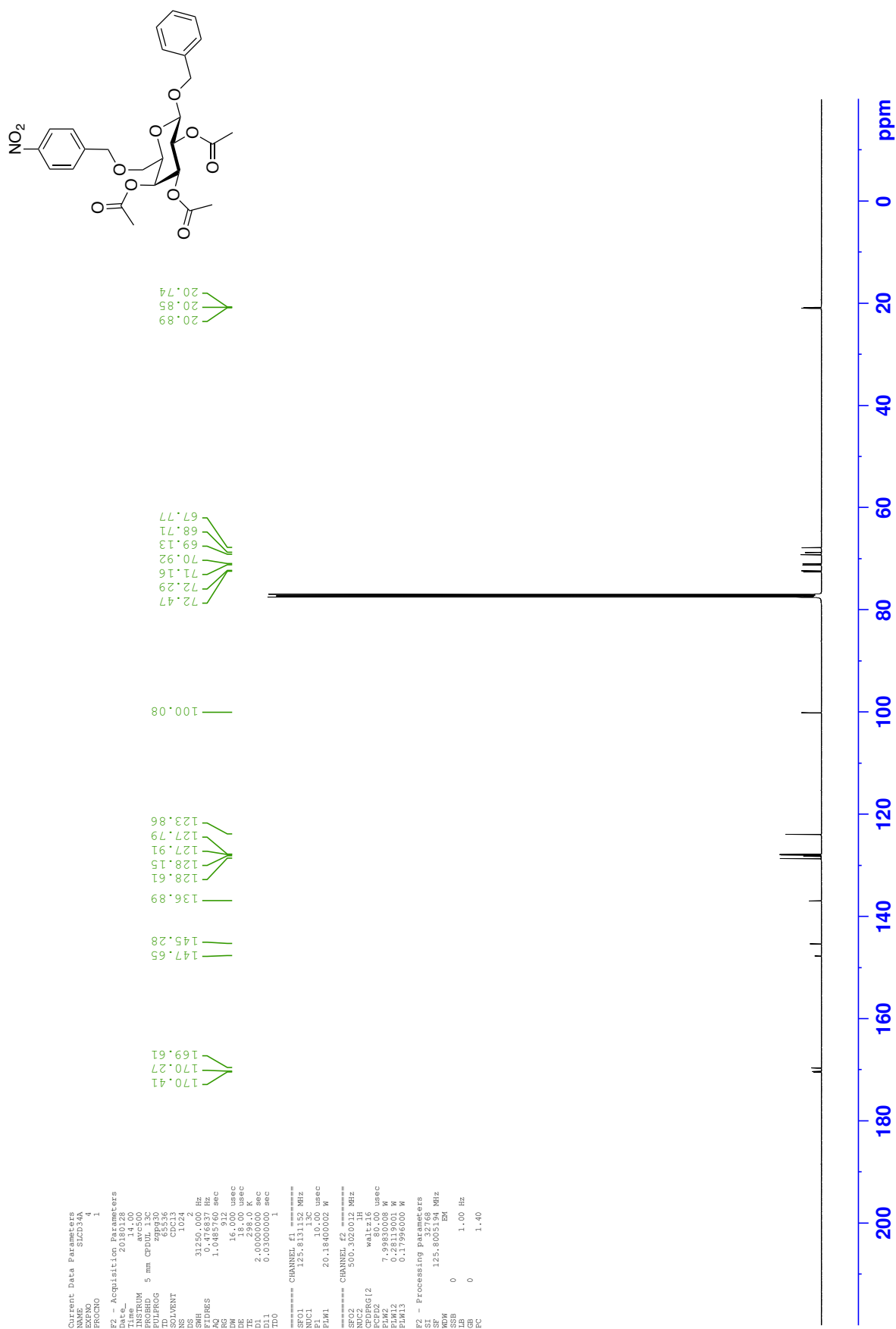
<sup>13</sup>C NMR - Benzyl 6-O-(4-nitrobenzyl)-β-D-galactopyranoside **126**



<sup>1</sup>H NMR - Benzyl 2,3,4-tri-O-acetyl-6-O-(4-nitrobenzyl)-β-D-galactopyranoside 247

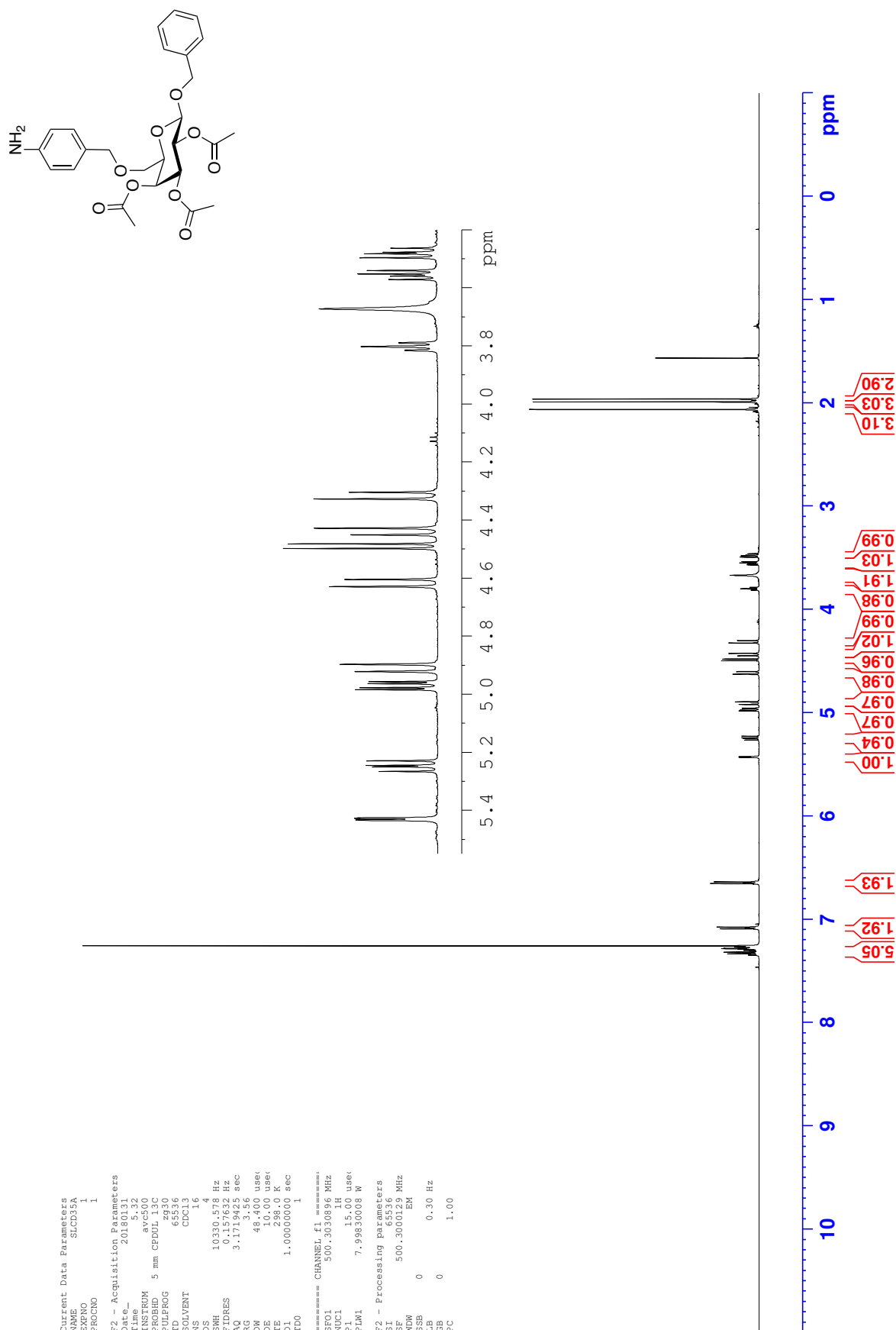


<sup>13</sup>C NMR - Benzyl 2,3,4-tri-*O*-acetyl-6-*O*-(4-nitrobenzyl)-β-D-galactopyranoside 247



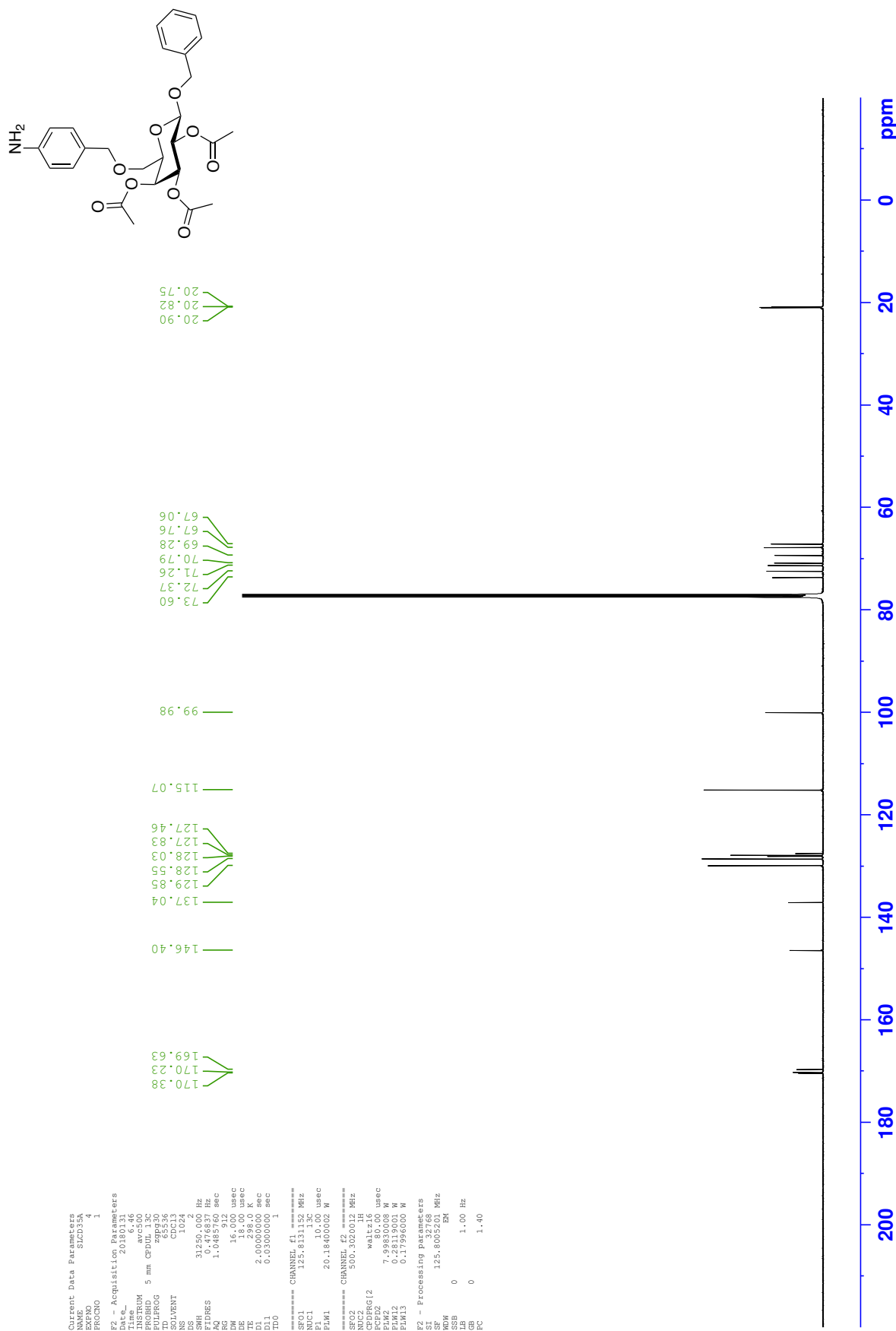
<sup>1</sup>H NMR - Benzyl 2,3,4-tri-*O*-acetyl-6-*O*-(4-aminobenzyl)-β-D-galactopyranoside **306**

Current Data Parameters  
 NAME: 306  
 EXNO: 1  
 PROCNO: 1  
 F2 - Acquisition Parameters  
 Date\_: 20180131  
 Time: 12.00  
 INSTRUM: av500  
 PROBHD: 5 mm CPDOL 13C  
 PULPROG: zg30  
 TD: 65536  
 SOLVENT: CDCl3  
 NS: 14  
 DS: 4  
 SWH: 10330.578 Hz  
 FIDRES: 0.157632 Hz  
 AQ: 3.1719425 sec  
 RG: 3.56  
 DW: 48.400 usec  
 DE: 0.000 usec  
 TE: 298.0 K  
 D1: 1.00000000 sec  
 TD0: 1  
 ===== CHANNEL f1 =====  
 SFO1: 500.3030856 MHz  
 NUC1: <sup>1</sup>H  
 P1: 15.00 usec  
 PLW1: 7.99830008 W  
 F2 - Processing parameters  
 SF: 500.300129 MHz  
 WDW: EM  
 SSB: 0  
 LB: 0.30 Hz  
 GB: 0  
 FC: 1.00

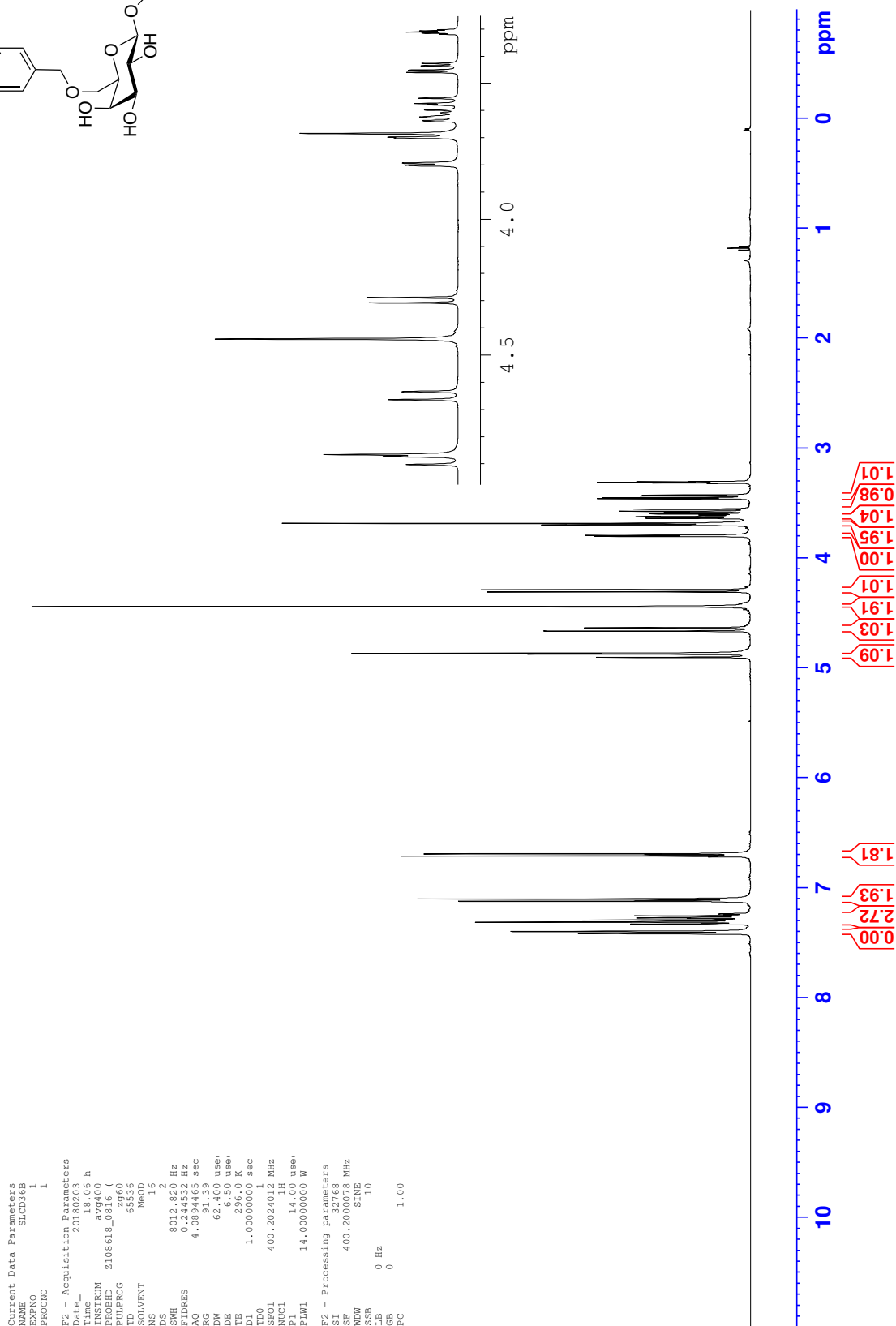
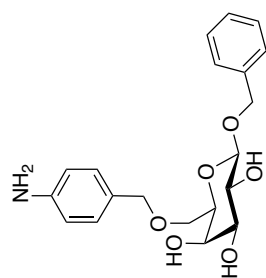




<sup>13</sup>C NMR - Benzyl 2,3,4,-tri-O-acetyl-6-O-(4-aminobenzyl)-β-D-galactopyranoside **306**

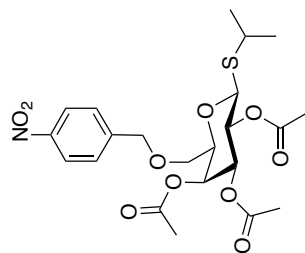


<sup>1</sup>H NMR - Benzyl 6-O-(4-aminobenzyl)-β-D-galactopyranoside **304**

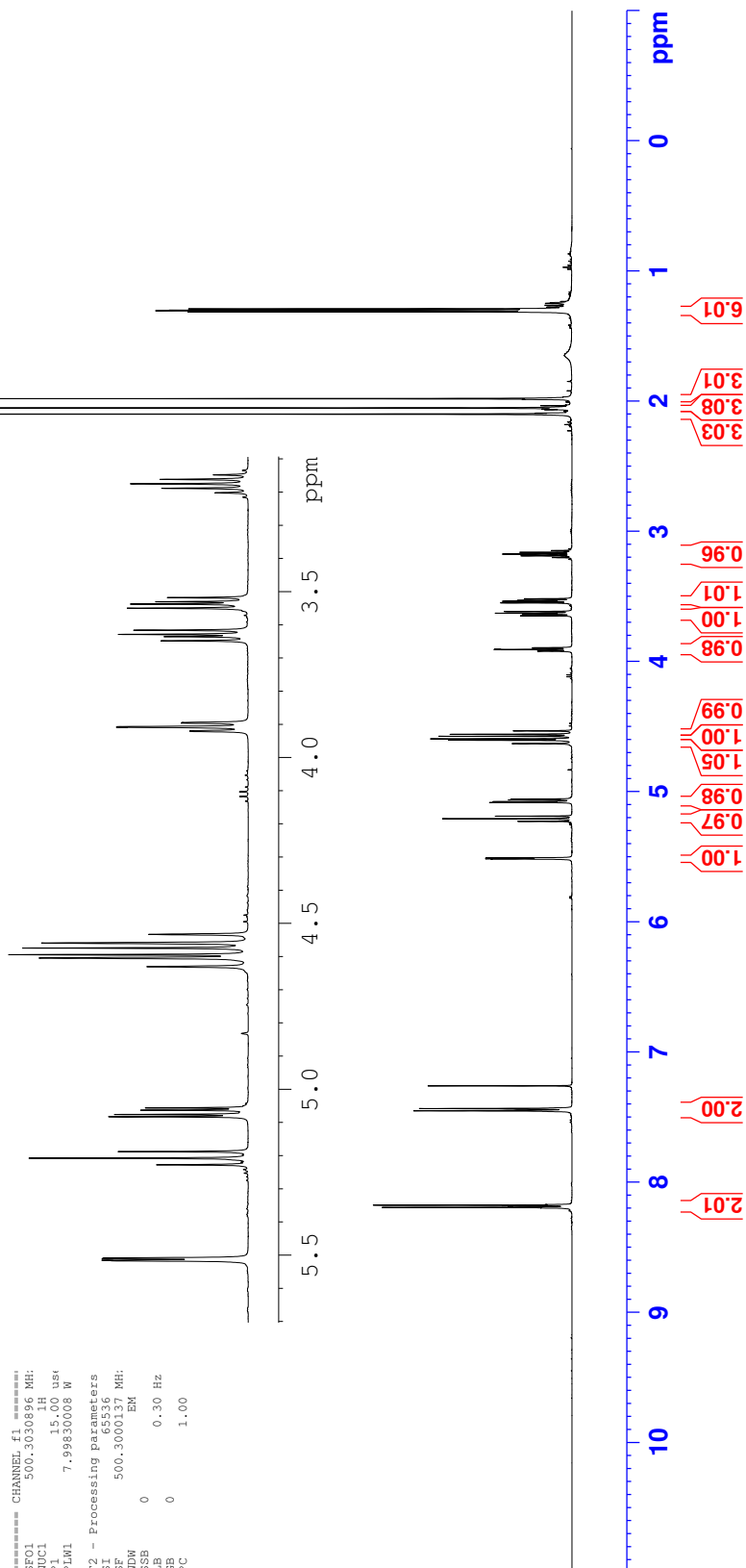




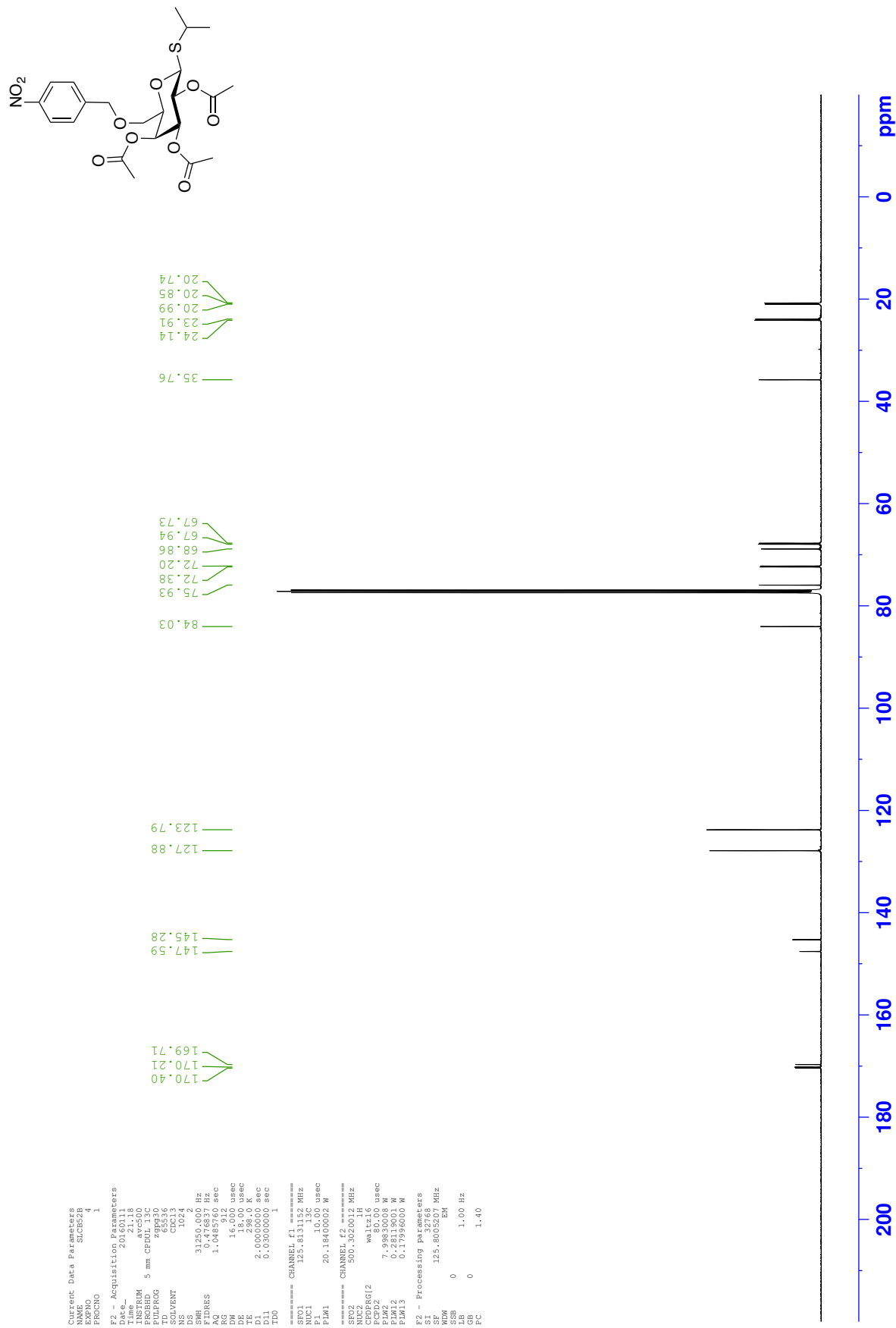
<sup>1</sup>H NMR - Isopropyl 2,3,4-tri-*O*-acetyl-6-*O*-(4-nitrobenzyl)-1-thio-β-D-galactopyranoside **248**



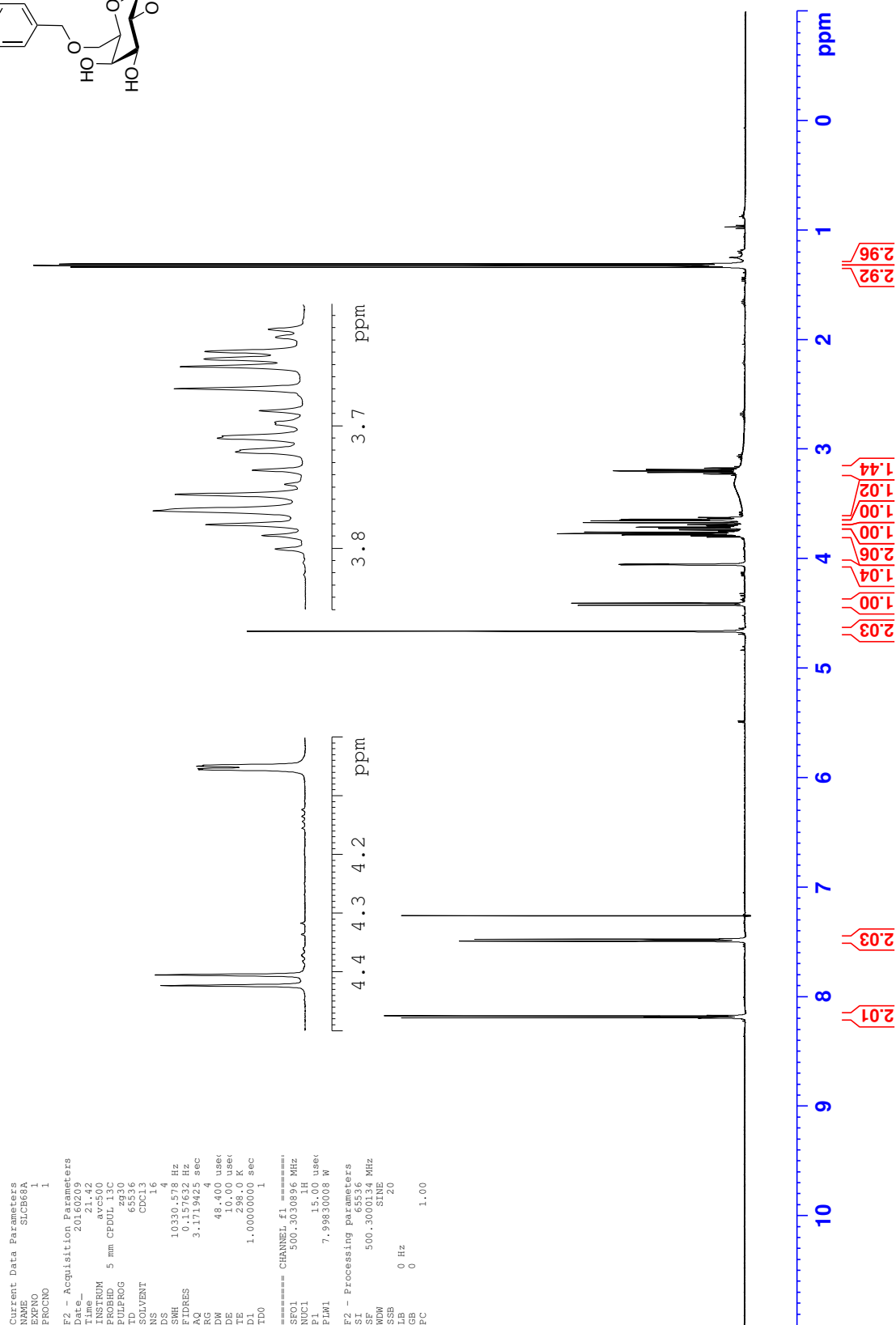
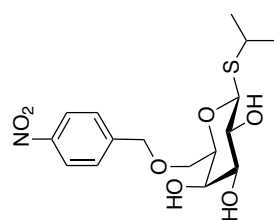
Current Data Parameters  
NAME SUC535B  
EXPNO 1  
PROCNO 1  
F2 - Acquisition Parameters:  
Date\_ 20160112  
Time 12:54  
INSTRUM spect  
PROBHD 5 mm CPDUI 13C  
PULPROG zgpg30  
TD 65536  
SOLVENT CDCl3  
NS 16  
DS 4  
SWH 10330.578 Hz  
FIDRES 0.157632 Hz  
AQ 3.1719425 sec  
RG 3.56  
DW 48.400 usec  
DE 15.00 usec  
TE 298.0 K  
D1 1.00000000 sec  
TD0 1  
===== CHANNEL f1 =====  
NUC1 13C  
P1 15.00 usec  
PLW1 7.99830008 W  
F2 - Processing parameters  
SI 32768  
SF 500.1300337 MHz  
WDW 0  
SSB 0  
LB 0.30 Hz  
GB 0  
PC 1.00



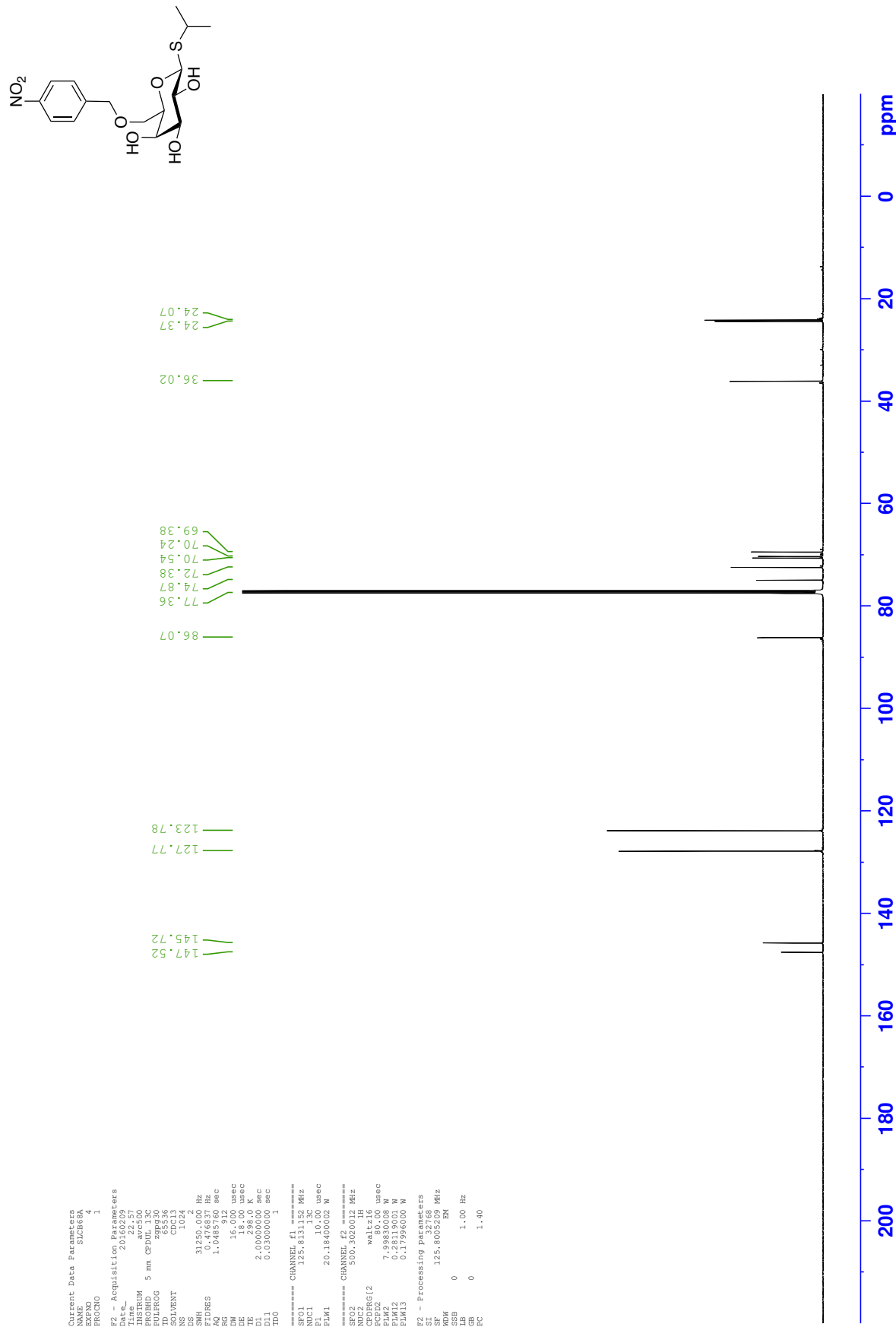
<sup>13</sup>C NMR - Isopropyl 2,3,4-tri-*O*-acetyl-6-*O*-(4-nitrobenzyl)-1-thio-β-D-galactopyranoside **248**



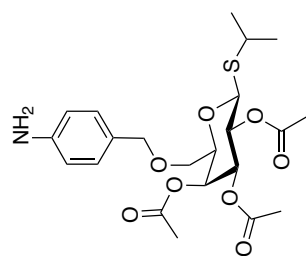
<sup>1</sup>H NMR - Isopropyl 6-O-(4-nitrobenzyl)-1-thio-β-D-galactopyranoside **89**



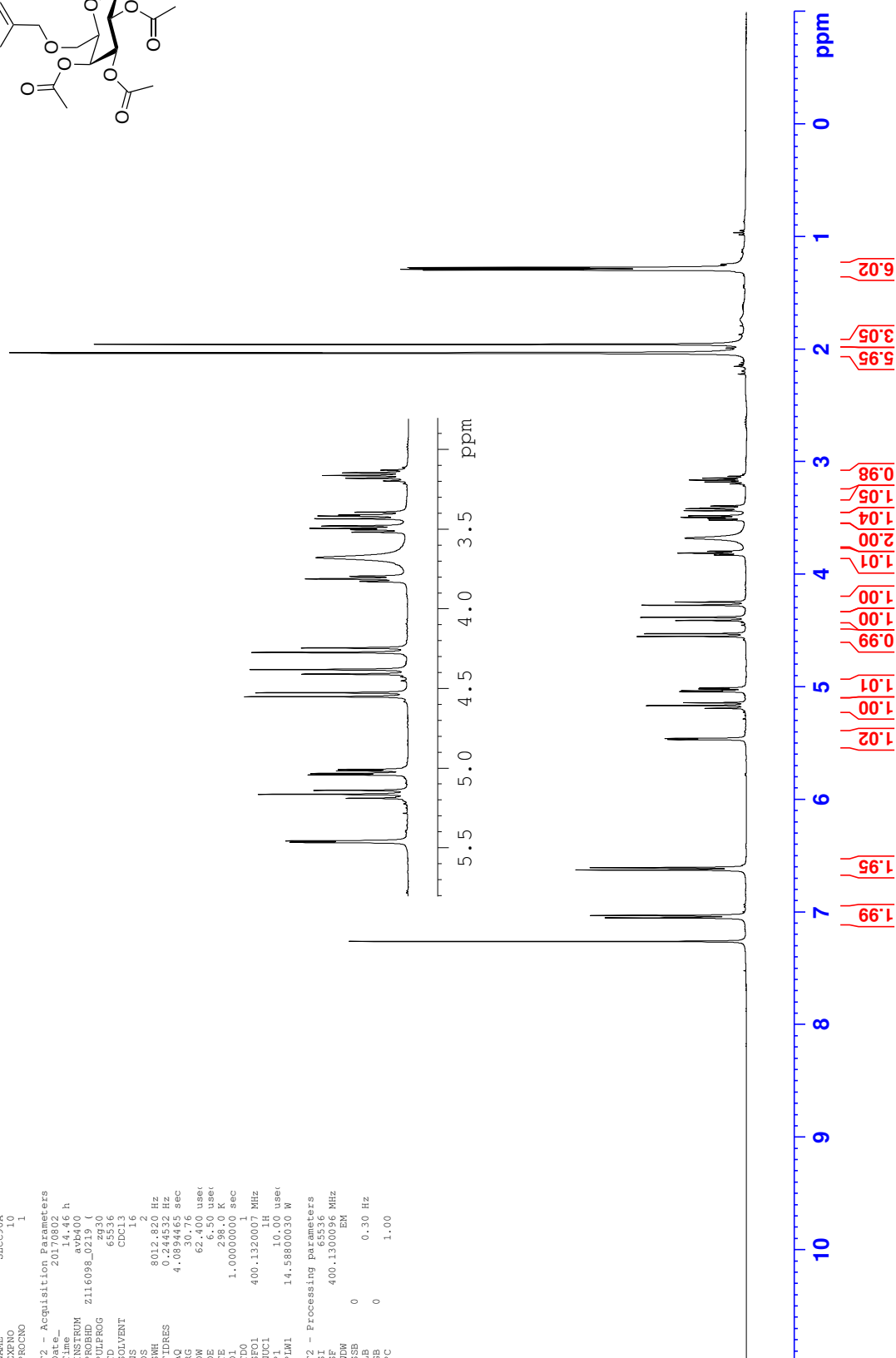
<sup>13</sup>C NMR - Isopropyl 6-O-(4-nitrobenzyl)-1-thio-β-D-galactopyranoside **89**



<sup>1</sup>H NMR - Isopropyl 2,3,4-tri-*O*-acetyl-6-*O*-(4-aminobenzyl)-1-thio-β-D-galactopyranoside **305**



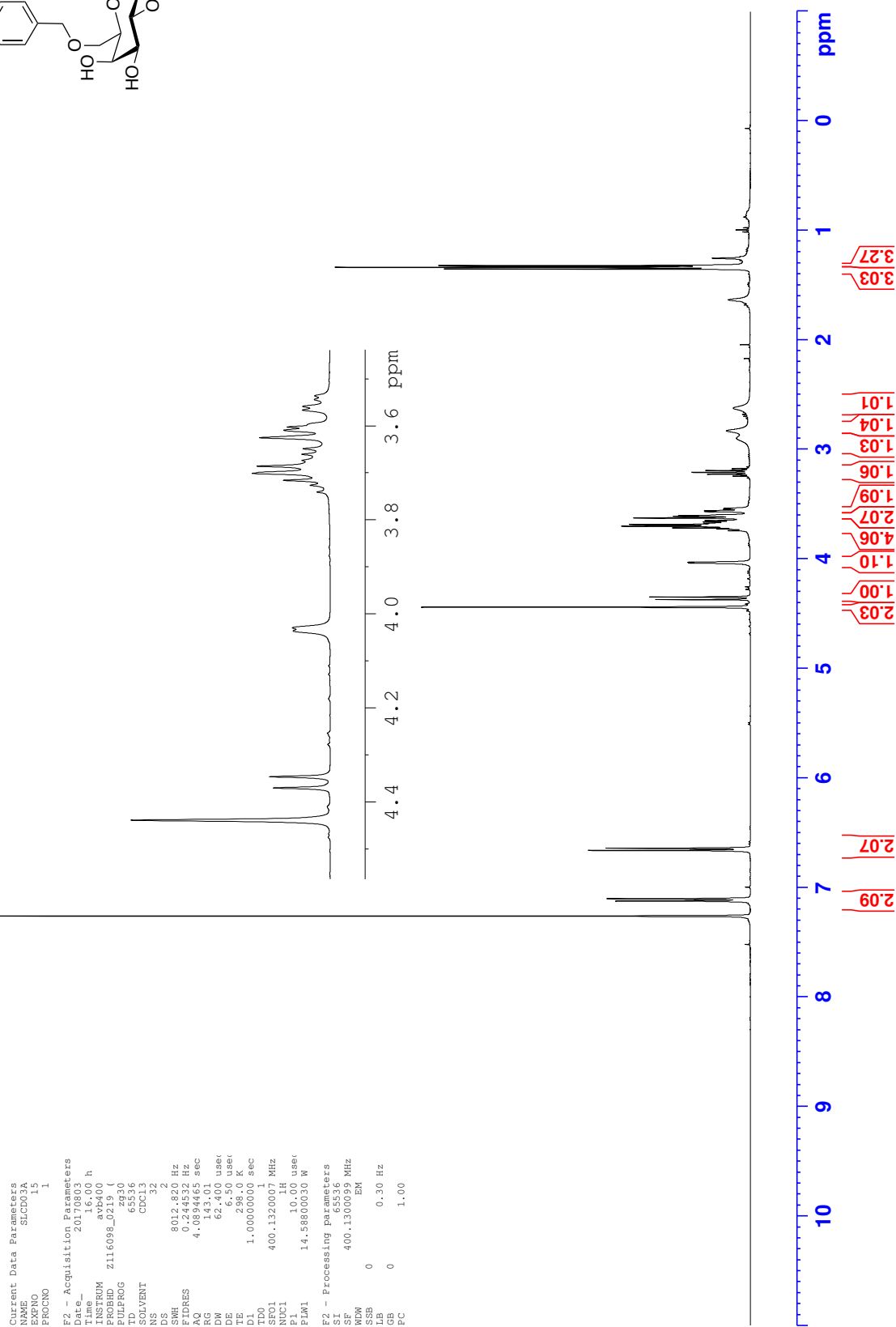
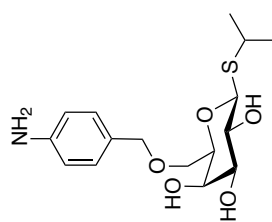
Current Data Parameters  
 NAME 305  
 EXNO 10  
 PROCNO 1  
 F2 - Acquisition Parameters  
 Date\_ 20170802  
 Time\_ 14:40  
 INSTRUM av400  
 PROBHD 2116098\_0219 (h  
 PULPROG zg30  
 TD 65536  
 SOLVENT CDCl3  
 NS 12  
 DS 2  
 SWH 8012.820 Hz  
 FIDRES 0.244532 Hz  
 AQ 4.0894465 sec  
 RG 30.76  
 DW 62.400 usec  
 DE 19.00 usec  
 TE 298.0 K  
 D1 1.00000000 sec  
 TD0 1  
 SFO1 400.1320007 MHz  
 NUC1 1H  
 P1 10.0 usec  
 PLW1 14.58800030 W  
 F2 - Processing parameters  
 SI 65536  
 SF 400.1300096 MHz  
 EQ 1  
 SSB 0  
 LB 0.30 Hz  
 GB 0  
 PC 1.00



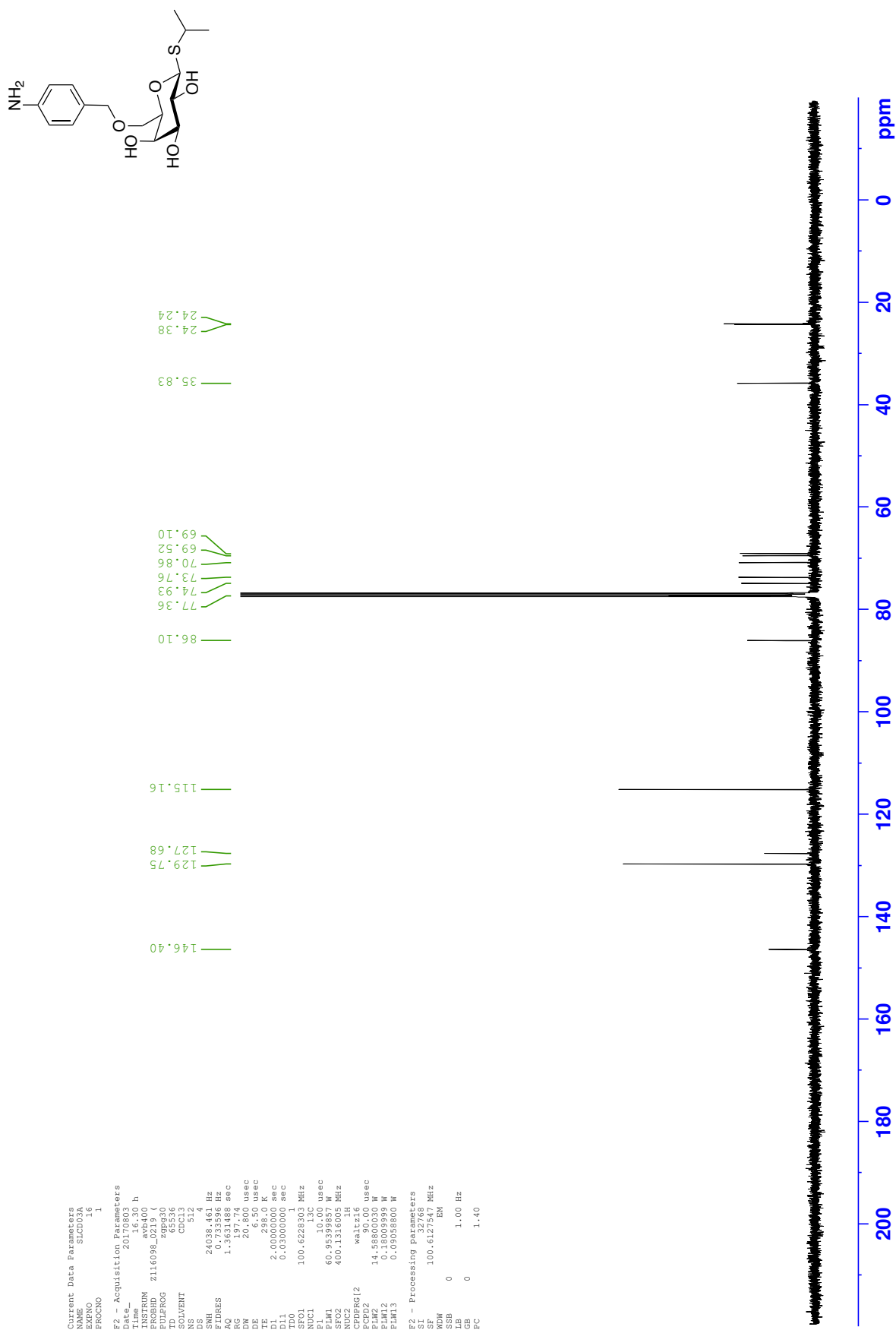




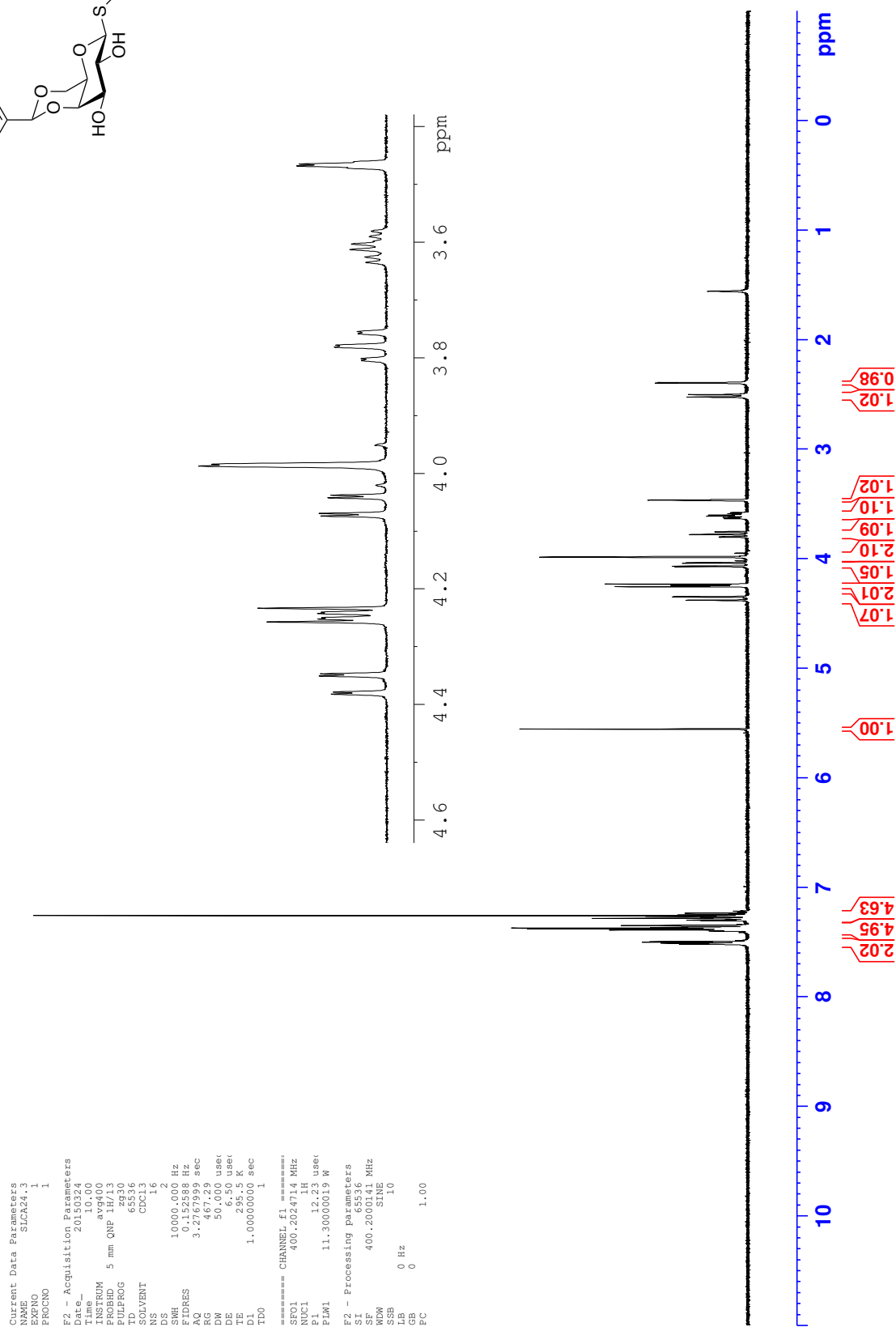
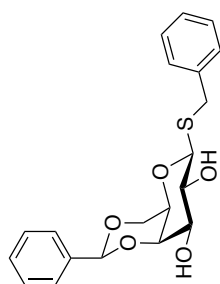
<sup>1</sup>H NMR - Isopropyl 6-O-(4-aminobenzyl)-1-thio-β-D-galactopyranoside **303**

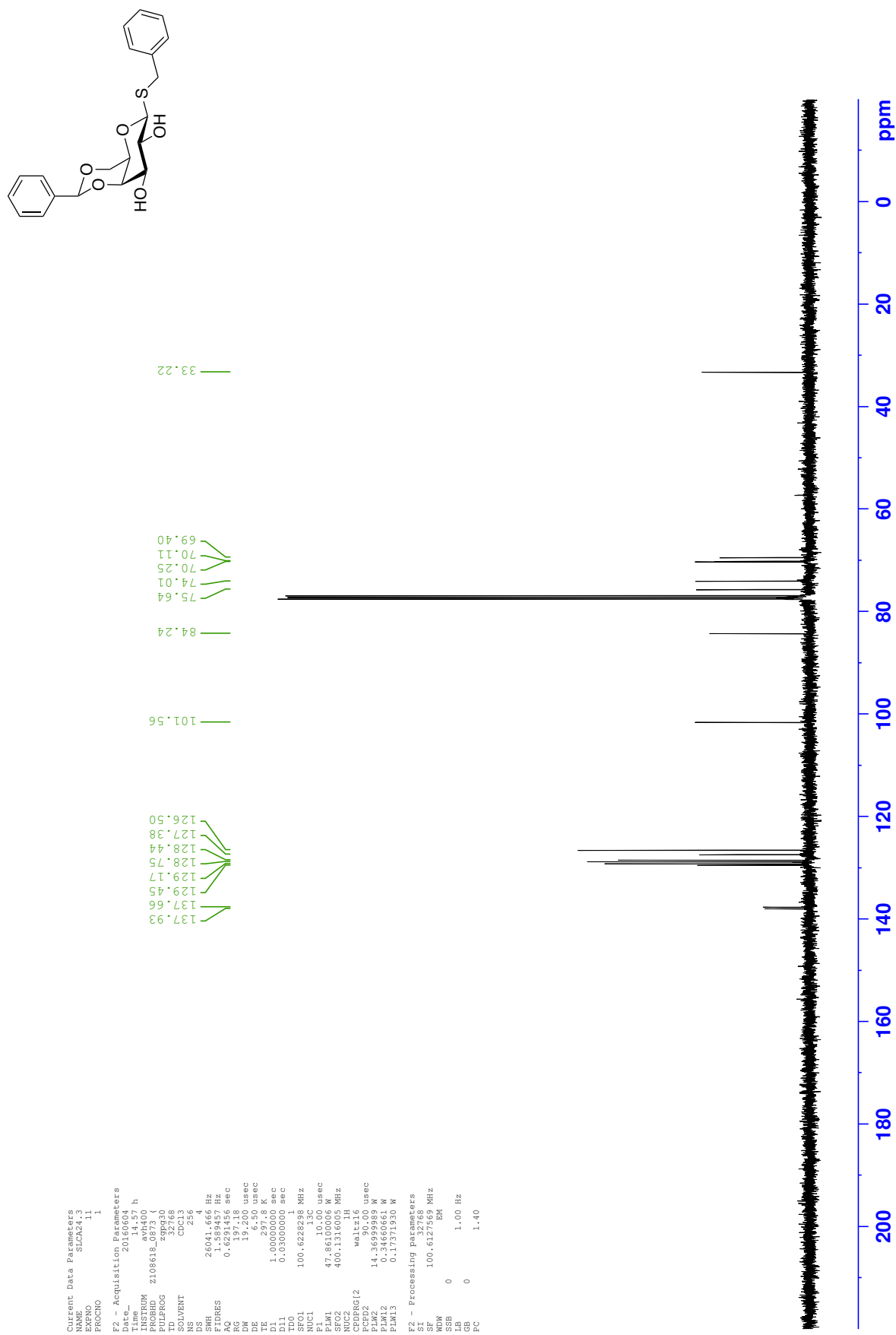


<sup>13</sup>C NMR - Isopropyl 6-*O*-(4-aminobenzyl)-1-thio-β-D-galactopyranoside **303**

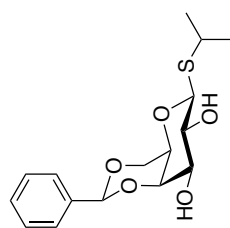


<sup>1</sup>H NMR - Benzyl 4,6-O-benzylidene-1-thio-β-D-galactopyranoside **256**

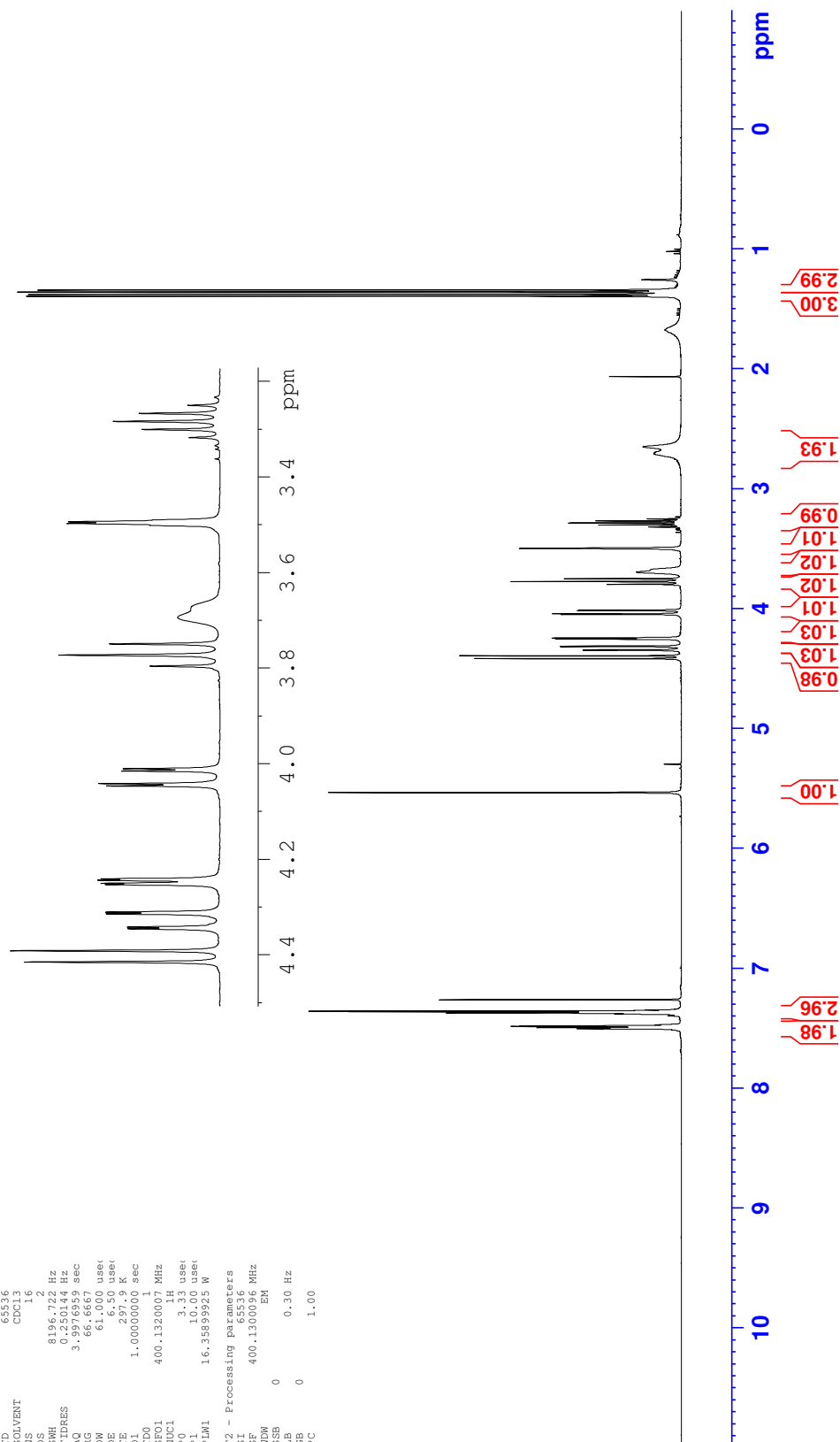


<sup>13</sup>C NMR - Benzyl 4,6-*O*-benzylidene-1-thio-β-D-galactopyranoside **256**

<sup>1</sup>H NMR - Isopropyl 4,6-O-benzylidene-1-thio-β-D-galactopyranoside 187

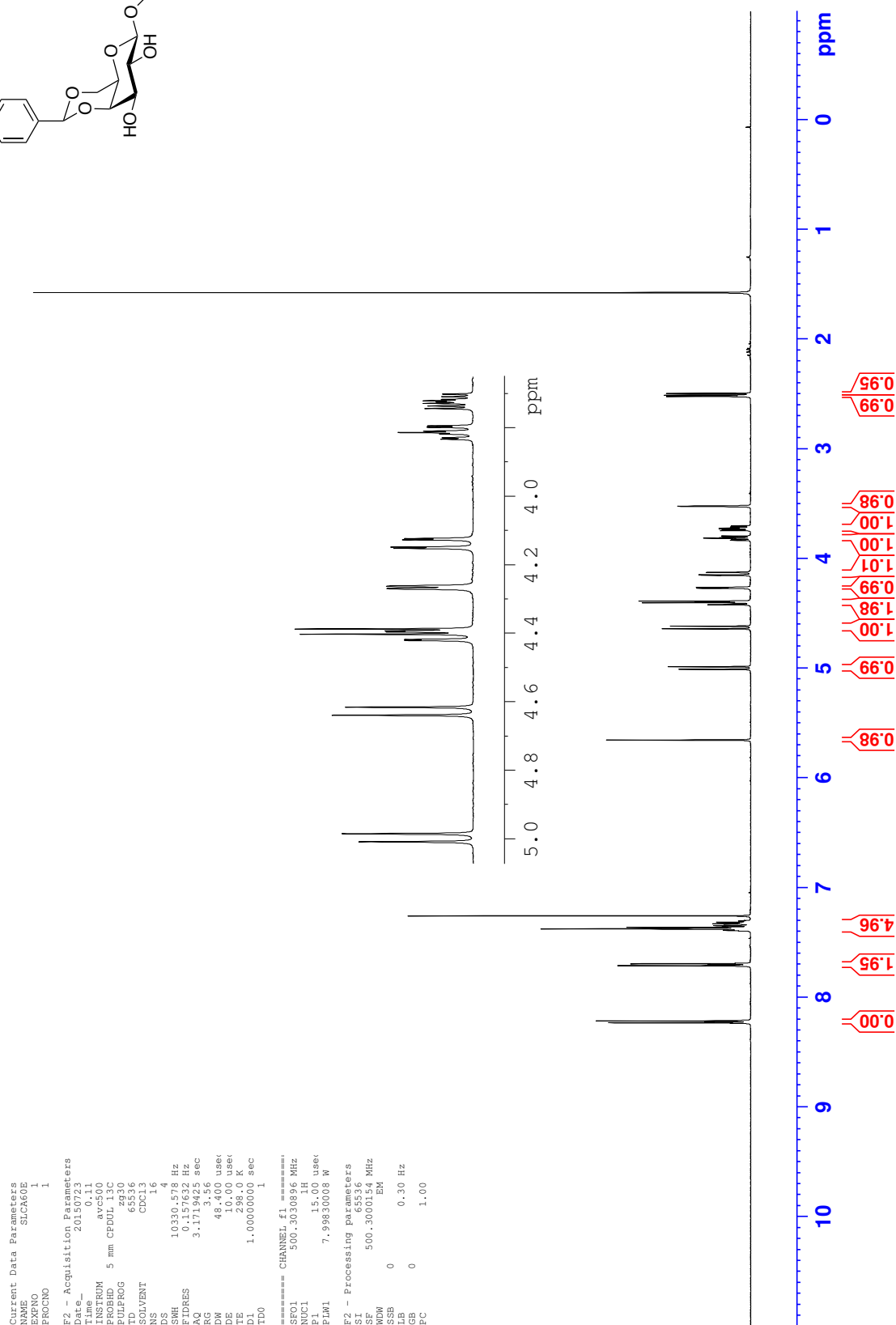
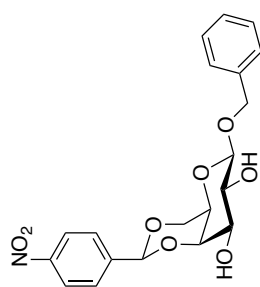


Current Data Parameters  
 NAME: 187  
 EXNO: 1  
 PROCNO: 1  
 F2 - Acquisition Parameters  
 Date\_: 20180626  
 Time: 14.52 h  
 INSTRUM: AVI9  
 PROBHD: 2116098\_0219 (16 mm QNP 1H/13  
 PULPROG: zg30  
 TD: 65536  
 SOLVENT: CDCl3  
 NS: 12  
 DS: 2  
 SWH: 8196.722 Hz  
 FIDRES: 0.250144 Hz  
 AQ: 3.9976959 sec  
 RG: 66.6667  
 DW: 61.000 usec  
 DE: 1.000 usec  
 TE: 297.9 K  
 D1: 1.00000000 sec  
 TD0: 1  
 SFO1: 400.1320007 MHz  
 NUC1: 1H user  
 P1: 10.00 usec  
 PL1: 0.00 dB  
 PLW1: 16.35899925 W  
 F2 - Processing parameters  
 SI: 65536  
 SF: 400.1300000 MHz  
 WDW: EM  
 SSB: 0  
 LB: 0.30 Hz  
 GB: 0  
 PC: 1.00



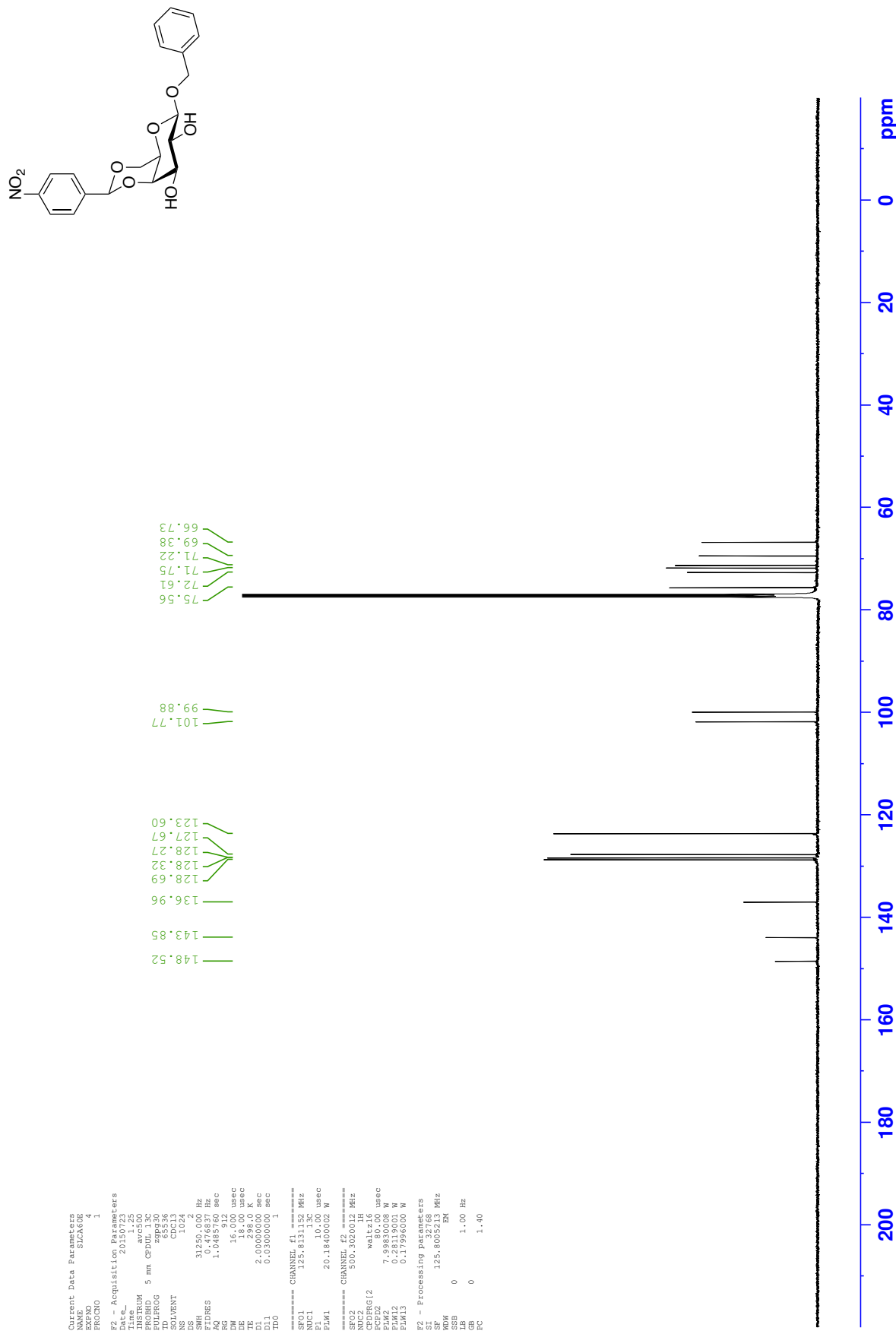


<sup>1</sup>H NMR - Benzyl 4,6-O-(4-nitrobenzylidene)-β-D-galactopyranoside 127

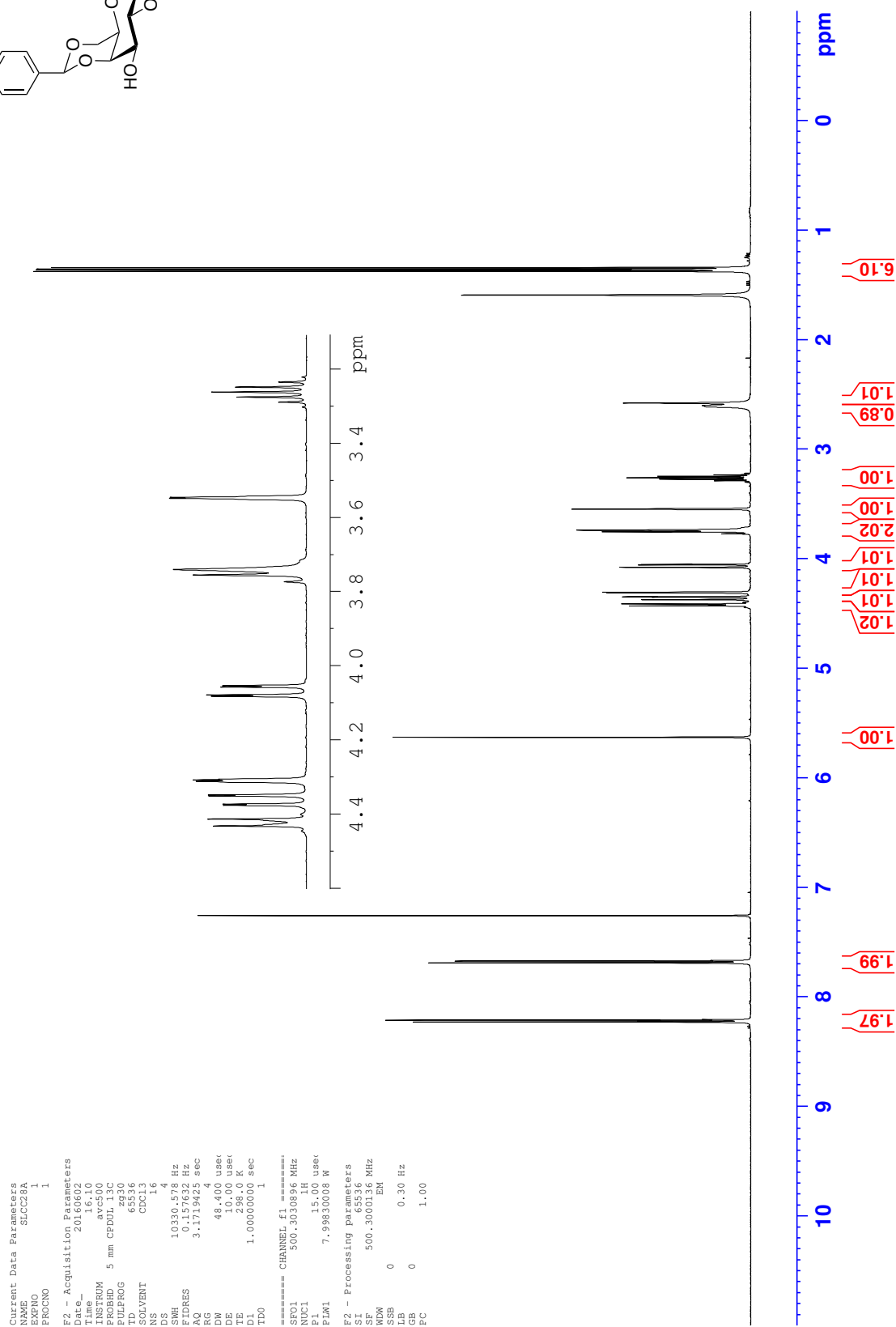
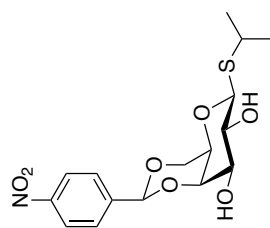




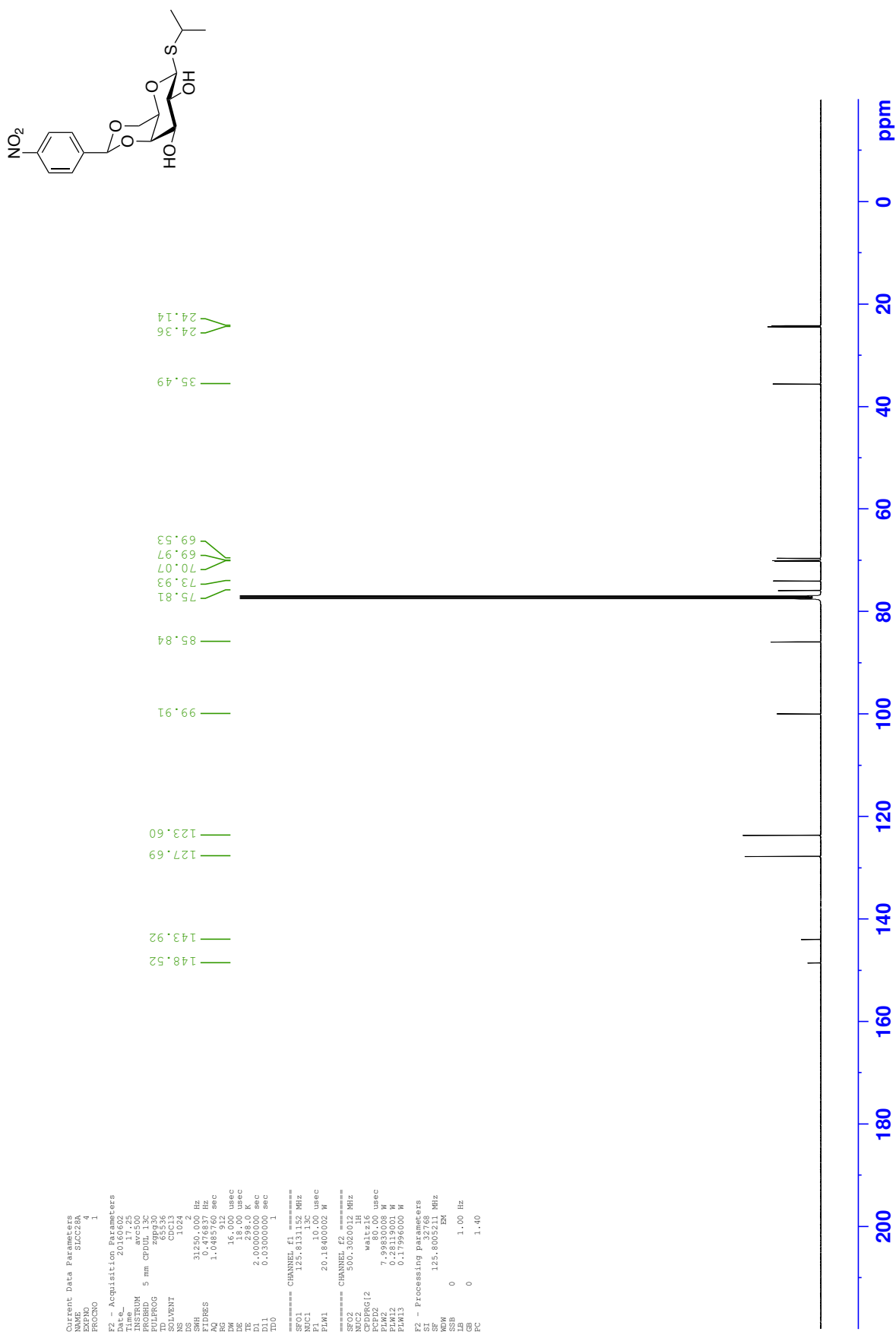
<sup>13</sup>C NMR - Benzyl 4,6-O-(4-nitrobenzylidene)-β-D-galactopyranoside **127**



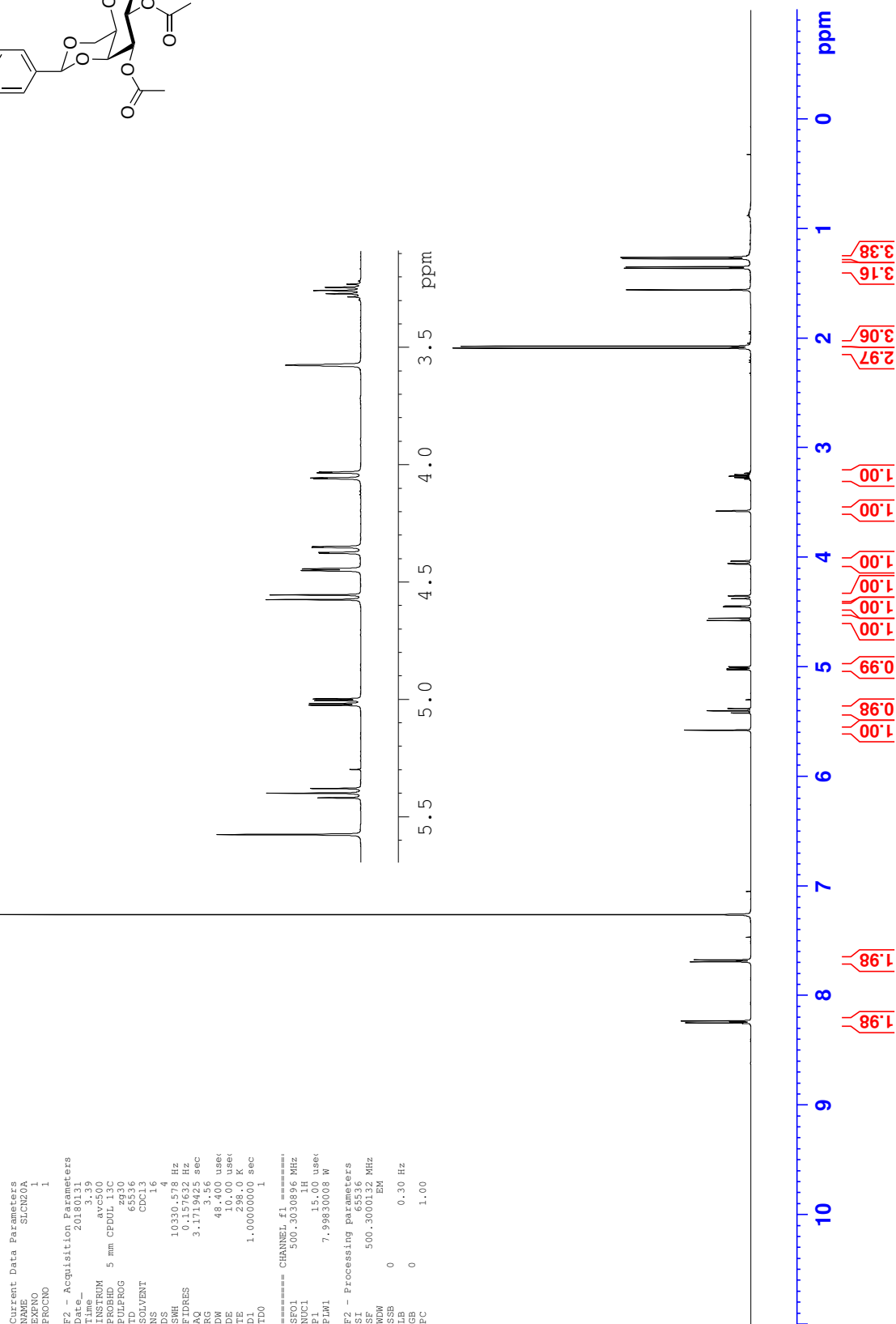
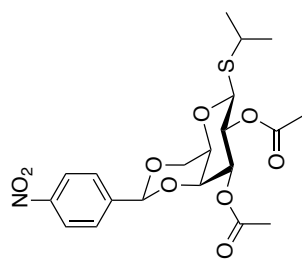
<sup>1</sup>H NMR - Isopropyl 4,6-O-(4-nitrobenzylidene)-1-thio-β-D-galactopyranoside **94**



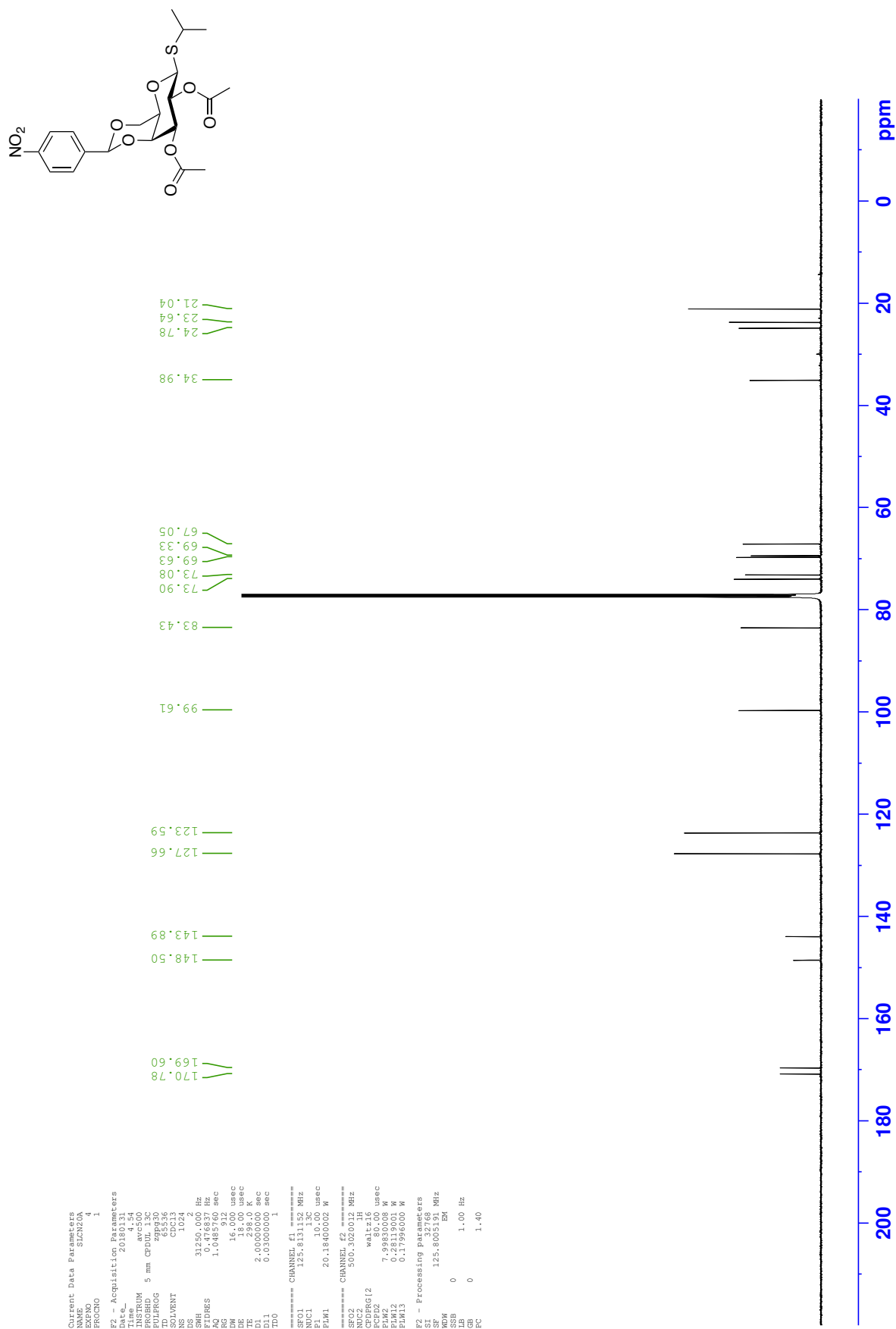
<sup>13</sup>C NMR - Isopropyl 4,6-*O*-(4-nitrobenzylidene)-1-thio-β-D-galactopyranoside **94**



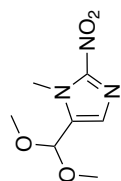
<sup>1</sup>H NMR - Isopropyl 2,3-di-*O*-acetyl-4,6-*O*-(4-nitrobenzylidene)-1-thio-β-D-galactopyranoside **308**



<sup>13</sup>C NMR - Isopropyl 2,3-di-*O*-acetyl-4,6-*O*-(4-nitrobenzylidene)-1-thio-β-D-galactopyranoside **308**



<sup>1</sup>H NMR - 5-(dimethoxymethyl)-1-methyl-2-nitro-1H-imidazole **268**



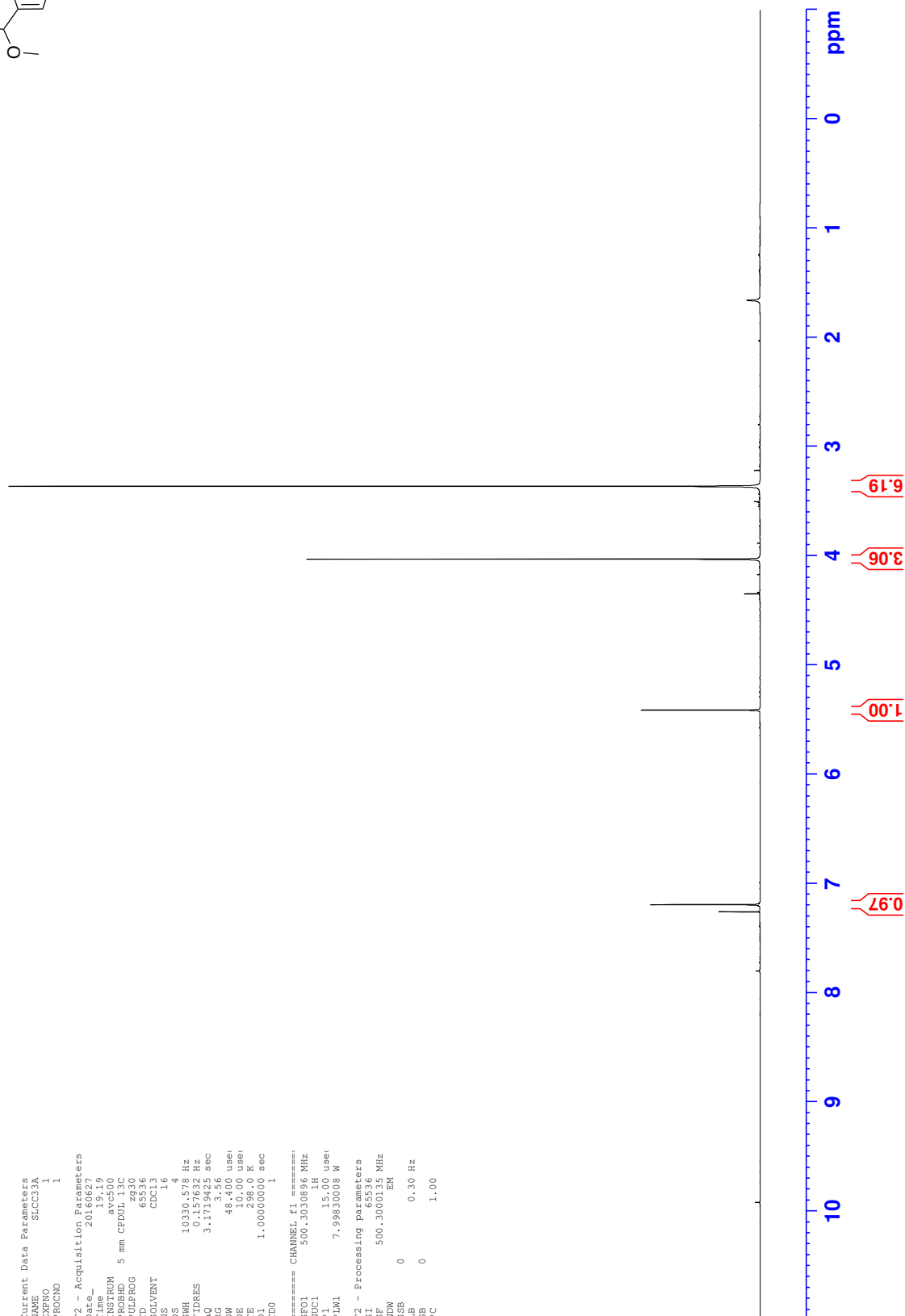
```

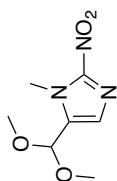
Current Data Parameters
NAME      268
EXPNO     1
PROCNO    1

F2 - Acquisition Parameters
Date_     20160627
Time      15.00
INSTRUM   spect
PROBHD    5 mm CPDUL 13C
PULPROG   zg30
TD         65536
SOLVENT   CDCl3
NS         16
DS         4
SWH        10330.578 Hz
FIDRES     0.157632 Hz
AQ          3.1719425 sec
RG          3.56
WDW         48.400 usec
SSB         0.000 usec
TE          298.0 K
D1          1.00000000 sec
TD0         1

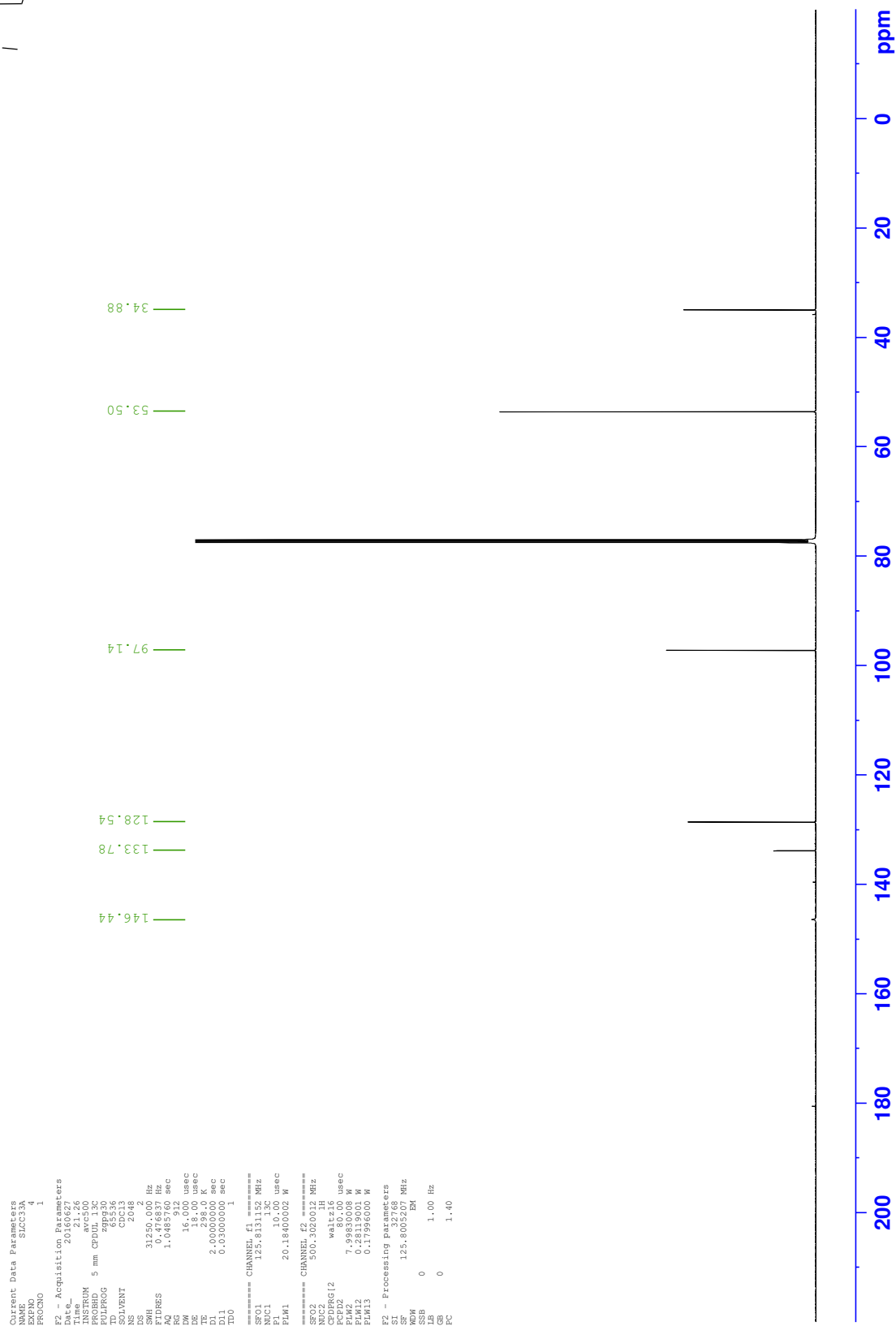
===== CHANNEL f1 =====
SFO1      500.3030856 MHz
NUC1       13C
P1         15.00 usec
PLW1       7.99830008 W

F2 - Processing parameters
SI         32768
SF          500.3000135 MHz
WDW         EM
SSB         0
LB          0.30 Hz
GB          0
PC          1.00
    
```

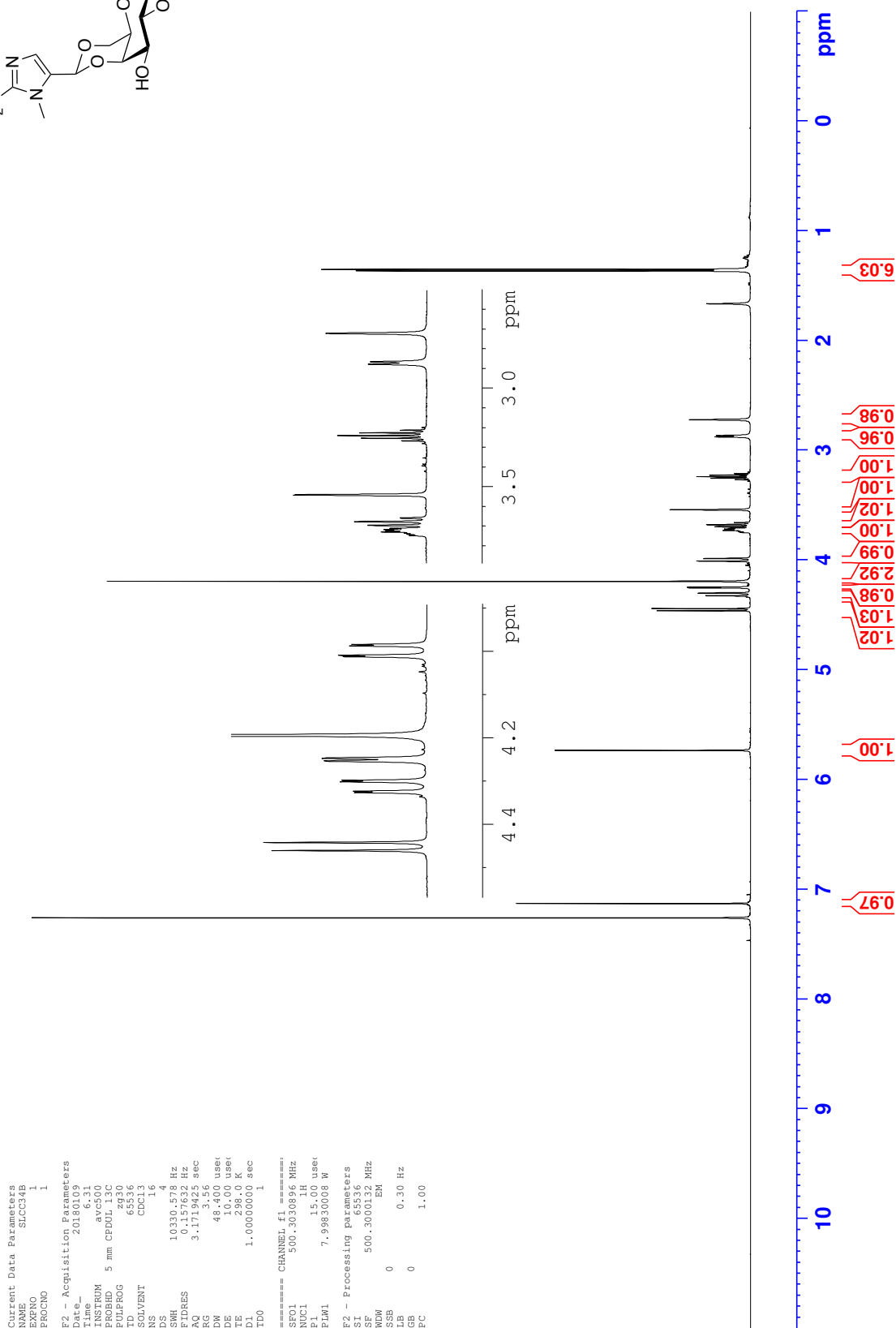
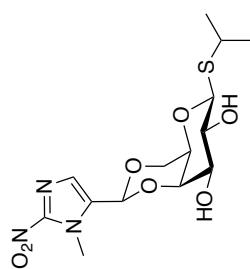




<sup>13</sup>C NMR - 5-(dimethoxymethyl)-1-methyl-2-nitro-1*H*-imidazole 268

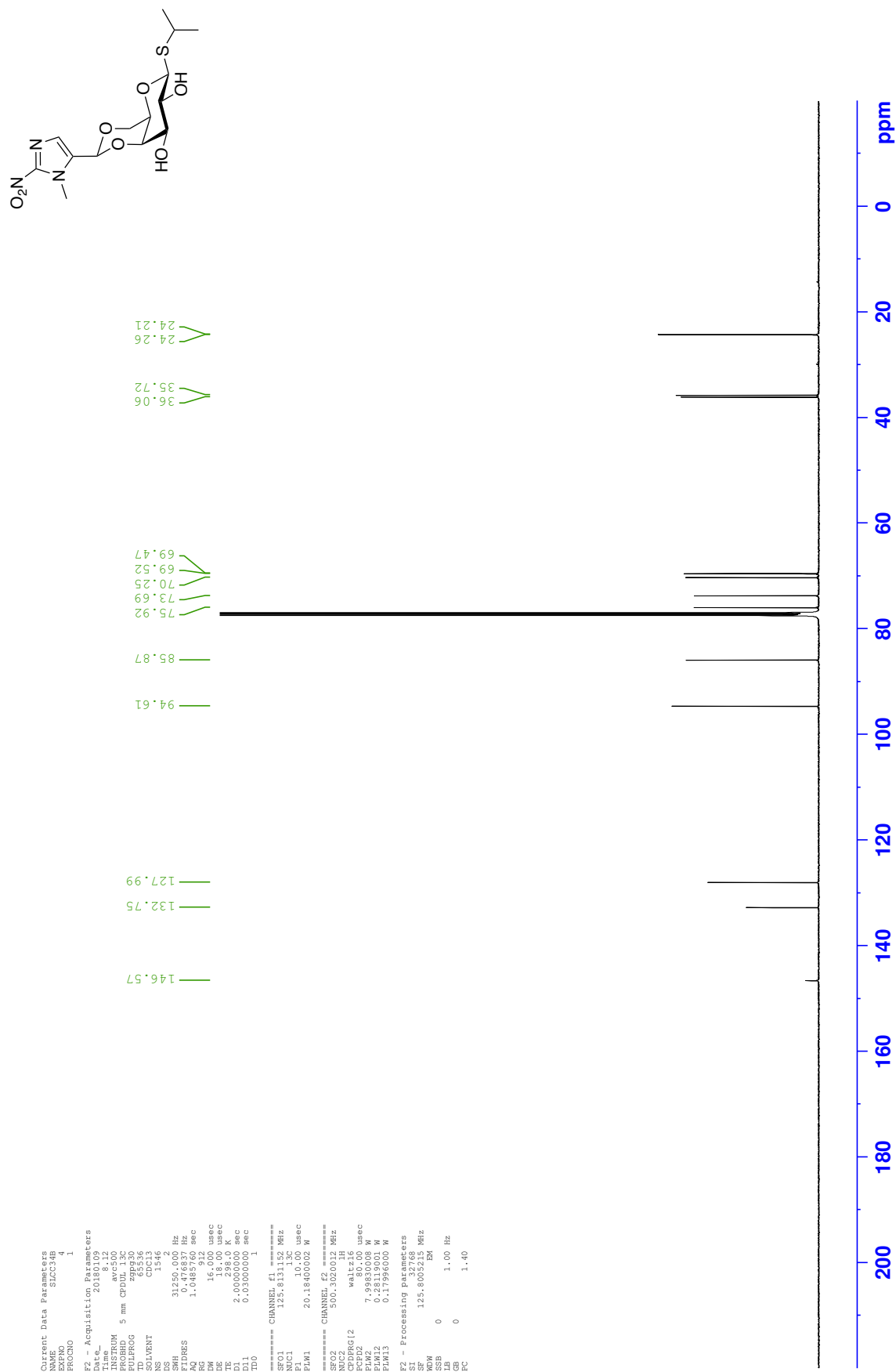


<sup>1</sup>H NMR - Isopropyl 4,6-O-(1-methyl-2-nitro-1*H*-imidazol-5-yl(methylidene))-1-thio-β-D-galactopyranoside **253**

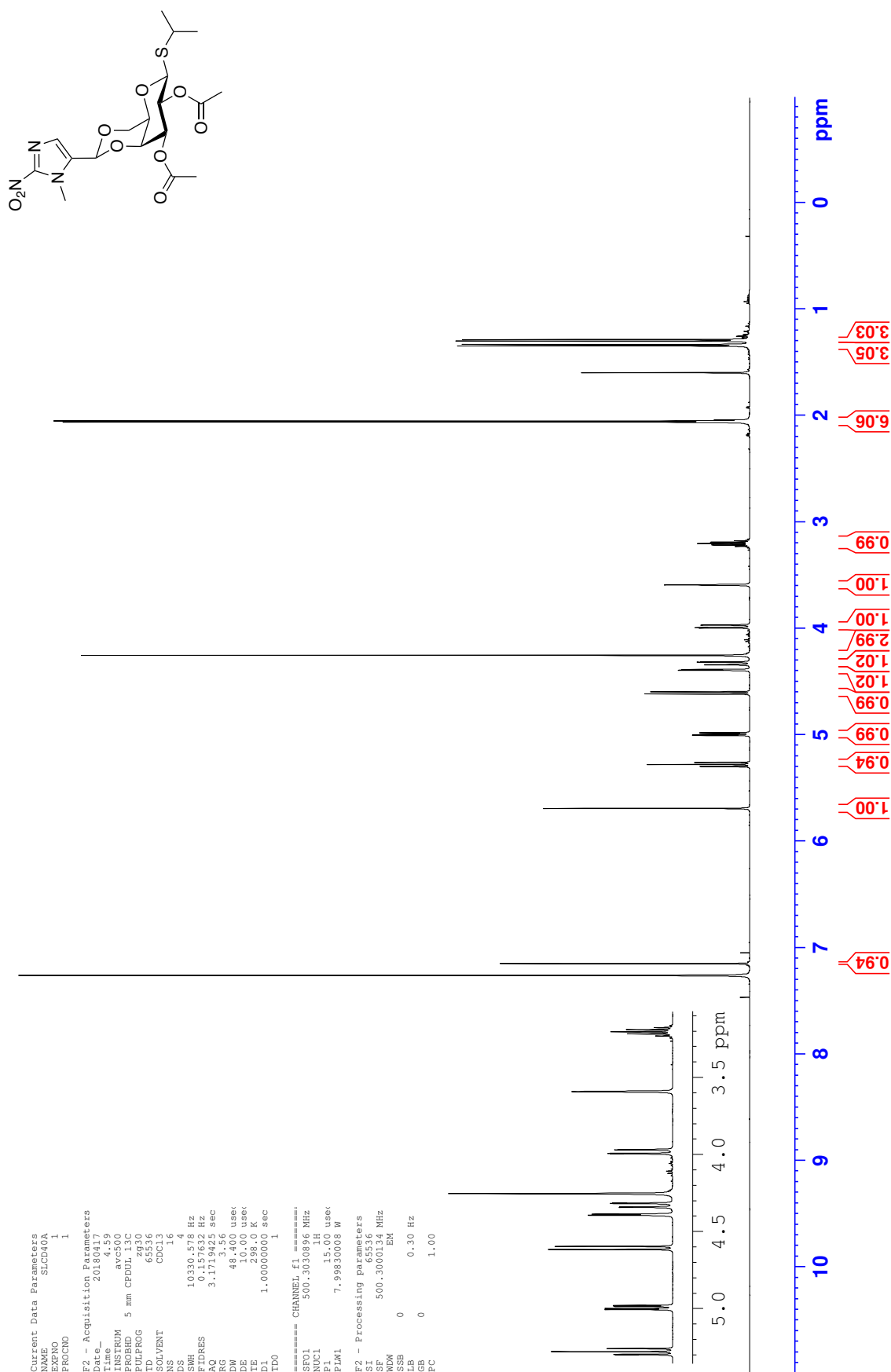




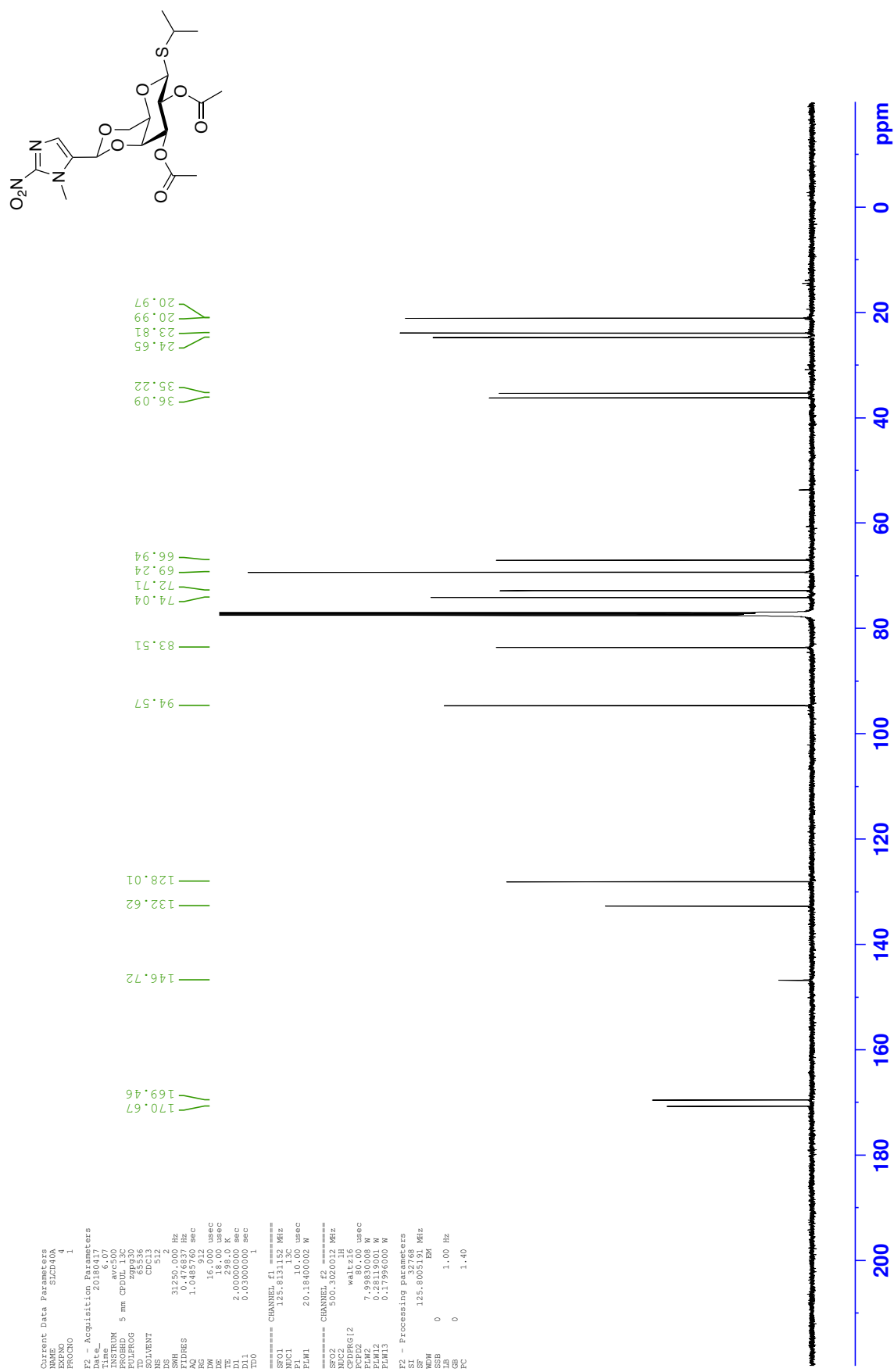
<sup>13</sup>C NMR - Isopropyl 4,6-*O*-(1-methyl-2-nitro-*H*-imidazol-5-yl(methylidene))-1-thio-β-D-galactopyranoside **253**



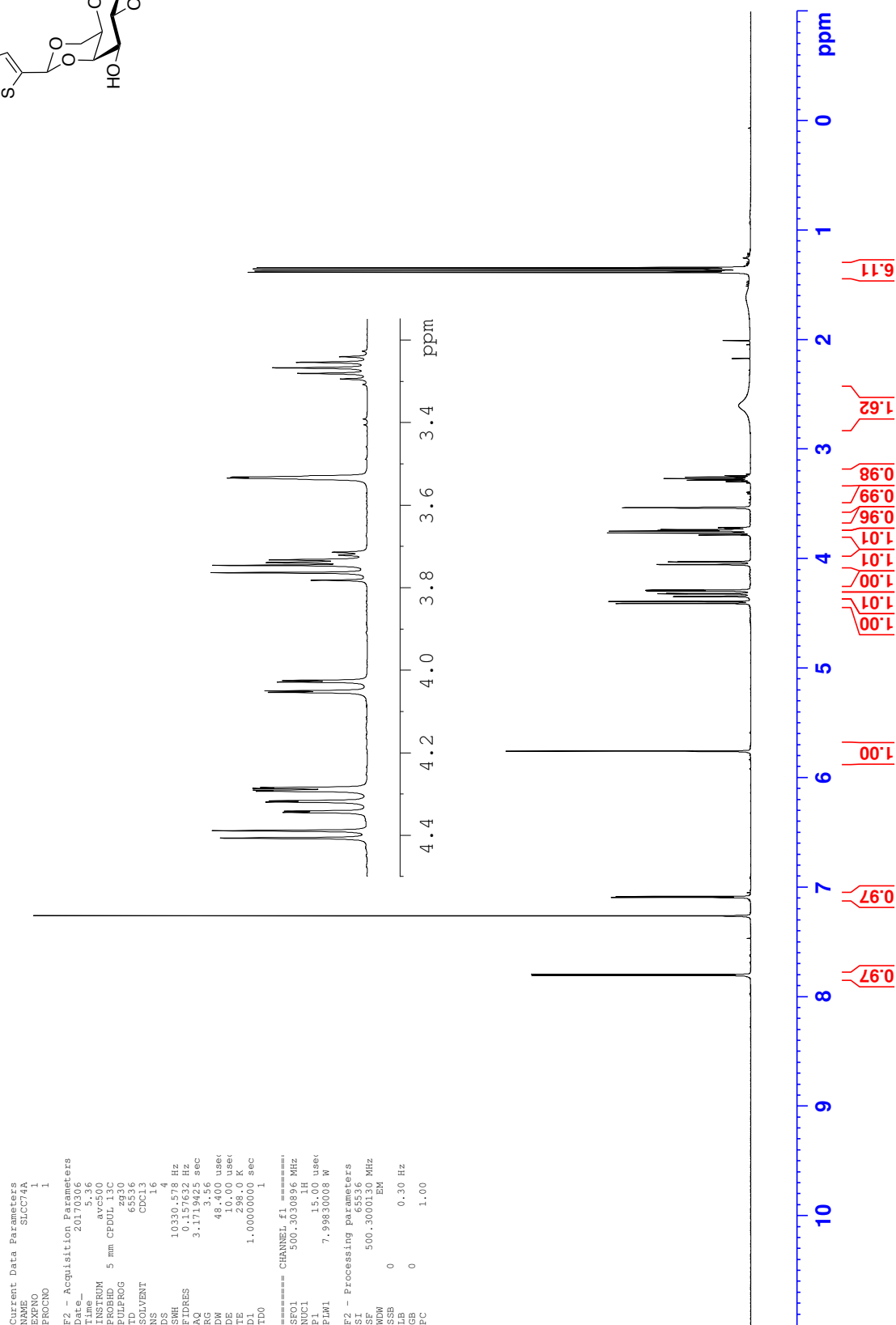
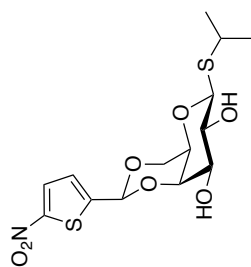
<sup>1</sup>H NMR - Isopropyl 2,3-di-O-acetyl-4,6-O-(1-methyl-2-nitro-1*H*-imidazol-5-yl(methylidene))-1-thio-β-D-galactopyranoside **309**



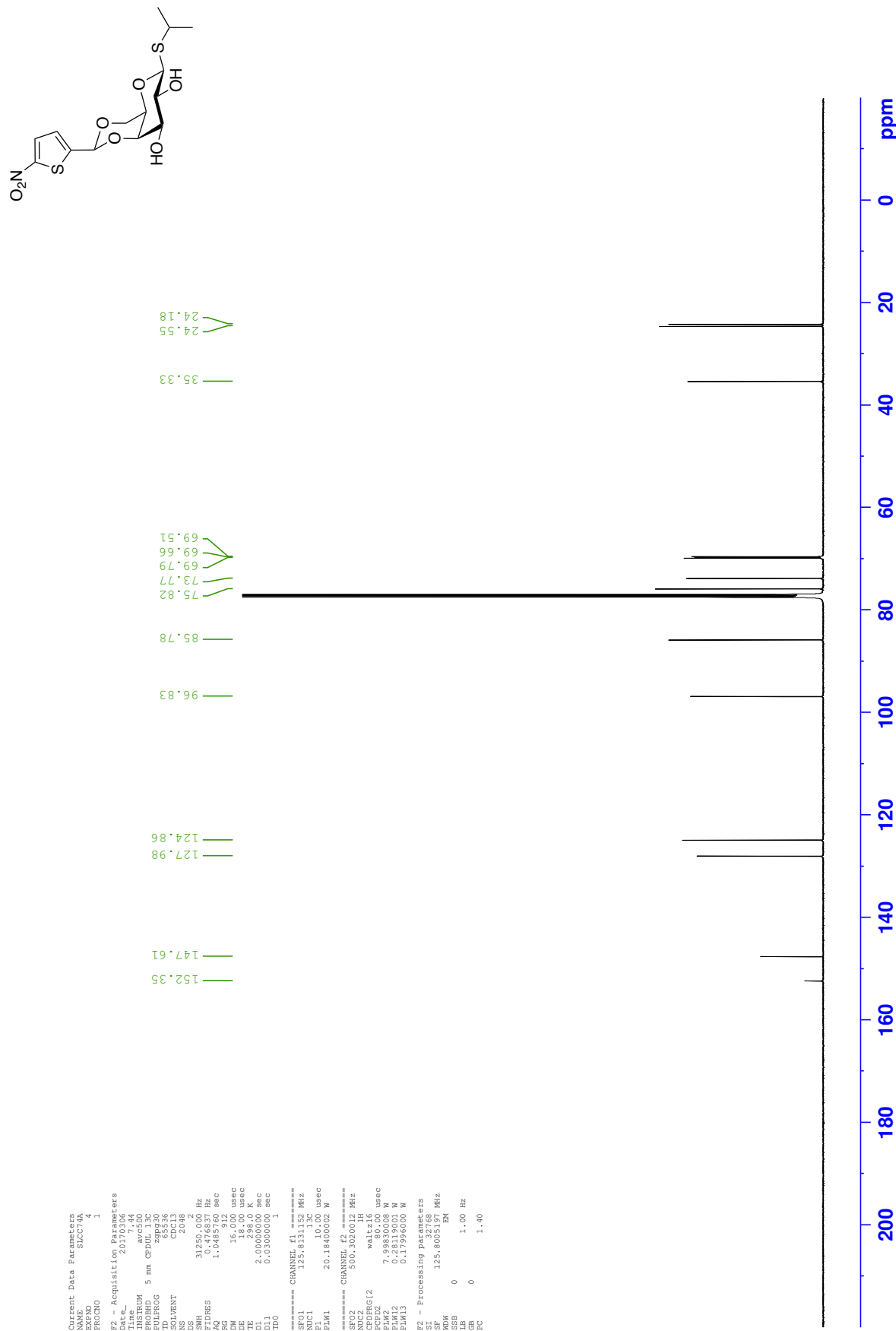
<sup>13</sup>C NMR - Isopropyl 2,3-di-*O*-acetyl-4,6-*O*-(1-methyl-2-nitro-1*H*-imidazol-5-yl(methylidene))-1-thio-β-D-galactopyranoside **309**



<sup>1</sup>H NMR - Isopropyl 4,6-O-(5-nitrothiophen-2-yl(methylidene))-1-thio-β-D-galactopyranoside **254**



<sup>13</sup>C NMR - Isopropyl 4,6-O-(5-nitrothiophen-2-yl(methylene))-1-thio-β-D-galactopyranoside **254**





20/09/2018

Reprints and Permissions | Science | AAAS

Complete issue reprints are not available, but we do offer **individual back issues of Science for purchase**.

## Requesting Permissions

Permission is required before reproducing any content (text, photos, tables, figures) from:

- *Science*
- *Science Advances* (for some uses)
- *Science Careers*
- *Science Immunology*
- *Science Robotics*
- *Science Signaling/STKE*
- *Science Translational Medicine*
- News from *Science*
- AIDScience
- SAGE KE

## Permission for authors

If you are the author of the article that was published in a *Science* journal or on a *Science* website, you retain the rights to use your paper and its contents as permitted under AAAS's **License to Publish**. If you wish to use your paper in ways that are not covered under the License to Publish, please submit your request to our Permissions Department in accordance with the guidelines below.

## Using AAAS material in a thesis or dissertation

**NOTE:** If you are the original author of the AAAS article being reproduced, please refer to your License to Publish for rules on reproducing your paper in a dissertation or thesis. AAAS permits the use of content published in its journals *Science*, *Science Immunology*, *Science Robotics*, *Science Signaling*, and *Science Translational Medicine*, but only provided the following criteria are met:

1. If you are using figure(s)/table(s), permission is granted for use in print and electronic versions of your dissertation or thesis.
2. A full-text article may be used only in print versions of a dissertation or thesis. AAAS does not permit the reproduction of full-text articles in electronic versions of theses or dissertations.

3. The following credit line must be printed along with the AAAS material: "From [Full Reference Citation]. Reprinted with permission from AAAS."
4. All required credit lines and notices must be visible any time a user accesses any part of the AAAS material and must appear on any printed copies that an authorized user might make.
5. The AAAS material may not be modified or altered except that figures and tables may be modified with permission from the author. Author permission for any such changes must be secured prior to your use.
6. AAAS must publish the full paper prior to your use of any of its text or figures.
7. If the AAAS material covered by this permission was published in *Science* during the years 1974–1994, you must also obtain permission from the author, who may grant or withhold permission, and who may or may not charge a fee if permission is granted. See original article for author's address. This condition does not apply to news articles.
8. If you are an original author of the AAAS article being reproduced, please refer to your License to Publish for rules on reproducing your paper in a dissertation or thesis.

Permission covers the distribution of your dissertation or thesis on demand by a third party distributor (e.g. ProQuest / UMI), provided the AAAS material covered by this permission remains in situ and is not distributed by that third party outside of the context of your thesis/dissertation.

Permission does not apply to figures/photos/artwork or any other content or materials included in your work that are credited to non-AAAS sources. If the requested material is sourced to or references non-AAAS sources, you must obtain authorization from that source as well before using that material. You agree to hold harmless and indemnify AAAS against any claims arising from your use of any content in your work that is credited to non-AAAS sources.

By using the AAAS material identified in your request, you agree to abide by all the terms and conditions herein.

AAAS makes no representations or warranties as to the accuracy of any information contained in the AAAS material covered by this permission, including any warranties of merchantability or fitness for a particular purpose.

Questions about these terms can be directed to the AAAS Permissions Department at [permissions@aaas.org](mailto:permissions@aaas.org).

## Reproducing AAAS material in other new works

### Get permission using RightsLink

If you are seeking permission to copy/reproduce/republish content from *Science* or *Science Translational Medicine* and are not the author of that content, you may use the Copyright Clearance Center's RightsLink service. If you are seeking permission to use content from one of the other AAAS publications listed above, please scroll down to the Special Request Guidelines below for further instructions.



19/09/2018

RightsLink - Your Account

## ELSEVIER LICENSE TERMS AND CONDITIONS

Sep 19, 2018

This Agreement between University of Oxford -- Sarah Collins ("You") and Elsevier ("Elsevier") consists of your license details and the terms and conditions provided by Elsevier and Copyright Clearance Center.

License Number	4423610377962
License date	Sep 07, 2018
Licensed Content Publisher	Elsevier
Licensed Content Publication	Cell
Licensed Content Title	Hallmarks of Cancer: The Next Generation
Licensed Content Author	Douglas Hanahan, Robert A. Weinberg
Licensed Content Date	Mar 4, 2011
Licensed Content Volume	144
Licensed Content Issue	5
Licensed Content Pages	29
Start Page	646
End Page	674
Type of Use	reuse in a thesis/dissertation
Portion	figures/tables/illustrations
Number of figures/tables/illustrations	1
Format	both print and electronic
Are you the author of this Elsevier article?	No
Will you be translating?	No
Original figure numbers	Figure 6
Title of your thesis/dissertation	Small Molecule Induced Hypoxia Activated Gene Expression
Expected completion date	Oct 2018
Estimated size (number of pages)	300
Requestor Location	University of Oxford 12 Mansfield Road  Oxford, Oxfordshire OX1 3TA United Kingdom Attn: University of Oxford
Publisher Tax ID	GB 494 6272 12
Total	<b>0.00 GBP</b>
Terms and Conditions	

20/09/2018

RightsLink - Your Account

## AMERICAN ASSOCIATION FOR CANCER RESEARCH LICENSE TERMS AND CONDITIONS

Sep 20, 2018

This Agreement between University of Oxford -- Sarah Collins ("You") and American Association for Cancer Research ("American Association for Cancer Research") consists of your license details and the terms and conditions provided by American Association for Cancer Research and Copyright Clearance Center.

License Number	4425301420715
License date	Sep 10, 2018
Licensed Content Publisher	American Association for Cancer Research
Licensed Content Publication	Cancer Research
Licensed Content Title	Association between Tumor Hypoxia and Malignant Progression in Advanced Cancer of the Uterine Cervix
Licensed Content Author	Michael Höckel,Karlheinz Schlenger,Billur Aral,Margarete Mitze,Uwe Schäffer,Peter Vaupel
Licensed Content Date	Oct 1, 1996
Licensed Content Volume	56
Licensed Content Issue	19
Type of Use	Thesis/Dissertation
Requestor type	academic/educational
Format	print and electronic
Portion	figures/tables/illustrations
Number of figures/tables/illustrations	1
Will you be translating?	no
Circulation	5
Territory of distribution	Worldwide
Title of your thesis / dissertation	Small Molecule Induced Hypoxia Activated Gene Expression
Expected completion date	Oct 2018
Estimated size (number of pages)	300
Requestor Location	University of Oxford 12 Mansfield Road  Oxford, Oxfordshire OX1 3TA United Kingdom Attn: University of Oxford
Billing Type	Invoice
Billing Address	University of Oxford 12 Mansfield Road  Oxford, United Kingdom OX1 3TA Attn: University of Oxford
Total	<b>0.00 GBP</b>
Terms and Conditions	



**Confirmation Number: 11748606**  
**Order Date: 09/14/2018**

#### Customer Information

**Customer:** Sarah Collins  
**Account Number:** 3001335724  
**Organization:** University of Oxford  
**Email:** sarah.collins@exeter.ox.ac.uk  
**Phone:** +44 7999332525  
**Payment Method:** Invoice

**This is not an invoice**

#### Order Details

**Current molecular medicine**

Billing Status:  
**N/A**

**Order detail ID:** 71552920

**ISSN:** 1566-5240

**Publication Type:** Journal

**Volume:**

**Issue:**

**Start page:**

**Publisher:** BENTHAM SCIENCE PUBLISHERS LTD.

**Permission Status:** **Granted**

**Permission type:** Republish or display content

**Type of use:** Thesis/Dissertation

**Order License Id:** 4427700610567

<b>Requestor type</b>	Academic institution
<b>Format</b>	Print, Electronic
<b>Portion</b>	chart/graph/table/figure
<b>Number of charts/graphs/tables/figures</b>	1
<b>The requesting person/organization</b>	Sarah Collins/University of Oxford
<b>Title or numeric reference of the portion(s)</b>	Figure 1
<b>Title of the article or chapter the portion is from</b>	Hypoxia and Radiation Therapy: Past History, Ongoing Research, and Future Promise
<b>Editor of portion(s)</b>	N/A
<b>Author of portion(s)</b>	Vu, Van Thuc ; et al
<b>Volume of serial or monograph</b>	9
<b>Issue, if republishing an article from a serial</b>	4
<b>Page range of portion</b>	442-458
<b>Publication date of portion</b>	May 1, 2009
<b>Rights for</b>	Main product
<b>Duration of use</b>	Life of current edition
<b>Creation of copies for the disabled</b>	no
<b>With minor editing privileges</b>	no

Copyright Clearance Center

20/09/2018, 12:17

<b>For distribution to</b>	U.K. and Commonwealth (excluding Canada)
<b>In the following language(s)</b>	Original language of publication
<b>With incidental promotional use</b>	no
<b>Lifetime unit quantity of new product</b>	Up to 499
<b>Title</b>	Small Molecule Induced Hypoxia Activated Gene Expression
<b>Instructor name</b>	Stuart Conway
<b>Institution name</b>	University of Oxford
<b>Expected presentation date</b>	Oct 2018

**Note:** This item was invoiced separately through our **RightsLink service**. [More info](#) **\$ 0.00**

---

<b>Total order items: 1</b>	<b>Order Total: \$0.00</b>
-----------------------------	----------------------------

[About Us](#) | [Privacy Policy](#) | [Terms & Conditions](#) | [Pay an Invoice](#)

Copyright 2018 Copyright Clearance Center



**Confirmation Number: 11748610**  
**Order Date: 09/14/2018**

#### Customer Information

**Customer:** Sarah Collins  
**Account Number:** 3001335724  
**Organization:** University of Oxford  
**Email:** sarah.collins@exeter.ox.ac.uk  
**Phone:** +44 7999332525  
**Payment Method:** Invoice

**This is not an invoice**

#### Order Details

**Annual review of plant biology**

Billing Status:  
**N/A**

**Order detail ID:** 71552925  
**ISSN:** 1545-2123  
**Publication Type:** e-Journal  
**Volume:**  
**Issue:**  
**Start page:**  
**Publisher:** ANNUAL REVIEWS  
**Author/Editor:** Annual Reviews, Inc

**Permission Status:** **Granted**  
**Permission type:** Republish or display content  
**Type of use:** Thesis/Dissertation  
**Order License Id:** 4427700866199

<b>Requestor type</b>	Academic institution
<b>Format</b>	Print, Electronic
<b>Portion</b>	chart/graph/table/figure
<b>Number of charts/graphs/tables/figures</b>	1
<b>The requesting person/organization</b>	Sarah Collins/University of Oxford
<b>Title or numeric reference of the portion(s)</b>	Figure 1
<b>Title of the article or chapter the portion is from</b>	oxygen sensing and signalling
<b>Editor of portion(s)</b>	N/A
<b>Author of portion(s)</b>	Joost T. van Dongen and Francesco Licausi
<b>Volume of serial or monograph</b>	66
<b>Issue, if republishing an article from a serial</b>	n/a
<b>Page range of portion</b>	345-367
<b>Publication date of portion</b>	12 January 2015
<b>Rights for</b>	Main product
<b>Duration of use</b>	Life of current edition
<b>Creation of copies for the disabled</b>	no
<b>With minor editing privileges</b>	no

Copyright Clearance Center

20/09/2018, 12:19

<b>For distribution to</b>	U.K. and Commonwealth (excluding Canada)
<b>In the following language(s)</b>	Original language of publication
<b>With incidental promotional use</b>	no
<b>Lifetime unit quantity of new product</b>	Up to 499
<b>Title</b>	Small Molecule Induced Hypoxia Activated Gene Expression
<b>Instructor name</b>	Stuart Conway
<b>Institution name</b>	University of Oxford
<b>Expected presentation date</b>	Oct 2018

**Note:** This item was invoiced separately through our **RightsLink service**. [More info](#) **\$ 0.00**

---

<b>Total order items: 1</b>	<b>Order Total: \$0.00</b>
-----------------------------	----------------------------

[About Us](#) | [Privacy Policy](#) | [Terms & Conditions](#) | [Pay an Invoice](#)

Copyright 2018 Copyright Clearance Center

20/09/2018

RightsLink - Your Account

## SPRINGER NATURE LICENSE TERMS AND CONDITIONS

Sep 20, 2018

This Agreement between University of Oxford -- Sarah Collins ("You") and Springer Nature ("Springer Nature") consists of your license details and the terms and conditions provided by Springer Nature and Copyright Clearance Center.

License Number	4426021475169
License date	Sep 11, 2018
Licensed Content Publisher	Springer Nature
Licensed Content Publication	Nature Reviews Cancer
Licensed Content Title	Targeting hypoxia in cancer therapy
Licensed Content Author	William R. Wilson, Michael P. Hay
Licensed Content Date	May 24, 2011
Licensed Content Volume	11
Licensed Content Issue	6
Type of Use	Thesis/Dissertation
Requestor type	academic/university or research institute
Format	print and electronic
Portion	figures/tables/illustrations
Number of figures/tables/illustrations	1
High-res required	no
Will you be translating?	no
Circulation/distribution	<501
Author of this Springer Nature content	no
Title	Small Molecule Induced Hypoxia Activated Gene Expression
Instructor name	n/a
Institution name	n/a
Expected presentation date	Oct 2018
Portions	Figure 1
Requestor Location	University of Oxford 12 Mansfield Road  Oxford, Oxfordshire OX1 3TA United Kingdom Attn: University of Oxford
Billing Type	Invoice
Billing Address	University of Oxford 12 Mansfield Road  Oxford, United Kingdom OX1 3TA Attn: University of Oxford
Total	<b>0.00 GBP</b>
Terms and Conditions	

20/09/2018

RightsLink - Your Account

## ELSEVIER LICENSE TERMS AND CONDITIONS

Sep 20, 2018

This Agreement between University of Oxford -- Sarah Collins ("You") and Elsevier ("Elsevier") consists of your license details and the terms and conditions provided by Elsevier and Copyright Clearance Center.

License Number	4427170951206
License date	Sep 13, 2018
Licensed Content Publisher	Elsevier
Licensed Content Publication	Bioorganic & Medicinal Chemistry
Licensed Content Title	Design of a bioreductively-activated fluorescent pH probe for tumor hypoxia imaging
Licensed Content Author	Eiji Nakata, Yoshihiro Yukimachi, Hirokazu Kariyazono, Seongwang Im, Chiaki Abe, Yoshihiro Uto, Hiroshi Maezawa, Toshihiro Hashimoto, Yasuko Okamoto, Hitoshi Hori
Licensed Content Date	Oct 1, 2009
Licensed Content Volume	17
Licensed Content Issue	19
Licensed Content Pages	7
Start Page	6952
End Page	6958
Type of Use	reuse in a thesis/dissertation
Intended publisher of new work	other
Portion	figures/tables/illustrations
Number of figures/tables/illustrations	1
Format	both print and electronic
Are you the author of this Elsevier article?	No
Will you be translating?	No
Original figure numbers	Figure 2
Title of your thesis/dissertation	Small Molecule Induced Hypoxia Activated Gene Expression
Expected completion date	Oct 2018
Estimated size (number of pages)	300
Requestor Location	University of Oxford 12 Mansfield Road  Oxford, Oxfordshire OX1 3TA United Kingdom Attn: University of Oxford
Publisher Tax ID	GB 494 6272 12
Total	<b>0.00 GBP</b>
Terms and Conditions	